

# Geologic Framework of Aquifer Units and Ground-Water Flowpaths, Verde River Headwaters, North-Central Arizona



Open-File Report 2004-1411

# **Geologic Framework of Aquifer Units and Ground-Water Flowpaths, Verde River Headwaters, North-Central Arizona**

Edited by Laurie Wirt, Ed DeWitt, and V.E. Langenheim

Prepared in cooperation with the Arizona Water Protection Fund Commission

Open-File Report 2004-1411

**U.S. Department of the Interior  
U.S. Geological Survey**

**U.S. Department of the Interior**  
Gale A. Norton, Secretary

**U.S. Geological Survey**  
P. Patrick Leahy, Acting Director

U.S. Geological Survey, Reston, Virginia: 2005

This publication is *only* available online at URL:

**<http://pubs.usgs.gov/of/2004/1411/>**

For information on other USGS products and ordering information:

World Wide Web: <http://www.usgs.gov/pubprod/>

Telephone: 1-888-ASK-USGS

For more information on the USGS—the Federal source for science about the Earth,  
its natural and living resources, natural hazards, and the environment:

World Wide Web: <http://www.usgs.gov/>

Telephone: 1-888-ASK-USGS

Any use of trade, product, or firm names in this publication is for descriptive purposes only  
and does not imply endorsement by the U.S. Government.

Although this report is in the public domain, permission must be secured from the individual  
copyright owners to reproduce any copyrighted materials contained within this report.

# Contents

The Verde River Headwaters, Yavapai County, Arizona.....	A
by Laurie Wirt	
Geologic Framework.....	B
by Ed DeWitt, Victoria E. Langenheim, and Laurie Wirt	
Geophysical Framework.....	C
by Victoria E. Langenheim, Ed DeWitt, and Laurie Wirt	
Hydrogeologic Framework.....	D
by Laurie Wirt, Ed DeWitt, and Victoria E. Langenheim	
Geochemistry of Major Aquifers and Springs.....	E
by Laurie Wirt and Ed DeWitt	
Sources of Base Flow in the upper Verde River.....	F
by Laurie Wirt	
Synthesis of Geologic, Geophysical, Hydrological, and Geochemical Evidence.....	G
by Laurie Wirt	
Glossary	
Appendix A	
Appendix B	

## Abbreviated Water-Quality Units

mg/L, milligrams per liter  
 µg/L, micrograms per liter  
 µS/cm, microsiemens per centimeter at 25 degrees Celsius  
 % meq/l, percent milliequivalents per liter  
 $\delta^{18}\text{O}$ , delta notation, for the ratio of oxygen-18/oxygen-16,  
 expressed in per mil or parts per thousand  
 $\delta\text{D}$ , delta notation for the ratio of hydrogen-2/hydrogen-1,  
 expressed in per mil or parts per thousand  
 ‰, notation for per mil, or parts per thousand  
 TU, tritium units  
 pCi/L, picocuries per liter  
 pmc, percent modern carbon

## Conversion Factors

### Inch/Pound to International Scientific Units (SI)

Multiply	By	To obtain
Length		
inch (in.)	2.54	centimeter (cm)
inch (in.)	25.4	millimeter (mm)
foot (ft)	0.3048	meter (m)
mile (mi)	1.609	kilometer (km)
Area		
square foot (ft <sup>2</sup> )	0.09290	square meter (m <sup>2</sup> )
square mile (mi <sup>2</sup> )	2.590	square kilometer (km <sup>2</sup> )
Volume		
gallon (gal)	3.785	liter (L)
gallon (gal)	0.003785	cubic meter (m <sup>3</sup> )
acre-foot (acre-ft)	1,233	cubic meter (m <sup>3</sup> )
Flow rate		
gallon per minute (gal/min)	0.06309	liter per second (L/s)
acre-foot per day (acre-ft/d)	0.01427	cubic meter per second (m <sup>3</sup> /s)
acre-foot per year (acre-ft/yr)	1,233	cubic meter per year (m <sup>3</sup> /yr)
cubic foot per second (ft <sup>3</sup> /s)	0.02832	cubic meter per second (m <sup>3</sup> /s)
Hydraulic conductivity		
foot per day (ft/d)	0.3048	meter per day (m/d)
Hydraulic gradient		
foot per mile (ft/mi)	0.1894	meter per kilometer (m/km)
Transmissivity*		
foot squared per day (ft <sup>2</sup> /d)	0.09290	meter squared per day (m <sup>2</sup> /d)

\*Transmissivity: The standard unit for transmissivity is cubic foot per day per square foot times foot of aquifer thickness [(ft<sup>3</sup>/d)/ft<sup>2</sup>]ft. In this report, the mathematically reduced form, foot squared per day (ft<sup>2</sup>/d), converted to gallons per day per foot (gpd/ft), is used for convenience.

Multiply	By	To obtain
Area		
acre	4,047	square meter (m <sup>2</sup> )
acre	0.004047	square kilometer (km <sup>2</sup> )
Volume		
million gallons (Mgal)	3,785	cubic meter (m <sup>3</sup> )
cubic foot (ft <sup>3</sup> )	0.02832	cubic meter (m <sup>3</sup> )
acre-foot (acre-ft)	1,233	cubic meter (m <sup>3</sup> )
Mass		
ounce, avoirdupois (oz)	28.35	gram (g)
pound, avoirdupois (lb)	0.4536	kilogram (kg)
Activities		
tritium unit	3.2	picocuries

Temperature in degrees Celsius (°C) may be converted to degrees Fahrenheit (°F) as follows:  
 $^{\circ}\text{F}=(1.8\times^{\circ}\text{C})+32$

Temperature in degrees Fahrenheit (°F) may be converted to degrees Celsius (°C) as follows:  
 $^{\circ}\text{C}=(^{\circ}\text{F}-32)/1.8$

## Cover Photograph

The photograph on the cover of this report overlooks Stillman Lake facing east toward the Verde River/Granite Creek confluence, north-central Arizona. The rocks are Devonian Martin Formation capped with Tertiary basalt. In the confluence area, ground water discharges along three distinct flowpaths to Stillman Lake, lower Granite Creek, and upper Verde River springs. This photograph is also figure 15A of this report.

## Author's Note

The Arizona Water Protection Fund Commission has provided a portion of funding for this report through grant #99-078WPF. The views or findings represented in this deliverable are the Grantee's and do not necessarily represent those of the Commission nor the Arizona Department of Water Resources.



# **The Verde River Headwaters, Yavapai County, Arizona**

*By* Laurie Wirt

Chapter A

## **Geologic Framework of Aquifer Units and Ground-Water Flowpaths, Verde River Headwaters, North-Central Arizona**

Edited by Laurie Wirt, Ed DeWitt, and V.E. Langenheim

Prepared in cooperation with the Arizona Water Protection Fund Commission

Open-File Report 2004-1411-A

**U.S. Department of the Interior  
U.S. Geological Survey**

**U.S. Department of the Interior**  
Gale A. Norton, Secretary

**U.S. Geological Survey**  
P. Patrick Leahy, Acting Director

U.S. Geological Survey, Reston, Virginia: 2005

For product and ordering information:  
World Wide Web: <http://www.usgs.gov/pubprod>  
Telephone: 1-888-ASK-USGS

For more information on the USGS--the Federal source for science about the Earth, its natural and living resources, natural hazards, and the environment:  
World Wide Web: <http://www.usgs.gov>  
Telephone: 1-888-ASK-USGS

Any use of trade, product, or firm names is for descriptive purposes only and does not imply endorsement by the U.S. Government.

Although this report is in the public domain, permission must be secured from the individual copyright owners to reproduce any copyrighted materials contained within this report.

This report has not been reviewed for stratigraphic nomenclature.

***Suggested citation:***

Wirt, L., 2005, The Verde River headwaters, Yavapai Count, Arizona *in* Wirt, Laurie, DeWitt, Ed, and Langenheim, V.E., eds., Geologic Framework of Aquifer Units and Ground-Water Flowpaths, Verde River Headwaters, North-Central Arizona: U.S Geological Survey Open-File Report 2004-1411, 33 p.



## Contents

Abstract.....	1
Introduction.....	1
Purpose and Scope .....	1
Overview of Report.....	6
Acknowledgments.....	7
Environmental Setting.....	7
History of Water Use .....	7
Threatened and Endangered Species.....	11
Physical Features.....	11
Climate .....	12
Overview of the Hydrology.....	13
Previous Hydrological Investigations.....	13
Predevelopment Conditions .....	16
Surface-Water Conditions.....	17
Big Chino Valley .....	20
Little Chino Valley.....	21
Upper Verde River Canyon .....	21
Ground-Water Conditions.....	27
Water Use .....	27
Little Chino Valley.....	27
Big Chino Valley .....	28
Upper Verde River.....	29
Conceptual Water Budget.....	29
References Cited.....	31

## Figures

<b>A1.</b> Shaded relief map showing upper Verde River watershed, locations of major physiographic features, and principal area for study investigations in this report.....	2
<b>A2.</b> Locations of known springs along the upper Verde River from Sullivan Lake to Sycamore Creek.....	3
<b>A3.</b> Shaded elevation map showing basin-fill aquifer boundaries. Basin-fill aquifer boundaries are dashed where likely interconnected with adjacent carbonate aquifer.....	5
<b>A4.</b> Photograph of Paleozoic rocks exposed on Big Black Mesa. Big Black Mesa forms the northern boundary of the Transition Zone with the Colorado Plateau .....	6
<b>A5.</b> Photograph of ancient fort ruin on bluff overlooking the upper Verde River .....	9
<b>A6.</b> Aerial photograph of heavily vegetated area surrounding Del Rio Springs (foreground), Tertiary volcanic rocks of the Sullivan Buttes volcanic field (middle ground), and Paleozoic sedimentary rocks of the Colorado Plateau (background) .....	9

<b>A7.</b>	Photographs showing construction of Sullivan Lake Dam, circa 1936. View is west. Sluice box in upper photo was used to divert perennial flow around the dam. Exposed rocks in gorge near the dam are 4.5 Ma basalt flows. Sullivan Buttes shown at skyline in upper photo. Note sediment filling channel upstream of the dam .....	10
<b>A8.</b>	Aerial photographs of lower Granite Creek. A, Lower Granite Creek and its confluence with the upper Verde River. View is north. Last mile of both Granite Creek and the Verde River above confluence are perennial. Canyon walls of Devonian Martin Formation and Chino Valley Formation (Cambrian?) capped by Tertiary basalt; B, Rugged bedrock canyon in lower Granite Creek. View is south toward Little Chino ground-water basin. Dipping strata are Proterozoic Mazatzal Quartzite .....	12
<b>A9.</b>	Map of upper Verde River watershed showing annual precipitation.....	14
<b>A10.</b>	Pre-1950 ground-water conditions inferred from 1947 U.S. Geological Survey topographic maps, indicating shallow water table in parts of Big and Little Chino Valleys. A, intermittent reach of upper Big Chino Wash between Partridge Creek and Wineglass Ranch (1947 Pichacho Buttes and Simmons quadrangles; 1:62,500 scale). Inset shows 1940 aerial photograph of Pine Creek and Big Chino Wash with cienaga; B, (facing page) .....	18
<b>A10.</b>	(Continued) B, ground-water conditions inferred from intermittent reaches in lower Big Chino Wash and Little Chino Creek (1947 USGS Paulden quadrangle, 1:62,500). Big Chino Wash is shown as a perennial segment from its confluence with Williamson Valley Wash to Sullivan Lake. Little Chino Creek is mapped as perennial from Del Rio Springs to Sullivan Lake, as is the upper Verde River downstream from Sullivan Lake to Stillman Lake .....	19
<b>A11.</b>	Aerial photograph of Sullivan Lake showing confluence of Little Chino Creek and Big Chino Wash. View is to the west. Rocks in foreground are 4.5-Ma basalt, and the background is valley-fill sediments overlying the basalt. Runoff in response to a regional storm, September 2003.....	20
<b>A12.</b>	Photographs of Walnut Creek (A) in perennial segment, and (B) near confluence with Big Chino Wash following regional storm of September 2003. Views to west and southwest.....	23
<b>A13.</b>	Photographs showing A, flood of February 20, 1993, at Sullivan Lake dam. View to southwest. Sullivan Buttes in background. Dam is behind hydraulic drop. B, Verde River gorge below the dam. View downstream to east. Canyon is carved from Tertiary basalt. Peak discharge of 23,200 ft <sup>3</sup> /s and daily mean discharge of 13,700 ft <sup>3</sup> /s are the sum of Big Chino Wash, Williamson Valley Wash, Little Chino Creek, and Granite Creek at Paulden gauge .....	24
<b>A14.</b>	Graph showing changes in base flow with distance along the upper Verde River .....	25
<b>A15.</b>	Photographs of Stillman Lake facing downstream (A) overlooking the confluence of Verde River canyon with Granite Creek , and (B) southeast from north canyon rim towards Little Thumb Butte; by R. Pope and L. Wirt, respectively. Stillman Lake is dammed by a natural levee of sediment from Granite Creek, which enters center right of upper photograph. Verde River canyon walls are predominantly Devonian Martin Formation (Dm), capped by the 4.5 Ma basalt flow (Tb). Rocks in background of lower photograph are Tertiary volcanic rocks in the Sullivan Buttes volcanic field (T1a) .....	26
<b>A16.</b>	Conceptual water budget for upper Verde River based on previously published estimates of recharge, as given in table A4.....	30

## Tables

<b>A1.</b>	Distance from Sullivan Lake dam to major springs, tributaries, and other geographic locations along the upper Verde River, Arizona .....	4
<b>A2.</b>	Summary of monthly climate records for stations in the Verde River headwaters study area .....	15
<b>A3.</b>	Summary of available surface-water data and characteristics of drainage basins for streamflow-gauging stations, Verde River headwaters, Arizona.....	21
<b>A4.</b>	Summary of predevelopment base-flow discharge and calculated recharge for major areas in the Verde River headwaters, Arizona.....	22

# The Verde River Headwaters, Yavapai County, Arizona

By Laurie Wirt

## Abstract

This study combines the results of geophysical, geologic, and geochemical investigations to provide a hydrogeologic framework of major aquifer units, identify ground-water flowpaths, and determine source(s) of base flow to the upper Verde River. This introductory chapter provides an overview of previous studies, predevelopment conditions, present surface-water and ground-water conditions, and a conceptual water budget of the hydrologic system. In subsequent chapters, this conceptual model will be evaluated and refined with respect to the results of each successive investigation. First, a compilation of mapping and field verification of the surficial geology, reinterpretation of driller's logs, and contour mapping of alluvial thicknesses and buried volcanic rocks provide new three-dimensional geologic information. Second, a suite of geophysical techniques—including aeromagnetic and gravity surveys and inverse modeling approaches—was used to interpret the deeper subsurface geology. Third, geologic, geophysical, and hydrological data were integrated to define basin boundaries, describe aquifer units in the basin-fill aquifers of Big and Little Chino valleys and the regional carbonate aquifer north of the upper Verde River, and develop a hydrogeologic framework. Water-level gradients were used to infer outlet flowpaths from the basin-fill aquifers through the carbonate aquifer toward the upper Verde River. Fourth, geochemical investigations employing analyses of dissolved major and trace elements and isotopes of  $\delta D$ ,  $\delta^{18}O$ ,  $^3H$ ,  $^{13}C$ , and  $^{14}C$  were used to characterize major aquifers, identify recharge areas, and determine evolution of water chemistry along ground-water flowpaths. Fifth, results of a tracer-dilution study and synoptic sampling identify locations of major spring inflows discharging to the upper Verde River, measure base-flow contributions, which were used to calculate the relative contributions from each aquifer to upper Verde River springs using inverse geochemical modeling. In the final chapter, synthesis of multiple lines of evidence improve understanding of the relationships between the three aquifers, regional ground-water flowpaths, and the proportion of flow from each aquifer to the upper Verde River. Collectively, data from many varied and independent sources improves confidence in the conceptual model of the hydrogeologic system.

## Introduction

The Verde River begins in a canyon below the confluence of two tributary basin-fill aquifers in Big and Little Chino valleys (fig. A1). The two basin-fill aquifers and an adjoining carbonate aquifer supply a network of springs that discharge about 25 cubic feet per second ( $ft^3/s$ ) of base flow to a 24-mi reach of river canyon between Granite Creek and Perkinsville (fig. A2, table A1). Most of the ground-water gains occur within the first few miles. Semiarid Big and Little Chino valleys are experiencing rapid population growth, which is entirely dependent on ground water. A detailed understanding of ground-water movement in the three aquifers is critical toward maintaining base flow in the upper Verde River.

Homeowners, municipalities, ranchers, environmental organizations, water utilities, and agencies responsible for resource management at the County, State, and Federal levels have a need to understand the geologic framework of major aquifers that are used for human water supply and that sustain the natural environment. Stakeholders recognize that an improved understanding of the hydrogeologic system is needed to manage water resources and to address the concerns of limited water supplies and environmental degradation. There is a need to understand not only the source of base flow to the Verde River but also the underlying geologic framework including the geometry, the geologic conduits and barriers that affect ground-water flowpaths, and the structure of the individual aquifer units where the greatest quantities of water are stored.

## Purpose and Scope

The area of investigation for the upper Verde River (figs. A1 and A2) was selected at the basin scale of the three principal aquifers (fig. A3) to include the Big and Little Chino valleys, the regional carbonate aquifer north of the Verde River, and surrounding upland areas. The upper Verde River is located in north-central Arizona, in Yavapai County, and begins about 20 mi north of Prescott. The river flows from west, near the town of Paulden; to east, near the town of Clarkdale. The study area is roughly bounded to the north by the

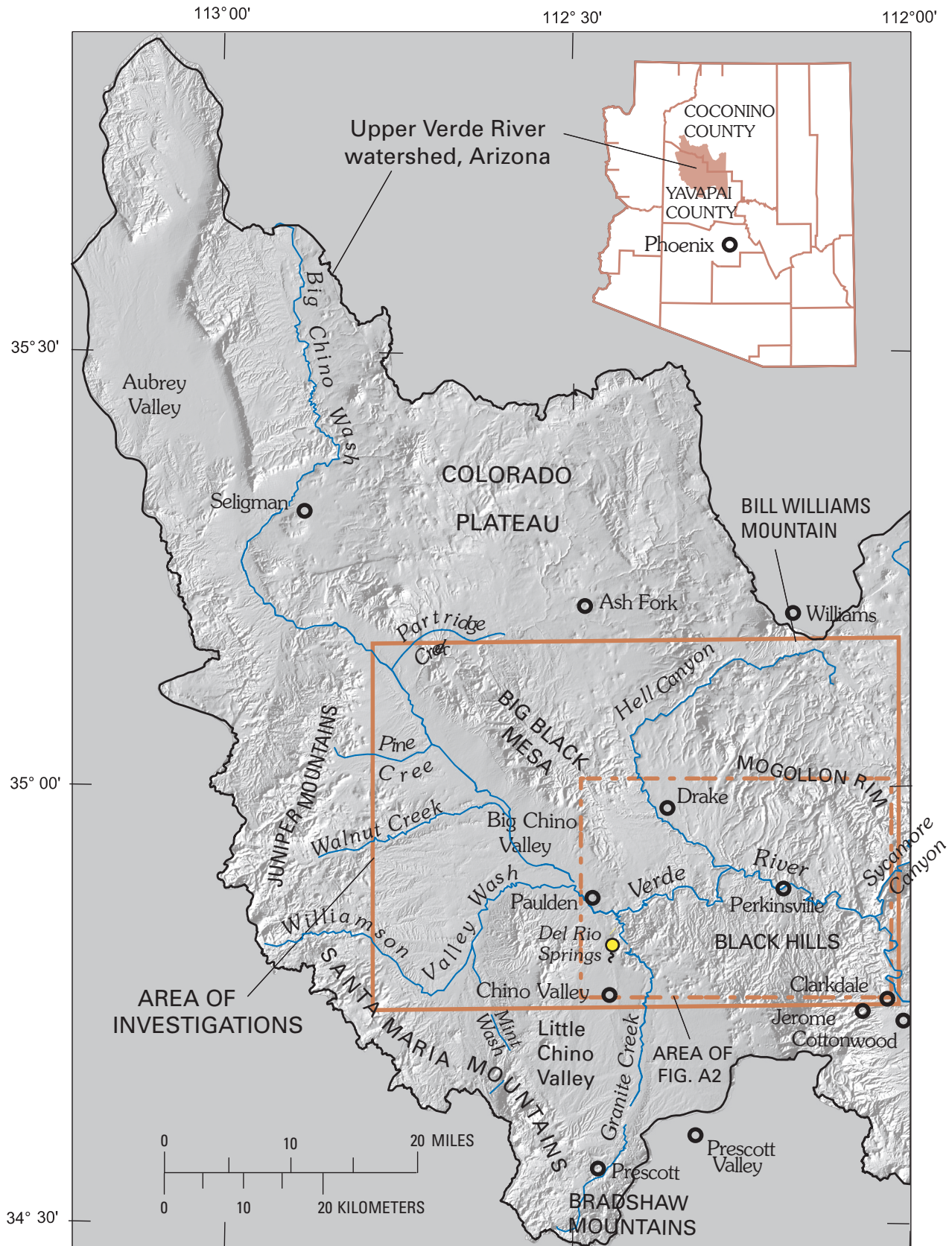


**Figure A1.** Shaded relief map showing upper Verde River watershed, locations of major physiographic features, and principal area for study investigations in this report. Base is from U.S. Geological Survey digital data 1:100,000; sun angle elevation is 45 degrees from southeast; azimuth is 120 degrees.

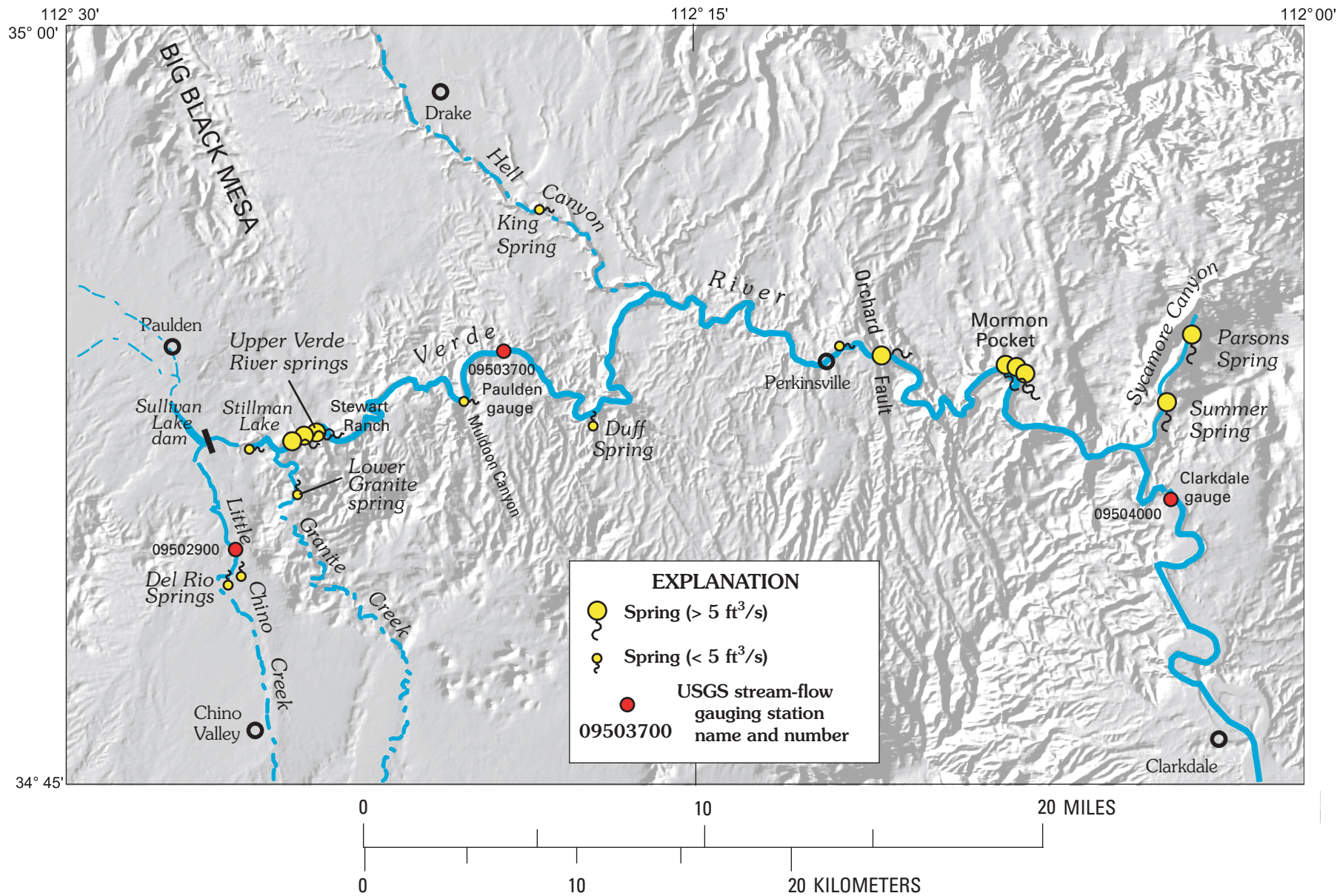


**Figure A2.** Locations of known springs along the upper Verde River from Sullivan Lake to Sycamore Creek. Base is from U.S. Geological Survey digital data 1:100,000; sun angle elevation is 45 degrees from southeast; azimuth is 120 degrees.

**Table A1.** Distance from Sullivan Lake dam to major springs, tributaries, and other geographic locations along the upper Verde River, Arizona.

[Distances are approximate and have not been surveyed]

<b>Major tributaries or physiographic features</b>	<b>Miles</b>	<b>Kilometers</b>
Del Rio Springs via Little Chino Creek	-3.0*	-4.8*
Lower Granite Spring*	1.0**	1.6**
Sullivan Lake Dam	0.0	0.0
Stillman Lake (upstream end)	1.0	1.6
Stillman Lake (downstream end)	1.9	3.1
Granite Creek confluence	2.0	3.2
Continuous flow begins	2.1	3.4
Upper Verde River springs (upstream end)	2.2	3.6
Stewart Ranch (west access)	3.2	5.1
Muldoon Canyon	8.0	12.9
Paulden gauge (09503700)	9.8	15.8
Verde Valley Ranch	10.3	16.6
Bull Basin Canyon	11.5	18.5
Duff Spring	13.9	22.4
Hell Canyon	18.0	29.0
U.S. Mine	19.4	31.2
Perkinsville diversion ditch	23.7	38.1
Perkinsville	24.0	38.6
Verde River near Orchard Fault	26.0	41.8
RR Crossing downstream of Perkinsville	26.6	42.8
Mormon Pocket springs	31.0	49.9
Sycamore Canyon	34.9	56.2
Clarkdale gauge (09504000)	36.6	58.9

\*Distance upstream from Sullivan Lake dam

\*\*Distance upstream from Granite Creek and Verde River confluence

Mogollon Rim and northwest by Big Black Mesa (fig. A4), and to the east by Sycamore Canyon. To the southeast, the boundaries are the Black Hills and Agua Fria watershed, and to the south and southwest, the study area includes the Bradshaw, Santa Maria, and Juniper Mountains. The westernmost boundary of the study area is the confluence of Big Chino Wash with Partridge Creek. For this report, the reach referred to as the “upper Verde River” is the 10-mi reach upstream from the U.S. Geological Survey streamflow gauging station near Paulden (station number 09503700 on fig. A2; river mi 10; referred to in this report as the “Paulden gauge”).

The common goal of the multi-disciplinary studies in this report is to provide a more detailed understanding of the hydrogeologic framework of the Verde River headwaters, especially the relation between major aquifers and the upper Verde River. Major aquifers contributing to the upper Verde

River include (A) the two Big and Little Chino basin-fill aquifers and adjoining carbonate aquifer underlying Big Chino Valley and Big Black Mesa, and (B) the part of the carbonate aquifer directly north of the upper Verde River between Big Black Mesa and Hell Canyon. As part of the geochemical investigations, some additional sampling was conducted downstream from the main study area to better characterize water chemistry of springs discharging from the carbonate aquifer between Perkinsville and Sycamore Creek.

The chapters in this report present geologic, geophysical, hydrogeologic, and geochemical interpretations for the Verde River headwaters study area. Surficial geologic maps are based on compilation of earlier studies and reconnaissance mapping. Sub-surface geologic interpretations are based on modeling of gravity measurements and high-resolution airborne geophysical data, and by interpreting available well

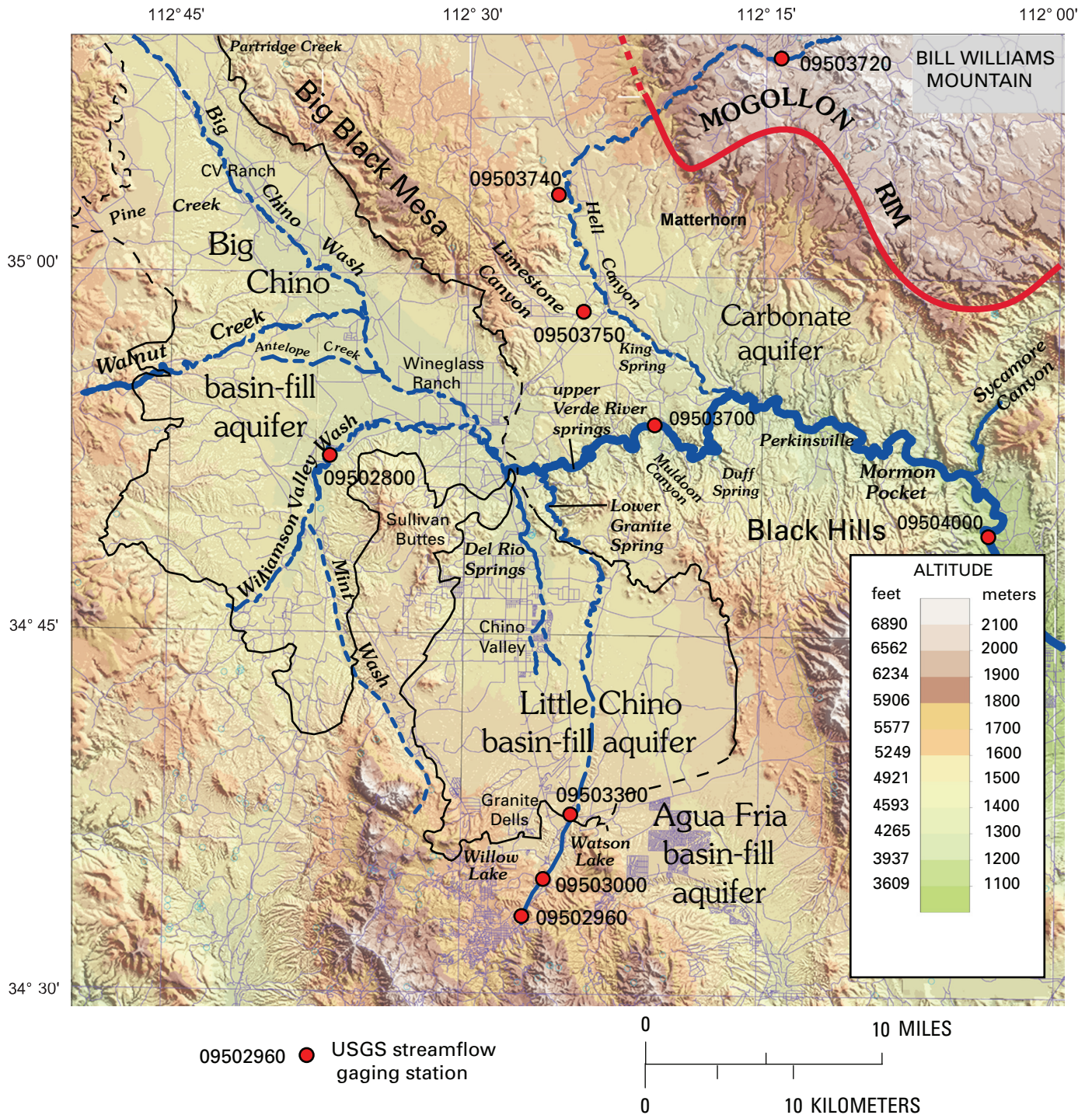


**Figure A3.** Shaded elevation map showing basin-fill aquifer boundaries. Basin-fill aquifer boundaries are dashed where likely interconnected with adjacent carbonate aquifer (Wirt and DeWitt, this volume; Chapter D). Base is from 1:100,000 U.S. Geological Survey digital data.





**Figure A4.** Photograph of Paleozoic rocks exposed on Big Black Mesa. Big Black Mesa forms the northern boundary of the Transition Zone with the Colorado Plateau. View is northwest. Rocks in foreground are Devonian Martin Formation capped by cliff-forming Mississippian Redwall Limestone. Prominent peak in distance is Picacho Butte.

logs and borehole data. An understanding of the hydrogeology was developed from the geology and from water-level data, surface-water data, and other hydrologic information. Interpretations of ground-water source areas and flowpaths were determined from geochemical and stable-isotope data from selected wells and springs and the relative age of ground water and the location of recharge areas is inferred from naturally occurring radioactive isotopes of tritium and carbon-14 ( $^{14}\text{C}$ ). Sources of ground-water inflow to the upper Verde River were characterized and quantified based on the results of a tracer study and synoptic sampling during low-flow conditions. Finally, multiple lines of geochemical evidence were integrated by inverse modeling using PHREEQC, a computer program for simulating chemical reactions and mixing (Parkhurst and Appelo, 1999).

The studies in this report were designed to address data gaps in earlier studies and in available geologic, geophysical, driller's log, water-level, water-chemistry, and stable-isotope

data. Ongoing geologic mapping efforts by the U.S. Geological Survey (USGS) in the Prescott National Forest was supplemented by field mapping and reinterpretation of driller logs from the ADWR database (Arizona Department of Water Resources, 2002). Ground-based gravity data and an airborne survey of magnetic and radiometric data were subcontracted in 1999 by World Geoscience (now Fugro) and in 2000 by Goldak Airborne Surveys. Geochemical studies include (a) geochemical analysis of wells and springs that were sampled for this study from 1999 to 2004, and (b) a June 2000 tracer-dilution study in the major gaining reach of the uppermost Verde River during low-flow conditions. Results of each study are presented sequentially and integrated with other studies to create a multidisciplinary conceptual model of the hydrogeology of the Verde River headwaters study area.

Collectively, the studies in this report yield information on geologic structures and basin geometry, ground-water flowpaths, relative rates of travel, and relative contributions from different aquifer sources that presently are needed by ground-water modelers and water-resource managers in State and Federal agencies, the Prescott Active Management Area, the Yavapai County Water Advisory Committee, and other stakeholders throughout the Verde River watershed.

## Overview of Report

Each chapter in this report presents the results of a different discipline or approach, with the final chapter serving as a synthesis and summary of all the results. As much as possible, chapters in this report are arranged in a logical sequence so that earlier chapters help provide a basis for subsequent interpretations made in following chapters. Geologic interpretations provide a framework for interpreting the geophysical investigations, as well as describing aquifer units. In much the same way, results of the geophysical surveys were used to interpret the basin geometry and subsurface geology. Both the geology and geophysics chapters provide background for the hydrogeology chapter. The hydrogeologic framework, in turn, helps constrain geochemical interpretations in water-chemistry chapters regarding ground-water flow directions and source areas of major springs discharging to the upper Verde River.

*Chapter A—The Verde River Headwaters:* This chapter provides an overview of study objectives as well as a compilation of background information about physical features, climate, and the hydrologic system as it is presently understood. Available data on predevelopment conditions, surface and ground-water conditions, water use, and a conceptual water budget based on recharge estimates from earlier studies also are presented.

*Chapter B—Geologic framework:* The regional geologic history and the physical nature of rock units and sediments are described. Geologic reinterpretation of driller's logs and contour mapping of buried volcanic rocks and overlying alluvium provides a three-dimensional understanding of the shallow geology, with emphasis near the outlets of the Big and Little Chino basins.

*Chapter C—Geophysical framework:* Geophysical modeling is used to estimate basement geometry in deeper parts of the alluvial basins and beneath adjoining upland areas, especially where deep well logs are unavailable. Aeromagnetic data are used to identify contrasts between rock and alluvium that promote or obstruct ground-water movement such as large faults and buried volcanic rocks. Gravity measurements are interpreted to estimate basin geometry, basin thickness, and structural features.

*Chapter D—Hydrogeologic framework:* The permeability and water-bearing characteristics of rock and sediment units within the major aquifers, basin geometry, aquifer boundaries, and nature of faults and buried volcanic rocks are described. Water-level gradients are integrated with geologic information to define ground-water flowpaths near the outlets of the basin-fill aquifers.

*Chapter E—Geochemistry of major aquifers and springs:* Trends in the concentrations of dissolved major and trace elements are used to characterize each major aquifer. Stable isotopes of hydrogen and oxygen are used to infer the altitude of recharge source areas. Naturally occurring radioactive isotopes of tritium and carbon-14 help to identify areas where modern recharge is occurring and indicate apparent ages of ground water. Changes in water chemistry are delineated along selected ground-water flowpaths.

*Chapter F—Sources of base flow in the upper Verde River:* A tracer-injection study and synoptic water-chemistry sampling were conducted during low-flow conditions to determine locations of diffuse springs and to quantify the relative contributions from each major aquifer source to base flow. Sources of inflows are identified on the basis of multiple lines of geochemical evidence, including field parameters, major and trace elements, and stable isotopes of hydrogen and oxygen. Multi-parameter inverse-geochemical modeling is used to determine the relative contribution from each major source, including the carbonate aquifer north of the Verde River.

*Chapter G, Synthesis of Geologic, Geophysical, Hydrogeological, and Geochemical Evidence:* The final chapter summarizes and integrates results of the earlier chapters to provide understanding of interconnections between the aquifers and the Verde River, directions of ground-water flowpaths, and relative contributions from each of the major source areas.

## Acknowledgments

Funding was provided by grant #99-078WPF from the Arizona Water Protection Fund Commission (AWPFC), administered by the ADWR. Partial support for these studies also was provided by Prescott National Forest, the Bureau of Land Management, and internal funding from the USGS.

Our work would not have been possible without access for sampling granted by Arizona Game and Fish, the Prescott National Forest, Billy Wells, and the Las Vegas, Alameda Cattle, Kieckheffer (K4), and Hitchcock (T2) Ranches. In addition, the Salt River Project Agricultural Improvement and Power District (SRP) donated the use of their helicopter to

obtain gravity measurements in inaccessible locations, and the Verde Scenic Railway loaned us a sidecar and crew to collect additional gravity measurements and water samples along the Clarkdale to Drake railroad line. Special thanks goes to Paul Lindberg (economic geologist, Sedona) for sharing his knowledge of the regional geology, to Christopher Eastoe and Ailang Gu (University of Arizona) for isotope analysis, and to Pierre Glynn (USGS) for his expertise in inverse modeling of the geochemistry. Aerial photography was artfully flown by Michael Collier of Flagstaff.

The following local residents graciously cooperated by providing access for water sampling activities: David Gipe, Don Varner and Ann Gipe, Harley and Patty Shaw, Billy Wells, Ann Harrington, and the Reeves, Wagner, Smith, Prucha, Schaible, and Arnold families. Without their cooperation, this study would not have been possible. Field support was provided by Susan Lane Matthes, Ann Harrington, David Christiana, Edessa Carr, Kay Lauster, Pam Sponholz, and Shaula Hedwall.

Technical reviewers included David Lindsey and John Hoffmann of the USGS, and Frank Corkhill, Keith Nelson, David Christiana, and Tracey Carpenter of the ADWR. Other USGS personnel who assisted the authors include Betsy Woodhouse, Ken Leib, John Evans, Christie O'Day, Rhonda Driscoll, Jeannie Bryson, Marilyn E. Flynn, Kyle Blasch, and Elizabeth Leon. Lisa Swanson, Maureen Freark, Amy Manning, and David Christiana of the ADWR helped to administer the grant.

## Environmental Setting

In a multidisciplinary study of this scope, it is necessary to examine the framework elements at a broad range of scales in order to evaluate major geologic features, topographic relief, and major aquifer units at the proper perspective. Framework components considered at the regional scale are physiographic features such as topography, climate, ecology, and geology. Components considered at the basin or aquifer scale include all of the regional factors plus well and spring data, surface-water runoff data, underlying basement geometry, and local structural features. Interrelations among these factors provide the context for movement of ground water from the principal recharge areas, through the major aquifers, to major springs.

Geology generally is a major topic in a discussion of environmental setting; however, because it is the major focus of the next three chapters, the regional geologic setting is not presented here. The following discussions of historical water use, threatened and endangered species, physical features, and climate provide background for hydrological information summarized in the remainder of this chapter.

## History of Water Use

The Verde River headwaters area has played an important role in Arizona history. Archeological artifacts indicate

ancestral native Americans lived here thousands of years ago, as evidenced by ruins throughout the upper Verde River canyon and its major tributaries (fig. A5). Gold mining and ranching brought settlers to the Prescott area in the 1850s and 1860s. Owing to its excellent water supply and tall grass for grazing, the provisional territorial capital of Arizona initially was established at Del Rio Springs in 1864 (fig. A6; Henson, 1965). After several months, the fort was moved to Prescott to be closer to gold mining and timber resources in the Bradshaw Mountains (fig. A1). Military forces were sent to protect miners and early settlers of the Arizona Territory from raids by Apache Indians. In the late 1800s, early white settlers successfully cultivated the area surrounding Del Rio springs, growing hay and vegetables for the miners and eventually shipping to more distant markets (Munderloh, 2000 and 2001; Allen, Stephenson & Associates, 2001). A ranching and farming settlement was established in Big Chino Valley by 1879 (Granger, 1985).

From 1901 through the 1930s, ranches and farms near Del Rio Springs supplied food and water for the railroad and tourism industry in Grand Canyon (Metzger, 1961), as well as the northern Arizona railroad towns of Ash Fork, Seligman, Williams, and Winslow. Ash Fork would be totally dependent on Del Rio water until 1956 (Allen, Stephenson & Associates, 2001). Trains stopped at Del Rio Springs to fill tank cars and transport farm produce. Also, the city of Prescott built a 21-mi pipeline from Del Rio Springs to Prescott in 1901 (Krieger, 1965; p. 115). The pipeline supplied 500,000 gallons per day (560 acre-ft/year; Baker and others, 1973) between 1904 and 1927 (Schwalen, 1967). Although the water supply was adequate for Prescott's needs, the cost of pumping was considered excessive, and the pipeline eventually was disassembled (Krieger, 1965). In the winter of 1925–26, the railroad drilled two wells at Del Rio Springs to replace the sump-pump system there (Matlock and others, 1973; p. 44). Beginning in the late 1930s, many deep wells were drilled for agricultural irrigation to tap the artesian aquifer underlying the town of Chino Valley. In 1947, the city of Prescott drilled two wells approximately 5 mi south of Del Rio Springs (Krieger, 1965), offering a much shorter pipeline. This event was the beginning of the main well field in Chino Valley that continues to supply most of the municipal water for the city of Prescott and the town of Chino Valley.

In the mid-1930s, Sullivan Lake was constructed as a public works project to offer recreation and fishing below the confluences of Williamson Valley Wash, Big Chino Wash, and Little Chino Creek. Perennial flow in Little Chino Creek and probably lower Big Chino Wash extended upstream from the dam at the time of its construction. Historical photos show a small sluice to divert base flow around the dam during construction (fig. A7). The lake filled with sediment by the early 1940s, and today its maximum depth is less than several feet. The small dam is a local landmark and generally is recognized as the beginning of the Verde River.

The upper Verde River is an important part of the water supply for downstream water users in Verde Valley communities and the city of Phoenix, and is particularly valued for its water quality. The Verde River generally is lower in total dissolved solids than other Phoenix water-supply sources, including the Salt River, Central Arizona Project water, and ground water from southeastern and western Salt River Valley (Greg Elliot, Salt River Project, written commun., 2004). Moreover, the Verde River is a precious supply of reliable water during prolonged droughts.

Accelerated development has led to increasing concern about water resource issues and the effects of pumping on base flow of the upper Verde River. Water use in the Tri-Cities area of Prescott, Prescott Valley, and Chino Valley is growing rapidly as the area becomes a suburban and retirement destination. The rural towns of Chino Valley and Paulden in Big Chino Valley are shifting away from an economy of irrigated agriculture and ranching to one of suburban land use, such as housing. The primary crops used to be cattle, corn, and alfalfa, but important agricultural products now include turf, hothouse flowers, and fresh produce. From 1980 to 1997, Yavapai County's population increased 108 percent from 68,145 to 142,075; or an average of 6.4 percent annually over the 17-year period (Arizona Department of Water Resources, 2000; Arizona Department of Economic Security, 1990; Arizona Department of Commerce, 1993–1997). In the year 1997, Yavapai County was one of three counties in the State that experienced an increase in population greater than 24.6 percent. In the Little Chino subbasin, the populations of Prescott and Chino Valley increased by 170 and 244 percent from 1980 to 1997, respectively (Arizona Department of Water Resources, 2000; table 2–2).

Water resources in both the Big and Little Chino basin-fill aquifers are under increasing pressure from population growth and residential development. The Little Chino basin-fill aquifer lies within the state-designated Prescott Active Management Area (PRAMA), which regulates ground-water withdrawals (Arizona Department of Water Resources, 1998). In 1999, the Arizona Department of Water Resources (ADWR) determined that the PRAMA was no longer at safe yield. Safe yield is an Arizona State water management goal that attempts to maintain a long-term balance between the amount of water withdrawn and the amount of water naturally and artificially recharged to the system. Since 1997, the PRAMA overdraft in excess of recharge has been estimated on the order of 6,610 to 9,830 acre-ft/year (Arizona Department of Water Resources, 1998, 1999a, 1999b, and 2000). To counterbalance the growing overdraft, the PRAMA plans to augment its water supplies from outside its watershed (Arizona Department of Water Resources, 1999b; Arizona State Legislature, 1991). Recently, the City of Prescott purchased a ranch in upper Big Chino Valley with the intent of building a pipeline to import 8,717 acre-ft/yr into the PRAMA (Southwest Groundwater Consultants, 2004). Concerns that future pumping of the Big Chino aquifer will decrease the flow of the Verde River are compounded by less restrictive development occurring outside the PRAMA in Big Chino Valley.



**Figure A5.** Photograph of ancient fort ruin on bluff overlooking the upper Verde River. Photograph by M. Collier.

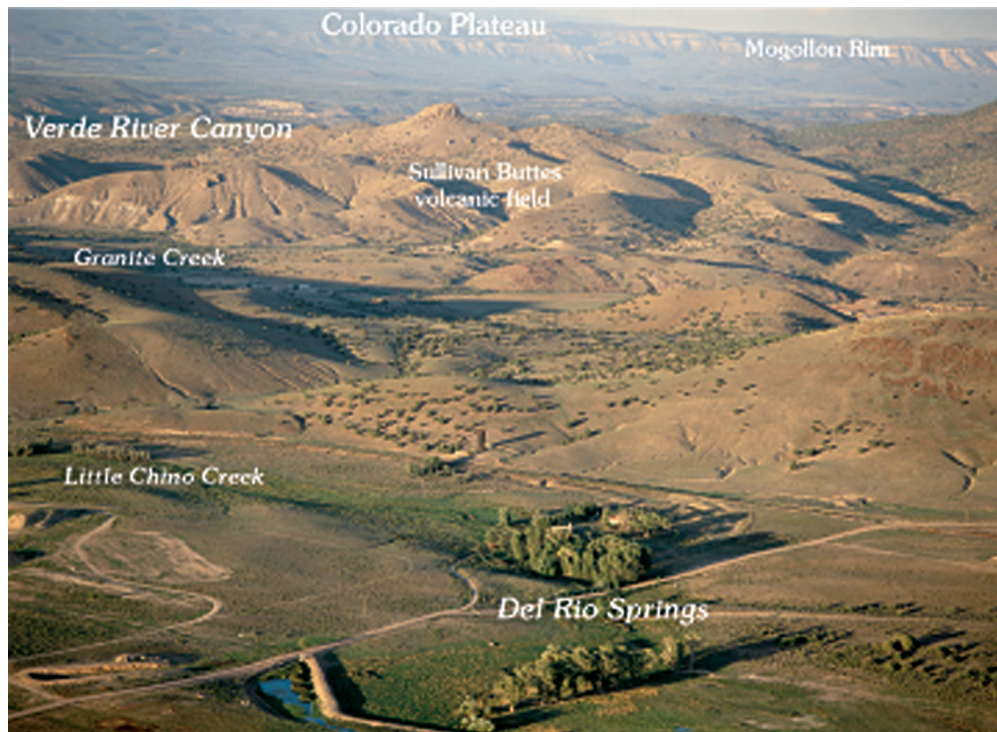


**Figure A6.** Aerial photograph of heavily vegetated area surrounding Del Rio Springs (foreground), Tertiary volcanic rocks of the Sullivan Buttes volcanic field (middle ground), and Paleozoic sedimentary rocks of the Colorado Plateau (background). View is to the northeast. Photograph by M. Collier.



**Figure A7.** Photographs showing construction of Sullivan Lake Dam, circa 1936. View is west. Sluice box in upper photo was used to divert perennial flow around the dam. Exposed rocks in gorge near the dam are 4.5 Ma basalt flows. Sullivan Buttes shown at skyline in upper photo. Note sediment filling channel upstream of the dam.

Since 1940, ground-water levels in Little Chino Valley have declined more than 75 ft in the north end of the basin—only a few miles from Del Rio Springs and the source springs of the Verde River (Arizona Department of Water Resources, 1999a and 2000; Corkhill and Mason, 1995; Remick, 1983). Decreasing ground-water storage trends have been observed in most parts of the PRAMA (Arizona Department of Water Resources, 1999). In 2003, the annual discharge of Del Rio Springs was about 1,000 acre-ft/year (Fisk and others, 2004)—less than one-half the 2,400–3,400 acre-ft/year of annual discharge when the spring was first gauged between 1940 and 1945 (Schwalen, 1967). Perennial flow in the Verde River historically began near Del Rio Springs (Henson, 1965; Krieger, 1965; p. 118), but year-round flow to Sullivan Lake via Little Chino Creek had disappeared by the early 1970s (A.L. Medina; U.S. Forest Service, oral commun., 1999), owing to agricultural diversions and ground-water pumping.

## Threatened and Endangered Species

The upper Verde River sustains important riparian habitat for fish and wildlife, including several threatened and endangered species. The U.S. Fish and Wildlife Service (2000) has designated the reach of the Verde River below Sullivan Dam as critical habitat for two threatened species, the spikedace minnow (*Meda fulgida*) and the extirpated loach minnow (*Tiaroga cobitis*). Native populations of spikedace minnow have been identified within this reach and elsewhere in the Verde River. Wildlife biologists consider lower Granite Creek, a perennial tributary to the upper Verde River, a particularly important expansion area for the recovery of spikedace (U.S. Fish and Wildlife Service, 2000).

Native fish populations in the upper Verde River are recognized as among the most diverse in Arizona (Arizona Game and Fish, 2004). Because of its outstanding native fish diversity and abundance as indicators of biotic integrity, Arizona Game and Fish acquired 796 acres along the upper Verde River and lower Granite Creek, now designated as the upper Verde River Wildlife area (Arizona Game and Fish, 2004). Arizona Game and Fish's primary management objective for this area is to monitor, manage, and maintain the extant native fish populations, which also include roundtail chub (*Gila robusta*), razorback sucker (*Xyrauchen texanus*), desert sucker (*Catostomus clarki*), Sonora sucker (*Catostomus insignis*), Longfin dace (*Agosia chrysogaster*), and speckled dace (*Rhinichthys osculus*).

Other wildlife of special concern that may occupy the upper Verde River and vicinity include Northern leopard frog (*Rana pipiens*), Mexican garter snake (*Thamnophis eques*), Arizona toad (*Bufo microscaphus*), belted kingfisher (*Ceryle alcyon*), Bald eagle (*Haliaeetus leucocephalus*), common black hawk (*Buteogallus anthracinus*), peregrine falcon (*Falco peregrinus*), southwestern willow flycatcher (*Empidonax trailii extimus*), red bat (*Lasiurus borealis*), spotted bat (*Euderma maculatum*), and southwestern river otter (*Lontra canadensis sonora*) (Arizona Game and Fish, 2004).

## Physical Features

The Verde River is part the Colorado River drainage basin which empties into the Gulf of California. The world famous Grand Canyon is the next major drainage to the north, and Phoenix's West Salt River basin is the next large valley to the south. The Verde River headwaters region covers 2,500 mi<sup>2</sup> of rugged mountains, steeply incised canyons, and rolling valleys, including Big and Little Chino valleys and Williamson Valley. Mountain ranges are predominantly oriented northwest to southeast with maximum elevations between 6,000 and 9,000 ft above mean sea level. The "headwaters" area is the source and upper part of a stream, especially of a large stream or river, including the upper drainage basin (Bates and Jackson, 1980). For the purposes of this report, the "Verde River headwaters" is defined as the part of the watershed upstream from the Paulden gauge (fig. A2). The largest spring inflows occur immediately downstream from the confluence of the Verde River and Granite Creek, which also is the confluence of the Big and Little Chino Valley topographical watersheds. At least 80 percent of the base flow at the Paulden gauge is supplied by upper Verde River springs (Wirt and Hjalmarson, 2000), also referred to as Big Chino Springs or Headwater Springs. The remaining inflow is derived from Stillman Lake, lower Granite Creek, and a small gain occurs near Muldoon Canyon (fig. A2). Duff Spring is the only known spring in the reach between the Paulden gauge and Perkinsville.

Major tributaries to Sullivan Lake and the upper Verde River (the reach upstream from the Paulden gauge) include Big Chino Wash, Williamson Valley Wash, Little Chino Creek, and Granite Creek. The reach of the Verde River upstream from Verde Valley begins at the Sullivan Lake dam and ends at the mouth of Sycamore Canyon (fig. A2, table A1). This 35-mi reach receives ephemeral tributary runoff in the narrow bedrock canyon between Granite Creek and the mouth of Sycamore Creek. On the north side of the Verde River, the largest tributary is Hell Canyon. South of the Verde River, this reach drains many low-lying canyons (altitudes are mostly between 4,000 and 5,000 ft).

The effective surface drainage of Big Chino Valley encompasses 1,850 mi<sup>2</sup> including Big Chino Valley, Williamson Valley, and at least 600 mi of watershed north of Interstate 40 between the towns of Seligman and Ashfork (fig. A1)—but does not include 357 mi<sup>2</sup> in Aubrey Valley, a closed basin (Schwab, 1995). Bill Williams Mountain is the highest peak at 9,256 ft, compared with 4,117 ft at the Paulden gauge. About 15 percent of the Big Chino watershed (about 280 mi<sup>2</sup>) exceeds an altitude of 6,000 ft, predominantly in the Bradshaw, Santa Maria, and Juniper Mountains (Wirt and Hjalmarson, 2000). Several peaks in these three mountain ranges exceed an altitude of 7,000 ft. The largest tributary is Williamson Valley Wash, with a drainage area of 255 mi<sup>2</sup>. Flow in lower Williamson Valley Wash is perennial for about 4.2 miles, from near its confluence with Mint Wash to the Williamson Valley Wash USGS streamflow gauging station near Paulden (09502800). Walnut Creek has perennial segments

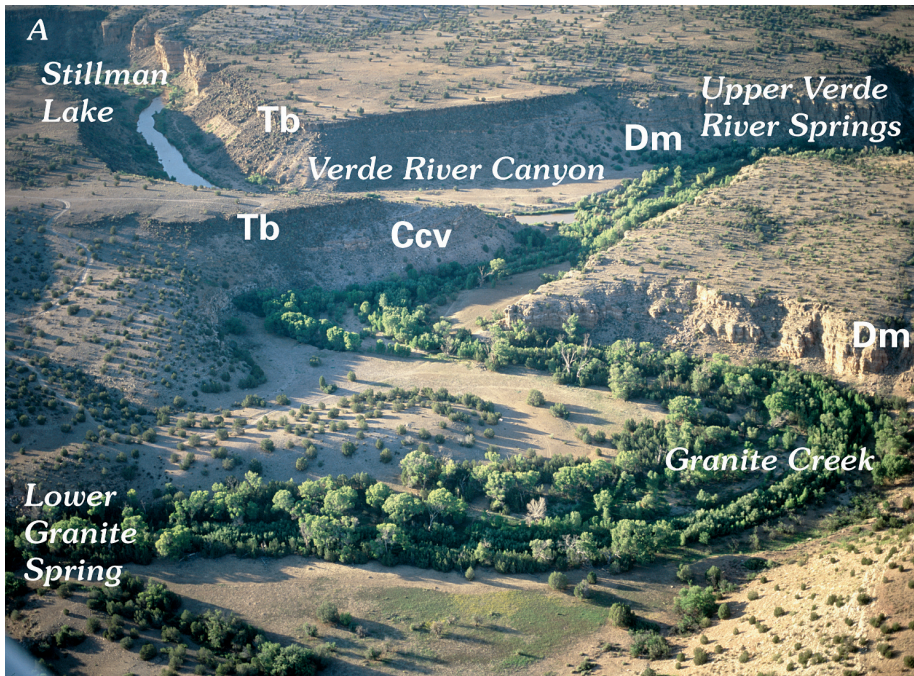
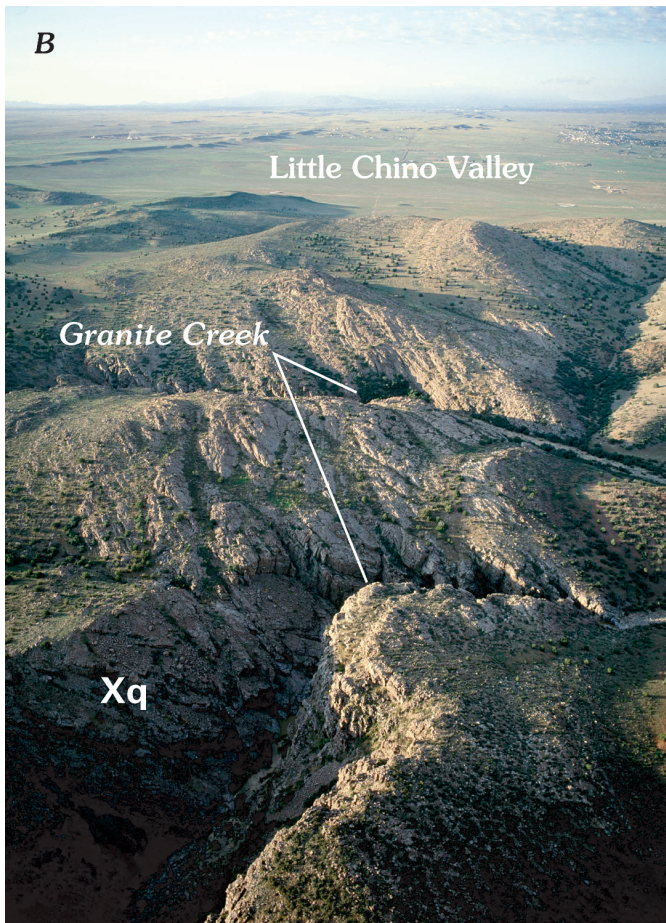


**Figure A8.** Aerial photographs of lower Granite Creek. A, Lower Granite Creek and its confluence with the upper Verde River. View is north. Last mile of both Granite Creek and the Verde River above confluence are perennial. Canyon walls of Devonian Martin Formation and Chino Valley Formation (Cambrian?) capped by Tertiary basalt; B, Rugged bedrock canyon in lower Granite Creek. View is south toward Little Chino ground-water basin. Dipping strata are Proterozoic Mazatzal Quartzite. Photographs by M. Collier.



and perennial tributaries west of the study area boundary, including North and South Forks and Apache Creek.

Little Chino Valley differs from Big Chino Valley in that it has not one but two surface-water outlets—Granite Creek and Little Chino Creek. The combined watershed area of Granite Creek and Little Chino Creek is about 300 mi<sup>2</sup> (Corkhill and Mason, 1995). Granite Creek has upper, middle, and lower reaches that are quite different in character. Granite Creek is perennial near Prescott where it is close to the Bradshaw Mountains. Middle Granite Creek is a wide, sandy, ephemeral wash north of the Granite Dells that accounts for the southern and eastern two-thirds of the Little Chino ground-water basin. In its lowermost reach above its confluence with the Verde River, Granite Creek changes character again and is a rugged bedrock channel with restricted ground-water underflow in the last 6 mi (fig. A8). Little Chino Creek drains a 40-mi<sup>2</sup> area surrounding the town of Chino Valley. The 220-mi<sup>2</sup> drainage area that corresponds with the ephemeral reach of Granite Creek and with Little Chino Creek approximately overlies the Little Chino basin-fill aquifer.

### Climate

The climate of the study area is arid to semiarid, with precipitation varying greatly from place to place and also by large differences from one year to the next. Two periods of warm and cold precipitation are related to seasonal atmospheric flow patterns and pressure systems (Western Regional Climate Center, 2004). From November through March, storm

systems from the Pacific Ocean cross the state. These winter storms occur more frequently at higher altitudes and sometimes bring snow. Summer rainfall usually begins early in July and lasts until mid-September. Moisture-bearing winds sweep into Arizona from the south or southeast, with their source in the Gulf of California or Gulf of Mexico. Summer rains occur in the form of thunderstorms which largely result from excessive heating of the ground and the lifting of moisture-laden air along main mountain ranges. Water from these brief, but often violent downpours can cause flash flooding. Winter storms tend to be less frequent but longer in duration.

Precipitation is governed to a great extent by elevation (fig. A9) and the season of the year (table A2). North of the Mogollon Rim, rain and snowfall on the southern edge of the Colorado Plateau is highly variable. At the northern edge of the study area, Bill Williams Mountain (9,256 ft) receives as much as 30 inches of precipitation, compared with less than 13 inches at nearby Ash Fork (5,130 ft). The greatest amounts of precipitation over the greatest areal extent occur at altitudes greater than 6,000 ft in the Bradshaw, Santa Maria, and Juniper Mountains. These mountain regions receive greater than 20 inches of precipitation annually, with some precipitation falling as snow. In contrast, the relatively dry valleys near the towns of Chino Valley (4,600 ft) and Paulden (4,400 ft) receive about 10–12 inches annually, predominantly during the summer monsoon season. Slightly separated from the rest of the Colorado Plateau and mostly lower than 6,000 ft in altitude, Big Black Mesa receives less rainfall than the other mountain ranges, between 12 and 18 inches per year.

Like rainfall, temperature varies greatly from season to season (table A2). Large spatial differences in temperature mainly result from differences in altitude. High temperatures are common throughout the summer months at the lower elevations. Cold air masses from Canada sometimes penetrate into the state, bringing temperatures well below zero in the high plateau and mountainous regions. In the summer, valley temperatures commonly exceed 95 degrees Fahrenheit (°F), and may reach 104°F (Ewing and others, 1994). Great extremes occur between day and night temperatures. During winter months, daytime temperatures may average 70 °F, with night temperatures often falling to freezing in the lower valleys. The minimum temperature of record is minus 12°F at Seligman, on the Colorado Plateau northwest of Big Chino Valley (Ewing and others, 1994).

The length of the growing season (period between freezes) typically lasts 4 to 5 months within the study area, ranging from less than 119 days in the higher parts of the Juniper and Santa Maria Mountains to an average of approximately 155 days in Big Chino Valley (Ewing and others, 1994). Annual free-water surface evaporation ranges between 50 and 60 inches per year (Ewing and others, 1994). Evaporation losses from small lakes such as Watson Lake and Willow Creek reservoirs (fig. A3) average 850 acre-ft/yr (Ewing and others, 1994; Appendix A, p. 2).

Flood conditions occur infrequently, although heavy thunderstorms during July and August at times cause floods

that do considerable local damage. Heaviest runoff usually occurs when moist tropical air from hurricanes dissipates over land. The heavy rains associated with these systems usually come during August or September but are likely to occur on the average of once every 10 years (Western Regional Climate Center, 2004).

## Overview of the Hydrology

The goal for the remainder of this chapter is to summarize all of the available hydrological information from previous studies in order to develop a working model of the hydrologic system. This will provide the necessary background for the data and interpretations presented in later chapters.

### Previous Hydrological Investigations

The earliest investigations in the headwaters of the Verde River were geologic maps by the U.S. Geological Survey (USGS) completed in the 1950s and 1960s. These investigations initially focused on mineral exploration, but gradually the emphasis shifted to include water resources. The Clarkdale quadrangle was mapped by Lehner (1958). Krieger (1965) mapped the geology of the Prescott and Paulden quadrangles and described the water resources of the Prescott area. Twenter and Metzger (1963) summarized the geologic framework in the Mogollon Rim region surrounding Verde Valley with respect to the ground-water hydrology.

From 1933 to 1967, detailed water-level surveys in Little Chino Valley were conducted by the University of Arizona (UA), including an accounting of discharge at Del Rio Springs and pumping withdrawals from the Little Chino basin-fill aquifer (Schwalen, 1967). These early UA studies were continued through the early 1970s (Matlock and others, 1973). Water-level monitoring of the Little Chino basin-fill aquifer was continued by ADWR and evolved from water-level contour maps (Remick, 1983) to ground-water models (Corkhill and Mason, 1995; Nelson, 2002). In the 1990s, the water-level monitoring program was expanded to include more wells, including a few in Big Chino Valley and the Paleozoic carbonate aquifer north of the upper Verde River. In 1996, the USGS resumed monitoring of gauges at Del Rio Springs and lower Williamson Valley Wash. Presently, water-level data from ADWR index wells and streamflow data from USGS gauges are continually updated and made available to the public through ADWR and USGS databases, annual data reports, and the internet.

In Big Chino Valley, the first water-level contour map was produced by Wallace and Laney (1976); this map was last updated by Schwab (1995). Predevelopment hydrologic conditions in the alluvial basins of Arizona, including those in the Verde River headwaters region, were compiled by Freethy and Anderson (1986). Other maps of hydrologic conditions by Levings and Mann (1980), and Owen-Joyce



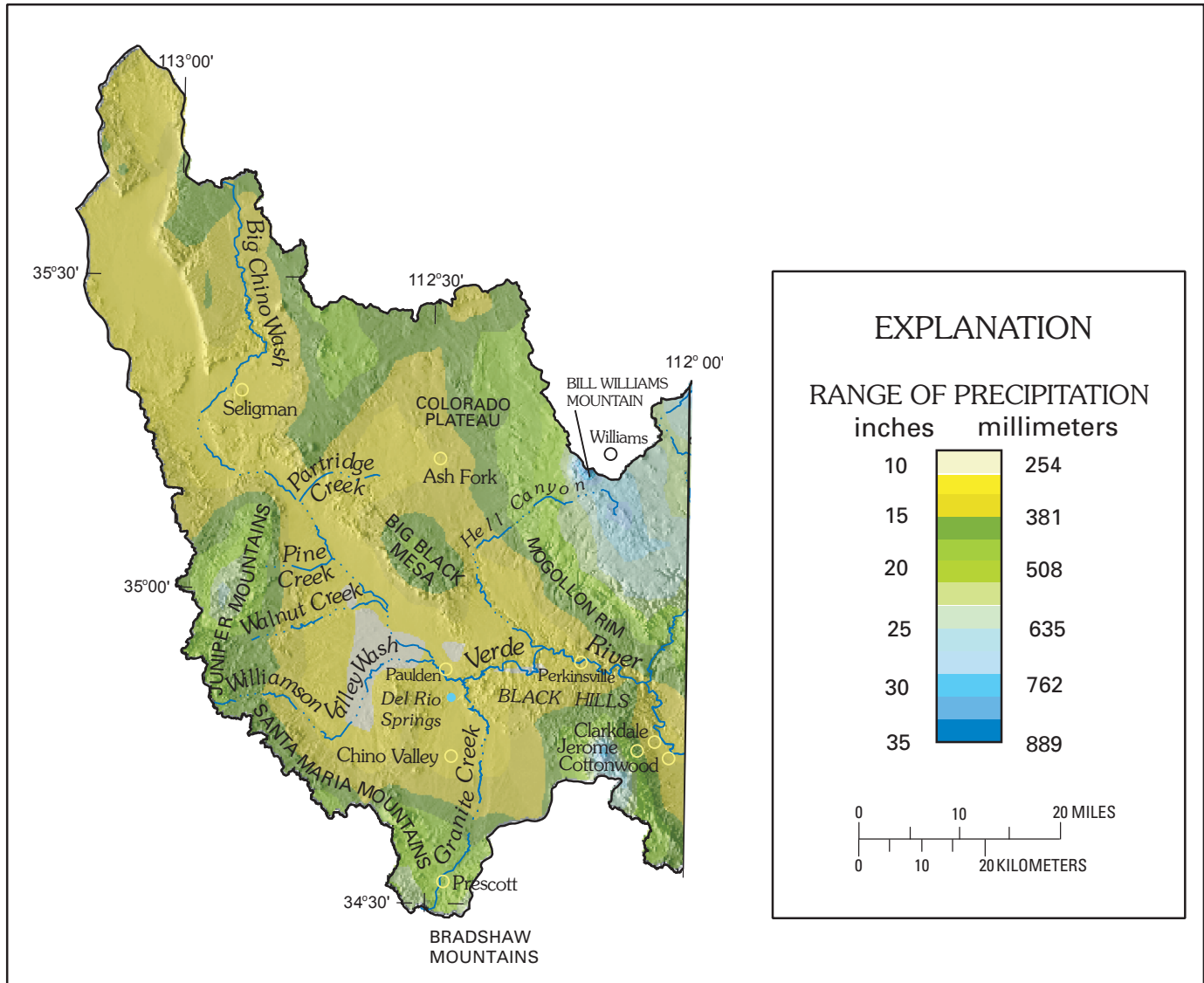


**Figure A9.** Map of upper Verde River watershed showing annual precipitation (Data source: U.S. Geological Survey website, <http://az.water.usgs.gov/rwi-ii/>; courtesy of Marilyn Flynn, based on PRISM dataset (1971-2000).

and Bell (1983) of the Verde Valley include some data for the region north of the Verde River between Paulden and Sycamore Canyon. Water Resource Associates (1990) conducted a hydrogeologic inventory of Big Chino Valley; the inventory consisted of a summary of hydrologic and geologic data, available well logs, and aquifer tests of candidate supply wells for the city of Prescott.

In the early 1990s, the Bureau of Reclamation carried out an extensive geologic and hydrologic investigation of the Big Chino Valley as a potential source of water supply for Prescott. The main objective was to examine the relation between ground water in Big Chino Valley and the upper Verde River. As part of the geological investigation,

ground-based geophysical surveys were conducted and three deep boreholes were drilled in the center of Big Chino basin (Ostenaar and others, 1993). Two ground-water models of the basin indicated that the ground water in the basin was connected to the river (Ewing and others, 1994; p. 7). Wirt and Hjalmarson (2000) compiled available hydrologic and geochemical data, including stable-isotope data, to consider the sources of ground water supplying base flow to upper Verde River springs and to examine historical water-budget relations between Big Chino Valley and the river. Arizona Department of Water Resources (2000) has compiled an overview of available data on water resources in the middle and upper Verde River watershed.

**Table A2.** Summary of monthly climate records for stations in the Verde River headwaters study area.

[Data source: Western Regional Climate Center, 2004]

CHINO VALLEY, ARIZONA (021654) Period of Record : 1971 to 2000													
Elevation 4,748 ft	Jan	Feb	Mar	Apr	May	Jun	Jul	Aug	Sep	Oct	Nov	Dec	Annual
Average max. temperature (F)	53.5	57.7	62.5	69.7	78.0	88.2	91.8	89.4	84.5	74.9	61.0	54.2	72.3
Average min. temperature (F)	22.9	25.5	29.5	35.2	42.9	51.0	58.8	57.9	50.5	39.1	27.2	22.3	38.7
Average total precipitation (in.)	1.2	1.3	1.2	0.6	0.5	0.4	1.7	2.2	1.6	1.1	0.9	0.9	13.4
PRESCOTT, ARIZONA (026796) Period of Record : 5/1/1898 to 12/31/2003													
Elevation 5,205 ft	Jan	Feb	Mar	Apr	May	Jun	Jul	Aug	Sep	Oct	Nov	Dec	Annual
Average max. temperature (F)	50.7	54.0	59.0	66.8	75.3	85.7	89.0	86.0	81.7	72.1	60.5	51.7	69.4
Average min. temperature (F)	21.2	24.0	28.2	34.0	40.6	48.9	57.4	56.0	48.5	37.1	27.3	21.9	37.1
Average total precipitation (in.)	1.7	1.9	1.8	0.9	0.5	0.4	2.9	3.3	1.7	1.1	1.3	1.6	19.1
Average total snowfall (in.)	6.2	5.0	5.2	1.3	0.2	0.0	0.0	0.0	0.0	0.2	2.2	4.8	25.0
WALNUT CREEK, ARIZONA (029158) Period of Record : 12/1/1915 to 12/31/2003													
Elevation 5,090 ft	Jan	Feb	Mar	Apr	May	Jun	Jul	Aug	Sep	Oct	Nov	Dec	Annual
Average max. temperature (F)	51.6	56.4	61.4	69.4	77.5	86.9	90.1	87.5	83.2	73.4	60.6	51.8	70.8
Average min. temperature (F)	21.0	23.2	26.0	30.3	36.9	44.0	53.7	53.1	44.9	34.1	25.3	20.0	34.4
Average total precipitation (in.)	1.5	1.6	1.4	0.7	0.5	0.4	2.3	2.8	1.5	1.0	0.9	1.4	16.2
Average total snowfall (in.)	3.7	2.8	1.7	0.6	0.1	0.0	0.0	0.0	0.0	0.0	0.4	2.4	11.8
SELIGMAN, ARIZONA (027716) Period of Record : 12/1/1904 to 12/31/2003													
Elevation 5,205 ft	Jan	Feb	Mar	Apr	May	Jun	Jul	Aug	Sep	Oct	Nov	Dec	Annual
Average max. temperature (F)	51.1	55.1	61.2	69.1	77.8	87.5	91.2	88.4	83.8	73.8	61.9	52.5	71.1
Average min. temperature (F)	21.2	24.0	26.9	32.0	38.8	46.3	55.1	54.1	46.8	36.5	26.9	21.6	35.8
Average total precipitation (in.)	0.9	1.0	1.0	0.5	0.4	0.3	1.8	2.1	1.1	0.7	0.7	0.9	11.4
Average total snowfall (in.)	3.3	2.8	1.8	0.4	0.2	0.0	0.0	0.0	0.0	0.1	1.2	2.8	12.6
ASH FORK 6 N, ARIZONA (020482) Period of Record : 4/ 2/1902 to 9/30/1987													
Elevation 5,130 ft	Jan	Feb	Mar	Apr	May	Jun	Jul	Aug	Sep	Oct	Nov	Dec	Annual
Average max. temperature (F)	51.5	55.2	61.0	68.9	77.9	87.8	91.7	88.9	84.5	74.3	63.0	53.8	71.5
Average min. temperature (F)	20.8	23.7	26.9	33.1	39.8	48.1	56.3	55.4	48.2	37.8	27.4	22.4	36.6
Average total precipitation (in.)	0.98	1.01	1.01	0.8	0.4	0.5	1.8	2.3	1.3	0.9	0.6	1.2	12.7
Average total snowfall (in.)	4.5	3.4	2.7	0.4	0.2	0.0	0.0	0.0	0.0	1.0	0.8	3.7	16.5
WILLIAMS, ARIZONA (029359) Period of Record : 3/26/1897 to 12/31/2003													
Elevation 6,750 ft	Jan	Feb	Mar	Apr	May	Jun	Jul	Aug	Sep	Oct	Nov	Dec	Annual
Average max. temperature (F)	45.1	47.5	52.3	61.0	69.9	80.4	83.6	80.9	75.9	66.4	55.0	47.1	63.8
Average min. temperature (F)	19.4	21.7	25.4	31.3	38.4	46.2	53.0	52.0	46.0	35.5	26.0	20.6	34.6
Average total precipitation (in.)	2.0	2.2	2.1	1.3	0.7	0.5	2.8	3.2	1.8	1.4	1.4	2.0	21.5
Average total snowfall (in.)	16.2	13.6	13.6	5.9	1.3	0.0	0.0	0.0	0.0	0.9	5.4	12.7	69.6

## Predevelopment Conditions

Early settlement of Little Chino Valley was described in the environmental setting of this chapter, and predevelopment conditions have been described by Schwalen (1967) and modelled by Corkhill and Mason (1995). Schwalen states that recharge to the artesian basin was in equilibrium with natural discharge before the construction of Watson Lake and Willow Creek dams in 1915 and 1937 (fig. A3). Ground-water pumping in Little Chino Valley began with the drilling of the first deep artesian well in 1930 (Schwalen, 1967). Schwalen (1967) notes that there was no appreciable pumping in the Little Chino basin or evidence that outflow was affected by reservoir storage until after 1937. Widespread water-level measurements in Little Chino Valley were first made in 1937 and have been used to simulate predevelopment conditions modeled by Corkhill and Mason (1995). The assumption that equilibrium conditions existed in the neighboring Agua Fria basin-fill aquifer prior to the 1940s also is reasonable (Corkhill and Mason, 1995).

Under predevelopment conditions, the ground-water system is assumed to be in long-term equilibrium in response to annual or longer-term climatic variations (Alley and others, 1999). Unfortunately, most ground- and surface-water data collection efforts in Williamson and Big Chino Valleys were initiated long after irrigated agricultural activities in the region began and, therefore, do not represent true predevelopment conditions. Although there are many historical accounts regarding the settlement of Del Rio Springs, Prescott, and Chino Valley dating back to the 1850s, little hydrologic information is available for Big Chino Valley prior to 1946. Big Chino Wash presently is ephemeral throughout its entire length, but there is evidence that some reaches may have been intermittent or perennial prior to agricultural development.

Among the earliest written descriptions of the landscape are the journals of the United States Army explorations. The Whipple expedition explored the length of Partridge Creek and upper Big Chino Valley for 23 days in 1854, describing the water, vegetation, and soils (Shaw, 1998). On January 19, the wagon party traveled down the valley to a point 8 mi and 20 degrees west of south from the confluence of Partridge Creek and Big Chino Wash. Lieutenant John Tidball wrote, "...*Good grass, no water. A messenger arrived from the advanced party stating that to the southwest of us were two running creeks besides a small lagoon and other water.*" The location described probably is the confluence of Pine Creek with Cienaga Creek, which had a large spring, later diverted for agricultural purposes (Shaw, 1998). Similar accounts of this site are repeated in journals by other expedition members. The expedition apparently crossed the main valley and explored the Pine Creek and Walnut Creek tributaries, eventually crossing over a pass at the head of Walnut Creek into the Bill Williams watershed. Thus, the expedition did not follow Big Chino Wash very far below the mouth of Partridge Creek. The journals of the Whipple expedition recommended Big Chino Valley for its good grass and promising agricultural potential. Before long "*settlement in the rich valley was steady, and by*

*1879 there was a need for a post office*" (Granger, 1985). The Big Chino post office closure in 1891 approximately coincides with a pattern of cattle overstocking and drought that wiped out many of the ranchers in the Prescott and Chino Valley areas in the 1890s (Henson, 1965).

Topographical maps published in 1947 (USGS 1:62,500 series), based on 1946 aerial photographs, show Big Chino Wash represented by a solid or double blue line between Partridge Creek and Antelope Wash (west of Wineglass Ranch), indicating either perennial or intermittent conditions (fig. A10). These maps are inconclusive because the aerial photography and field checking may have occurred during a wetter timeframe. In addition, flow may have varied greatly from season to season. Evidence that there were pools capable of withstanding droughts, however, is provided by biologists who collected fish in the vicinity of CV Ranch. Several native fish species were taken from upper Big Chino Wash in 1897 (Gilbert and Scofield, 1898) and again in 1950 (Winn and Miller, 1954). Species identified in 1897 included Roundtail Chub (*Gila Robusta intermedia*), Spikedace (*Meda fulgida*), Speckled dace, (*Rhinichthys osculus*) and loach minnow (*Tiaroga cobitis*). Roundtail chub and Sonora sucker (*Catostomus insignis*) were identified in 1950. Weedman and others (1996) describe the collection site as 2 mi southeast of K4 Farm, which is near the meandering confluence of Big Chino Wash with Pine Creek. An oblique aerial photograph taken in 1940 of this area shows a large dark area interpreted as a large marsh or cienaga between Pine Creek and Big Chino Wash (fig. A10A). The photograph shows water in both Pine Creek and Big Chino Wash, a diversion dam on lower Pine Creek with impounded water, roads and irrigation ditches, and irrigated fields. Pine Creek and Big Chino Wash are now ephemeral.

Comparisons of water-level contour maps by Wallace and Laney (1976) and Schwab (1995) indicate that historical pumping for irrigated agriculture has, at times, had a measurable effect on water levels in parts of Big Chino Valley. Although water levels in lower Big Chino Valley downstream from Walnut Creek were similar in February 1992 (Schwab, 1995) to what they were in March 1975 (Wallace and Laney, 1976); large declines have been observed near irrigated farmland in the upper Big Chino Valley. The water table along Big Chino Wash between its confluences with Partridge Creek and Pine Creek apparently was near or at land surface prior to 1950 (fig. A10A). In 1975, water levels along this reach were approximately 30 to 100 ft below land surface (Wallace and Laney, 1976). Agricultural activity decreased after 1975, and in 1992 water levels along this reach were approximately 20 to 80 ft below land surface. The largest rises in water level were clustered along a narrow strip of irrigated farmland. The rise for some individual wells was as much as 40 ft from 1975 to 1992 (Schwab, 1995). Wirt and Hjalmarson (2000, p. 32) identify an inverse correlation between decreased pumping (mostly in northern or "upper" Big Chino Valley) and an increase in Verde River base flow between the 1960s and the 1990s.

Although little predevelopment hydrological information is available for Williamson Valley Wash, roundtail chub and an unidentified sucker species were found by Arizona Game and Fish in authorized surveys of Williamson Valley Wash in 1990, 1992, and 2001 (Weedman and others, 1996; Girmendonk and others, 1997; Clark, 2002). Roundtail chub are abundant in the reach between the Williamson Valley Road and the Williamson Valley Wash streamflow gauging station (Clark, 2002). This 4.2-mi stream segment presently is about the same length as indicated as perennial on the 1947 USGS Simmons quadrangle, which lends additional credibility to the segments of Big Chino Wash mapped as perennial. In addition, speckled dace are common in Walnut Creek and several of its tributaries (Kevin Morgan, Arizona Game and Fish, written commun., November 2000).

The Sullivan Lake dam was built below the confluence of Little Chino Creek and Big Chino Wash in the late 1930s (fig. A6). In Little Chino Valley, a 6-mi perennial reach in Little Chino Creek originated 2 mi south of the Puro railroad siding at Del Rio Springs (fig. A10B). Base flow in Little Chino Creek was the primary source of water to Sullivan Lake (and the Verde River between Sullivan Lake and Stillman Lake) until the early 1970s (A.L. Medina; U.S. Forest Service, oral commun., 1999). Presently, the creek is perennial for about 0.5 mi north and 0.5 mi south of the Puro railroad siding at Del Rio Springs. Part of the original cienaga is still present in this reach.

As mentioned earlier, ground-water discharge from Del Rio Springs to Little Chino Creek is declining, and at present is less than one half of what it was 60 years ago. Average annual discharge was  $2,828 \pm 455$  acre-ft per year (acre-ft/yr) between 1939 and 1945, when first measured by Schwalen (1967). Between 1997 and 2002, average annual discharge was  $1,360 \pm 150$  acre-ft/yr (McCormack and others, 2003). All base flow in Little Chino Creek currently is diverted or infiltrates to irrigated pasture and several ponds that are part of the cattle ranch (Allen, Stephenson & Associates, 2001). About 150 acre-ft/yr of the discharge from Del Rio Springs bypasses the USGS gauge (Allen, Stephenson & Associates, 2001) as does runoff from Big Draw, an ephemeral tributary. Big Draw joins Little Chino Creek about one mi north of Del Rio Springs.

The historical decrease in ground-water discharge near Del Rio Springs is largely attributed to ground-water pumping in Little Chino Valley and to surface-water diversions from Del Rio Springs and Little Chino Creek (Wirt and Hjalmanson, 2000). Drought conditions (Betancourt, 2003) are thought to account for the decline from about 1,500 to 1,000 acre-ft/yr during the 1997 through 2003 water years. The 2003 water year had the lowest mean daily discharge of any year on record ( $0.85\text{--}1.0$  ft<sup>3</sup>/s during 14 consecutive days in July; Fisk and others, 2004). Because there is no longer perennial flow from either Big Chino Wash or Little Chino Creek, the size of Sullivan Lake (fig. A11) is usually considerably smaller than depicted in 1947 (fig. A10B), and usually looks more like a large meadow than a lake. Impounded runoff generally is retained for extended periods of several months or longer

following large storms, but the author has observed a dry lake on several occasions.

In an early account of lower Big Chino Valley, the Bureau of Reclamation (1946) described the relation of streams in the Verde River headwaters as follows: “the head of the Verde, formed by the junction of Chino Creek (*Big Chino Wash?*) and Williamson Valley Wash, is fed by permanent ground water.” The confluence of Big Chino Wash and Williamson Valley Wash at that time was located about 1 mi upstream from Sullivan Lake. This segment of Big Chino Wash is now ephemeral, and aggraded with sediment above Sullivan Lake dam (fig. A11). The 1947 USGS map shows this segment of lower Big Chino Wash as perennial or intermittent (fig. A10B); however, for reasons described earlier this assignment is considered questionable. Because of the inflow from the Little Chino basin, the water table would have been at lake level between Sullivan Lake and the confluence of Williamson Valley Wash with Big Chino Wash (elevation 4,350 ft) in 1947. In 1990, the water level of a nearby production well was reported as 4,255 ft in 1990 (Dugan well at (B-17-02) 04 CDA; Water Resource Associates, 1990). In addition, Schwab (1995) reports the water-level elevation of several nearby wells as ranging between 4,246 and 4,270 ft. Thus, the water table in the vicinity of Sullivan Lake apparently had declined by more than 80 ft since 1947, and was about 20 ft higher than upper Verde River springs during the early 1990s (the upper range of elevation used for upper Verde River springs in this study is  $4,235 \pm 1$  ft; Wirt and DeWitt, this volume; Chapter D).

To summarize ground-water conditions prior to about 1950, upper Big Chino Wash probably was intermittent or perennial in a few segments between Partridge Creek and Antelope Wash. During droughts, there must have been at least enough water for fish to survive in isolated pools. The water table would have been at land surface or near land surface over much of this reach. The water table is still fairly shallow, between about 20 and 70 ft below land surface (Schwab, 1995). In lower Big Chino Valley, the water table was near or at the land surface between the confluence of Big Chino Wash and Williamson Valley Wash and present-day Sullivan Lake dam. Water levels near Sullivan Lake appear to have declined more than 80 ft since 1947 and are presently about 20 ft higher than the maximum elevation for upper Verde River springs. Since 1950, about 6 mi of perennial stream segments surrounding Sullivan Lake became ephemeral—at least 4 mi in Little Chino Creek, 1 mi in lower Big Chino Wash, and 1 mi of the Verde River between Sullivan and Stillman Lakes. These changes are broadly attributed to a combination of surface-water diversions, ground-water pumping, and climatic factors such as prolonged and reoccurring droughts.

## Surface-Water Conditions

Streamflow has two components—storm runoff and base flow. Storm runoff occurs in direct response to rainfall and snowmelt, typically over brief periods of time or having a relatively short seasonal duration. Base flow is the amount of

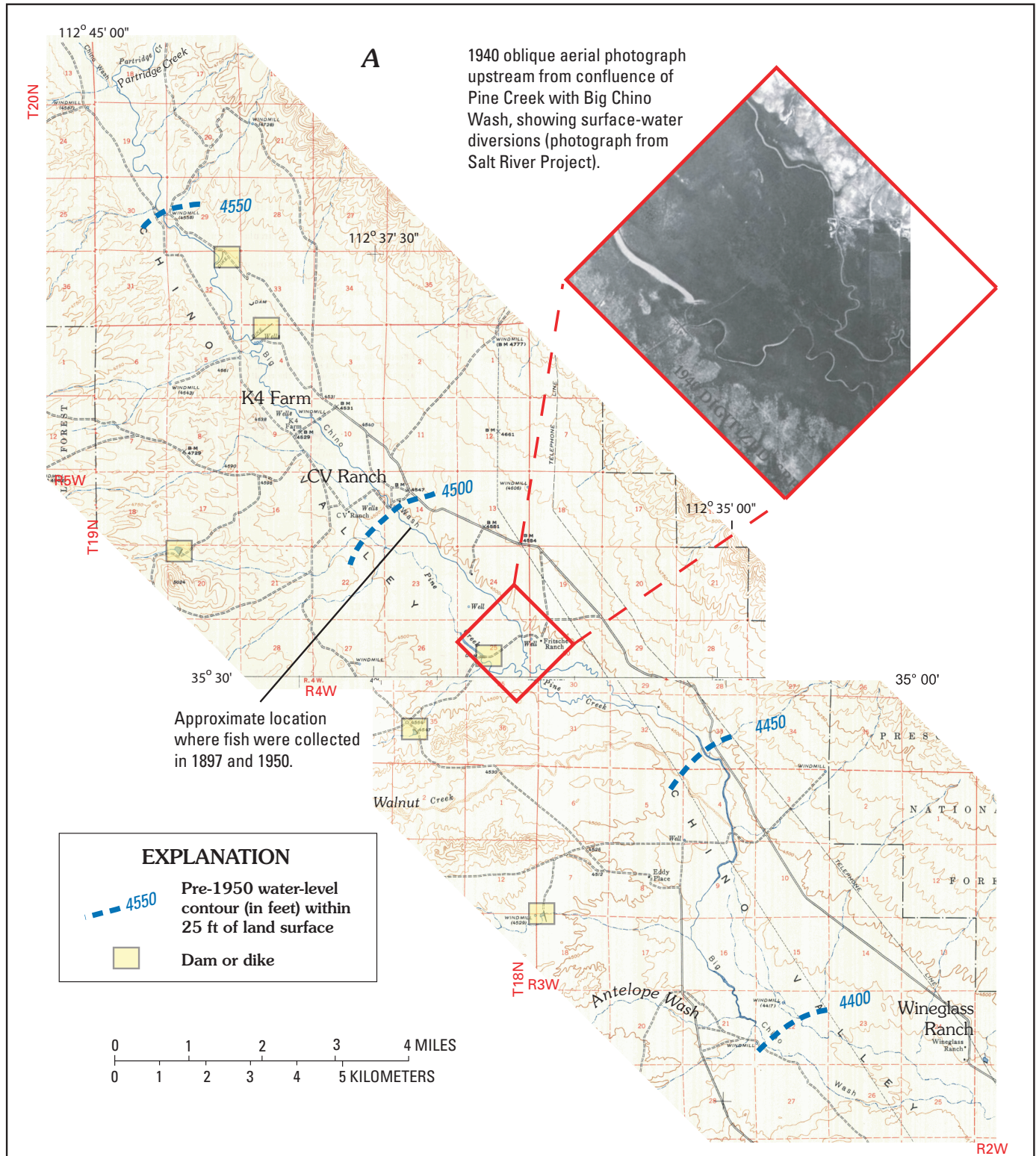


**Figure A10.** Pre-1950 ground-water conditions inferred from 1947 U.S. Geological Survey topographic maps, indicating shallow water table in parts of Big and Little Chino Valleys. A, intermittent reach of upper Big Chino Wash between Partridge Creek and Wineglass Ranch (1947 Pichacho Buttes and Simmons quadrangles; 1:62,500 scale). Inset shows 1940 aerial photograph of Pine Creek and Big Chino Wash with cienaga; B, (facing page).

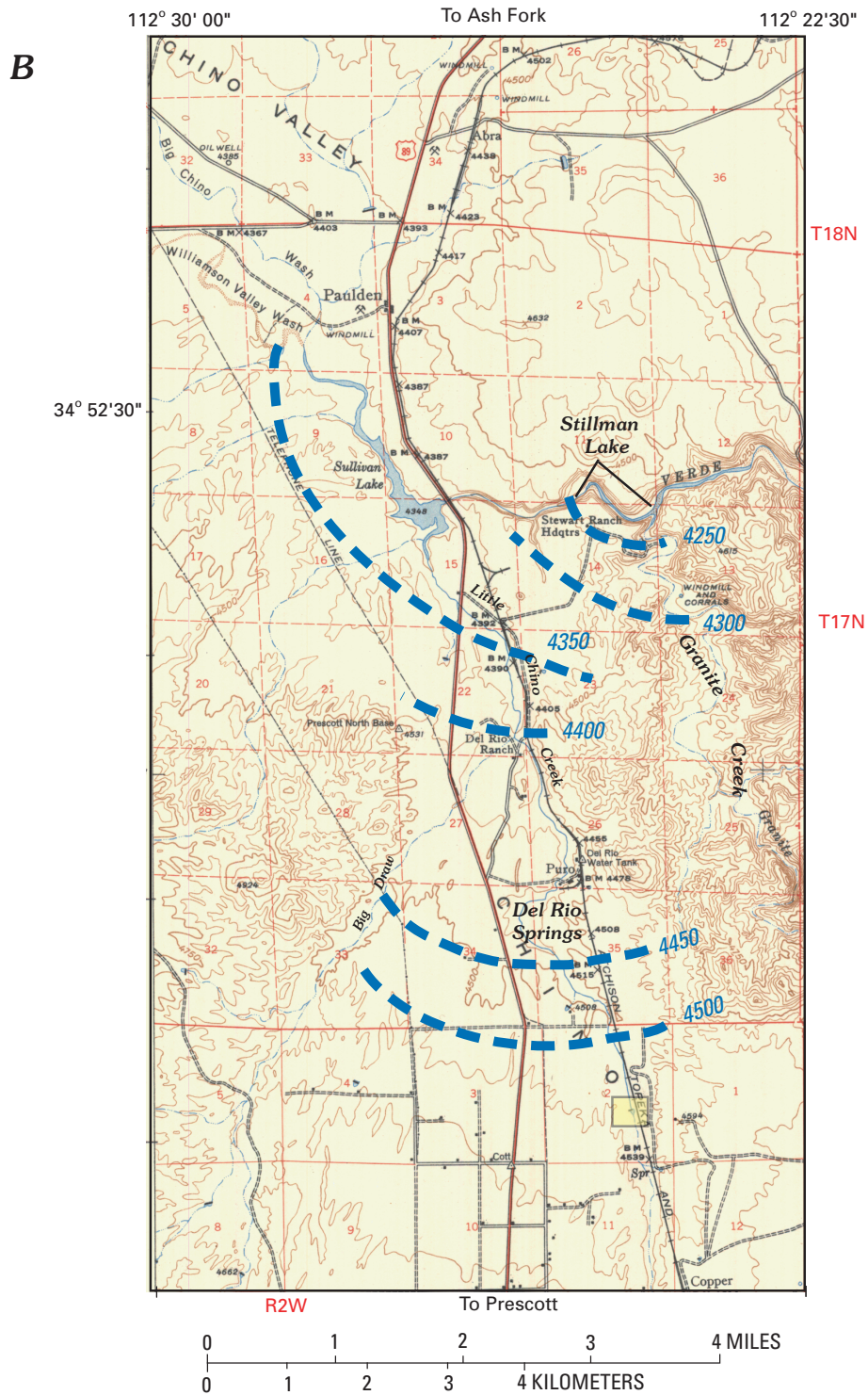


**Figure A10.** (Continued) B, ground-water conditions inferred from intermittent reaches in lower Big Chino Wash and Little Chino Creek (1947 USGS Paulden quadrangle, 1:62,500). Big Chino Wash is shown as a perennial segment from its confluence with Williamson Valley Wash to Sullivan Lake. Little Chino Creek is mapped as perennial from Del Rio Springs to Sullivan Lake, as is the upper Verde River downstream from Sullivan Lake to Stillman Lake.

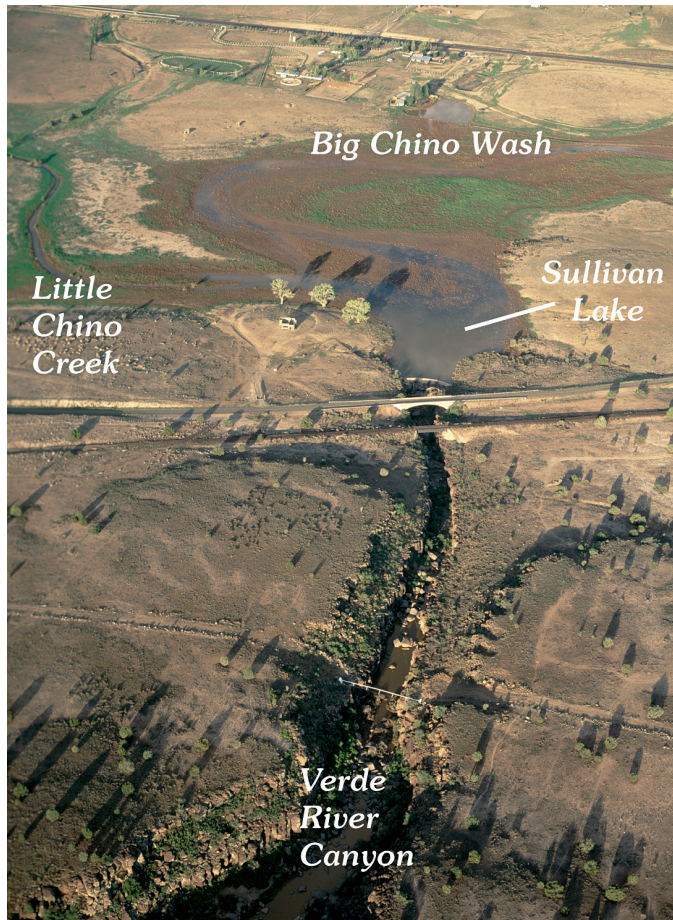


**Figure A11.** Aerial photograph of Sullivan Lake showing confluence of Little Chino Creek and Big Chino Wash. View is to the west. Rocks in foreground are 4.5-Ma basalt, and the background is valley-fill sediments overlying the basalt. Runoff in response to a regional storm, September 2003. Photograph by M. Collier.

streamflow sustained by discharge of ground water. Long-term changes in base flow indicate changes in the volume of water stored in the aquifer and how discharge from the aquifer is distributed among pumpage, streamflow, and evapotranspiration losses, which depend on rainfall and land use (Alley and others, 1999).

Base flow and storm-runoff characteristics are highly variable in time and space for different parts of the Verde River headwaters study area. Direct comparisons between streamflow gauges are difficult because of differences in the period of the gauge record, elevation, precipitation, recharge, water use, and the uneven distribution of rock types. Stream gauges are operated for different objectives and timeframes, resulting in widely different periods of record (table A3). Many large streams or intermittent tributaries, such as Big Chino Wash or lower Granite Creek, have no continuous streamflow records at all.

In general, the larger the drainage area the larger the base flow, as well as the peak runoff. For example, the Verde River near Paulden gauge (drainage area = 2,507 mi<sup>2</sup>) has a 50th percentile daily mean flow duration of 25 ft<sup>3</sup>/s, compared to that of 82 ft<sup>3</sup>/s for the Verde River near Clarkdale (drainage area = 3,503 mi<sup>2</sup>) (Fisk and others, 2004). Flow duration of daily mean discharge, expressed in a percentage of time, are specified daily flows that are equaled or exceeded for a given percentage of time, expressed in percentiles (Pope and others, 1998). The “50th percentile” represents a flow value that is equaled or exceeded 50 percent of the time throughout the period of annual record. A 10th percentile daily mean flow at the Paulden gauge of 29 ft<sup>3</sup>/s is likely to be exceeded less than 10 percent of the time; whereas the 90th percentile daily mean flow of 22 ft<sup>3</sup>/s is likely to be exceeded 90 percent of the time (Fisk and others, 2004). In contrast, the maximum recorded discharge (or daily peak discharge) values, which represent almost entirely storm water runoff, is 23,200 ft<sup>3</sup>/s for the Paulden gauge and 53,200 ft<sup>3</sup>/s for the Clarkdale gauge. The exceedance probability for flows of this magnitude is within a recurrence interval of 25 to 50 years (Pope and others, 1998), indicating that most surface-water runoff occurs during large but infrequent floods. These statistics are cited here to illustrate that ground-water discharge (or base flow) accounts for nearly all of the water in the upper Verde River, nearly all of the time.

## Big Chino Valley

Walnut Creek (fig. A12) and Williamson Valley Wash are the two largest tributaries to Big Chino Valley with perennial reaches (fig. A1). Ewing and others (1994) operated a U.S. Forest Service gauge on Walnut Creek from August 1991 to July 1992 and reported a mean discharge of 1,500 acre-ft/yr, reported as 2.07 ft<sup>3</sup>/s for those 10 months (table A4). They also estimated average runoff from Williamson Valley Wash gauge at 11,583 acre-ft/yr (mean annual discharge of 15.7 ft<sup>3</sup>/s for the 1965–1985 water years). This compares with a mean annual discharge of 14.5 ft<sup>3</sup>/s over the period from 1965 to 2003, with a daily mean flow of 1.7 ft<sup>3</sup>/s and no flow measured on some days (table A3; Fisk and others, 2004).

Few, if any, streamflow data are available for Pine Creek, Partridge Creek, or Big Chino Wash, which (along with smaller ephemeral tributaries and areal recharge in upland areas) were assumed by Ewing and others (1994) to contribute the remaining fraction of base flow to the upper Verde River. In their ground-water model, Ewing and others (1994) assumed that surface-water runoff and, therefore, direct recharge from Partridge Creek was insignificant. Areal recharge in upland areas was estimated between 0.43 and 0.83 inches per year (Ostenaar and others, 1993).

Because there is no gauge for Big Chino Wash, its peak discharge of record can only be indirectly inferred, but probably exceeds 15,000 ft<sup>3</sup>/s. The peak of the largest recorded flood at the Paulden gauge was 23,200 ft<sup>3</sup>/s on February 20, 1993, which also included an unknown amount of inflow from

**Table A3.** Summary of available surface-water data and characteristics of drainage basins for streamflow-gauging stations, Verde River headwaters, Arizona.

[Data from annual USGS water data reports, 1997 to 2003; Pope and others, 1998; ft, feet; mi<sup>2</sup>, miles squared; ft<sup>3</sup>/s, cubic feet per second; --, no data]

Station name	Station no.	Mean basin elevation (ft)	Drainage area (mi <sup>2</sup> )	Mean annual basin precipitation (in.)	Stream length (mi <sup>2</sup> )	Maximum discharge (ft <sup>3</sup> /s)	Minimum discharge (ft <sup>3</sup> /s)	Daily mean flow <sup>1</sup> (ft <sup>3</sup> /s)	Mean annual discharge (ft <sup>3</sup> /s)	Period of record
Williamson Valley Wash near Paulden	09502800	5,120	255	17.3	19.2	14,800	no flow	1.7	14.5	March 1965 to 2003
Granite Creek at Prescott	09502960	5,285	30			6,600 <sup>2</sup>	no flow	no flow	4.2	1994 to 2003
Granite Creek near Prescott	09503000	5,900	36.3	22.1	7.3	3,200	no flow	no flow	5.8	July 1932 to Sept 1943; Oct 1994 to Sept 2003
Granite Creek below Watson Lake	09503300	5,020	--	--	--	247	no flow	no flow	0.57	1999 to 2003
Del Rio Springs	09502900	4,430	40.9	--	--	652	0.85	1.82	1.83	1996 to 2003
Verde River near Paulden	09503700	5,410	2,507 <sup>3</sup>	16.3	78.4	23,200	15	25	42.0	1963 to 2003
Hell Canyon near Williams	09503720	7,110	14.9	24.1	5.3	1,080	no flow	no flow	--	1966 to 1979
Hell Canyon tributary near Ash Fork	09503740	5,180	0.75	17.2	1.7	84	no flow	no flow	--	1969 to 1980
Limestone Canyon near Paulden	09503750	5,310	14.5	15.5	8.4	1,100	no flow	no flow	--	1969 to 1980
Verde River near Clarkdale	09504000	5,490	3,503 <sup>3</sup>	19.1	115	53,200	55	82	177	1915 to 2003

<sup>1</sup>Discharge which was equaled or exceeded 50% of the time.

<sup>2</sup>Flood occurred outside of period of record.

<sup>3</sup>364 mi<sup>2</sup> generally is considered noncontributing, including 357 mi<sup>2</sup> in Aubrey Valley playa, a closed basin. Actual noncontributing area is thought here to be much higher (Wirt and DeWitt, Chapter D).

### Little Chino Valley

There is a large gap in the period of record for the gauge at Del Rio Springs on Little Chino Creek. The initial gauge was washed out by a peak flood of 65 ft<sup>3</sup>/s on August 4, 1946 (Schwalen, 1967). Fifty years later the USGS installed a new gauge at a nearby location in August, 1996. Mean annual discharge for this gauge was 1.83 ft<sup>3</sup>/s between 1996 and 2003 (table A3). There is no gauge for lower Granite Creek near its confluence with the Verde River, but there are three long-term gauges in the upper Granite Creek watershed near Prescott.

Prior to the construction of dams for Watson Lake and Willow Creek reservoirs in 1915 and 1937 (fig. A3), upper Granite Creek contributed about 6 ft<sup>3</sup>/s of mean annual discharge to Little Chino Valley through a narrow canyon in the Granite Dells (Schwalen, 1967; table A4). The discharge to the two reservoirs between 1933 to 1947, which is considered here to be representative of predevelopment inflow from the upper Granite Creek watershed to Little Chino Valley, averaged 6,250 acre-ft/yr from 1933 to 1947 (Schwalen, 1967; p. 20) with a median value of 3,200 acre-ft/yr (Corkhill and Mason, 1995).

The maximum recorded discharge for Granite Creek near Prescott was 6,600 ft<sup>3</sup>/s on August 19, 1963 (Fisk and others, 2004; table A3). The total predevelopment recharge for the Little Chino ground-water basin, assuming flow-through runoff and evaporative losses, is estimated at about 4,500 acre-ft/yr (table A4; Schwalen, 1967; Matlock and others, 1973).

### Upper Verde River Canyon

Base flow in the upper Verde River is steady—changing little in response to precipitation or lack thereof—from year to year, and within a year. Base flow for the Verde River near Paulden has been nearly constant over its historical period of record (July 1963 to present), and generally ranges between 22 and 26 ft<sup>3</sup>/s (Owen-Joyce and Bell, 1983; Pope and others, 1998). Using a hydrograph separation approach, Wirt and Hjalmarson (2000) determined a mean base flow for the Paulden gauge of 25 ft<sup>3</sup>/s or 18,000 acre-ft/yr. This compares reasonably well with a mean base flow of 16,000 acre-ft/yr calculated by Freethey and Anderson (1986), using a different period of record (table A4). In this report, the base flow value that will be used for the Verde River near Paulden is the mean for the two hydrograph separation estimates, or 17,000



**Table A4.** Summary of predevelopment base-flow discharge and calculated recharge for major areas in the Verde River headwaters, Arizona.

[mi<sup>2</sup>, miles squared; acr-ft/yr, acre feet per year; bold indicates mean where n is total number of estimates]

Basin	Subbasin	Drainage area (mi <sup>2</sup> )	Base flow discharge <sup>2</sup> (acre-ft/yr)	Predevelopment calculated recharge (acre-ft/yr)	Recharge as percent of total calculated recharge <sup>6</sup>	Data source	
Big Chino Valley		1,850		21,600 <sup>5</sup> 21,500	78.9	Ewing and others (1994); Ford (2002) Freethy and Anderson (1986) <sup>4</sup>	
				<b>21,550</b>		<b>Average of above (n = 2)</b>	
	Williamson Valley Wash Walnut Creek	255	11,583 1,500			Ewing and others (1994) Ewing and others (1994)	
Little Chino Valley	Granite Creek and Little Chino Creek watersheds	300		5,000 4,000 4,500	16.5	Schwalen (1967) Matlock and others (1973) Freethy and Anderson (1986) <sup>4</sup>	
						<b>4,500</b>	<b>Average of above (n = 3)</b>
	Del Rio Springs Willow Creek Granite Creek near Prescott (above Watson Lake)	41 36	2,849 1,420 4,830			Schwalen (1967) Schwalen (1967) Schwalen (1967)	
Big Black Mesa		100		1,250	4.6	Ford (2002)	
Verde River gage near Paulden		2,507 <sup>1</sup>	18,000 <sup>3</sup> 16,000 <sup>3</sup>	<b>27,300<sup>6</sup></b>	100.0	Wirt and Hjalmarson (2000) Freethy and Anderson (1986) <sup>4</sup>	
			<b>17,000</b>			<b>Average of above (n = 2)</b>	

<sup>1</sup>Includes 357 mi<sup>2</sup> of noncontributing area in Aubrey Valley.

<sup>2</sup>Base-flow discharge is same as mean annual discharge, except as noted.

<sup>3</sup>Base-flow discharge determined by hydrograph separation for period of record at time of study.

<sup>4</sup>Data from Freethy and Anderson (1986) are the raw values used to construct the pie charts in their report.

<sup>5</sup>Value of 23,700 acre-ft/yr of recharge for upper Verde River watershed (Ewing and others, 1994) minus 2,100 acre-ft/year of inflow in 1990 from Little Chino Valley (ADWR, 2000) equals 21,600 acre-ft/year (Ford, 2002).

<sup>6</sup>Sum of average calculated recharge for Big and Little Chino Valleys and Big Black Mesa.

acre-ft/yr (table A4). This mean value compares favorably with the annual mean discharge of 16,370 acre-ft per year during the 2000 water year at the Paulden gauge (MacCormack and others, 2002), a year without any storm runoff and which currently is the lowest annual discharge of record.

Surface-water runoff in the upper Verde River and its bedrock canyon tributaries may exceed daily base flow by three to four orders of magnitude. The maximum flow of record at the Paulden gauge was 23,200 ft<sup>3</sup>/s in 1993 (fig. A13). The lowest mean daily flow of record was 15 ft<sup>3</sup>/s during May 13–23, 1964, which coincided with pumping to fill artificial lakes constructed for real estate promotion near Wineglass Ranch in Big Chino Valley (Wirt and Hjalmarson, 2000). This response to pumping suggests a hydraulic connection between the Big Chino basin-fill aquifer, Verde River base flow, and the part of the regional carbonate aquifer that lies in between. When pumping ceased, the base flow quickly recovered to 23 ft<sup>3</sup>/s in June 1964—a period with little, if any, rainfall runoff. In comparison, the lowest mean daily flow measured since May 1964 was 19 ft<sup>3</sup>/s for several weeks in June and July of 2003, following several years of extended drought conditions.

The USGS conducted synoptic surveys of base flow in 1979, 1991, 1999, and 2000 to define base-flow conditions and sources of inflow to the upper reach (Owen-Joyce and Bell, 1983; Ewing and others, 1994; and U.S. Geological Survey, 2000 and 2001; fig. A14). Perennial base flow in the Verde River canyon presently begins downstream from the Sullivan Lake dam as an impounded section of river channel that is informally known as Stillman Lake (between river mi 1.0 and 2.0), where the river canyon intersects the water table (fig. A15). This reach is dammed by a natural levee of sand deposited by Granite Creek, currently vegetated with cattails. Although the lower reach of Granite Creek also is perennial, the reach immediately downstream from Stillman Lake and Granite Creek was ephemeral from 1999 to 2001. In June 2000, the dry reach extended more than 500 ft downstream from Stillman Lake, although this area has since been impounded by beaver dams. Base flow from Stillman Lake and lower Granite Creek travels beneath the surface through shallow alluvium in this reach (Wirt, Chapter F, this volume).

Perennial discharge in the upper Verde River reemerges near mi 2.1 and increases to about 19 ft<sup>3</sup>/s by Stewart Ranch

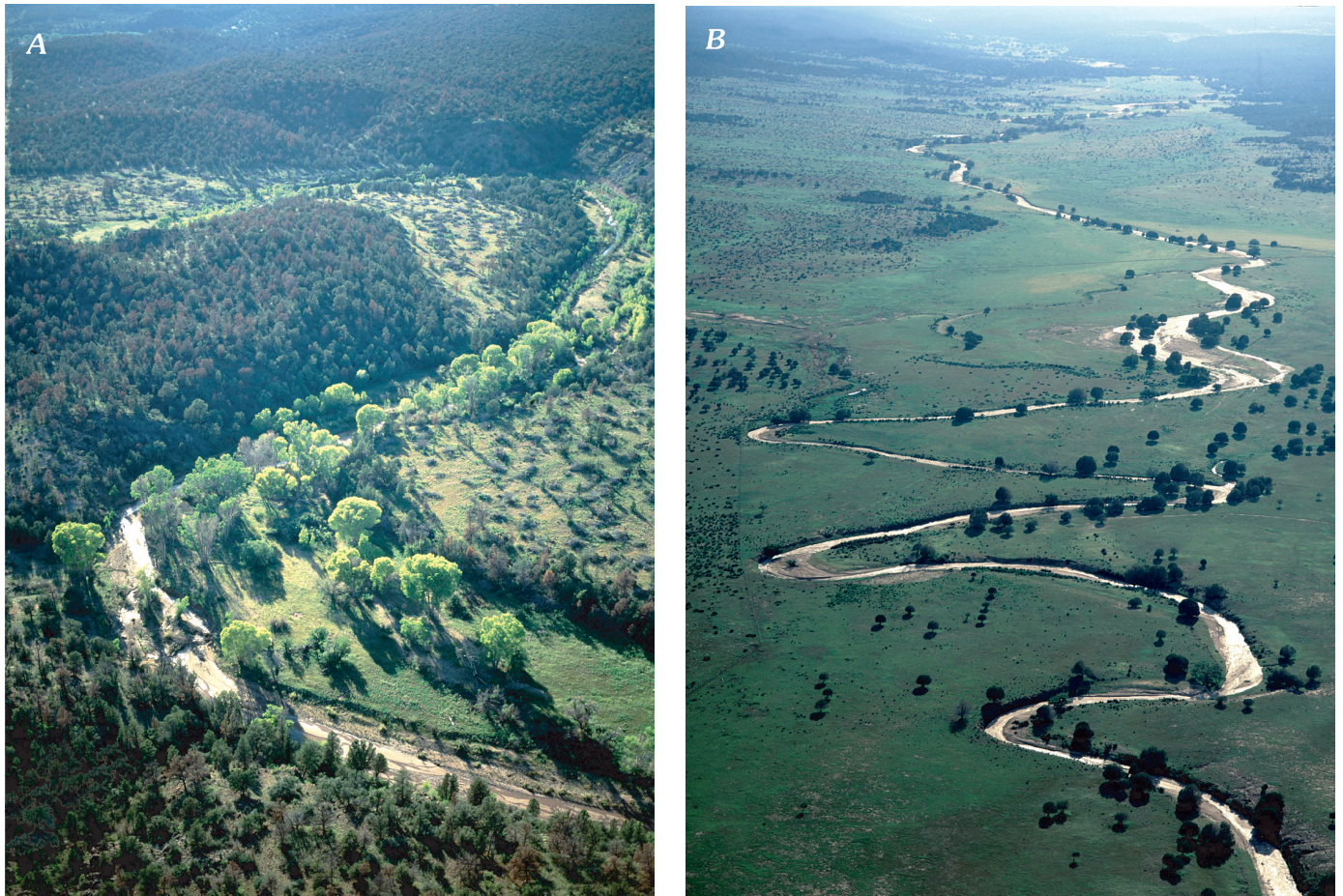


**Figure A12.** Photographs of Walnut Creek (A) in perennial segment, and (B) near confluence with Big Chino Wash following regional storm of September 2003. Views to west and southwest. Photographs by M. Collier.



**Figure A13.** Photographs showing A, flood of February 20, 1993, at Sullivan Lake dam. View to southwest. Sullivan Lake dam is behind hydraulic drop. B, Verde River gorge below the dam. View downstream to east. Canyon is carved from Tertiary basalt. Peak discharge of 23,200 ft<sup>3</sup>/s and daily mean discharge of 13,700 ft<sup>3</sup>/s are the sum of Big Chino Wash, Williamson Valley Wash, Little Chino Creek, and Granite Creek at Paulden gauge. Photographs by E. Carr.



(river mi 3.2; fig. A14, located on fig. A2). Most of the gain occurs from a large, diffuse spring network discharging from the Martin Formation near river mi 2.2, formerly referred to as “Big Chino Springs” (Wirt and Hjalmarson, 2000) and here referred to throughout this report as “upper Verde River springs.” Since 2000, beavers have intermittently dammed the Verde River near upper Verde River springs, creating a series of ponds and flooding the major spring outlet.

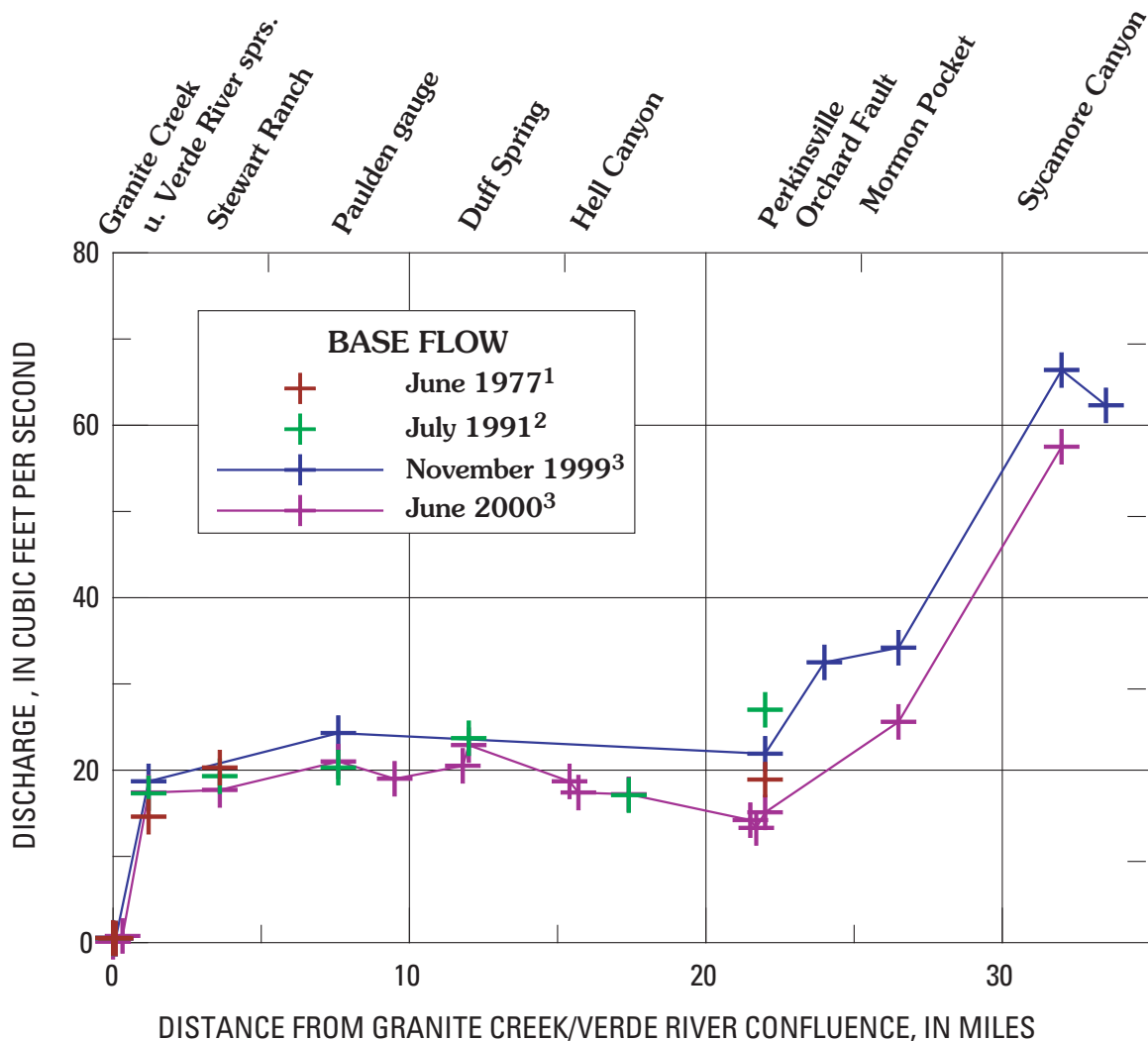
Below river mi 3.0, the upper Verde River typically is a narrow, free-flowing stream about 10- to 20-ft wide and less than 3-ft deep; with deeper and wider pools present in a few locations. At least 2 ft<sup>3</sup>/s of inflow occurs from small seeps on both banks of the Verde River near the mouth of Muldoon Canyon (river mi 8; fig. A14; located on fig. A2). An additional 2.5 ft<sup>3</sup>/s of gain below the Paulden gauge is derived from Duff Spring (river mi 14; fig. A14; located on fig. A2). Beavers have been active in some localities.

Although Hell Canyon receives as much as 25 inches of annual rainfall in its headwaters near Bill Williams Mountain, the Verde River experiences no change in base flow in the vicinity of Hell Canyon (fig. A14). This suggests that ground water does not travel beneath Hell Canyon to reach the Verde River. Three streamflow gauges on the Colorado Plateau—in upper Hell Canyon, a small tributary of Hell Canyon, and in Limestone Canyon—have small drainage areas less than 15 mi<sup>2</sup>, with mean annual basin precipitation ranging from 15.5 to 24.1 inches (table A3). These stream segments are ephemeral and usually dry, although individual flash floods have exceeded 1,000 ft<sup>3</sup>/s.

Base flow in June 2000 decreased more than 30 percent in the 10-mi reach between Duff Spring and Perkinsville (fig. A14). The loss is attributed to a variety of potential factors including evaporation from water surfaces, plant transpiration, losses to the underlying limestone, and seasonal diversions to an irrigation ditch upstream from the Perkinsville bridge.

The Verde River gains about 10 ft<sup>3</sup>/s between the State Route 72 bridge at Perkinsville (river mi 24) and the railroad bridge (river mi 27). This gain is attributed in part to groundwater inflows from small springs and in part to possible seepage inflows from local irrigation returns. The largest of these

inflows is an unnamed spring at the intersection of the Verde River and the Orchard Fault (fig. A2). Here, fault breccia and rubble zones have been observed in Redwall Limestone north of the Verde River. Farther downstream, base flow increases to 57 ft<sup>3</sup>/s downstream from a large spring at Mormon Pocket. A large tributary inflow (Sycamore Creek) occurs at Sycamore Canyon, with an annual low flow for the USGS streamflow gauging station near Clarkdale (09504000, hereto referred to as the Clarkdale gauge) of 71 ft<sup>3</sup>/s. Based on a discontinuous record (1916, 1918–20; 1966–1996), the mean monthly minimum values for the Clarkdale gauge range from 61.6 to 73.8 ft<sup>3</sup>/s (Fisk and others, 2004).



**DATA SOURCES**

<sup>1</sup>Owen-Joyce and Bell, 1983

<sup>2</sup>Ewing and others, 1994

<sup>3</sup>U.S. Geological Survey database

**Figure A14.** Graph showing changes in base flow with distance along the upper Verde River.

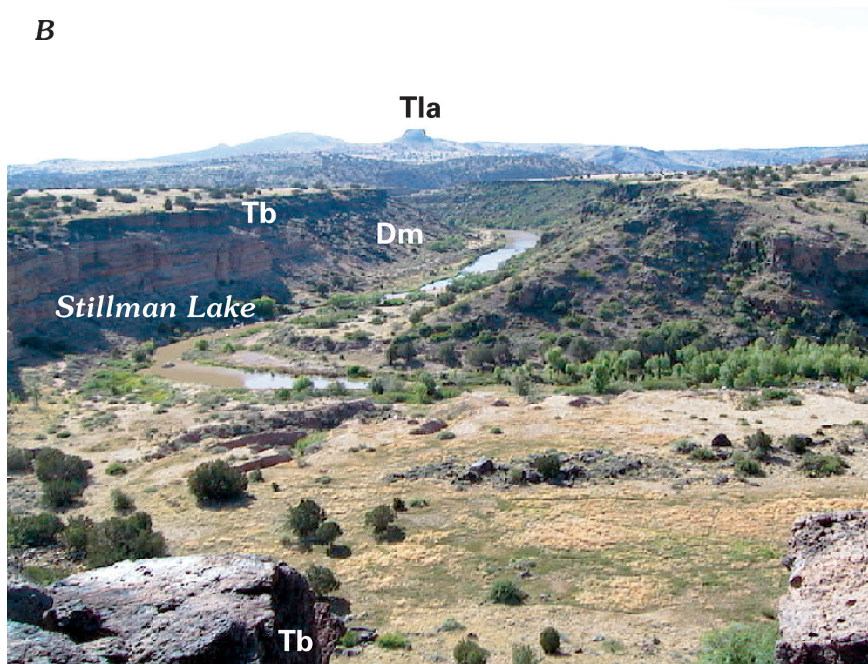


**Figure A15.** Photographs of Stillman Lake facing downstream (A) overlooking the confluence of Verde River canyon with Granite Creek, and (B) southeast from north canyon rim towards Little Thumb Butte; by R. Pope and L. Wirt, respectively. Stillman Lake is dammed by a natural levee of sediment from Granite Creek, which enters center right of upper photograph. Verde River canyon walls are predominantly Devonian Martin Formation (Dm), capped by the 4.5 Ma basalt flow (Tb). Rocks in background of lower photograph are Tertiary volcanic rocks in the Sullivan Buttes volcanic field (Tla).

## Ground-Water Conditions

Basin-fill aquifers in Big and Little Chino valleys serve as a ground-water reservoir and distribution system. Recharge and discharge are the inflow and outflow terms of the storage system. Recharge is the percentage of precipitation that becomes ground water. The amount of recharge that occurs is dependent on many factors including climate, runoff characteristics of the soil and rock, and the amount and type of vegetation. Recharge usually travels through an unsaturated zone to reach the water table, but also can occur directly beneath wetlands, lakes, or losing stream reaches. Recharge and discharge can occur at the same locality under different runoff conditions.

The term “discharge” refers to the flow in a stream as well as to the outflow from an aquifer. Discharge in a stream is naturally derived from ground-water discharge, precipitation runoff, or a combination of both. As discussed previously, the discharge in a stream during low-flow conditions is entirely from ground-water discharge and is referred to as “base flow.” In the study area, ground-water movement through the aquifer is driven by gravity to points of discharge—to springs (for example, Del Rio Springs), natural lakes and ponds (for example, Stillman Lake and King Spring), or gaining streams (for example, the upper Verde River from Granite Creek to Stewart Ranch).

Variations in predevelopment base flow are attributed solely to seasonal or long-term changes in climate. Variations in historical base-flow measurements also result from surface-water diversions or impoundments, ground-water withdrawals (pumping), and land use, as well as climatic variability. Human activities such as surface-water diversions and large-scale pumping of ground water have a direct impact on the base flow downstream. The delay of impact from pumping may be years or even decades, particularly with increasing distance from the stream. Other nonpoint-source changes in land use such as suburban development, agricultural practices, and altering the type of vegetation can result in a gradual impact on base flow that is difficult to distinguish from natural climate variability.

In Big Chino Valley, present ground-water conditions no longer reflect true predevelopment conditions. This is evident by comparing modern water-level contour maps (Schwab, 1995) with fig. A10, in which predevelopment ground-water conditions have been inferred from 1947 USGS maps and historical aerial photographs. The vertical accuracy of predevelopment water-level contours is estimated at one-half the 50-ft contour interval or to within 25 ft of land surface. For predevelopment conditions in Little Chino Valley, the reader is referred to water-level contour maps in Schwalen (1967) and modeled predevelopment conditions in Corkhill and Mason (1995). Modern water levels in Big and Little Chino valleys are discussed in greater detail in Chapter D (Wirt and DeWitt, this volume), in regard to the major aquifer boundaries and hydrogeologic framework.

## Water Use

As of 1997, water use in the Verde River headwaters was about 81 percent agricultural and 11 percent residential, with the remaining fraction of use by commerce and industries located primarily in the Prescott and Chino Valley areas (Arizona Department of Water Resources, 2000). A great deal of current municipal, residential, agricultural, industrial, and commercial water use information is available for upper Verde River watershed in general, and the Little Chino basin in particular, which has recently been summarized for 1997 conditions by Arizona Department of Water Resources (2000). Unfortunately, the water-use data are often confusing in that they are sometimes reported for the Verde watershed as a whole, or for the Middle and Upper Verde River basins combined, or for the Prescott Active Management Area (PRAMA) only (which may or may not include the upper Agua Fria watershed). Water-use data are not always easily broken out for individual subbasins. In addition, past water use has been reported by different agencies using different approaches over different timeframes. Estimates of agricultural water use vary widely in part depending on whether a consumptive use or water-duty reporting method is taken. Consumptive use generally means the amount of water consumed by the crop itself, whereas a water-duty approach is the total amount of water supplied. The water-duty factor could include water lost due to field inefficiencies such as conveyance losses, evaporation, crop leaching requirements, and so forth; in addition to the amount of water consumed by the crop. Water-use information generally is thought to be fairly accurate for Little Chino Valley, but considerably less accurate for Big Chino Valley. The greater accuracy of water-use data for the Little Chino Valley is attributed to early hydrological studies by Schwalen (1967) and Matlock and others (1973), and lately because of detailed reporting requirements for the PRAMA by ADWR (Arizona Department of Water Resources, 1998, 1999a, 1999b, 2000; Corkhill and Mason, 1995; Nelson, 2002).

### Little Chino Valley

As discussed earlier, water demand in the Prescott Active Management Area is increasing as a consequence of rapid population growth (Arizona Department of Water Resources, 2000). Water use in excess of safe yield for the combined Little Chino Valley and upper Granite Creek watersheds was estimated at about 13,000 acre-ft/yr in 1990 by Corkhill and Mason (1995). This estimate is now reported differently for the entire PRAMA instead of for just the Little Chino basin-fill aquifer and has been revised to include recharge beneath Granite Creek (Nelson, 2002). Since 1997, the PRAMA overdraft in excess of recharge has been reported variously between 6,610 and 9,830 acre-ft/year (Arizona Department of Water Resources; 1998, 1999a, 1999b, and 2000). Predictive ground-water model simulations by Nelson (2002) presume that surface-water discharge from Del Rio Springs will be

gone by 2025. The Arizona Department of Water Resources (2000) estimated Little Chino inflow to the upper Verde River in 1990 at about 2,100 acre-ft/year, compared with 4,500 acre-ft/yr during predevelopment (table A4).

Water use in Little Chino Valley in 1997 was about one-half municipal (including residential, commercial, and industrial demand) and one-half agricultural (Arizona Department of Water Resources, 2000). In general, agricultural use is diminishing as residential use is expanding. Because municipal water use generally is metered for billing purposes, the amount delivered can be determined quite accurately. Major water providers in Prescott and Little Chino Valley supplied about 6,750 acre-ft/yr in 1997 (Arizona Department of Water Resources, 2000). The largest agricultural user is the Chino Valley Irrigation District (CVID). In 1998, the city of Prescott entered into an agreement with the CVID and acquired their surface-water rights. The diversion volume to satisfy these rights averaged 3,250 acre-ft/yr from 1991–1997 (Arizona Department of Water Resources, 2000). In 1997, agricultural demand within Little Chino Valley was 6,610 acre-ft/yr for 2,170 irrigated acres (Arizona Department of Water Resources, 2000).

In order to compare different methods, ADWR tried a consumptive use approach with a weighted water duty of 6.6 acre-ft for the same 2,170 acres where the amount of water use was known accurately. Based on their consumptive use method, ADWR estimated total agricultural water use for Little Chino Valley at 14,310 acre-ft/yr (Arizona Department of Water Resources, 2000; p. 3–34 and p. 6–5)—or more than twice the 6,610 acre-ft/yr reported by more direct approaches, such as gauging of irrigation ditches or metering of wells. The large degree of error in the consumptive use estimate reflects large uncertainties in many of the assumptions the analysis is based on (Frank Corkhill, written communication, 2005). In the following section on Big Chino Valley, it is important to note that the less accurate consumptive-use approach is the only method used, which does not take into consideration the practice of deficit irrigation. Pasture is the predominant crop grown in the upper Verde River watershed and is typically deficit irrigated (Arizona Department of Water Resources, 2000, p. 3–20). Deficit irrigation applies whatever limited amount of water that is available to keep the crops alive, resulting in reduced crop yield. A deficit application rate generally is substantially lower than the recommended application rate for a given crop type.

## Big Chino Valley

Any discussion of past water use in Big Chino Valley should consider the discussion of predevelopment hydrology presented earlier in this chapter, as well as information in studies by the Arizona Crop and Livestock Reporting Service (1974), annual reports on ground-water conditions by the USGS such as Anning and Duet (1994), Wallace and Laney (1976), Schwab (1995), Ewing and others (1994), and the Arizona Department of Water Resources (2000).

To evaluate historical changes in water use, one must look at changes in land-use patterns in Williamson Valley, upper Big Chino Valley, and Walnut Creek, as well as the study or method used to produce the estimate. Ranching and irrigated agriculture in Big Chino Valley, Walnut Creek, and Williamson Valley started with settlement in the 1860s and probably peaked in the 1950s and 1960s. Accounts prior to 1967 vary considerably, and few direct measurements are available. From the mid 1970s through the mid 1990s, ground-water pumping for irrigated agriculture decreased to less than a tenth of that reported for 1975 (Anning and Duet, 1994). Since 1998, land actively cultivated in upper Big Chino Valley has reportedly increased by 1,350 acres (Arizona Department of Water Resources, 2000; p. 3–31).

Water use throughout Big Chino Valley is more than 90 percent agricultural. Although the amount of water used by private wells in lower Big Chino Valley is growing rapidly, the amount of residential use after subtracting for septic tank recharge was estimated at about 348 acre-ft/yr in 1997 (Arizona Department of Water Resources, 2000). Arizona Department of Water Resources reports that Abra Water Company, the largest municipal supplier, delivered 56 acre-ft/yr to its customers in 1997. Water demand for town of Ash Fork in the northern part of the watershed, although thought to be part of the Colorado Plateau aquifer system, was 81 acre-ft/yr. The sum of this municipal and residential water use is still far less than 10 percent of total water use for the basin.

Williamson Valley was settled in 1865, and irrigated acreage and cropping patterns have not changed substantially since reporting began in the 1960s. About 1,300 acres are actively irrigated, with more than 90 percent in pasture (Arizona Department of Water Resources, 2000). Water-duty estimates of the amount of water pumpage, however, vary widely depending on the report. Active irrigation was reported as 2,000 acre-ft/yr between 1950 and 1974 (Wallace and Laney, 1976). Although land-use patterns did not change substantially, Ewing and others (1994) recalculated water use as about 3,000 acre-ft/yr in 1990. Using a weighted duty factor, Arizona Department of Water Resources (2000) estimated 1997 agricultural water use in Williamson Valley at 5,204 acre-ft/yr. During this timeframe, water levels in Williamson Valley appear to have dropped slightly. Water levels in a few wells were a few feet lower in 1992 (Schwab, 1995) than when water levels were measured in those wells in 1975 (Wallace and Laney, 1976). The amount of residential water use is unknown, but the number of new homes has increased substantially since the 1980s.

Seventy percent of ground-water pumping prior to 1967 was in northern or “upper” Big Chino Valley, according to Bob Wallace (USGS hydrologist, oral commun. in 1989; in Water Resource Associates, 1990, p. 6). Reports of water use in upper Big Chino Valley generally are combined with water use in Walnut Creek. Water diversions for ranching operations started in Walnut Creek around 1869 and peaked in the late 1950s and early 1960s (Arizona Department of Water Resources, 2000). Estimates of ground-water pumping for Big Chino Valley of

20,000 acre-ft/yr prior to 1967 (Wallace and Laney, 1976; Schwab, 1995) are unsubstantiated and are considered here as inaccurate. The USGS, in cooperation with A. Allen, County Agricultural Agent, field checked the land under active irrigation in 1967. As a result of these inspections, ground-water pumpage for upper Big Chino Valley was downwardly revised from 20,000 to 9,000 acre-ft/yr, beginning in 1967 (H.W. Hjalmarson, written commun., 2004; based on his USGS field notes dated June 8, 1967). There is little indication that water use for Big Chino Valley ever exceeded 15,000 acre-ft/yr prior to 1967 (H.W. Hjalmarson, written commun., 2004). Estimates of early ground-water pumping in Big Chino Valley vary considerably in other studies, which may reflect different consumptive use factors or that the amount of land actively under cultivation kept changing. A study by the Bureau of Reclamation (Ewing and others, 1994) states that water use was 5,200 acre-ft/yr in 1960. An earlier appraisal report by the Bureau of Reclamation (1974) lists the amount of agricultural water use in Big Chino Valley at the time of that study at 994 acre-ft. Anning and Duet (1994) report 11,000 acre-ft for 1974. The large differences among these estimates suggests either that reporting practices or the amount of irrigated land may have changed greatly from year to year.

Annual pumping estimates reported by the USGS from 1967 to 1990 (Anning and Duet, 1994) were estimated by multiplying the irrigated acreage by an annual water duty of 5 acre ft. Ground-water pumping in upper Big Chino Valley decreased from about 12,000 acre-ft/yr in 1975 to 2,000 acre-ft/yr in 1982-83 (Wallace and Laney, 1978; Anning and Duet, 1994). Water use remained low through the 1980s and early 1990s. Recently, active irrigation in upper Big Chino Valley and Walnut Creek has reportedly more than doubled—from about 1,130 acres in the mid 1990s to a total of 2,480 acres in 1998 (Arizona Department of Water Resources, 2000; p. 3–31). Using their weighted-water duty approach, Arizona Department of Water Resources estimated agricultural water use for both Big Chino Valley and Walnut Creek in 1998 at 9,924 acre-ft/yr. This estimate is about 5 times greater than the 1990 estimate of 2,000 acre-ft/yr by Ewing and others (1994), and is 2.5 times greater than the 4,000 acre-ft/year reported by Anning and Duet (1994). Again, the large differences among the Big Chino agricultural estimates for the 1990s brings into question the accuracy of the various water-use data.

In summary, the amount of agricultural water use in Big Chino Valley has varied greatly. The amount of agricultural demand steadily decreased from its peak in 1975 through the early 1990s (Anning and Duet, 1994). Since about 1998 demand has probably increased, but by an unknown factor. ADWR's water-duty estimates based largely on historical aerial photography have been more than twice as high as those obtained by more direct accounting methods in Little Chino Valley. Large discrepancies among various studies are attributed to differences in consumptive use factors, soil types, farming practices, delivery methods, and system efficiencies, as well as differences in estimating the amount of land under

cultivation. More accurate and direct methods such as metering to calculate agricultural water use in this basin are sorely needed.

## Upper Verde River

The total amount of water use in the carbonate aquifer north of the upper Verde River is unknown, but is minor relative to water use in Big and Little Chino valleys. Between Paulden and Clarkdale, several wells in the carbonate aquifer north and south of the Verde River are used for ranching and domestic use. Return flows from irrigated pasture at Perkinsville may account for part of the observed inflows to the Verde River in this reach. Total water use probably is less than a few hundred acre-ft/yr.

## Conceptual Water Budget

Developing a conceptual water budget for the upper Verde River watershed involves balancing ground-water inflows and outflows. Inflows include recharge from infiltrating precipitation and runoff, ground-water underflow from adjacent basins (if any), and stream inflow into the basin that is lost to the aquifer (not applicable in this case study). Outflows include evapotranspiration, stream base flow out of the basin, and ground-water underflow out of the basin (if any). Of these inflows and outflows, only base flow can be measured directly and accurately. Ground-water recharge generally is calculated as the sum of inflows and outflows to the aquifer system, which includes base flow from streams entering and exiting the aquifer, evapotranspiration, and ground-water underflow out of the basin of interest. Calculating the relative ground-water contribution from each subbasin involves a substantial amount of uncertainty.

Several studies have used various approaches and statistical methods to develop estimates of recharge for the Verde River headwaters and its major subbasins. The hydrologic data compiled in table A4 are publically available and come from reputable sources recognized for their scientific expertise, including the USGS, Bureau of Reclamation, and University of Arizona. For the Verde River headwaters, Freethey and Anderson (1986) presumed that underflow past the Paulden gauge was relatively insignificant, accounting for less than 3 percent (500 acre-ft/yr) of outflow from Big Chino Valley. Evapotranspiration was estimated at 7,000 acre-ft/year for Big Chino Valley, and 2,000 acre-ft/yr for Little Chino Valley (Freethey and Anderson, 1986). Because few predevelopment data are available for Big Chino Valley, the recharge estimates by Freethey and Anderson (1986) and Ewing and others (1994) are largely based on historical base flow at the Paulden gauge, which began operation in 1963. Base flow at the Paulden gauge is estimated at about 17,000 acre-ft/yr (table A4). Water-budget components such as base flow that are reliably known were considered fixed in order to estimate the remaining components (Freethey and Anderson, 1986). Differences



among estimates from different studies are largely attributed to slightly different statistical approaches (for example, using the mean versus the median), or to different periods of record. For a more detailed understanding of these approaches, the reader is referred to the original data sources. These estimates are compiled here to develop a conceptual understanding of the primary inflow and outflow components in the hydrologic system rather than a detailed budget analysis.

Base flow in the upper Verde River is supplied by Big and Little Chino valleys and the carbonate aquifer in the vicinity of Big Black Mesa. During predevelopment conditions, ground-water inflow to the upper Verde River from Little Chino Valley was about 4,500 acre-ft/yr (table A4), but was about 2,100 acre-ft/yr during the 1990s (Arizona Department of Water Resources, 2000). Ford (2002) estimated Big Black Mesa recharge at 1,250 acre-ft/yr based the land area of the mesa exceeding 5,000 ft above sea level and a rate of precipitation between 16 and 18 inches. Because some recharge on the north side of the Big Black Mesa may be tributary to the Colorado Plateau, this estimate is considered a maximum value. Most recharge for Big Black Mesa area probably discharges

directly to ground water in Big Chino Valley, or to the carbonate aquifer north of the Verde River, and is estimated to provide about 5 percent of base flow at the Paulden gauge (Ford, 2002). Mean annual discharge from Williamson Valley Wash and Walnut Creek can account for two-thirds to three-fourths of base flow at the Paulden gauge. The remainder is attributed to discharge from Little Chino Valley, Big Black Mesa, and other Big Chino Valley nonperennial tributaries such as Pine Creek and Partridge Creek, as well as recharge in upland areas or recharge from storm runoff beneath ephemeral streams (Ewing and others, 1994).

By assuming that predevelopment recharge is proportionate to modern base flow, Big Chino Valley contributes 78.9 percent, or about 13,400 of the 17,000 acre-ft/yr of mean annual discharge at the Paulden gauge (fig. A16). If we include Big Black Mesa as part of Big Chino Valley, these combined areas contribute about 14,200 acre-ft/yr of base flow. Using the predevelopment value of 4,500 acre-ft/yr, Little Chino Valley originally contributed about 16.5 percent of recharge to the upper Verde River but presently is thought to deliver about half its predevelopment value, or 8.4 percent,

### SOURCES OF RECHARGE TO THE UPPER VERDE RIVER

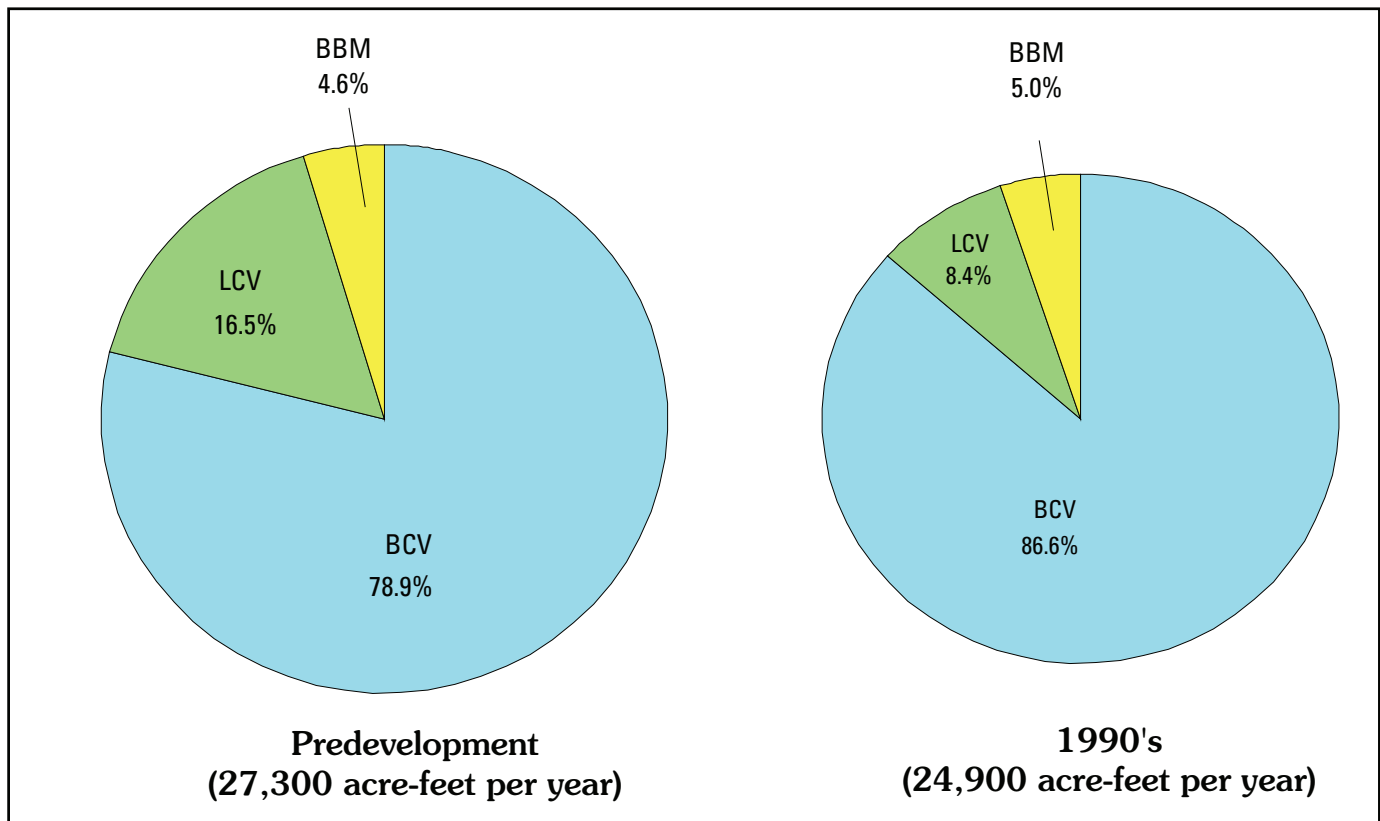


**Figure A16.** Conceptual water budget for upper Verde River based on previously published estimates of recharge, as given in table A4. (LCV = Little Chino Valley, BCV = Big Chino Valley, BBM = Big Black Mesa). Note that pie diagram on the right is proportionately smaller (91 percent) than the one on the left.

with Big Chino Valley and Big Black Mesa combined contributing the remaining 92 percent of base flow at the Paulden gauge. This overly simplistic water budget is compiled from several studies using various approaches—therefore, no precision or accuracy can be assigned to these percentages. Moreover, current water consumption in Big Chino Valley is unknown and therefore neglected. Nevertheless, this water-budget exercise provides a rough conceptual framework that summarizes much of the earlier work that has been done and provides a basis for comparison with new information presented in the following chapters in this report.

## References Cited

- Allen, Stephenson & Associates, 2001, Hydrogeology study of The Ranch at Del Rio Springs: prepared for The Bond Ranch at Del Rio Springs, LLC; available from Allen, Stephenson & Associates, Phoenix, Arizona, 88 p. plus appendices.
- Alley, W.M., Reilly, T.E., and Franke, O.L., 1999, Sustainability of ground-water resources: U.S. Geological Survey Circular 1186, 79 p.
- Anning, D.W., and Duet, N. R., 1994, Summary of ground-water conditions in Arizona 1987–90: U.S. Geological Survey Open-File Report 94–476, 1 map.
- Arizona Crop and Livestock Reporting Service, 1974, Crop-land atlas of Arizona: Phoenix, Arizona Crop and Livestock Reporting Service report, 68 p.
- Arizona Department of Commerce, 1993–1997, County profiles: Coconino, Gila, and Yavapai Counties, Arizona.
- Arizona Department of Economic Security, 1990, Housing unit data for Arizona, counties, places, and Indian reservations: April 1, 1990, Census.
- Arizona Department of Water Resources, 1998, Preliminary report on the Safe-Yield Status of the Prescott Active Management Area: 44 p. plus appendices.
- Arizona Department of Water Resources, 1999a, Report on the final decision and order that the Prescott Active Management area is no longer at safe-yield: January 12, 1999, 31 p.
- Arizona Department of Water Resources, 1999b, Third management plan for Prescott Active Management Area 2000–2010: [http://www.water.az.gov/adwr/Content/Publications/files/ThirdMgmtPlan/tmp\\_final/prescott/pre-toc.pdf](http://www.water.az.gov/adwr/Content/Publications/files/ThirdMgmtPlan/tmp_final/prescott/pre-toc.pdf)
- Arizona Department of Water Resources, 2000, Verde River Watershed Study: Arizona Department of Water Resources report, 208 p. plus appendices.
- Arizona Department of Water Resources, 2002, Arizona Registry of Wells 55 CD-ROM, updated March 2002.
- Arizona Game and Fish, accessed on May 19, 2004, [http://www.gf.state.az.us/outdoor\\_recreation/wildlife\\_area\\_upper.shtml](http://www.gf.state.az.us/outdoor_recreation/wildlife_area_upper.shtml)
- Arizona State Legislature, 1991, Groundwater Transportation Act: Article 8.1, Withdrawals of groundwater for transportation to Active Management area; Section 45-555; Transportation of groundwater withdrawn in Big Chino subbasin of the Verde River groundwater basin to initial active management area; exception; definitions.
- Baker, T.L., Rae, S.R., Minor, J.E., and Connor, S.V., 1973, Water for the Southwest—historical survey and guide to historic sites: American Society of Civil Engineers, Historical Publication no. 3, 205 p.
- Bates, R.L., and Jackson, J.A., ed., 1980, Glossary of Geology: American Geological Institute, Falls Church, Virginia, p. 286.
- Betancourt, J.L., 2003, The current drought (1999–2003) in historical perspective: 2003 Southwest Drought Summit report, May 12–13, 2003, Northern Arizona University, Flagstaff, Arizona, [http://www.mpcer.nau.edu/megadrought/drought\\_summit\\_report/](http://www.mpcer.nau.edu/megadrought/drought_summit_report/)
- Bureau of Reclamation, 1946, Chino Valley project, Arizona: U.S. Department of Interior, Project Planning Report No. 3-8b.9-0, April 1946, Appendix C.
- Bureau of Reclamation, 1974, Chino Valley Unit Appraisal Report, U.S. Department of Interior, April 1974, table 9, p. 79.
- Clark, R.J., 2002, Comments prepared in support of the proposed rule listing the Gila Chub as endangered with critical habitat: Department of the Interior, Fish and Wildlife Service, 50 CFR Part 17, Proposed Rules, Federal Register, v. 67, no. 154, August 9, 2002.
- Corkhill, E.F. and Mason, D.A., 1995, Hydrogeology and simulation of ground-water flow: Prescott Active Management Area, Yavapai County, Arizona: Arizona Department of Water Resources Modeling Report No. 9, 143 p.
- Ewing, D.B., Osterberg, J.C., Talbot, R.W., 1994, Ground-water Study of the Big Chino Valley—Hydrology and hydrogeology: Bureau of Reclamation Technical Report, Denver, Colorado, Sections I through III, including 6 appendices.
- Fisk, G.G., Duet, N.R., Evans, D.W., Angerth, C.E., Castillo, N.K., and Longworth, S.A., 2004, Arizona Water Resources Data—Water Year 2003: U.S. Geological Survey Water-Data Report AZ-03-1, 328 p.
- Ford, J.R. 2002, Big Chino Valley ground water as the source of the Verde River *in* Ground Water/Surface Water Interactions, July 1–3, 2002, American Water Resources Association summer specialty conference, 6 p.

- Freethy, G.W., and Anderson, T.W., 1986, Predevelopment hydrologic conditions in the alluvial basins of Arizona and adjacent parts of California and New Mexico: U.S. Geological Survey Hydrologic Investigations Atlas HA-664.
- Gilbert, C.H., and Scofield, N.B., 1898, Notes on a collection of fishes from the Colorado Basin in Arizona. Proceedings U.S. National Museum, v. 20, p. 287-499 (plates XXXVI-XXXIX).
- Girmendonk, A.L., and Young, K.L., 1997, Status review of Roundtail Chub, *Gila robusta*, in the Verde River Basin: Arizona Game and Fish Department, Technical Report 114, 68 p.
- Granger, B.H., 1985, Arizona Place Names: University of Arizona Press, Tucson, p. 338.
- Henson, Pauline, 1965, Founding a wilderness capital, Northland Press, Flagstaff, 261 p.
- Krieger, M.H., 1965, Geology of the Prescott and Paulden quadrangles, Arizona. U.S. Geological Survey Professional Paper 467, 127 p.
- Lehner, R.E., 1958, Geology of the Clarkdale quadrangle, Arizona: U.S. Geological Survey Bulletin 1021-N, p. 511-592 with plates.
- Levings, G.W., and Mann, L.J., 1980, Maps showing ground-water conditions in the upper Verde River area, Yavapai and Coconino Counties, Arizona-1978: U.S. Geological Survey Water-Resources Investigations, Open-File Report 80-726, maps.
- Matlock, W.G., Davis, P.R., and Roth, R.L., 1973, Groundwater in Little Chino Valley, Arizona: University of Arizona Agricultural Experiment Station, Technical Bulletin 201, 19 p.
- McCormack, H.F., Fisk, G.G., Duet, N.R., Evans, D.W., Roberts, W.P., and Castillo, N.K., 2003, Arizona Water Resources Data—Water Year 2002: U.S. Geological Survey Water-Data Report AZ-02-1, 337 p.
- Metzger, D.G., 1961, Geology in relation to availability of water along the South Rim, Grand Canyon National Park, Arizona: *in* Hydrology of the Public Domain, U.S. Geological Survey Water-Supply Paper 1475-C, p. 105-135, with plates.
- Munderloh, Terry, 2000, Del Rio's quick brush with the seat of government: The Daily Courier, Days Past, October 19, 2000, Prescott, Arizona.
- Munderloh, Terry, 2001, Del Rio Springs after Fort Whipple moved on: The Daily Courier, Days Past, February 20, 2000, Prescott, Arizona.
- Nelson, Keith, 2002, Application of the Prescott Active Management Area—Ground-water flow model planning scenario 1999-2025: Arizona Department of Water Resources Modeling Report No. 12, 49 p.
- Ostenaar, D.A., Schimschal, U.S., King, C.E., Wright, J.W., Furgerson, R.B., Harrel, H.C., and Throner, R.H., 1993, Big Chino Valley Groundwater Study—Geologic Framework Investigations Seismotectonic Report 93-2, Bureau of Reclamation, Denver Office, 31 p.
- Owen-Joyce, S.J., and Bell, C.K., 1983, Appraisal of water resources in the Upper Verde River area, Yavapai and Coconino Counties, Arizona: Arizona Department of Water Resources Bulletin 2, 219 p.
- Parkhurst, D.L., and Appelo, C.A.J., 1999, User's guide to PHREEQC (Version 2)—A computer program for speciation, batch-reaction, one-dimensional transport, and inverse geochemical calculations. U.S. Geological Survey Water-Resource Investigations Report 99-4259, 312 p.
- Pope, G.L., Rigas, P.D., and Smith, C.F., 1998, Statistical summaries of streamflow data and characteristics of drainage basins for selected streamflow-gauging stations in Arizona through Water Year 1996: U.S. Geological Survey, Water-Resources Investigations Report 98-4225, 907 p.
- Remick, W.H., 1983, Maps showing ground-water conditions in the Prescott Active Management Area, Yavapai County, Arizona—1982. Arizona Department of Water Resources Hydrologic Map Series, Phoenix, Report Number 9.
- Schwab, K.J., 1995, Maps showing ground-water conditions in the Big Chino sub-valley of the Verde River Valley, Coconino and Yavapai Counties, Arizona—1992: Department of Water Resources, Hydrologic Map Series Report Number 28, Phoenix, Arizona, 1 sheet.
- Shaw, H.G., 1998, Wood Plenty, Grass Good, Water None: The Juniper Institute, unpublished draft manuscript, 150 p.
- Schwalen, H.C., 1967, Little Chino Valley artesian area and ground-water basin: Technical Bulletin 178, Agricultural Experiment Station, University of Arizona, Tucson, Arizona, 63 p.
- Southwest Ground-Water Consultants, 2004, C.V./C.F. Ranch Acquisition hydrology report: prepared for the City of Prescott, June, 2004, 6 chapters plus Appendix.
- Twenter, F.R., and Metzger, D.G., 1963, Geology and ground water in Verde Valley—the Mogollon Rim region Arizona: U.S. Geological Survey Bulletin 1177, 132 p.
- U.S. Fish and Wildlife Service, 2000, Endangered and threatened wildlife and plants; final designation of critical habitat for the Spikedace and Loach Minnow: Federal Register 65(80): p. 24328-24372.
- U.S. Geological Survey, 1997 to 2004, Arizona Water Resources Data: U.S. Geological Survey Water-Data Reports AZ-97-1 through AZ-03-1.
- Wallace, B. L. and Laney, R. L., 1976, Maps showing ground-water conditions in the lower Big Chino Valley and

- Williamson Valley areas, Yavapai and Coconino Counties, Arizona—1975–76: U.S. Geological Survey Open-File Report Water Resources Investigations 76–78, 2 maps.
- Weedman, D.A., Girmendonk, A.L., and Young, K.L., 1996, Status review of Gila Chub, *Gila intermedia*, in the United States and Mexico: Arizona Game and Fish Department, Technical Report 91, 100 p.
- Western Regional Climate Center, <http://www.wrcc.dri.edu/narratives/ARIZONA.htm>, accessed on 6/18/2004.
- Winn, H.E., and Miller, R.R., 1954, Native post-larval fishes of the lower Colorado River Basin, with a key to their identification: California Fish and Game, v. 40, p. 273–285.
- Wirt, Laurie, and Hjalmarson, H.W., 2000, Sources of springs supplying base flow to the Verde River headwaters, Yavapai County, Arizona: U.S. Geological Survey Open-File Report 99–0378, 50 p.



# Geologic Framework

By Ed DeWitt, Victoria E. Langenheim, and Laurie Wirt

Chapter B

## **Geologic Framework of Aquifer Units and Ground-Water Flowpaths, Verde River Headwaters, North-central Arizona**

Edited by Laurie Wirt, Ed DeWitt, and Victoria E. Langenheim

Prepared in cooperation with the Arizona Water Protection Fund Commission

Open-File Report 2004–1411-B

**U.S. Department of the Interior**  
**U.S. Geological Survey**

**U.S. Department of the Interior**

Gale A. Norton, Secretary

**U.S. Geological Survey**

P. Patrick Leahy, Acting Director

U.S. Geological Survey, Reston, Virginia: 2005

For product and ordering information:

World Wide Web: <http://www.usgs.gov/pubprod>

Telephone: 1-888-ASK-USGS

For more information on the USGS--the Federal source for science about the Earth, its natural and living resources, natural hazards, and the environment:

World Wide Web: <http://www.usgs.gov>

Telephone: 1-888-ASK-USGS

Any use of trade, product, or firm names is for descriptive purposes only and does not imply endorsement by the U.S. Government.

Although this report is in the public domain, permission must be secured from the individual copyright owners to reproduce any copyrighted materials contained within this report.

This report has not been reviewed for stratigraphic nomenclature.

***Suggested citation:***

DeWitt, E., Langenheim, V. E., and Wirt, L., 2005, Geologic framework: *in* Wirt, Laurie, DeWitt, Ed, and Langenheim, V.E., eds., Geologic Framework of Aquifer Units and Ground-Water Flowpaths, Verde River Headwaters, North-Central Arizona: U.S. Geological Survey Open-File Report 2004-1411-B, 28 p.

# Contents

Abstract.....	1
Introduction.....	1
Acknowledgments.....	1
Rock Units .....	2
Proterozoic Rocks.....	2
Paleozoic rocks.....	3
Tertiary rocks.....	7
Lati-andesite.....	7
Hickey Formation and Older Basalt and Sedimentary Rocks.....	9
Younger Basalt and Sedimentary Rocks.....	12
Tertiary and Quaternary sediment in Big and Little Chino Valleys .....	15
Structural Features.....	19
Quaternary to Late Tertiary Faults.....	21
Conclusions.....	26
References Cited.....	26

# Figures

<b>B1.</b> Location map of north-central Arizona showing location of study area and location of figures B2 and B3. ....	2
<b>B2.</b> Geologic map of the northern part of Little Chino Valley .....	5
<b>B3.</b> Geologic map of the southeastern part of Big Chino Valley.....	6
<b>B4.</b> Major-element classification diagrams for 21-27-Ma volcanic rocks in the Sullivan Buttes volcanic field (units Tlal, Tlau, and Tla) near Chino Valley.....	8
<b>B5.</b> Maps showing location of buried lati-andesite centers .....	10
<b>B6.</b> Major-element classification diagrams for 10-15 Ma volcanic rocks of the Hickey Formation (units Thb, and Tha) and 8-10 Ma volcanic rocks (unit Tbo) near Prescott and Chino Valley .....	13
<b>B7.</b> Map showing extent of 10-15-Ma flows in the Hickey Formation, Little Chino Valley.....	14
<b>B8.</b> Maps showing thickness of 4-6-Ma basalt flows in southeastern Big Chino Valley .....	17
<b>B9.</b> Major-element classification diagrams for 4-6-Ma volcanic rocks (unit Tby) near Paulden .....	18
<b>B10.</b> Lithologic logs showing mineralogy of playa deposits and other basin-fill units, Big Chino Valley.....	20
<b>B11.</b> Map showing thickness of Quaternary and Tertiary basin fill above 4-6-Ma basalt flows in southeastern Big Chino Valley.....	23
<b>B12.</b> Maps showing thickness of Quaternary and Tertiary basin fill above youngest Tertiary volcanic units in northern Little Chino Valley.....	25

# Geologic Framework

By Ed DeWitt, Victoria E. Langenheim, and Laurie Wirt

## Abstract

The basins underlying by Big and Little Chino Valleys developed in late Tertiary time (10 Ma to the present) by crustal extension in central Arizona and in the Basin-and-Range province to the south. Big Chino Valley, which is the larger of the two basins, is a northwest-trending, 45-km-long graben bordered by the Quaternary Big Chino Fault on the northeast side of the valley. Big Chino Valley contains at least 700 m of Quaternary and late Tertiary sediment near the deepest part of the basin. Fine-grained carbonate sediment, containing analcime and bloedite(?), indicates that the central part of the basin was a playa. Alluvial fans contributed sediment to the margin of the playa from the south and west. Basalt flows entered the valley from the north, west, and southeast from 6.0 to 4.5 Ma.

The basin underlying Little Chino Valley is smaller and contains a thinner sequence of Quaternary and late Tertiary sediment. The deepest part of the basin trends northwest and is 18 km long. Maximum sediment thickness is about 200 m. Alluvial fans contributed sediment from the west, south, and southeast. The valley lacks any proven playa deposits. No young (4-6 Ma) basalt flows are known in the valley. Beneath the Quaternary and late Tertiary sediments are abundant flows, domes, and intrusive centers of 24-Ma latite-andesite, and some extensive basalt flows of the 10-15-Ma Hickey Formation. These volcanic rocks formed an irregular topographic surface on which the Quaternary and late Tertiary sediment was deposited. Consequently, isopachs of sediment thickness in Little Chino Valley are complex and mirror the underlying relief on the Tertiary volcanic rocks.

## Introduction

Tertiary basins in north-central Arizona formed as the Basin-and-Range province was extended to the southwest, away from the Colorado Plateau. Within the Transition Zone, Big and Little Chino Valleys are the northernmost of such valleys that were formed from 10 Ma to the present (fig. B1). Although not as extensive nor as deep as Basin-and-Range basins, the basins underlying Big and Little Chino Valleys share common characteristics, such as fault-bounded margins, incorporation of volcanic material in the basin fill,

and facies variations within the sediment fill. Knowledge of the geologic material in the basin, deposited over space and time, is necessary for an understanding of the evolution of the basin.

Studies of the geology of Big Chino Valley include regional reconnaissance mapping (Krieger, 1965; 1967a; 1967b; 1967c), investigations of water resources in the western and southeastern part of the valley (Water Resource Associates, 1989), and an integrated study of water resources (Ostenaar and others, 1993a, 1993b; Ewing and others, 1994). Geologic mapping since the 1970's has been limited to the far western end of the valley (Goff and others, 1983) and the far southeastern end (Tyner, 1984 and Ward, 1993), where Tertiary volcanic rocks were studied. The geology of Little Chino Valley has been studied in less detail than Big Chino Valley. Mapping includes detailed work in the far northern and southern ends of the valley (Krieger, 1965) and reconnaissance investigations in Little Chino and Lonesome Valleys (Schwalen, 1967).

Detailed knowledge of the geology of the mountains and basins is necessary in order to determine aquifer boundaries, hydraulic characteristics, and the ground-water flow paths, which are discussed in Chapter D (this volume). This investigation builds on previous ones and includes new mapping in parts of the two valleys, chemical analysis and X-ray diffraction studies of Tertiary sedimentary and volcanic units, compilation and synthesis of well logs in both valleys, and construction of preliminary longitudinal and cross sections in parts of the valleys. Mapping was compiled at 1:100,000 scale and is part of a regional map of the Prescott National Forest-Verde headwaters region (DeWitt and others, in press).

## Acknowledgments

John Hoffmann, D.A. Lindsey, Keith Nelson, Frank Corkhill, Pat O'Hara, Dean Ostenaar, and William Wellendorf, provided constructive criticism of the manuscript. Dean Ostenaar provided drill cuttings of the three Bureau of Reclamation wells in Big Chino Valley. William Wellendorf provided drill cuttings of wells from northern Little Chino Valley. Discussions with Pat O'Hara, Steve Reynolds, Dean Ostenaar, and William Wellendorf improved the first author's understanding of the Tertiary volcanic rock units and geometry of basins in the Chino Valley area.



## Rock Units

Early and Middle Proterozoic plutonic and metamorphic rocks constitute the basement to the mountains and valleys in the region. Exposures of the basement are limited in the study area, but are abundant in the Bradshaw Mountains to the south and the Black Hills to the southeast (fig. B1). Paleozoic sedimentary rocks overlie the basement and are exposed throughout the area except where removed by erosion during Tertiary time. Rocks include sandstone, limestone, dolomite, and minor shale. Tertiary volcanic rocks are locally abundant both in mountain ranges and within the basins. Tertiary to Quaternary sediments and rocks are abundant in both basins and include conglomerate, other alluvial deposits, and playa deposits, all of which interfinger in complex patterns.

## Proterozoic Rocks

Proterozoic rocks are well exposed west of the town of Chino Valley and along Granite Creek, northeast of Chino Valley (fig. B2). Other exposures of these units throughout the area are smaller and discontinuous, including some near the confluence of Granite Creek and the Verde River (fig. B2),

near Table Mountain southwest of Chino Valley, (fig. B2), and west of Sullivan Buttes (fig. B3). Metabasalt (unit Xb) that includes minor metaandesite and iron-formation forms a prominent outcrop west of Chino Valley and a much smaller outcrop east of Del Rio Springs. Metatuff and associated volcaniclastic rocks (unit Xt) are exposed southeast of Lower Granite Spring in a faulted sliver of bedrock. Metamorphosed pelitic sediments and wacke (unit Xp) crops out west of the metabasalt (fig. B2) and underlies much of the Sullivan Buttes (DeWitt and others, in press). Similar metapelitic rocks are present in cuttings from wells north of Paulden (logs by E.D. McKee of well in B(18-2)20 CA, as supplied by Tom McGarvin, written commun., 2000).

These three rock units have been regionally metamorphosed to greenschist facies and deformed, and possess a northeast-striking foliation that dips steeply. Zones of high strain are locally apparent in the metamorphic rocks. Rocks of similar composition, metamorphic grade, and fabric development are exposed in the Bradshaw Mountains, south of Prescott (Krieger, 1965; Anderson and Blacet, 1972a; DeWitt and others, in press) and in the Black Hills, west of Jerome (Anderson and Creasey, 1958; 1967). Although an isotopic age for these rock units has not been determined in the study area, similar metabasalt and metatuff to the south in the Bradshaw

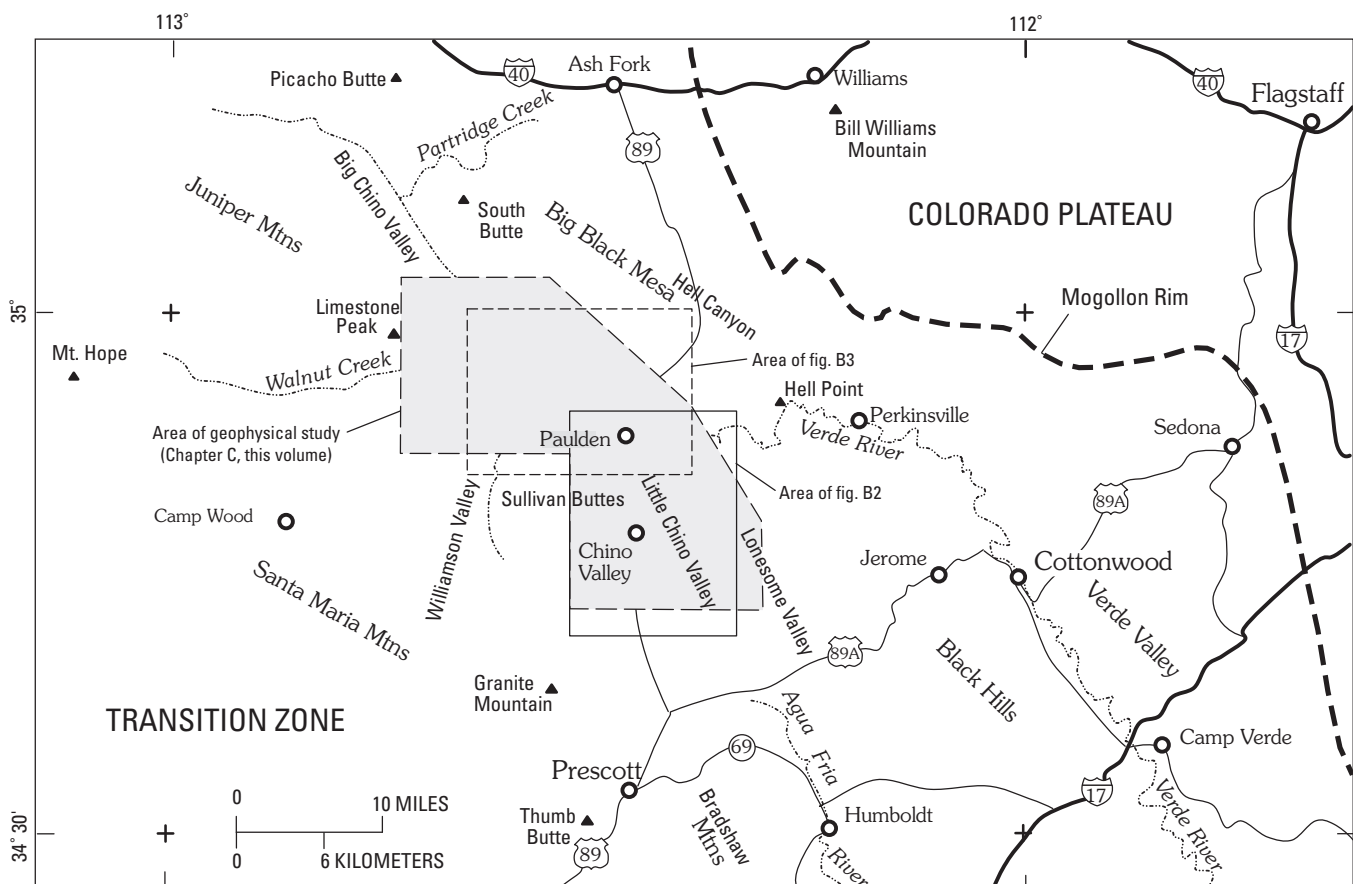


**Figure B1.** Location map of north-central Arizona showing location of study area and location of figures B2 and B3.

Mountains are as old as 1.76 Ga and metapelitic rocks are about 1.76-1.74 Ga (DeWitt and others, in press). Regional magnetic patterns (Langenheim and others, 2000; Langenheim and others, Chapter C, this volume) reveal that the foliation and rock units strike north in the eastern part of the study area (fig. B2) and northeast in the western part (fig. B3). Therefore, much of Little Chino Valley is probably underlain by metabasalt and metatuff. Much of the far southeastern end of Big Chino Valley is probably underlain by metapelitic rocks.

Four Proterozoic plutonic units intrude the metavolcanic and metasedimentary rocks, but none forms large outcrops. Gabbro (unit Xgb) is recognized east of Table Mountain (fig. B2). Coarse-grained gabbro, cumulate-texture gabbro, and ultramafic rocks are present as inclusions in Tertiary latite-andesite throughout the eastern Sullivan Buttes (Arculus and Smith, 1979; Tyner, 1984; Ward, 1993). Gravity data (Langenheim and others, 2000; Langenheim and others, this volume) suggest that abundant gabbro and associated ultramafic rocks may underlie the western side of Little Chino Valley. The long-wavelength nature of the gravity anomaly suggests that the gabbro is deeply buried. The gabbro is similar in composition to abundant gabbro in the central Bradshaw Mountains (Anderson and Blacet, 1972a; 1972b), and probably is 1.74-1.76 Ga (DeWitt and others, in press).

The Williamson Valley Granodiorite (unit Xwv; DeWitt and others, in press) intrudes metabasalt and metapelitic rocks west of Chino Valley (fig. B2) and is medium grained, equigranular, undeformed in most outcrops, and contains distinctive yellow-stained quartz grains (DeWitt, 1989). A mixture of aplite and pegmatite dikes and irregularly shaped bodies (unit Xap) intrudes metapelitic rocks west of Sullivan Buttes (fig. B3). The aplite-pegmatite is medium to coarse grained and highly variable, texturally. Pegmatite bodies in drill cuttings from a well north of Paulden probably are from this unit (logs by E.D. McKee of well in B(18-2)20 CA, as supplied by Tom McGarvin, written commun., 2000).

Small bodies mapped as Prescott Granodiorite (Krieger, 1965) east of Table Mountain and east of Granite Creek (fig. B2) contain variably foliated biotite granodiorite (unit Xpr). The Prescott Granodiorite is about 1.68 Ga (DeWitt and others, in press). Magnetic and gravity data (Langenheim and others, 2000; Langenheim and others, this volume) suggest that much of southern Little Chino Valley may be underlain by Prescott Granodiorite. Some well logs from the area of Sullivan Lake area (fig. B2) report "granite" at depth, but it cannot be proven if this "granite" is equivalent to the Prescott Granodiorite, Williamson Valley Granodiorite, or other known plutonic units in the Prescott-Jerome area.

The Mazatzal Group (unit Xq) unconformably overlies metabasalt and metatuff along lower Granite Creek (fig. B2), at the northern end of Little Chino Valley (Krieger, 1965; Bradshaw, 1974). Abundant quartzite and lesser conglomerate and argillite are deformed about northeast-striking axial planes into open anticlines and synclines. The Mazatzal Group east of Del Rio Springs could be slightly younger (Chamberlain and others, 1991) than the type Mazatzal Group in central Arizona

(Silver and others, 1986). Quartzite of the Mazatzal Group extends to the north, in isolated outcrops, to the Verde River. Magnetic data (Langenheim and others, 2000; Langenheim and others, this volume) suggests that the quartzite probably extends to the south, in the subsurface, beneath the northern end of Little Chino Valley.

A fifth plutonic unit, the granite of Chino Valley (DeWitt and others, in press) underlies much of central Big Chino Valley (fig. B3), but is exposed only northwest of the study area near South Butte and Partridge Creek (fig. B1). The granite is medium to coarse grained, slightly to strongly porphyritic, and contains potassium-feldspar phenocrysts. Undeformed in many outcrops, the granite is deformed in zones of high strain that strike northeast and dip steeply. The granite coincides with an aerially extensive high-amplitude magnetic anomaly centered over Big Black Mesa.

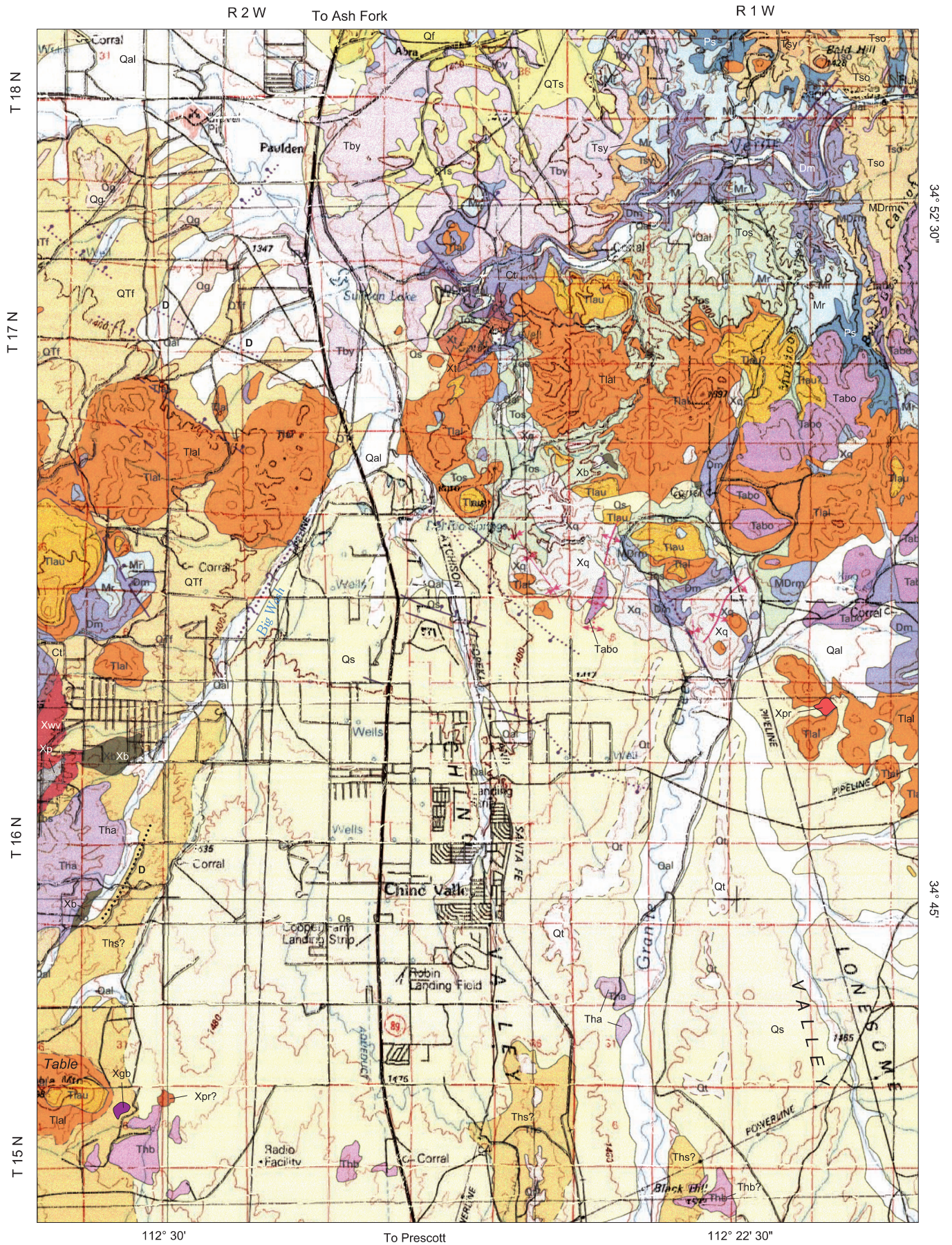
A simplified depiction of the basement rocks, from west to east, is: (1) a large body of granite underlies much of central Big Chino Valley, northwest of figure B3; (2) metasedimentary rocks contact the granite to the east in a northeast-striking belt that extends from the western Sullivan Buttes to north of Paulden (fig. B3); (3) metavolcanic rocks contact the metasedimentary rocks to the east and may be present throughout much of Little Chino Valley (fig. B2); (4) a large body of gabbro and ultramafic rocks is present in the upper crust beneath the western part of Little Chino Valley; (5) small bodies of granite to granodiorite cut the metavolcanic rocks in the far southern part of Little Chino Valley and may form a large pluton farther to the south; and (6) quartzite of the Mazatzal Group locally overlies the metavolcanic rocks in an irregularly shaped belt that extends from the Verde River, southwest, to beneath the northern end of Little Chino Valley.

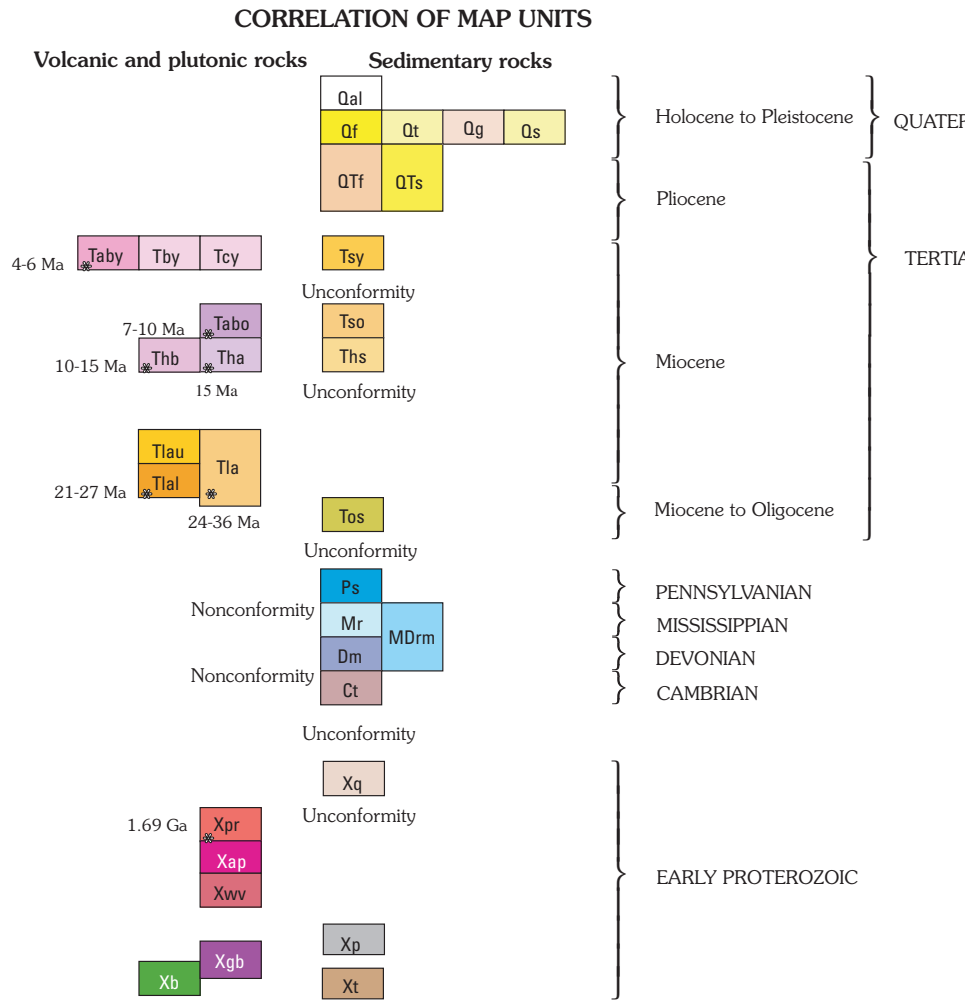
## Paleozoic rocks

Cambrian Tapeats Sandstone (unit Ct) is the basal Paleozoic rock unit in the area, lying unconformably on Proterozoic rocks west of the town of Chino Valley and in fault contact with the Proterozoic rocks along lower Granite Creek (fig. B2). Farther down the Verde River the Tapeats crops out beneath the Devonian Martin Formation (fig. B2). Outcrops of Tapeats are tentatively identified north of the Big Chino Fault, along the base of Big Black Mesa. Rocks in that area could be part of the Devonian Chino Valley Formation, as discussed below. The Tapeats consists of a basal quartz-pebble conglomerate, strongly cemented sandstone and quartzite, and minor dolomitic sandstone (Krieger, 1965). Near topographic highs created by erosion-resistant basement rocks such as the quartzite of the Mazatzal Group, the Tapeats was not deposited. Thickness of the Tapeats ranges from 30 to 50 meters and increases to the west (Krieger, 1965).

Cambrian Bright Angel Shale is exposed west of the study area, in western Big Chino Valley, at the base of the Juniper Mountains (Krieger, 1967a; fig. B1). There the unit is composed of shale, dolomitic shale, and unusual K<sub>2</sub>O-rich rocks that are 10-20-m thick and that underlie the Martin

**B4 Geologic Framework**

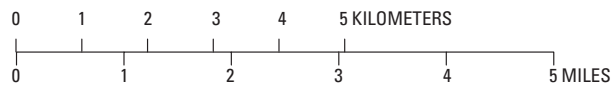




### EXPLANATION OF MAP SYMBOLS

- Contact — Dotted where concealed. Queried where indeterminate
- Fault — Dashed where approximately located or dotted where concealed by younger units. Bar and ball on downthrown side
- Monocline — Dotted where concealed. Both axes shown
- \* Radiometrically determined age
- CV-DH-3 Location and name of selected well discussed in text

Base from U.S. Geological Survey 1:100,000 Williams and Prescott



Scale 1:100,000

**Figure B2 (above and facing page).** Geologic map of the northern part of Little Chino Valley. Geology from DeWitt and others (in press).

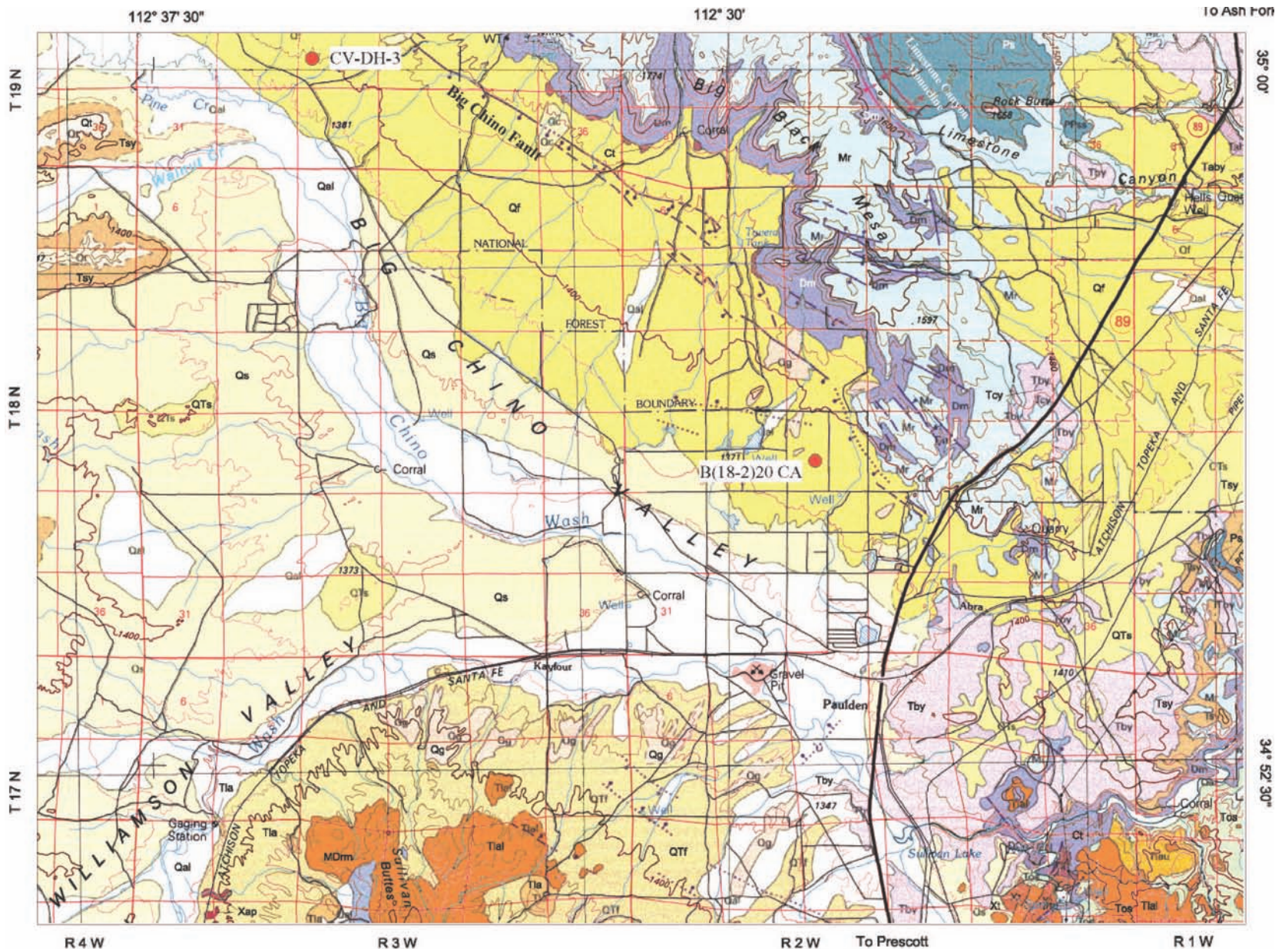


Figure B3. Geologic map of the southeastern part of Big Chino Valley. Geology from DeWitt and others (in press).

Formation.  $K_2O$  concentrations as high as 10.0 weight percent and boron concentrations as high as 280 ppm (Miesch, unpub. data in Baedeker and others, 1998) suggest that the Bright Angel Shale may contain a component of felsic tuff that was deposited in a shallow-water marine setting (Bowie and others, 1966, 1967; Hutcheon and others, 1998). However, rocks of such unusual chemical composition have not been documented in regional geologic mapping of Big Chino Valley (DeWitt, this study).

The Devonian Martin Formation (unit Dm) is extensively exposed on Big Black Mesa north of the Big Chino Fault (fig. B3), and east of Granite Creek and along the Verde River (fig. B3). The Martin is composed of thickly bedded dolomite and minor impure limestone that are about 130-m thick (Krieger, 1965). Karst features are noted near the base of the Martin, along northwest-striking, high-angle fractures (this study). For purposes of this study, the Chino Valley Formation (Hereford, 1975) is grouped within the basal Martin Formation. The Chino Valley consists of sandstone, conglomerate, and dolomitic shale (Beus, 1989) that are 5-10-m thick near Jerome (Wolfe, 1983). Aluminous rocks in the Chino Valley Formation have an unusual chemical composition characterized by  $K_2O$  concentrations as high as 8.5 weight percent (Hereford, unpub. data in Baedeker and others, 1998). These aluminous rocks are similar, compositionally, to shale-rich rocks in the Bright Angel Shale and probably were formed by felsic tuff deposition in a marine basin ((Bowie and others, 1966, 1967; Hutcheon and others, 1998).

Mississippian Redwall Limestone (unit Mr) overlies the Martin Formation and is exposed extensively on the top of Big Black Mesa (fig. B3) and to a lesser extent east of Muldoon Canyon and north of the Verde River (fig. B2). The Redwall is a high-calcium limestone (contains less than 1.1% equivalent MgO) containing variable amounts of chert in thin, discontinuous beds. Karst features, including interconnected caves, are well developed in the Redwall, particularly in the middle part of the unit. Thickness of the Redwall varies according to the amount of karst and collapse in the unit, but averages about 80 m.

The Pennsylvanian Supai Formation (unit Ps), a predominantly quartz-rich clastic rock that contains minor amounts of conglomerate, limestone, and evaporite beds (unit Ps), overlies the Redwall and is exposed north of Big Black Mesa (fig. B3), and north of the Verde River and east of Muldoon Canyon (fig. B2). Much of the Supai is poorly cemented and weathers to recessive outcrops. Regionally the Supai is as much as 180 m thick (Krieger, 1965); only about 40 m of Supai is exposed in the study area. The upper part has been removed by erosion prior to Tertiary time.

## Tertiary rocks

The oldest Tertiary rock unit is a distinctive and important sequence of fluvial gravels and alluvial fan deposits (unit Tos) that were derived from a regional uplift to the southwest. These gravels contain cobbles of Early Proterozoic rock

units common in the Bradshaw Mountains to the south, and of Paleozoic carbonate rocks and sandstone (Krieger, 1965). Imbrication directions show northeast transport, toward the present-day Mogollon Rim. The gravels are poorly to moderately well sorted and poorly cemented, and crop out in a paleochannel, about 6.5 km wide, that extends from near Highway 89 at Del Rio Springs on the west to Muldoon Canyon on the east. The paleochannel coincides with map unit Tos in fig. B2. Maximum thickness of the unit is about 75 m (Krieger, 1965). The gravel deposits extend beneath Little Chino Valley and the town of Chino Valley and form part of the productive artesian aquifer (Schwalen, 1967). The extent of the channel north of the Verde River cannot be determined because of erosion and cover by younger gravel deposits. Because the gravels are preserved beneath 24-Ma lati-andesite flows, the unit is Oligocene or older. The Tertiary tectonic history of the Basin-and-Range province south of the Bradshaw Mountains suggests that the channel deposits are probably no older than 34 Ma (Spencer and Reynolds, 1989).

No other gravel of this age is known in the study area, but other similar deposits are exposed farther west in Big Chino Valley, near South Butte (fig. B1). There, conglomerate containing clasts of Early Proterozoic gabbro and metasedimentary rocks, and Middle Proterozoic granite, as well as Paleozoic sandstone and carbonate rocks, unconformably overlies Martin Formation and Redwall Limestone. Clast imbrications indicate transport to the northeast. Streams in that area eroded Proterozoic basement and Paleozoic strata on the south side of present-day Big Chino Valley and transported the clasts across the site of the future valley to the northeast. Locally, lati-andesite flows cap South Butte at an elevation higher than the Tertiary conglomerate. The extent of this paleochannel and associated gravels cannot be determined due to extensive erosion of the conglomerate.

## Lati-andesite

Lati-andesite (a rock composition intermediate between latite and andesite) and associated volcanic rocks (units Tla, Tlal, Tlau) are exposed northeast and northwest of Little Chino Valley (fig. 2) and in the Sullivan Buttes area, south of Big Chino Valley (fig. B3). Eruptions began with formation of mafic cones and flows (part of unit Tlal); younger flows, domes, and breccias of intermediate composition followed (also part of unit Tlal); late eruptions were of locally thick mafic flows (unit Tlau). Both extrusive sheets and intrusive necks and plugs are well preserved, some in large ring dikes (Krieger, 1965; Tyner, 1984; Ward, 1993). Individual eruptive centers produced extrusive sheets whose partially eroded remnants are less than 1,500 m in diameter and less than 200 m thick. Preserved plugs are less than 300 m in diameter.

The most mafic rock types are alkali-calcic alkali basalt; least mafic rock types are alkali-calcic dacite (fig. B4A). Very low A/CNK ratios (fig. B4B), potassic to very potassic nature (fig. B4C), and very Mg-rich to Mg-rich nature (fig. B4D) allow the lati-andesite to be distinguished from Miocene and

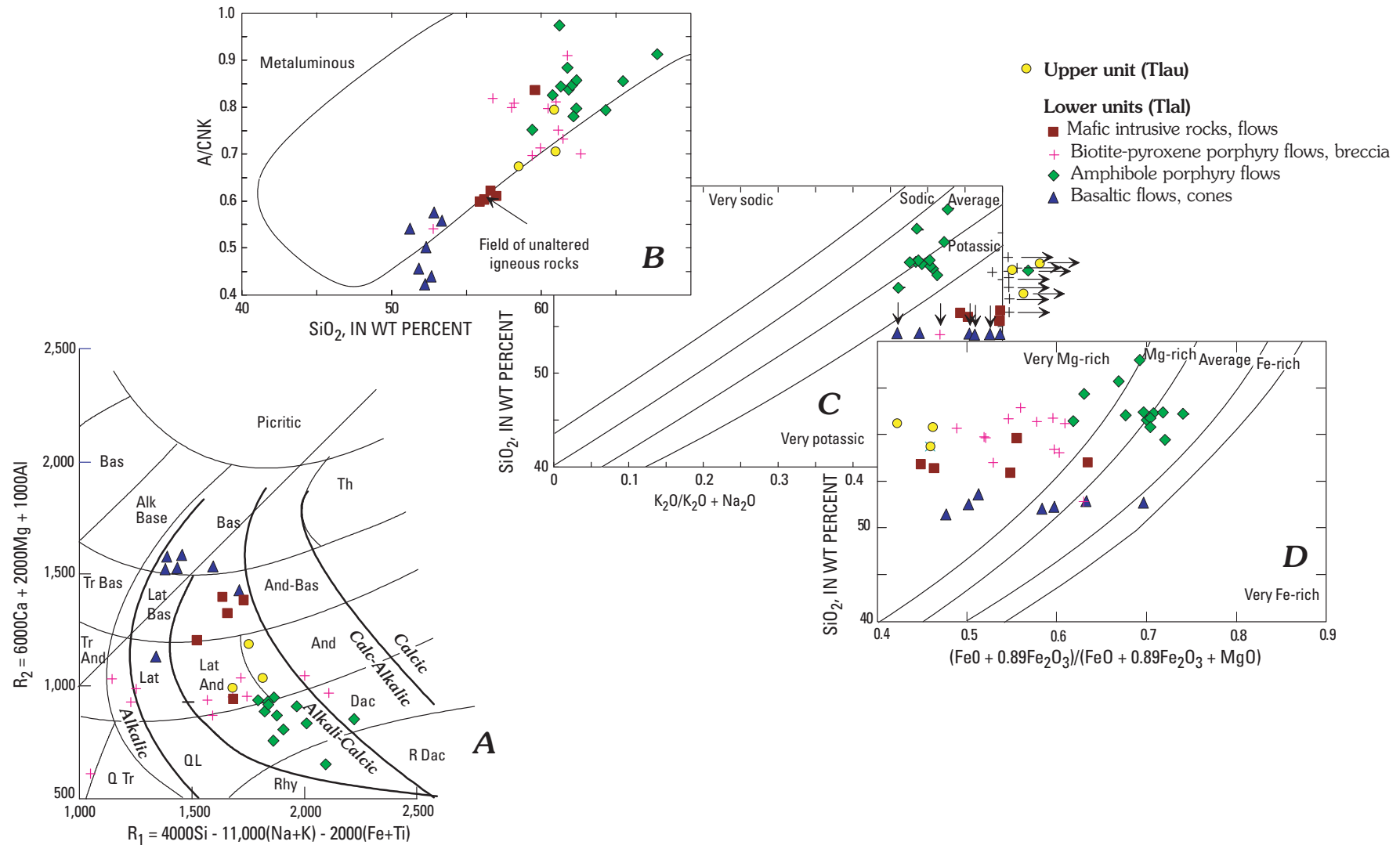


**Figure B4.** Major-element classification diagrams for 21-27-Ma volcanic rocks in the Sullivan Buttes volcanic field (units Tlal, Tlau, and Tla) near Chino Valley. Data from Tyner (1984), Ward (1993), and this study. (A),  $R_1$ ,  $R_2$  major-element classification diagram (De la Roche and others, 1980). Picritic, ultramafic composition; Bas, basinite; Alk Bas, alkali basalt; Bas, basalt; Th, tholeiite; Tr Bas, trachybasalt; Lat Bas, lati-basalt; And-Bas, andesitic basalt; Tr And, trachyandesite; Lat, latite; Lat And, lati-andesite; And, andesite; Q Tr, quartz trachyte; QL, quartz latite; Dac, dacite; Rhy, rhyolite; R Dac, rhyodacite. Fields of alkalinity from Fridrich and others (1998). (B), Alumina saturation diagram ( $\text{SiO}_2$  versus  $\text{A/CNK}$ ). A, molar  $\text{Al}_2\text{O}_3$ ; C, molar  $\text{CaO}$ ; N, molar  $\text{Na}_2\text{O}$ ; K, molar  $\text{K}_2\text{O}$ . Field of unaltered igneous rocks from DeWitt and others (2002). (C), Alkali classification diagram ( $\text{K}_2\text{O}/(\text{K}_2\text{O} + \text{Na}_2\text{O})$  versus  $\text{SiO}_2$ ). Field boundaries from Fridrich and others (1998). Samples with horizontal arrows plot far to the right of the outline of (C). Samples with vertical arrows plot in the very potassic field, below the outline of (C). (D), Iron enrichment classification diagram ( $(\text{FeO} + 0.89\text{Fe}_2\text{O}_3)/(\text{FeO} + 0.89\text{Fe}_2\text{O}_3 + \text{MgO})$  versus  $\text{SiO}_2$ ). Field boundaries from DeWitt and others (2002).

younger basaltic rocks. Lati-andesite and associated rocks have elevated Th and U concentrations, and are easily distinguished from other Tertiary volcanic rocks on radiometric maps (Langenheim and others, 2000). Although the youngest flows physically resemble Miocene and younger basalts, elevated Th and U concentrations allow differentiation from Miocene and younger basalt. Remnants of the oldest basaltic latites, recognized by elevated Th and U concentrations, were remapped (this study) in areas previously thought to be covered by younger basalt, especially in the area northeast of Granite Creek (fig. B2).

The lati-andesite forms a volcanic field that overlies a dissected surface underlain by rocks ranging in age from the Early Proterozoic Mazatzal Group through the Permian Supai Formation. Much of the lati-andesite was erupted onto the Martin Formation. The age of volcanism appears to be about 24 Ma, as determined by limited K-Ar dating of hornblende and biotite (Krieger and others, 1971). The original extent of the volcanic field was larger than the remnant preserved in the study area. The volcanic field extended into the northern part of Little Chino and Lonesome Valleys and occupied a considerable part of the southeastern part of Big Chino Valley as evidenced by magnetic data (Langenheim and others, 2000; Langenheim and others, this volume). Intrusive centers are consistently reversely magnetized, leading to a pattern of conspicuous magnetic lows on magnetic maps (Langenheim and others, this volume). Locations of such lati-andesite centers buried beneath basin fill can be accurately determined (fig. B5A and B). Outcrops of lati-andesite and related rocks to the west of Big Chino Valley, in the Camp Wood area (Ash, 1997), suggest continuity of the volcanic field across much of Williamson Valley Wash and some of southern Big Chino Valley.

In Bureau of Reclamation drillhole CV-DH-3, located in central Big Chino Valley (fig. B3), biotite-rich volcanic rock was encountered at about 698 m (2290 ft) depth, but was identified as basalt (Ostenaa and others, 1993b). X-ray diffraction data corroborate the presence of biotite and indicate significant potassium feldspar. Chemical data confirm that the rock is a lati-andesite, we tentatively correlate it with lati-andesite in the Sullivan Buttes area.

## Hickey Formation and Older Basalt and Sedimentary Rocks

The Miocene Hickey Formation, consisting of regionally extensive basalt flows and less extensive sedimentary rocks, crops out in the surrounding mountain ranges, especially in the Black Hills, and in the Bradshaw Mountains (fig. B1). Basalt flows in the Hickey Formation that erupted from the northern Black Hills are present just east of Lonesome Valley and probably underlie much of eastern Lonesome Valley. No flows of Hickey age are recognized in the Big Chino Valley area.

West of the town of Chino Valley, a locally thick hornblende-bearing trachyandesite to trachybasalt (unit Tha) overlies Early Proterozoic basement rocks. This hornblende-rich rock is mineralogically similar to trachyandesite at Thumb Butte, west of Prescott, which has a  $^{40}\text{Ar}/^{39}\text{Ar}$  groundmass

date of 14.8 Ma (Nichols Boyd, 2001). Rocks of similar mineralogy are exposed along Granite Creek southeast of the town of Chino Valley (Krieger, 1965) and are included in the Hickey Formation for this report. Samples of this rock contain calcite and plot above the field of those at Thumb Butte (fig. B6A), but the sample containing the least calcite has similar A/CNK ratio (fig. B6B) and Fe/Fe+Mg ratio (fig. B6D) to the Thumb Butte rocks. The top surface of the trachyandesite flow can be traced using interpreted well logs toward the town of Chino Valley for a distance of about 5.5 km (fig. B7), and probably extended farther northeast before formation of the basin in northeastern Little Chino Valley after about 7 Ma.

Discontinuously exposed basalt flows (unit Thb), thought to be in the Hickey Formation (Krieger, 1965), extend from Table Mountain to Black Hill. Chemistry of one sample from Black Hill is similar to many samples in the Prescott area (fig. B6). The upper surface of the flow(s) can be traced toward the town of Chino Valley by the interpretation of well logs (fig. B7). Prior to development of the basin in northeastern Little Chino Valley, the flow(s) could have extended farther northeast.

Sedimentary rocks tentatively assigned to the Hickey Formation (unit Ths) crop out between Black Hill and Table Mountain (fig. B2). Rock types include poorly sorted conglomerate, fluvial sandstone, and minor clay-rich beds. East of Granite Creek these sedimentary rocks underlie the basalt flow on Black Hill. The base of the sedimentary rocks is not exposed. A partial thickness in excess of 35 m is indicated.

One distinctive and extensive basalt flow (unit Tabo) extending from King Tank to Muldoon Canyon (fig. B2) is believed to be younger than the Hickey Formation (< 10 Ma), but older than younger basalt flows (4-6 Ma). This basalt is extremely magnetic (about 10 volume-percent magnetite-equivalent), crops out over a large area, and extends to the northeast of Bull Basin Canyon (fig. B2). Originally considered a part of the lati-andesite (Krieger, 1965), this basalt is characterized by its low eU (equivalent uranium) and Th concentrations (Langenheim and others, 2000) and alkalic chemistry (fig. B6), and is presumed to be unrelated to the lati-andesite. Its present topographic position, at an elevation lower than the Hickey Formation, but higher than younger basalt flows, suggests an intermediate age of 7-10 Ma, but the flow could be within the range of the Hickey Formation.

Beneath the magnetic basalt flow along Bull Basin Canyon (fig. B2) are sedimentary rocks consisting of distal conglomerate, fluvial conglomerate, and minor sandstone (unit Tso). Clasts in the conglomerate were derived, predominantly, from the southwest, as indicated by clast imbrication and composition. Originally mapped as sedimentary rocks beneath lati-andesite (Krieger, 1965), we interpret the rocks to be filling an 7-10-Ma channel that cut down to the present-day elevation of the Verde River southeast of Bald Hill, near the Paulden gage (fig. B2). Similar rocks crop out on the north side of the river, but some of them may have been derived from the northwest or were locally reworked. Thickness of the sedimentary rocks along the northern part of Bull Basin Canyon is as much as 90 m.



**B10 Geologic Framework**

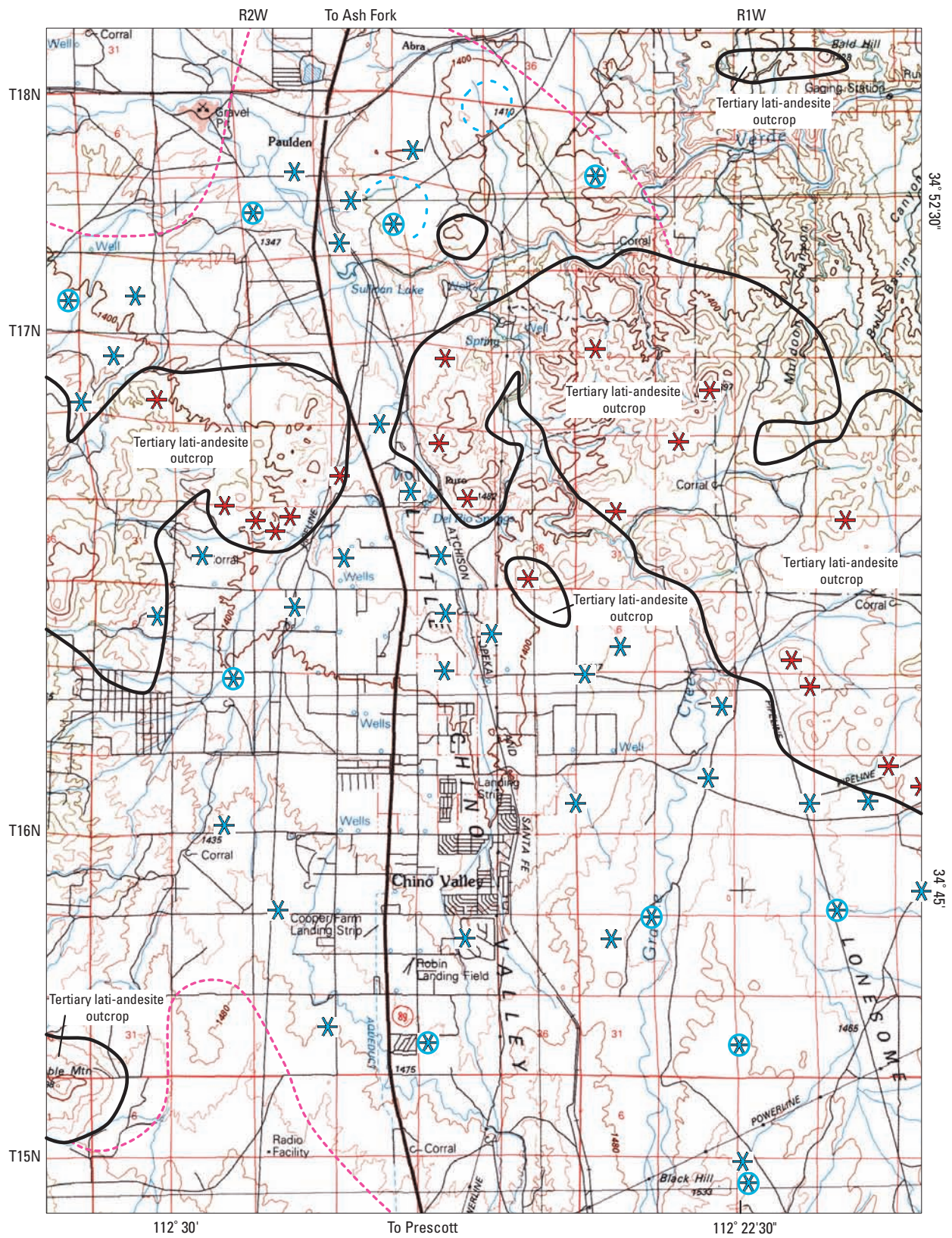


**Figure B5 (above and facing page).** Maps showing location of buried latite-andesite centers. (A), Little Chino Valley; (B), Big Chino Valley.

112° 37' 30"

112° 30'

To Ash Fork

T19N

35° 00'

T18N

T17N

35° 00'

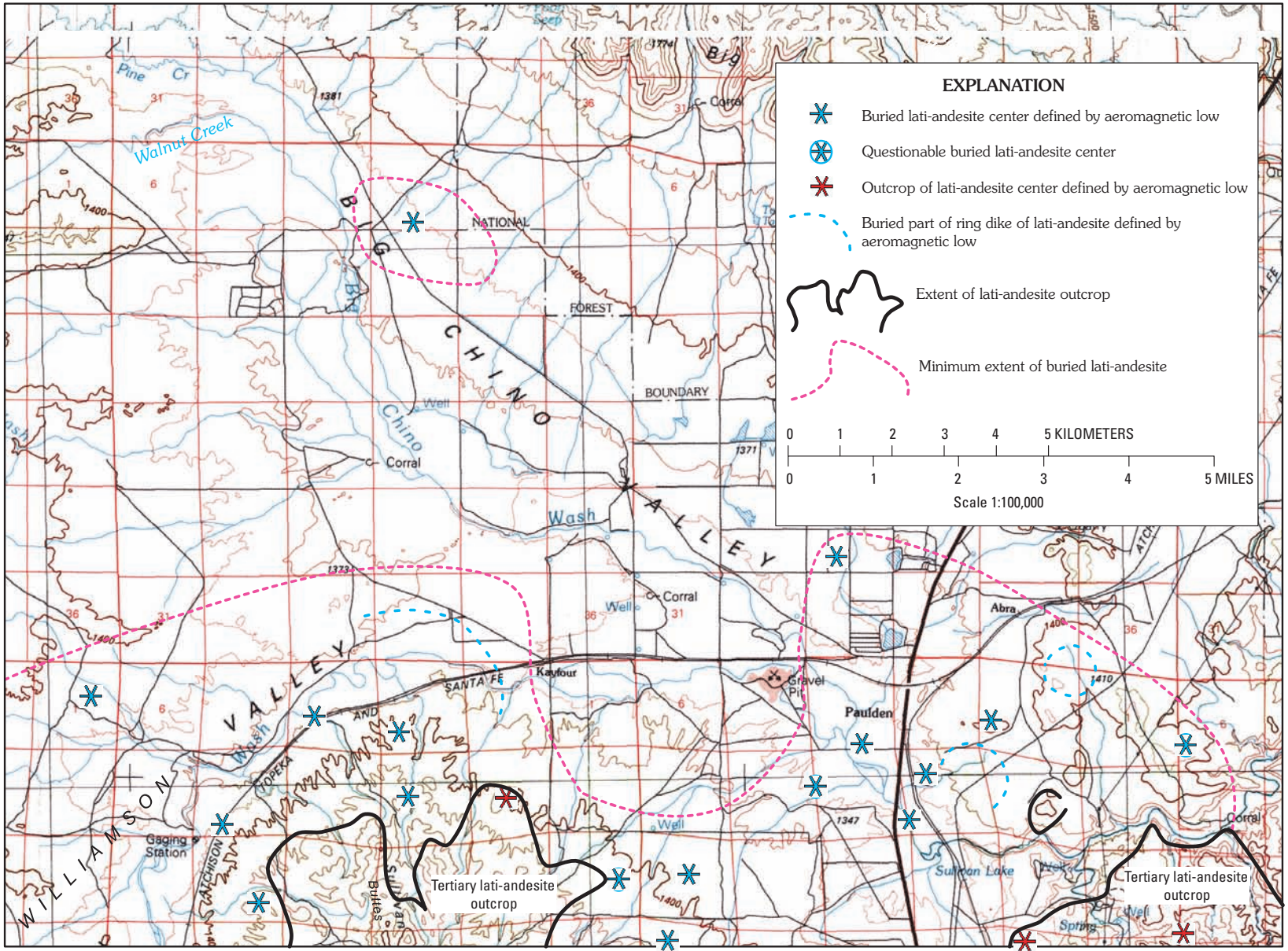
R4W

R3W





R2W

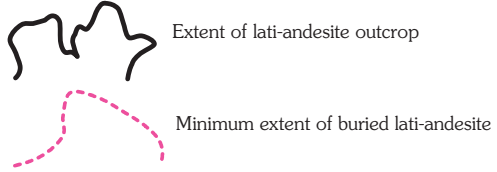
To Prescott

R1W



**EXPLANATION**

-  Buried lati-andesite center defined by aeromagnetic low
-  Questionable buried lati-andesite center
-  Outcrop of lati-andesite center defined by aeromagnetic low
-  Buried part of ring dike of lati-andesite defined by aeromagnetic low



0 1 2 3 4 5 KILOMETERS  
 0 1 2 3 4 5 MILES  
 Scale 1:100,000

## Younger Basalt and Sedimentary Rocks

Extensive basalt flows (units Tby and Taby), derived primarily from eruptive centers on the Colorado Plateau to the north, flowed over the Mogollon Rim and into Big Chino Valley and the present-day area of the Verde River east of Paulden from about 4 to 6 Ma (fig. B2). Cinder cones (unit Tcy), such as the one northeast of Paulden (fig. B3) provided local sources for some of the flows. These flows are part of the Miocene Perkinsville Formation (Lehner, 1958), defined to the east of the map area. Northeast of Hells Well (fig. B3), a flow near the Drake railroad siding is 6.0 Ma (K-Ar whole rock, McKee and Anderson, 1971). This flow probably extends southeast toward Hell Point (fig. B1). Extensive basalt flows (unit Tby) east and south of Paulden are 4.5 Ma (K-Ar whole rock, McKee and Anderson, 1971) and provide important limitations on the configuration of basin fill beneath the basalt.

The 4.5-Ma basalt outcrop east and south of Paulden consists of three flows, two of which fill a paleocanyon in the gorge of the Verde River east of Sullivan Lake. An arcuate paleocanyon (fig. B8A), having a steep southeastern wall, is partially filled by the lowest flow, which is a minimum of 30-m thick. The middle flow, which is about 40-m thick, fills the rest of the paleocanyon and is separated from the lowest flow by less than 1 m of conglomerate derived from latite-andesite to the south. This middle flow has the 4.5-Ma age determination. The top flow is exposed north of the gorge; its eroded thickness is less than 10 m. A 1-m-thick conglomerate containing clasts of latite-andesite separates the top flow from the middle flow. Location of the paleocanyon can be determined to the west, beneath Quaternary and Tertiary valley fill in Big Chino Valley, by the greatest thickness of basalt (fig. B8B). Well logs document the presence of buried basalt at least 8 km northwest of Paulden, at a depth of greater than 175 m (570 ft). Magnetic data (Langenheim and others, 2000; Langenheim and others, this volume) confirms the presence of basalt in the subsurface slightly farther to the northwest. The thickest accumulation of basalt, in excess of 125 m (400 ft) south of Abra, fills the paleocanyon cut into Paleozoic bedrock. This thick section of basalt was interpreted to result from a narrow, buried graben (Water Resource Associates, Inc., 1991). To the northeast, location of the paleocanyon is approximately indicated by logs of water wells; the canyon appears to curve to the north and northwest, and may have drained Limestone Canyon during the time of basalt eruptions.

Basalt in the paleocanyon and beneath Big Chino Valley to the west of Paulden may have been derived, in part, from the cinder cone northeast of Paulden along Highway 89 (fig. B2), but much of the basalt south of Paulden could have had local, concealed sources, most likely northwest-striking, high-angle feeder dikes. Abundant cinders noted in well logs southwest of Sullivan Lake (Arizona Department of Water Resources, 2003) suggest a buried cinder cone that could have fed some of the flows from the south. The present dip of the top surface of the flows beneath Big Chino Valley, to the northwest, averages only one degree (fig. B8B). Subsidence

since 4.5-Ma must account for part of that dip, leaving a dip surface of less than one degree down the valley during basalt eruption. A local source for the basalt would aid flow down a surface of such minimal dip.

North of Abra (fig. B3) basalt flowed over Paleozoic strata and into the basin of Big Chino Valley. A small, sinuous canyon may have been cut in Paleozoic bedrock north of Abra where basalt is locally more than 30-m thick (fig. B8B). East of Paulden the basalt flowed over Paleozoic bedrock before encountering Tertiary sediments in Big Chino Valley. In DRM-2 (fig. B8A), a well west of Paulden (B17-2)4 CAD, basalt overlies 75 m of Tertiary fine-grained sediment that is part of the valley fill in Big Chino Valley (Water Resource Associates, Inc., 1990). Given the thickness and fine grain size of sediment beneath the basalt at this location, the margin of the Big Chino basin must be east of Highway 89 and be buried by basalt. South of Sullivan Lake, basalt flows thin against a buttress of latite-andesite flows. Decreasing thickness to the south (fig. B8B), in the region 2 km north of Del Rio Springs (fig. B3), suggests that the basalt flows never reached Little Chino Valley, but were deflected to the west into the deeper part of Big Chino Valley (fig. B8B). Logs from wells are lacking north of Del Rio Springs, but wells south of Del Rio Springs show no evidence of 4-6-Ma basalt flows in northern Little Chino Valley.

Chemistry of all the younger basalt flows in the area is similar (fig. B9). The middle and top flows of the 4.5-Ma sequence near Paulden are identical, within uncertainty, to the cinder cone northeast of Paulden. Magnetic susceptibility measurements of all three flows are similar, and are higher than basalt from the cinder cone. The 6.0-Ma flows near Drake and Hell Point also are chemically similar to the flows near Paulden (fig. B9).

These 4.5-Ma basalt flows are present, at the same elevation, on both sides of the present-day Verde River downstream from Sullivan Lake (fig. B2). An ancestral Verde River was not present in that area at 4.5 Ma. Similarly, the flow at Hell Point (fig. B1; Krieger, 1965) extends across the Verde River, indicating that neither the river nor Hell Canyon were developed in that area at 6.0 Ma. Stream cobbles found on top of the 4.5-Ma basalt flow on the north side of the Verde River north of Lower Granite Spring were derived from the south, in the Bradshaw Mountains, not from the west in the Juniper and Santa Maria Mountains (DeWitt, this study). Therefore, after 4.5 Ma, the ancestral Verde River appears to have flowed to the north from the Bradshaw Mountains to the present-day confluence of Granite Creek and the Verde River. The location of present-day Granite Creek may have been the site of the ancestral Verde River.

Basalt-cobble conglomerate and limestone-cobble conglomerate (unit Tsy) are locally interbedded with the basalt flows, especially in the area 7 km south of Hells Well (Krieger, 1965). Regionally, such fluvial systems were flowing from north to south, off the Mogollon Rim (McKee and McKee, 1972). Locally, fluvial systems were draining uplifts such as Big Black Mesa, where limestone-cobble conglomerate was

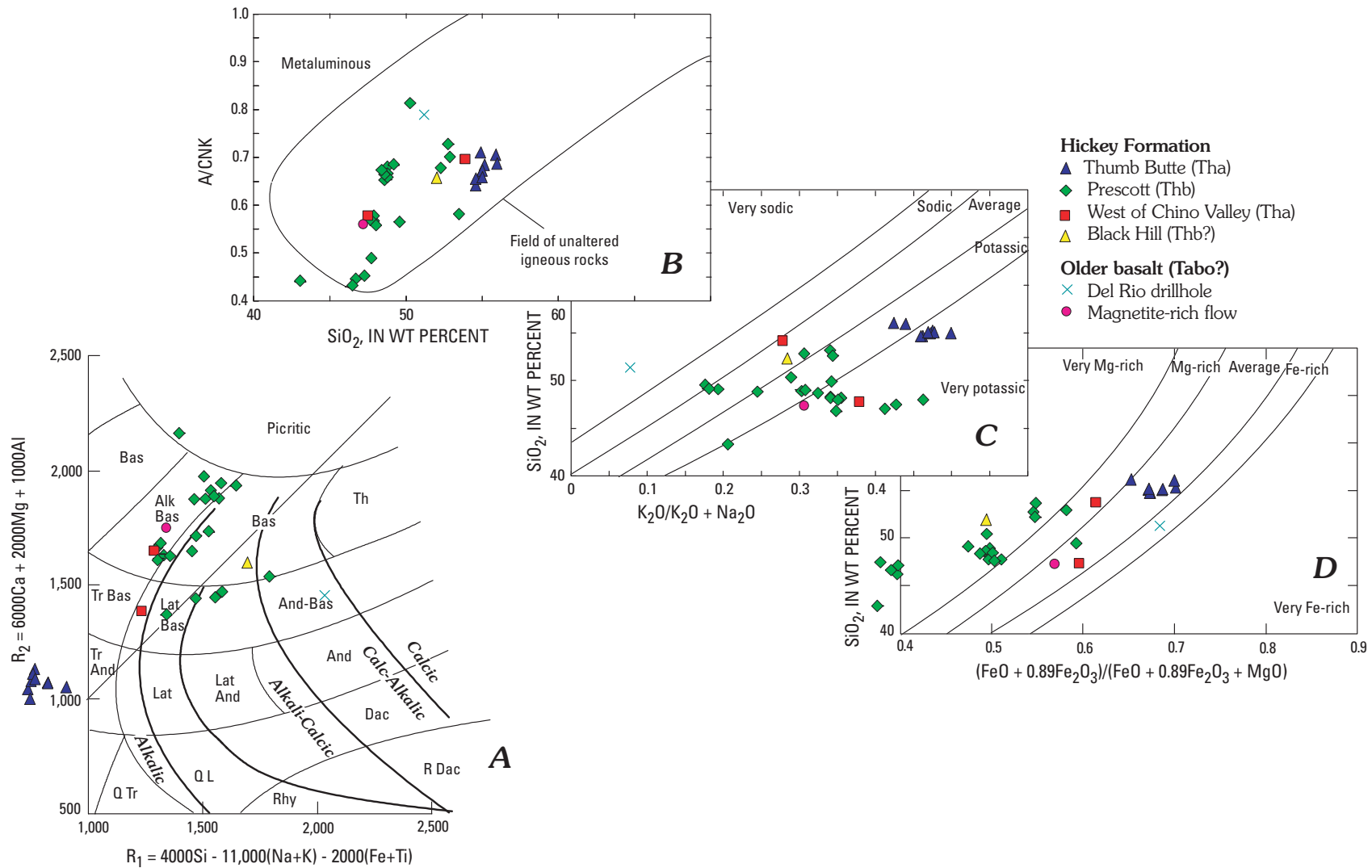


**Figure B6.** Major-element classification diagrams for 10-15 Ma volcanic rocks of the Hickey Formation (units Thb, and Tha) and 8-10 Ma volcanic rocks (unit Tbo) near Prescott and Chino Valley. Data from this study, McKee and Anderson (1971), and Nichols Boyd (2001). Rock abbreviations and field boundaries defined in figure B4. Samples from Thumb Butte are in the trachyandesite field, and are plotted correctly, but are to the left of the outline of (A). Samples from near Prescott are in the very Mg-rich field, and are plotted correctly, but are to the left of the outline of (D).

**B14 Geologic Framework**

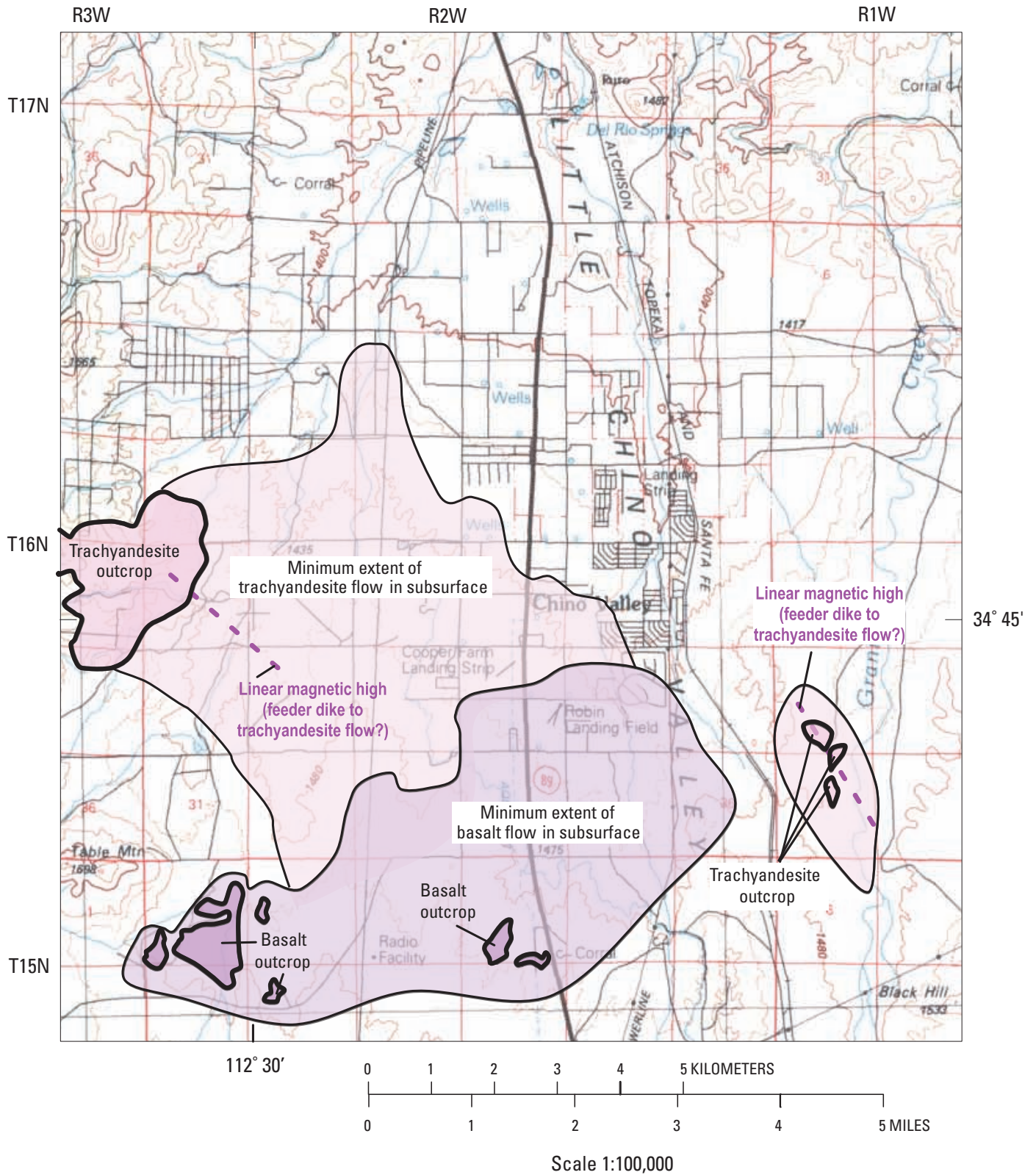


**Figure B7.** Map showing extent of 10-15-Ma flows in the Hickey Formation, Little Chino Valley.

shed to the southeast and was intermixed with the basalt flows. These younger sedimentary rocks are discernible from the sedimentary rocks older than the lati-andesite by virtue of the abundance of basalt cobbles and virtual lack of Early Proterozoic basement clasts.

## Tertiary and Quaternary sediment in Big and Little Chino Valleys

Tertiary and Quaternary sediments consist of proximal and distal alluvial fan deposits (units Qf, QTf), fine-grained alluvial sediments (units Qs, QTs), terrace gravels (unit Qt), thin sheet-like deposits of gravel (unit Qg), and alluvial material in present-day streams (unit Qal). Alluvial fans are most abundant in Big Chino Valley where they extend away from Big Black Mesa and radiate from the Sullivan Buttes (fig. B3). Fine-grained alluvial sediments are common in the central parts of Little and Big Chino Valleys (figs. B2 and B3). Terrace gravels are common along Granite Creek in Little Chino Valley (fig. B2) and Walnut Creek in Big Chino Valley (fig. B3). Sheets of gravel (unit QTf) are restricted to the area radiating away from the Sullivan Buttes (figs. B2 and B3). Alluvial material is present in the modern drainages of Granite Creek (fig. B2), Big Chino Wash, and Williamson Valley Wash (fig. B3). The distribution of surficial deposits shown in figures B2 and B3 has been simplified from previous investigations (Ostenaar and others, 1993b, plate 1).

Extensive alluvial fans composed primarily of carbonate clasts and detritus extend away from outcrops of Paleozoic carbonate rocks along Big Black Mesa (fig. B3). Fans are of low slope, but extend as much as 5 km into Big Chino Valley. Cobbles as large as 1 m near the mountain front give way to pebble-size clasts near the bottom of the fans. These carbonate-rich fans are recognized on eU and Th radiometric maps (Langenheim and others, 2000) by their very low concentrations of radioactive elements. Distal parts of the fans may contain a significant amount of fine-grained basin fill. Fans are thickest near the mountain front. About 150 m (500 ft) of alluvial fan sediment overlies playa sediments in the Bureau of Reclamation drill hole CV-DH3 near the Big Chino Fault (Ostenaar and others, 1993b) in Big Chino Valley (fig. B10).

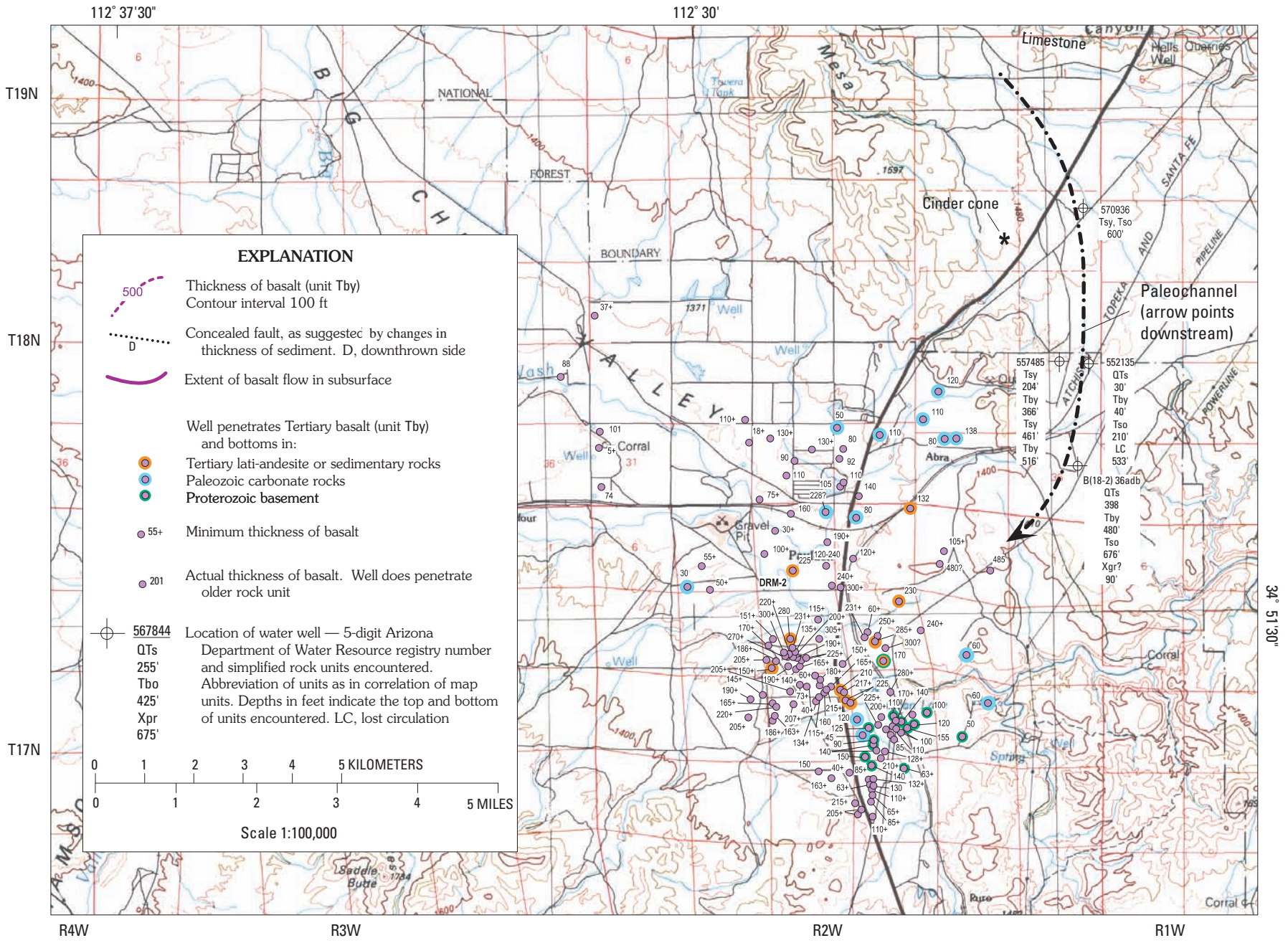
Alluvial fans composed primarily of clasts of lati-andesite and minor Paleozoic carbonate rock radiate from Sullivan Buttes (fig. B3). These fans have moderate slope and extend as much as 3.5 km away from outcrop in the Sullivan Buttes. Cobble- to pebble-size clasts of lati-andesite are common along the length of the fans, as the lati-andesite is more resistant to transport than carbonate material. Because of the abundance of lati-andesite, the alluvial fans have high concentrations of eU and Th, and stand out on radiometric maps (Langenheim and others, 2000) as distinct from fans containing abundant carbonate clasts. Radiometric logs of a well north of Sullivan Buttes (Ostenaar and others, 1993b) indicate that the fans extend into southeastern Big Chino Valley to depths of greater than 220 m. Fans of this nature are not recognized at the northern margin of Little Chino and

Lonesome Valley, and probably were never formed in that area. Remnants of such fans would be preserved in some of the valleys draining south into present-day Lonesome Valley if they had formed in Quaternary to Tertiary time.

Fine-grained alluvial sediment in the centers of Big and Little Chino Valleys is diverse in composition. Material in western Big Chino Valley and Williamson Valley contains pebbles of Proterozoic basement rocks, lati-andesite, and basalt in a carbonate-poor to carbonate-rich matrix. Clasts decrease in abundance toward the central part of Big Chino Valley, where sediment at the surface is carbonate rich and fine grained. The western side of Little Chino Valley contains sediment similar in composition to that in Williamson Valley, as it was derived from bedrock of similar composition in the eastern Sullivan Buttes and the Bradshaw Mountains to the southwest (fig. B1). Eastern Little Chino Valley and Lonesome Valley contain carbonate-rich fine-grained sediments derived from weathering of Paleozoic strata in the Black Hill to the east (fig. B1). Beds containing high concentrations of clay minerals are more common in Lonesome Valley than in the western part of Little Chino Valley.

**Playa deposits in Big Chino Valley.** In order to understand the mineralogy and distribution of sediments in central Big Chino Valley, archived samples from Bureau of Reclamation drillholes (Ostenaar and others, 1993b) were analyzed by x-ray diffraction techniques. Samples were analyzed at 30-m (100-ft) intervals in the three drillholes; selected qualitative mineral abundances are shown for various depths (fig. B10). Caution is urged in the interpretation of the results because the holes were drilled using muds containing clay minerals, and only chips are available from the drilling. Although care was exercised in washing drilling mud from the chips, some could have adhered to the chips (Ostenaar and others, 1993b). Also, chips may circulate up and down the hole during drilling, creating a sample that is a composite of an interval of sediment. Grain size of the sediment cannot be determined from the chips because of the small size of the chips and because dissolution of carbonate-cemented and sulfate-bearing materials could take place during drilling. Depths and thicknesses are noted in feet (meters in parentheses) in the following discussion because original depths, thicknesses, and descriptions of the drillholes are in feet (Ostenaar and others, 1993b).

Two minerals were found in deposits interpreted to have been deposited in a playa environment in Big Chino Valley. Analcime, a zeolite mineral, is recognized in all three drillholes. Bloedite, a sodium sulfate mineral, is tentatively identified from selected samples from the three drillholes. Other minerals, predominantly feldspars, interfere with a positive identification of bloedite(?). Chemical analyses or scanning electron imaging may be needed to corroborate the presence of bloedite(?). From 500 foot depth (150 m) to 2300 foot depth (700 m) in CV-DH-3 both minerals are noted and analcime is abundant. In CV-DH-1 an interval from 50 foot depth (15 m) to 850 foot depth (260 m) contains both minerals. Only one sample in CV-DH-2 contains the minerals, at about 220 foot depth (67 m). Analcime can be formed by the diagenetic



34° 51' 30"

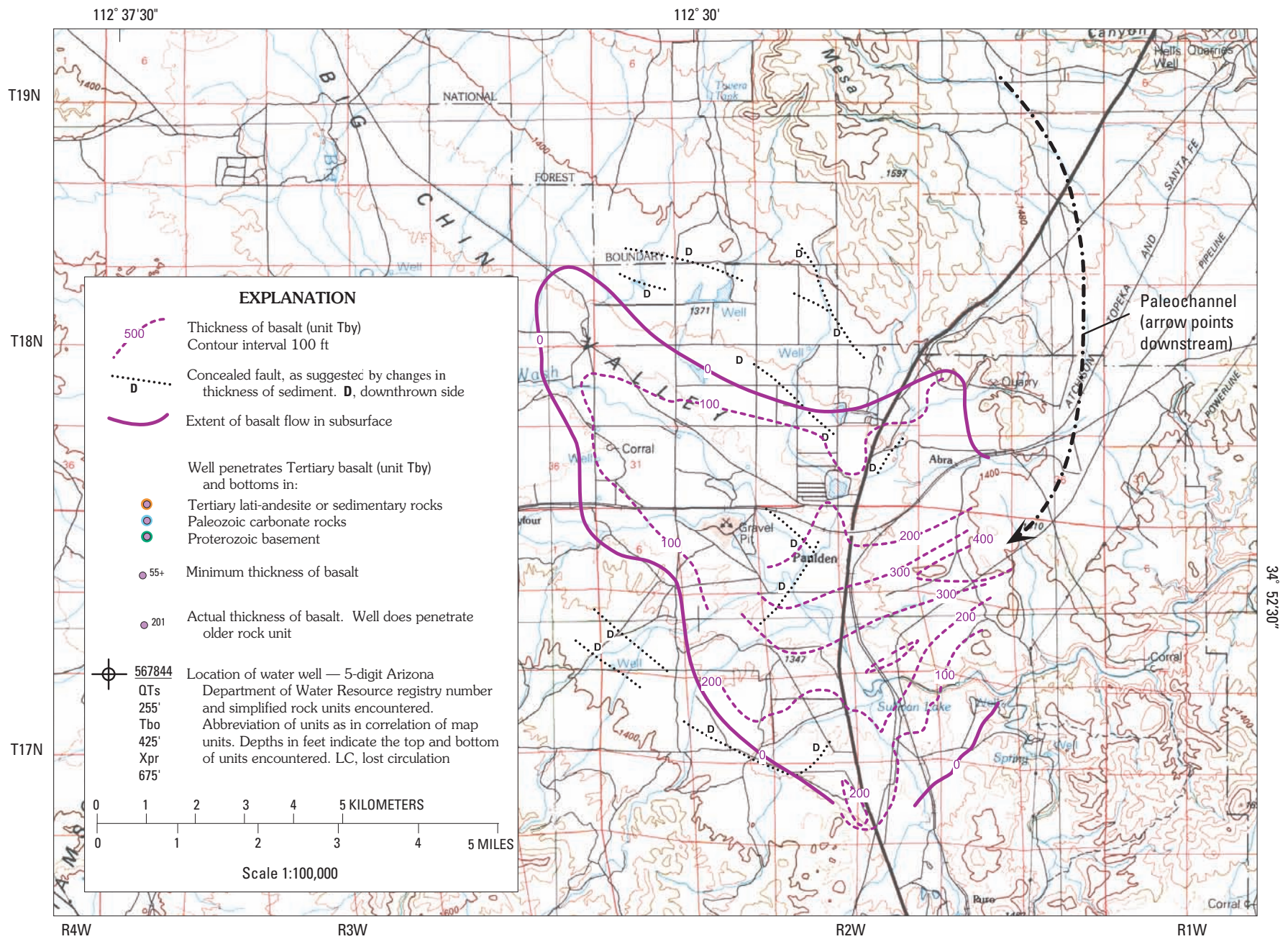


**Figure B8 (above and facing page).** (A), Maps showing thickness of 4-6-Ma basalt flows in southeastern Big Chino Valley. (A) Well locations and thickness determinations. (B), Isopachs of basalt thickness and locations of buried faults.



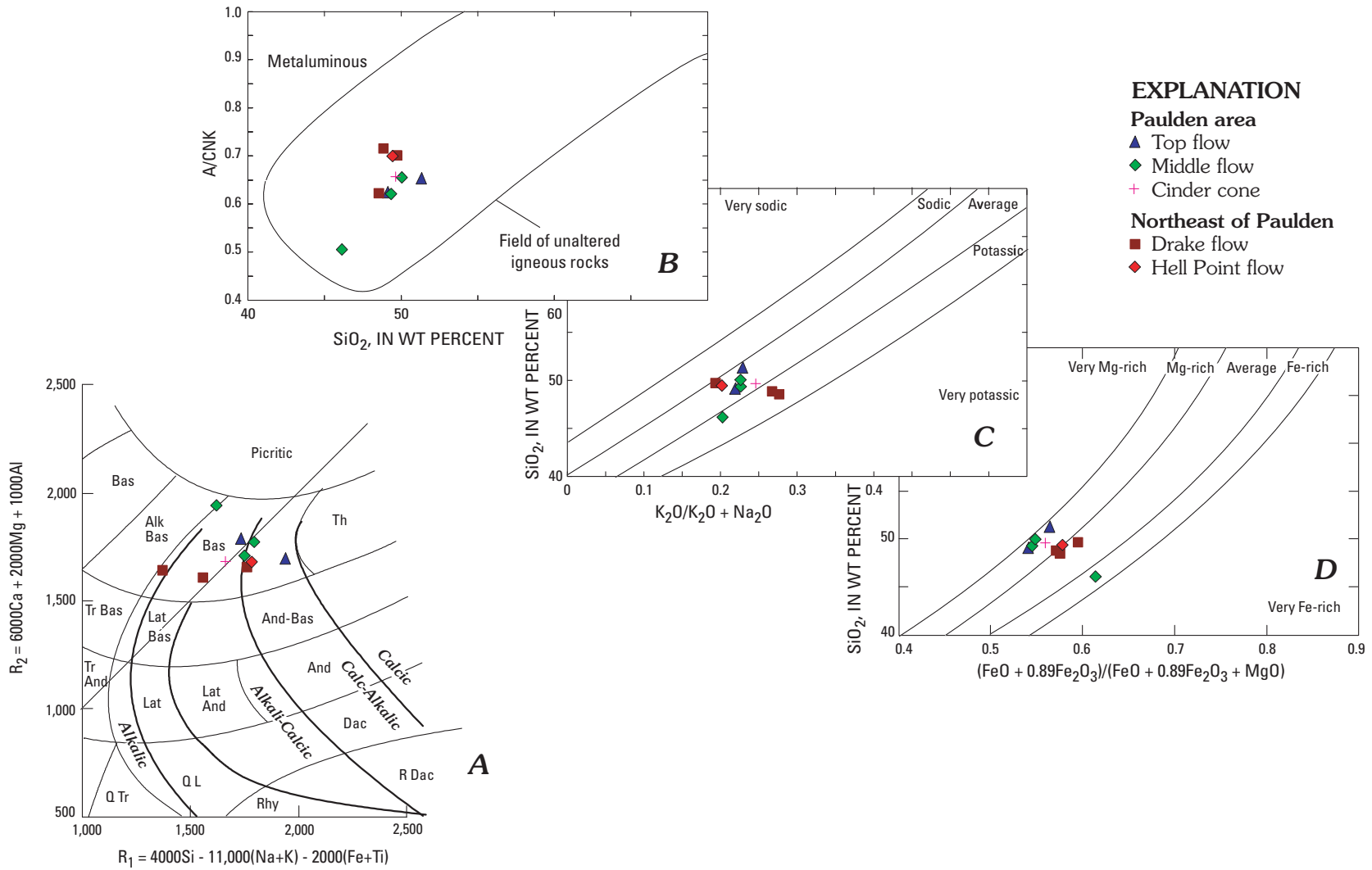


**Figure B9.** Major-element classification diagrams for 4-6-Ma volcanic rocks (unit Tby) near Paulden. Data from this study, McKee and Anderson (1971), and Witke and others (1989). Rock abbreviations and field boundaries defined in figure B4.

breakdown of albite at elevated pH, or can be a primary mineral deposited in alkaline lakes such as those that formed the Green River Formation in Wyoming and Utah (Meddaugh and Salotti, 1983; Remy and Ferrell, 1989). Bloedite(?) forms from evaporation of dilute brines in marine, playa, or closed-basin settings (Palache and others, 1957; Rosen, 1994). The presence of both minerals, coupled with the fine grain size of the sediment (Ostenaar and others, 1993b), and the predominance of calcite and dolomite in all analyzed sediments, is evidence of deposition in a playa setting.

Thickness of the playa deposits decreases from 1800 feet (550 m) near the Big Chino Fault (CV-DH-3) to 800 feet (244 m) near the axis of the valley, farther southeast (CV-DH-1), to less than 100 feet (30 m) on the southwest side of Big Chino Wash (CV-DH-2). Calcareous siltstone interrupts the playa sediments in CV-DH-1 over an interval of 150 feet (46 m). From CV-DH-3, the playa sediments are interpreted to inter-finger with siltstone and silty dolomite to the southeast. This interfingering probably is the result of fluctuating shoreline of the playa and periodic flooding of the playa by alluvial fan sediment from the south and southeast. From CV-DH-1 to CV-DH-2, the interval of playa sediments thins to less than 100 feet (30 m). Alluvial sediment from Williamson Valley, including calcareous siltstone and calcareous sand and gravel were shed onto the margins of the playa, restricting its growth to the south and west.

An approximate timeline within the basin can be determined from the thickness of sediment overlying the 4.5-Ma basalt flow northwest of Paulden (figs. B11A and B11B). The top surface of the basalt flow dips uniformly to the northwest at 1 degree. North-northeast of Kayfour, in the center of the valley, the 500-foot isopach of sediment above the basalt flow is well located. From that point to CV-DH-3 is a distance of 6.5 miles. Given a drop of 100 feet per mile (approximately 1 degree dip), the projected top surface of the basalt (a 4.5-Ma timeline) would be found in CV-DH-3 at a depth of 1150 feet (350 m). Because the rate of subsidence in the deepest part of the basin is probably greater than that near Kayfour, the projected depth of the 4.5-Ma timeline at CV-DH-3 is probably a minimum. Therefore, at least the upper 1000 feet of sediment in CV-DH-3 could be younger than 4.5 Ma.

Preliminary qualitative ranking, based on X-ray diffraction peaks of minerals in the playa sediments, shows, in general, carbonate minerals greater in concentration than analcime, which is greater in concentration than clay minerals, which are greater in concentration than bloedite(?) and quartz (fig. B10). Exceptions are noted to this general order. Only a qualitative estimation of mineral concentrations was undertaken due to the nature of the chip samples. Relative order of the four most abundant minerals could be amended by further investigations, primarily by chemical analyses. An altered illite is the predominant clay mineral identified in the playa sediments. Potassium appears to be deficient in the illite, resulting in peaks of reduced intensity and broadened width at low 2-theta measurements. A comparison of the qualitative abundance of clay minerals in non-playa sediments to

that in playa sediments suggests greater concentration of clay minerals in the playa sediments, in agreement with previous work (Ostenaar and others, 1993b, Water Resource Associates, Inc., 1989, 1990, and 1991). Carbonate minerals and analcime are more abundant than clay minerals in the playa sediments. Dolomite-to-calcite ratios vary in the playa, dolomite being more abundant at depth and calcite being more abundant shallower in the playa (fig. B10). This variation could be primary or it could reflect dolomitization of the lower parts of the playa sediments.

Sediment in Little Chino Valley. Compared to central and northwestern Big Chino Valley, Little Chino Valley contains much thinner Quaternary and Tertiary sediment that is younger than the youngest volcanic rocks (fig. B12A). Significantly, the pattern of isopachs of sediment is very irregular compared to those in southeastern Big Chino Valley (fig. B12B). Sediment in Little Chino Valley was deposited on an irregular topography created by underlying lati-andesite flows, domes, and intrusive necks, and by valleys partially filled by flows of the Hickey Formation. In general, sediment increases in thickness from southwest to northeast, and exceeds 600 feet (180 m) only south of Del Rio Springs. Between Table Mountain and Black Hill, thickness of sediment younger than the youngest volcanic rocks is less than 20 m. Areas of least sediment fill coincide with resistant intrusive centers of lati-andesite (fig. B12B). Topography on the eroded lati-andesite surface locally exceeds 70 m, especially at inferred buried intrusive centers (fig. B12B). East of Granite Creek there are too few drillholes to define thickness of the sediment.

## Structural Features

The Limestone Canyon monocline, exposed on Big Black Mesa (fig. B3), is believed to be of Laramide (60-80 Ma) age because of its similarity in structure to monoclines on the Colorado Plateau (Davis, 1978). This monocline strikes northwest and faces northeast; the Martin Formation and Redwall Limestone are present on the southwestern side of the monocline and the Supai Formation crops out on the northeast (Krieger, 1965). Structural relief along the monocline ranges from 70 to 120 m; the monocline dies out to the southeast near the mouth of Limestone Canyon (fig. B3). A small, north-striking monocline along Bull Basin Canyon (Krieger, 1965; fig. B2) probably is a Laramide structure. The monocline is truncated and overlain by undeformed Tertiary volcanic rocks, chiefly older(?) Tertiary basalt (unit Tabo) and is therefore older than about 10 Ma.

The regional dip of Paleozoic strata on Big Black Mesa and the area north of the Verde River is gently to the northeast, and probably is the result of deformation related to monocline formation. Such deformation resulted in a series of basement-cored blocks that dipped gently to the northeast and that were bounded by the northwest-striking monoclines. Northwest-striking normal faults having displacement down to the south were formed between monoclines, but none are recognized in the study area. The combination of monocline formation and

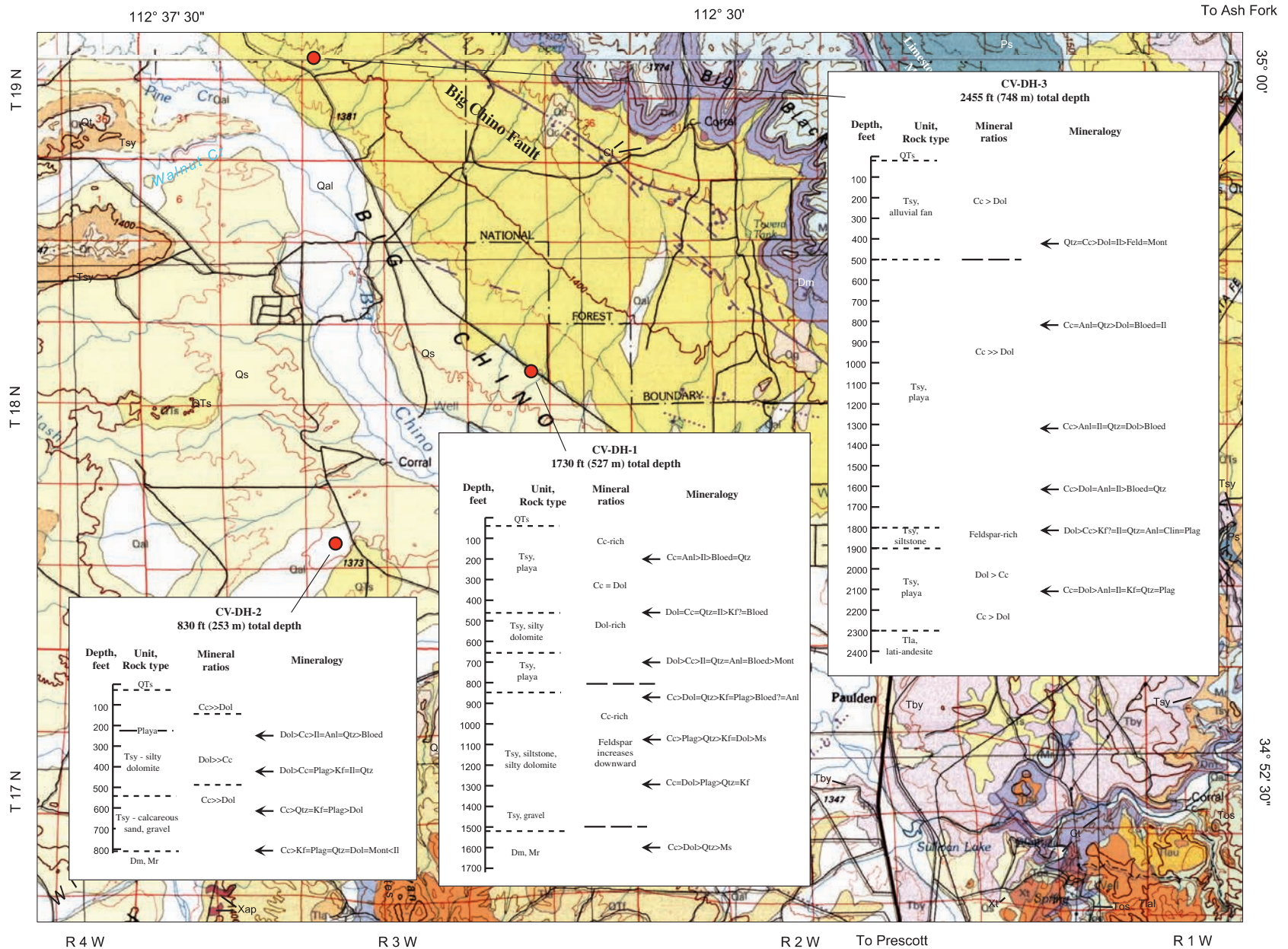


**Figure B10.** Lithologic logs showing mineralogy of playa deposits and other basin-fill units, Big Chino Valley. Location of Bureau of Reclamation drill holes (Ostenaa and others, 1933b) shown. Abbreviation of units as in figures 2 and 3. Cc, calcite; Dol, dolomite; Il, illite; Anl, analcime; Qtz, quartz; Bloed, bloedite(?); Plag, plagioclase; Kf, potassium feldspar; Mont, montmorillonite; Ms, muscovite; Feld, feldspar; Clin, clinoptilolite.

normal faulting created a dip slope of Paleozoic strata that rose gently to the southwest, away from the Colorado Plateau. Paleozoic rocks therefore were stripped from the basement in the southern part of the study area.

A northeast-striking pair of high-angle reverse faults cuts the Paleozoic rocks and Proterozoic basement between Lower Granite Spring and the Verde River (Krieger, 1965). The faults project beneath undeformed Tertiary latite to the northeast, and must, therefore, be older than about 24 Ma. The extent of these faults to the southwest is unknown. A concealed normal fault having displacement down to the east is suggested west of the town of Chino Valley, along or slightly east of Big Wash (fig. B2). On the northwestern side of the fault, trachyandesite of the Hickey Formation rests on Proterozoic basement. On the southeastern side of the fault, logs of water wells suggest a minimum of 70 m of sediment and latite separating the trachyandesite from underlying basement. The fault would be pre-Hickey in age, as the trachyandesite does not appear to be offset.

### Quaternary to Late Tertiary Faults

Big Chino Valley is a northwest-trending late Tertiary graben that is bordered on the northeast by the Big Chino Fault. Only about one-third of the total length of the fault is in the study area. At the northern margin of the study area, near CV-DH-3, the fault has at least 1100 m of displacement (fig. B3). The fault decreases in displacement to the southeast and dies in a series of horsetail splays north of Paulden. Latest movement on the fault is pre-Holocene (Menges and Pearthree, 1983; Pearthree, 1998). At the surface, the Big Chino Fault displaces alluvial fan material 8-10 m down toward the basin over a length of more than 45 km.

The Big Chino Fault is only 1.6 km northeast of CV-DH-3, but there is little evidence of fault-related sediments in the well log (fig. B10). From the base of latite to the covering alluvial fan, there are no conglomerates such as would be expected from erosion of the uplifted block along a normal fault. Instead, the entire interval contains fine-grained playa sediments. In the Verde Valley to the southeast, conglomeratic sediments shed from the uplifted block of the Verde Fault are numerous in the basin sediments near the fault (Anderson and Creasey, 1967; Nations and others, 1981). Perhaps displacement on the Big Chino Fault during the time of playa development did not produce a significant topographic block on the upthrown side. Rather, uplift on the northeastern side may have kept pace with subsidence on the southwestern side. Significant topographic relief on the upthrown side of the fault is signaled by the appearance of alluvial fan deposits overlying the playa sediments, at a depth of about 150 m (fig. B10).

The southwestern side of the valley north of Sullivan Buttes contains a number of small faults having various senses of displacement (fig. B11B). The southernmost of these faults increases in displacement from about 100 m (in T17N, R2W, Sec. 7) to the northwest. Northwest of Kayfour the presumed northwestern extension of the fault has a minimum of 300 m

of offset, as determined from displacement of latite to the west in drillhole B(18-3) 35DA, drilled to a depth of 260 m (Ostenaar and others, 1993b). Across Williamson Valley to the northwest, a lack of deep water wells hinders interpretation of buried faults. Northwest of the study area, near Limestone Peak (fig. B1), displacement on a concealed normal fault that may border the basin on the south is about 220 m, as calculated from displacement of the Redwall Limestone.

The inception and duration of normal faulting in Big Chino Valley and along the Big Chino Fault is difficult to determine. Regional extension took place after deposition of the youngest flows in the Hickey Formation at 10 Ma. The Big Chino basin probably started to form at about 8-10 Ma. By 6 Ma, parts of the basin had a topographic form similar to its present-day shape, with cliffs of Paleozoic strata on the north side. Basalt flowed over these cliffs and into the valley northeast of the map area, south of Picacho Butte (fig. B1), by about 6 Ma. At 5.5 Ma basalt flowed into the northwestern end of the valley from sources in the northeastern Juniper Mountains (Goff and others, 1983; Arney and others, 1985), and at 4.5 Ma, basalt flowed into the southeastern end of the basin. Central parts of the valley may have continued to subside slowly and form playa deposits after 4.5 Ma. The first significant topographic relief across the fault is indicated by thick alluvial fan material that overlies the playa deposits.

The northern end of Little Chino Valley, south of outcrops of the Mazatzal Group, likely is bounded by a largely concealed normal fault(s) that strikes northwest (fig. B2). Part of the fault(s) is mapped southeast of Del Rio Springs and has displacement down to the west, as would be expected for a basin-bounding fault. The fault(s) may step to the south, away from bedrock exposures (fig. B12B), as suggested by logs of water wells near Granite Creek. Displacement across the fault segments is difficult to determine, as no wells are drilled deep enough to penetrate both sediment fill and latite, but may exceed 180 m near Del Rio Springs. Farther southeast, near Granite Creek, displacement appears to be less, about 100 m. A concealed normal fault that forms part of the southwestern side of the basin is suggested by logs of water wells (fig. B12B). The northwest-striking fault, which may have less than 50 m of displacement, passes beneath the town of Chino Valley and extends toward Lonesome Valley.

Two small, northwest-striking faults that are exposed south of Del Rio Springs (fig. B2) have displacement, determined from surface ruptures (Pearthree, 1998), of down to the north, opposite to that of the basin-bounding fault(s). Although this opposing sense of displacement could suggest formation of a local graben, groundwater withdrawal in far northern Little Chino Valley (Schwalen, 1967) also could be causing surface ruptures that have displacement down to the north.

The western side of northern Little Chino Valley west of Del Rio Springs may not be bounded by a laterally continuous late Tertiary fault, as suggested by some previous work (Ostenaar and others, 1993b). Rather, alluvial fans extend away from latite flows and intrusive rocks and thicken into Little Chino Valley. A buried normal fault could be concealed

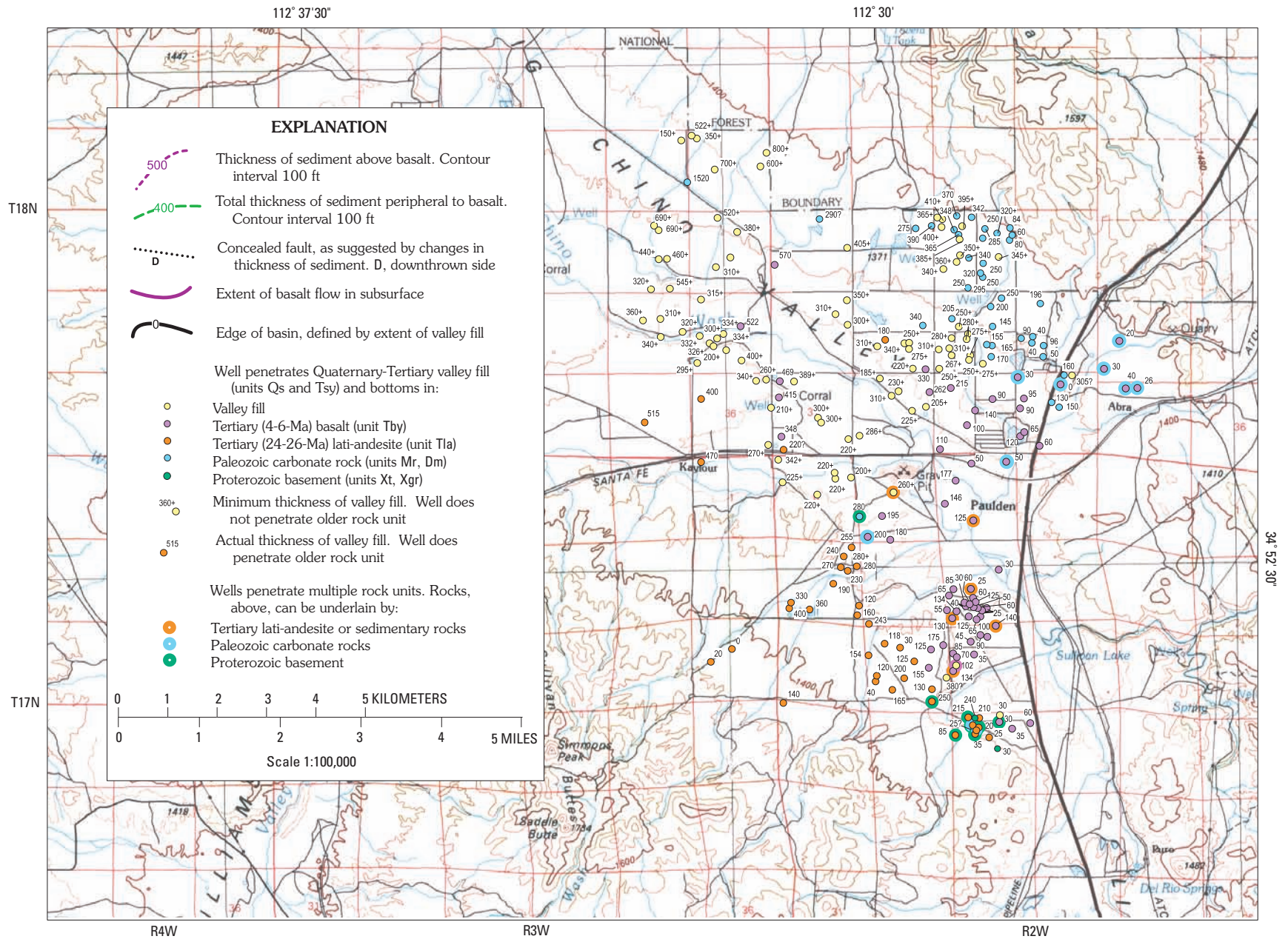


**Figure B11 (above and facing page).** (A), Map showing thickness of Quaternary and Tertiary basin fill above 4-6-Ma basalt flows in southeastern Big Chino Valley. (A) Locations of wells and thickness determinations. (B), Isopachs of sediment thickness above basalt and locations of buried faults.



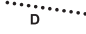












112° 37' 30"

112° 30"

T18N

T17N

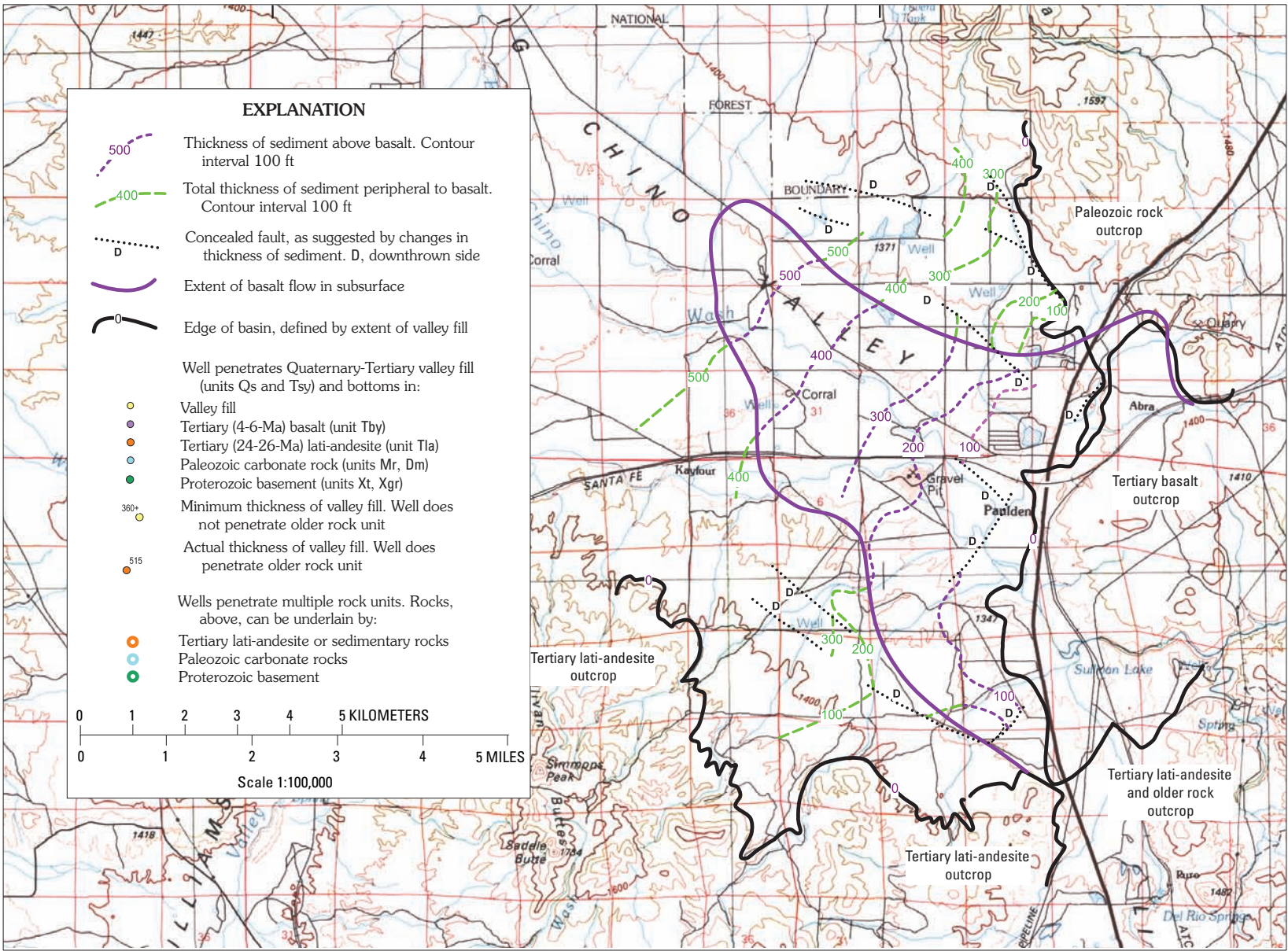
### EXPLANATION

-  Thickness of sediment above basalt. Contour interval 100 ft
-  Total thickness of sediment peripheral to basalt. Contour interval 100 ft
-  Concealed fault, as suggested by changes in thickness of sediment. D, downthrown side
-  Extent of basalt flow in subsurface
-  Edge of basin, defined by extent of valley fill
- Well penetrates Quaternary-Tertiary valley fill (units Qs and Tsy) and bottoms in:
  -  Valley fill
  -  Tertiary (4-6-Ma) basalt (unit Tby)
  -  Tertiary (24-26-Ma) lati-andesite (unit Tla)
  -  Paleozoic carbonate rock (units Mr, Dm)
  -  Proterozoic basement (units Xt, Xgr)
-  360+ Minimum thickness of valley fill. Well does not penetrate older rock unit
-  515 Actual thickness of valley fill. Well does penetrate older rock unit
- Wells penetrate multiple rock units. Rocks, above, can be underlain by:
  -  Tertiary lati-andesite or sedimentary rocks
  -  Paleozoic carbonate rocks
  -  Proterozoic basement

0 1 2 3 4 5 KILOMETERS

0 1 2 3 4 5 MILES

Scale 1:100,000



R4W

R3W

R2W

36° 52' 30"

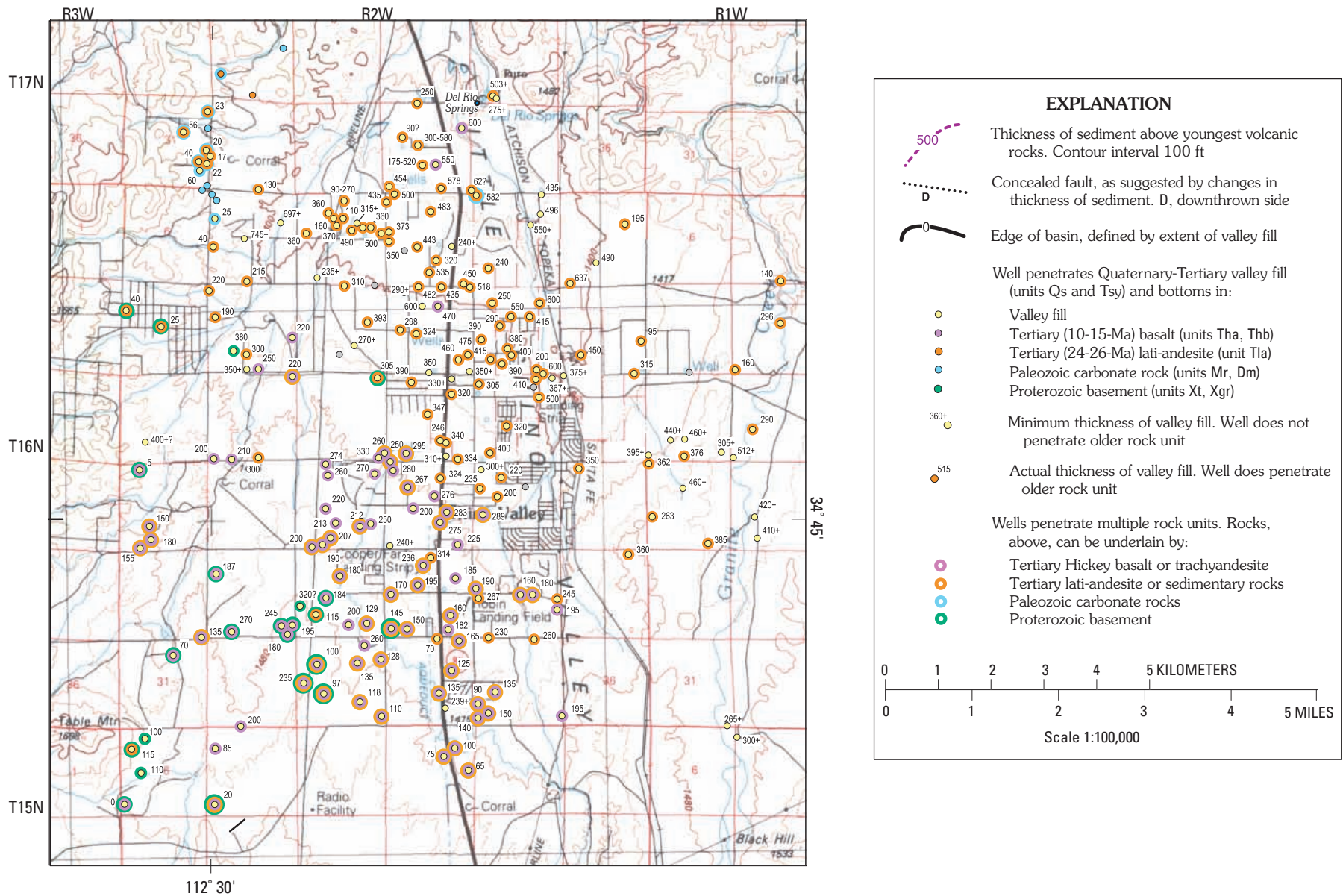
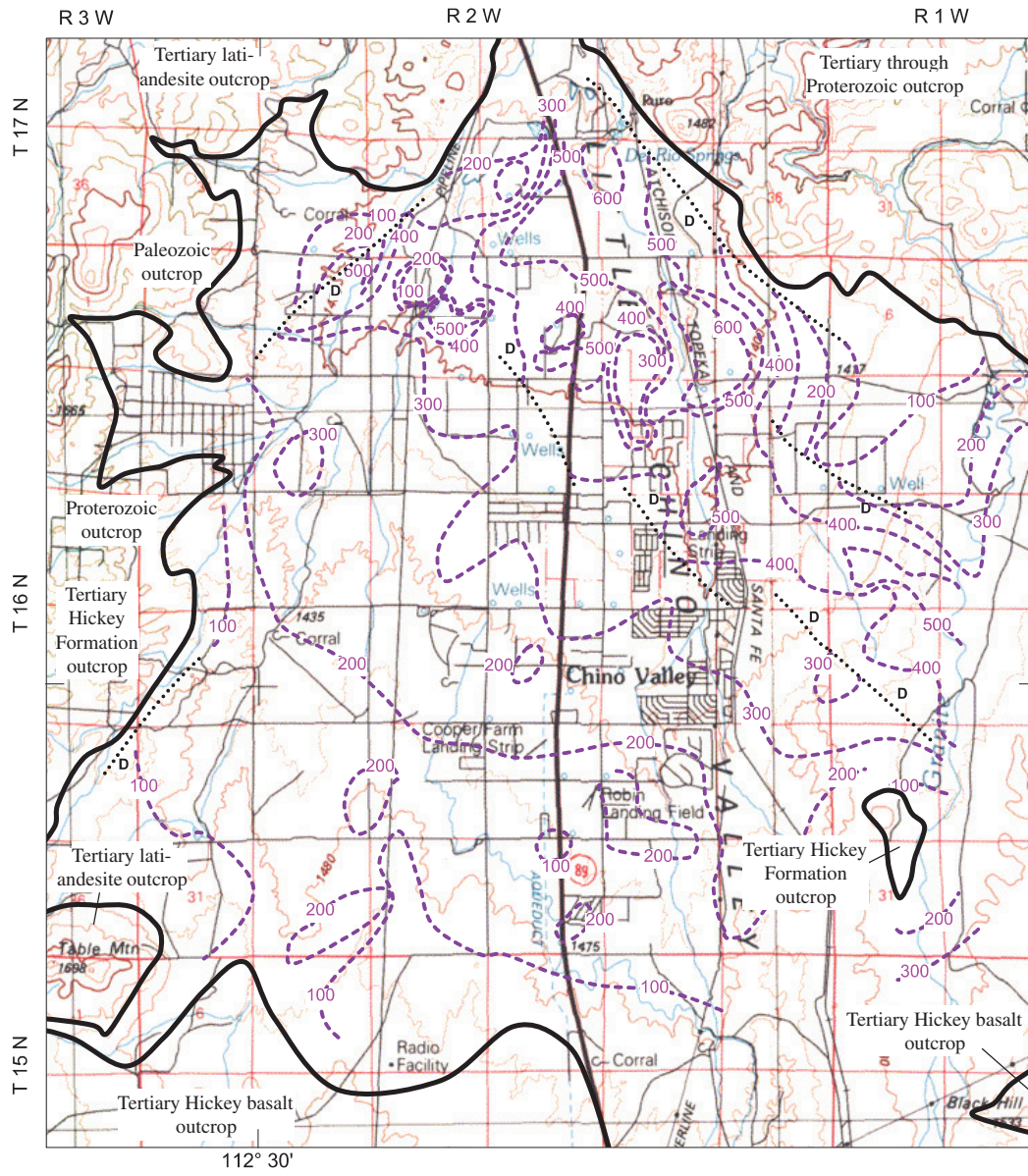


**Figure B12 (above and facing page).** Maps showing thickness of Quaternary and Tertiary basin fill above youngest Tertiary volcanic units in northern Little Chino Valley. (A), Location of wells and schematic logs showing thickness of Quaternary and Tertiary basin fill above youngest Tertiary volcanic units. (B), Isopachs of thickness of Quaternary and late Tertiary basin fill above youngest Tertiary volcanic units, and locations of buried faults, northern Little Chino Valley



**EXPLANATION**

- Thickness of sediment above youngest volcanic rocks. Contour interval 100 ft
- Concealed fault, as suggested by changes in thickness of sediment. D, downthrown side
- Edge of basin, defined by extent of valley fill

Wells penetrate Quaternary-Tertiary valley fill (units Qs and Tsy) and bottoms in:

- Valley fill
- Tertiary (10-15-Ma) basalt (units Tha, Thb)
- Tertiary (24-26-Ma) lati-andesite (unit Tla)
- Paleozoic carbonate rock (units Mr, Dm)
- Proterozoic basement (units Xt, Xgr)

Minimum thickness of valley fill. Well does not penetrate older rock unit

Actual thickness of valley fill. Well does penetrate older rock unit

Wells penetrate multiple rock units. Rocks, above, can be underlain by:

- Tertiary Hickey basalt or trachyandesite
- Tertiary lati-andesite or sedimentary rocks
- Paleozoic carbonate rocks
- Proterozoic basement

0 1 2 3 4 5 KILOMETERS  
0 1 2 3 4 5 MILES  
Scale 1:100,000



beneath the fans, toward the center of the basin, but drillhole data are lacking to prove the continuity of such a fault. To the south, Big Wash is a linear, north-northeast striking feature that has been suggested to be underlain by a fault. North of Table Mountain, along Big Wash, a pre-Hickey, northeast-striking normal fault is present (fig. B12B). Because of the presence of this fault, we cannot dismiss the possibility that the northern part of Big Wash could be underlain by a pre-Hickey fault.

## Conclusions

Synthesis of the geology, geochemistry, and geophysics of rock units in the area resulted in significant additions to understanding of how Miocene basins formed in both Big and Little Chino valleys. Geologic mapping enabled Proterozoic basement rocks to be projected beneath the basins from surrounding outcrops. Geochemical investigations and aerial radiometric data allowed the separation of Oligocene latite from Miocene and younger basalt. X-ray diffraction data substantiated the presence of playa deposits containing fine-grained carbonate-rich sediments rich in analcime and possibly containing bloedite(?) in the deepest part of Big Chino Valley. Aerial magnetic data revealed the location of buried Proterozoic basement rocks. Synthesis of data from well logs enabled mapping of buried Oligocene latite and Miocene and younger basaltic rocks beneath basin fill in Big and Little Chino valleys. Locations of probable concealed normal faults in the two basins were interpreted from rapid apparent thickness changes of sediment. Data from aerial magnetic surveys revealed the location of buried intrusive centers of latite and basalt.

Within the study area, the basin underlying Big Chino Valley contains at least 700 m of Miocene and younger basin fill that rests regionally on Paleozoic strata, and locally on Oligocene latite. Much of the deepest part of the basin contains sediment deposited in a playa. Alluvial fans supplied clastic sediment to the playa from the west and south. The basin probably had internal drainage from its inception at about 8-10 Ma through 4-5 Ma, when basalt flows from the Colorado Plateau entered the valley from the west, north, and southeast. Continued subsidence in the central part of the basin after 4-5 Ma resulted in deposition of additional playa sediments. Coarse-grained fanglomerate deposited adjacent to the Big Chino Fault overlies the playa sediment and indicates significant topographic relief across the fault only late in its movement history.

The basin underlying northern Little Chino Valley contains less than 200 m of Miocene and younger basin fill that rests on a buried volcanic field of Oligocene latite and Miocene and younger basalt. The complex pattern of buried latite and basalt reveals paleovalleys and topographic highs concealed by the Miocene and younger basin fill. No playa sediments are documented in the basin fill, which is characterized by fanglomerate and finer-grained alluvial

sediment derived from the south, west, and southeast. Formation of the basin is believed to have taken place during the same interval as the basin in Big Chino Valley, but direct geochronologic data are lacking. No 4.5-6-Ma basalt flows are known in the northern part of the valley. A normal fault along the northeast margin of the basin has at least 180 m of displacement, and probably was active during formation of the basin.

## References Cited

- Anderson, C.A., and Blacet, P.M., 1972a, Precambrian geology of the northern Bradshaw Mountains, Yavapai County, Arizona: U.S. Geological Survey Bulletin 1336, 82 p.
- Anderson, C.A., and Blacet, P.M., 1972b, Geologic map of the Mount Union quadrangle, Yavapai County, Arizona: U.S. Geological Survey Geologic Quadrangle Map GQ-997, scale 1:62,500.
- Anderson, C. A., and Creasey, S.C., 1958, Geology and ore deposits of the Jerome area, Yavapai County, Arizona, *with sections on the United Verde Extension mine by G.W.H. Norman and on the Cherry Creek mining district by R.E. Lehner*: U.S. Geological Survey Professional Paper 308, 185 p.
- Anderson, C.A., and Creasey, S.C., 1967, Geologic map of the Mingus Mountain quadrangle, Yavapai County, Arizona: U.S. Geological Survey Map GQ-715, scale 1:62,500.
- Arculus, R.J., and Smith, D., 1979, Eclogite, pyroxenite and amphibolite inclusions in the Sullivan Buttes latite, Chino Valley, Yavapai County, Arizona, *in* Boyd, F.R., and Meyer, H.O.A., eds., *The mantle sample; inclusions in kimberlites and other volcanics: Proceedings of the second international kimberlite conference*; v. 2, p. 309-317.
- Arizona Department of Water Resources, 2003, Arizona Registry of Wells 55 CD-ROM, updated June, 2003.
- Arney, Barbara, Goff, Fraser, and Eddy, A.C., 1985, Chemical, petrographic, and K-Ar age data to accompany reconnaissance geologic strip map from Kingman to south of Bill Williams Mountain, Arizona: Los Alamos National Laboratory Report LA-10409-HDR, 26 p.
- Ash, Nathan, A., 1997, Physical volcanology of the Santa Maria Mountains volcanic field, Yavapai County, Arizona: Flagstaff, Northern Arizona University, M.S. thesis, 102 p.
- Baedecker, P.A., Grossman, J.N., and Buttleman, K.P., 1998, National Geochemical Data Base; PLUTO Geochemical data base for the United States: U.S. Geological Survey Digital Data Series DDS-47, CD-ROM.
- Bates, R.L., and Jackson, J.A., ed., 1980, *Glossary of Geology*: American Geological Institute, Falls Church, Virginia, 286 p.

- Beus, S.S., 1989, Devonian and Mississippian geology of Arizona, *in* Jenney, J.P., and Reynolds, S.J., eds., *Geologic evolution of Arizona: Tucson, Arizona Geological Society Digest 17*, p. 287-312.
- Bowie, S. H. U., Dawson, J., Gallagher, M. J., Ostle, D., Lambert, R., St J., Lawson, R. I., 1966, Potassium-rich sediments in the Cambrian of northwest Scotland: Institution of Mining and Metallurgy, Transactions, Section B: Applied Earth Science, vol.75, p.125-145.
- Bowie, S. H. U., Dawson, J., Gallagher, M. J., Ostle, D., 1967, Potassium-rich sediments in the Cambrian of northwest Scotland [discussion]: Institution of Mining and Metallurgy, Transactions, Section B: Applied Earth Science, vol.76, p.60-69.
- Bradshaw, E.D., 1974, Structure in Mazatzal quartzite, Del Rio, Arizona [abs.]: Geological Society of America Abstracts with Programs, v. 6, p. 426-427.
- Chamberlain, K.R., Karlstrom, K.E., and Bowring, S.A., 1991, U-Pb age constraints on deposition of the quartzite at Del Rio and 1.72 Ga deformation in the Chino Valley area, northern Yavapai County, Arizona [abs.]: Geological Society of America Abstracts with Programs, v. 23, p. no. 4, p. 11.
- Davis, G.H., 1978, Monocline fold pattern of the Colorado Plateau, *in* Matthews, V. III, ed., *Laramide folding associated with basement block faulting in the western United States: Geological Society of America Memoir 151*, p. 215-233.
- De la Roche, H., Leterrier, J., Grandclaude, P., and Marchal, M., 1980, A classification of volcanic and plutonic rocks using  $R_1R_2$ -diagram and major-element analyses--its relationships with current nomenclature: *Chemical Geology*, v. 29, p. 183-210.
- DeWitt, Ed, Langenheim, V.E., Force, Eric, Vance, Kelly, and Lindberg, P.A., *with* a digital database by Doug Hirschberg, Guy Pinhassi, and Nancy Shock, *in press*, Geologic map of the Prescott National Forest and headwaters of the Verde River, Yavapai and Coconino Counties, Arizona: U.S. Geological Survey Miscellaneous Investigations Map I-xxxx, scale 1:100,000, two sheets.
- DeWitt, Ed, Zech, R.S., Chase, C.G., Zartman, R.E., Kucks, R.P., Bartelson, Bruce, Rosenlund, G.C., and Earley, Drummond, III., 2002, Geologic and aeromagnetic map of the Fossil Ridge area and vicinity, Gunnison County, Colorado: U.S. Geological Survey, Geologic Investigations Series Map I-2738, scale 1:30,000 and pamphlet.
- DeWitt, Ed, 1989, Geochemistry and tectonic polarity of Early Proterozoic (1700-1750 Ma) plutonic rocks, north-central Arizona, *in* Jenney, J.P., and Reynolds, S.J., eds., *Geologic evolution of Arizona: Tucson, Arizona Geological Society Digest 17*, p.149-163.
- Ewing, D.B., Osterberg, J.C., Talbot, R.W., 1994, Groundwater Study of the Big Chino Valley—hydrology and hydrogeology: Bureau of Reclamation Technical Report, Denver, Colorado, 14 p. plus 6 appendices.
- Fridrich, C.J., DeWitt, Ed, Bryant, Bruce, and Smith, R.P., 1998, Geologic map of the Collegiate Peaks Wilderness Area and the Grizzly Peak caldera, central Sawatch Range, Colorado: U.S. Geological Survey Miscellaneous Investigations Map I-2565, scale 1:50,000, 1 sheet and pamphlet.
- Goff, F.E., Eddy, A.C., and Arney, B.H., 1983, Reconnaissance geologic strip map from Kingman to south of Bill Williams Mountain, Arizona: Los Alamos National Laboratory Map LA-9202, scale 1:48,000.
- Hereford, Richard, 1975, Chino Valley Formation (Cambrian?) in northwestern Arizona: Geological Society of America Bulletin, v. 86, p. 677-682.
- Hutcheon, Ian, Bloch, John, de Caritat, Patrice, Shevalier, Maurice, Abercrombie, Hugh, Longstaffe, Fred J.A.F., 1998, What is the cause of potassium enrichment in shales?, *in* Schieber, Juergen, Zimmerle, Winfried, Sethi, Parvinder S., editors, *Shales and mudstones: II, Petrography, petrophysics, geochemistry, and economic geology: E. Schweizerbart'sche Verlagsbuchhandlung Naeglele u. Obermiller, Stuttgart, Federal Republic of Germany*, 60 p.
- Krieger, M.H., 1965, Geology of the Prescott and Paulden quadrangles, Arizona: U.S. Geological Survey Professional Paper 467, 127 p.
- \_\_\_\_\_, 1967a, Reconnaissance geologic map of the Turkey Canyon quadrangle, Yavapai County, Arizona: U.S. Geological Survey Miscellaneous Geologic Investigations Map I-501, scale 1:62,500.
- \_\_\_\_\_, 1967b, Reconnaissance geologic map of the Picacho Butte quadrangle, Yavapai and Coconino Counties, Arizona: U.S. Geological Survey Miscellaneous Geologic Investigations Map I-501, scale 1:62,500.
- \_\_\_\_\_, 1967c, Reconnaissance geologic map of the Simmons quadrangle, Yavapai County, Arizona: U.S. Geological Survey Miscellaneous Geologic Investigations Map I-503, scale 1:62,500.
- Krieger, M.H., Creasey, S.C., and Marvin, R.F., 1971, Ages of some Tertiary andesitic and latitic volcanic rocks in the Prescott-Jerome area, north-central Arizona, *in* Geological Survey Research 1971-U.S. Geological Survey Professional Paper 750-B, p. B-157-B160.
- Langenheim, V.E., Duval, J.S., Wirt, Laurie, and DeWitt, Ed, 2000, Preliminary report on geophysics of the Verde River headwaters region, Arizona: U.S. Geological Survey Open-File Report 00-403, 28 p.

- Lehner, R.E., 1958, Geology of the Clarkdale quadrangle, Arizona: U.S. Geological Survey Bulletin 1021-N, p. 511-592, 1 plate, scale 1:48,000.
- McKee, E.D., and McKee, E.H., 1972, Pliocene uplift of the Grand Canyon region – time of drainage adjustment: Geological Society of America Bulletin, v. 83, p. 1923-1932.
- McKee, E.H., and Anderson, C.A., 1971, Age and chemistry of Tertiary volcanic rocks in north-central Arizona and relation of the rocks to the Colorado Plateau: Geological Society of America Bulletin, v. 82, p. 2767-2782.
- Meddough, W.S., and Salotti, C.A., 1983, Mineralogy and geochemistry of Green River Formation oil shales, C-A tract, Colorado: Oil Shale Symposium Proceedings, v. 16, p. 113-123.
- Menges, C.M., and Pearthree, P.A., 1983, Map of neotectonic (latest Pliocene-Quaternary) deformation in Arizona: Arizona Bureau of Geology and Mineral Technology, Open-File Report 83-22, 48 p.
- Nations, J.D., Hevly, R.H., Blinn, D.W., and Landye, J.J., 1981, Paleontology, paleoecology, and depositional history of the Miocene-Pliocene Verde Formation, Yavapai County, Arizona, *in* Stone, Claudia, and Jenney, J.P., eds.: Arizona Geological Society Digest, v. 13, p. 133-149.
- Nichols Boyd, Beth, 2001, Thumb Butte; a latite among Tertiary basalts, *in* Erskine, M.C., Faulds, M.E., Bartley, J.M., and Rowley, P.D., eds., The geologic transition, high plateaus to Great Basin; a symposium and field guide; the Mackin volume: Utah Geological Association publication 30, Pacific Section AAPG Guidebook GB78, p. 305-312.
- Ostenaar, D.A., Schimschal, U.S., King, C.E., Wright, J.W., Furgerson, R.B., Harrel, H.C., and Throner, R.H., 1993a, Big Chino Valley groundwater study: Geologic framework investigations: Bureau of Reclamation, Denver, CO, 31 p.
- Ostenaar, D.A., Schimschal, Ulrich, King, C.E. Jr., and Wright, J.W., 1993b, Big Chino Valley groundwater study – geologic framework investigations: U.S. Bureau of Reclamation Seismotectonic Report 93-2, vol. 1, Report and plates, 31 p., 9 plates, scale about 1:40,000, vol. 2, Appendices.
- Palache, Charles, Berman, Harry, and Frondel, Clifford, 1957, The System of Mineralogy: John Wiley and Sons, London, v. II, 1124 p.
- Pearthree, P.A., 1998, Quaternary fault data and map for Arizona: Arizona Geological Survey Open-File Report 98-24, 122 p., 1 sheet, 1:750,000 scale.
- Remy, R.R., and Ferrell, R.E., 1989, Distribution and origin of analcime in marginal lacustrine mudstones of the Green River Formation, south-central Uinta Basin, Utah: Clays and Clay Minerals, v. 37, p. 419-432.
- Rosen, M.R., 1994, The importance of groundwater in playas; a review of playa classifications and the sedimentology and hydrology of playas: Geological Society of America Special Paper 289, 18 p.
- Schwalen, H.C., 1967, Little Chino Valley artesian area and groundwater basin: Technical Bulletin 178, Agricultural Experiment Station, University of Arizona, Tucson, Arizona, 63 p.
- Silver, L.T., Conway, C.M., and Ludwig, K.R., 1986, Implications of a precise chronology for Early Proterozoic crustal evolution and caldera formation in the Tonto Basin-Mazatzal Mountains region, Arizona [abs.]: Geological Society of America Abstracts with Programs, v. 18, p. 413.
- Spencer, J.E., and Reynolds, S.J., 1989, Middle Tertiary tectonics of Arizona and adjacent areas, *in* Jenney, J.P., and Reynolds, S.J., eds., Geologic evolution of Arizona: Tucson, Arizona Geological Society Digest 17, p.539-574.
- Tyner, Grace Nell, 1984, Geology and petrogenesis of the Sullivan Buttes latite, Yavapai County, Arizona; field and geochemical evidence: Austin, University of Texas, Ph.D. dissertation, 286 p.
- Ward, Sonja, A., 1993, Volcanic stratigraphy of a portion of the Sullivan Buttes latite, Chino Valley, Arizona: Flagstaff, Northern Arizona University, M.S. Thesis, 60 p.
- Water Resource Associates, Inc., 1991. Application for a Subdivision Water Adequacy Statement, Headwaters Ranch Project, Paulden, Arizona: Certified by Stephen Noel, May 10, 1991.
- Water Resource Associates, Inc., 1990, Hydrogeology investigation of Big Chino Valley, Yavapai County, Arizona: Phase II, Volume III, 42 p. plus well logs. Reports for city of Prescott, City Attorney's Office, Prescott; available from city of Prescott.
- Water Resource Associates, Inc., 1989, Hydrogeology investigation, Big Chino Valley, Yavapai county, Arizona, Phase I, Volumes I & II: Reports for city of Prescott, City Attorney's Office, Prescott; available from city of Prescott.
- Witke, J.H., Smith, Douglas, and Wooden, J.L., 1989, Origin of Sr, Nd, and Pb isotopic systematics in high-Sr basalts from central Arizona: Contribution to Mineralogy and Petrology, v. 101, p. 57-68.
- Wolfe, E.W., 1983, Geologic map of the Arnold Mesa Roadless Area, Yavapai County, Arizona: U.S. Geological Survey Miscellaneous Field Studies Map MF- 1577-B, scale 1:24,000.



# **Geophysical Framework Based on Analysis of Aeromagnetic and Gravity Data, Verde River Headwaters, North-Central Arizona**

By V.E. Langenheim, Ed DeWitt, and Laurie Wirt

Chapter C

## **Geologic Framework of Aquifer Units and Ground-Water Flowpaths, Verde River Headwaters, North-Central Arizona**

Edited by Laurie Wirt, Ed DeWitt, and V.E. Langenheim

Prepared in cooperation with the Arizona Water Protection Fund Commission

Open-File Report 2004–1411-C

**U.S. Department of the Interior  
U.S. Geological Survey**

**U.S. Department of the Interior**  
Gale A. Norton, Secretary

**U.S. Geological Survey**  
P. Patrick Leahy, Acting Director

U.S. Geological Survey, Reston, Virginia: 2005

For product and ordering information:

World Wide Web: <http://www.usgs.gov/pubprod>

Telephone: 1-888-ASK-USGS

For more information on the USGS--the Federal source for science about the Earth, its natural and living resources, natural hazards, and the environment:

World Wide Web: <http://www.usgs.gov>

Telephone: 1-888-ASK-USGS

Any use of trade, product, or firm names is for descriptive purposes only and does not imply endorsement by the U.S. Government.

Although this report is in the public domain, permission must be secured from the individual copyright owners to reproduce any copyrighted materials contained within this report.

***Suggested citation:***

Langenheim, V.E., DeWitt, E., and Wirt, L., 2005, Geophysical Framework Based on Analysis of Aeromagnetic and Gravity Data, Verde River Headwaters, North-Central Arizona: *in* Wirt, Laurie, DeWitt, Ed, and Langenheim, V.E., eds., Geologic Framework of Aquifer Units and Ground-Water Flowpaths, Verde River Headwaters, North-Central Arizona: U.S. Geological Survey Open-File Report 2004-1411-C, 25 p.

## Contents

Abstract.....	1
Introduction.....	1
Acknowledgments .....	1
Data and Methods .....	1
Aeromagnetic and Gravity Data .....	1
Filtering Techniques .....	3
Wavelength Separation .....	3
Geophysical Boundaries .....	3
Drill Holes and Physical Properties .....	3
Geophysical Anomalies .....	14
Depth to Basement Method .....	15
Results .....	16
Depth to Basement.....	16
Playa Deposit/Alluvial Fans.....	22
Distribution of Volcanic Rocks in Subsurface.....	22
Conclusions and Recommendations .....	24
References Cited.....	24

## Figures

<b>C1.</b> Shaded-relief topographic map of study area.....	2
<b>C2.</b> Aeromagnetic (reduced to pole) map of the study area .....	4
<b>C3.</b> Isostatic gravity.....	5
<b>C4a.</b> Aeromagnetic filtered bandpass-filtered to enhance shallow sources.....	6
<b>C4b.</b> Aeromagnetic field bandpass-filtered to enhance deep sources.....	7
<b>C5.</b> First vertical derivative of the magnetic field.....	8
<b>C6.</b> Aeromagnetic field filtered to enhance shallow sources.....	9
<b>C7.</b> Filtered gravity field to enhance shallow sources .....	10
<b>C8.</b> Pseudogravity map of the study area.....	11
<b>C9.</b> Density and magnetic boundaries .....	12
<b>C10.</b> Average densities of Tertiary sedimentary rocks derived from various methods .....	15
<b>C11.</b> Schematic representation of basin-basement separation.....	16
<b>C12a.</b> Thickness of Cenozoic sedimentary and volcanic fill using the density-depth function of Tucci and others (1982).....	18
<b>C12b.</b> Thickness of Cenozoic sedimentary and volcanic fill using a density-depth function derived from resistivity logs .....	19
<b>C13.</b> Mismatch between basin thickness encountered in wells that did not encounter pre-Cenozoic bedrock and predicted basin thickness from the gravity inversion.....	20
<b>C14.</b> Basement gravity (Model 2) based on density-depth function derived from resistivity.....	21
<b>C15.</b> Interpretive map of study area. Geology on shaded-relief topography with magnetic boundaries .....	(oversized)

## Tables

<b>C1.</b> Densities ( $\text{g/cm}^3$ ) and magnetic susceptibilities ( $10^{-3}$ cgs units) .....	13
<b>C2.</b> Density-depth function .....	16

# Geophysical Framework Based on Analysis of Aeromagnetic and Gravity Data

By V.E. Langenheim, Ed DeWitt, and Laurie Wirt

## Abstract

Analysis of aeromagnetic and gravity data provides new insights on the geometry of geologic structures in the Verde River headwaters region. Magnetic anomalies reveal hidden volcanic rocks lying at shallow depths beneath the ground surface. For example, semicircular magnetic lows can be used to map the extent of shallowly buried (less than 200–300 meters) latite-andesite plugs. In contrast, Tertiary basalts produce worm-like anomaly patterns. The geophysical data also can be used to detect concealed faults within the study area. The Big Chino fault has the largest amount of vertical throw of any fault in the study area based on gravity, magnetic, and limited well data. The pervasive magnetic grain within Little Chino Valley is northeast- and northwest-striking, but apparently none of the structures responsible for this grain appear to have large vertical offsets like the Big Chino fault. Gravity data indicate 1–2 kilometers of basin fill beneath Big Chino Valley. Based on gravity inversions for basin thickness, the volume of total sediment in Big Chino Valley within the study area is estimated to be 140.2 to 158.4 cubic kilometers (1.14 to 1.29 x 10<sup>8</sup> acre-feet). The areal extent of the Big Chino gravity low coincides with a thick playa deposit delineated by analysis of well data. The lack of a distinct gravity low in Little Chino Valley suggests that the sedimentary and volcanic fill is much thinner (less than 1 kilometer) than that of Big Chino Valley.

## Introduction

The goal of this geophysical study is to improve understanding of the subsurface geologic framework of the Verde River headwaters region (fig. C1). This work builds upon two earlier studies (Ostenaar and others, 1993; Water Resource Associates, 1989) that compiled well data and collected profiles of geophysical data. This study includes a more quantitative and detailed interpretation of aeromagnetic and gravity data collected by the U.S. Geological Survey in 1999–2000 than that presented in Langenheim and others (2000). The emphasis of this chapter is analysis of aeromagnetic and gravity data and how these data provide information on the geometry of geologic structures in the study area. Radiometric

data are more useful for mapping surficial deposits and thus are discussed in Chapter B. The first part of the chapter deals with data methods, analysis, and description; the second part emphasizes the interpretation of the data; their hydrogeologic significance will be discussed in Chapter D.

The aeromagnetic data can be used to detect Tertiary volcanic rocks and certain rock types within the Proterozoic crystalline basement. The gravity data reflect the density contrast between basin sediments and pre-Cenozoic bedrock and density contrasts within the Proterozoic crystalline basement rocks. The analysis of these datasets is an effective tool in defining hidden structures important to ground-water studies, such as the configuration and structural fabric of basement and volcanic rocks beneath Tertiary sedimentary deposits.

## Acknowledgments

We would like to thank the Arizona Water Protection Fund Commission for financial support (Arizona Water Protection Fund Grant 99-078). We appreciate the helpful comments of reviewers Tom Hildenbrand and Bob Jachens (U.S. Geological Survey, Menlo Park, Calif.), John Hoffmann (U.S. Geological Survey, Tucson, Ariz.) and Frank Corkhill (Arizona Dept. of Water Resources).

## Data and Methods

### Aeromagnetic and Gravity Data

Details of the processing techniques of the high-resolution aeromagnetic (and radiometric) data collected for the study are given in Langenheim and others (2000). Flight lines were oriented east-west, spaced 150 meters (.093 mile) apart, and flown at a nominal altitude of 150 meters (500 feet) above terrain, or as low as permitted by the Federal Aviation Administration and safety considerations. North-south control lines were spaced 3.0 kilometers (1.83 miles) apart. Total flight distance was 5,600 kilometers (3,480 miles). To shift anomalies over their respective sources, the magnetic data were reduced to the pole (fig. C2; Blakely, 1996). Accuracy of the data is estimated to be on the order of 0.5 to 1 nanoTesla (nT).



C2 Geophysical Framework of Verde River Headwaters, Arizona

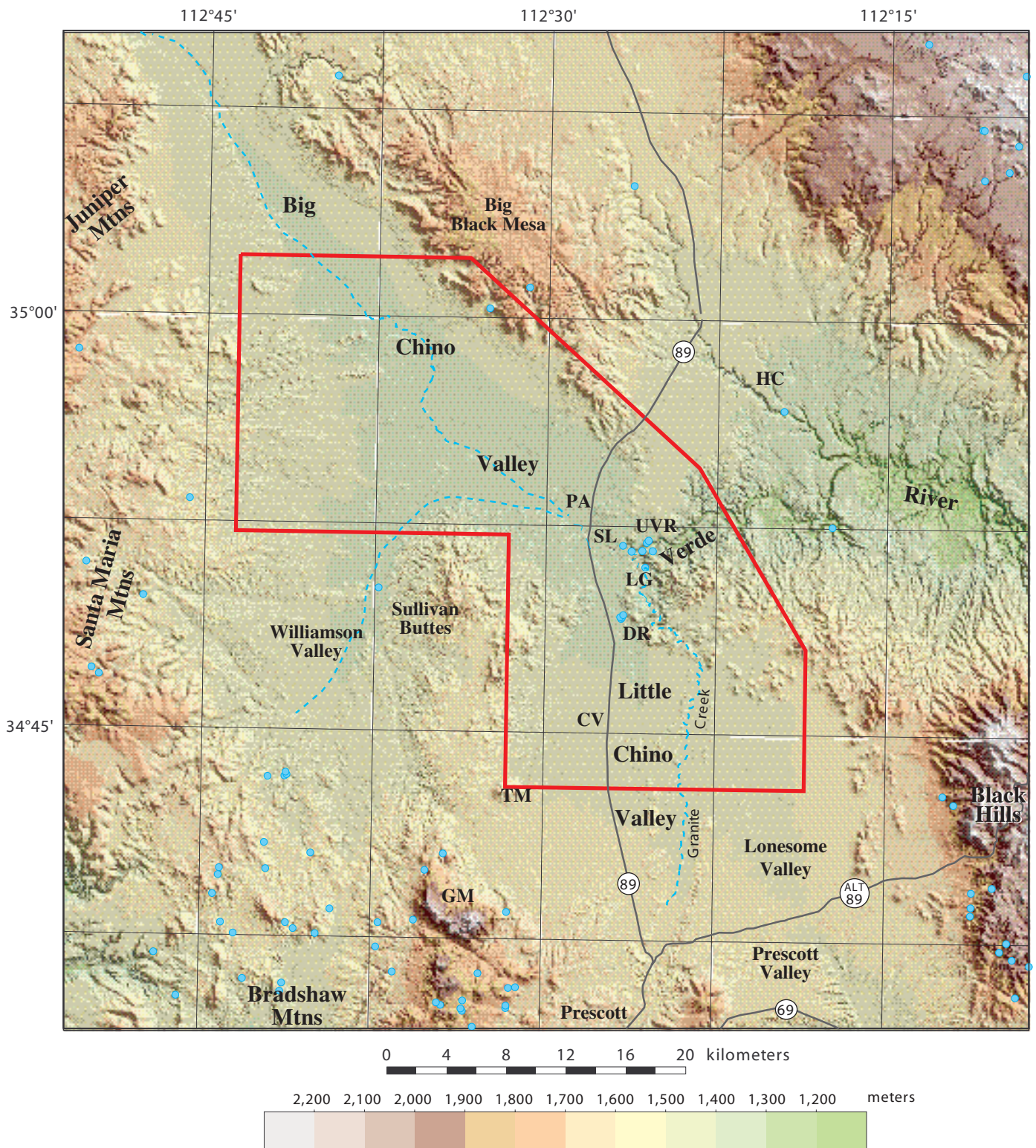


**Figure C1.** Shaded-relief topographic map of the study area. Aeromagnetic survey boundary is shown in red. Blue circles are spring locations. Dashed blue lines, ephemeral streams. UVR, upper Verde River springs; CV, town of Chino Valley; DR, Del Rio springs; GM, Granite Mountain; HC, Hell Canyon; LG, lower Granite Spring; PA, Paulden; SL, Sullivan Lake, TM, Table Mountain. Illumination direction from the northeast.

About 1,160 gravity stations were used to produce an isostatic gravity map of the region (Langenheim and others, 2000; Water Resource Associates, 1989). The isostatic gravity data reflect density variations within the middle and upper crust (fig. C3; Simpson and others, 1986). Details on the processing of these data are given in Langenheim and others (2000). Gravity stations are nonuniformly distributed in the region (fig. C3). Station spacing is on average one station per 2 cubic kilometers, although the station spacing is as low as one station per 10 cubic kilometers even within parts of the Big Chino and Little Chino Valleys. Accuracy of the data is estimated to be on the order of 0.1 to 0.5 milligal (mGal).

## Filtering Techniques

Magnetic and gravity anomalies are produced by a variety of sources that range in size and depth. Superposition of anomalies from multiple sources can result in interpretational ambiguities. For example, both Proterozoic crystalline and Tertiary volcanic rock types are magnetic, but they are characterized by different anomaly wavelengths. Shallow sources typically cause short-wavelength anomalies, whereas deep sources cause long-wavelength anomalies. Generally, Tertiary volcanic rocks, which are comparatively thinner and shallower than Proterozoic crystalline rock, should produce shorter-wavelength anomalies. Several analytical techniques were applied to the geophysical data to enhance particular anomaly characteristics, such as wavelength or trend.

## Wavelength Separation

To emphasize both short-wavelength anomalies caused by shallow sources (for example, Tertiary volcanic rock) and long-wavelength anomalies (for example, Proterozoic crystalline rock), a match filter was applied (Phillips, 2001). Match filtering separates the data into different wavelength components by modeling the observed spectra using two distinct equivalent source layers at increasing depths (see Phillips, 2001). Figures C4a and C4b show the resulting separated fields produced by the dipole equivalent-source layers at 0.320 kilometer and 3.88 kilometers depth, associated with shallow and deep sources, respectively. Another method, the first vertical derivative of the magnetic data (fig. C5) suppresses longer-wavelength trends caused by more deeply buried magnetic rock types (Blakely, 1996). A third method to sharpen the effects of near-surface sources involves analytically upward continuing the magnetic or gravity field by a small interval (100 meters for the magnetic data; 1 kilometer for the gravity data because of the nonuniform distribution of gravity stations). The method of upward continuation is the transformation of magnetic or gravity data measured on one surface to data that would be measured on a higher surface; this operation tends to smooth the data by attenuation of short-wavelength anomalies (Dobrin and Savit, 1988). This smoothed field then is subtracted from the unfiltered field to produce a

residual field. The unfiltered and residual fields (figs. C2, C4, and C6 for the magnetic field; figs. C3 and C7 for the gravity field) illustrate the effectiveness of this approach to highlight subtle geologic features.

To help emphasize the more voluminous magnetic sources (such as those residing in the Proterozoic crystalline basement), the aeromagnetic anomalies are mathematically transformed into pseudogravity (or magnetic potential) anomalies (Baranov, 1957). This procedure effectively converts the magnetic field to the “gravity” field that would be produced if all magnetic material were replaced by proportionately dense material. The transformation (a) removes the dipolar effect of the magnetic field, thereby shifting the anomalies to a position directly over their sources, and (b) amplifies the long-wavelength features at the expense of short-wavelength anomalies (Blakely, 1996). The pseudogravity map is not independent of the map of the magnetic field, but simply a filtered rendition of the magnetic field that emphasizes long-wavelength anomalies (fig. C8).

## Geophysical Boundaries

To help delineate structural trends and gradients expressed in the gravity field, a computer algorithm is used to locate the maximum horizontal gravity gradient (Blakely and Simpson, 1986; fig. C9). Gradient maxima occur approximately over vertical or near-vertical contacts that separate rocks of contrasting densities. For moderate to steep dips (45 degrees to vertical), the horizontal displacement of a gradient maximum from the top edge of an offset horizontal layer is always less than or equal to the depth to the top of the source (Grauch and Cordell, 1987). Magnetization boundaries (fig. C9) were calculated in a similar way as described in Blakely and Simpson (1986), by using the pseudogravity field produced from the residual magnetic field shown in figure C6.

## Drill Holes and Physical Properties

Most of the drill holes in the study area are shallow (less than 100 meters) and do not have detailed or reliable lithologic logs. Well logs can provide critical geologic constraints needed in geophysical modeling and interpretation, but uncertainties in well log data quality limit their utility. This analysis used most of the well logs compiled by Krieger (1965) and Ostenaar and others (1993), augmented by well logs obtained from the Arizona Department of Water Resources (unpublished data). Figure C6 shows locations of utilized wells and illustrates their relatively uneven areal distribution.

Magnetic and gravity data reflect the subsurface distribution of magnetization and density. Magnetization ( $\text{emu}/\text{cm}^3$ ) is the sum of induced and remanent components. The induced component depends on magnetic susceptibility (cgs unit) that is easily measured in the field. Magnetic susceptibility and density information of exposed rock types is critical to determine the sources of gravity and magnetic anomalies. Table C1

**C4 Geophysical Framework of Verde River Headwaters, Arizona**

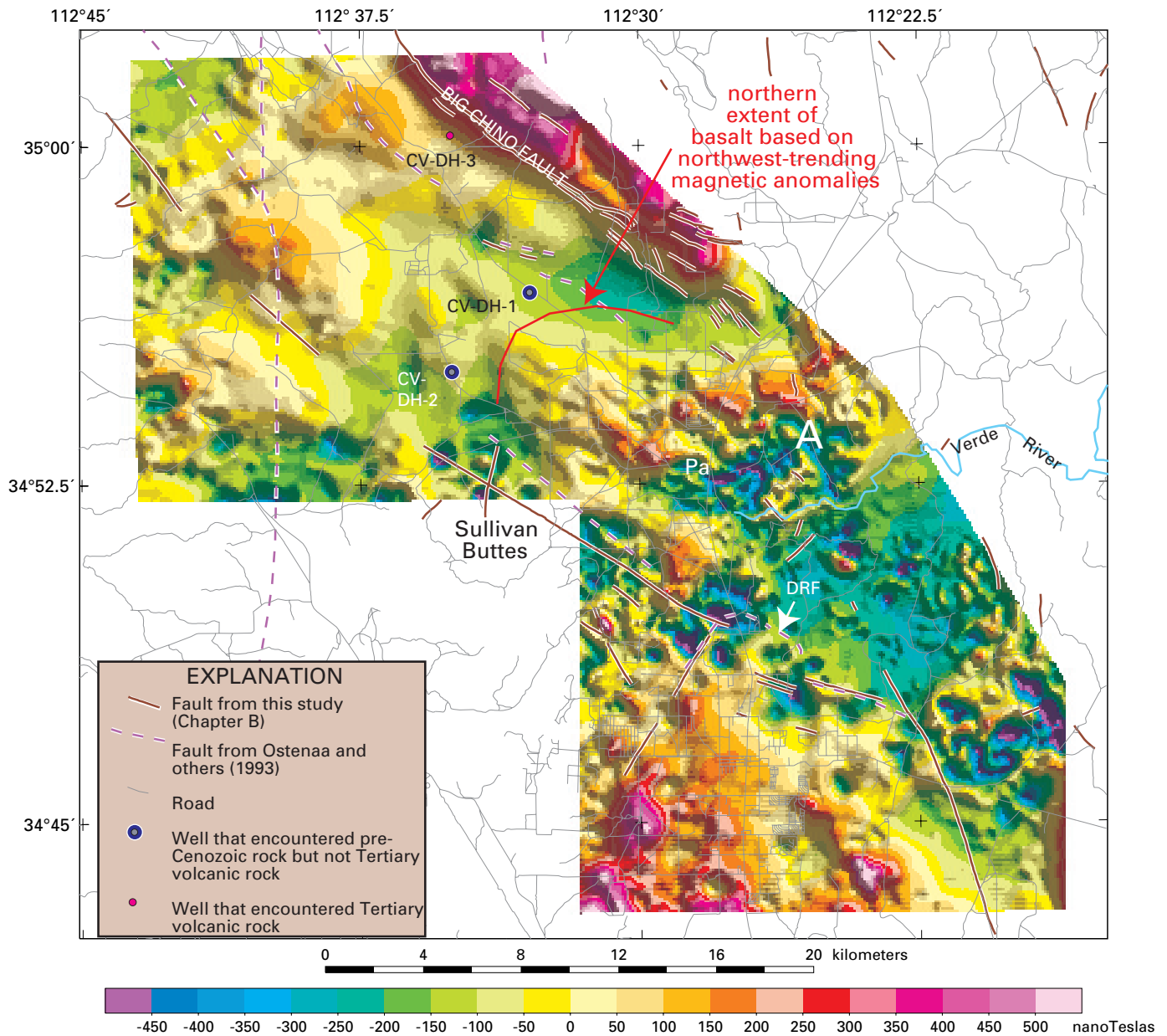


**Figure C2.** Aeromagnetic (reduced to pole) map of the study area. Anomalies are located over their sources if remanent magnetization is absent. "A" is an example of "worm-like" magnetic anomaly pattern produced by Tertiary basalt. DRF, Del Rio fault; Pa, Paulden.

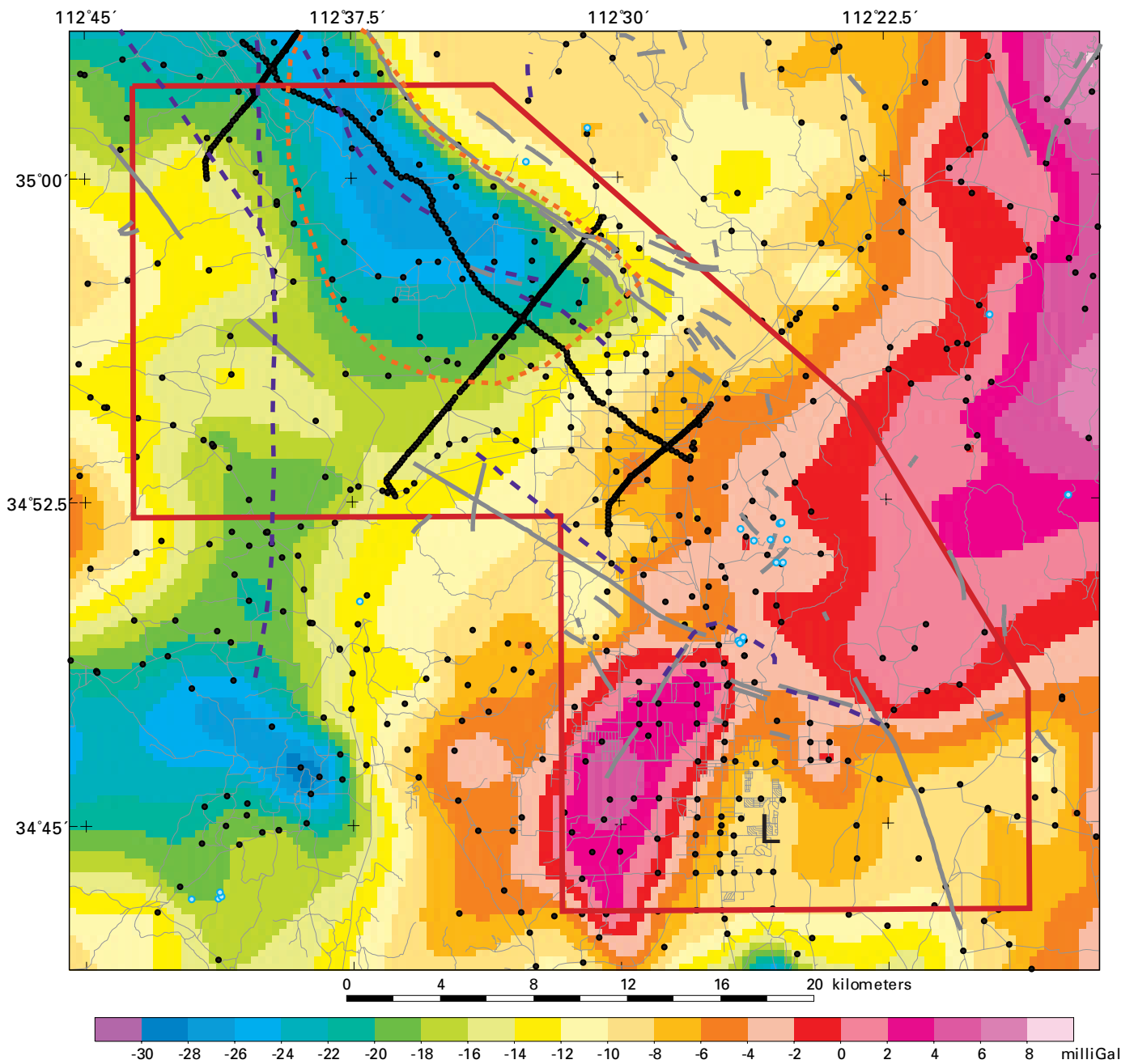


**Figure C3.** Isostatic gravity map. Black circles are gravity stations. Thick red line marks extent of aeromagnetic survey. Dashed orange line is approximate extent of the playa deposit that was interpreted as a clay deposit by Schwab (1995). Dark gray lines are faults determined in this study (Chapter B); dashed purple lines, faults from Ostenaar and others (1993). Blue circles are springs. "L" is small gravity low west of Granite Creek.

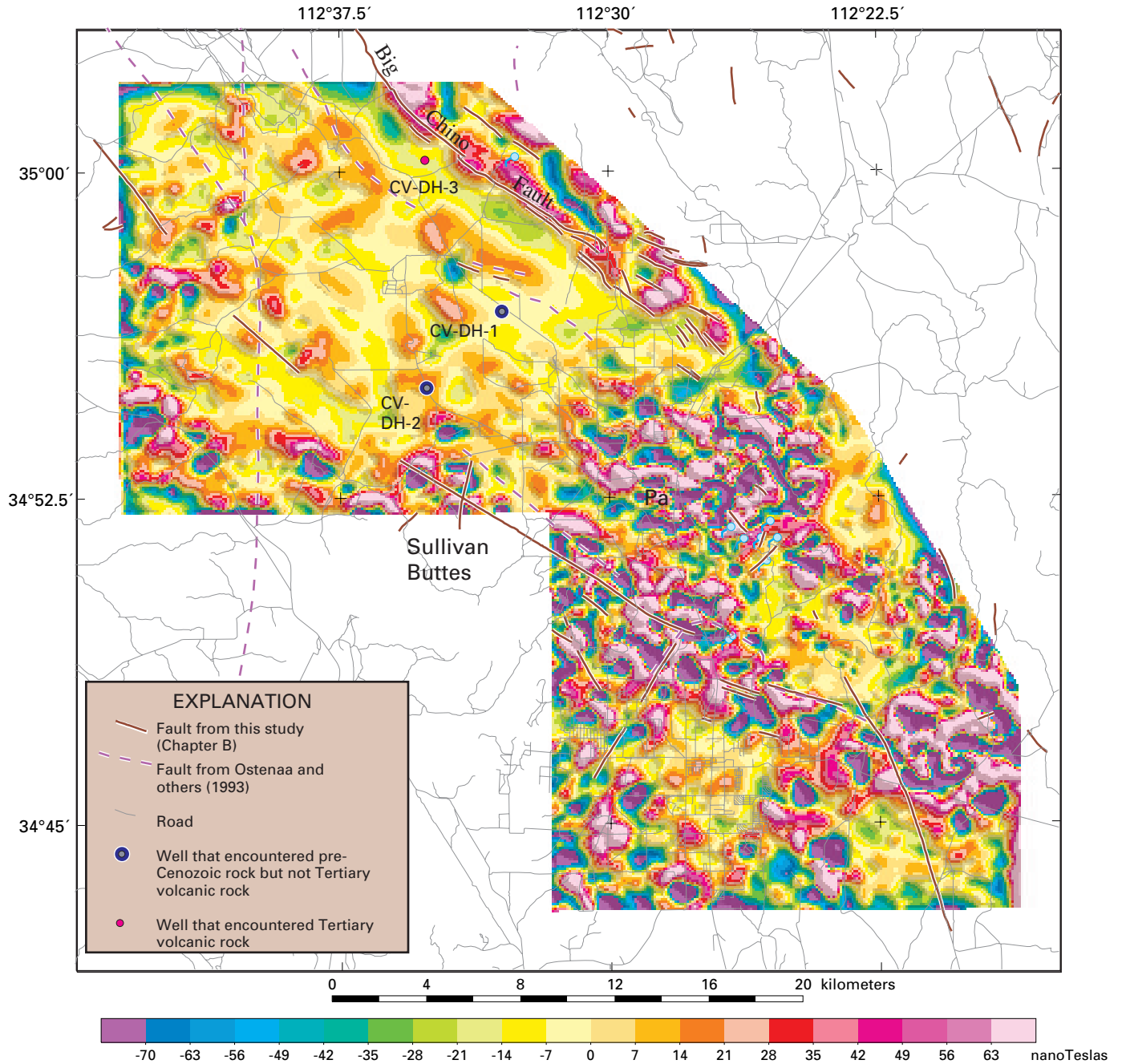


**Figure C4a.** Map of aeromagnetic field bandpass-filtered to enhance shallow sources (most lying <1km). Springs shown as blue circles with tails. Pa, Paulden.

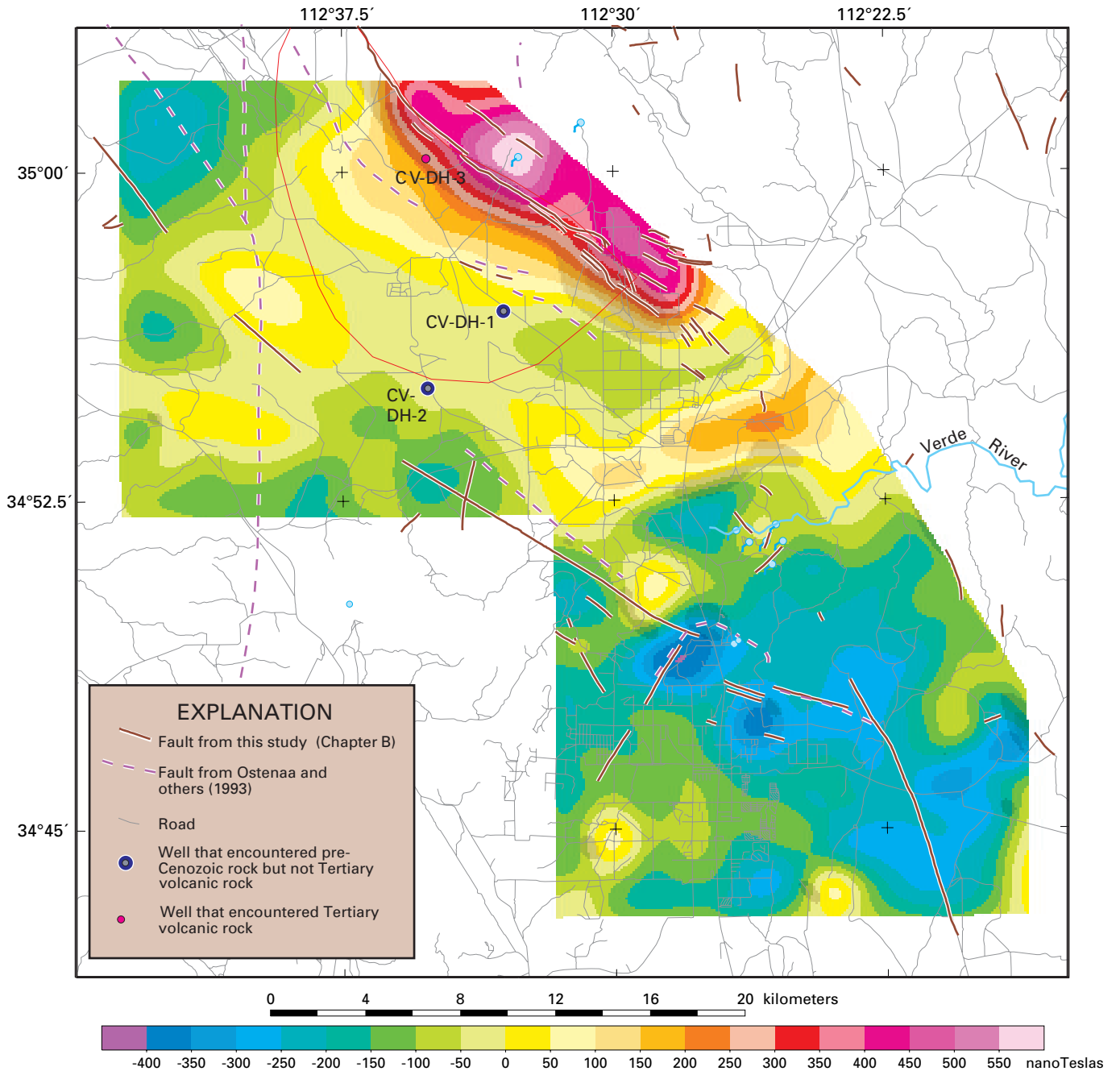


**Figure C4b.** Map of aeromagnetic field bandpass-filtered to enhance deep (approximately greater than 1-2 km) sources.

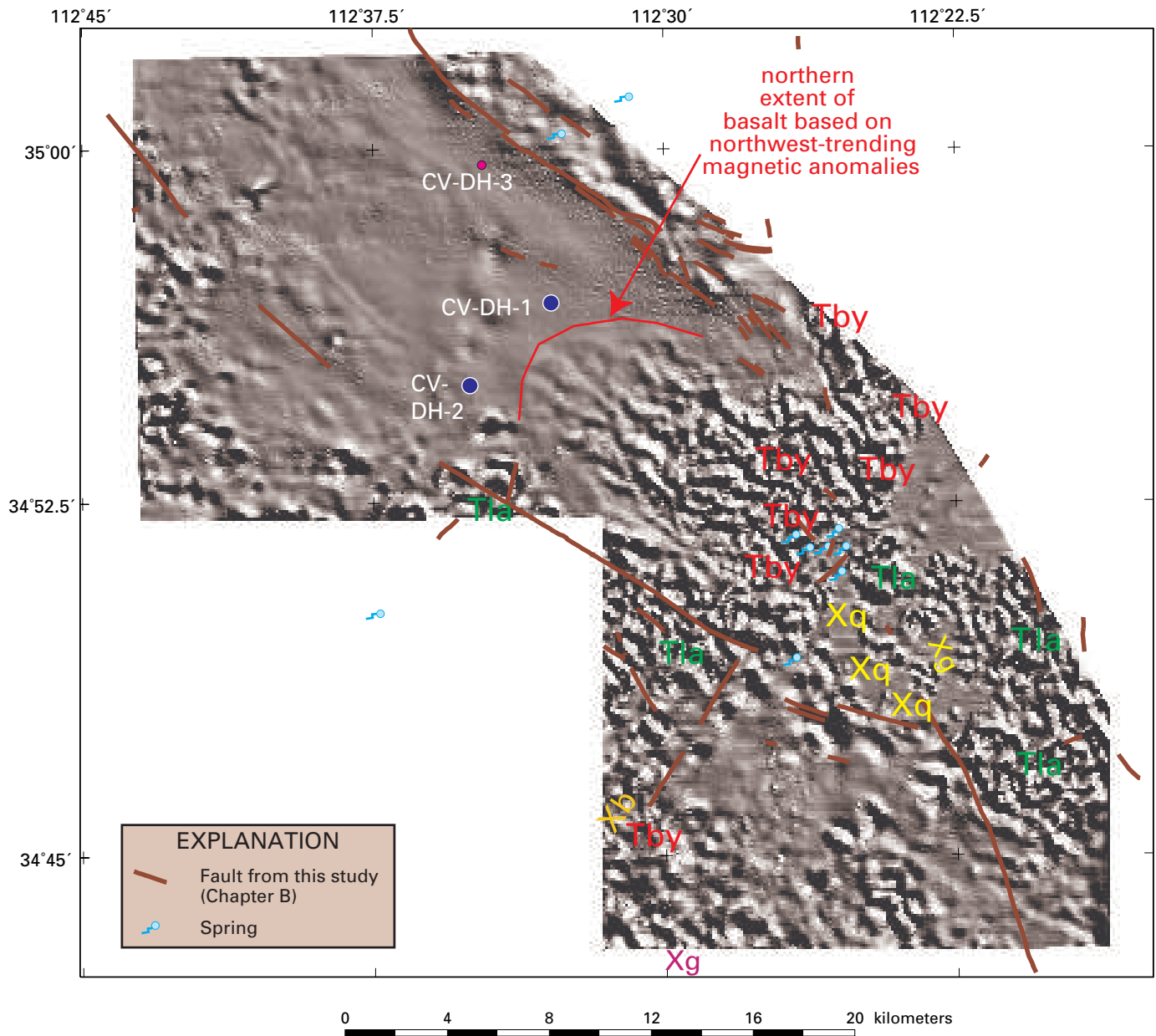


**Figure C5.** Map of first vertical derivative of the magnetic field. Xq, Xg, and Xb are exposed Proterozoic quartzite, granite and metabasalt, respectively; Tby, Tertiary basalt; Tla, Tertiary latite-andesite.

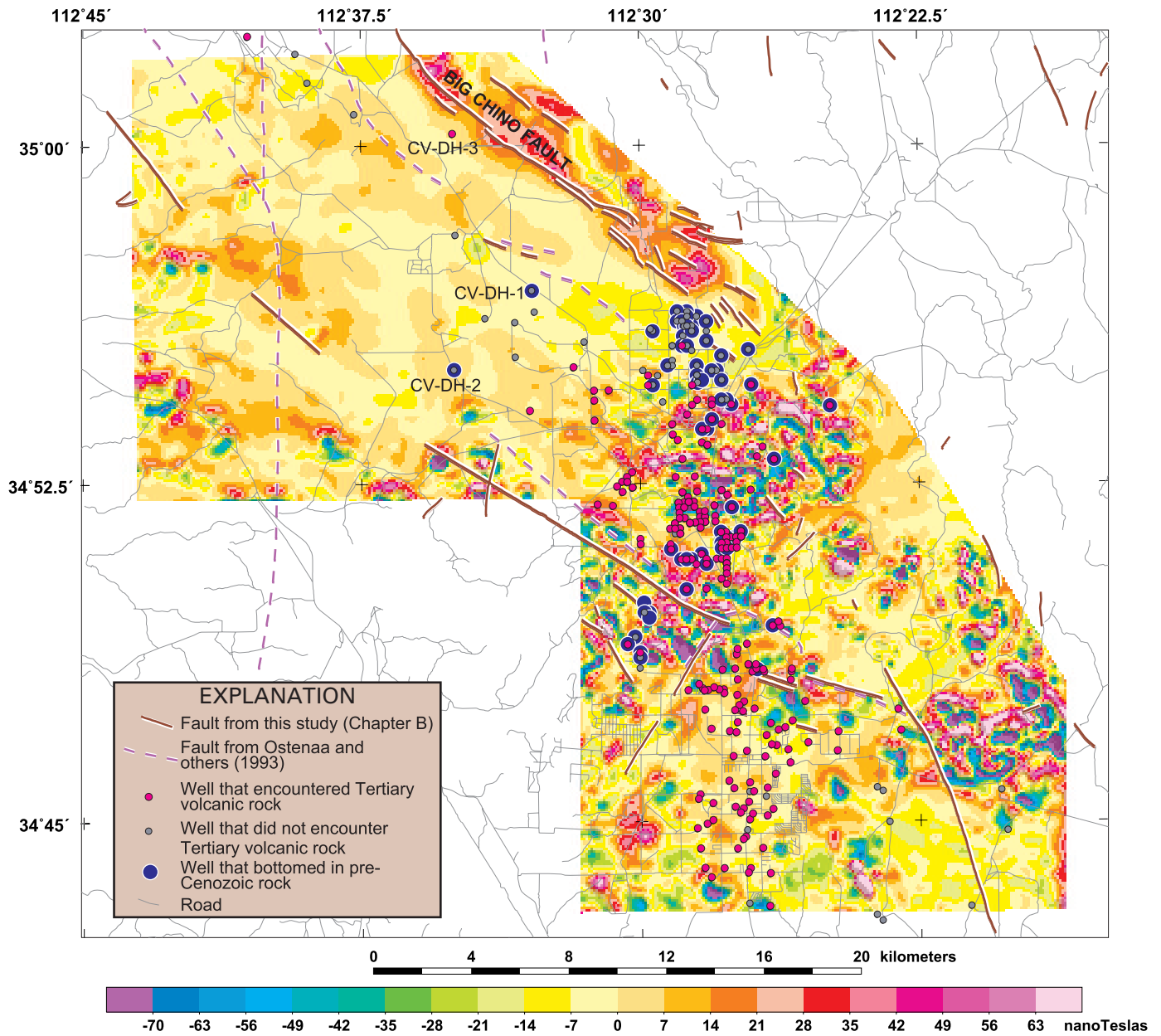


**Figure C6.** Map of aeromagnetic field filtered (by subtraction of upward continuation of magnetic field) to enhance shallow sources. Wells are from Krieger (1965), Ostenaar and others (1993), and ADWR unpublished data. Note that wells that did not encounter Tertiary volcanic rock may have been too shallow to encounter Tertiary volcanic rock; only those wells that bottom in pre-Cenozoic rock without penetrating Tertiary volcanic rock indicate an absence of Tertiary volcanic rock at that location.



C10 Geophysical Framework of Verde River Headwaters, Arizona

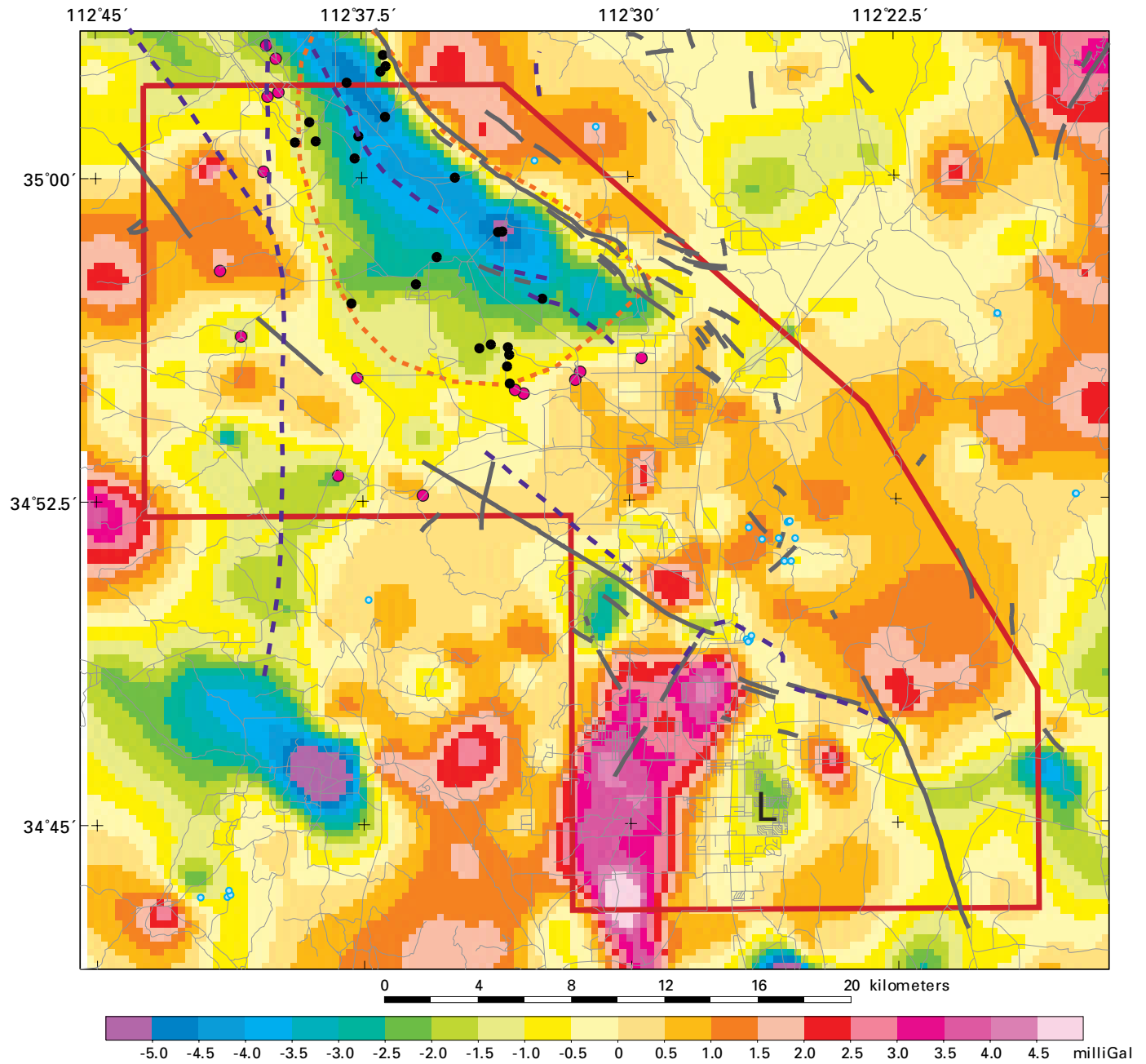


**Figure C7.** Map of filtered gravity field to enhance shallow sources. See Figure C3 caption for explanation of map. Black circles are wells within the playa deposit, magenta circles are wells around perimeter of playa deposit (from Schwab, 1995). "L" is small gravity low west of Granite Creek.

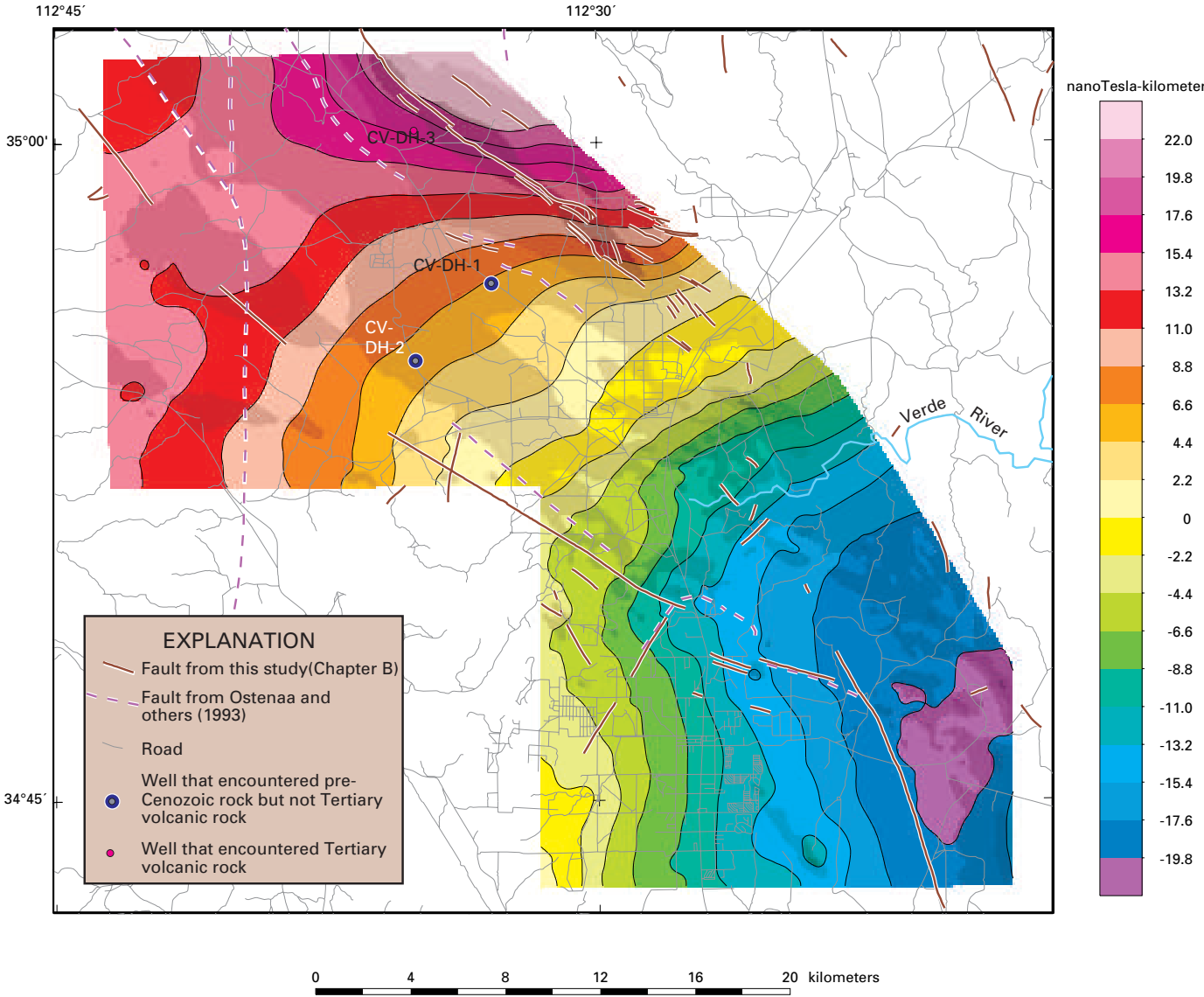


**Figure C8.** Shaded-relief pseudogravity map of the study area. The map emphasizes longer-wavelength anomalies (such as those residing in the Proterozoic crystalline basement). Illumination direction from the northeast.

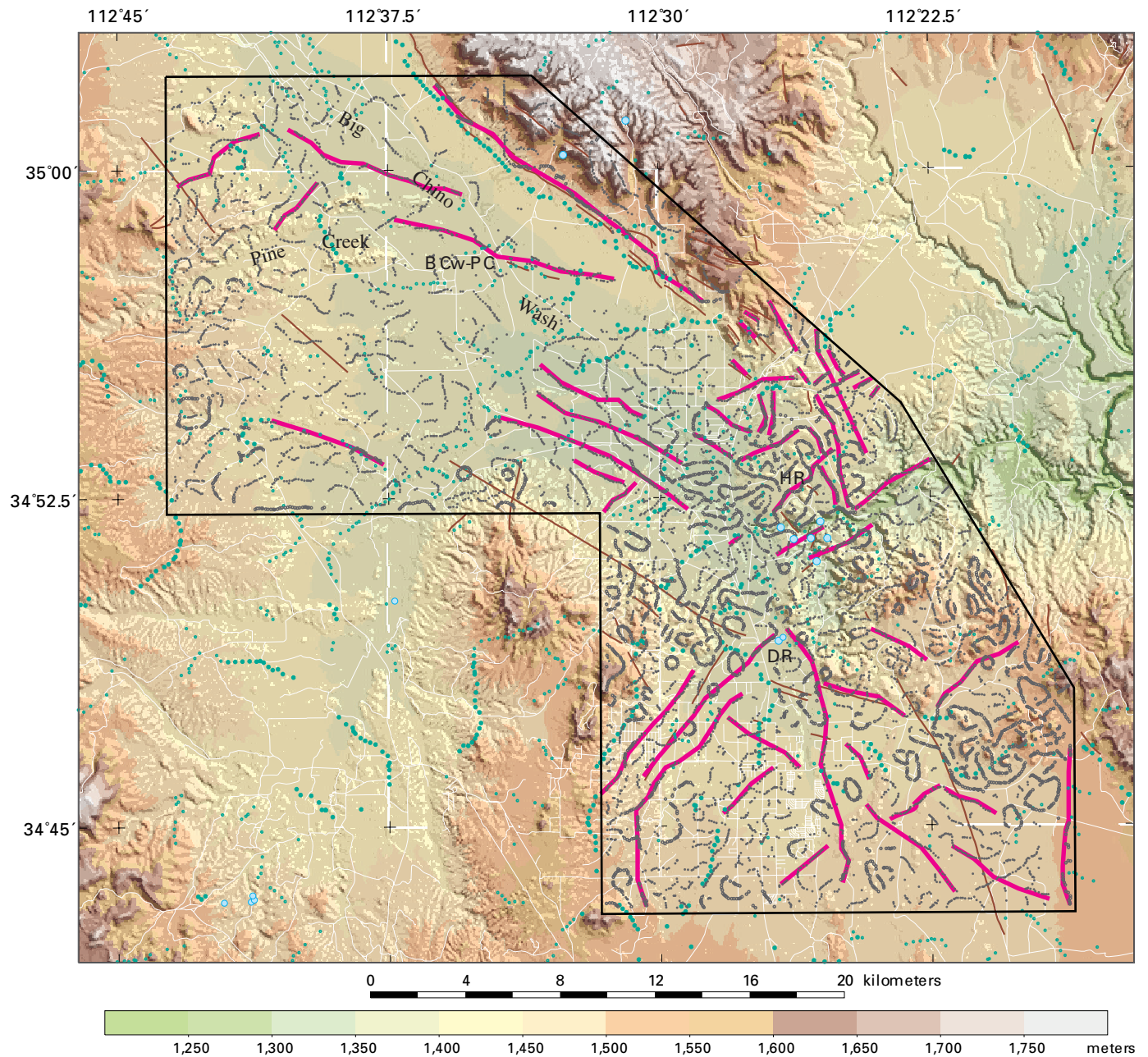


**Figure C9.** Map of density (green) and magnetic (gray) boundaries. Smaller dots reflect weaker gradients in gravity or magnetic data than those shown by larger dots. Magenta lines are inferred major magnetic lineaments. Magnetic lineament marked “BCw-PC” is nearly coincident with a dashed fault scarp near the junction of Big Chino wash and Pine Creek. Note that Del Rio Springs (DR) is located at the intersection of two magnetic lineaments. Brown lines are faults from this study. Blue circles are springs. HR, Headwaters Ranch area.

summarizes the magnetic susceptibility and density data of various rock types collected for this study.

The most magnetic rock types are Tertiary basalt and Tertiary lati-andesite, with average magnetic susceptibilities of  $1.20$  and  $0.74 \times 10^{-3}$  cgs units, respectively. The lati-andesites have the widest range in magnetic properties, ranging from  $0.04 \times 10^{-3}$  cgs units for oxidized lati-andesites to  $5.04 \times 10^{-3}$  cgs units for a Tertiary hornblende-bearing latite.

Limited physical property data related to Tertiary sedimentary rocks (4 samples) suggest that these rocks can produce measurable magnetic anomalies, although their average susceptibility is  $0.26 \times 10^{-3}$  cgs units, which is considerably less than those of the Tertiary basalt and lati-andesite. Detritus from the volcanic rocks probably is responsible for the magnetic properties of the sedimentary rocks. The most magnetic Tertiary sedimentary sample was breccia primarily composed of lati-andesite.

because of their age (more likely for the original remanence to have decayed) and grain size (coarser grain sizes indicating that original remanence may have been subjected to greater thermal changes; Tarling, 1983). Individual basalt flows in the Verde River region may have a uniform direction of magnetization, either of normal or reversed polarity (McKee and Elston, 1980). Steeply dipping faults that offset subhorizontal units, such as basalt flows, often produce magnetic anomalies that appear as linear trends on aeromagnetic maps (for example, Bath and Jahren, 1984, for the Yucca Mountain region, Nevada). The lati-andesites, on the other hand, often are extruded from volcanic plugs and thus tend to produce intense, somewhat circular magnetic anomalies. For this study, the magnetic remanence of a lati-andesite exposed in the Sullivan Buttes area was measured; its direction is reversed (declination (D) of  $149^\circ$  and inclination (I) of  $-58^\circ$ ; note present-day direction has  $D=13^\circ$  and  $I=61^\circ$ ) and the intensity of the remanent magnetization is about  $3 \times 10^{-6}$  emu/cm<sup>3</sup>. This information

**Table C1.** Densities (grams/cubic centimeter) and magnetic susceptibilities ( $10^{-3}$  cgs units) of hand samples collected for this study

[ $\pm$ , standard deviation; n, number of samples]

Rock Type	Density Range	Average Density	Susceptibility Range	Average Susceptibility
<b>Tertiary basalt</b>	2.59—2.97	2.78 $\pm$ 0.10 (n=24)	0.14—3.98	1.20 $\pm$ 0.99 (n=24)
<b>Tertiary sedimentary rocks</b>	2.35—2.57	2.46 (n=2)	0.16—0.32	0.26 $\pm$ 0.07 (n=4)
<b>Tertiary lati-andesite</b>	2.27—2.91	2.59 $\pm$ .13(n=20)	0.04—5.04	0.74 $\pm$ 1.05 (n=20)
<b>Paleozoic sedimentary rocks</b>	2.45—2.84	2.67 $\pm$ 0.13(n=15)	0.00—0.00	0.00 (n=10)
<b>Proterozoic rocks</b>	2.59—3.06	2.73 $\pm$ 0.12(n=26)	0.00—0.95	0.15 $\pm$ 0.26 (n=41)

The magnetic properties of the Paleozoic sedimentary rocks (table C1), consisting of the Redwall Limestone, Martin Formation, and Tapeats Sandstone, are usually weak, resulting in low-amplitude magnetic anomalies generally undetectable by airborne surveys. Proterozoic rocks have a range of measured susceptibilities from 0 to  $0.95 \times 10^{-3}$  cgs units; metasedimentary rocks, such as the Mazatzal quartzite ( $0 \times 10^{-3}$  cgs units), generally are incapable of producing detectable magnetic anomalies. However, metavolcanic rocks, gabbros, and some intrusive rocks can produce prominent magnetic anomalies. In the study area and vicinity, Prescott granodiorite ( $0.95 \times 10^{-3}$  cgs units) and Chino Valley granite ( $0.88 \times 10^{-3}$  cgs units; exposed just north of the survey area) have the highest magnetic susceptibility values of the intrusive rocks.

Magnetic susceptibility is one part of the total magnetization of a rock (as mentioned above) and primarily is a function of the amount of magnetite in the rock. The other component, the remnant magnetization, is determined by the direction and strength of the Earth's magnetic field when the rock acquired its magnetization. It can be an important component of the magnetization of the Tertiary volcanic rocks, but is unlikely to contribute to the magnetization of the Precambrian rock types

supports the interpretation that many of the circular magnetic lows in figures C2, C4, C5, and C6 are caused by reversely magnetized lati-andesite plugs.

The density measurements of this study (table C1) are consistent with earlier data (Cunion, 1985; Frank, 1984). Proterozoic rocks are dense (approximately 2.73 grams/cubic centimeter (g/cm<sup>3</sup>)), but exhibit a wide range in values. For instance, gabbro and metavolcanic rocks are very dense (2.75 to 3.06 g/cm<sup>3</sup>); however, representative density values of aplites and pegmatites are low (2.59 g/cm<sup>3</sup>). The metasedimentary and granitic rocks are characterized by intermediate densities. The density of the Paleozoic rocks is indistinguishable from those of the Proterozoic granitic rocks, although the carbonate lithologies (Martin Formation and Redwall Limestone) are denser than the Tapeats Sandstone (2.62—2.84 g/cm<sup>3</sup> versus 2.45—2.49 g/cm<sup>3</sup>, respectively). Similarly, the Tertiary basalts may be difficult to distinguish from the pre-Cenozoic rocks, with an average density of 2.78 g/cm<sup>3</sup>. The lati-andesites are less dense (average 2.59 g/cm<sup>3</sup>), although densities of vesicular basalts in the study area are as low as the average lati-andesite density.

Only two direct density measurements of the Tertiary sedimentary sequence were made in the study area; these measurements are undoubtedly biased towards higher densities because of the difficulty in obtaining a hand sample in unconsolidated materials. They are significantly less dense ( $\sim 2.46 \text{ g/cm}^3$ ) than most of the other rock types. No measurements were made on Quaternary sedimentary deposits for this study. Because of the difficulty of obtaining direct density measurements on Quaternary and Tertiary sedimentary rocks, one must rely on indirect information.

Indirect information on densities of Tertiary sedimentary rocks comes from sonic velocities measured in the Bureau of Reclamation drill holes (Ostenaar and others, 1993). Using the relation of Gardner and others (1974) developed for sedimentary rocks,

$$\rho = 0.23v^{0.25} \quad (1)$$

one can estimate the density,  $\rho$  ( $\text{g/cm}^3$ ), from the sonic velocity,  $v$  (feet/second or ft/s). Sonic velocities measured on Quaternary and Tertiary sedimentary rocks in drillhole CV-DH-1 (Ostenaar and others, 1993) average from about 1.8 kilometers/second ( $\text{km/s}$ ;  $6,000 \text{ ft/s}$ ) between depths of 240–300 meters (800–1,000 feet) to as high as  $3.7 \text{ km/s}$  ( $12,000 \text{ ft/s}$ ) between depths of 380–410 meters (1,250–1,350 feet). In drillhole CV-DH-2, average velocities increase from  $2.4 \text{ km/s}$  ( $8,000 \text{ ft/s}$ ) at depths of 100–150 meters (320–500 feet) to as high as  $4.9 \text{ km/s}$  ( $16,000 \text{ ft/s}$ ) near the bottom of the hole. Corresponding densities for the young sedimentary deposits range from  $2.02$  to  $2.59 \text{ g/cm}^3$ , averaging about  $2.24 \text{ g/cm}^3$  from 90–168 meters (300–550 feet) for CV-DH-2 and  $2.20 \text{ g/cm}^3$  from 240–460 meters (800–1,520 feet) for CV-DH-1. Unfortunately, the deepest well studied by Ostenaar and others (1993), CV-DH-3, was not logged for velocity, although all three were logged for resistivity.

Another indirect method to estimate density is to calculate velocity from the resistivity and then use the empirical relationship shown in equation (1). All three physical properties—density, velocity, and true resistivity—are linked by a common dependence on porosity. Limitations to use of this method are described in Faust (1953). If the apparent resistivity ( $R_a$ ) measured in the wells approximates the true resistivity of the rock, then Faust's (1953) empirical relationship between velocity ( $v$ ) and apparent resistivity ( $R_a$ ) and depth ( $Z$ ) can be written

$$v = \delta(Z * R_a)^{0.1667} \quad (2)$$

where  $\delta$  is an empirical constant (1948), which is applicable to most geologic sections. Using equation (1) and equation (2), average densities for the depth ranges discussed above for drillholes CV-DH-1 and CV-DH-2 are about  $2.27 \text{ g/cm}^3$  and  $2.20 \text{ g/cm}^3$ , respectively. For CV-DH-3, densities based on this method range from  $2.01 \text{ g/cm}^3$  to  $2.31 \text{ g/cm}^3$ , but average about  $2.10 \text{ g/cm}^3$  for depths of 61–213 meters (200–700 feet),  $2.05 \text{ g/cm}^3$  for 213–396 meters (700 to 1,300 feet), and  $2.27 \text{ g/cm}^3$  for 396–640 meters (1,300 to 2,100 feet).

Perhaps a better, more direct measure of the density of the sedimentary sequence comes from borehole gravity surveys

outside the study area (Tucci and others, 1982). Densities derived from borehole gravity data probably are more representative of the basin rock and sediment densities because the method measures a larger volume than that of isolated hand samples or borehole velocity and resistivity logs. Another advantage of the method is that it can measure density at different depths beneath the ground surface. The mean densities from borehole gravity surveys from several scattered localities in Arizona range from approximately  $1.97$  to  $2.32 \text{ g/cm}^3$  for the upper 366 meters (1,200 feet) of basin-fill deposits (Tucci and others, 1982; *their* figure 3). Figure C10 summarizes average densities derived from these various methods for Quaternary and Tertiary sedimentary rocks.

## Geophysical Anomalies

The aeromagnetic anomaly patterns over Little and Big Chino Valleys (fig. C2) differ. Little Chino Valley is characterized by short-wavelength magnetic anomalies. The magnetic anomalies in Big Chino Valley tend to be broader and smoother. Little Chino Valley (except for its southwestern quarter) generally has lower magnetic values (less than  $0 \text{ nT}$ ) than those over Big Chino Valley (more than  $0 \text{ nT}$ ). This difference is clearly expressed in the pseudogravity field (fig. C8) and occurs roughly in the area of the Verde River canyon east of Paulden. Higher values typically occur north of the River (see for example, fig. C2, C4b, C8). The lower magnetic values in Little Chino Valley are likely caused by less magnetic Proterozoic basement (as suggested by fig. C4b and fig. C8 if these maps truly reflect deeper sources in the Proterozoic basement). Tertiary volcanic rocks, exposed or shallowly buried ( $< 1$  kilometer), are the source of many of the very high-amplitude, short-wavelength anomalies in much of Little Chino Valley, the area around Paulden and near Sullivan Buttes. Many of the Tertiary latite-andesites coincide with very strong circular magnetic lows indicative of volcanic plugs. Tertiary basalts generally produce a “worm-like” magnetic anomaly pattern (“A” on Fig. C2). The broader, longer-wavelength anomalies in Big Chino Valley likely express deeper sources. A prominent magnetic high coincides with Paleozoic carbonate rocks exposed on Big Black Mesa (fig. C2). Because these rocks are weakly magnetic, the source of the anomaly most likely is concealed Proterozoic granitic rocks exposed just northwest of the study area. The magnetic basement on Big Black Mesa is buried by as much as 260–280 meters based on the average unit thicknesses of the Paleozoic sedimentary sequence exposed there. Sources of broader magnetic highs in the adjacent Big Chino Valley probably express Proterozoic granitic rocks deeply buried beneath the valley fill. In contrast, the Proterozoic basement beneath much of Little Chino Valley probably is metavolcanic and metasedimentary rocks, which apparently are less magnetic than the granite underlying much of Big Chino Valley and Big Black Mesa. For example, the area of exposed Proterozoic Mazatzal quartzite is a magnetically quiet region (“Xq” on fig. C5) with lower magnetic values (fig. C2).

AVERAGE DENSITY OF QUATERNARY AND TERTIARY SEDIMENTARY ROCKS  
(grams/cubic centimeter)

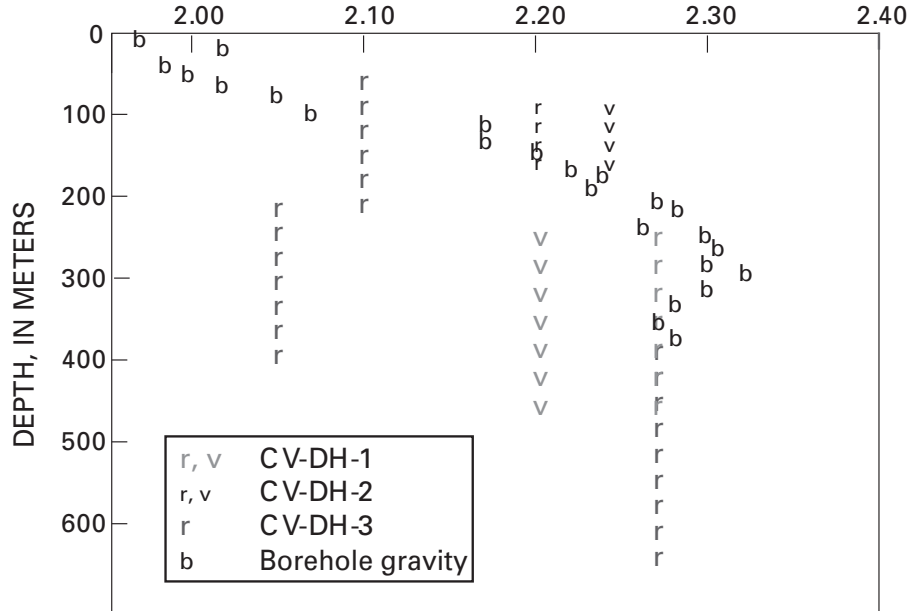


**Figure C10.** Average densities of Quaternary and Tertiary sedimentary rocks derived from various methods. r, derived from resistivity; v, derived from velocity; b, from borehole gravity of Tucci and others (1982; *their* figure 3).

Big Chino Valley, characterized by a gravity low, is bounded on the east by the Big Chino Fault (fig. C3). The deepest part of the basin, as suggested by the lowest gravity value within the valley, is about 5 kilometers south of the northern boundary of the study area. Gravity values increase to the southeast towards Sullivan Lake, indicating thinning of the basin-fill deposits.

Little Chino Valley is characterized by higher gravity values than those over Big Chino Valley, suggesting that Little Chino Valley basin is not as deep. South of the study area near the intersection of Highway 89 and alternate route 89 (fig. C1), a gravity low most likely reflects a thick stock of Prescott granodiorite rather than a deep basin (Cunion, 1985). The northern margin of this low is along the southern margin of the study area (fig. C3). Prescott granodiorite (and Granite Dells granite) is less dense than the some of the more mafic metavolcanic and gabbros within Proterozoic basement. This low may mask more subtle gravity lows caused by locally thick accumulations of basin fill (for example, “L” on fig. C3). Because the gravity field is affected both by changes in thickness of the Cenozoic deposits and density variations in the underlying Paleozoic and Proterozoic rocks, a method described below attempts to separate these two sources.

## Depth to Basement Method

In this section, depth to pre-Cenozoic bedrock is calculated for Big Chino Valley and Little Chino Valley and to determine the geometry of bounding and internal faults.

The method used in this study to estimate the thickness of Cenozoic rocks was developed by Jachens and Moring (1990) and modified to incorporate drill hole and other geophysical data (Bruce Chuchel, U.S. Geological Survey, written commun., 1996; fig. C11). The inversion method allows the density of bedrock to vary horizontally as needed, whereas the density of basin-filling deposits is specified by a predetermined density-depth relation. Two density-depth functions listed in table C2 were used. A first approximation of the bedrock gravity field is derived from gravity measurements made on exposed pre-Cenozoic rocks, augmented by appropriate bedrock gravity values calculated at sites where depth to bedrock is known. This approximation (which ignores the gravity effects of nearby basins) is subtracted from the observed gravity, which provides a first approximation of the basin gravity field. Repeating the process using the specified density-depth relation, the thickness of the basin-fill deposits is calculated. The gravitational effect of this first approximation of the basin-fill layer is computed at each known bedrock station. This effect is, in turn, subtracted from the first approximation

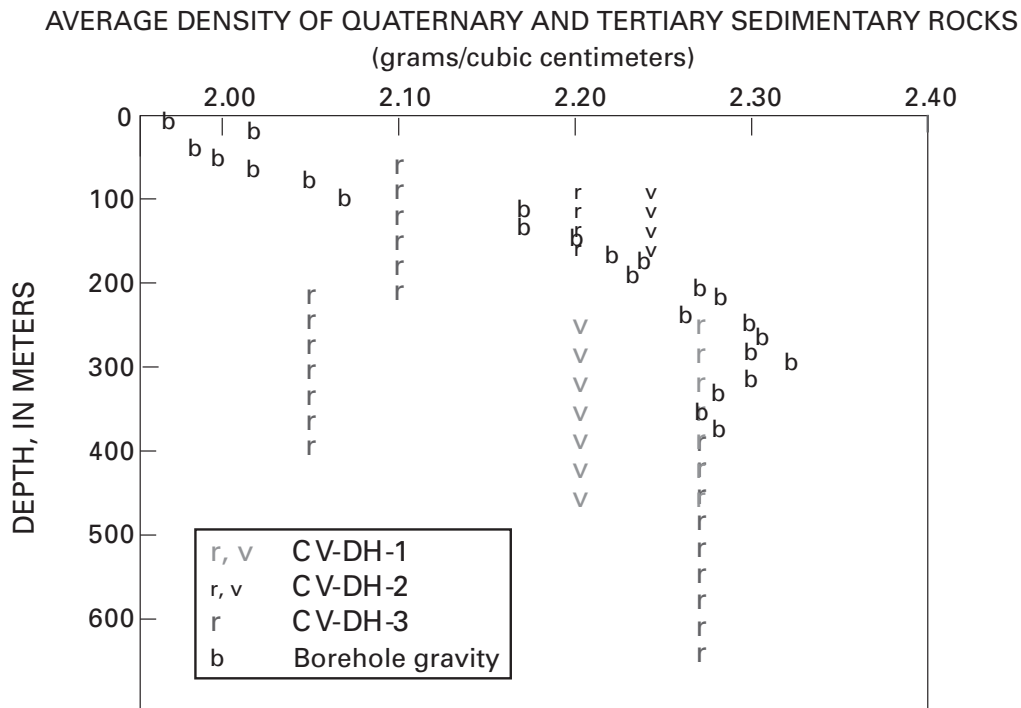


Figure C11. Schematic representation of basin-basement separation.

of the bedrock gravity field and the process is repeated until successive iterations produce no substantial changes in the bedrock gravity field.

The inversion presented here does not take into account lateral variations in the density of Cenozoic deposits, which may be an important source of error in the study area, particularly where it is underlain by thick, dense basalt flows.

Table C2. Density-depth function.\*

Depth Range	Based on Arizona Borehole Gravity	Determined from Resistivity
0—100 meters	-0.67	-0.57
100—200 meters	-0.47	-0.60
200—600 meters	-0.37	-0.47
>600 meters	-0.25	-0.25

\*density contrast (g/cm<sup>3</sup>) relative to underlying pre-Cenozoic bedrock

This method has been shown to be effective in determining the general configuration of the pre-Cenozoic bedrock surface in Nevada (Phelps and others, 1999). Phelps and others (1999) showed that the model bedrock surface of Yucca Flat

(Nevada Test Site, northwest of Las Vegas, Nev.) was a reasonable approximation of the true surface based on comparison with calculated basin depths from closely spaced drill holes. The predicted shape of the basin did not change significantly with additional well control. Furthermore, it seems that lateral variations in basin density, unless abrupt, do not change the overall modeled shape of the basin. Although the method is a good tool for predicting the shapes of basins, it can be less effective in estimating the magnitude of basin thickness, especially in basins containing thick basalt flows or in areas of poor well control. Below is a discussion of the sources of error in the depth-to-basement calculations.

## Results

### Depth to Basement

Two basin models (fig. C12) were created using two different density-depth functions (table C2). Figure C12a shows the basin model using a density-depth function based on data from Tucci and others (1982); figure C12b is the basin model using a density-depth function based on the resistivities measured in the Bureau of Reclamation drill holes (Ostenaa

and others, 1993). Because of the wide density range of the local Cenozoic volcanic rocks and their limited thickness (basalts generally less than 30 meters thick), the same density-depth relationship was assumed for Cenozoic volcanic rocks as for the Cenozoic sedimentary deposits. One might consider including the basalts with the pre-Cenozoic bedrock, but the difficulty of distinguishing dense basalt from lower-density latite-andesite in driller's logs and the presence of gravel beneath both the basalts and latite-andesites made this approach intractable. The models utilize bedrock gravity stations and well data to constrain the thickness of Cenozoic sediment.

The models were tested by comparing the predicted basin thickness with the minimum thickness of Cenozoic deposits found in wells that did not bottom in pre-Cenozoic rock (fig. C13). In Big Chino Valley, the basin thickness predicted by the models generally is greater than that found in these wells (fig. C13; pink areas are where model thickness is supported by these wells). In Little Chino Valley, the basin models agree with the well data in the central part of the valley, where the deepest part of the basin is modeled and where the lowest isostatic gravity values ("L" on fig. C3) are located. Along the western margin of the valley where wells did not encounter pre-Cenozoic rock, the models underestimate basin-fill thickness by as much as 250 meters. The western part of the valley coincides with a large positive gravity anomaly (fig. C3, C7; dashed gray line on fig. C13). Without well control to constrain the bedrock gravity, the modeling process will not show a basin in the vicinity of the gravity high. Another substantial underestimate of basin fill (269 meters or 881 feet) is 3 kilometers east of the deepest part of the Little Chino Valley basin, where the thickest Tertiary volcanic rock was encountered in drillholes. The basin model using the density-depth function based on Tucci and others (1982) produces fewer underestimates in Little Chino Valley. However, both models are poorly constrained in Little Chino Valley because of the limited wells that penetrate pre-Cenozoic rock (thus constraining the bedrock gravity component; see fig. C14) and because of the thickness of volcanic rock within the sediments (resulting in inaccurate density-depth functions and possibly in substantial lateral variations in the density of rock and sediment units).

The basin models appear to be more accurate for Big Chino Valley, even though wells that bottomed in pre-Cenozoic rock are limited to its southern margin. The northernmost wells that penetrated pre-Cenozoic bedrock (CV-DH-1 and CV-DH-2) did not encounter Tertiary volcanic rock. Northwest-trending magnetic anomalies (fig. C2) suggest that the Tertiary basalt deepens to the northwest from exposures near Paulden and terminates southeast of these two drill holes. Thus, the presence of shallowly buried, thick basalt flows, which can introduce error in the inversion method, is unlikely in the central part of Big Chino Valley. No information on bedrock gravity variations is available for central Big Chino Valley, but bedrock gravity values at CV-DH-1 and CV-DH-2 are comparable to those measured on Big Black Mesa (fig. C14). The lack of evidence for significant variations in bedrock gravity could indicate similar basement rock beneath Big Chino Valley

and Big Black Mesa. The aeromagnetic data suggest that the magnetic basement of Big Black Mesa does extend southwest of the Big Chino fault (fig. C2, fig. C4), at least as far as the scarp near the intersection of Big Chino Wash and Pine Creek (BCw-PC on fig. C9). Thus, large variation in bedrock density is not anticipated at least beneath the eastern part of Big Chino Valley.

Another test of the basin model is a comparison of the basin depths with those predicted from resistivity depth soundings (Ostenaa and others, 1993; Water Resources Associates, 1989). Of the 19 soundings within the study area (Ostenaa and others, 1993), only 2 soundings (Z7 and Z10) disagree substantially with the basin models (depths to Paleozoic rock from resistivity, 600 and 780 meters, depths predicted by basin models, 1,100 and 1,400 meters). These soundings flanking CV-DH-3 lie in the deeper part of the basin. The modeled resistivities interpreted as Paleozoic rock at these two sites are indistinguishable from resistivities measured at the bottom of CV-DH-3, which encountered Tertiary latite-andesite, suggesting that the resistivity method may not be capable of distinguishing Paleozoic rock from Tertiary latite-andesite. The depth soundings presented in Water Resources Associates (1989) are all consistent with basement depths estimated by the gravity inversion method. Thus, the basin models predicted from the gravity inversion are in substantial agreement with the resistivity soundings.

Another test of the basin model was made after the models were created; deep wells in Big Chino, Little Chino, and Williamson Valleys were completed and reached bedrock. In all cases, the predicted basin depths within the study area were deeper than the depths at which bedrock was encountered. Two of the wells drilled in Big Chino Valley (fig. C12; CVR-1, bedrock at 149 meters; CVR-2, bedrock at 494 meters) agree within 1-21 percent of the predicted basin depths (resistivity model, 179 and 500 meters; Tucci model, 181 and 563 meters, respectively). The third well (fig. C12; CVR-3) penetrated bedrock substantially above both of the predicted basin thicknesses (512 meters versus 1,224 and 1,444 meters). One well in Little Chino Valley (16N/1W/23aca) hit bedrock at a depth of 148 meters, within 25 percent of the predicted basin depths (both 185 m). Two deep wells (fig. C12) were drilled in the Williamson Valley, outside of the study area. One well within the gravity low did not penetrate basement at a depth of 457 meters (BH-1), which is consistent with the predicted basin thicknesses. The well outside the gravity low (BH-3) penetrated bedrock at a depth of 429 meters. The basin depth calculated with the resistivity derived density-depth function (569 meters) was closer to the actual bedrock surface than the basin depth calculated with the Tucci density-depth function (755 meters). The consistent overestimation of basin thickness by the models at wells that did penetrate bedrock suggests that a lighter density-depth function should be used for future work, especially for Big Chino and Williamson Valleys.

Both models show similar shapes for the basin configuration in the study area, but predict slightly different thicknesses. For example, at CV-DH-3, the modeled basin depth



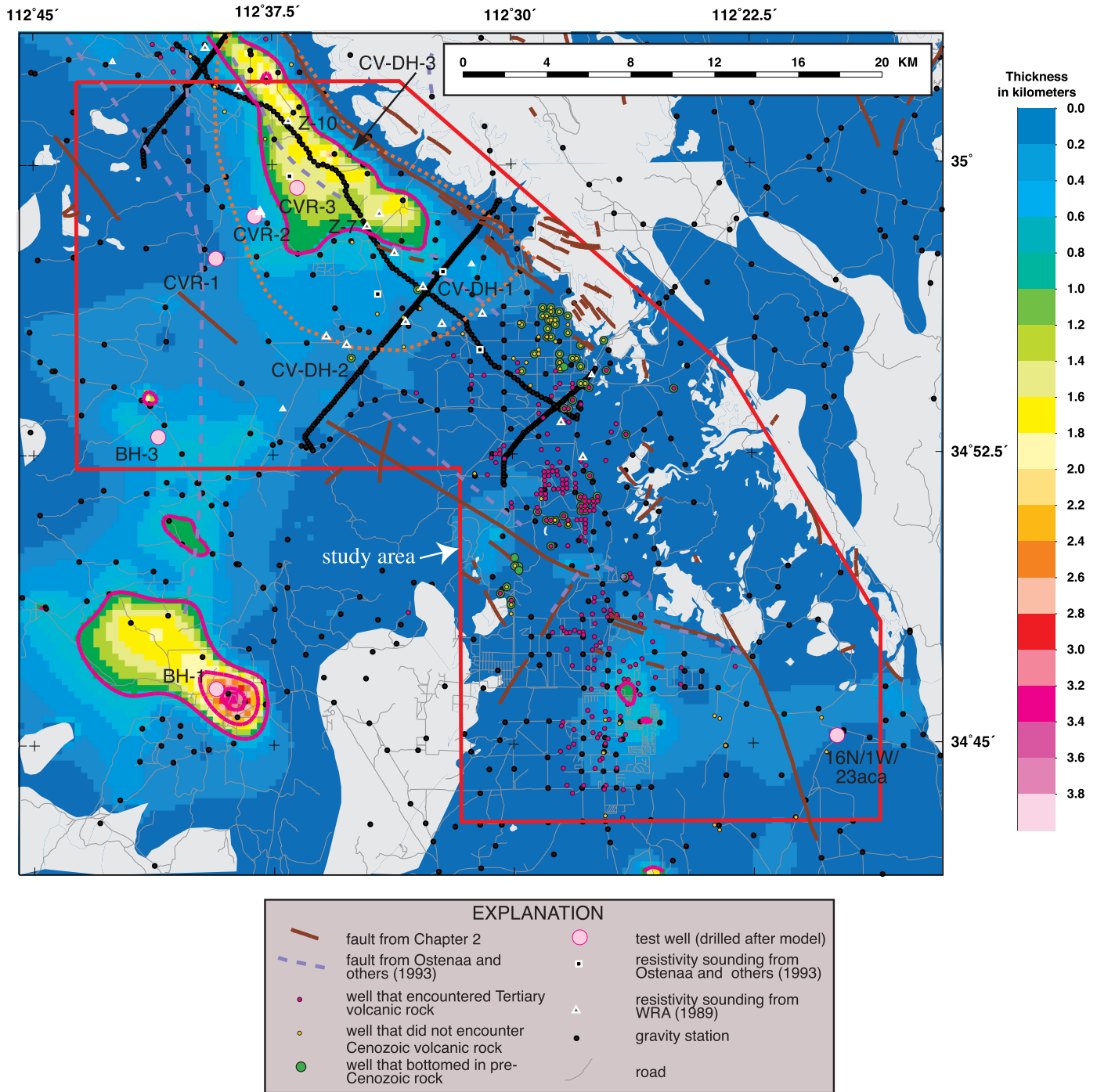


**Figure C12a.** Map of modeled thickness of Cenozoic sedimentary and volcanic fill using the density-depth function of Tucci and others (1982). Thick magenta lines are 1-kilometer contours. Dashed orange line outlines extent of playa deposit from Schwab (1995). Pale gray areas are pre-Cenozoic outcrops.

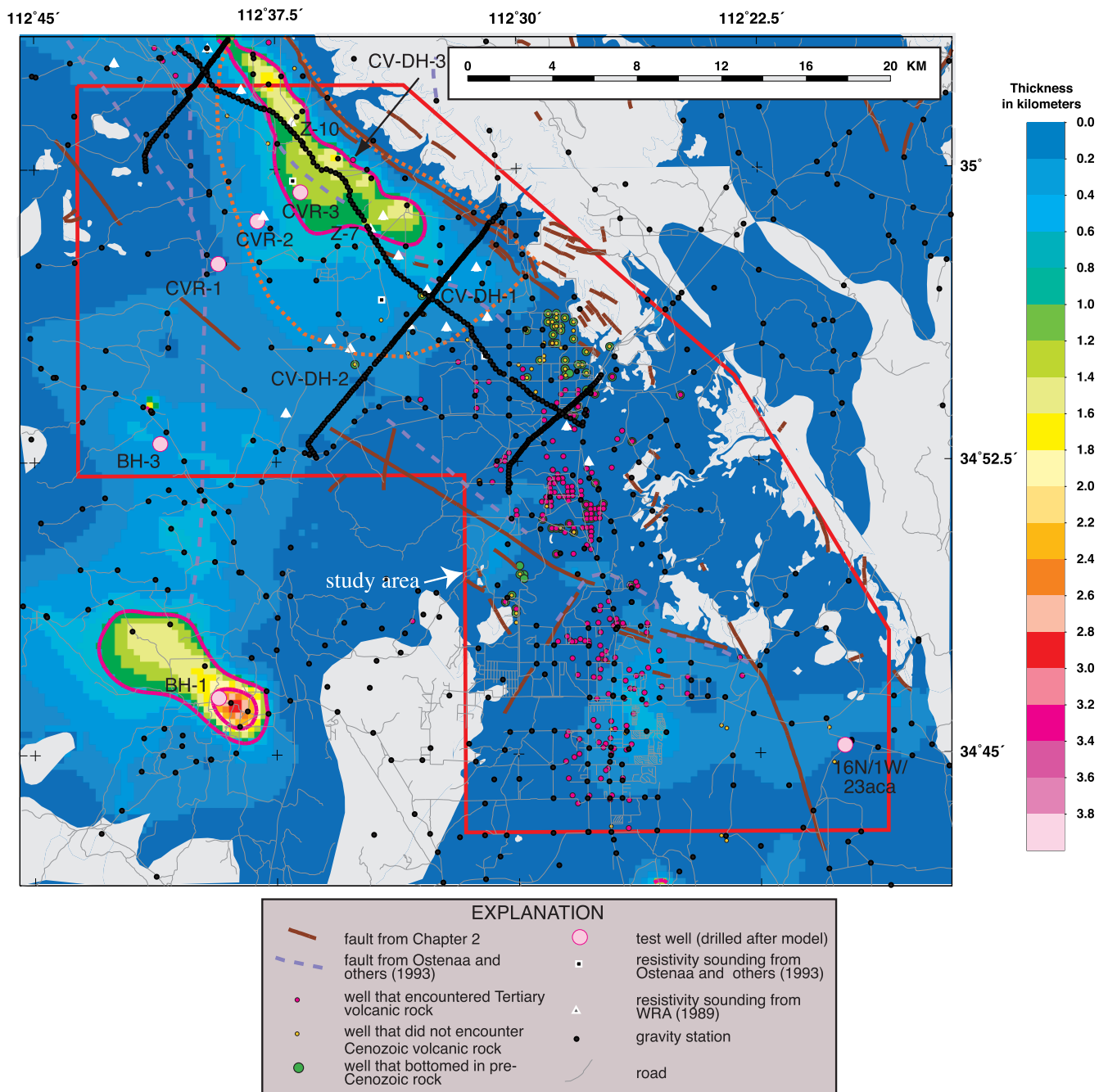


**Figure C12b.** Map of modeled thickness of Cenozoic sedimentary and volcanic fill using a density-depth function derived from resistivity logs. Thick magenta lines are 1-kilometer contours. Dashed orange line outlines extent of playa deposit from Schwab (1995). Pale gray areas are pre-Cenozoic outcrops.

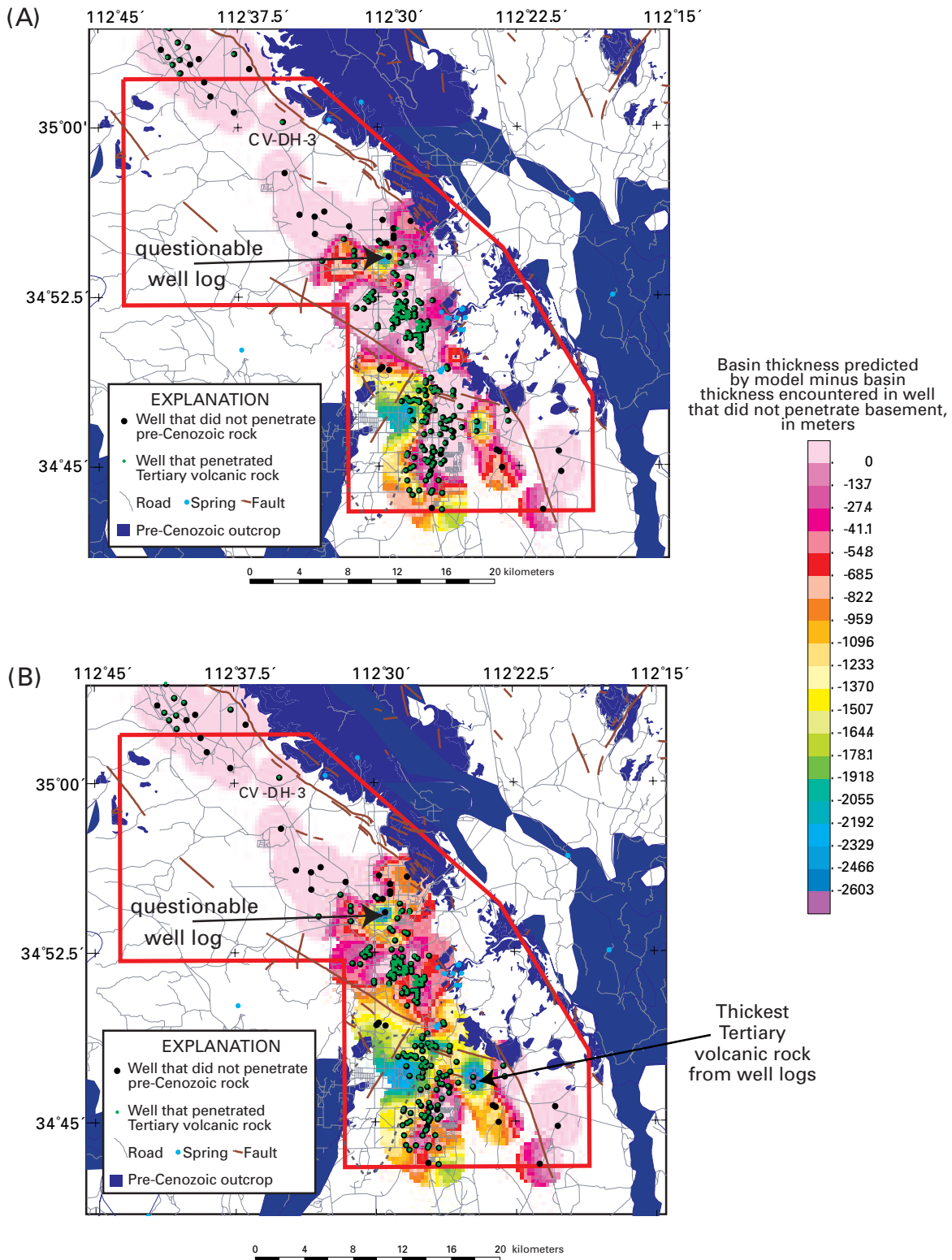


**Figure C13.** Maps of mismatch between basin thickness encountered in wells that did not encounter pre-Cenozoic bedrock and predicted basin thickness from gravity inversion models. Thick red line is survey boundary. Gray dashed line shows extent of gravity high. White areas are basin areas that do not have wells. Pink areas are where basin model thickness agrees with thickness encountered by well. Questionable well log is inconsistent with geology interpreted from adjacent well logs. (A) Mismatch for model using Tucci and others (1982) density-depth function. (B) Mismatch for model using density-depth function based on resistivity.

is 1 kilometer in figure C12a, but about 800 meters in figure C12b. CV-DH-3 bottomed in 50 meters (165 feet) of “basalt” (lati-andesite; Chapter B) at a depth of 748 meters (2455 feet). The basin models suggest that there is another 50—250 meters of Cenozoic volcanic (and presumably sedimentary) deposits below the bottom of the drill hole. Because lati-andesite underlain by Tertiary gravel is exposed on the upthrown side of the Big Chino fault on South Butte (approximately 10 kilometers northwest of the northeast corner of the aeromagnetic survey) gravel most likely underlies the lati-andesite at CV-DH-3.

The thickness of the gravel on the downthrown block could be greater than that of the upthrown block if a substantial portion of the topographic relief associated with Big Black Mesa existed at the time of gravel deposition, as inferred by Ostenaar and others (1993). The gravity inversion models suggest an additional thickness of gravel and lati-andesite of 50—250 meters beneath the bottom of CV-DH-3; the lower bound is consistent with geologic inference (Chapter B).

Estimates of the total sediment volume for the two models for the area of Big Chino Valley within the study area

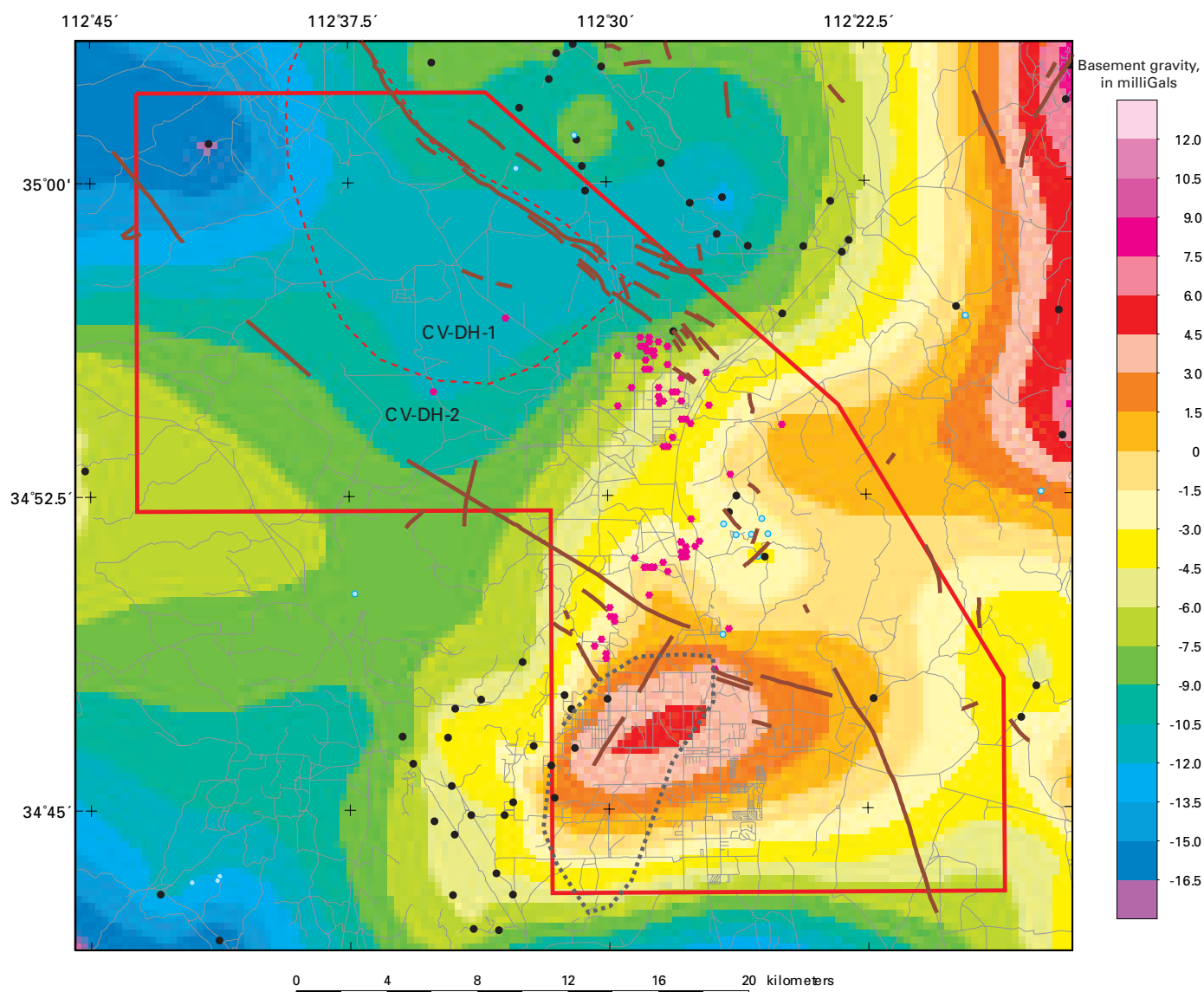


**Figure C14.** Basement gravity map (Model 2 based on density-depth function from resistivity). Black circles are gravity stations measured on bedrock. Magenta circles are wells that encountered bedrock. Gray dotted line outlines extent of isostatic gravity high that underlies western part of Little Chino Valley. The gravity inversion shows a basement gravity high in roughly the same area, but poorly matches the orientation of the high. This mismatch will introduce error in the basin thickness model. Alternatively, the source of the gravity high could reflect a great thickness of Tertiary high-density basalts within the fill (representing a large lateral change in basin-fill density that is not accounted for in the basin inversion method).

range from 140.2 to 158.4 cubic kilometers (1.14 to 1.29 x 10<sup>8</sup> acre-feet). The models show the basin beneath Big Chino Valley as asymmetric, with the deepest part of the basin along the northeastern margin of the valley and generally elongated parallel to the trend of the Big Chino fault. The deepest part of the basin is 3—4 kilometers wide; however, the western margin of the basin in the central part of the valley is not well defined because of the paucity of gravity stations. Detailed gravity profiles are limited to only the extreme northern and southern ends of the basin (fig. C3, C12). Thus, the western margin (presumably fault controlled) may trend parallel to the Big Chino fault (as suggested by Ostenaar and others, 1993). Alternatively, the western margin may trend more westerly and parallel to the scarp near Big Chino Wash and its coincident magnetic edge (BCw-PC; fig. C9).

### Playa Deposit/Alluvial Fans

One feature that has figured prominently in discussions concerning ground-water flow within Big Chino Valley is a deposit of fine-grained sediment in the center of the basin. The fine-grained sediments were deposited in a playa environment, formed by damming of from Big Chino Valley by basalt flows east of Paulden (Chapter B; Ostenaar and others, 1993). Preservation of the deposit may have been facilitated by downdropping of the basin by the Big Chino fault during late Tertiary and Quaternary time (Menges and Pearthree, 1983; Ostenaar and others, 1993).

The lateral extent of the playa deposit is approximately known from water well logs (Schwab, 1995; dashed orange line on fig. C3). The thickest part of the playa deposit is found in drill hole CV-DH-3 (~ 670 meters or 2,200 feet; Ostenaar and others, 1993; Chapter B). The playa deposit thickens towards the center of Big Chino Valley (Schwab, 1995; Ostenaar and others, 1993; and Chapter B). Gravity and resistivity methods may be a viable tool to map the distribution of playa deposits because fine-grained sediment is characterized by high porosities (thus low densities) and by low resistivities (less than 10 ohm-m).

A resistivity log indicates very low resistivities (as low as 1—2 ohm-m) in CV-DH-3 (Ostenaar and others, 1993, their fig. 3.A-2). Low resistivities (10 ohm or less) suggest the presence of saturated playa sediment. Resistivity depth soundings 3—4 kilometers northwest and southeast of the drillhole show higher resistivities. Part of this difference between the logged resistivities in CV-DH-3 and adjacent soundings can be attributed to the limited area probed by the logging method, possible contamination by drilling fluids, or irregularities on the bore surface. In other studies, a comparison of soundings derived from well logs and coincident sounding data often shows similar curves, but the log resistivities are 25 to 40 percent lower than the sounding data (R. Bisdorf, USGS, written commun., 2001). Adjusting the log resistivities at CV-DH-3 produces resistivities of less than 10 ohm-m. A resistivity profile along the southern margin of the basin, perpendicular to the axis of the valley, indicates resistivities of 10 ohm-m or

less near the eastern margin of the valley (Ostenaar and others, 1993, their fig. 3.A-3).

The resistivity soundings are limited areally as are the wells used by Schwab (1995) to delineate the outline of the playa (dashed orange line on fig. C3). Because density and resistivity are linked by a dependence on porosity, the gravity field may be useful in mapping the extent of the playa deposit. The extent of the playa deposit (fig. C3) matches much of the gravity low of Big Chino Valley. Gravity data filtered to enhance shallow sources, such as those within the basin, show low values concentrated along the eastern margin of the basin (fig. C7). Assuming that these anomalies reflect high-porosity basin fill, then one can map thickness variations in the fill. Thus, the basin thickness models can serve as a proxy for the thickness of the playa deposit, assuming that the deposit is continuous throughout the basin between depths of 100 and 700 meters (the depth range of playa deposit encountered in CV-DH-3). However, the gravity inversion method does not have the resolution to map thin lenses of gravel within the deposit, and fails to account for possible lateral variations in density within the basin (for example, coarse-grained alluvial fan deposits that lie adjacent to the Big Chino fault). Note, however, that if coarse-grained deposits are present along the fault zone, they are restricted to less than 1 or 2 kilometers southwest of the fault zone (see Ostenaar and others, 1993, their cross-section F-F'). Gravity models constrained by CV-DH-3 do not indicate a large volume of dense, coarse-grained deposits between CV-DH-3 and the Big Chino fault. However, these models provide nonunique answers. A multitude of geometries can produce the same observed gravity anomaly. Resistivity or high-resolution seismic surveys that cross the fault may help define the dimensions of lens-shaped or thin bodies of coarse-grained deposits along the fault zone and possibly within the playa deposit.

### Distribution of Volcanic Rocks in Subsurface

Magnetic anomalies reflect the presence of magnetic rock types within Tertiary volcanic rock and Proterozoic basement. Exposed volcanic rock produces either “wormlike” or semicircular anomaly patterns, as delineated by the magnetic boundaries on Figures C9 and C15. The magnetic boundaries often coincide with topographic relief on the volcanic rock, shown as dark blue lines on figure C15. Semicircular anomalies characterize exposed Tertiary lati-andesite; the anomalies usually are intense magnetic lows indicating reversely magnetized rock. Semicircular magnetic lows over areas covered by young sedimentary deposits are probably Tertiary lati-andesite plugs (annotated with “p” on fig. C15). Some of the semicircular magnetic highs (“p+”) also could be caused by lati-andesite plugs that are normally polarized or by semicircular hills of normally polarized basalt (see “b?” on fig. C15). A magnetic high at Table Mountain in the extreme southwest corner of the study area coincides with lati-andesite. A corresponding radiogenic anomaly rules out interpretation as a mafic rock such as basalt or metagabbro; see Chapter B. A circular magnetic high

1.5 kilometers north-northeast of Table Mountain also could indicate latite-andesite; alternatively, the source of the positive anomaly could be Proterozoic basement or Tertiary basalt. Tertiary basalt and Proterozoic basement are exposed immediately south of the survey boundary 2 kilometers east of Table Mountain (Krieger, 1965; Billingsley and others, 1988).

Exposed Tertiary basalt (Tby on fig. C15) produces a complicated “wormlike” magnetic anomaly pattern. In the area east of Paulden and immediately north of the Verde River, exposed basalt produces high-frequency magnetic anomalies. Some magnetic boundaries associated with the Tertiary basalt coincide with topographic relief of the exposed basaltic surface; others coincide with the contact of the basalt with weakly magnetic Paleozoic limestone. The basalt seems to be reversely polarized in the Headwaters Ranch area (HR on fig. C9), where exposed limestone coincides with a magnetic high and the surrounding basalt coincides with pronounced magnetic lows. The magnetic high is caused by the underlying Proterozoic basement (possibly granite similar to that beneath Big Black Mesa). The basalt has been dated at 4.5 Ma (McKee and Anderson, 1971) and according to the magnetostratigraphic timescale (Harland and others, 1982), should be reversely polarized. Water well logs indicate that the basalt is 148 meters (485 feet) thick about 1 kilometer north of the limestone outcrop and within the magnetic low. The increase in thickness of the basalt from 0 meters at the limestone to 148 meters at HR-2 (Ostenaar and others, 1993, their table F) would produce a negative magnetic anomaly if the basalt were predominantly reversely polarized. This change in thickness may reflect a buried fault (with a northeast strike) or topography on the pre-basalt surface (such as a paleochannel). The magnetic boundaries elsewhere within this magnetically complicated area may thus reflect abrupt changes in thickness of the basalt. The variations in thickness of basalt could have resulted from flow around topographic features produced by erosion, faulting/fracturing, or a combination of both (light blue lines on fig. C15). Other explanations for the complicated variations in the magnetic field include relief on the Proterozoic surface and variations in magnetization within either the basalt or Proterozoic basement. Without more physical property information, deeper drill holes with reliable logs, and hydrologic data, one can only point to these areas marked by strong magnetic boundaries as potential sites underlain by fractures, faults, or channel margins that likely influence the movement of ground water in this area.

West and northwest of the exposed basalt in the Verde River gorge area, strong magnetic boundaries over young sedimentary deposits (units Qal and Qs on fig. C15) may be extensions of those over exposed basalt. Well logs indicate shallow volcanic rock (generally less than 50 meters deep). About 4 kilometers northwest of the exposures of Tertiary basalt, the magnetic anomalies are less intense and strike predominantly northwest (parallel to the Big Chino fault; fig. C2, C5). Wells (150 meters or deeper) bottom in Tertiary volcanic rock in this area. Relief on the upper surface of the volcanic rock probably is the source of these northwest-striking anomalies. The

anomalies and, thus, the basalt cannot be traced more than 10 kilometers northwest from outcrops (red line on fig. C5). Thus, these northwest-striking magnetic boundaries most likely delineate faults that offset the volcanic rock or channelways (also probably fault controlled) that the volcanic rock flowed down. Tilting of the basalt could produce these anomalies; however, evidence indicates little tilting of the basalt, and well data indicate little stratigraphic separation between basalt flows (Chapter B). These features most likely are related to faulting because their strike is parallel to the most prominent fault in the study area, the Big Chino fault.

The gravity and magnetic data in Little Chino Valley do not indicate deep basins or steeply-dipping, large-offset normal faults, in contrast to the anomaly patterns in Big Chino Valley. Nor do these data detect the presence of the horseshoe-shaped Del Rio fault as inferred by Ostenaar and others (1993), although Del Rio springs is located near the intersection of magnetic lineaments (fig. C9). Almost all of the mapped faults shown in figure C15 in Little Chino Valley cut across magnetic boundaries, suggesting that fault displacements are small (less than 100 meters). Several semicircular magnetic anomalies may express concealed latite-andesite plugs, whose tops lie 300 meters or shallower based on the method of Peters (1949). Well logs indicate that several of the plugs are buried less than 200 meters. The plugs tend to be located along the margins of the valley. The maximum calculated depth to the top of an individual plug is on the order of 700 meters, based on inspection of residual anomalies after upward continuation of the magnetic field 700 and 800 meters (the depth to the top of the latite-andesite found in CV-DH-3 in Big Chino Valley). It is possible that the relative absence of plug-related anomalies in the central part of the valley west of Granite Creek is caused by a greater depth of burial to the top of the plugs. Part of this area coincides with a local gravity low (“L” on fig. C3, C7) that has north-striking edges, the eastern edge of which corresponds with a subtle magnetic gradient. The middle part of this magnetic gradient coincides roughly with a change in water-table elevation (highlighted by dashed light blue line on fig. C15). Another north-south trending gradient in the southeastern part of the survey area (dashed light blue line on fig. C15) coincides with a large change in water-level elevation (60 to more than 120 meters or 200 to more than 400 feet depths; Arizona Department of Water Resources, 2001, written communication). The magnetic gradient overlies alluvial deposits, but the source of the anomaly probably is in Proterozoic basement. North-striking magnetic, gravity and radiometric gradients caused by exposed Proterozoic basement are 5 kilometers east of the survey boundary (Langenheim and others, 2000). Thus, magnetic and gravity lineaments, even if caused by physical property variations in Proterozoic basement, also may locate potential groundwater pathways (fractures or faults within the impermeable crystalline basement). Inferred major lineaments are shown in magenta on figures C9 and C15. The relation of ground-water flow and these lineaments, if any, needs to be determined by acquiring additional data, such as hydrologic data from existing and new wells.

## Conclusions and Recommendations

The aeromagnetic and gravity data provide new insights on the distribution of and structures associated with Tertiary volcanic rock and Proterozoic basement beneath Big and Little Chino Valleys. Some of these concealed structures may act as potential pathways or barriers for groundwater movement. Of particular interest are the shallowly buried latite-andesite plugs in northern Little Chino Valley, manifested as semicircular magnetic lows. Magnetic data, as well as limited well data, indicate that these plugs lie as much as 200 to 300 meters beneath valley fill. The plugs are mostly likely barriers to ground-water flow, based on the relatively unfractured and impermeable nature of exposed intrusive centers, compared to the fractured and permeable nature of the flows and volcaniclastic aprons.

The gravity data provide additional information on basin thickness in Big Chino Valley. By using a gravity inversion method, estimates of the total sediment volume for the area of Big Chino Valley within the study area range from 140.2 to 158.4 cubic kilometers (1.14 to 1.29 x 10<sup>8</sup> acre-feet). Additional constraints, such as wells that penetrate the entire basin sequence in both valleys and more detailed gravity, electric or seismic surveys, would reduce uncertainty in estimates presented here. New wells also could test whether the structures identified here influence ground-water movement. For example, are northwest-trending fractures (inferred from geologic and geophysical data) more open to fluid flow, as proposed for these fractures throughout the Colorado Plateau (Thorstenson and Beard, 1998)?

## References Cited

- Baranov, V., 1957, A new method for interpretation of aeromagnetic maps: Pseudo-gravimetric anomalies: *Geophysics*, v. 22, p. 359-383.
- Bath, G.D., and Jahren, C.E., 1984, Interpretations of magnetic anomalies at a potential repository site located in the Yucca Mountain area, Nevada Test Site: U.S. Geological Survey Open-File Report 82-536, 27 p.
- Billingsley, G.H., Conway, C.M., and Beard, L.S., 1988, Geologic map of the Prescott 30 by 60-minute quadrangle, Arizona: U.S. Geological Survey Open-File Report 88-372, scale 1:100,000.
- Blakely, R.J., 1996, *Potential Theory in Gravity and Magnetic Applications*: Cambridge University Press, 441 p.
- Blakely, R.J., and Simpson, R.W., 1986, Approximating edges of source bodies from magnetic or gravity anomalies: *Geophysics*, v. 51, p. 1494-1498.
- Cunio, Edward Joseph, Jr., 1985, Analysis of gravity data from the southeastern Chino Valley, Yavapai County, Arizona: Northern Arizona University Master's thesis, 110 p.
- Davis, S.N., and DeWeist, R.J.M., 1966, *Hydrogeology*: John Wiley & Sons, p. 374-380.
- Dobrin, M.B., and Savit, C.H., 1988, *Introduction to Geophysical Prospecting*: McGraw-Hill Book Company, 867 p.
- Faust, L.Y., 1953, A velocity function including lithologic variation: *Geophysics*, v. 18, no. 2, p. 271-288.
- Frank, A.J., 1984, Analysis of gravity data from the Picacho Butte area, Yavapai and Coconino counties, Arizona: Northern Arizona University Master's thesis, 91 p.
- Gardner, G.H., Gardner, L.W., and Gregory, A.R., 1974, Formation velocity and density: the diagnostic basis for stratigraphic traps: *Geophysics*, v. 39, p. 770-780.
- Grauch, V.J.S., and Cordell, Lindrith, 1987, Limitations of determining density or magnetic boundaries from the horizontal gradient of gravity or pseudogravity data: *Geophysics*, v. 52, no. 1, p. 118-121.
- Harland, W. B., Cox, Allan, Llewellyn, P. G., Pickton, C. A. G., Smith, A. G., Walters, R., and Fancett, K. E., 1982, *A geologic time scale*: Cambridge University Press, 131 p.
- Jachens, R.C., and Moring, B.C., 1990, Maps of the thickness of Cenozoic deposits and the isostatic residual gravity over basement for Nevada: U.S. Geological Survey Open-File Report 90-404, 15 p., 2 plates.
- Krieger, M.H., 1965, *Geology of the Prescott and Paulden quadrangles, Arizona*: U.S. Geological Survey Professional Paper 467, 127 p.
- Langenheim, V.E., Duval, J.S., Wirt, Laurie, and DeWitt, Ed, 2000, Preliminary report on geophysics of the Verde River headwaters region, Arizona: U.S. Geological Survey Open-File Report 00-403, 28 p. (<http://wrgis.wr.usgs.gov/open-file/of00-403>).
- Langenheim, V.E., and Jachens, R.C., 1996, Thickness of Cenozoic deposits and groundwater storage capacity of the westernmost part of the Las Vegas Valley, inferred from gravity data: U.S. Geological Survey Open-File Report 96-259, 29 p.
- McKee, E.H., and Anderson, C.A., 1971, Age and chemistry of Tertiary volcanic rocks in north-central Arizona and relation of the rocks to the Colorado plateaus: *Geological Society of America Bulletin*, vol.82, no.10, p.2767-2782.
- McKee, E.H., and Elston, D.P., 1980, Reversal chronology from a 7.9-11.5 m.y. old volcanic sequence in central Arizona: Comparison with ocean floor polarity record: *Journal of Geophysical Research*, v. 85, p. 327-337.

- Menges, C.M., and Pearthree, P.A., 1983, Map of neotectonic (latest Pliocene-Quaternary) deformation in Arizona: Arizona Bureau of Geology and Mineral Technology, Open-File Report 83-22, 48 p.
- Ostenaar, D.A., Schimschal, U.S., King, C.E., Wright, J.W., Furgerson, R.B., Harrel, H.C., and Throner, R.H., 1993, Big Chino Valley groundwater study: Geologic framework investigations: Bureau of Reclamation, Denver, CO, 31 p.
- Peters, L.J., 1949, The direct approach to magnetic interpretation and its practical application: *Geophysics*, v. 14, p. 290-320.
- Phelps, G.A., Langenheim, V.E., and Jachens, R.C., 1999, Thickness of Cenozoic deposits of Yucca Flat inferred from gravity data, Nevada Test Site, Nevada: U.S. Geological Survey Open-File Report 99-310, 33 p.
- Phillips, J.D., 2001, Designing matched bandpass and azimuthal filters for the separation of potential-field anomalies by source region and source type: Australian Society of Exploration Geophysicists, 15th Geophysical Conference and Exhibition, Expanded Abstracts CD-ROM, 4 p.
- Schwab, K.J., 1995, Maps showing groundwater conditions in the Big Chino Sub-Valley of the Verde River valley, Coconino and Yavapai counties, Arizona—1992: Department of Water Resources, Hydrologic Map Series Report Number 28, Phoenix, Arizona, 1 sheet.
- Simpson, R.W., Jachens, R.C., Blakely, R.J., and Saltus, R.W., 1986, A new isostatic residual gravity map of the conterminous United States with a discussion on the significance of isostatic residual anomalies: *Journal of Geophysical Research*, v. 91, p. 8348-8372.
- Tarling, D.H., 1983, *Paleomagnetism: Principles and Applications in Geology, Geophysics, and Archaeology*: Chapman and Hall, Ltd: New York, 379 p.
- Thorstenson, D.J., and Beard, L.S., 1998, Geology and fracture analysis of Camp Navajo, Arizona Army National Guard, Arizona: U.S. Geological Survey Open-File Report 98-242, 42 p.
- Tucci, Patrick., Schmoker, J.W., and Robbins, S.L., 1982, Borehole-gravity surveys in basin-fill deposits of central and southern Arizona: U.S. Geological Survey Open-File Report 82-473, 24 p.
- Water Resources Associates, Inc., 1989, Hydrogeology investigation, Big Chino Valley, Yavapai county, Arizona, Phase I, Volumes I & II: consultants reports for City of Prescott, City Attorney's Office, Prescott, Arizona, November 29, 1989, 2 volumes.
- Wirt, Laurie, and Hjalmarson, H.W., 2000, Sources of springs supplying base flow to the Verde River headquarters, Yavapai County, Arizona: U.S. Geological Survey Open-File Report 99-0378, online release (<http://pubs.usgs.gov/of/1999/ofr-99-0378>), 54 p.



# EXPLANATION

112° 45'                      112° 37.5'                      112° 30'                      112° 22.5'                      112° 15'

## Quaternary

- Qal-Alluvium
- Qs-Sediment
- Qt-Terrace gravel
- Qg-Gravel
- Qf-Fanglomerate
- Qc-Colluvium
- QTs-Sedimentary rocks (Quaternary and Tertiary)
- QTf-Fanglomerate (Quaternary and Tertiary)

## Tertiary

- Taby-Alkali basalt )
- Tby-Basalt (Tertiary)
- Thb-Hickey Formation
- Tlau-Lati-andesite
- Tlal-Lati-andesite
- Tov-Volcanic rocks
- Tbu-Basalt, undivided
- Tsy-Sedimentary rocks
- Tso-Sedimentary rocks
- Tos-Sedimentary rocks
- Tso-Sedimentary rocks, undivided)

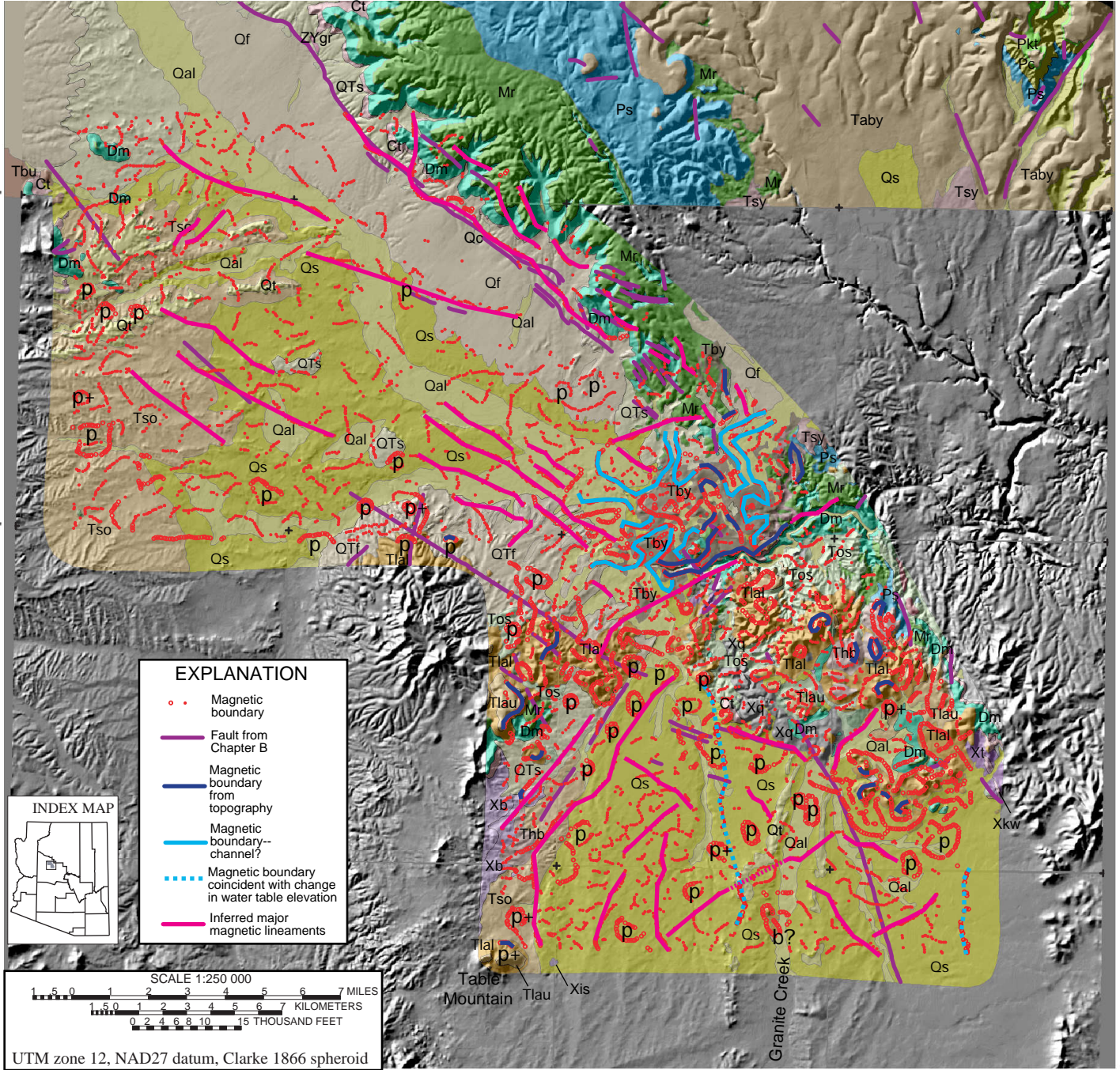
## Paleozoic

- Pkt-Kaibab and Torowep Formations (Lower Permian)
- Pc-Coconino Sandstone (Lower Permian)
- Ps-Supal Formation (Lower Permian and Upper Pennsylvanian)
- Mr-Redwall Limestone (Upper and Lower Mississippian)
- Dm-Martin Formation (Upper and Middle? Devonian)
- Ct-Tapeats Sandstone (Middle and Lower Cambrian)

## Precambrian

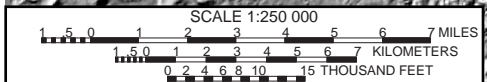
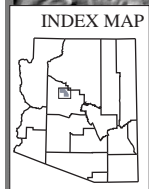
- ZYgr-Granite (Middle? Proterozoic)
- Xq-Mazatzal Formation (early Proterozoic)
- Xkw (Xap)-Alaskite of King Wash (early Proterozoic)
- Xis-Granite of Iron Springs (early Proterozoic)
- Xu-Granitic and metamorphic rocks, undivided (early Proterozoic)
- Xt-Tuffaceous metasedimentary rocks (early Proterozoic)
- Xb-Basaltic metavolcanic rocks (early Proterozoic)

35° 00'  
34° 52.5'  
34° 45'



**EXPLANATION**

- Magnetic boundary
- Fault from Chapter B
- Magnetic boundary from topography
- Magnetic boundary--channel?
- Magnetic boundary coincident with change in water table elevation
- Inferred major magnetic lineaments



UTM zone 12, NAD27 datum, Clarke 1866 spheroid



# Hydrogeologic Framework

By Laurie Wirt, Ed DeWitt, and V.E. Langenheim

Chapter D

## **Geologic Framework of Aquifer Units and Ground-Water Flowpaths, Verde River Headwaters, North-Central Arizona**

Edited by Laurie Wirt, Ed DeWitt, and V.E. Langenheim

Prepared in cooperation with the Arizona Water Protection Fund Commission

Open-File Report 2004–1411-D

**U.S. Department of the Interior**  
**U.S. Geological Survey**

**U.S. Department of the Interior**  
Gale A. Norton, Secretary

**U.S. Geological Survey**  
P. Patrick Leahy, Acting Director

U.S. Geological Survey, Reston, Virginia: 2005

For product and ordering information:  
World Wide Web: <http://www.usgs.gov/pubprod>  
Telephone: 1-888-ASK-USGS

For more information on the USGS--the Federal source for science about the Earth, its natural and living resources, natural hazards, and the environment:  
World Wide Web: <http://www.usgs.gov>  
Telephone: 1-888-ASK-USGS

Any use of trade, product, or firm names is for descriptive purposes only and does not imply endorsement by the U.S. Government.

Although this report is in the public domain, permission must be secured from the individual copyright owners to reproduce any copyrighted materials contained within this report.

***Suggested citation:***

Wirt, F.N., DeWitt, Ed, and Langenheim, V.E., 2005, Hydrogeologic Framework, *in* Wirt, Laurie, DeWitt, Ed, and Langenheim, V.E., eds., Geologic Framework of Aquifer Units and Ground-Water Flowpaths, Verde River Headwaters, North-Central Arizona: U.S. Geological Survey Open-File Report 2004-1411-D, 27 p.

## Contents

Abstract.....	1
Introduction.....	1
Geologic Setting.....	1
Permeability of Rock Units .....	6
Proterozoic Rocks.....	6
Paleozoic Rocks .....	6
Tertiary Rocks and Sediment.....	8
Basement Geometry and Aquifer Boundaries.....	8
Recharge Areas and Spring Locations .....	9
Water-Bearing Characteristics of Major Aquifer Units.....	10
Carbonate Aquifer.....	10
Carbonate Aquifer Underlying Basin-Fill Deposits .....	13
Carbonate Aquifer North of Upper Verde River .....	13
Basin-fill Deposits.....	17
Big Chino Basin-Fill Aquifer .....	17
Tertiary Basalt Flows.....	18
Playa Deposit.....	18
Other Basin-Fill Alluvium .....	19
Little Chino Basin-Fill Aquifer .....	19
Paleozoic Rocks.....	20
Older Sedimentary Rocks.....	20
Lati-andesite .....	20
Hickey Formation Volcanic and Sedimentary Deposits .....	20
Quaternary to Late Tertiary Alluvial Deposits .....	21
Water-Level Gradients of Major Aquifers.....	21
Big Chino Basin-fill Aquifer .....	21
Little Chino Basin-fill Aquifer .....	22
Carbonate Aquifer.....	22
Big Black Mesa and the Ground-Water Divide .....	23
Carbonate Aquifer North of Upper Verde River .....	23
Summary and Conclusions.....	24
References Cited.....	25

## Figures

- |  |   |
|--|---|
| <b>D1.</b> Schematic diagram of Colorado Plateau and Transition Zone geologic provinces and prominent geographical features, upper Verde River watershed .....                           | 2 |
| <b>D2.</b> Schematic diagram of basin-fill aquifer boundaries in relation to geologic provinces and different parts of the regional carbonate aquifer, upper Verde River watershed ..... | 3 |

<b>D3.</b>	Geologic map of the Verde River headwaters study area .....	4
<b>D4.</b>	Shaded elevation map showing basin-fill aquifer boundaries and the location of high-altitude (red) and low-altitude (yellow) springs .....	5
<b>D5.</b>	Photograph of King Spring in Hell Canyon .....	9
<b>D6.</b>	Columnar section of Verde River headwaters region, north-central Arizona .....	11
<b>D7.</b>	Photograph of large solution features in Redwall Limestone in upper Verde River canyon .....	12
<b>D8.</b>	Compilation of water-level contours in the Verde River headwaters area (after Schwab, 1995; Corkhill and Mason, 1995).....	14
<b>D9.</b>	Water-level contour map for carbonate aquifer north of upper Verde River .....	15

## Tables

<b>D1.</b>	Water-bearing characteristics of major aquifer units.....	7
<b>D2.</b>	Range in hydraulic conductivity of sediment and rock types found in Big and Little Chino basins .....	16
<b>D3.</b>	Water-level measurements for wells north of the upper Verde River .....	17

# Hydrogeologic Framework

By Laurie Wirt, Ed DeWitt, and V.E. Langenheim

## Abstract

The upper Verde River watershed drains the northwestern Transition Zone and southwestern Colorado Plateau geologic provinces. Proterozoic igneous rocks largely define the basin geometry and boundaries of the Big and Little Chino basin-fill aquifers. Big and Little Chino Valleys contain gently sloping reservoirs of ground water that drain toward large springs near their basin outlets. The ground-water flow direction of basin-fill aquifers is from the basin margins and tributaries toward the basin center and then down the major axes of the valleys. Spring flow in the river canyon emerges from Paleozoic carbonate rocks downstream from the confluence of the Big and Little Chino basin-fill aquifers.

In Little Chino Valley, a complex sequence of alluvial and volcanic deposits forms a highly productive aquifer having confined and unconfined ground-water conditions. Artesian flow near the town of Chino Valley can be produced from (a) trachyandesite overlying small pockets of irregularly distributed sediment, (b) volcanic-clastic sequences within the latite-andesite, (c) latite-andesite over sedimentary rock or alluvium, (d) permeable basalt beneath strongly cemented alluvium, and (e) unconsolidated alluvium beneath strongly cemented alluvium. Buried plugs of latite-andesite increase in abundance north of Del Rio Springs. The narrow basin outlet and low permeability of the plugs restrict northern movement of ground water, contributing to discharge at Del Rio Springs. From Del Rio Springs, the most reasonable flowpath is northeast through faulted Paleozoic rock and latite-andesite toward spring-fed Stillman Lake and Lower Granite Spring.

In Big Chino Valley, ground-water flowpaths and rates of flow are influenced by the heterogeneous distribution of alluvial deposits (including a fine-grained playa deposit) and buried basalt flows. At the ground-water outlet near Paulden, a highly permeable basalt flow straddles both sides of the basin margin, and a moderately permeable carbonate aquifer shallowly underlies the basin-fill deposits. The Big Chino basin-fill aquifer and the carbonate aquifer north of the upper Verde River are hydraulically connected, as indicated by a water-level gradient of less than 10 ft per mi across the basin boundary. The regional ground-water flow direction between Paulden and Hell Canyon is east or southeast, consistent with the Big Chino aquifer as the major source of discharge to upper Verde River springs. Potential contributions from carbonate units to the Big Chino basin-fill aquifer, if any, are most

likely to occur (a) beneath the Big Chino basin-fill aquifer, (b) through alluvial fans along the base of Big Black Mesa, or (c) near the outlet of the basin-fill aquifer along fractures parallel to the northwest-striking Big Chino Fault.

## Introduction

Three major aquifers in the headwaters study area contribute base flow to the upper Verde River. They are the Big and Little Chino basin-fill aquifers and the adjoining carbonate aquifer. This chapter describes the geologic setting, aquifer boundary conditions, water-bearing characteristics, and regional water-level gradients. Local heterogeneities within each major subbasin or aquifer are described, including differences in permeability of rock types, water-bearing characteristics of aquifer units, stratigraphic relations, and structures that control local movement of ground water. The objective of this chapter is to provide a conceptual hydrogeologic framework for ground-water flowpaths in the upper Verde River headwaters region.

## Geologic Setting

Big and Little Chino Valleys are part of the Transition Zone, a physiographic and tectonic transition between the relatively undeformed Colorado Plateau province to the northeast, and the severely faulted Basin and Range province to the southeast (Pierce, 1985; Ostenaar and others, 1993). The Verde River watershed drains nearly equal parts of the Transition Zone and the southwestern edge of the Colorado Plateau (fig. D1). The Transition Zone developed in response to tectonic uplift, rifting, and extensional movements that formed the Basin and Range province during the Tertiary period. These profound structural changes had little effect on the flat-lying rocks of Colorado Plateau (Lucchitta, 1989). Big and Little Chino Valleys (and Verde Valley to the east) are among the first in a series of alluvial basins extending outward from the eroded southwestern margin of the Colorado Plateau. Transition Zone basins tend to be smaller and shallower than Basin and Range basins farther south and west. Their average elevation is intermediate between the plateau rim and the southern desert basins.

D2 Hydrogeologic Framework

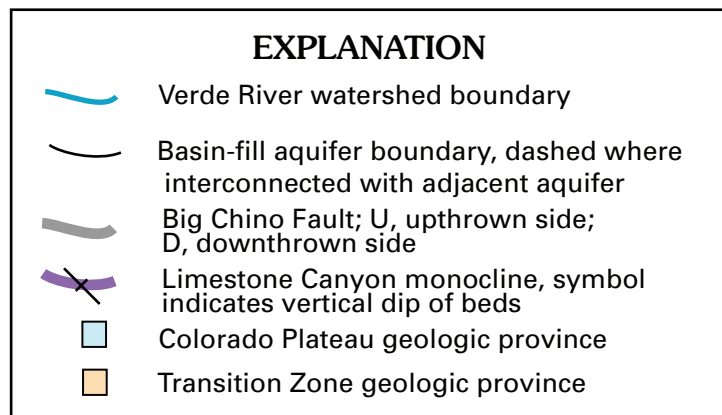
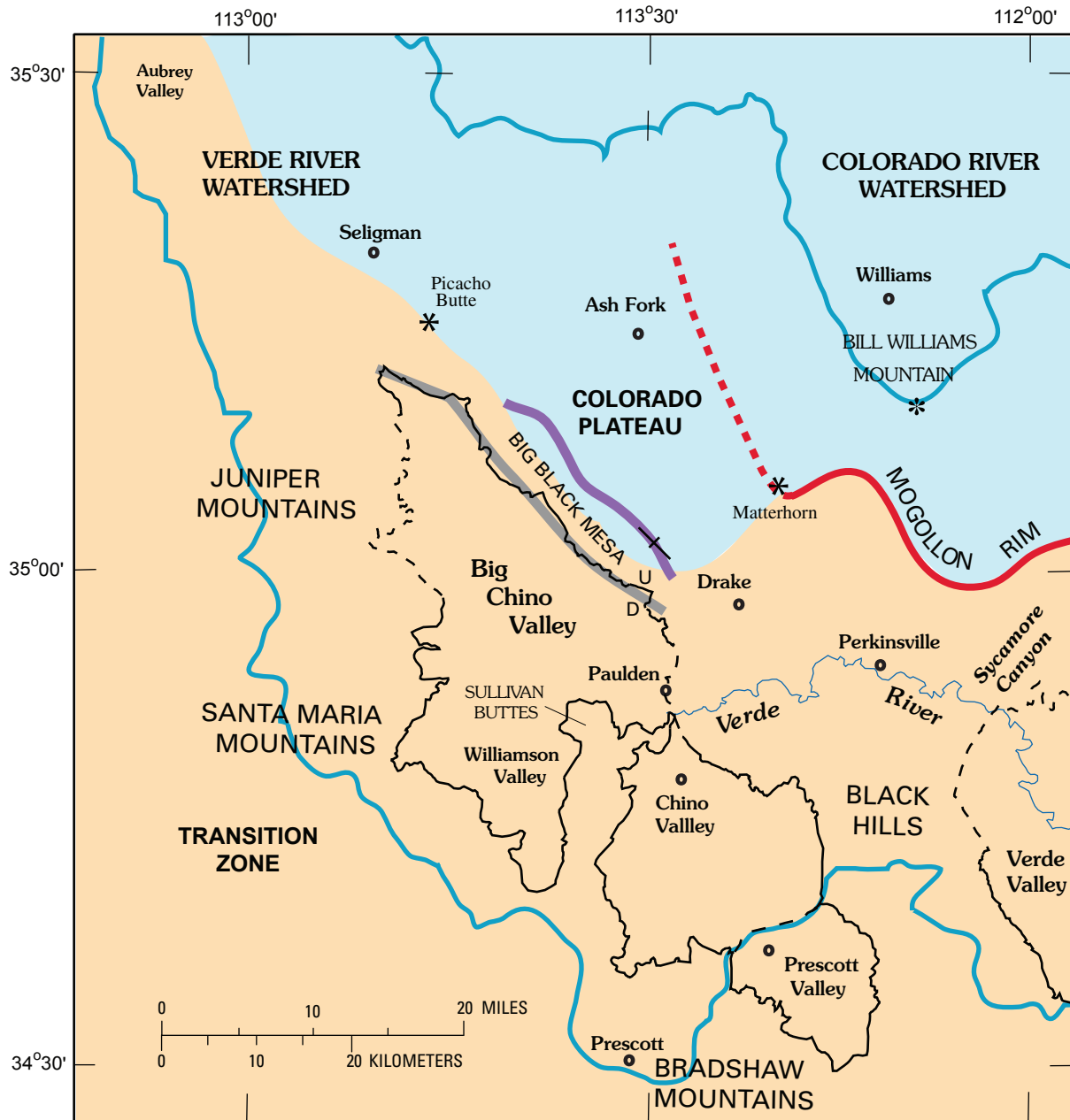
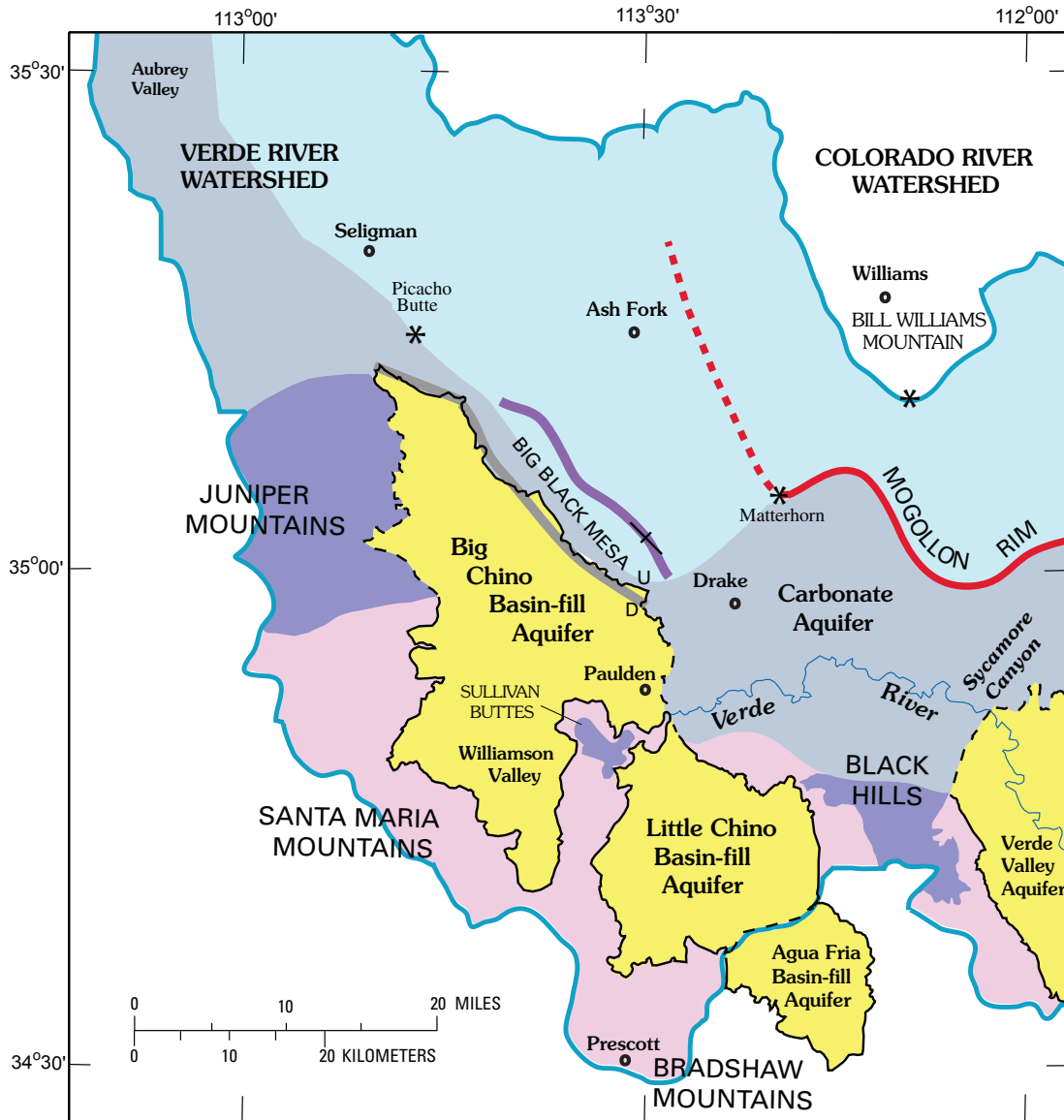


**Figure D1.** Schematic diagram of Colorado Plateau and Transition Zone geologic provinces and prominent geographical features, upper Verde River watershed. Base is from U.S. Geological Survey digital data 1:100,000.



**EXPLANATION**

	Carbonate aquifer; moderate to high permeability; beneath Colorado Plateau
	Carbonate aquifer; moderate to high permeability; Transition Zone; connected to Colorado Plateau
	Carbonate remnant; moderate to high permeability; Transition Zone; disconnected from Colorado Plateau
	Igneous and metamorphic rocks; low permeability
	Basin-fill aquifer, moderate to high permeability; Transition Zone, boundary dashed where likely interconnected with adjacent aquifer
	Verde River watershed boundary
	Big Chino Fault; U, upthrown side; D, downthrown side
	Limestone Canyon monocline, symbol indicates vertical dip of beds

**Figure D2.** Schematic diagram of basin-fill aquifer boundaries in relation to geologic provinces and different parts of the regional carbonate aquifer, upper Verde River watershed. Base is from U.S. Geological Survey digital data 1:100,000.



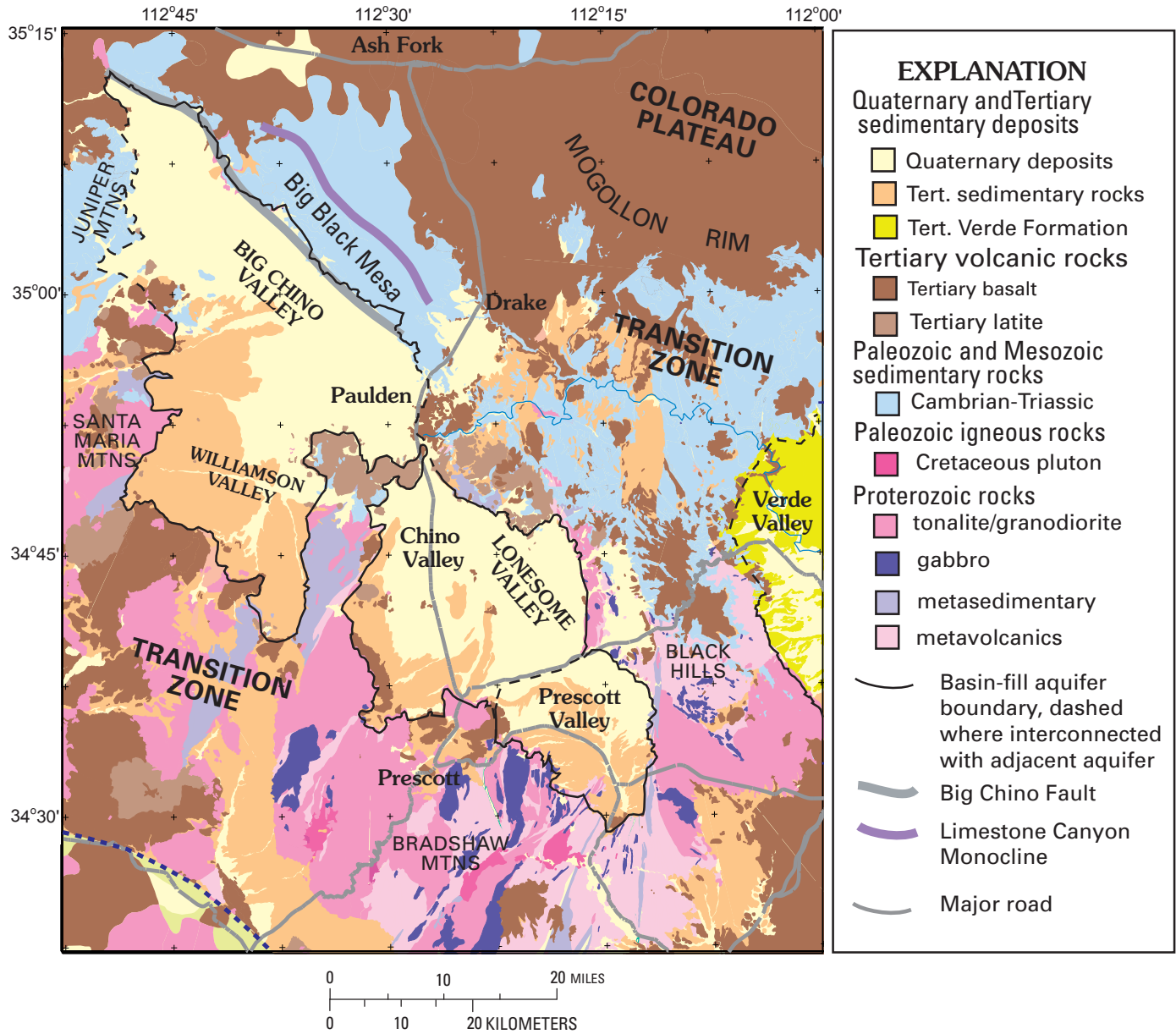
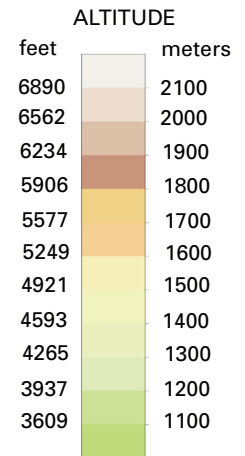
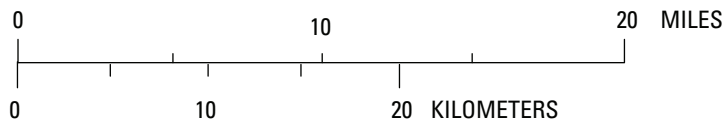
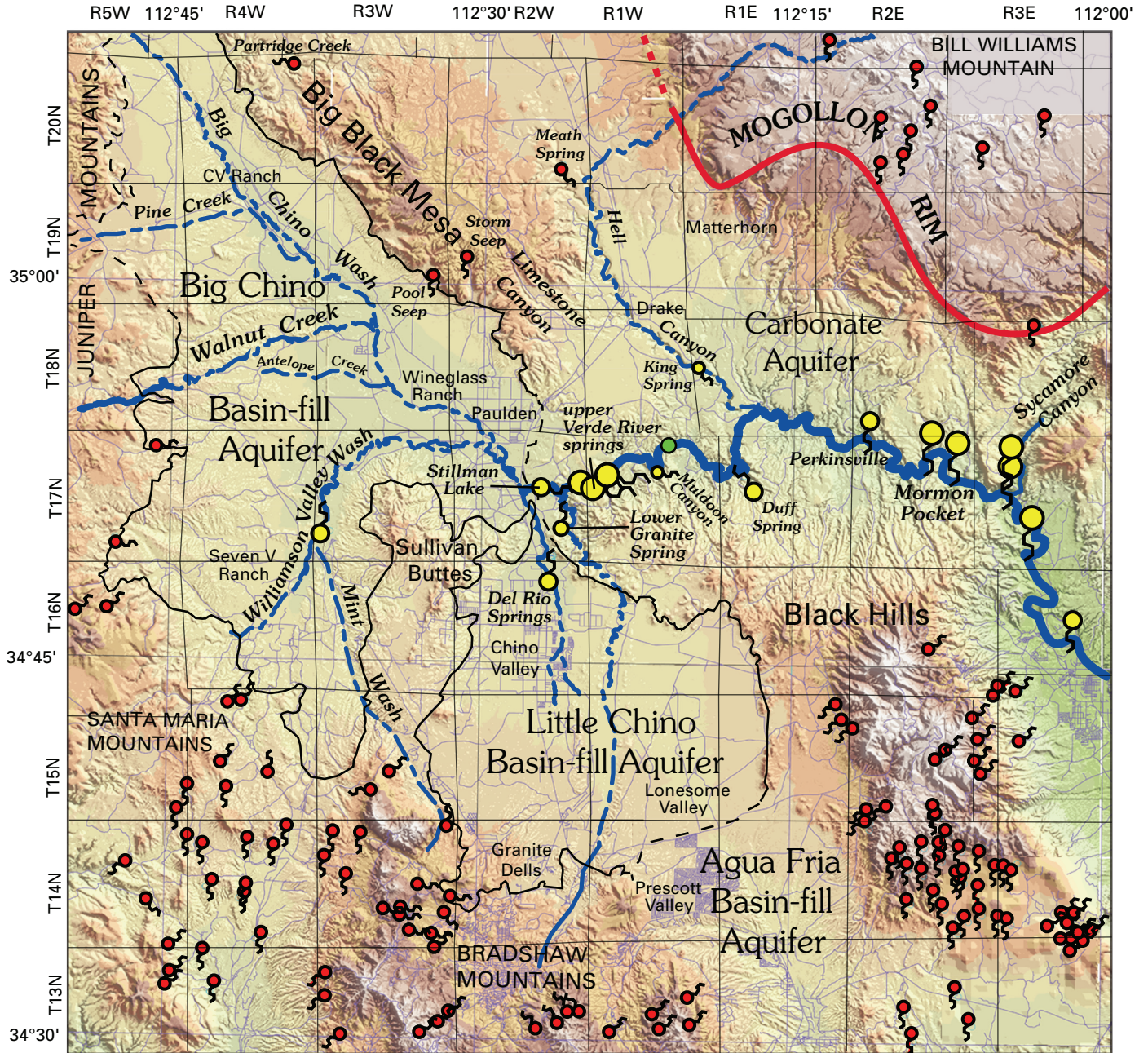


**Figure D3.** Geologic map of the Verde River headwaters study area (simplified from DeWitt and others, in press). Geology outside of thick dotted blue line is abridged from Reynolds (1988) and Richard and Kneale (1993). Base is from U.S. Geological Survey digital data 1:100,000.

**Figure D4 (facing page).** Shaded elevation map showing basin-fill aquifer boundaries and the location of high-altitude (red) and low-altitude (yellow) springs. Aquifer boundaries are dashed where likely interconnected with adjacent aquifer. Base is from 1:100,000 U.S. Geological Survey digital data.



**EXPLANATION**

	Low-altitude spring (< 4,550 ft; > 5 ft <sup>3</sup> /s)		Basin-Fill Aquifer boundary; dashed where interconnected
	Low-altitude spring (< 4,550 ft; 1 to 5 ft <sup>3</sup> /s)		USGS Paulden gage (station 09502800)
	Low-altitude spring (< 4,550 ft; < 1 ft <sup>3</sup> /s)		High-altitude spring (>5,000 ft; < 1 ft <sup>3</sup> /s)

All basins and ranges south and west of the margin of the Colorado Plateau are in the Transition Zone (Pierce, 1985). Within the study area, the southern boundary of the Colorado Plateau is defined, in part, by the erosional scarp of the Mogollon Rim (figs. D1–D4). The Mogollon Rim is well-defined near the Matterhorn, a prominent topographic feature northeast of Drake. The Rim is a steep escarpment east of the Matterhorn in Sycamore Canyon and north of Verde Valley. West of the Matterhorn, the Rim extends northward toward Ash Fork, where it is partially to completely buried by Tertiary basalt flows (DeWitt and others, in press), and lacking in topographic definition. The southern boundary of the Colorado Plateau west of Drake is defined by the crest of Big Black Mesa north of Big Chino Valley. North of Drake, the southern boundary of the Colorado Plateau is offset between the Matterhorn and the anticlinal crest of Big Black Mesa. Thus, the southern and western boundary of the Colorado Plateau within the study area is defined by Big Chino Valley and the crest of Big Black Mesa, which define the northern boundary of fault-bounded basins of middle Tertiary age.

As evidenced by the extremely rugged topography of canyons, cliffs, and buttes, the upper Verde River is actively eroding the southern margin of the Colorado Plateau. Given enough geologic time and the right conditions, the rim of the Colorado Plateau predictably will recede farther north toward the Grand Canyon. Sycamore Canyon, Hell Canyon, and Partridge Creek are among the largest of many deeply incised canyons eroding the edge of the plateau within the Verde River watershed (fig. D4). Prominent head cuts occur at the confluence of Big and Little Chino Valleys at Sullivan Lake and in Hell Canyon north of Drake. Erosion along Partridge Creek and Limestone Canyon has nearly severed Big Black Mesa from the rest of the Colorado Plateau. Other erosional remnants of Paleozoic strata that were once connected to the Colorado Plateau are located in the Juniper Mountains, Sullivan Buttes, and in the Black Hills (fig. D2).

Basement rocks in the Transition Zone have undergone regional Basin and Range extensional faulting. Mountain ranges are the uplifted blocks, and the down-dropped basins form grabens. Proterozoic igneous and metamorphic rocks are presumed to underlie Paleozoic sedimentary rocks beneath the basin-fill material in most of Big and Little Chino basins (fig. D3). Where Proterozoic rocks are exposed in the bottoms of canyons, they display irregular relief beneath the Paleozoic strata.

The three major aquifers in the study area—the Big and Little Chino basin-fill aquifers and the adjoining carbonate aquifer—have aquifer characteristics intermediate to those of the Colorado Plateau and the Basin and Range. The two basin-fill aquifers contain alluvial sediments and Tertiary volcanic rocks that resulted from Basin and Range faulting and extension. The regional carbonate aquifer is partly capped by Tertiary basalt, which in some areas has filled incised paleochannels. The Big and Little Chino basin-fill aquifers have the large storage capacity of typical Basin and Range basin-fill aquifers and deliver steady, reliable discharge to their

outlets. The carbonate aquifer in the Transition Zone north of Big Chino Valley and the upper Verde River is the broken and eroded margin of a large regional carbonate aquifer that lies more than 3,000 ft beneath much of the southwestern Colorado Plateau. Karst plays an important role in ground water movement not only for the carbonate aquifer north of the upper Verde River, but underneath and along the margins of the Big Chino basin-fill aquifer where it is shallowly underlain by carbonate rocks.

## Permeability of Rock Units

Permeability is the capacity of a porous rock or sediment to transmit fluid. Overall permeability of rock types in the study area is a function of primary and secondary porosity. Primary porosity is the percentage of pore space in a rock or sediment at the time of deposition or following cementation. Secondary porosity develops after emplacement of a stratigraphic unit through processes such as fracturing or dissolution. Secondary porosity greatly increases the overall permeability because of the presence of fractures, joints, karst features, and other structures, such as faults, which are likely to be connected and allow fluid flow.

## Proterozoic Rocks

Most Proterozoic rocks types of igneous and metamorphic origin have low to very low porosity (table D1). Such rocks lack pore space because of their crystalline nature and include granodiorite (units Xpr, Xwv), aplite-pegmatite (unit Xap), and gabbro (unit Xgb). The Mazatzal Group consists of quartzite that is strongly cemented by secondary quartz, thereby destroying any primary porosity that the sandstone had prior to metamorphism. All these rock units and similar granite and granodiorite to the west, beneath Big Chino Valley, contain few fractures, joints, and faults, and have low permeability.

Strongly foliated rock units such as metabasalt (unit Xb), metatuff (unit Xt), and metamorphosed pelitic sediments (unit Xp) have an increased secondary porosity due their prominent northeast-striking foliation, which creates zones of weakness along which joints and fractures locally form. At some places, these rocks have been deeply weathered before deposition of the Tapeats Sandstone, and their overall permeability may be markedly increased. Some water wells southeast of Sullivan Lake report yields of 50–100 gallons per minute (gpm) from zones within metatuff (Arizona Department of Water Resources, 2002).

## Paleozoic Rocks

Most Paleozoic rocks have moderate permeability (table D1). Only the Tapeats Sandstone (unit Ct) has low permeability, due to its strongly cemented nature. The Bright Angel Shale and the Chino Valley Formation, found

**Table D1.** Relative porosity and permeability of stratigraphic units.

Period	Map unit	Stratigraphic unit	Primary porosity	Secondary porosity	Overall permeability
Quaternary	Qal	alluvium	high		high
	Qf	fanglomerate	high		high
	Qt	gravel	high		moderate
	Qg	gravel	high		high
	Qs	undivided sediment	moderate		moderate
	QTf	fanglomerate	moderate		moderate
	QTs	undivided sediment	moderate		moderate
	Taby	alkali basalt	low	high	high
	Tby	basalt	low	high	high
	Tcy	cinders	high		high
	Tsy	conglomerate	high		high
	Tabo	alkali basalt	low	high	moderate
	Tso	conglomerate	high		high
	Thb	basalt	low	high	moderate
Tertiary	Tha	trachyandesite	low	moderate	moderate
	Ths	conglomerate	high		high
	Tlau	upper lati-andesite	low	moderate	moderate
	Tlal	lower lati-andesite	low	moderate	moderate
	Tla	undivided lati-andesite	low	moderate	moderate
	Tla	lati-andesite intrusive centers	low	low	low
	Tla	breccia	moderate		moderate
	Tla	cinders	moderate		moderate
	Tos	conglomerate	high		high
	Permian	Ps	sandstone	moderate	
Mississippian	Mr	limestone	moderate	high	high
Devonian	Dm	dolomite	moderate	moderate	moderate
Cambrian	Ct	sandstone	low		low
Proterozoic	Xq	quartzite	very low		very low
	Xpr	granodiorite	very low		very low
	Xap	aplite-pegmatite	very low		very low
	Xwv	granodiorite	very low		very low
	Xp	pelitic schist	very low	moderate	low
	Xgb	gabbro	very low		very low
	Xb	metabasalt	low	moderate	low
	Xt	metatuff	very low	moderate	moderate

above the Tapeats, are inferred to have low porosity owing to the clay origin of shale. The Martin Formation contains abundant northwest-striking high-angle joints near its base, thereby enhancing its overall permeability. Locally, the base of the Martin includes dissolution cavities and other small karst features. The middle part of the Redwall Limestone is strongly modified by karst solution, creating connected caves and collapse features. Hence, its overall permeability is among the highest of any rock type for the study area (table D1). Sandstone in the Supai Formation is poorly cemented, giving it moderate overall permeability.

The Tapeats, due to its low overall porosity, forms a resistive layer to vertical movement beneath the overlying Paleozoic units. For this reason, springs such as those along the upper Verde River are preferentially localized at the base of the Martin. Productive water wells near Drake (Southwest Groundwater Consultants; 2002) and in the carbonate aquifer north of Paulden (Water Resources Associates, 1990) attest to the moderate permeability of the lower part of the Martin.

### Tertiary Rocks and Sediment

Conglomerate beneath lati-andesite (unit Tso) contains poorly lithified and cemented gravel and sandstone, all of which have high primary porosity and high permeability (table D1). Overlying lati-andesite flows (units Tla, Tlal, and Tlau) have low primary porosity due to their igneous nature, but interbedded breccia and cinders have an increased permeability. Lati-andesite flows contain intersecting cooling fractures and joints that give the lati-andesite a moderate overall permeability. Strongly cemented lati-andesite may form a confining layer in the central part of Little Chino Valley. Intrusive centers of lati-andesite have very low permeability.

Conglomerate beneath flows in the Hickey Formation (unit Ths) contains poorly cemented and lithified gravel and sandstone, all of which have high secondary porosity and permeability (table D1). Overlying basalt flows (unit Tby) contain abundant intersection columnar joints which give the basalt a moderate overall permeability. Trachyandesite in the Hickey (unit Tha) contains fewer columnar joints, and a somewhat lower overall permeability, but a classification of moderate is assigned (table D1). Because the trachyandesite in the Hickey contains fewer columnar joints than basalt, it may form a confining layer between the town of Chino Valley and outcrops in the Sullivan Buttes to the west.

Conglomerate beneath highly magnetic basalt flows (unit Tso) is poorly sorted and lithified and has high permeability. Underlying highly magnetic alkali basalt (unit Tabo) is presumed to have high secondary porosity and overall moderate permeability similar to flows in the Hickey Formation.

Basalt flows derived from the Colorado Plateau or erupted within the study area (units Taby and Tby) have high overall permeability (table D1), due in large part to extensive intersecting columnar joints. Highly productive water wells near Paulden, some yielding thousands of gpm (Water Resource Associates, 1989, 1990), attest to the high permeability of the

basalt flows. Interbedded deposits of cinders (unit Tcy) have high permeability, as shown by driller's logs of water wells located south and west of Paulden (Arizona Department of Water Resources, 2002). Conglomeratic sediment interbedded with the basalt flows (unit Tsy) has a high permeability due to the uncemented nature of the sediment.

Tertiary and Quaternary sedimentary rocks and sediments in Big and Little Chino Valleys have moderate to high primary porosity and overall permeability (table D1). High permeability is indicated for alluvium (unit Qal), fanglomerate along the southwestern face of Big Black Mesa (unit Qf), and well-sorted gravel (units Qg and Qt). Distal deposits of fanglomerate, near the center of Big Chino Valley, should have reduced permeability compared to proximal deposits near Big Black Mesa. Moderate permeability is estimated for mixed types of sedimentary rocks and sediments (units Qs, QTs) and fanglomerate that surrounds Sullivan Buttes (unit QTf). This fanglomerate is locally strongly cemented in layers tens-of-ft thick, unlike fanglomerate along the southwestern face of Big Black Mesa. The strongly cemented fanglomerate may form a local confining layer in the northern part of Little Chino Valley.

Playa deposits in Big Chino Valley (time equivalent of unit Tsy and Tso) in all likelihood have a lower overall permeability than most surficial units (Qal, Qf, Qt and Qg), but an accurate estimation is difficult due to a lack of representative samples. Most cuttings of playa materials are contaminated with drilling mud and probably represent the most resistant rock types in the playa; the softer and water-soluble material was destroyed during drilling. Representative core samples of the playa deposit would be needed to determine its overall permeability.

### Basement Geometry and Aquifer Boundaries

Proterozoic basement rocks define the basin geometry and areal extent of basin-fill aquifers in the Verde River headwaters region (fig. D3). The basin-fill deposits and Paleozoic sedimentary rock overlie an irregular topography of Proterozoic igneous and metamorphic rocks. The most common basement rocks are granite, gabbro, metavolcanic and metasedimentary schist, in decreasing order of abundance. Water yields in such rocks generally are poor and depend on the presence, if any, of fractures and their degree of interconnection. These rocks play an important role hydrologically, because they define the low permeability boundaries of the basins and increase runoff potential in upland areas where they are exposed. They also provide a source of solutes and detrital minerals to alluvium and soil.

Aquifer boundaries (figs. D1–D4) are drawn as solid lines where the basin-fill deposits abut Proterozoic basement rocks having low permeability. Dashed lines indicate potential connections between the basin-fill aquifers and adjoining carbonate or basin-fill aquifers. Dashed boundaries

occur in four locations. First, the northwest boundary of the Big Chino aquifer along the Juniper Mountains is in contact with an erosional remnant of the carbonate aquifer. Second, the Big Chino aquifer north of Paulden is in contact with carbonate rock along part of the Big Chino fault, where there is little vertical displacement. Displacement along the fault increases to the northwest, where basin-fill sediments are in faulted contact with relatively impermeable Proterozoic rock (DeWitt and others, Chapter B, this volume), indicated by a solid-line boundary. Third, the southeast boundary of the Little Chino basin-fill aquifer adjoins the Agua Fria basin-fill aquifer. And fourth, the northeastern boundary of the Little Chino aquifer (north of Del Rio Springs) adjoins the carbonate aquifer near Stillman Lake and lower Granite Creek. In all four cases where aquifer boundaries are dashed, the adjoining aquifers are interpreted as connected, indicating that ground water can potentially move between one aquifer and the other. The basin-fill aquifer boundaries presented here are largely consistent with those interpreted by Robson and Banta (1995) at the 1:100,000 scale.

## Recharge Areas and Spring Locations

Recharge from snowmelt and rainfall runoff is conveyed by gravity from upland areas to basin-fill aquifers and then through connected bedrock openings to reach springs near the topographic outlets of Big and Little Chino Valleys. The size and location of springs depend on many factors, including climate, the nature and relation of permeable and impermeable strata, the extent of upland drainage areas, and the position of the water-level gradient relative to the land surface. Springs identified from USGS 1:24,000 scale maps (fig. D4) in this study have been broadly subdivided into two groups—high-altitude springs (in red) and low-altitude springs (in yellow). These groupings will be conceptually useful in the forthcoming discussion of water chemistry (Wirt and DeWitt, Chapter E; this volume).

High-altitude springs are defined here as springs in bedrock areas at elevations greater than 5,000 ft above sea level. These springs are not part of a large aquifer system and generally discharge small volumes relative to low-altitude springs (defined here as springs at elevations below 4,550 ft above sea level). Ground water supplying high-altitude springs is stored in small-volume secondary openings, such as fractures, catchments of colluvium, or pockets of stream alluvium. High-altitude springs tend to respond more quickly to temporal changes in precipitation than low-altitude springs. Having limited storage capacity, they are more likely to dry up during extended periods of drought. Despite their smaller volume, high-altitude springs sustain intermittent and perennial stream segments in Mint Wash, Williamson Valley Wash, Walnut Creek, Pine Creek, and their tributaries.

Streams and washes in Big and Little Chino Valleys are predominantly ephemeral except where the ground-water table is shallow and intercepted by the land surface, such as near the

topographic outlets of the valleys. These low-altitude springs often create cienagas, or spring-fed marshes. The largest low-altitude spring in Little Chino Valley is Del Rio Springs. A 4-mi reach of lower Williamson Valley Wash is supplied by ground water, or spring fed, as are reaches of Walnut Creek, lower Granite Creek, and lower Sycamore Creek. The largest spring network downstream from the Verde River/Granite Creek confluence (upper Verde River springs) lies below the topographical outlets of both Big and Little Chino valleys. Ground water in the Paleozoic carbonate aquifer usually discharges to the base of incised limestone canyons, such as upper Verde River springs, Stillman Lake, and King Spring in Hell Canyon (fig. D5). Ground water travels preferentially through networks of fractures and solution zones in limestone, although seepage from limestone beneath streambed alluvium will appear diffuse.

Within the Transition Zone, the Paleozoic sedimentary rocks that form the carbonate aquifer typically are incised, with as much as 2,000 ft of vertical relief north of the upper



**Figure D5.** Photograph of King Spring in Hell Canyon. View is north. Rocks are Supai Formation capped with Tertiary basalt. The spring discharges from the carbonate aquifer where the land surface intersects the water table. (Photograph by L. Wirt, U.S. Geological Survey.)

Verde River and along Big Black Mesa. Because the topography is so irregular, the depth of the water table beneath the land surface is highly variable. For example, the land surface intersects the water table at King Spring, a permanent spring in the bottom of Hell Canyon about 2 mi southeast of Drake (fig. D4). At the base of the vertical walled canyon between Drake and King Spring, the saturated zone is between 0 and about 25 ft beneath the stream channel. Perpendicular to this reach in either direction, the aquifer is overlain by 400 ft of unsaturated rock. Artesian conditions have been encountered near Drake, indicating the aquifer is confined, at least locally.

The amount of surface-water runoff and ground-water recharge at any location is a function of precipitation, vegetation, slope, and the capacity of water-bearing rock and sediment units to absorb, store, and transmit water. High-altitude springs are most numerous where precipitation is great and rocks are relatively impermeable, particularly in the granite and gneissic rocks of the Bradshaw, Santa Maria, and Juniper Mountains, and the Black Hills (fig. D4). Only four small springs are present around the perimeter of Big Black Mesa, which is attributed in part to lesser amounts of precipitation and in part to the greater permeability of the carbonate rocks. Ground-water recharge is very efficient in karst terrain because precipitation readily infiltrates secondary rock openings that intersect the land surface (Winter and others, 1999; p. 50). Volcanic rocks also have a high degree of secondary porosity caused by uneven cooling fractures and unconformities. High-altitude springs are relatively common draining from basalt south of Bill Williams Mountain and in the headwaters of Sycamore Canyon. These high areas receive some of the greatest amounts of precipitation in the study area (Chapter A; fig. A9).

In a study of southern Coconino County, McGavock and others (1986, p. 13) found the least amount of surface-water runoff (and greatest recharge potential) where permeable volcanic cinders were exposed at land surface. Infiltration also tended to be higher at lower altitudes, such as in relatively flat parts of Cataract Canyon and Little Colorado River drainages. Runoff was greatest where topography was steep and rocks were least permeable, such as igneous rocks and schist. Based on these findings it is expected that infiltration in the study area is greatest for Paleozoic carbonate rocks and Tertiary volcanic rocks. Recharge also is expected to be high for low-gradient runoff flowing over alluvium. In addition, recharge occurs as seepage losses beneath losing reaches of major tributaries.

## Water-Bearing Characteristics of Major Aquifer Units

Water-bearing units range from Paleozoic to Quaternary in age and are presented in ascending order from oldest to youngest. At any given location, an aquifer may consist of one or more water-bearing units, spanning a broad range in age (fig. D5). Not all units are available in all locations. The

carbonate aquifer is comprised of several Paleozoic sedimentary units, ranging in age from Cambrian to Permian. The carbonate aquifer is locally overlain by thick Tertiary basalt flows and sediments, which can fill incised paleochannels to depths that extend below the water table. Similarly, the Big and Little Chino basin-fill aquifers, which are predominantly comprised of Tertiary and Quaternary sediment, commonly include Tertiary basalt, latite-andesite, and conglomerate facies.

## Carbonate Aquifer

Nearly the entire region north of the Big Chino Fault and the upper Verde River (in the Transition Zone and extending beneath the Colorado Plateau) is comprised of a continuous expanse of Paleozoic sedimentary rocks, overlain in some areas by Tertiary basalt flows. In addition, eroded remnants of Paleozoic rocks south of the Big Chino Fault are concealed beneath Big Chino Valley and part of northern Little Chino Valley (DeWitt and others, Chapter B, this volume). Southward, the carbonate rocks are uplifted and exposed in the Juniper Mountains, Sullivan Buttes, and Black Hills (fig. D2). Paleozoic remnants beneath the basins and in mountain ranges to the south are mostly separated from carbonate rocks beneath the Colorado Plateau by faulting and erosion. Thus, some Transition Zone carbonate rocks are stratigraphically continuous with the carbonate rocks beneath the Colorado Plateau, and some are not. In the northwestern part of Big Chino Valley, the basin-fill aquifer north of Walnut Creek is bounded by carbonate rocks that are partly capped with basalt. These carbonate rocks are considered an erosional remnant of the Colorado Plateau (fig. D2), because they are stratigraphically discontinuous. Little hydrologic information is available for the Juniper Mountain area adjoining the Big Chino basin-fill aquifer.

The carbonate aquifer consists of several hydraulically connected limestone, dolomite, sandstone, and shale formations. The formations, in ascending order, include the Tapeats Sandstone and Bright Angel Shale of Cambrian age; the Martin Formation of Devonian age; the Redwall Limestone of Mississippian age; and the Supai Formation of Pennsylvanian and Permian age. The primary water-bearing unit in the study area is the Martin, followed to a lesser degree by the Redwall. Together these units are known as the regional carbonate aquifer.

Owing to variations in uplift and erosion, not all Paleozoic units are preserved at all locations in the study area. In the southern and western parts of the area where Paleozoic units are exposed, the Martin usually is the uppermost unit. On Big Black Mesa and north of the upper Verde River (toward Drake and east of Hell Canyon), the Redwall is the uppermost unit. Although exposed in just a few locations in Hell Canyon and along the upper Verde River canyon, the Supai is an important unit in the regional aquifer farther east in Verde Valley (Twenter and Metzger, 1963; Owen-Joyce and Bell, 1983).

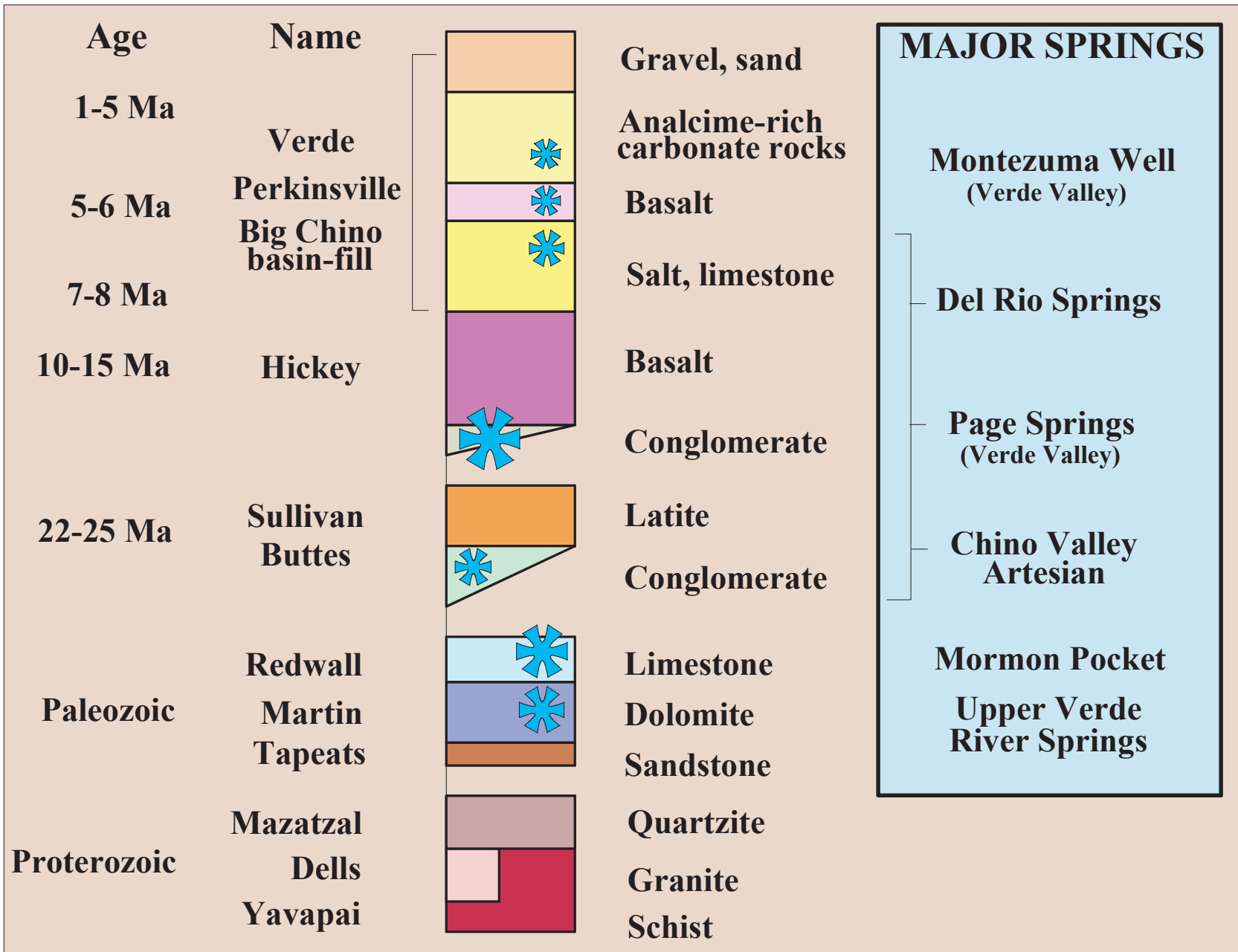


**Figure D6.** Columnar section of Verde River headwaters region, north-central Arizona. Water-bearing units that host springs are indicated by blue asterisks. Source of water may be different than host unit.



## D12 Hydrogeologic Framework

The Tapeats Sandstone is the basal aquifer unit, consisting of medium-to-coarse grained feldspathic sandstone ranging in thickness from 0 to 300 ft. This formation is exposed along the base of Big Black Mesa and the Juniper Mountains and in lower Granite Creek. In the northwestern part of Big Chino Valley, the Tapeats Sandstone is overlain by the Bright Angel Shale. In the southeastern part Big Chino Valley and near the mouth of Granite Creek, the Tapeats is overlain by interbedded carbonate and clastic rocks of unknown age known as the Chino Valley Formation (shown in fig. A8, Chapter A; Hereford, 1975; Beus, 1989). Three facies are recognized in the Chino Valley Formation—a lithic sandstone, a pebble conglomerate, and a red shaly dolomite.

The overlying Martin Formation is composed predominantly of dolomite, followed by minor limestone, interbedded shale and sandstone, and minor amounts of limey siltstone and sandstone. It is easily distinguished by its gray color and evenly-bedded, step-like outcrops (Krieger, 1965). Within the study area, the Martin ranges in thickness from 300 to 400 ft. The Martin crops out on Big Black Mesa, in the Juniper Mountains, and throughout much of the upper Verde River

canyon between Stillman Lake and the Paulden gauge. The Martin contains fractures and solution features, which are evident in Verde River canyon exposures near upper Verde River springs (Knauth and Greenbie, 1997).

The Martin is unconformably overlain by the Mississippian Redwall Limestone, except where eroded near the surface. The Redwall Limestone, which has a thickness of about 200 ft in the study area, is a massive, cliff-forming unit (fig. D7). In the Grand Canyon region it is well known for its large caverns, collapse features, and extensive caves and springs (Stanton's Cave, Redwall Cavern, and Vasey's Paradise, for example).

Large springs at Mormon Pocket and Summers Spring in Sycamore Canyon emerge through the Redwall near its lower contact with underlying Martin. Earlier studies recognized that the water-bearing Paleozoic rock formations are hydraulically connected laterally and vertically by connected fractures and dissolution cavities (Twenter and Metzger, 1963; Owen-Joyce and Bell, 1983). Dissolution openings, known as karst, offer the potential for water to travel rapidly through the subsurface (White, 1969, 1988, 1999; Ford, 1999; Ford and Williams,



**Figure D7.** Photograph of large solution features in Redwall Limestone in upper Verde River canyon. (Photograph by L. Wirt, U.S. Geological Survey.)

1989). Solution channels and saturated caverns are capable of storing and transmitting large amounts of water.

The irregular distribution of fractures can produce confined aquifer conditions. This concept is demonstrated by a 700-ft well at Drake (fig. D8 and D9; SB0001; B-19-01 33cca), which was drilled through unsaturated basalt, Redwall, and Martin into what is probably the Chino Valley Formation or upper Tapeats. Upon penetrating the lower Martin, the water level rose nearly 300 ft within the borehole (Southwest Groundwater Consultants, 2002; William G. Wellendorf, written commun., 2002). Subsequent inspection with a down-hole camera showed a pronounced increase in the number of fractures and solution features near the base of the Martin relative to the overlying units. The static water level of the well (4,244 ft; table D3; Southwest Groundwater Consultants, written commun., 2004) is about the same as the stream elevation in nearby Hell Canyon.

The lower Martin Formation is host to several prominent springs in the Verde River watershed, including upper Verde River springs and spring-fed Stillman Lake near Paulden, Haskell Spring near Cottonwood (Thiele, 1961), and Allen Springs on Mingus Mountain, which are the water supply for the town of Jerome (Paul Lindberg, oral commun., 2002). The Martin is similar in composition and thickness to the Cambrian Muav Limestone that is host to many springs in the Grand Canyon. In the Grand Canyon, most springs in the lower Paleozoic section generally discharge above the Bright Angel Shale, which is a relatively impermeable rock unit. A small quantity of water evidently penetrates the shale, as evidenced by smaller springs in the shale and underlying rock. The Bright Angel Shale is recognized for its properties in retarding the downward percolation of ground water (Metzger, 1961; Twenter, 1962; Huntoon, 1977; Myers, 1987). The shale in the Bright Angel and the highly-cemented sandstone layers in the Tapeats impede downward movement and cause ground water to move laterally above the contact. This accounts for the accumulation of ground water in the overlying formation, the Muav Limestone. In the Verde River watershed, the relation between the Martin and the underlying Chino Valley Formation and Tapeats Sandstone units is hydrologically analogous to the relation between the Muav Limestone and the Bright Angel Shale.

## Carbonate Aquifer Underlying Basin-Fill Deposits

Some of the highest-yield water wells in Big Chino Valley are located along the base of Big Black Mesa north of Paulden where the basin-fill deposits are thin. These wells penetrate Paleozoic limestone beneath 50 to 400 ft of Tertiary basin-fill sediment (fig. B11; DeWitt and others, Chapter B, this volume). The “Weber Well” north of Paulden (B-18-02-28abb) is an example of such a well, reportedly yielding as much as 5,000 gpm (Water Resources Associates, 1990). This well is 385 ft in depth. Although few wells fully penetrate the basin-fill deposits to produce from the carbonate aquifer, Paleozoic rocks are presumed to underlie most or all of the Big

Chino basin-fill aquifer (Ostenna and others, 1993; DeWitt and others, Chapter B, this volume). In earlier studies, water-level contour maps did not distinguish among wells producing from carbonate rocks underlying the basin-fill versus those producing from Tertiary basin-fill sediment or volcanic rocks (fig. D8; Wallace and Laney, 1976; Schwab, 1995). Water-levels for the carbonate aquifer near Paulden are not substantially different from those in alluvium or basalt in the basin-fill aquifer, suggesting that the “upper” basin-fill aquifer and “lower” carbonate aquifer are strongly connected in the basin outlet region. Additional work is needed to better understand the interrelation between the upper and lower aquifers.

## Carbonate Aquifer North of Upper Verde River

The depth of wells in the carbonate aquifer north of the Verde River ranges from 480 to 720 ft (table D3). Based on the small number of well logs, reported water yields are highly variable. A few wells are productive, and some are not. Dry holes north of the Bar Hart Ranch have been drilled as deep as 700 ft, and well drilling in this region is considered risky (Don Varner and David Gipe, local ranchers, oral commun., 2002).

A highly productive well near Drake (SB0001; B-19-01 33cca), discussed earlier, is completed in the lower Martin near the contact of the Chino Valley or Tapeats (Southwest Groundwater Consultants, 2002). This stratigraphic interval was observed to have a pronounced increase in the number of fractures and solution features relative to overlying units. The same stratigraphic interval is exposed at the base of the upper Verde River canyon where there is spring discharge; at river mi 2.3 (upper Verde River springs), and at river mi 8.0 (unnamed spring near Muldoon Canyon).<sup>1</sup> The well log of a 620-ft stock well 2 mi south of Drake at B-18-01 17aa is fairly similar to well SB0001. The borehole penetrated unsaturated basalt in the near surface (from 96 to 138 ft), which is underlain by conglomerate and limestone. A 720-ft stock well 2 mi northeast of Drake at B-19-01 16acb is completed almost entirely in basalt. Both stock wells typically are pumped at a rate of about 10 gpm (Don Varner and David Gipe, local ranchers, oral commun., 2002). No aquifer tests are available for any of the wells in the carbonate aquifer near Drake.

A second highly productive well (HR-2 in fig. D9) in the carbonate aquifer is located just outside of the Big Chino basin, 1.5-mi north of upper Verde River springs and the Verde River. At this location, the well penetrates a basalt-filled paleochannel that is cut into Paleozoic rock (DeWitt and others, this volume). The driller’s log indicates that the HR-2 borehole initially penetrated 200 ft of basalt, lost circulation for 265 ft, and bottomed in what was described as sand, sandstone, or limestone. The lowermost part of the log is interpreted as penetrating buried Tertiary alluvium,

<sup>1</sup> Locations along Verde River in river miles shown in fig. A2 and listed in Table A1, Chapter A, this volume.

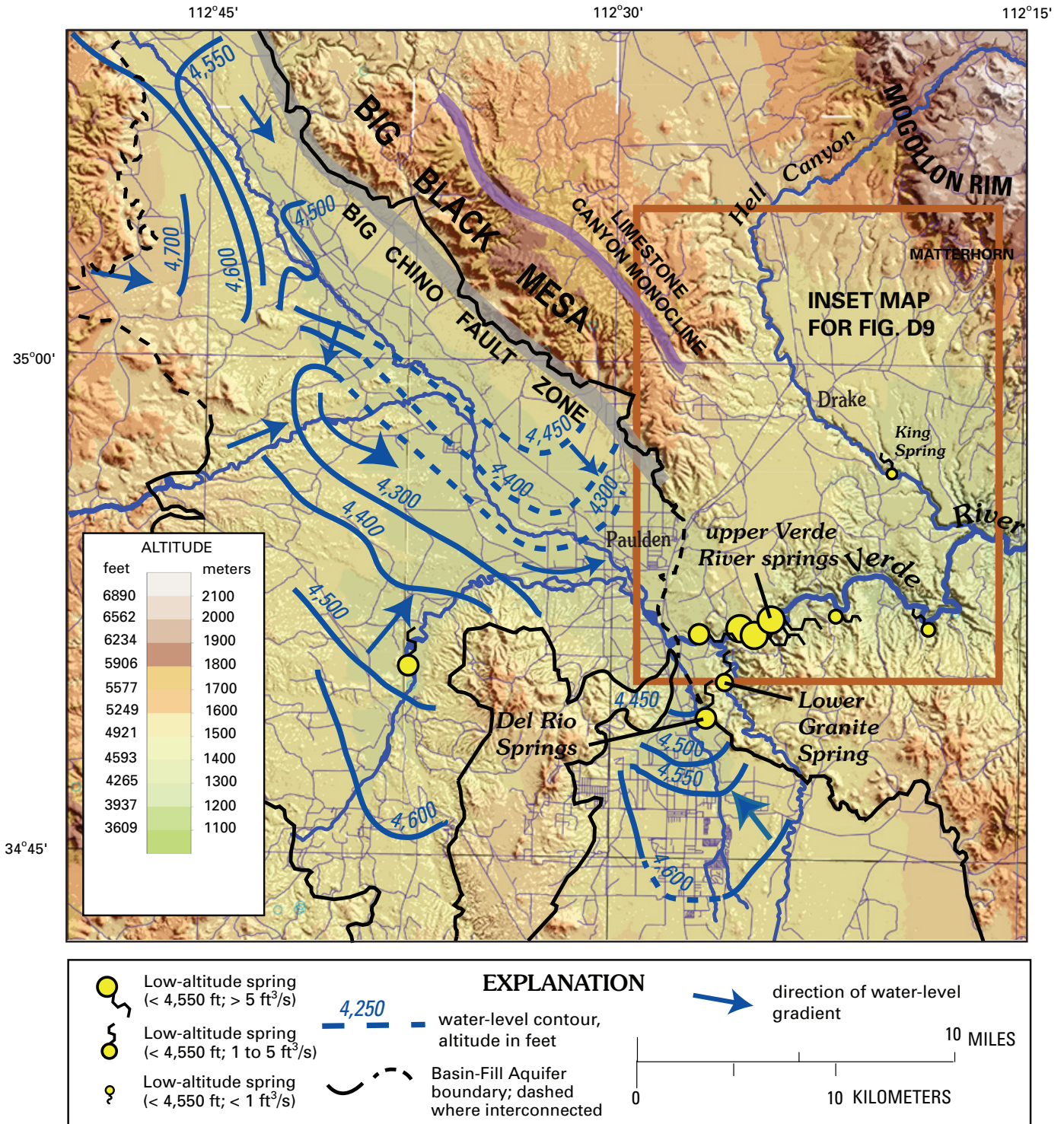


**Figure D8.** Compilation of water-level contours in the Verde River headwaters area (after Schwab, 1995; Corkhill and Mason, 1995). Dashed contours and arrows are the author's interpretation. Low-altitude springs shown as yellow circles, water-level contour elevations given in feet.

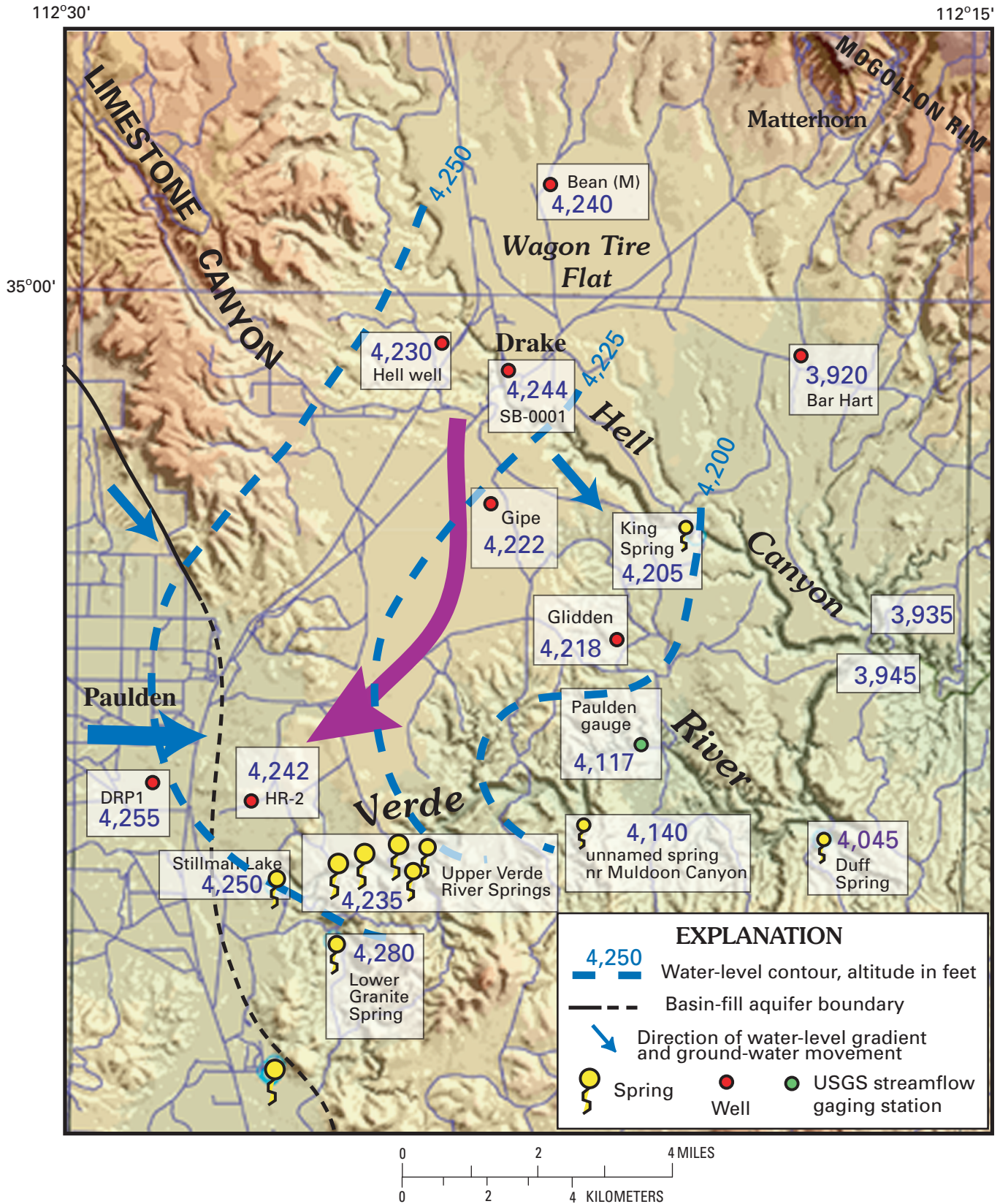


**Figure D9.** Water-level contour map for carbonate aquifer north of upper Verde River. Blue arrows indicate direction of ground-water movement. Two-sigma accuracy of water-level data within 20 ft (data in table D3). Purple arrow is approximate location of buried basalt-filled paleochannel (DeWitt and others, Chapter B, this volume). Base is from U.S. Geological Survey digital data 1:100,00.

## D16 Hydrogeologic Framework

**Table D3.** Water-level measurements for wells north of the upper Verde River. Well locations shown on fig. D9.

[ADWR = Arizona Department of Water Resources (2002), USGS = U.S. Geological Survey (Bills and Flynn, 2002),  
SGC = Southwest Groundwater Consultants (2002), WRA = Water Resources Associates (1990, 1991)]

Local ID	Well Name	Data Source	Registration No./Name	Land Surface Altitude	Well Depth	Water Level Date	Water Level Depth (feet)	Water Level Altitude (feet)
B-19-01 16aca	Bean	ADWR	55-645843	4790	720	8/4/1994	552.8	4237
	"	ADWR				3/19/1996	552.8	4237
	"	ADWR				11/1/1996	553.1	4237
	"	ADWR				10/17/1997	553.4	4237
	"	ADWR				10/23/1998	553.0	4237
	"	ADWR				5/21/1999	553.6	4236
	"	ADWR				10/22/1999	553.8	4236
	"	ADWR				3/28/2001	553.7	4236
A-19-01 33bbd	Bar Hart	ADWR		4460	585	7/26/1994	533.6	3926
	" "	ADWR				5/19/1999	540.1	3920
B-19-01 33ccc	SB-0001/Drake	SGC	55-586901	4650	700	7/1/2001	400.0	4244
B-18-01 06aba	Hells well	ADWR	55-631892	4631	460	2/22/2001	401.0	4230
B-18-01 17aaa	Gipe	ADWR	55-511557	4643	620	4/6/1993	420.6	4222
	" "	ADWR				4/12/1994	420.0	4223
	" "	ADWR				10/4/1995	419.8	4223
	" "	ADWR				3/19/1996	420.1	4223
	" "	ADWR				11/1/1996	420.7	4222
	" "	ADWR				10/17/1997	421.2	4222
	" "	ADWR				10/23/1998	421.1	4222
	" "	ADWR				4/19/1999	422.1	4221
	" "	ADWR				10/22/1999	422.2	4221
	" "	ADWR				3/28/2001	422.6	4220
B-18-01 27abc	Glidden	ADWR	55-631886	4407		4/12/1994	189.0	4218
	"	ADWR				4/19/1999	189.3	4218
B-17-02W02dcc1	HR-2	WRA	55-527679	4565.33	500	7/13/1990	323.3	4242
	"	ADWR		4570		6/12/2001	325.1	4245
	"	ADWR				10/15/2001	325.1	4245
B-17-02W02dcc2	HR-1	ADWR		4565	397	6/12/2001	319.0	4246
	"	ADWR				10/10/2001	318.9	4246
B-17-2 04cda	DRP1	WRA		4457	400	8/11/1989	102.0	4255
B-21-02 14bcc	Ash Fork #1, AF-06	USGS		5110	1700	12/1/1974	1000	4110
	" "	USGS				5/1/1984	999	4111
	" "	USGS				2/7/1986	1000	4110
	" "	USGS				2/13/1987	988	4122
	" "	USGS				1/27/1988	999	4111
	" "	USGS				10/17/1997	997	4113

or Martin, Chino Valley, or Tapeats at the bottom of the paleochannel (DeWitt and others, this volume). Any of these units typically would have maximum hydraulic conductivities comparable to fractured basalt, ranging from  $1 \times 10^2$  to  $1 \times 10^3$  (table D2). An aquifer test was conducted for 2 days at approximately 600 gpm, with 3.04 ft of drawdown (Water Resource Associates, 1991). Transmissivity was estimated to be 122,800 gallons per day per foot (gpd/ft) by the Theis type-curve method. The large transmissivity at well HR-2 is thought here to indicate a line source or boundary condition at constant head, such as recharge from a perennial stream (Lohman, 1979; p. 58-61; Theis, 1941), which in this case would be the nearby Verde River.

In short, well yields in the carbonate aquifer tend to be improved where the well intercepts basalt-filled drainages or the base of the Martin, or both. The Martin/Chino Valley/Tapeats stratigraphic interval is host to most of the springs in this region.

**Table D2.** Range in hydraulic conductivity of sediment and rock types found in Big and Little Chino basins (after Ewing and others, 1993).

Rock Type	Hydraulic conductivity (feet per day)	
	minimum	maximum
unfractured limestone	$5 \times 10^{-4}$	$5 \times 10^0$
fractured limestone	$5 \times 10^{-3}$	$5 \times 10^2$
unfractured basalt	$1 \times 10^{-8}$	$1 \times 10^{-4}$
fractured basalt	$1 \times 10^{-2}$	$1 \times 10^3$
unfractured sandstone	$1 \times 10^{-3}$	$1 \times 10^2$
coarse sand and gravel	$1 \times 10^3$	$1 \times 10^5$
medium sand	$1 \times 10^2$	$1 \times 10^4$
fine sand	$1 \times 10^{-1}$	$1 \times 10^2$
playa deposits	$1 \times 10^{-6}$	$1 \times 10^{-2}$

### Basin-fill Deposits

Principal water-bearing units within Big and Little Chino basin-fill deposits consist of Tertiary volcanic rock and Quaternary and Tertiary sediment.

Tertiary deposits include alluvial fans, floodplain or playa sediments, basalt flows, lati-andesite flows, and intrusive lati-andesite. Tertiary sediment varies in particle size from clay to gravel depending on the environment of deposition and may be poorly consolidated. Floodplain and playa deposits near the center of the basins are fine-grained and difficult to distinguish from one another. The mineralogy of basin sediment varies substantially according to source area. Big Black Mesa and Juniper Mountains supply predominantly carbonate minerals, whereas the Bradshaw and Santa Maria mountain ranges and Sullivan Buttes provide predominantly silicate minerals.

Quaternary deposits include alluvial fans, colluvium covering hill slopes, floodplain terraces, and stream gravels. In the center of the basins, these young Quaternary surface deposits are commonly less than 50-ft thick. Thick alluvial-fan deposits are prevalent along the valley margins. Some of the largest fans along Big Black Mesa were initiated in the Late Tertiary and extend at least 500-ft deep (Bureau of Reclamation borehole CV-DH-3; in Ostenaar and others, 1993, and shown in Chapter B, fig. B3).

All of the stratigraphic facies described above are unevenly distributed, creating a heterogeneous aquifer. For example, buried Tertiary basalt flows facilitate movement of ground water in northwest and southeast Big Chino Valley. The presence of lati-andesite intrusives in Little Chino Valley may confine older sediment, creating artesian conditions. Paleozoic carbonate rocks may be hydrologically connected with alluvial sediments and Tertiary basalt flows in areas where they underlie and adjoin the basins. The hydraulic conductivity of different rock types and alluvium varies greatly within each major aquifer.

Table D2 lists hydraulic conductivity values compiled from the literature by Ewing and others (1994) for the Big Chino basin-fill aquifer and adjoining carbonate aquifer. The hydraulic conductivity, reported in feet per day (ft/d), is the rate at which a rock or sediment unit transmits water. These values span more than ten orders of magnitude. Within the Verde headwaters, the hydraulic conductivity may be as high as  $1 \times 10^3$  ft/d (basalt) or  $5 \times 10^2$  ft/d (limestone). Hydraulic conductivity for coarse sand and gravel ranges from  $1 \times 10^3$  ft/d to  $1 \times 10^5$  ft/d. Tertiary basalt ranges in texture from unfractured and relatively impermeable, to columnar and extremely fractured. Karst solution features are commonly observed in Paleozoic limestone and dolomite. Secondary porosity in the limestone and basalt accounts for several high-yielding wells in the Paulden area.

### Big Chino Basin-Fill Aquifer

Big Chino Valley is an elongate, fault-bounded basin that is at least 2,300 ft deep in the center and shallower around the northwest, southeast, and southwestern margins (Langenheim and others, Chapter C, this volume). Big Chino Valley owes its long, narrow configuration to the northwesterly strike of the Big Chino Fault. Displacement along the fault places basin deposits against granitic basement rock, creating a relatively impermeable basin boundary along most of Big Black Mesa, except where there is little displacement against Paleozoic carbonate rocks north of Paulden. Extensive fine-grained carbonate in the center of Big Chino Valley is interpreted as having formed in a lacustrine playa (DeWitt and others, this volume). Williamson Valley, the largest tributary subbasin, is at least 1,500 ft deep in the center and shallower near its edges (Langenheim and others, Chapter C, this volume). Depth to water in both Big Chino and Williamson Valleys is typically between a few ft and 200 ft below land surface (Wallace and Laney, 1976; Schwab, 1995). The Big Chino basin-fill aquifer

is capable of storing large amounts of ground water (Krieger, 1965; Water Resource Associates, 1990; Ostenaar and others, 1993; Ewing and others, 1994).

The major lithological units within the Big Chino basin-fill aquifer include (a) buried basalt flows in the northwest and southeast parts of the basin, (b) thick fine-grained playa sediment in the basin center, and (c) other basin-fill sediment. These are discussed in greater detail next.

### Tertiary Basalt Flows

Basalt flows in southeast Big Chino Valley originated north of Paulden or east of Sullivan Lake (DeWitt and others, this volume). Three flows are exposed east of Sullivan Lake in the modern Verde River canyon. A 4.5-Ma basalt flowed down a paleochannel (penetrated by well HR-2) in the carbonate aquifer. The basalt is as much as 400-ft thick within a narrow paleochannel about 1 mi north of the upper Verde River. The basalt flows widened and thinned as they flowed into Big Chino Valley and were subsequently buried by younger Tertiary alluvium (DeWitt and others, this volume, fig. B8). Basalt can be traced in well logs sloping toward the center of the basin, to a depth greater than 500-ft west of Wineglass Ranch. The basalt thins to less than 90 ft where last detected. Basalt flows reached the Sullivan Buttes latite andesite on the south and the Paleozoic rock along the Big Chino Fault to the north.

Wells that penetrate the basalt flow in southeast Big Chino Valley are capable of very large yields, as demonstrated by a 400-ft uncased supply well (known as the Dugan well or DRP1) located inside the basin about 1 mi northeast of Sullivan Lake at (B-17-02) 04cda (fig. D9 and table D3). Water Resources Associates (1990) conducted an aquifer test of DRP1 with a pumping rate of 5,000 gpm for 7 days that resulted in 3.31 ft of total drawdown. The calculated rate of transmissivity and specific yield are 220,000 gpd/ft and 0.29, respectively (Water Resource Associates, 1990; phase IV, v. V, p. 14), which makes this well one of the highest yielding in Big Chino Valley.

The hydrogeologic setting for DRP1 is best interpreted from the deeper monitoring well (DRM2) at the site that was drilled to a depth of 600 ft. The borehole encountered alluvium from land surface to 125 ft, followed by an upper and a lower basalt flow between 125 and 350 ft, underlain by Tertiary alluvium from 350 to 600 ft. From 185 to 285 ft the driller lost circulation in a reddish-brown basalt layer. Lost circulation is often an indication of openings, such as columnar fractures or rubble zones. The three piezometers that were nested inside the monitoring well casing were screened in the upper basalt, lower basalt, and underlying alluvium, respectively. During the aquifer test, the difference in water levels for the three stratigraphic units was slight (< 0.52 ft), and amount of the drawdown for each well was similar in response to pumping stress (Water Resources Associates, 1990), an indication that the upper and lower basalt flows are hydrologically connected with one another, as well as with the underlying Tertiary alluvium.

The DRP1 and HR-2 supply wells are interpreted as penetrating the same sequence of basalt flows, although DRP1 is completed within the basin-fill aquifer, and HR-2 penetrates a basalt-filled paleochannel in the carbonate aquifer north of the Verde River. Both are highly productive wells that lost circulation at approximately the same elevation during drilling and produce water predominantly from fractured basalt. At both locations, the small amount of drawdown during aquifer testing is an indication that the basalt units are hydrologically connected with adjoining carbonate or sediment units.

Buried basalt also is present in northwestern Big Chino Valley. The basalt originated either in the Partridge Creek or Juniper Mountain areas and flowed into Big Chino Valley, where it subsequently has been buried by younger alluvial deposits (DeWitt and others, this volume). In upper Big Chino Valley, there are no drillers' logs for wells that fully penetrate or produce directly from the buried basalt. At (B-19-04)03bcd on CV Ranch, a well intercepted basalt at about 730-ft below land surface. The well is screened in the overlying alluvium, thus little can be said about the water-bearing characteristics of the basalt at this location.

### Playa Deposit

The center of the basin contains a thick sequence of fine-grained carbonate sediment formed in a playa environment (Ostenaar and others, 1993; DeWitt and others, Chapter B, this volume). The center of the basin is thought to contain at least 2,300 ft of sediment, but basin thickness (and inferred playa thickness) diminishes toward the margins of the basin. The fine-grained carbonate sediment is composed of as much as 80 percent calcite, dolomite, and analcime, and <15 percent quartz, feldspar, illite, and bloedite(?) (DeWitt and others, this volume). Bloedite is a sulfate mineral that forms under evaporative conditions. A lack of halite and gypsum in the sediment suggests less saline conditions than those that formed the closed-basin playa in Verde Valley during deposition of the Verde Formation, however, mineralogical analyses have been completed only for selected cuttings from three Bureau of Reclamation deep boreholes.

The playa has a lower hydraulic conductivity than other alluvial deposits (table D2) but does not extend far enough across the valley to create a barrier to ground-water movement, either down the axis of Big Chino Valley or across the outlet of Williamson Valley (Ostenaar and others, 1993; Ewing and others, 1994; p. 28). Coarser-grained material was found above latite in the bottom of borehole CVDH-3 penetrating the playa (Chapter B, this volume), suggesting more permeable sediment may be present beneath the playa. In addition, the playa deposit presumably is underlain by Paleozoic carbonate rock in some places, and thus movement of water beneath the playa through karst openings is possible. The lack of change in the slope of water levels between northwest and southeast Big Chino Valley (Wallace and Laney, 1976; Schwab, 1995; fig. D8) is considered compelling evidence that the playa does not form an impassable barrier between these areas.

### Other Basin-Fill Alluvium

With the exception of the playa deposit, other types of alluvial basin-fill deposits in the Big Chino aquifer are fairly heterogeneous with respect to grain size, ranging from clay to boulders. Williamson Valley supplies mostly silicate minerals (quartz) and feldspar from the granites, gneisses, and volcanic rocks in the Santa Maria Mountains, Mint Wash, and Sullivan Buttes areas. Physical and chemical weathering of quartz and feldspar tends to produce relatively sandy, permeable sediment. Partridge Creek and the Juniper Mountains contribute both carbonate detritus and basalt to upper Big Chino Wash. Big Black Mesa is the largest source of carbonate sediment. In general, carbonate rocks dissolve to produce finer-grained, relatively less permeable sediment than sediment derived from silicate sources. Grain size also is related to other factors, however, such as the length of time and intensity of surficial weathering and the distance the particle has been physically transported from its source area. Stream sediment in southeast Big Chino Wash is an integrated mixture of granitic, volcanic, and carbonate debris from upland source areas.

Hydraulic conductivity of unconsolidated sand and gravel may span five orders of magnitude, ranging from 0.1 to 10,000 ft/day (table D2). Alluvial fans, colluvium covering hill slopes, stream gravels, and flood-plain terraces are common along major stream drainages. Quaternary surface deposits are commonly less than 50-ft thick. Most driller's logs that would be described as "alluvial wells" typically penetrate the shallow surficial deposits to produce from underlying Tertiary sediments. Substantial quantities of ground water may be produced from wells completed in these deposits.

Large diameter production wells near Big Chino Wash in upper Big Chino Valley commonly produce between 1,000 and 4,000 gpm (Water Resources Associates, 1990). Many of these irrigation wells are old and lack driller's logs. In general, most of these wells are less than 700 ft in depth. The wells probably are screened in alluvial deposits above the buried basalt units (where present), but some wells may intercept basalt layers in the part of the valley upgradient from the confluence of Pine Creek and Big Chino Wash. Water Resources Associates (1990) drilled a monitoring well and conducted an aquifer test on a relatively deep supply well on the CV Ranch at (B-19-04)03bcd. This aquifer test provides some of the best descriptions regarding water-bearing characteristics of alluvial wells in upper Big Chino Valley.

A 7-day aquifer test of production well CVP1 was conducted at a rate of 3,000 gpm and resulted in 63.12 ft of drawdown. The calculated rate of transmissivity and specific yield are 157,000 gpd/ft and 0.36 (dimensionless), respectively (Water Resource Associates, 1990; p. 13 phase IV, v. V). The 700-ft production well is 55 ft north of the monitor well (CVM1). CVP1 has a screened interval from 107 to 698 ft, and a saturated thickness of 638 ft. CVM1 was drilled to a total depth of 744 ft, penetrating basalt at 730 ft (Water Resources Associates, 1990). The upper 710 ft of sediment were mostly described as "silty clay" or "clayey silt." The basalt is overlain

by 20 ft of "granitic and basaltic sand and gravel." The monitoring well was completed at a bottom depth of 700 ft, and is screened from 612 to 697 ft below land surface. Although both wells are screened in mostly fine-grained alluvium, it is not clear whether the high well yield should be entirely attributed to the fine-grained sediment. Some of the high yield could be derived from underlying coarse-grained basalt gravels or possibly from high secondary porosity in basalt.

Little is known about the extensive basin-fill deposits below about 700 ft in Big Chino Valley, including grain size, degree of consolidation, and degree of hydraulic confinement, if any. Nor is much known about the extent of interfingering between the playa deposit and basin-fill alluvium, or the full occurrence of the buried basalt flows. Less is directly known about a presumed hydraulic connection with the underlying carbonate aquifer at the base of the basin-fill deposits. Most wells are relatively shallow compared to total basin depth, and no wells fully penetrate the center of the playa or the basalt flows in middle and northwestern Big Chino Valley.

### Little Chino Basin-Fill Aquifer

In general, the Little Chino basin-fill aquifer is not as deep or narrow as Big Chino Valley. Thickness of the aquifer increases from southwest to northeast, with its greatest thickness locally in excess of about 700 ft near Del Rio Springs (Langenheim and others, Chapter C; fig. C3). Many drillers' logs are available surrounding the town of Chino Valley (ADWR, 2002); however, the subsurface geology is quite complex owing to the irregular distribution of buried volcanic extrusive rocks, volcanic-clastic sedimentary rocks, and basalt flows (DeWitt and others, Chapter B, this volume).

Ground-water movement across the basin-fill aquifer boundary is known to occur in two locations where basement rock is absent. Along the southeastern aquifer boundary, the interface between the Little Chino and Agua Fria basin-fill aquifers consists of about 700-ft of predominantly sedimentary deposits. Overpumping in the Chino Valley and Prescott Valley areas may be shifting the ground-water divide between these two aquifers. The second location of ground-water movement across the basin-fill aquifer boundary is the ground-water outlet northeast of Del Rio Springs and Little Chino Creek. Not all ground water discharges at Del Rio Springs; some underflow continues north. The northeastern boundary of the basin-fill aquifer with the carbonate aquifer consists of moderately permeable rocks that are exposed along Stillman Lake and Lower Granite Creek (DeWitt and others, Chapter B, this volume; figure B8; see also Chapter A, figs. A8 and A15).

Depth to water ranges from land surface at Del Rio Springs (elevation 4,450 ft) to about 100 ft (elevation 4,550 ft) beneath the town of Chino Valley (Corkhill and Mason, 1995, *their* fig. 17). The main artesian zone beneath Chino Valley extends north to Del Rio Springs for a distance of at least 6.5 mi and has a width of about 4 mi (Schwalen, 1967). The artesian part of the aquifer is highly productive, with many wells discharging 1,000 to 3,000 gpm (Corkhill and Mason, 1995).



In the northern part of Little Chino Valley, water from artesian wells used to flow at the land surface. Remick (1983) reported seven flowing wells in the winter of 1981–82. Historically, hydraulic head in the main artesian zone has been approximately 100 ft higher than the shallow unconfined part of the aquifer near the town of Chino Valley, although water levels have been steadily declining (Arizona Department of Water Resources, 2000).

A correlation has been observed between pumping from wells in the artesian zone and discharge at Del Rio Springs. Schwalen (1967) describes a lag time of 6 hours between pumping of deep wells near Del Rio Springs and a 0.74 ft<sup>3</sup>/s reduction in streamflow near the present-day USGS gauge (09502900; see Chapter A, table A3; shown on fig. A6). In addition, Allen, Stephenson & Associates (2001) evaluated USGS gauge data, metered wells, recorded irrigation activities, and a series of aquifer tests to assess whether water pumped from the confined aquifer on other parts of the Del Rio Ranch had a direct relation with flow at Del Rio Springs. Their study concluded that pumping in the northern part of the basin had a “direct, immediate, and quantifiable impact” on the discharge at the gauge.

Corkhill and Mason (1995) divided the Little Chino basin-fill deposits into an upper alluvial unit and a lower volcanic unit. The upper unit was considered a water-table aquifer, and the lower aquifer unit was considered hydrologically distinct and artesian. DeWitt and others (this volume) have identified confining conditions in shallow alluvium, as well as in underlying volcanic and sedimentary rock units. These confining conditions are irregularly distributed and discontinuous. Therefore, the shallow alluvium and underlying stratigraphic units are presumed hydrologically connected, and the single aquifer system is complex. Depending on location, ground water within the basin-fill aquifer is under either confined or unconfined conditions. Artesian flow can be produced from several different geologic settings. These settings include (a) trachyandesite overlying small pockets of irregularly distributed sediment, (b) volcanic-clastic sequences within the lati-andesite, (c) lati-andesite over sedimentary rock or alluvium, (d) permeable basalt beneath strongly cemented alluvium, and (e) unconsolidated alluvium beneath cemented alluvium. The Little Chino basin-fill deposits are discussed in detail next, in order from oldest to youngest formation.

### Paleozoic Rocks

Few wells penetrate Paleozoic rocks in the northern part of Little Chino Valley, and regional interpretation by DeWitt and others (in press) indicates that only minor thicknesses (less than 100 ft) of Paleozoic rocks should be found in the subsurface of far northern Little Chino Valley. South of the town of Chino Valley, and extending to Prescott, Paleozoic rocks are unknown in southern Little Chino Valley and in Lonesome Valley.

### Older Sedimentary Rocks

A paleochannel 4-mi wide and as much as 230 ft thick underlies lati-andesite in outcrop east and north of Del Rio Springs, outside the basin boundary (DeWitt and others, this volume; fig B2 unit Tos). The channel is filled with poorly-sorted to well-sorted conglomerate, gravel, and finer-grained sediment derived from the southwest. The paleochannel is vertically offset by faulting at the basin boundary. Within the basin, the paleochannel extends southwest beneath northern Little Chino Valley and the town of Chino Valley. Its full extent farther southwest is unknown because of cover by younger rock units. Sediment in the paleovalley is poorly and moderately cemented and is interpreted to have high permeability. In southern Little Chino Valley, these sediments are thought to be hydrologically connected to overlying sediment in the Hickey Formation, which extends south to Prescott and the Bradshaw Mountains.

### Lati-andesite

Flows, breccias, and intrusive centers of 24-Ma lati-andesite underlie much of northern Little Chino Valley at depth, below the Hickey Formation. Locally, rocks of the Hickey may be absent where topographic highs related to intrusive centers of lati-andesite are present. Thickness of lati-andesite is highly variable, but is greatest (~650 ft) near intrusive centers that are resistant to erosion. Breccias, deposits of cinders, and tuffaceous rocks of lati-andesite composition are moderately permeable and are interbedded with flows that are much less permeable. Intrusive centers are interpreted to have low permeability, due to their unfractured nature. Very few wells go completely through the lati-andesite. Impermeable lati-andesite probably confines the underlying older Tertiary sedimentary rocks. Intrusive centers form impermeable plugs that divert water flow up and away from underlying Tertiary sedimentary rocks and from deposits of breccia, cinders, and tuffaceous rocks. Some of the central artesian field near the town of Chino Valley probably is created by barriers of unfractured lati-andesite.

### Hickey Formation Volcanic and Sedimentary Deposits

Flows of basalt and trachyandesite underlie the alluvial deposits in parts of the basin. In the southwestern part of the basin, southwest of the town of Chino Valley, a trachyandesite flow can be traced from outcrop in the Sullivan Buttes to the southern limit of the artesian field (DeWitt and others, Chapter B, this volume, fig. B7). The 130-ft thick flow appears to have been derived from a northwest-striking, high-angle feeder dike. Trachyandesite does not contain as many cooling cracks and through-going fractures as basalt, so the flow serves as a local confining layer to uncemented sediment in the Hickey Formation beneath the flow. Farther south, a basalt flow extends, at the surface, from near Table Mountain to highway 89. The flow is as much as 330 ft thick and overlies sediment in the Hickey. Some deep wells south of Del Rio

Springs penetrate as much as 150 ft of basalt in paleovalleys cut into the underlying lati-andesite. This basalt could be Hickey in age or it could be 8–10 Ma. Alluvial deposits within the Hickey were deposited in sinuous, narrow valleys whose locations are difficult to map. Sediment thickness varies from 30 to 100 ft.

Thin lenses of poorly sorted sediment probably underlie Hickey trachyandesite in the southern part of Little Chino Valley. The trachyandesite may form a confining layer above this sediment and above volcanoclastic sediments associated with lati-andesite. Many of the shallowest artesian wells in middle Little Chino Valley appear to have penetrated the trachyandesite and produced water from pockets of alluvium and lati-andesite below. These volcanic units are irregularly distributed, and there are not enough deep drillers' logs to make detailed interpretations in these areas.

#### Quaternary to Late Tertiary Alluvial Deposits

Diverse sedimentary units in northern Little Chino Valley above the youngest Tertiary volcanic units include proximal and distal fanglomerate, fine-grained clastic valley fill, and local alluvium distributed along old stream courses. Thickness of the sedimentary units is highly variable due to the underlying volcanic field of Hickey basalt and lati-andesite (DeWitt and others, Chapter B, fig. B12) and varies from less than 100 ft southwest of the town of Chino Valley to more than 650 ft near Del Rio Springs. Much of the fine-grained sedimentary fill is poorly lithified and cemented and is inferred to have moderate or higher permeability. Fanglomerates derived from the Sullivan Buttes west of Del Rio Springs are locally highly cemented in discontinuous zones as much as 30 ft thick on the northwestern side of northern Little Chino Valley. These highly cemented units form locally confining layers above clastic sediment of late Tertiary age. Wells in (B-17-02)34 and (B-16-02)3 produce from sediment beneath the cemented fanglomerate.

Most wells completed in the shallow alluvium are used for domestic and stock purposes, and well yields cannot be determined (Allen, Stephenson & Associates, 2001). Estimated hydraulic conductivities range from 1 to 200 ft/day and average 9 ft/day (Corkhill and Mason, 1995). Historically, the shallow alluvium has received recharge from irrigation return flows (Schwalen, 1967).

## Water-Level Gradients of Major Aquifers

Water-level gradients provide an indication of the directions of ground-water flow in an aquifer. Water-level contour maps of the Big and Little Chino basin-fill aquifers that were constructed in the early 1990s are represented in fig. D8. Water-level data are sparse for the carbonate aquifer north of the upper Verde River, shown within the area of the inset map rectangle (Levings and Mann, 1980; Owen-Joyce and Bell,

1983). In the following section, available water-level data and gradients are evaluated in relation to the hydrogeologic framework of the major aquifers, as presented thus far in this chapter.

### Big Chino Basin-fill Aquifer

Ground-water movement in Big Chino Valley follows a curved axis from northwest to southeast (fig. D8). From an elevation of about 4,525 ft near the mouth of Partridge Creek to 4,255 ft near Paulden (Schwab, 1995; Water Resources Associates, 1990), the water-level gradient is gentle, dropping about 270 ft in 22 mi or an average of 12 ft/mi. In Williamson Valley, the gradient drops from 4,600 ft near the northeast flank of Granite Mountain to 4,455 ft at the USGS gauge on Williamson Valley Wash, or an average of 28 ft/mi in 5 mi. The depth to ground water in Big Chino Valley, Williamson Valley, and Walnut Creek ranges from the surface to 250 ft below land surface (Schwab, 1995). Depth to water is largely dependent on topography and, therefore, is shallow near the center and increases towards the basin margins. Ground water typically is less than 25 ft below land surface beneath Big Chino Wash from its confluence with Pine Creek to Antelope Creek, and beneath Williamson Valley Wash from the Seven V Ranch to the USGS streamflow gauging station 09502800 (Schwab, 1995). The direction of ground-water movement is perpendicular to water-level contours, as indicated by the arrow directions in fig. D8. Around the perimeter of Big Chino Valley, ground-water flowpaths generally follow major surface-water inflows (such as Williamson Valley and Pine Creek) from the margins toward the valley center. In the center of the basin, ground water travels above, around, and possibly beneath the playa deposit.

Large alluvial fans along Big Black Mesa overlie the playa deposit in the center of the basin. The fans extend basinward from Big Black Mesa for 2.4 mi (DeWitt and others, this volume). Alluvial fans overlie the playa deposit from a depth of less than 30 ft in the center of the basin to as much as 500 ft along the Big Chino Fault (Ostenaar and others, 1993). Most of the wells on the alluvial fans are relatively shallow and produce from above the playa deposit. Depth to water in the alluvial fan area overlying the playa is relatively shallow, ranging from 11 to 170 ft below land surface (Schwab, 1995). Ground-water contours approximately follow the topography of the coalescing fans, sloping away from Big Black Mesa toward Big Chino Wash.

On the southwest side of Big Chino Valley, the sandier sediments across the wide outlet of Williamson Valley provide greater permeability and a faster rate of ground-water flow than would a direct route through the center of the playa. Here, the main ground-water flowpath down the axis of the valley is west of Big Chino Wash and the edge of the playa. Few data are available to demonstrate whether a secondary component of ground-water movement occurs through Tertiary volcanic rocks and Paleozoic sedimentary rocks that underlie the playa, or through alluvial fan deposits along the down-dropped side of the Big Chino Fault.

The main ground-water flowpath approximately underlies Big Chino Wash in the upper part of the basin but deviates from Big Chino Wash in the center and southeastern part of the basin. Ground-water contours curve gently south and west of Big Chino Wash from its confluence with Pine Creek to Antelope Creek, where the main axis of flow again curves back towards the valley center. There is a narrow low-lying region, or saddle, in the water table trending from southwest to northeast between Wineglass Ranch and Paulden, possibly caused by well pumping. The saddle is too small to show with 100 ft contour intervals (fig. D8), but is defined by eight wells with measured water levels < 4,260 ft (Schwab, 1995).

The lowest point of the water table is in the southeastern part of the basin north of Paulden where basalt and carbonate rocks are concealed by alluvium (DeWitt and others, this volume; fig. B8). In addition to buried basalt, ground-water movement down the valley is probably influenced by eastward thinning of the basin-fill deposits, and by the shallow underlying carbonate aquifer (DeWitt and others, this volume; fig. B8). North of Paulden along the horsetail splays that mark the terminus of the Big Chino Fault, the thickness of basin-fill deposits overlying the carbonate aquifer is less than 400 ft.

The Big Chino basin-fill aquifer drains through the carbonate aquifer north and east of Paulden, rather than southeast beneath the surface-water outlet at Sullivan Lake. The flowpath may be diverted northward by mounding of the water table beneath Sullivan Lake (Water Resource Associates, 1990). The mounding is caused by from recharge of impounded surface-water runoff from Big and Little Chino Valleys. Proterozoic basement is relatively shallow south of Sullivan Lake (DeWitt and others, Chapter D, this volume) and is thought to block much of the northward flow from the Little Chino basin-fill aquifer. The water-level elevation for the Big Chino basin-fill aquifer near Paulden is about  $4,255 \pm 10$  ft, (for a well at (B-17-02)04cda; Water Resource Associates, 1990; table D3); which is about 20 ft higher than the altitude of upper Verde River springs ( $4,235 \pm 1$ ; river mi 2.3).

The elevation of first perennial flow at upper Verde River springs that is used in this report is  $4,235 \pm 1$  ft as determined by a high-vertical resolution, or "survey grade" global positioning survey (Maurice Tatlow, Arizona Department of Water Resources, written commun., 1999). This compares favorably with a measured elevation of  $4,233 \pm 1$  for the water surface of the upper Verde River on April 29, 1991 with a level and rod survey, at an imprecise location described as below the confluence of Granite Creek at river mi 2.5 (Water Resources Associates, 1991). The elevation of the largest spring, located against the north canyon wall, is a few ft higher than the water surface of the river indicating artesian conditions. The water-level gradient between the Big Chino basin-fill aquifer and upper Verde River springs is less than 10 ft/mi.

### Little Chino Basin-fill Aquifer

Granite Creek is the major surface-water drainage, and the largest potential source of ground-water recharge to

the Little Chino basin-fill aquifer. The main ground-water flowpath is from south to north beneath Granite Creek in the central part of the alluvial basin (4,600 ft contour; fig. D8). Northward movement is blocked by rugged outcrops of Proterozoic rocks along lower Granite Creek, including Mazatzal Quartzite and Tertiary lati-andesite (Wirt, this volume; fig. A8). Ground water travels northwest towards Chino Valley, and then north toward Del Rio Springs (4,425 ft), a gradient of about 175 ft in 3 mi, or about 58 ft/mi. Del Rio Springs and Little Chino Creek are the discharge zone for both the artesian and unconfined aquifer units, with hydraulic head in the artesian parts of aquifer higher than that under water-table conditions (Schwalen, 1967; Matlock and others, 1973; Corkhill and Mason, 1995; Allen, Stephenson & Associates, 2001). During predevelopment conditions, the hydraulic head in the deepest part of the aquifer was as much as 100 ft greater than the head in shallow part of the aquifer (Corkhill and Mason, 1995; Remick, 1983). The difference in head indicates that deeper water-bearing units receive recharge at higher altitudes, which is consistent with a major recharge area beneath the ephemeral reach of Granite Creek southeast of the town of Chino Valley.

Buried plugs of lati-andesite increase in abundance north of Del Rio Springs. The lower permeability of these intrusive rocks restricts subsurface movement of ground water in the lati-andesite and paleochannel conglomerate, partly accounting for discharge at Del Rio Springs. In addition, there is an abrupt decrease in the width and thickness of the aquifer system. The occurrence of younger alluvium north of Del Rio Springs is limited to a narrow neck of shallow alluvium along Little Chino Creek, underlain by lati-andesite and shallow basement. The least restrictive ground-water flowpath is northeast of Del Rio Springs (elevation 4,425) toward moderately permeable Paleozoic rock and lati-andesite exposed along Stillman Lake and lower Granite Spring (at elevations 4,250 and 4,280 ft, respectively). The beginning of the spring-fed reach in lower Granite Creek coincides with the location of two small northeast-striking faults in Paleozoic rocks shown at the 1:48,000 scale by Krieger (1965). Between Del Rio Springs and springs in lower Granite Creek and Sullivan Lake, the water table or potentiometric surface drops 145 ft over a distance of 1.5 to 2 mi, a gradient of 70 to 100 ft/mi.

### Carbonate Aquifer

The regional carbonate aquifer north of the upper Verde River and Big Chino Valley straddles the Colorado Plateau and the Transition Zone provinces (fig. D2). North of the Transition Zone boundary, sedimentary rocks are relatively flat and unbroken, and movement of ground water is north or northeast toward Cataract Canyon and the Colorado River. South of the Transition Zone boundary, ground water in the carbonate aquifer is captured by the upper Verde River and Big Chino Valley. In comparison to the Colorado Plateau, carbonate rocks in the Transition Zone have undergone a greater intensity of faulting, folding, and erosion. Consequently, ground water within the

aquifer is more likely to be compartmentalized or confined in some locations.

In northern Arizona, prominent northwest-striking fractures throughout the Colorado Plateau area tend to be open to fluid flow (Thorstenson and Beard 1998; L. S. Beard, oral commun., 1999). In the study area, the largest structures most likely to influence ground-water movement include the Big Chino Fault and Limestone Canyon Monocline—which roughly parallel one another and strike northwest. These structural flexures and faults have influenced topography and drainage patterns of the exposed sedimentary rocks within the Transition Zone. Stratigraphic contacts and bedding planes also may provide conduits for flow.

Secondary porosity from fractures and karst near the base of the Martin are recognized as an important pathway. The pattern of subsurface karst dissolution is nearly impossible to discern, however, except where large caves allow underground exploration, such as in nearby Grand Canyon (Huntoon, 1970). Karst often approximately follows major faults and dominant fracture patterns, which here include northwest-striking structures such as the Big Chino Fault and the Limestone Canyon Monocline. Alternately, some karst pathways may follow primary depositional features such as the collapse and rubbles zones in the Redwall Limestone. Preferential dissolution also could have occurred along segments of basalt-filled paleochannels that are exposed in the walls of Hell Canyon and noted in driller's logs north of the upper Verde River (DeWitt and others, this volume). Paleocanyon walls would have been weathered before the basalt was emplaced. In addition, permeability of the basalt is high (table D1). Any combination of these pathways through the carbonate aquifer is possible.

Ground water in a large carbonate aquifer typically will discharge to one or a few large springs. Within the study area, the carbonate aquifer discharges to the base of incised limestone canyons at Storm Seep on Big Black Mesa, upper Verde River springs, King Spring in Hell Canyon, Mormon Pocket, and Sycamore Canyon. Although the pattern of karst may seem random, the source area must be upgradient from the point of discharge. Ground-water flowpaths within the carbonate aquifer can be inferred in part from topography, geologic framework, well information, and the locations of springs.

## Big Black Mesa and the Ground-Water Divide

The crest of Big Black Mesa is a ground-water divide for the carbonate aquifer between the Colorado Plateau and the Transition Zone. The location of the ground-water divide is inferred here on the basis of the geologic framework and limited water-level data. Relevant features important to the hydrogeologic framework include (a) northwest-striking faults, monclines, and fracture trends, (b) the stratigraphy and dip of the sedimentary rock units, and (c) karst dissolution openings.

Displacement along the Big Chino Fault places basin deposits against granitic basement rock, creating a relatively impermeable basin boundary along most of the base of Big Black Mesa except near Paulden. The large area north of the

Big Black Mesa has the topographic and structural characteristics of the Colorado Plateau. Streams and washes flow toward Partridge Creek and upper Big Chino Wash, which are ephemeral (Myers, 1987). North of I-40, ground water follows the gentle northeast dip of the Paleozoic strata, more or less perpendicular to the regional strike (Twenter, 1962, p. 22; Myers, 1987; McGavock, 1986; Montgomery and Associates, 1996). This direction may be locally modified by karst or structural features. Surface-water runoff on the Colorado Plateau overlying the carbonate aquifer infrequently reaches Big Chino Valley. Little if any ground-water recharge to Big Chino Valley is likely north of the ground-water divide, which approximately follows the crest of Big Black Mesa.

High-altitude springs on Big Black Mesa may or may not be perched, but their presence above the floor of Big Chino Valley suggests that the water table or the potentiometric surface is mounded beneath topographic highs. Four high-altitude springs around the perimeter of Big Black Mesa range in elevation from 5,000 to 5,700 ft (fig. D4). There are no wells on Big Black Mesa, although water-level measurements from eight wells northwest of Big Black Mesa near Partridge Creek and Pichacho Butte range from 4,541 to 4,636 ft (Bills and Flynn, 2002). Water-level measurements from deep municipal wells along I-40 near the towns of Ash Fork (4,095 to 4,114 ft) and Williams (between 3,900 and 4,100 ft) (Arizona Department of Water Resources, 2002; Bills and Flynn, 2002; Pierce, 2003) are substantially lower than water-level altitudes ranging between 4,205 ft at King Spring and 4,230 to 4,244 ft near Drake (table D3).

In comparison, measured water levels throughout Big and Little Chino Valleys and in the carbonate aquifer north of the upper Verde River all exceed  $4,235 \pm 1$  ft in altitude—at least 100 ft greater than the elevation of measured water levels in the carbonate aquifer near Ash Fork and Williams. The ground-water divide between the Transition Zone and the Colorado Plateau is inferred to continue northeast of Big Black Mesa, toward the Matterhorn and Bill Williams Mountain, approximately following the northern boundary of the Transition Zone (figs. D1 and D2). The precise location of the ground-water divide between Drake and Ash Fork is uncertain, but is thought to approximately follow the northern Transition zone boundary for the carbonate aquifer (shown in fig. D2). This interpretation agrees with the northern aquifer boundary for the Big Chino basin-fill aquifer as depicted by Robson and Banta (1995). Water levels surrounding Bill Williams Mountain range from about 3,860 for the regional aquifer to 4,900 ft for perched conditions (Arizona Department of Water Resources, 2002; Bills and Flynn, 2002; Pierce, 2003).

## Carbonate Aquifer North of Upper Verde River

In the Transition Zone north of the upper Verde River, the regional direction of ground-water movement in the carbonate aquifer is east or southeast, as inferred from water-level altitudes of gaining reaches of the upper Verde River (see fig. A14, Chapter A), springs, and wells in the carbonate aquifer

north of the river (fig. D9 and table D3). New water-level measurements collected since 1993 include twice as many wells and spring locations for this area than in previous studies (Owen-Joyce and Bell, 1983; Levings and Mann, 1980). The vertical accuracy of most land-surface elevations was estimated from USGS 7.5-minute quadrangle maps having 20-ft topographic contours, and, therefore, individual water-level data are presumed accurate to within  $\pm 10$  ft. Two of the new sites are index wells in the Arizona Department of Water Resources monitoring program, which are measured annually. The index measurements have changed little from year to year, varying less than 2.0 ft over an 8-year period.

Water-level elevations in the carbonate aquifer directly north of upper Verde River springs vary between 4,244 and 4,205 ft in elevation, a range of about  $40 \pm 10$  ft. This area, which lies between the 4,250 and 4,200 ft contours (fig. D9), extends from Paulden on the west to Drake on the north, and from King Spring on the east to the upper Verde River to the south. The small range in variability of the water-level measurements for this area is notable despite the fact that different parties collected data in different years, using different methods and equipment, and in that topographic relief varies more than 400 ft (fig. D9 and table D3). From west to east along the gaining reach of the Verde River, the water-level gradient slopes from about 4,255 ft near Paulden to 4,130 ft near Muldoon Canyon, a gradient of about 25 ft/mi. From north to south, the water-level gradient changes less than 5 ft/mi between Drake and upper Verde River springs. Owing to little well control, the 4,250 ft contour could extend farther north of Drake, or farther northwest beneath Big Black Mesa, but is well constrained to the east and south.

Near Drake, the water-level gradient slopes southeast toward King Spring, parallel to Hell Canyon. King Spring is a local point of discharge for this part of the carbonate aquifer, with evapotranspiration and seepage losses to the shallow alluvium approximately equal to discharge. East of Hell Canyon, the water-level gradient declines abruptly by more than 300 ft in less than a mi. To the east from King Spring to Mormon Pocket and Sycamore Canyon (a distance about 20 mi) the total decline in the water-level gradient is about 500 ft or an average of 25 ft/mi. The major ground-water flow direction between the town of Paulden and Hell Canyon is west to east; or northwest to southeast—parallel to the northwest-striking faults, monoclines, and fracture patterns. Underflow from Big and Little Chino Valleys past the mouth of Hell Canyon is presumed to be insignificant (Freethy and Anderson, 1986). Proterozoic rocks with low permeability crop out at river level between the Paulden gauge and Hell Canyon, which may contribute to the lack of measurable ground-water inflow to the upper Verde River between Hell Canyon and Perkinsville (Wirt, Chapter A, this volume; fig. A14).

Ground water exits Big Chino Valley north and east of Paulden (figs. D8 and D9; Wallace and Laney, 1976; Owen-Joyce and Bell, 1983; Freethy and Anderson, 1986; Schwab, 1995), through Tertiary basalt, or Paleozoic sedimentary rocks, or both. The lack of an abrupt change in gradient across the

basin boundary between the Big Chino basin-fill aquifer and the carbonate aquifer is a strong indication that these two aquifers are hydraulically connected. Less than a mi northwest of upper Verde River springs (4,235+1 ft), well HR-2 in the basalt paleochannel is 500-ft deep and has a water-level elevation of 4,242+1 ft (Water Resource Associates, 1991).

The water-level gradient along the first 8 mi of the upper Verde River (25 ft/mi) is about twice that of the gradient over Big Chino Valley (12 ft/mi). The regional gradient and flow direction are consistent with the Big Chino aquifer as the primary source of discharge to upper Verde Springs, although it is possible that a small fraction of base flow could be derived from the carbonate aquifer. This possibility will be addressed further in Chapters E and F (this volume). Based on the regional water-level gradients in the basin-fill and carbonate aquifers (figs. D8 and D9), all inflow is derived west or northwest of upper Verde River springs. As mentioned earlier, discharge from the carbonate aquifer, if any, could potentially contribute to upper Verde River springs from Paleozoic rocks (a) beneath the Big Chino basin-fill aquifer, (b) through alluvial fans along the base of Big Black Mesa, or (c) near the outlet of the basin-fill aquifer along joints parallel to the northwest-striking Big Chino Fault.

Ground water from the Big Chino aquifer passes through about 2 mi of basalt and carbonate rock before reaching upper Verde River springs. Some ground water discharges farther east near the confluence of Muldoon Canyon with the Verde River (river mi 8). On the basis of the regional ground-water gradient, the source of this seepage is from the west or northwest, which could include the Big Chino basin-fill aquifer, as well as the carbonate aquifer in the Drake area. An alternate possibility is that all or part of the seepage could be derived from the vicinity of Muldoon Canyon to the south, where little water-level information is available.

## Summary and Conclusions

The Transition Zone geologic province within the Verde River headwaters region contains three major aquifers, the Big and Little basin-fill aquifers, and a compartmentalized carbonate aquifer. Basin and Range faulting created the down-dropped structural basins that contain large basin-fill aquifers in Big and Little Chino valleys. Tertiary volcanic rocks are an important component of the basin-fill material, particularly in Little Chino Valley. North of Big Chino Valley and the Verde River, essentially flat-lying Paleozoic carbonate rocks are considered part of the Colorado Plateau. Within the Transition Zone, Paleozoic carbonate rocks lack continuity, and have been faulted and in some areas folded. Carbonate rocks are present beneath Big Chino Valley and in northern Little Chino Valley and crop out as erosional remnants in mountain ranges to the south. North of the upper Verde River and in the Granite/Verde confluence area, sedimentary rock units are deeply incised and partly buried. Near the confluence area, at least two paleocanyons are concealed

by Tertiary basalt flows, one east of Del Rio Springs and one northeast of Paulden.

Ground-water recharge to basin-fill aquifers in the Verde River headwaters is from mountain recharge and from direct stream runoff within the basins in areas having the greatest precipitation, favorable topography, and permeable rock or sediments. The water table is usually shallow beneath incised canyons, where recharge to the carbonate aquifer likely is greatest in areas having well-developed karst or fracture systems. Tertiary basalts also have a high degree of secondary porosity and recharge potential. In contrast, surface-water runoff is greatest in high-altitude areas underlain by relatively impermeable Proterozoic rocks.

Big and Little Chino Valleys contain gently sloping reservoirs of ground water that drain by gravity toward large springs near their outlets. The ground-water flow direction of basin-fill aquifers generally is from the basin margins and tributaries toward the center and down valley axes. In Big Chino Valley, ground-water conditions are typically unconfined. In Little Chino Valley ground water flows under both unconfined and a variety of confining conditions. Despite these complexities, each basin-fill aquifer is interpreted as a single, connected system.

Big Chino Valley owes its elongate, asymmetric configuration to the northwesterly strike of the Big Chino Fault. Displacement along the fault places basin deposits against Proterozoic rocks, creating an impermeable boundary along most of Big Black Mesa. The fault ends in a series of horse-tail splays north of Paulden, where Paleozoic carbonate rocks shallowly underlie and abut basin-fill sediments. Ground-water flowpaths and rates of flow are influenced by lateral and vertical changes in grain size of alluvial sediments (such as permeable stream gravels versus the fine-grained playa deposits) and buried basalt flows. High-yielding wells along Big Chino Wash have been developed from heterogeneous basin-fill sediments. In upper Big Chino Valley, high yielding wells in basin-fill alluvium are underlain by a basalt flow. At the basin outlet near Paulden, a basalt unit with high overall permeability straddles the basin-fill aquifer boundary, facilitating the movement of ground water into the carbonate aquifer. In addition, the lower Martin Formation shallowly underlies the basin-fill deposits north of Paulden (< 400 ft in depth). High-yielding supply wells near Paulden have been developed in Tertiary basalt and karst on both sides of the basin boundary.

Little Chino Valley is not as deep or elongate in any direction as Big Chino Valley. Alluvial and volcanic basin fill directly overlies Proterozoic basement rock and Paleozoic strata in the deepest part of the basin, forming a highly productive artesian aquifer. Buried plugs of latite-andesite increase in abundance north of Del Rio Springs. The narrowing of alluvial deposits toward the basin outlet and low permeability of the plugs restricts northern movement of ground water, which in part accounts for discharge at Del Rio Springs. From Del Rio Springs, the most reasonable ground-water flowpath is northeast through faulted Paleozoic rock and latite-andesite in the carbonate aquifer near Stillman Lake and Lower Granite Creek.

The crest of Big Black Mesa is interpreted as a ground-water divide separating the Big Chino basin-fill aquifer and the regional carbonate aquifer beneath the Colorado Plateau. A large part of the carbonate aquifer north of the divide (nearly half of the upper Verde River watershed) probably contributes little, if any, ground water tributary to Big Chino Valley or the Verde River. Between the Verde River and Drake, the regional ground-water flow direction in the carbonate aquifer is to the southeast, and appears to follow the dominant northwest-southeast structural orientation of Big Chino Valley and Big Black Mesa. On a more local scale, ground-water movement likely is influenced by the presence of basalt flows, faults and connected fractures, karst, stratigraphic contacts and bedding planes, and differences in the grain size of sediment. Fractures and karst near the base of the Martin Formation are important conduits.

The Big Chino basin-fill aquifer and the carbonate aquifer north of the upper Verde River are strongly connected near Paulden. This is evidenced by a gently sloping water-level gradient east of Paulden that extends north of Drake, and east as far as Hell Canyon. Gradient and flow direction are entirely consistent with the Big Chino aquifer providing the major source of discharge to upper Verde River springs, although it is possible that a minor fraction of inflow could be derived from the carbonate aquifer. Potential contributions from the carbonate aquifer to the Big Chino basin-fill aquifers are most likely from carbonate rocks (a) beneath the Big Chino basin-fill aquifer, (b) through alluvial fans along the base of Big Black Mesa, or (c) near the outlet of the basin-fill aquifer along solution-enhanced fractures parallel to the northwest-striking Big Chino Fault.

## References Cited

- Allen, Stephenson & Associates, 2001, Hydrogeology study of The Ranch at Del Rio Springs: prepared for The Bond Ranch at Del Rio Springs, LLC; available from Allen, Stephenson & Associates, Phoenix, Arizona, 88 p. plus appendices.
- Arizona Department of Water Resources, 2000, Verde River Watershed Study: Arizona Department of Water Resources report, 208 p. plus appendices.
- Arizona Department of Water Resources, 2002, Arizona Registry of Wells 55 CD-ROM, updated March 2002.
- Beus, Stanley, 1989, Devonian and Mississippian Geology of Arizona: *in* Jenney, J.P., and Reynolds, S.J., Geologic evolution of Arizona: Tucson, Arizona Geological Society Digest 17, p. 287–311.
- Bills, D.J., and Flynn, M.E., 2002, Hydrogeologic data for the Coconino Plateau and adjacent areas, Coconino and Yavapai Counties, Arizona: U. S. Geological Survey Open-File Report 02-265, 29 p. with CD-ROM.

- Corkhill, E.F. and Mason, D.A., 1995, Hydrogeology and simulation of groundwater flow: Prescott Active Management Area, Yavapai County, Arizona: Arizona Department of Water Resources Modeling Report No. 9, 143 p.
- DeWitt, Ed, Langenheim, V.E., Force, Eric, Vance, Kelly, and Lindberg, P.A., *with* a digital database by Doug Hirschberg, Guy Pinhassi, and Nancy Shock, *in press*, Geologic map of the Prescott National Forest and headwaters of the Verde River, Yavapai and Coconino Counties, Arizona: U.S. Geological Survey Miscellaneous Investigations Map I-xxxx, scale 1:100,000, two sheets.
- Ewing, D.B., Osterberg, J.C., Talbot, R.W., 1994, Groundwater Study of the Big Chino Valley—Hydrology and hydrogeology: Bureau of Reclamation Technical Report, Denver, Colorado, 14 p. plus 6 appendices.
- Ford, D.C., 1999, Perspectives in karst hydrogeology and cavern genesis: *in* Karst Modeling, Karst Waters Institute Special Publication 5, p.17–29.
- Ford, D.C., and Williams, P.W., 1989, Karst geomorphology and hydrogeology: London, Unwin and Hynman, 601 p.
- Freethy, G.W., and Anderson, T.W., 1986, Predevelopment hydrologic conditions in the alluvial basins of Arizona and adjacent parts of California and New Mexico: U.S. Geological Survey Hydrologic Investigations Atlas HA-664.
- Hereford, Richard, 1975, Chino Valley Formation (Cambrian?) in northwestern Arizona: Geological Society of America Bulletin, v. 86, p. 677–682.
- Huntoon, P.W., 1970, The hydro-mechanics of the groundwater system in the southern portion of the Kaibab Plateau, Arizona: University of Arizona Ph.D thesis, Department of Geosciences, Tucson, Arizona, 251 p. with maps.
- Huntoon, P.W., 1977, Relationship of tectonic structure to aquifer mechanics in the western Grand Canyon District, Arizona: University of Wyoming, Water Resources Series No. 66, 51 p.
- Knauth, L. P., and Marnie Greenbie, 1997, Stable isotope investigation of ground-water-surface-water interactions in the Verde River headwaters area: Arizona State University Department of Geology report in fulfillment of Arizona Water Protection Fund Grant #95-001, administered by Arizona Department of Water Resources, 28 p.
- Krieger, M.H., 1965, Geology of the Prescott and Paulden quadrangles, Arizona. U.S. Geological Survey Professional Paper 467, 127 p.
- Levings, G.W., and Mann, L.J., 1980, Maps showing ground-water conditions in the upper Verde River area, Yavapai and Coconino Counties, Arizona-1978: U.S. Geological Survey Water-Resources Investigations, Open-File Report 80-726, maps.
- Lohman, S. W., 1979, Ground-Water Hydraulics: U.S. Geological Survey Professional Paper 708, 70 p.
- Lucchitta, Ivo, 1989, History of the Grand Canyon and of the Colorado River in Arizona, *in* Jenney, J.P., and Reynolds, S.J., 1989, Geologic Evolution of Arizona: Arizona Geological Society Digest 17, p. 701–715.
- Matlock, W.G., Davis, P.R., and Roth, R.L., 1973. Groundwater in Little Chino Valley, Arizona: University of Arizona Agricultural Experiment Station, Technical Bulletin 201, 19 p.
- Myers, S.M., 1987, Map showing ground-water conditions in the Peach Springs basin, Arizona: Arizona Department of Water Resources, Hydrologic Map Series Report no.15.
- McGavock, E.H., Anderson, T.W., Moosburner, Otto, and Mann, L.T., 1986, Water Resources of southern Coconino County, Arizona: Arizona Department of Water Resources Bulletin 4, 53 p.
- Metzger, D.G., 1961, Geology in relation to availability of water along the South Rim, Grand Canyon National Park, Arizona: *in* Hydrology of the Public Domain, U.S. Geological Survey Water-Supply Paper 1475-C, p. 105–135, with plates.
- Montgomery, E.L., and Associates, Inc., 1996, Assessment of hydrogeologic conditions and potential effects of proposed groundwater withdrawal for Canyon Forest Village, Coconino County, Arizona: E.L. Montgomery and Associates, Inc., 64 p.
- Ostenaar, D.A., Schimschal, U.S., King, C.E., Wright, J.W., Furgerson, R.B., Harrel, H.C., and Throner, R.H., 1993, Big Chino Valley Groundwater Study—Geologic Framework Investigations Seismotectonic Report 93-2, Bureau of Reclamation, Denver Office, 31 p.
- Owen-Joyce, S.J., and Bell, C.K., 1983, Appraisal of water resources in the Upper Verde River area, Yavapai and Coconino Counties, Arizona: Arizona Department of Water Resources Bulletin 2, 219 p.
- Pierce, W.H., 1985, Arizona's backbone: the transition zone: Arizona Bureau of Geology and Mineral Technology Field-notes: v. 15, no. 3, 6 p.
- Pierce, H.A., 2003, Structural controls on ground-water conditions and estimated aquifer properties near Bill Williams Mountain, Williams, Arizona: U.S. Geological Survey, Water-Resources Investigations Report 01-4058, 41 p.
- Remick, W.H., 1983, Maps showing ground-water conditions in the Prescott Active Management Area, Yavapai County, Arizona—1982. Arizona Department of Water Resources Hydrologic Map Series, Phoenix, Report Number 9.

- Robson, S.G., and Banta, E.R., 1995, Ground water atlas of the United States; Segment 2, Arizona, Colorado, New Mexico, and Utah: U.S. Geological Survey, Hydrologic Investigations Atlas 0375-7978, 18 sheets.
- Schwab, K.J., 1995, Maps showing ground-water conditions in the Big Chino Sub-Valley of the Verde River Valley, Coconino and Yavapai Counties, Arizona—1992: Department of Water Resources, Hydrologic Map Series Report Number 28, Phoenix, Arizona, 1 sheet.
- Schwalen, H.C., 1967, Little Chino Valley artesian area and ground-water basin: Technical Bulletin 178, Agricultural Experiment Station, University of Arizona, Tucson, Arizona, 63 p.
- Southwest Groundwater Consultants, 2002, Hydrogeology of proposed Stirling Bridge project, Drake, Arizona: Southwest Groundwater Consultants, August 8, 2002, 11 p.
- Theis, C.V., 1941, The effect of a well on the flow of a nearby stream: *Am. Geophys. Union Trans.*, v. 22, p. 734-738.
- Thiele, H.J., 1961, Groundwater hydrological and geophysical survey, Haskell Spring area, Clarkdale, Arizona: Consulting hydrologist's report prepared for Clarkdale Realty Co., Scottsdale, Arizona, 14 p.
- Thorstenson, D.J., and Beard, L.S., 1998, Geology and fracture analysis of Camp Navajo, Arizona Army National Guard, Arizona: U.S. Geological Survey Open-File Report 98-242, 42 p.
- Twenter, F.R., and Metzger, D.G., 1963, Geology and ground water in Verde Valley—the Mogollon Rim region of Arizona: U.S. Geological Survey Bulletin 1177, 132 p.
- Twenter, F.R., 1962, Geology and promising areas for ground-water development in the Hualapai basin area, Arizona: U.S. Geological Survey Water Supply Paper 1576-A, 38 p.
- Wallace, B.L. and Laney, R.L., 1976, Maps showing ground-water conditions in the lower Big Chino Valley and Williamson Valley areas, Yavapai and Coconino Counties, Arizona - 1975-76: U.S. Geological Survey Open-File Report Water Resources Investigations 76-78, 2 maps.
- Water Resources Associates, 1989, Hydrogeology investigation of Big Chino Valley, Yavapai County, Arizona: Phase I, Consultants reports for city of Prescott, City Attorney's Office, Prescott, Arizona, November 29, 1989, 2 volumes.
- Water Resources Associates, 1990, Hydrogeology investigation of Big Chino Valley, Yavapai County, Arizona: Phase II, Consultants reports for city of Prescott, City Attorney's Office, Prescott, Arizona, February 5, 1990, 3 volumes.
- Water Resources Associates, 1991, Application for a Subdivision Water Adequacy Statement Headwaters Ranch Project, Paulden, Arizona: Water Resources Associates, Inc., certified by Stephen Noel, May 10, 1991.
- White, W.B., 1999, Conceptual models for karstic aquifers: *in* Karst Modeling, Karst Waters Institute Special Publication 5, p. 11-16.
- White, W.B., 1988, Geomorphology and hydrology of karst terrains: New York, Oxford University Press, 464 p.
- White, W.B., 1969, Conceptual models for carbonate aquifers: *Ground Water*, v. 7, p. 15-21.
- Winter, T.C., Harvey, J.W., Franke, O.L., and Alley, W.M., 1999, Ground water and surface water—A single resource: U.S. Geological Survey Circular 1139, 79 p.





# **Geochemistry of Major Aquifers and Springs**

By Laurie Wirt and Ed DeWitt

Chapter E

## **Geologic Framework of Aquifer Units and Ground-Water Flowpaths, Verde River Headwaters, North-Central Arizona**

Edited by Laurie Wirt, Ed DeWitt, and V.E. Langenheim

Prepared in cooperation with the Arizona Water Protection Fund Commission

Open-File Report 2004–1411-E

**U.S. Department of the Interior**  
**U.S. Geological Survey**

**U.S. Department of the Interior**  
Gale A. Norton, Secretary

**U.S. Geological Survey**  
P. Patrick Leahy, Acting Director

U.S. Geological Survey, Reston, Virginia: 2005

For product and ordering information:  
World Wide Web: <http://www.usgs.gov/pubprod>  
Telephone: 1-888-ASK-USGS

For more information on the USGS--the Federal source for science about the Earth, its natural and living resources, natural hazards, and the environment:  
World Wide Web: <http://www.usgs.gov>  
Telephone: 1-888-ASK-USGS

Any use of trade, product, or firm names is for descriptive purposes only and does not imply endorsement by the U.S. Government.

Although this report is in the public domain, permission must be secured from the individual copyright owners to reproduce any copyrighted materials contained within this report.

***Suggested citation:***

Wirt, Laurie, DeWitt, Ed, 2005, Geochemistry of Major Aquifers and Springs, *in* Wirt, Laurie, DeWitt, Ed, and Langenheim, V.E., eds., Geologic Framework of Aquifer Units and Ground-Water Flowplaths, Verde River Headwaters, North-Central Arizona: U.S. Geological Survey Open-File Report 2004-1411-E, 44 p.

# Contents

Abstract.....	1
Introduction.....	1
Purpose and Scope .....	2
Previous Investigations.....	2
Acknowledgments .....	4
Methods of Investigation.....	4
Sampling Strategy.....	4
Field Methods .....	5
Analytical Methods.....	6
Isotope Characterization and Apparent Age-Dating Techniques.....	6
Hydrogen and Oxygen Stable Isotopes.....	6
Tritium .....	7
Carbon-13 and -14.....	7
Water-Quality Sampling Results.....	8
Major-Ion Chemistry.....	8
Trace-element Chemistry .....	10
Marine Shale Origin of Arsenic, Lithium, and Boron .....	10
Igneous and Sedimentary Sources of Strontium .....	12
Isotope Chemistry .....	14
Evaporation and Characterization of Major Aquifers and Springs .....	14
Apparent Age of Ground Water.....	21
Tritium .....	21
Carbon-14 and Carbon-13.....	21
Multiple Lines of Geochemical Evidence along a Flowpath.....	25
References Cited.....	27
Appendix A. Water chemistry data for wells and springs (1981 to present), Verde River headwaters, Arizona.....	33
Appendix B. Isotope data for wells and springs (1986 to present), Verde River headwaters, Arizona .....	42

## Figures

<b>E1.</b> Major water-chemistry sample groups characterized in this study, Verde River headwaters region, Arizona.....	3
<b>E2.</b> Trilinear diagrams (Piper, 1944) showing major-ion proportions in percent milliequivalents per liter (%meq/l). Plot <i>A</i> shows proportions for high-altitude springs and basin-fill aquifer; plot <i>B</i> shows proportions for low-altitude springs and the carbonate aquifer.....	9
<b>E3.</b> Box- and whisker plots (SAS Institute, 1998) of selected major and trace elements characterizing major aquifers and springs, Verde River headwaters, Arizona. Plot <i>A</i> , major element concentrations; Plots <i>B</i> and <i>C</i> , trace-elements concentrations .....	11

<b>E4.</b>	Graph showing $\delta D$ versus $\delta^{18}O$ for springs contributing to the upper Verde River, including upper Verde River springs, Stillman Lake, Lower Granite Creek, and Del Rio Springs. All spring samples were collected June 15–17, 2000.....	16
<b>E5.</b>	Graphs showing $\delta D$ versus $\delta^{18}O$ for sample groups in the Verde River headwaters (1986–2004); (A) major springs discharging to the upper Verde River versus wells and springs in the carbonate aquifer, and (B) upper Verde River springs versus Big and Little Chino basin-fill aquifers and high-altitude springs, tributaries and wells.....	18
<b>E6.</b>	Box- and whisker plot (SAS Institute, 1998) of $\delta^{18}O$ for sample groups upgradient of upper Verde River springs .....	20
<b>E7.</b>	Map showing tritium activities measured in this study, upper Verde River headwaters region .....	22
<b>E8.</b>	Map showing carbon-14 activities measured in this study, upper Verde River headwaters region .....	23
<b>E9.</b>	Graphs showing changes in water chemistry along regional water-level gradient from upper to lower Big Chino Valley and from the Big Chino basin-fill aquifer near Paulden through the carbonate aquifer to upper Verde River springs .....	25

## Tables

<b>E1.</b>	Chemistry of major rock types exposed in Verde River headwaters region, Arizona.....	13
<b>E2.</b>	Statistical summary of stable-isotope samples grouped by major aquifers and springs, and surrounding upland areas .....	15

# Geochemistry of Major Aquifers and Springs

By Laurie Wirt and Ed DeWitt

## Abstract

In this chapter, graphical methods to plot geochemical and isotopic data are used to characterize major aquifers and springs discharging to the upper Verde River and to identify changes in water chemistry along the main ground-water flowpath from Big Chino Valley to upper Verde River springs. Samples were analyzed for major and trace elements,  $\delta^{18}\text{O}$ ,  $\delta\text{D}$ ,  $^3\text{H}$ ,  $^{14}\text{C}$ , and  $^{13}\text{C}$ . Ground-water samples are grouped by aquifer, altitude, and geographic location to identify important processes and trends. Sample groups include (a) high-altitude areas west and south of Big Chino Valley, (b) the carbonate aquifer north of Big Chino Valley and the upper Verde River (Mississippian-Devonian, or M-D sequence), (c) the Little Chino basin-fill aquifer, (d) the Big Chino basin-fill aquifer, (e) the carbonate aquifer near the outlet of the Big Chino basin-fill aquifer (Devonian-Cambrian, or D-C zone), and (f) low-altitude springs discharging to the upper Verde River.

Limitations of the stable-isotope data used in this study include not being able to volumetrically weight contributions from different areas of the ground-water system. Also, evaporation has had a significant effect on the stable-isotope composition of spring-fed lakes and some samples from the M-D carbonate aquifer. Despite these drawbacks, the Little Chino basin-fill aquifer and the M-D sequence still could be largely excluded as major sources to upper Verde River springs. Low-altitude springs discharging from the Little Chino basin-fill aquifer are  $\sim 0.4$  per mil (‰) enriched in  $\delta^{18}\text{O}$ , with high dissolved strontium ( $> 450 \mu\text{g/L Sr}$ ) resulting from contact latite-andesite in northern Little Chino Valley. In contrast, the M-D sequence is depleted by about  $1.3\text{‰}$   $\delta^{18}\text{O}$  and  $7.9\text{‰}$   $\delta\text{D}$  and is low in strontium (less than  $120 \mu\text{g/L Sr}$ ), compared to moderate values for upper Verde River springs ( $346$  to  $440 \mu\text{g/L Sr}$ ).

Water chemistry of upper Verde River springs has characteristics of both the Big Chino basin-fill aquifer and the D-C zone of the carbonate aquifer near Paulden. Values of  $-10.3 \pm 0.2\text{‰}$   $\delta^{18}\text{O}$  and  $-74.4 \pm 2.0\text{‰}$   $\delta\text{D}$  were used to trace a flowpath from the Big Chino basin-fill aquifer near Paulden through the D-C zone to upper Verde River springs. Disproportionate increases of the boron and lithium along the flowpath of 274 percent B versus 188 percent Li (with no corresponding change in  $\delta^{18}\text{O}$ ,  $\delta\text{D}$ , Ca, and Sr values) indicate the major process responsible for increases in trace elements is water-rock interaction. The upper Verde River springs samples

have moderately high values of  $17\text{--}29 \mu\text{g/L As}$ ,  $136\text{--}270 \mu\text{g/L B}$ , and  $28\text{--}49 \mu\text{g/L Li}$ , attributed to water-rock contact with marine shale within the D-C zone. The highest concentrations in the study area of  $33\text{--}38 \mu\text{g/L As}$ ,  $330\text{--}460 \mu\text{g/L B}$ , and  $54\text{--}86 \mu\text{g/L Li}$  are found in the D-C zone.

The presence of measurable tritium and elevated  $^{14}\text{C}$  activity near the outlets of the basins indicates that recharge is occurring beneath major drainages, including Williamson Valley Wash, lower Big Chino Wash, Granite Creek, and Little Chino Creek. Carbon-14 activities along the flowpath between the Big Chino basin-fill aquifer near Paulden area and upper Verde River springs range between 55 and 42 percent modern carbon, compared with 18 percent modern carbon for a well in the D-C zone north of Paulden. Along the final leg of the flowpath to upper Verde River springs, the  $^{14}\text{C}$  activity decreases slightly from  $55.5 \pm 0.6$  to  $42 \pm 0.3$  percent modern carbon, which is attributed either to water-rock interaction or a small amount of mixing.

No mixing of the Big Chino basin-fill aquifer with a second source is needed to account for the stable-isotope composition and trace-element chemistry at upper Verde River springs. Despite the lack of compelling geochemical evidence to support mixing between the carbonate aquifer and the Big Chino basin-fill aquifer, however, a standard analytical uncertainty of  $0.2 \delta^{18}\text{O}\text{‰}$  would allow approximately 15 percent of the total discharge to upper Verde River springs to be derived from the M-D sequence of the carbonate aquifer. Multiple lines of geochemical evidence are consistent with a basin outlet flowpath from the Big Chino aquifer near Paulden through the D-C zone of the carbonate aquifer to upper Verde River springs.

## Introduction

The goal of the geochemical and isotopic studies in this chapter is to identify ground-water flowpaths and source(s) of springs discharging to the upper Verde River. From 2000 to 2004, water-chemistry samples were collected from the Big and Little Chino basin-fill aquifers, from high-altitude springs and tributaries of the Bradshaw, Santa Maria, and Juniper Mountains, and from the carbonate aquifer north of Big Chino Valley and the upper Verde River (fig. E1). A variety of geochemical methods were used to infer recharge sources, define ground-water flowpaths, and to show differences in the

## E2 Geochemistry of Major Aquifers and Springs

apparent ages of ground water contributing to the upper Verde River. Geochemical and stable isotope results of past studies also were utilized when appropriate.

Geochemical approaches used in this study include major- and trace-element concentrations, stable (or nonradioactive) isotopes of oxygen, hydrogen, and carbon, and radioactive tritium and carbon-14. Concentrations of major ions and trace elements help to define processes related to water-rock interactions and possible mixing of end members. Stable isotopes of oxygen and deuterium provide information about the altitude of ground-water recharge areas and the degree of evaporation. Tritium and carbon-14 are used to identify changes in the apparent age of ground water along major flowpaths. Hydrologic and geologic information developed in the conceptual hydrogeologic framework (Chapter D, this volume) was utilized in sampling strategy and helped to constrain ground-water flow directions, evaluate spatial differences in solutes and environmental isotopes, and infer probable sources of dissolved species. Geochemical trends are particularly useful for delineating flowpaths through fractured rock aquifers and for evaluating whether concentrations of certain elements are caused by water-rock interactions or by ground-water mixing.

### Purpose and Scope

The purpose of this chapter is to identify geochemical trends for the Big and Little Chino basin-fill aquifers, the regional carbonate aquifer, and for springs discharging to the upper Verde River. Geochemical and isotope methods are used (1) to characterize the water chemistry of major aquifers, recharge areas, and springs in the upper Verde River, (2) to identify water-rock interactions along flowpaths through fractured rock near the outlets of Big and Little Chino Valleys, (3) to delineate areas where recharge is occurring, and (4) to determine whether ground water discharging to upper Verde River springs is derived from a single source (e.g. the Big Chino basin-fill aquifer) or is comprised of a mixture of ground water from the Big Chino aquifer with the adjacent carbonate aquifer.

### Previous Investigations

Previous hydrological investigations of the headwaters have used concentrations of major elements to describe water quality. In 1946 and 1947, H.B. Babcock of the U.S. Geological Survey (USGS) collected what are perhaps the earliest water-quality analyses for wells in Little Chino Valley (Krieger, 1965; table 18). Several other studies have plotted chemical parameters on maps to compare and to characterize similar and dissimilar types of water. In Big Chino Valley, Wallace and Laney (1976) plotted specific conductivity, and Schwab (1995) plotted chemical-quality diagrams of major cations and anions. Remick (1983) mapped total-dissolved solids for Big and Little Chino Valleys. These studies surmise

that ground water in the headwaters region generally is of excellent quality and suitable for most uses, except for the occurrence of moderate to high amounts of dissolved arsenic in samples from the southeastern end of Big Chino Valley (Schwab, 1995).

Several studies have used water chemistry and stable-isotope analyses to characterize ground water in the headwaters. In 1986–87, the USGS collected six ground-water samples in Big and Little Chino Valleys as part of a regional aquifer-system analysis of basins in the southwestern United States (Robertson, 1991). In the summer of 1991, the USGS collected stream samples and conducted a seepage study of base flow in the upper Verde River. Twelve samples also were collected from wells and springs in Big and Little Chino basins in cooperation with Arizona Department of Water Resources. The joint effort was part of a hydrologic and geologic study by the Bureau of Reclamation to investigate the Big Chino aquifer as a possible source of water for the city of Prescott (Ewing and others, 1994).

Past stable-isotope interpretations have been a basis for conflicting conclusions about the source of upper Verde River springs. Arizona State University (ASU) conducted a 2-year stable-isotope ( $^2\text{H}$  and  $^{18}\text{O}$ ) investigation of ground and surface-water in the Verde River headwaters (Knauth and Greenbie, 1997). They concluded that the source of discharge to upper Verde River springs was the carbonate aquifer north of the upper Verde River. This interpretation was largely based similarities between samples collected from the upper Verde River and the Glidden well (fig. E1). Wirt and Hjalmarsen (2000) compiled and interpreted  $^{18}\text{O}$ ,  $^2\text{H}$ ,  $^3\text{H}$ , and  $^{13}\text{C}$  data compiled from earlier studies, along with new samples from upper Verde River springs. These stable-isotope data were used in a mass balance calculation to estimate the relative proportion of inflow to the Verde River from the Big and Little Chino aquifers. On the basis of the mass balance results, Wirt and Hjalmarsen (2000) concluded that the Big Chino aquifer supplied at least 80 percent of the base flow in the upper Verde River. This estimate was compared with their water budget for the upper Verde River based on historical precipitation, stream discharge, ground-water levels, and pumping records. Data used in their study came from the water-quality and stream-gauge databases of the USGS, the Arizona Department of Water Resources ground-water monitoring network, National Weather Service climate records, ASU stable-isotope data (Knauth and Greenbie, 1997), and USGS databases. The different conclusions reached by the ASU and USGS studies over the origin of springs in the upper Verde River have remained a source of controversy and are a major focus of this study.

### Acknowledgments

The authors thank John Hoffman and David Lindsey of the USGS, and Frank Corkhill, Keith Nelson, David Christiana, and Tracy Carpenter of the Arizona Water Resources for their thoughtful reviews which helped to improve this

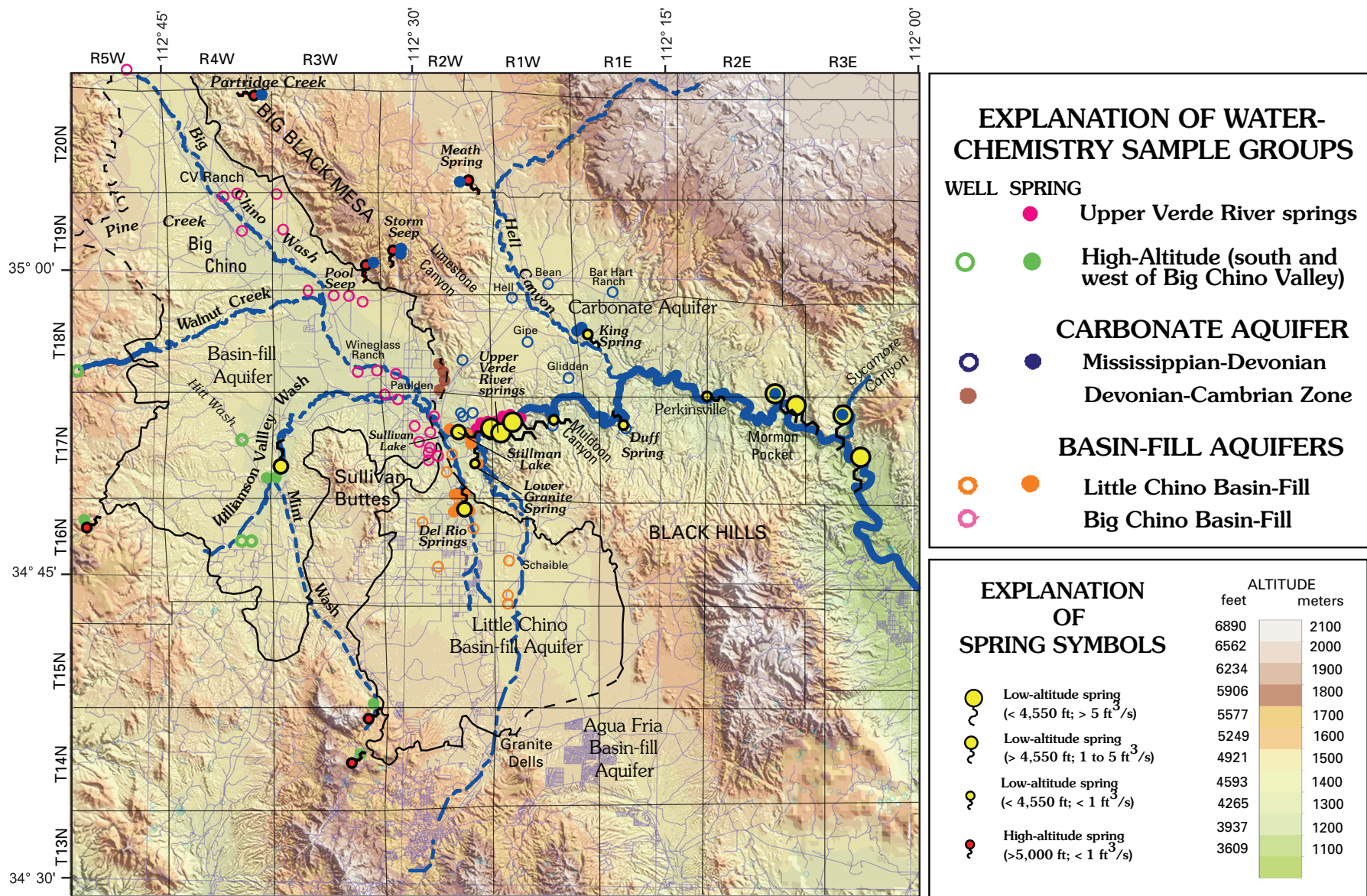
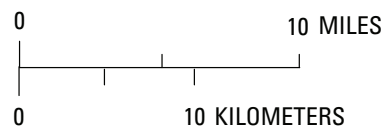


**Figure E1.** Major water-chemistry sample groups characterized in this study, Verde River headwaters region, Arizona. Water chemistry and isotope data are reported in Appendixes A and B, respectively. Aquifer boundaries are dashed where likely interconnected with adjacent aquifer (Wirt and DeWitt, this volume; Chapter D). Base is from 1:100,000 U.S. Geological Survey digital data.



manuscript. The following local residents also granted permission and provided access for water sampling activities: Billy Wells, David Gipe, Don Varner and Ann Gipe, Harley and Patty Shaw, Billy Wells, Ann Harrington, and the Reeves, Wagner, Smith, Prucha, Schaible, and Arnold families. Prescott National Forest, Arizona Game and Fish, and the Las Vegas, Alimeda Cattle, Kieckheffer (K4), and Hitchcock (T2) Ranches also provided access for sampling. Field support was provided at various times by Susan Lane Matthes, Ann Harrington, Eddessa Carr, Kay Lauster, and by Pam Sponholz and Shaula Hedwall of the U.S. Fish and Wildlife Service. USGS personnel who assisted the authors in the field include Betsy Woodhouse and Christie O'Day.

## Methods of Investigation

Sample sites were selected to characterize aquifers, to show spatial variations in the concentrations of selected solutes of interest, to identify recharge areas, and to define changes in apparent age along major ground-water flow directions. Targeted flowpaths for sampling were chosen from water-level contour maps and water-level data (Schwab, 1995; Corkhill and Mason; 1995; Wallace and Laney, 1976; and Chapter D, this volume, figs. D6 and D7).

Sampling also targeted gaps in coverage by previous studies. Gaps in previous studies were geographic and analytical. Earlier investigations by the USGS (Wirt and Hjalmarson, 2000), and Knauth and Greenbie (1997, Arizona State University) focused on the Big and Little Chino basin-fill aquifers and major springs in the upper Verde River. Few samples had been collected from the carbonate aquifer north of Big Chino Valley and the upper Verde River, particularly in the area surrounding Big Black Mesa. Also, relatively few samples had been collected from springs and tributaries in mountain-front recharge areas such as the Bradshaw, Santa Maria, and Juniper Mountains. Knauth and Greenbie (1997) measured stable isotopes but did not analyze for major ions, trace elements, tritium, or carbon isotopes. In addition, earlier studies by the USGS did not routinely include several trace elements of interest in this study, notably boron, lithium, and arsenic.

Sampling sites, ranging from upland springs to lowland points of ground-water discharge, are grouped on figure E1, using a color and symbol scheme that is followed in subsequent figures. Strategy for sample-site selection and how samples were assigned to groups for the purpose of interpretation is explained in the following section.

## Sampling Strategy

In order to characterize the water chemistry of major aquifers and springs discharging to the upper Verde River, ground-water samples were grouped by major aquifer or by altitude and geographic location (fig. E1). Major sample

groups include (a) the Big Chino basin-fill aquifer, (b) the Little Chino basin-fill aquifer, (c) the carbonate aquifer north of Big Chino Valley and the upper Verde River, (d) high-altitude areas west and south of Big Chino Valley, and (e) upper Verde River springs. These groups correspond with the hydrogeologic framework presented in Chapter D (this volume). Basin-fill aquifer samples typically include well samples and low-altitude springs near the outlets of the basins. Carbonate aquifer samples include high- and low-altitude springs and deep wells located north of the upper Verde River and Big Chino Valley. The high-altitude sample group includes shallow well and spring samples in probable recharge areas near the Bradshaw, Santa Maria, and Juniper Mountains where precipitation and runoff are the greatest within the study area. Samples from upper Verde River springs comprise their own sample group.

An important consideration was how to select samples that best represent each aquifer. In stream sampling, a standard procedure is to collect a horizontal and vertical composite of streamflow, representing a flow-weighted composite. In ground-water sampling, it is nearly impossible to collect a flow-weighted composite representing the cross-sectional width, depth, and average flow rate of the aquifer. Each well represents a point sample; or at best, a vertical composite that often does not fully penetrate the thickness of the aquifer. In addition, the problem of representatively sampling an aquifer is different for an alluvial aquifer versus a fractured rock aquifer. For these reasons, it was not possible to collect a volumetric composite at different points within each aquifer along major flowpaths. A large spring discharging from the downgradient end of an aquifer could, however, be considered a volumetric composite—as long as no substantial mixing with an adjacent aquifer has occurred upgradient from the spring.

In this study, low-altitude springs near topographical basin outlets were considered representative of outflow from the upgradient aquifer. For example, Del Rio Springs and Lower Granite Spring samples were grouped as part of the Little Chino basin-fill aquifer, and samples from King Spring, Mormon Pocket spring, and Summers Spring in Sycamore Canyon were considered part of the Mississippian-Devonian (M-D) sequence in the carbonate aquifer. In contrast, although upper Verde River springs is the largest low-altitude spring downgradient from Big Chino Valley, the springs could not be grouped as part of Big Chino basin-fill aquifer sample group because a major objective of this study was to test whether a smaller amount of mixing with the carbonate aquifer occurs prior to discharge to the upper Verde River. Thus the upper Verde River spring samples were grouped separately from Big Chino basin-fill aquifer samples. For the same reason, Stillman Lake samples initially could not be grouped with any aquifer, although the lake was subsequently interpreted to have a Little Chino source on the basis of several lines of geochemical evidence that will be presented later in this chapter.

Springs and wells north of Big Chino Valley and the upper Verde River—from Partridge Creek on the west to Sycamore Canyon on the east—were sampled to represent



the regional carbonate aquifer. In this region, there are so few wells and springs in the carbonate aquifer that nearly all available sites were sampled. There are no wells on Big Black Mesa, but four springs were sampled around its perimeter at elevations greater than 4,500 ft. Three wells and three springs were sampled between Big Black Mesa and Sycamore Canyon. Most of the carbonate aquifer samples are from the Martin Formation or overlying Redwall Limestone, which have been grouped as part of the M-D sequence of the carbonate aquifer. North of Paulden, four wells produce from the Devonian-Cambrina (D-C) zone of the carbonate aquifer beneath the Big Chino basin-fill aquifer (Chapter D, this volume). As results will show, these four samples have distinct water-quality characteristics related to differences in the geology and have been interpreted as a subgroup of the carbonate aquifer. Throughout this report, the two stratigraphic intervals are referred to as the D-C zone and the M-D sequence of the carbonate aquifer.

High-altitude springs and major tributary inflows to the Big Chino and Williamson Valley basin-fill aquifer include perennial (or spring-fed) reaches in lower Williamson Valley Wash and Mint Wash, shallow wells in the Williamson Valley and Walnut Creek watersheds, and several high-altitude springs at elevations greater than 4,500 ft in the Bradshaw, Santa Maria, and Juniper Mountains. In general, these high-altitude samples have small catchment areas. An exception is the perennial reach of lower Williamson Valley Wash, which occupies a position intermediate to high-altitude and low-altitude springs at 4,500 to 4,450 ft in elevation. The reach is downgradient of a large subbasin composed of alluvium and buried volcanic rocks, and has been interpreted as a representative composite of high-altitude recharge to Williamson Valley. Thus, samples along Williamson Valley Wash were included in the high-altitude sample group, but also could have been included as a tributary of the Big Chino basin-fill aquifer. Big Chino basin-fill wells were selected along the longitudinal valley axis between high-altitude recharge areas and the upper Verde River.

Lastly, an attempt was made to sample springs emerging from a variety of rock types. Springs in the Bradshaw and Santa Maria Mountains generally are in contact with Proterozoic granites and gneisses. Springs in the Juniper Mountains and Big Black Mesa emerge from Paleozoic carbonate rocks or Tertiary basalt flows. Perennial segments of major tributaries, such as lower Williamson Valley Wash and Walnut Creek, emerge from stream alluvium that is a composite of upgradient rock types.

Sources of alluvium in Big Chino Valley include Proterozoic igneous or metamorphic rock from the Bradshaw and Santa Maria Mountains, carbonate rock from the Juniper Mountains and Big Black Mesa, and Tertiary volcanic rocks in the basin-fill deposits, Sullivan Buttes, and surrounding upland areas. Basin-fill deposits in Little Chino Valley include most of the same rock types found in Big Chino Valley, although in somewhat different proportions. Little Chino basin-fill deposits contain a much higher fraction of volcanic extrusives, particularly latite-andesite (Chapter D, this volume). The source of alluvium in Little Chino Valley is predominantly

Proterozoic igneous or metamorphic rock from the Bradshaw Mountains and Granite Dells and Tertiary volcanic rock from Sullivan Buttes. Sediment in the northeastern part of the basin originating from Paleozoic rock in the Black Hills contains a large fraction of carbonate material. Variations in the concentrations of solutes in the basin-fill aquifers can sometimes be explained by association with certain rock types. In such instances, it generally is easier to discuss spatial variability of a few individual samples within the group, rather than to add a new subgroup or classification.

## Field Methods

Well and spring discharges were monitored at least 20 minutes prior to sample collection to allow stabilization of water temperature, specific conductance, pH, and dissolved oxygen. Well samples were collected after at least three well volumes had been purged or after field measurements had stabilized, or both—as prescribed by USGS standard sampling methods (Wilde and others, 1999). Livestock and irrigation wells typically were sampled after running a generator-operated pump overnight (12 hours or longer), in cooperation with the rancher. Windmills were sampled from outlet pipes following sufficiently windy conditions, that is if it was observed that the blades were turning and the stock tank was overflowing. No well samples were collected from stagnant stock tanks, because substantial evaporation could have occurred.

Small diffuse springs and spring-fed pools of water were problematic to sample for a variety of reasons. Springs discharging to a gaining stream typically emerge through the streambed and mix with streamwater. This makes it difficult to sample the inflow directly or to get a flow-weighted composite of diffuse inflows through a gaining reach. Most of the inflow to upper Verde River springs occurs through the streambed. The eight samples collected June 17-18, 2000 (Appendix A), each represent a discrete inflow that had not yet entered or mixed with the Verde River. Thus, averaged values for the group of samples cannot be considered a true volumetric composite. Moreover, if a spring-fed pond is large and stagnant or slow-moving (such as Stillman Lake or King Spring) then it often was difficult to identify the point of ground-water inflow and the best sampling location. In these cases, evaporation and chemical reactions with atmosphere may affect the water chemistry. Spring sampling locations were selected by looking for sites with clear water (not cloudy), visible current, and relatively low dissolved oxygen and water temperature values. In a few instances, springs appeared currentless or stagnant (notably King Spring, Stillman Lake, an unnamed spring in Tucker Canyon, and Meath Spring) and it was not always possible to find field evidence for ground-water inflow. Consequently these spring data were interpreted with the knowledge that evaporation could have occurred prior to sampling. In addition, water chemistry of some of these high-altitude springs appears to vary seasonally. An understanding of field-sampling conditions was an important consideration in the interpretation of the stable-isotope results.

## Analytical Methods

Separate aliquots of ground-water samples were analyzed for major and trace ions,  $^{18}\text{O}$ ,  $^2\text{H}$ ,  $^3\text{H}$ ,  $^{13}\text{C}$ , and  $^{14}\text{C}$ . Aliquots for cation analyses were filtered in the field using a cellulose-nitrate 0.45-micron pore-size filter and acidified using ultrapure nitric acid. Aliquots for anion analyses were filtered with no acidification. On rare occasions that spring water was visibly cloudy, isotope samples were filtered. Isotope samples were always unacidified and usually unfiltered. Alkalinity was measured in the field by incremental titration with 1.6N  $\text{H}_2\text{SO}_4$  (Wilde and others, 1999).

Major- and trace-element concentrations were measured at the USGS Mineral Resources Program laboratory in Denver, Colorado. Major elements were determined by inductively coupled plasma-atomic emission spectrometry (ICP-AES; Briggs and Fey, 1996) and by inductively coupled plasma-mass spectrometry (ICP-MS; Lamothe and others, 1999). Concentrations of chloride, bromide, and fluoride were determined by ion chromatography (d'Angelo and Ficklin, 1996). Analytical detection limits by laboratories used in this study are reported in Lamothe and others (1999) and d'Angelo and Ficklin (1996). Analytical results for major and trace-element chemistry for this and other USGS Verde River watershed studies are reported in Appendix A, grouped by major aquifer or geographical region.

Samples for  $^{18}\text{O}$ ,  $^2\text{H}$ ,  $^{13}\text{C}$ ,  $^{14}\text{C}$ , and  $^3\text{H}$  were analyzed by the Laboratory of Isotope Geochemistry at the University of Arizona in Tucson, Arizona. Analyses for stable isotopes of oxygen and hydrogen were performed by mass spectrometer (Craig, 1957; Coleman and others, 1982; Gehre and others, 1996). Isotopic data, grouped by aquifer or geographical region, are reported in Appendix B.

Samples for  $^{14}\text{C}$  analysis were collected in 50-liter plastic carboys with minimal headspace and kept indoors to minimize temperature changes and to avoid exposure to direct sunlight. It usually was impractical to filter large volumes of water in the field; but if the water had obvious cloudiness from suspended material, it was filtered with a 0.45-micron pore-sized filter capsule. The carboys were transported to the University of Arizona (UA) Laboratory of Isotope Geochemistry within 72 hours of collection. At the UA laboratory, dissolved inorganic carbon was separated from the large volume of water by precipitation as barium or strontium carbonate ( $\text{BaCO}_3$ , or  $\text{SrCO}_3$ , respectively). The  $^3\text{H}$ ,  $^{13}\text{C}$ , and  $^{14}\text{C}$  activities were determined by liquid scintillation counting (Polach and others, 1973; , 1996). In several instances where site access for large sample volumes was poor, 1-liter samples were submitted for  $^{14}\text{C}$  analysis by accelerator mass spectrometry (AMS) at the Arizona AMS Laboratory at the University of Arizona, Tucson ([http://www.physics.arizona.edu/ams/education/ams\\_principle.htm](http://www.physics.arizona.edu/ams/education/ams_principle.htm)). Accelerator mass spectrometry costs about twice as much as liquid scintillation, but requires a substantially smaller volume of precipitate and has a smaller uncertainty of < 0.3 percent modern carbon (pmc).

The reported analytical precision for tritium generally was between 0.6 and 0.9 tritium units (TU) with a detection limit of about 0.5 TU, depending on the length of counting and the level of enrichment. Analytical detection limits varied from 0.4 to 1.2 TU, depending upon the counting time and activity of each sample. The analytical uncertainty for  $^{14}\text{C}$  was reported as < 0.8 pmc for liquid scintillation (Christopher J. Eastoe, written commun., 2003).

## Isotope Characterization and Apparent Age-Dating Techniques

The following is an overview of the stable-isotope and radioactive-isotope techniques used by this study. Stable isotopes were used to identify sources of water, to estimate ground-water quality changes along a flowpath, to determine the amount of mixing (if any), and to identify water that has undergone evaporation since precipitation in the source area.

Radioactive isotopes were used to indicate the amount of time that ground water has been isolated from the atmosphere. Abundances of radioactive isotopes are expressed as activities because counting methods measure energy emissions from a given volume of sample, rather than the concentration of an individual isotope. The activity of a radioactive nuclide is related to the number of atoms, its decay constant, and the counting efficiency of the radiation detector.

## Hydrogen and Oxygen Stable Isotopes

The isotopic composition of the hydrogen ( $^1\text{H}$  and  $^2\text{H}$ ) and oxygen ( $^{16}\text{O}$  and  $^{18}\text{O}$ ) in the water molecules of the ground water and surface water is used in hydrologic studies to determine sources of water, to trace water along a flowpath, and to identify water that has undergone evaporation since precipitation in the source area (Coplen, 1993; Coplen and others, 2000). These isotopes are particularly useful in tracing ground-water flowpaths, because they are part of the water molecule and can be assumed to behave conservatively once the water has reached the saturated zone and no longer has contact with the atmosphere. Evaporation and condensation of atmospheric precipitation and moisture in the unsaturated zone are the most significant physical processes that affect the proportions of these isotopes.

Isotopes are atoms of the same element that differ in mass because of a difference in the number of neutrons in the nucleus (Fritz and Fontes, 1980). For example, deuterium ( $^2\text{H}$ ) is hydrogen with one proton and one neutron in the nucleus and is distinguished from hydrogen ( $^1\text{H}$ ) that has one proton and no neutrons in the nucleus. Stable-isotope ratios are expressed in per mil units, or parts per thousand (‰), to represent the deviation of the isotope ratio to a reference standard using delta notation ( $\delta$ ), according to equation 1:

$$\delta = \left( \frac{R_x}{R_{\text{std}}} - 1 \right) 1,000 \quad (1)$$

where

$R_x$  = ratio of isotopes in the sample, and  
 $R_{std}$  = ratio of isotopes in the standard.

R is the measured isotopic ratio. Per mil values are presented relative to a standardized reference compound, which is different for different isotopes. In this report the standardized reference compound used is Vienna Standard Mean Ocean Water (SMOW) for hydrogen ( $\delta^2\text{H}$ ) and oxygen ( $\delta^{18}\text{O}$ ) (Coplen, 1994). The delta symbol is followed by the chemical symbol for the heavier isotope of the isotope pair (for instance  $\delta^{18}\text{O}$ , because  $^{18}\text{O}$  is heavier than  $^{16}\text{O}$ ). Larger (or less negative) values show the sample to be enriched in the heavy isotope species relative to the standard, and smaller (or more negative) values show the sample to be depleted in the heavy isotope species relative to the standard.

Isotopic variations in  $\delta^2\text{H}$  and  $\delta^{18}\text{O}$  usually are covariant because they are part of the water molecule. The vapor pressure of water containing the lighter isotopes of hydrogen and oxygen ( $^1\text{H}$  and  $^{16}\text{O}$ ) is greater than that of water containing the heavier isotopes, deuterium, and oxygen-18 ( $^2\text{H}$  and  $^{18}\text{O}$ ). Therefore,  $^1\text{H}$  and  $^{16}\text{O}$  evaporate more readily than  $^2\text{H}$  and  $^{18}\text{O}$ . Atmospheric water vapor becomes progressively depleted in the heavier isotopes as the vapor travels from near the equator toward the poles, from the coast inland, or from lower to higher altitudes. In general, the isotopic composition of precipitation varies globally according to the World Meteoric Water Line (WMWL) (Craig, 1961), computed by equation 2:

$$\delta^2\text{H (per mil)} = 8 \delta^{18}\text{O (per mil)} \pm 10 \quad (2)$$

Equation 2 shows that the isotopic composition of globally averaged precipitation typically varies with a slope of 8 on plots of  $\delta^{18}\text{O}$  at ‰. The intercept, known as the deuterium excess, has been observed to vary widely depending on local climatic conditions (Dansgaard, 1964). During the kinetic fractionation effect of evaporation, the isotopic composition of residual water is shifted toward greater enrichment of  $^2\text{H}$  and  $^{18}\text{O}$  as a function of temperature, humidity, salt concentration, and other factors (Coplen, 1993). A slope between three and less than eight is typical of water that has undergone substantial evaporation (Ingraham, 1998, p.93; Coplen, 1993, p. 235). In Arizona, significant variations in the  $^2\text{H}$  and  $^{18}\text{O}$  of precipitation and subsequent runoff are caused by (1) seasonal variability between winter storms and summer monsoons, (2) local differences in altitude, and (3) evapotranspiration of surface-water runoff prior to direct recharge (Kalin, 1994; Van Metre and others, 1997, p. 29-30; and Wright, 2001). The  $\delta^2\text{H}$  and  $\delta^{18}\text{O}$  contents of a ground-water sample are composites of prevailing climate conditions in the recharge area. So far as recharge and discharge conditions are averaged over the long-term, stable-isotope ratios in ground water discharging near the distal end of the aquifer (in the absence of evaporation) are expected to remain constant through time.

## Tritium

Tritium ( $^3\text{H}$ ) has a half-life of 12.42 years (Lucas and Unterweger, 2000) and is produced naturally in the atmosphere by cosmic-ray bombardment of nitrogen and oxygen in the atmosphere (International Atomic Energy Agency, 1994). From 1952 to 1969, large amounts of tritium were released into the atmosphere by the testing of thermonuclear weapons. The average tritium activity for Arizona precipitation during the period 1962–1965 (International Atomic Energy Agency, 1994) was 1,140 tritium units [one tritium unit (TU) = one  $^3\text{H}$  atom per  $10^{18}$  H atoms]. Since the end of above-ground testing in 1963, the tritium activity in precipitation has decreased as a consequence of radioactive decay and atmospheric fallout. Background levels of tritium in southern Arizona have ranged from about 5 to 10 TU since 1994 (C. J. Eastoe, oral commun., 2004). For the timeframe of this study, water with detectable tritium probably has been recharged since 1953 or else has mixed with a fraction of water that is post-1953. Tritium in ground water recharged before 1953 has now decayed to an activity that is below a detection limit of 0.4–0.7 TU. Water exceeding modern background levels of 5 to 10 TU has been in equilibrium with the atmosphere since 1953 (Ingraham, 1998) and before 1994 (C. J. Eastoe, oral commun., 2004). A tritium activity below 5 TU is ambiguous in that some of the ground water could have recharged since 1953 and mixed with predominantly older water. Because of decreasing levels of tritium in modern precipitation and uncertainties due to possible mixing, in this study, tritium was not used to date ground water precisely. Tritium activities primarily are used to indicate areas where recent recharge may be occurring and to assist with the interpretation of  $^{14}\text{C}$  results.

## Carbon-13 and -14

Carbon has two stable isotopes ( $^{12}\text{C}$  and  $^{13}\text{C}$ ) and one radioactive isotope ( $^{14}\text{C}$ ). Carbon-14 has a half-life of 5,730 years, making it a useful dating tool for ground water that is thousands of years old (Fritz and Fontes, 1980). Carbon-14 undergoes radioactive decay to  $^{14}\text{N}$  so that once isolated from the atmosphere, the amount of  $^{14}\text{C}$  decreases in direct relation to its half-life. Like tritium,  $^{14}\text{C}$  is produced in the upper atmosphere by interaction of cosmic rays, and also was introduced in large amounts by nuclear weapons testing. Inorganic carbon enters the ground water via recharge of precipitation, dissolution of  $\text{CO}_2$  in the unsaturated zone, and dissolution of carbonate minerals. Dissolved bomb-related  $^{14}\text{C}$  may mix with older water, causing ages to appear younger if not corrected. The initial activity of  $^{14}\text{C}$  and the abundance nonradioactive carbon ( $\delta^{13}\text{C}$ ) in the recharge area, and at a downgradient point in the flow system, must be known or estimated to date the carbon and estimate ground-water ages.

Carbon-13 in ground water provides insight into sources of carbon and carbonate reactions in the flow system. Also,  $\delta^{13}\text{C}$  data are used to adjust ground-water ages determined by modeling of  $^{14}\text{C}$  data. Carbon isotope ratios ( $^{13}\text{C}/^{12}\text{C}$  values, or  $\delta^{13}\text{C}$ )

reflect the conditions of the unsaturated zone and the type of substrate through which the water has flowed. The range of  $\delta^{13}\text{C}$  in ground water is largely determined by the  $\delta^{13}\text{C}$  of soil gas and reactions of carbonate minerals in the aquifer (Bullen and Kendall, 1998). Oxidation of organic matter and plant respiration in the soil zone introduces relatively light carbon. Dissolution of carbonate rocks introduces relatively heavy carbon. The  $\delta^{13}\text{C}$  is measured against a standard, which is a marine fossil belemnite of the Cretaceous Peedee Formation in South Carolina. The ratio of dissolved carbonate species in the ocean (and most marine carbonate rocks) is typically about 0‰.

The primary source of  $\delta^{13}\text{C}$  in ground water is from  $\text{CO}_2$  in the soil atmosphere of the recharge zone (Bullen and Kendall, 1998). Soil gas  $\delta^{13}\text{C}$  results from atmospherically derived ( $\delta^{13}\text{C} = -7‰$ ) and microbially respired  $\text{CO}_2$ . The contribution of carbon as dissolved inorganic carbon from precipitation is negligible for most catchment systems (Bullen and Kendall, 1998). Few  $\delta^{13}\text{C}$  soil gas values for arid areas have been reported. A mean value of  $-15.12 \pm 2.88‰$  for five samples near Tucson, Arizona was determined by Wallick (1973, p. 122). Also,  $\delta^{13}\text{C}$  of  $\text{CO}_2$  in desert soil near Tucson averaged  $-20‰$  (Parada, 1981). Partial pressure of  $\text{CO}_2$  ( $P_{\text{CO}_2}$ ) values reported in that study ranged from 0.001 to 0.05 atmospheres. Values of  $-15$  to  $-19‰$  have been measured for the soil gas of arid west Texas (Pearson and Hanshaw, 1970). Soil-gas samples collected from the Dripping Springs basin in central Arizona had a typical value of about  $-18.0‰$   $\delta^{13}\text{C}$  (Pierre Glynn, unpub. data, oral commun., 2005).

The  $\delta^{13}\text{C}$  of carbonate rock may vary slightly. Marine carbonate rocks normally have the same  $\delta^{13}\text{C}$  value as dissolved ocean carbonate, but ratios can vary substantially within a single formation. For example, a  $6.28‰$  range in the  $\delta^{13}\text{C}$  of the Mooney Falls Member of the Redwall Limestone was reported for 36 rock samples from three sites in the Grand Canyon and six sites along the Verde River between Chino Valley and Perkinsville (Muller and Mayo, 1986). The overall average for the nearly pure limestone samples was  $-1.85‰$  and ranged from a maximum of  $\pm 2.44‰$  and a minimum of  $-3.84‰$ . The  $\delta^{13}\text{C}$  of the Devonian Martin Limestone is unknown, but it is reasonable to assume that it should be similar to the overlying Redwall Limestone of Mississippian age. In the headwaters area, the main mineral carbon sources include limestone and dolomite, as well as secondary calcite deposited as pedogenic carbonate in unconsolidated sediments or as fracture fillings within volcanic rocks.

## Water-Quality Sampling Results

For this study, 64 water samples were analyzed for concentrations of major ions and selected metals, and ratios of stable isotopes of oxygen ( $\delta^{18}\text{O}$ ), hydrogen ( $^2\text{H}$ , or  $\delta\text{D}$ ), and carbon ( $^{13}\text{C}$ ); and for tritium ( $^3\text{H}$ ). Fourteen samples were analyzed for carbon-14 ( $^{14}\text{C}$ ). These new data are interpreted

here in combination with earlier USGS data compiled by Wirt and Hjalmanson (2000) and the  $\delta^{18}\text{O}$  and  $\delta\text{D}$  data of Knauth and Greenie (1997).

From 1986 to present, a total of 91 water samples have been analyzed for concentrations of major ions in the upper Verde River watershed by the USGS (Appendix A). About 90 percent of these samples were analyzed by atomic emission spectroscopy for trace elements that routinely occur at the parts per million level. About 60 percent of the sample group was analyzed using mass spectroscopy, which has lower detection limitations for trace elements occurring at parts per billion levels. Consequently, there are fewer analyses available for As than for B and Li. In addition, a total of 124 well and spring samples were analyzed for stable isotopes (Appendix B). Sample results in Appendices A and B have been grouped according to the strategy outlined in the section on "Sampling Strategy" and outlined in the explanation of figure E1.

Results of major-ion, trace-element, stable-isotope, tritium, and carbon isotope data are presented sequentially in this section. In the end of the chapter, these multiple lines of evidence will be integrated by looking at variations in the geochemistry along selected ground-water flowpaths from upper Big Chino Valley to Paulden through the basin-fill aquifer, and from Paulden to upper Verde River springs through the carbonate aquifer.

## Major-Ion Chemistry

Trilinear plots (Piper, 1944) are used to show relative proportions of major cations and anions, reported in percent milliequivalents per liter (% meq/l). The two trilinear plots for samples from the major aquifer groups and major springs discharging to the upper Verde River (fig. E2) show predominantly calcium-bicarbonate waters with variable proportions of magnesium and sodium. In general, calcium (Ca) is the predominant cation, and bicarbonate ( $\text{HCO}_3^-$ ) is the predominant anion. Sample groups having a relatively large degree of visual scatter are plotted on figure E2A; groups that cluster more tightly are plotted on figure E2B.

For all of the basin-fill and high-altitude spring samples (fig. E2A); the major cations are Ca (30 to 70% meq/l) and magnesium (Mg) (15 to 65% meq/l), with relatively small amounts of sodium (Na) and potassium (K) (5 to 30 % meq/l). The variation in proportions of major ions in the Big and Little basin-fill aquifers and the high-altitude springs of the Bradshaw, Santa Maria, and Juniper Mountains is attributed to the ground water having contact with a wide variety of rock types; hence, a more variable chemistry. Based on of the range of major-ion proportions, it is not possible to distinguish the Big Chino basin-fill aquifer from the Little Chino basin-fill aquifer, nor is it possible to distinguish basin-fill aquifer samples from high-altitude springs and tributaries, although some of Big Chino basin-fill samples have slightly higher concentrations of chloride (Cl).

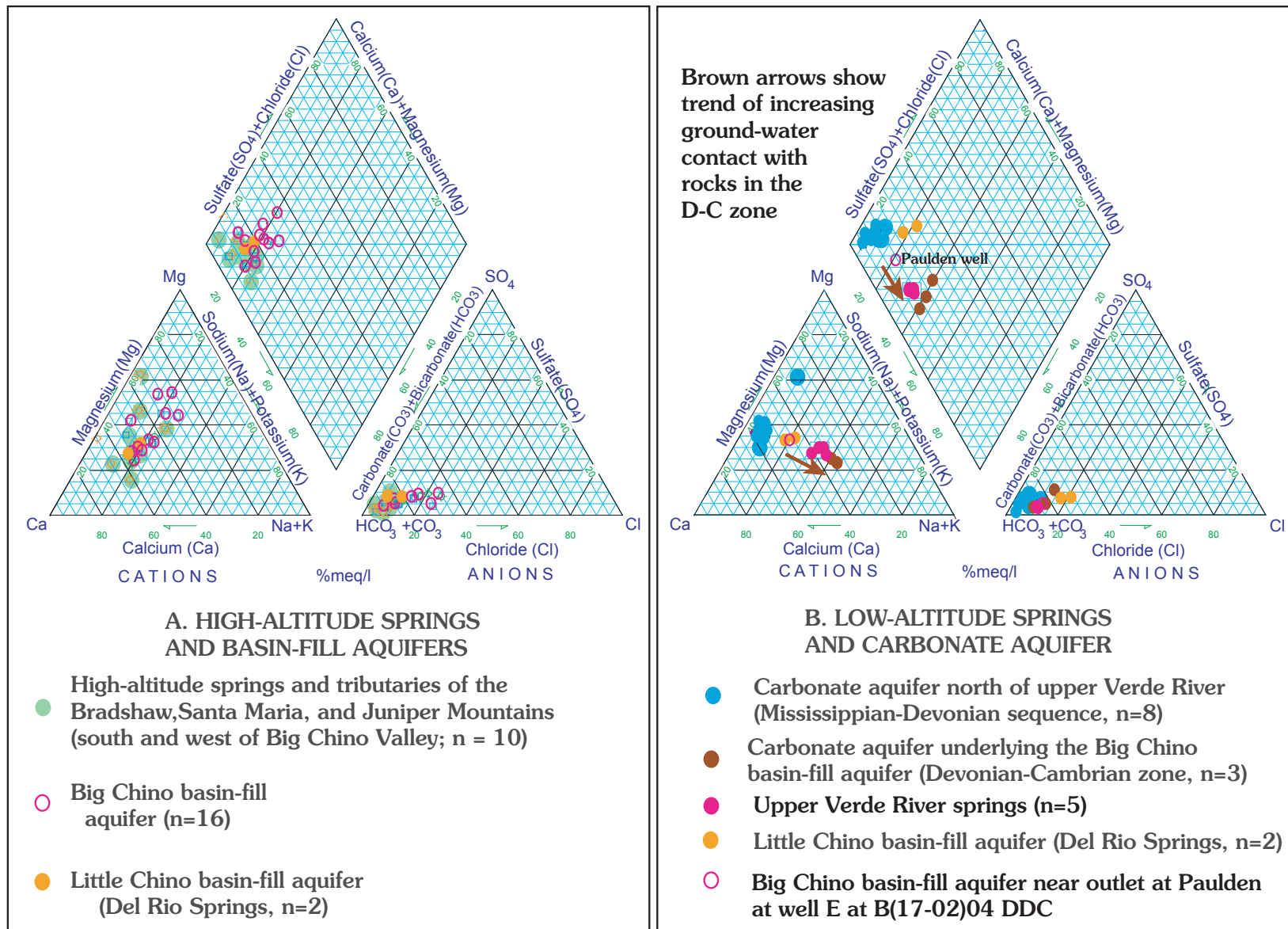


**Figure E2.** Trilinear diagrams (Piper, 1944) showing major-ion proportions in percent milliequivalents per liter (%meq/l). Plot A shows proportions for high-altitude springs and basin-fill aquifer; plot B shows proportions for low-altitude springs and the carbonate aquifer. Samples plotted have cation-anion balances within 5 percent. Data are reported in Appendix A; n, number of samples.

On figure E2B, the tighter clustering for upper Verde River springs is attributed to repeated sampling of a single low-altitude spring location, or in the case of the carbonate aquifer, to the two carbonate aquifer subgroups having little spatial variation in major-ion chemistry. Samples from the M-D sequence of the carbonate aquifer (blue circles, fig. E2B); plot in a fairly tight cluster on the left side of the diamond-shaped graph. The major cation is Ca (55 to 60% meq/l), followed by Mg (35 to 45% meq/l), with less than 10% meq/l of Na and K.

In contrast, the D-C zone of the carbonate aquifer underlying the Big Chino basin-fill aquifer (brown circles, fig. E2B) has distinct major-ion proportions, plotting to the lower right of all other sample groups. The major cation for this sample group is Na, rather than Ca. These samples have among the highest concentrations of Na, Cl, sulfate ( $\text{SO}_4$ ), and silica (Si) in the study area, as shown by the brown box- and whisker plot of major-element concentrations (fig. E3A). The samples were collected from four wells >285 ft in depth northeast of Paulden and east of Wineglass Ranch (B-18-02, sections 21, 27 and 28; see Appendix A for well depths). Each well penetrates a thin veneer of basin-fill sediment into the underlying Paleozoic rocks (DeWitt and others, this volume) and is interpreted as producing from the water-bearing zone near the base of the Martin Formation or top of the Bright Angel Shale.

Like the four wells in the D-C zone, ground water from upper Verde River springs also discharges near the base of the Martin Formation. Water from upper Verde River springs has nearly equal major-ion proportions of Ca, Mg, and Na, which plot intermediate to those for the Big Chino basin-fill aquifer and the D-C zone. A brown arrow shows the evolution of increasing water-rock interaction, from the outlet of Big Chino basin-fill aquifer at well B(17-02)04 DDC toward samples from upper Verde River springs and the D-C zone. The change in major-ion proportions primarily results from an increase in Na, Cl,  $\text{SO}_4$ , and Si concentrations as opposed to a small increase in the Ca concentration (fig. E3A). The range of Ca values for upper Verde River springs compares more closely with the range of Ca values for the Big Chino basin-fill aquifer than with the range for the D-C zone. Ground water of the D-C zone is moderately mineralized and characterized by consistently higher concentrations of Na, K, Cl,  $\text{SO}_4$ , and Si, than all other sample groups (figs. E2B and E3A). Intermediate concentrations of these elements in ground water discharging to upper Verde River springs may result either from water-rock interaction of Big Chino basin-fill ground water as it travels through the D-C zone or from mixing of the Big Chino basin-fill aquifer with ground water from the D-C zone. Both of these hypotheses and the geology of the outlet flowpath are addressed next.

## Trace-element Chemistry

Trace elements are useful indicators of water-rock reactions. In this section, box- and whisker plots (SAS Institute, 1998) were used to visually summarize the differences in

selected major-ion and trace-element concentrations for each of the sample groups of interest. The elements shown on fig. E3 (with the exception of Ca) were selected to best illustrate the differences among sample groups. Calcium concentrations are shown to provide a frame of reference, because with few exceptions it is the major cation. The majority of analytes which were not selected typically have overlapping ranges in concentrations that vary little among the different groups (much like Ca). The box- and whisker plots show the median and 10th, 25th, 75th, 90th percentiles for each statistical grouping. Outlier values above the 90th and below the 10th percentiles were omitted. In all three plots, the vertical axis has a log scale.

## Marine Shale Origin of Arsenic, Lithium, and Boron

With the exception of samples from upper Verde River springs and the D-C zone, dissolved arsenic (As), boron (B), and lithium (Li) concentrations are relatively low throughout most of the study area (fig. E3B and 5.3C). The source of these elements is of particular interest because they indicate the nature of water-rock interactions along the major ground-water flowpath from the outlet of the Big Chino basin-fill aquifer near Paulden to upper Verde River springs. Perennial flow in the upper Verde River emerges from the D-C zone, near its confluence with Granite Creek. Discharge to upper Verde River springs (river mi 2.3 to 2.9) is from the lower Martin Formation (Devonian), which overlies the the Chino Valley Formation (Devonian?) above the Tapeats Sandstone (Cambrian). Box- and whisker plots of dissolved As, Li, and B for the upper Verde River springs sample group are higher than all other sample groups, with the exception of the four wells penetrating the D-C zone. Well samples from the D-C zone have concentrations of 33–38  $\mu\text{g/L}$  As, 330–460  $\mu\text{g/L}$  B, and 54–86  $\mu\text{g/L}$  Li, compared with those from upper Verde River springs of 17–29  $\mu\text{g/L}$  As, 136–270  $\mu\text{g/L}$  B, and 28–49  $\mu\text{g/L}$  Li (fig. E3B; Appendix A). In addition, As, Li, and B values for the D-C zone correlate positively with Na, K, Cl,  $\text{SO}_4$ , and Si, values (fig. E3A). Shales of marine or lacustrine origin are a possible sedimentary source for all of these elements. Silicate minerals in igneous rocks are a possible source of Na, K, and Si.

The occurrence of elevated As, Li, and B is unusual, because few sedimentary rocks contain this suite of trace elements. The three elements typically are found together in volcanic gases and geothermal water (Hem, 1985; Shaw and Sturchio, 1991); however, there are no known geothermal springs in the study area. In addition, volcanic rocks in the study area contribute relatively low concentrations of these trace elements to water of basin-fill aquifers and do not appear to be a major source. Ground water at Del Rio Springs, for example, has had extensive contact with a variety of volcanic rocks in the Little Chino basin-fill aquifer, yet contains comparatively low concentrations of As, Li, and B. In contrast, ground water discharging to upper Verde River springs has had extensive contact with the D-C zone of the carbonate aquifer.

### Dissolved Major and Trace-Element Concentrations, Verde River Headwaters, Arizona

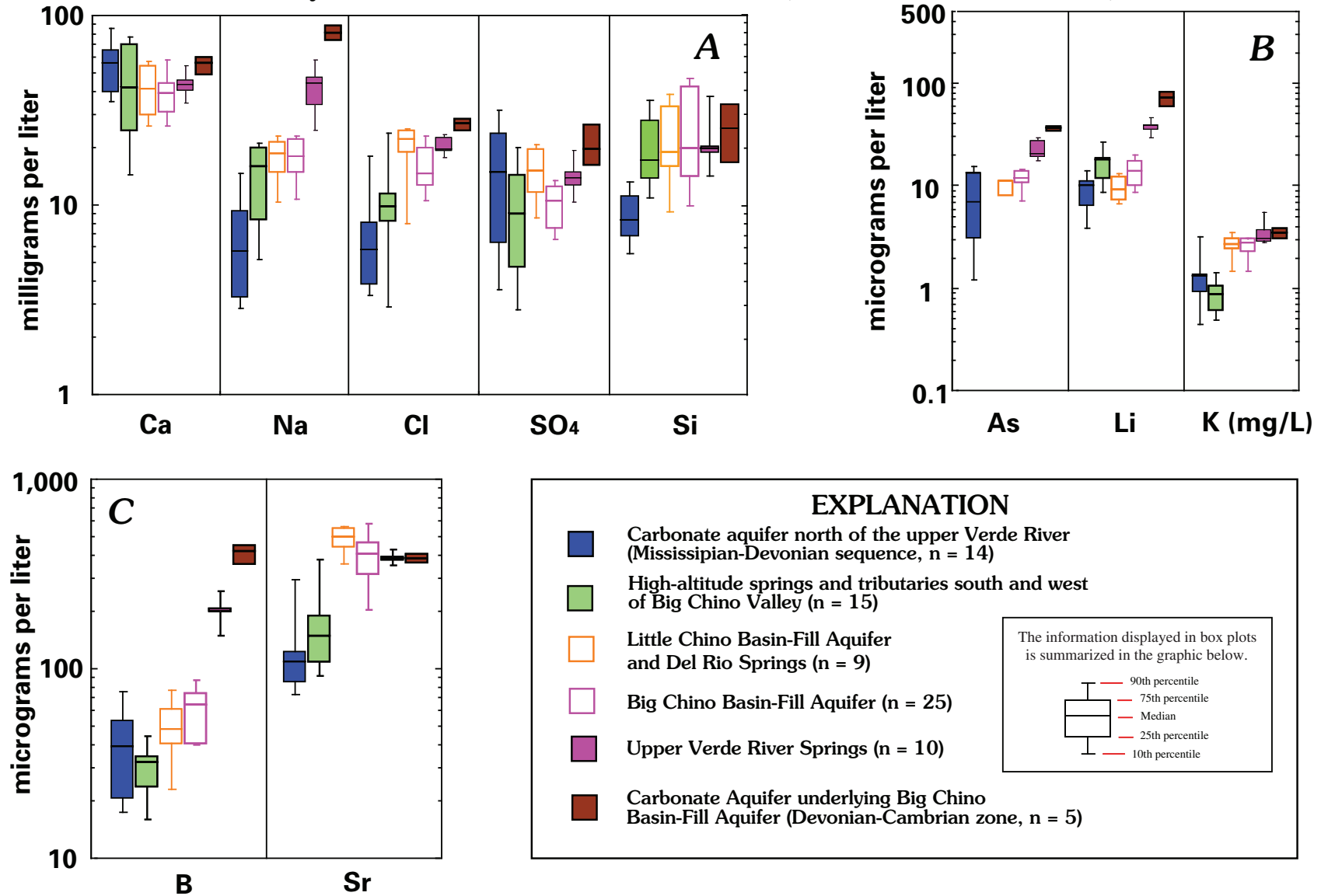


**Figure E3.** Box- and whisker plots (SAS Institute, 1998) of selected major and trace elements characterizing major aquifers and springs, Verde River headwaters, Arizona. Plot A, major element concentrations; Plots B and C, trace-elements concentrations. Order of box- and whisker plots is the same as in explanation; n, number of samples; all data reported in Appendix A. Not all samples were analyzed for all constituents. Outliers above and below the 10th and 90th percentile are not shown.

The Chino Valley Formation, the most likely source of these elements in the D-C zone, is a pebble conglomerate, mudstone, and siltstone unit between the Martin Formation and the Tapeats, probably of Devonian age (Hereford, 1975; Chapter D, this volume). Exposures are found near the mouth of Granite Creek and also along the base of Big Black Mesa east of Partridge Creek (Hereford, 1975). The Chino Valley Formation occupies the same stratigraphic interval and has chemical similarities to the Cambrian Bright Angel Shale (table E1), which crops out farther west in northwestern Big Chino Valley (Krieger, 1967; DeWitt and others, Chapter B, this volume, fig. B1). Potassium concentrations as high as 10.0 weight percent (as  $K_2O$ ) and B concentrations as high as 280 parts per million (ppm) for the Bright Angel Shale (Miesch, unpub. data in Baedeker and others, 1998) suggest that the shale may contain a component of felsic tuff that was deposited in a shallow-water marine setting (Bowie and others, 1966, 1967; Hutcheon and others, 1998). Marine shale formed from K-rich ash is a reasonable source of As, Li, and B. These elements are present in ocean water at concentrations of 4.41 ppm B, 0.17 ppm Li, and 1.45 to 1.75 parts per billion (ppb) As (Emsley, 1991), and would tend to be concentrated by sorption to fine-grained sediment and clay.

Solid-phase concentrations as high as 8.6 weight percent  $K_2O$  in the Chino Valley Formation (Hereford, 1975) also suggest a submarine ash depositional environment similar to that for the Bright Angel Shale. We note a comparative lack of solid-phase potassium in other permeable rocks within the study area (table E1). Elevated concentrations of dissolved As, Li, and B in upper Verde River springs and well samples from the D-C zone north of Paulden suggest contact with a sedimentary unit similar in genesis to the Bright Angel Shale or Chino Valley Formation. Ground-water contact with Paleozoic-age shale would explain elevated concentrations of dissolved As, B, and Li; although solid-phase data for As and Li in Paleozoic shale are lacking.

An alternative hypothesis is that the elevated dissolved As, B, and Li could be derived from the playa deposit in Big Chino Valley. Economic deposits of boron commonly are found in playa deposits as borax (Emsley, 1991), although little is known about As or Li occurrence or behavior in a playa environment. In this scenario, ground water in contact with the playa in the Big Chino basin-fill aquifer travels along the Big Chino Fault zone and through karst of the underlying and adjoining D-C zone. Although plausible, there are no dissolved or solid-phase chemistry data from the playa deposit to directly support or refute this hypothesis. In both scenarios, ground water from the Big Chino basin-fill aquifer travels through the D-C zone to reach upper Verde River springs.

Not all ground water in the carbonate aquifer has had extensive contact with the D-C zone. Waters having among the lowest concentrations of As, B, and Li (fig. E3B) include the M-D sequence of carbonate aquifer and high-altitude springs south and west of Big Chino Valley in contact with a variety of rock types. Arsenic, B, and Li concentrations for the Big Chino basin-fill aquifer group are highest near the

southeastern end of the basin, which could be an indication of upwelling or mixing with deeper circulating ground water from the underlying carbonate aquifer near the outlet of the aquifer. On average, the Big Chino aquifer sample group contains slightly higher concentrations of As, Li, and B than samples from the Little Chino basin-fill aquifer and Del Rio Springs. The highest As, Li, and B concentrations in Little Chino ground water are found near the Granite Creek/Verde River confluence where the Chino Valley Formation is present. In general, elevated As, Li, and B concentrations provide a distinct tracer for ground water that has been in contact with the D-C zone.

## Igneous and Sedimentary Sources of Strontium

Strontium (Sr) in ground water is derived from weathering of rocks undergoing weathering and dissolution in the drainage basin (Benson and Peterman, 1995; Bullen and Kendall, 1998, Bierman and others, 1998). The amount of strontium in ground water is related to the initial Sr content of rock-forming minerals and its chemical availability, which is a function of leaching, dissolution, degree of weathering, and residence time. Strontium is similar in chemistry to the alkaline-earth element calcium and replaces calcium and potassium in silicate and carbonate minerals in minor amounts (Hem, 1985). In any given catchment, Sr may be released at different rates; for example, from carbonates by dissolution, plagioclase by leaching, and clay minerals by ion-exchange processes (Bierman and others, 1998).

High concentrations of Sr are common in brines and evaporates (Hem, 1985), as well as in playa deposits of the western Great Basin (Benson and Peterman, 1995; Lin, 1996). Strontium concentrations probably are elevated in the vicinity of playa deposit near the center of Big Chino Valley, although both water and solid-phase data are lacking. Rocks having the lowest concentrations of Sr are the Paleozoic Redwall Limestone and Martin Formation, with less than 100 ppm. Other Paleozoic units have slightly higher Sr concentrations, but generally are less than 220 ppm. Most Proterozoic rocks are moderately low in Sr, with between 200 and 500 ppm.

With the possible exception of the playa, strontium-rich volcanic rocks are the major source of dissolved Sr in the headwaters study area. Strontium-rich rocks in the study area include Tertiary basalts and lati-andesite, with the Hickey basalt averaging 1,700 ppm (table E1). Two Sr-rich volcanic units are exposed north of Del Rio Springs and the area surrounding Sullivan Lake and the Sullivan Buttes. These are 4.5-Ma basalt flows near Paulden with an average concentration of 660 ppm Sr; and the Sullivan Buttes lati-andesite in northern Little Chino Valley with an average concentration of 960 ppm Sr (table E1). Water samples from Del Rio Springs, Lower Granite Springs, and Stillman Lake are substantially elevated in strontium, having dissolved concentrations ranging from 460 to 620  $\mu\text{g/L}$  (fig. E3C). Dense plugs of Sullivan Buttes lati-andesite that become more abundant in the northern part of the basin are the most likely source of dissolved Sr at



**Table E1.** Chemistry of major rock types exposed in Verde River headwaters region, Arizona. Solid-phase rock data from U.S. Geological Survey PLUTO database, except as noted.

(nd, not determined; <, less than; n, is number of samples)

Map unit	Rock type	Number of samples (n)	weight percent								parts per million					
			Silica as SiO <sub>2</sub>	Aluminum as Al <sub>2</sub> O <sub>3</sub>	Iron as Fe <sub>2</sub> O <sub>3</sub> <sup>5</sup>	Iron as FeO	Magnesium as MgO	Calcium as CaO	Sodium as Na <sub>2</sub> O	Potassium as K <sub>2</sub> O	Manganese as MnO	Carbon Dioxide as CO <sub>2</sub>	Barium	n	Strontium	n
Tby	Younger basalt	47	50	15.7	4.0	7.2	6.7	9.3	3.3	1.3	0.17	0.34	470	8	660	32
Tbo	Older basalt	3	51	14.1	0.0	0.0	6.9	8.5	3.1	1.5	0.14	0.02	540	2	960	3
Thb	Hickey basalt	56	50	14.4	5.3	4.5	7.7	8.6	3.4	1.9	0.14	0.06	1340	45	1700	47
Tla	Sullivan Buttes latite andesite <sup>1</sup>	60	60	14.1	3.5	2.5	4.2	5.4	3.0	4.4	0.08	0.19	1660	54	960	60
Ps	Supai, undivided	3	nd	6.4	1.6	nd	6.7	9.7	0.4	2.4	0.05	nd	270	3	163	3
Mr	Redwall Limestone <sup>2</sup>	21	1	<0.010	0.1	nd	6.0	49.1	<.15	<.02	0.03	44.84	26	18	61	23
Dm	Martin Formation <sup>2</sup>	9	2.8	<0.010	0.4	nd	20.3	29.9	<.15	<.02	0.02	46.10	18	8	74	9
Dcv	Chino Valley Fm <sup>3</sup>	10	39	10.2	2.9	0.6	9.1	12.9	<0.2	5.2	0.05	19	nd	0	nd	0
Cba	Bright Angel Shale <sup>4</sup>	16	53	18.0	5.0	0.7	1.0	0.9	0.3	8.8	0.05	0.36	510	16	219	16
Ct	Tapeats Sandstone	33	73	2.3	0.7	0.1	0.3	1.6	0.1	1.0	0.01	0.15	120	33	119	33
Cm	Muav Formation	32	18	3.2	1.6	1.4	5.3	22.0	0.5	1.8	0.12	nd	360	44	162	44
Yg	1.4-Ga plutons <sup>2</sup>	4	69	13.9	4.1	nd	0.9	2.3	2.7	4.9	0.14	nd	840	4	242	4
Xfg	1.7-Ga felsic plutonic rocks <sup>2</sup>	9	70	14.3	2.7	nd	0.8	1.6	3.3	4.9	0.07	nd	720	7	287	9
Xmg	1.7-Ga mafic plutonic rocks <sup>2</sup>	41	55	15.5	5.0	5.7	5.5	7.7	2.9	1.3	0.15	nd	580	27	497	27
Xfv	1.7-Ga felsic metavolcanic rocks <sup>2</sup>	3	68	13.7	3.0	4.4	1.1	2.2	4.7	1.1	0.07	nd	220	1	244	2
Xmv	1.7-Ga mafic metavolcanic rocks <sup>2</sup>	80	52	15.5	3.1	9.2	4.7	7.4	3.1	0.6	0.19	nd	360	55	294	73

<sup>1</sup>Tyner (1984); Ward (1993)

<sup>2</sup>DeWitt, unpub. Data (2002)

<sup>3</sup>Hereford (1975)

<sup>4</sup>Mean boron concentration for Bright Angel Shale is 180 ppm (n = 23); lithium concentration for one sample is 220 ppm.

<sup>5</sup>Bold value indicates percent total iron expressed as FeTO<sub>3</sub>

Del Rio Springs (460 to 540  $\mu\text{g/L}$ ). Ground water discharging to Stillman Lake and lower Granite Creek has slightly higher dissolved Sr concentrations (540 to 620  $\mu\text{g/L}$ ), which are acquired through contact with fractured volcanic rocks along the flowpath between the Little Chino basin-fill aquifer and the Granite Creek confluence area. In addition to water-rock contact with lati-andesite, Sr concentrations at Stillman Lake and lower Granite Spring could be partly derived from the 4.5-Ma basalt flow exposed at Sullivan Lake.

In general, dissolved Sr concentrations greater than about 350  $\mu\text{g/L}$  probably indicate exposure to Tertiary volcanic rock, although the playa deposit in Big Chino Valley should not be ruled out as a possible source in that location. Direct analytical evidence to support or eliminate a playa source of strontium is not available. No ground water has been sampled directly from the playa deposit, nor are there solid-phase Sr analyses from well cuttings. The maximum concentration of 720  $\mu\text{g/L}$  Sr measured for the study area, however, was collected from a 334-ft well near the buried playa along Big Chino Wash south of Wineglass Ranch (well B-18-03 25cda) (Appendix A). A volcanic source of strontium is unlikely at this location, because the closest buried basalt unit is more than 200 ft below the bottom of the well (DeWitt and others, Chapter B, this volume; fig. B8).

A volcanic source of Sr is more plausible for the second and third highest Sr values in the Big Chino basin-fill aquifer sample group (fig. E3C). A moderately high value of 440  $\mu\text{g/L}$  Sr was measured near the confluence of Williamson Valley Wash with Hitt Wash (fig. E1, well B-16-04 15acd). This occurrence is downgradient from lati-andesite exposed in upper Hitt Wash (Chapter D; fig. D3). A concentration of 360  $\mu\text{g/L}$  Sr from northwestern Big Chino Valley (well B-19-03 30bcb) is downgradient from young basalt flows exposed in Tucker Canyon. The well log intercepts these basalt flows beneath several hundred ft of alluvium. In addition, much of the stream sediment deposited by Big Chino Wash contains basalt clasts from the upper part of the basin. In summary, the maximum Sr concentration for Big Chino Valley might be related to the playa deposit, but most other high concentrations of strontium appear to be related to the occurrence of igneous rocks. Better understanding of trace-element chemistry near the playa is needed.

In the area surrounding Sullivan Lake, which is the northern surface-water outlet for Del Rio Springs, Big Chino basin-fill wells have fairly high concentrations of Sr (between 400 and 620  $\mu\text{g/L}$ ) (Appendix A; B-17-02, sections 2, 4, 9, 10, and 15). In this area, the basin-fill aquifer consists of Sr-rich 4.5 Ma basalt inter-layered with alluvium, although other sources of Sr are possible. This area is also downgradient from the playa deposit, Sullivan Buttes, and alluvial fans predominantly composed of lati-andesite cobbles.

Water samples from upper Verde River springs contain between 346 and 440  $\mu\text{g/L}$  Sr, compared with 70 to 120  $\mu\text{g/L}$  Sr for samples from the carbonate aquifer (M-D sequence), and with 460 to 620  $\mu\text{g/L}$  for the Little Chino basin-fill aquifer (fig. E3C; Appendix A). In comparison, strontium

concentrations for the D-C zone range from 350 to 420  $\mu\text{g/L}$ , closely matching the range measured for upper Verde River springs. The Sr concentration could be related either to the length of the flowpath or the residence time through Sr-rich rocks. Also, the clay-rich shale in the Chino Valley Formation may be more permeable or more easily leached than igneous rocks, in which Sr would be held in the crystalline lattice of feldspar minerals.

Strontium concentrations for upper Verde River springs are indistinguishable from those in the Big Chino basin-fill aquifer near Paulden and from the nearby D-C zone of the carbonate aquifer. The broad range of Sr concentrations shown by the box- and whisker plot for the Big Chino basin-fill aquifer (fig. E3C) is misleading, because it represents a range of values collected from well samples throughout the aquifer, rather than a volumetric composite measured at the aquifer outlet. Some Big Chino ground water is in contact with the 4.5 Ma basalt-filled paleochannel that straddles the aquifer boundary north of Sullivan Lake (Chapter D, this volume, fig. D8), which is an additional likely source of Sr. Because of difficulties in obtaining representative samples, the mean Sr concentration of ground water exiting Big Chino Valley through the carbonate aquifer is not known. Discharge to upper Verde River springs appears to lack extensive water-rock interaction with lati-andesite, which tends to produce Sr concentrations greater than 460  $\mu\text{g/L}$ . Thus, a Little Chino source of ground water is unlikely. Mixing with a substantial fraction of ground water from the carbonate aquifer directly north of the upper Verde River (M-D sequence) also is unlikely based on typical dissolved concentrations of less than 120  $\mu\text{g/L}$ , which would be expected to dilute or lower Sr concentrations. Ground-water contributions from Mississippian and Devonian rocks (M-D sequence) of the carbonate aquifer, if any, would need to first travel through the Devonian-Cambrian contact (D-C zone) and acquire higher concentrations of strontium and trace elements, or be so minor as not to substantially affect the water chemistry. The case for ground-water mixing will be further tested by inverse modeling in Chapter F (Wirt, this volume).

## Isotope Chemistry

### Evaporation and Characterization of Major Aquifers and Springs

Stable isotopes of hydrogen and oxygen in the ground water and surface water of the study area were used to (1) indicate the degree of evaporation, (2) characterize and compare the isotope composition of major aquifers and springs, (3) trace water along flowpaths, and (4) evaluate mixing. From 1986 to 2003, one hundred-thirty seven well and spring samples were collected and analyzed by three different stable-isotope laboratories (USGS in Reston, University of Arizona in Tucson, and Arizona State University in Tempe). Two standard deviation analytical precisions of 0.2‰ for  $\delta^{18}\text{O}$  and 2.0‰ for  $\delta\text{D}$  are assumed for all of data used in this study

**Table E2.** Statistical summary of stable-isotope sample groups by major aquifers, springs, and surrounding upland areas.[ $\delta$ , delta; Std Dev, standard deviation of the mean; ND, not determined; n, number of samples; all isotope values reported in per mil]

Sample Group	$\delta^{18}\text{O}$		$\delta^{18}\text{O}$		$\delta\text{D}$		$\delta\text{D}$		Count (n)
	Mean	Std Dev <sup>3</sup>	Minimum	Maximum	Mean	Std Dev <sup>3</sup>	Minimum	Maximum	
Carbonate Aquifer north of Verde River (Mississippian–Devonian) <sup>1</sup>	–11.5	ND	–12.0	–10.9	–82.1	ND	–85.0	–78.0	8
High–Altitude springs, tributaries, and wells (south and west of Big Chino Valley)	–10.7	0.4	–11.1	–10.0	–75.6	2.1	–79.4	–71.8	12
Big Chino Basin–Fill wells	–9.9	0.3	–10.5	–8.8	–71.5	3.0	–78.0	–65.0	35
Little Chino Basin–Fill wells <sup>2</sup>	–10.0	0.4	–11.2	–8.9	–70.7	3.8	–78.0	–61.0	22
Carbonate Aquifer underlying Big Chino Basin–Fill Aquifer (Devonian–Cambrian zone)	–10.4	ND	–10.7	–10.3	–74.5	ND	–77.0	–74.0	7
upper Verde River springs	–10.3	0.1	–10.4	–10.1	–74.3	0.7	–75.0	–73.2	10

<sup>1</sup>Includes Bean, Gipe, and Bart Hart wells; and Mormon Pocket and Sycamore Canyon springs. King, Meath, and Tucker springs were highly evaporated and not included.<sup>2</sup>Includes Del Rio Springs but not Lower Granite Spring or Stillman Lake.<sup>3</sup>Standard deviations not reported for sample groups < 10. In such instance, a 2-sigma analytical precision of 0.2 per mil for  $\delta^{18}\text{O}$ , and 2.0 per mil for  $\delta\text{D}$  are assumed (Kendall and Caldwell, 1998; p. 75; Christopher J. Eastoe, oral commun., 2003).

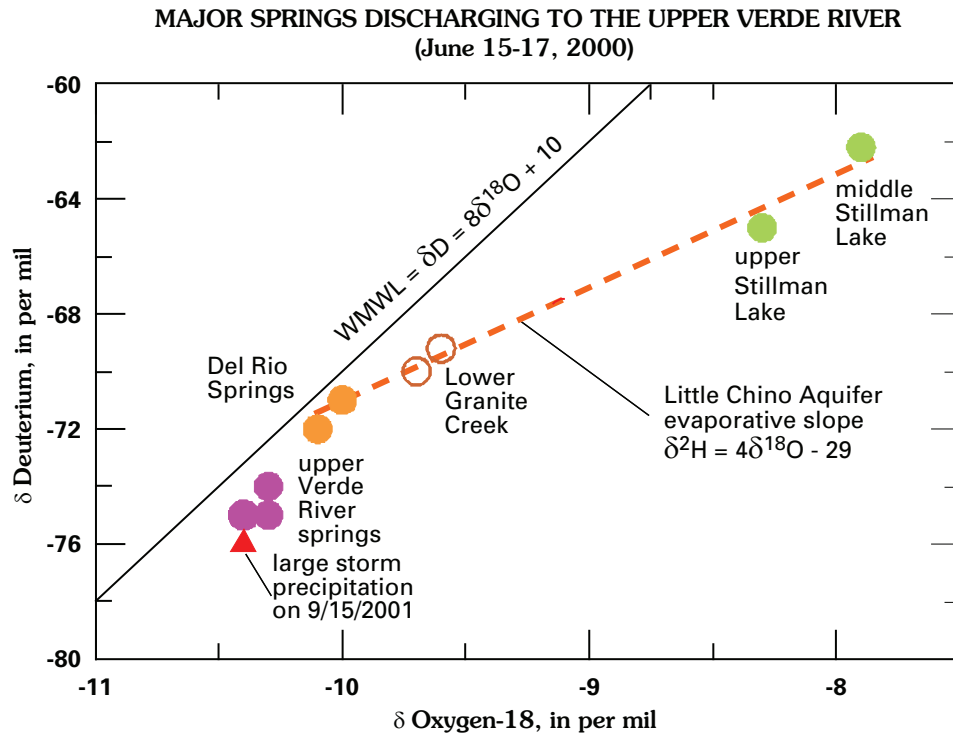


**Figure E4.** Graph showing  $\delta D$  versus  $\delta^{18}O$  for springs contributing to the upper Verde River, including upper Verde River springs, Stillman Lake, Lower Granite Creek, and Del Rio Springs. All spring samples were collected June 15–17, 2000. WMWL = World Meteoric Water Line. Data are reported in Appendix B.

(Kendall and Caldwell, 1998; p. 75; Christopher J. Eastoe, oral commun., 2003).

Variations in  $^2H$  and  $^{18}O$  were evaluated to characterize and to compare the isotope composition of low-altitude springs with ground water near the outlets of Big and Little Chino Valleys (table E2 and fig. E4). Low-altitude spring samples (fig. E4) were collected during the tracer-dilution synoptic study of June 15–17, 2000 (Chapter F, this volume). Thus, the variations in  $\delta^{18}O$  and  $\delta D$  reflect spatial differences, as opposed to time-related differences. In general, the low-altitude spring samples plot below and to the right of the World Meteoric Water Line (WMWL).

Stillman Lake is a water-table lake that infrequently receives runoff overtopping the dam at Sullivan Lake. The lake drains through stream alluvium near the mouth of Granite Creek to the upper Verde River (Chapters A and F, this volume; fig. A15). Unlike Sullivan Lake, which changes greatly in size in response to local runoff (of lack thereof); the water

surface at Stillman Lake stays fairly constant through droughts and immediately following floods. Based on the author's observations over the past decade, the surface of Stillman Lake during low-flow conditions appears to have varied by less than a foot. Because all samples on figure E4 were collected following an extended period of little if any rainfall (U.S. Geological Survey, 1999–2003), it is unlikely that the lake samples are a mixture of ground water and surface-water runoff.

Water in Stillman Lake has a substantial residence time and experiences a considerable amount of evaporation. Samples from Stillman Lake, Granite Creek, and Del Rio Springs plot along a dashed regression line with a slope of 4, indicative of water that has undergone evaporation. Samples with the greatest length of exposure to the atmosphere are progressively enriched in  $^2H$  and  $^{18}O$  along the regression line from Del Rio Springs (least evaporated), to Lower Granite Spring (intermediate), and Stillman Lake (most evaporated). The  $\delta^{18}O$  and  $\delta D$  values for upper Verde River springs ( $n = 6$ ) are substantially

more depleted than the least evaporated samples from Del Rio Springs and appear to be derived from a different aquifer source.

To evaluate whether the Stillman Lake samples are a mixture of residual surface-water runoff from wetter conditions and ground water, local precipitation was collected. During the summer of 2001, roof runoff was collected by a local resident of Chino Valley from several rain storms. A composite of several small thunderstorms from that monsoon season was highly evaporated ( $\delta^{18}\text{O} = -3.3\text{‰}$  and  $\delta\text{D} = -28\text{‰}$ ). The composite precipitation plots off the scale of the graph, on the extension of the dashed regression line for the Little Chino aquifer spring samples (fig. E4). In contrast, a single large regional storm on September 15, 2001, produced enough runoff to partially fill Sullivan Lake, with a  $\delta^{18}\text{O}$  of  $-10.4\text{‰}$  and  $\delta\text{D}$  of  $-76\text{‰}$ . The stable-isotope ratio for the large rainfall event does not appear to have been affected by evaporation and is  $0.4\text{‰}$  more depleted in  $\delta^{18}\text{O}$  than Del Rio Springs. Coincidentally or not, this storm sample is isotopically identical (within laboratory precision) to upper Verde River springs (fig. E4, table E2). While more long-term data are needed to define seasonal variations in  $\delta^{18}\text{O}$  and  $\delta\text{D}$  in precipitation throughout the study area, it is evident that large regional storms produce less evaporated runoff than small ones and are more likely to generate greater amounts of surface-water runoff and ground-water recharge. No rainfall runoff is known to have topped Sullivan Lake dam for more than 6 months proceeding June, 2000. If Stillman Lake had contained a mixture of ground water and runoff in June 2000, the stable-isotope ratio of the residual runoff would have had to coincidentally fall on the same regression line as the Del Rio Springs and Granite Creek samples. In summary, Stillman Lake water does not appear to have been a mixture at the time of sampling.

As indicated by a statistical summary of stable-isotope data for the sample groups (table E2), the mean  $\delta^{18}\text{O}$  value for upper Verde River springs ( $-10.3\pm 0.1\text{‰}$ ) most closely resembles the mean for the four wells penetrating the D-C zone along the basin margin ( $-10.4\pm 0.3\text{‰}$ ). The mean  $\delta^{18}\text{O}$  value for the Big Chino sample group ( $-9.9\pm 0.3$ ) and its range between the maximum of  $-8.8\text{‰}$  and minimum of  $-10.5\text{‰}$  is misleading, however, in that it does not accurately represent a flow-weighted composite of ground water near the outlet of the basin-fill aquifer, such as at Del Rio Spring or the spring fed reach in lower Williamson Valley Wash. The mean instead represents 35 random well locations that were sampled on different dates from different screened intervals in the upper 700 ft of the aquifer. Upper Verde River springs would seem to represent a flow-weighted composite of Big Chino ground water, however, the possibility of mixing with a small fraction of the M-D sequence along the final leg of the flowpath first must still be ruled out.

In addition, the  $^2\text{H}$  and  $^{18}\text{O}$  content of shallow ground water beneath Big Chino Wash, Williamson Valley Wash, and near Sullivan Lake is potentially influenced by local recharge and likely enriched relative to the aquifer as a whole. Compelling evidence for direct recharge to the valley floor is based on tritium results presented in the following section.

Consequently, the group mean may be biased. Big Chino well samples near the outlet of the basin-fill aquifer are substantially more depleted in  $\delta^{18}\text{O}$  and  $\delta^2\text{H}$  than the group mean, and their isotope composition is indistinguishable from that of upper Verde River springs. This helps to explain why the  $\delta^{18}\text{O}$  of  $-10.3\text{‰}$  for ground water near Paulden (well E at (B-17-02)04 DDC; Appendix B) is isotopically identical to the mean  $\delta^{18}\text{O}$  value for upper Verde River springs (table E2), but differs from the group mean.

A  $\delta^{18}\text{O}$  value of approximately  $-10.3\pm 0.2\text{‰}$  can be used to trace the main flowpath upgradient from upper Verde River springs through the D-C zone to the outlet of the basin-fill aquifer near Paulden. By this approach, no mixing of the Big Chino basin-fill aquifer with another source is required to account for the  $\delta^{18}\text{O}$  composition of ground water discharging to upper Verde River springs, within the limits of analytical precision. Trends in water chemistry along this flowpath, including the stable-isotope data, will be further discussed in the final section of this chapter entitled "Multiple Lines of Evidence along a Flowpath."

Figure E5A compares variations in the  $^2\text{H}$  and  $^{18}\text{O}$  isotopic composition of upper Verde River springs with different geographical regions of the carbonate aquifer, including high-altitude springs on Big Black Mesa, deep wells north of the Verde River near Drake, large springs at Mormon Pocket and Sycamore Canyon, and the D-C zone beneath the margin of the Big Chino basin-fill aquifer. Figure E5B compares samples from upper Verde River springs with those from the two basin-fill aquifers and the high-altitude springs, tributaries, and wells west and south of Big Chino Valley. Most of the samples in the two graphs plot above the WMWL (International Atomic Energy Agency, 1994), suggesting that  $\delta^{18}\text{O}$  and  $\delta\text{D}$  of local precipitation that is recharged along the Mogollon Rim is more enriched than the global average.

Like the samples from Stillman Lake, the  $^2\text{H}$  and  $^{18}\text{O}$  isotopic composition of four samples collected from King Spring (Chapter D, fig. D4) between May 2000 and June 2002 have undergone varying degrees of evaporation, as indicated by a slope of approximately 4 (fig. E5A). The dashed blue regression line for the King Spring samples is parallel to the regression line for Stillman Lake, Granite Creek, and Del Rio Spring samples, also with a slope of 4. Left of the WMWL, the King Spring regression line intercepts several other spring samples from the carbonate aquifer near Big Black Mesa. Variation in  $^2\text{H}$  and  $^{18}\text{O}$  for three samples from Storm Seep, collected on different dates, probably are caused by seasonal variations in evaporation. A sample from Pool Seep plots within  $-0.4\pm 0.1\text{‰}$   $\delta^{18}\text{O}$  of the Storm Seep sample, which were both collected on April 19, 2001. Isotopically depleted water at small springs such as Storm Seep and Pool Seep was collected near the point of ground-water discharge, and typically have undergone less evaporation than larger water bodies such as King Spring or Stillman Lake, where the point of ground-water discharge is difficult to detect. The regional water-level gradient (fig. D7, Chapter D, this volume) and the

stable-isotope data indicate that the source of water to King Spring is from the northwest.

Many spring samples and some of the well samples collected during previous studies from stock tanks have undergone evaporation or were not purged prior to sampling, and these samples are not be considered representative of the carbonate aquifer. Two samples from Tucker Canyon and Meath Spring were collected from stagnant pools (fig. E1; Appendix B) and are not included on figure E5A because they are too highly evaporated and plot off scale to the upper right of the graph. Three stable-isotope samples in the carbonate aquifer north of the Verde River are included on figure E5A from previous studies, although the wells apparently were not adequately purged prior to sampling. These include two samples from the Glidden well at B(18-01)27AAC (depth unknown), which were collected from a stock tank by ASU

(Marnie Greenbie, oral commun., 2002), and a sample from the Hell well at B(18-01)06 ABB (depth = 460 ft) which was sampled from a stock tank by the USGS during a previous study (shown on fig. E1; Appendix B; see also Chapter D, this volume, table D3 and fig. D7). In addition, no driller's logs are available for the Hell Well or the Glidden well, making any interpretation uncertain.

The two Glidden well samples are within 2-sigma analytical precision of the  $\delta^{18}\text{O}$  analyses for upper Verde River springs (table E2; Appendix B), leading to Knauth and Greenbie's (1997) interpretation that the source of upper Verde River springs is the carbonate aquifer north of the upper Verde River. The two  $\delta\text{D}$  values, however, fall off the WMWL and are isotopically different from those for upper Verde River springs, although if averaged together they would produce a value nearly identical to upper Verde River springs. No explanation

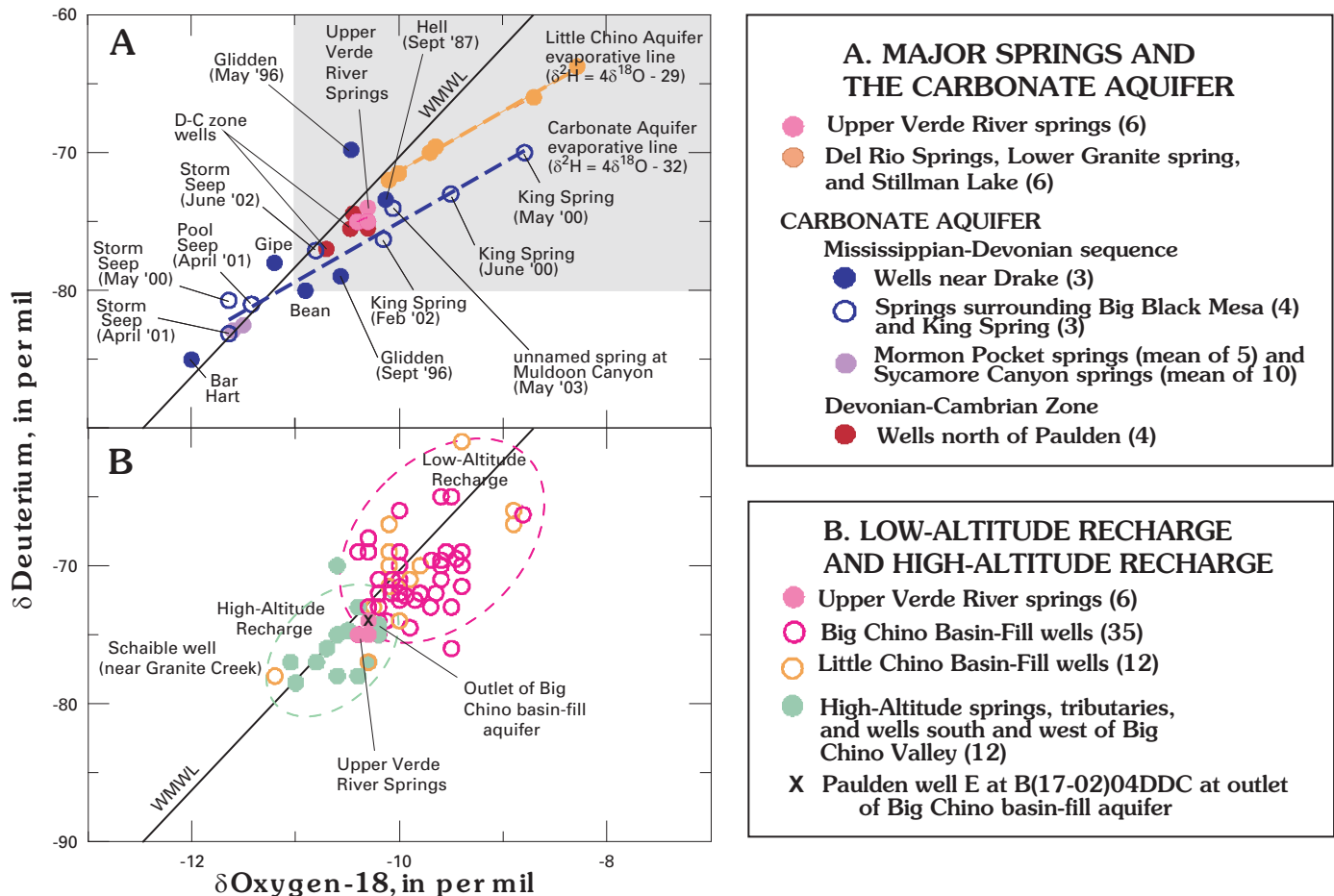


**Figure E5.** Graphs showing  $\delta\text{D}$  versus  $\delta^{18}\text{O}$  for sample groups in the Verde River headwaters (1986–2004); (A) major springs discharging to the upper Verde River versus wells and springs in the carbonate aquifer, and (B) upper Verde River springs versus Big and Little Chino basin-fill aquifers and high-altitude springs, tributaries and wells. In graph A, all analyses were used to illustrate seasonal variability of evaporative trends for surface water. In the graph B, in cases where multiple analyses were available for a single well location, the median values were used to minimize sample distribution bias. All data are reported in Appendix B. Shaded area in upper graph represents the graph area shown in figure E4. Number in parentheses in the explanation is number of samples in group. WMLW = World Meteoric Water Line ( $\delta\text{D} = 8\delta^{18}\text{O} \pm 10$ ).

is made here for the large disparity between the two  $\delta D$  values with the  $\delta^{18}O$  values essentially remaining constant. Compared with the new data from this study, the stable-isotope signature of the Glidden sample collected in September 1996 more closely resembles that of the Gipe and Bean samples than that for upper Verde River springs. The Glidden sample collected in May 1996 plots above the WMWL, and is different than all the other samples. Because of the differences in the  $\delta D$  values, a lack of other lines of geochemical evidence, and the absence of a well log, interpretation of the Glidden well is considered inconclusive.

Samples in the carbonate aquifer which have not undergone substantial evaporation include three wells north of the upper Verde River (Bean, Gipe, and Bar Hart wells shown on figs. E1 and E5A) and large low-altitude springs at Sycamore Canyon and Mormon Pocket. The wells range in depth from 585 to 720 ft and all three were pumped extensively before sampling. The Sycamore Canyon and Mormon Pocket springs, with steady discharge exceeding  $5\text{ft}^3/\text{s}$ , have been sampled repeatedly with little variation. All these M-D sequence samples are more depleted than upper Verde River springs (on average 1.3‰, table E2) plotting near or left of the WMWL. Thus, the M-D sequence of this part of the carbonate aquifer is substantially depleted in  $^2\text{H}$  and  $^{18}\text{O}$  compared to upper Verde River springs and based on water-level gradients could not contribute to the upper Verde River upstream from Perkinsville (Chapter D, this volume). Likely sources of recharge near Drake include direct recharge of runoff along Limestone Canyon and Hell Canyon, which are deeply incised to just above the water table in some reaches. The evident source of recharge to springs at Mormon Pocket and Sycamore Canyon is the extensive high-altitude region surrounding Bill Williams Mountain to the north (Wirt, 1993; Bryson and others, 2004).

Well samples from the two basin-fill aquifers plotted on fig. E5B show a broad scatter pattern of stable-isotope ratios. Samples from the Big Chino basin-fill aquifer (open pink circles) plot to the upper right of upper Verde River springs (solid pink circles), a pattern overlapping with and similar to the pattern of samples for the Little Chino basin-fill aquifer and Little Chino low-altitude springs (orange open and solid circles, respectively). Both Big and Little Chino basin samples generally are enriched in  $\delta^{18}O$  and  $\delta D$  compared to upper Verde River springs—a trend attributed to a higher fraction of recharge at lower altitudes derived from losing tributary streams and seepage beneath ephemeral streams. In contrast, high-altitude samples from springs in the Bradshaw, Santa Maria, and Juniper Mountains (elevations  $> 4,500$  ft) and major tributaries including Williamson Valley Wash and Walnut Creek (solid green circles) are substantially more depleted and plot in a scatter pattern overlapping with and to the lower left of upper Verde River springs. High-elevation samples represent ground water that is recharging the edges of the basins. An exception is a highly-depleted sample from the Schaible well in Little Chino Valley (figs. E1 and E5B; B-16-01 17 CCB), which plots similarly to the high-altitude well

and spring samples. The well is less than  $\frac{1}{4}$  mi from Granite Creek and probably receives direct recharge from high-altitude runoff during exceptionally large but infrequent storms.

Thus, two types of recharge appear to be occurring within the study area. High-altitude recharge is depleted relative to upper Verde River springs, owing to greater precipitation and cooler temperatures (Chapter A, this volume; fig. A9 and table A2). Low-altitude recharge to the basins is enriched relative to upper Verde River springs, owing to warmer temperatures and evaporation of overland flow on the valley bottoms. Ground water near the outlets of the Big and Little Chino basin-fill aquifers is a volumetric composite of both types of recharge. Samples from upper Verde River springs, the four D-C zone well samples, and basin-fill well E at (B-17-02)04 DDC near Paulden plot between the two oval-shaped scatter patterns for the basin-fill aquifers and high-altitude area samples (fig. E5B), as would be expected for a composite of high- and low-altitude recharge.

At the risk of redundancy, we reiterate that an important limitation of the stable-isotope data used in this study is not being able to volumetrically weight contributions from various parts of the ground-water system. As mentioned previously, most of the ground-water samples were collected from springs and wells that are less than 700 ft in depth. The basin-fill aquifer in Big Chino Valley is at least 2,000 ft deep in the center of the basin (Langenheim and others, Chapter C, this volume). Deep ground water in the centers of large basins is likely to have been recharged during a cooler and wetter climatic period (Robertson, 1991) or may be comprised of mostly high-altitude recharge. Deep ground water, which is largely unsampled, is expected to be more depleted in  $\delta^{18}O$  and  $\delta D$  than the relatively shallow well water sampled in this study. Deep ground water eventually must flow toward the outlet of the basin-fill aquifer. The hypothesis that mixing occurs between the basin-fill aquifer and underlying carbonate aquifer as deep and shallow flowpaths converge near the outlet will be evaluated by inverse modeling in Chapter F (this volume).

The range in  $\delta^{18}O$  data for each sample group has been summarized using box- and whisker plots (fig. E6). The box- and whisker plots for upper Verde River springs and the D-C zone of the carbonate aquifer underlying Big Chino Valley are nearly identical, suggesting that the two ground waters have a similar source. The  $\delta^{18}O$  box- and whisker plots for upper Verde River springs and the D-C zone are more depleted than that for the Big Chino basin-fill aquifer sample group, but closely match the sample from well E at (B-17-02)04 DDC, which is representative of ground water at the outlet of the Big Chino basin-fill aquifer near Paulden.

Wells between Paulden in the basin-fill aquifer and upper Verde River springs in the D-C zone have similar  $\delta^{18}O$  content because they essentially lie along the same flowpath. Water-level gradients indicate the direction of ground-water movement near Paulden is east, from the basin-fill aquifer into the carbonate aquifer and then southeast toward the upper Verde River (Chapter D, this volume, fig. D7). Large well yields

in wells penetrating limestone is an indication of solution features and preferential flow along the extension of the Big Chino Fault trend and basin-fill aquifer boundary (Chapter D, this volume). Secondary fractures and joint sets in basalt and Paleozoic sedimentary rocks provide yet another conduit out of the basin-fill aquifer.

The stable-isotope data do not convincingly indicate that upper Verde River springs is a mixture of two sources, unless both sources have fairly similar  $\delta^2\text{H}$  and  $\delta^{18}\text{O}$  isotopic composition, or unless the contribution from one source is relatively minor. On average, the carbonate aquifer north of the Verde River (M-D sequence) typically is 1.3‰ more depleted in  $\delta^{18}\text{O}$  than upper Verde River springs (table E2), or—particularly in the case of the Glidden and Hell wells, and the King Spring samples—so enriched by evaporation

or having sampling uncertainties such that no conclusive interpretation can be made. Based on the regional water-level gradients, some mixing with the carbonate aquifer could occur west or north of upper Verde River springs (Chapter D, this volume; figs. D6 and D7). Using a mass-balance approach, the maximum hypothetical contribution from the M-D sequence of the carbonate aquifer north of the Verde River that could occur, without affecting the  $\delta^{18}\text{O}$  content of upper Verde River springs by more than 0.2‰ (the analytical precision of the technique), is about 15 percent. Ford (2002) estimated recharge from the carbonate aquifer underlying Big Black Mesa at about 5 percent of the base flow to the upper Verde River (Chapter A, this volume; fig. A16 and table A4). A 5-percent mix with the carbonate aquifer would be too small to produce a statistically significant shift in the

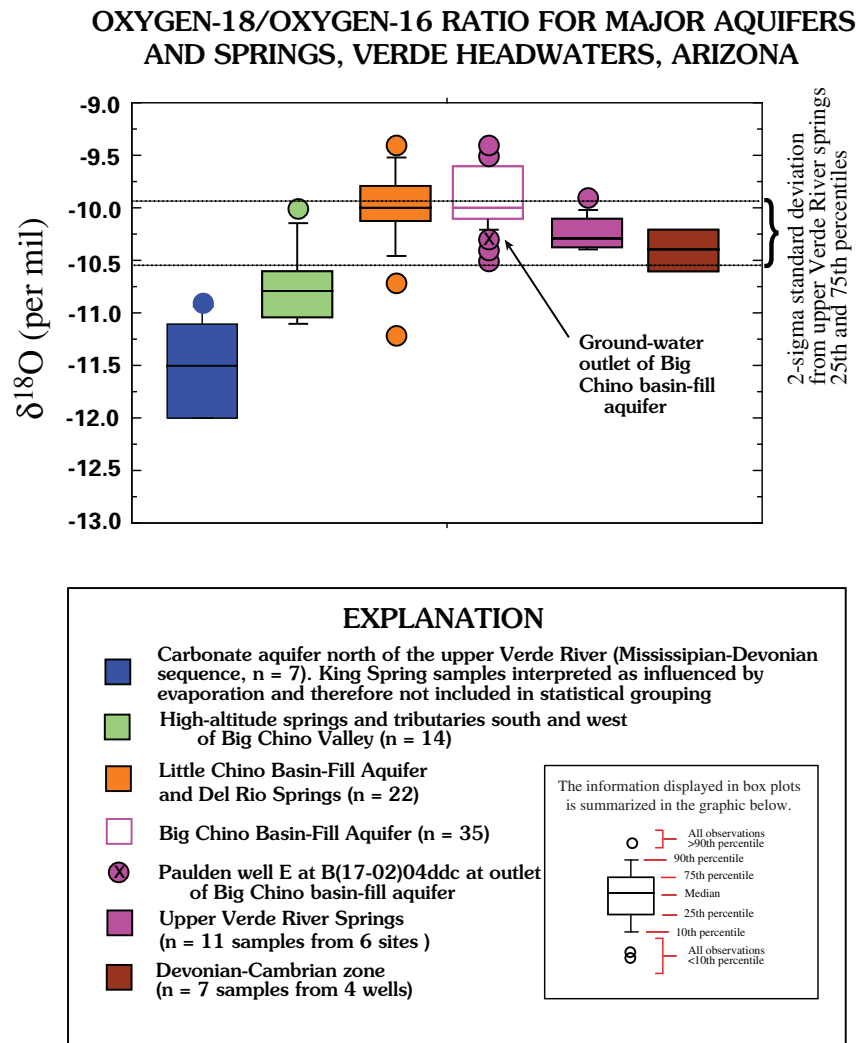


**Figure E6.** Box- and whisker plot (SAS Institute, 1998) of  $\delta^{18}\text{O}$  for sample groups upgradient of upper Verde River springs. Order of box- and whisker plots is the same as in explanation; n, is number of samples. Data are summarized in table E2.



$\delta^2\text{H}$  and  $\delta^{18}\text{O}$  composition. Thus, no indisputable conclusion can be reached based on stable-isotope evidence alone except that the amount of mixing, if any, is less than about 15 percent. The mixing hypothesis will be further evaluated by inverse geochemical modeling in the following chapter (Chapter F, this volume).

## Apparent Age of Ground Water

Tritium and  $^{14}\text{C}$  data provide a useful means of estimating apparent age and degree of mixing and for delineating ground-water movement. Spatial differences in the activities of tritium and  $^{14}\text{C}$  on figs. E7 and E8 illustrate flowpath directions and areas where recharge is occurring. Detectable tritium values are interpreted to mean that the water is either modern in age, or contains a fraction of modern water. Ground water having a low  $^{14}\text{C}$  activity, expressed as percent modern carbon (pmc), is presumed older than waters having a higher percentage of modern carbon. Ground-water ages have not been calculated for this study.

### Tritium

Tritium activities in ground water (fig. E7) are interpreted relative to modern local precipitation. Two precipitation samples in the study area were analyzed for tritium during the summer of 2001. A composite of summer rain collected from roof runoff by a local resident of Chino Valley contained  $9.1 \pm 0.41$  tritium units (TU). The composite sample was collected by transferring runoff into a large sealed container immediately following each storm. In no instance did the roof runoff exceed the capacity of the collection container. A large regional storm on September 15, 2001, contained  $5.0 \pm 0.36$  TU. Both activities are consistent with background values for modern precipitation in southern Arizona ranging from about 5 to 10 TU (Christopher J. Eastoe, oral commun., 2004; Wright, 2001). The highest tritium values in the study area are samples from high-altitude springs on Big Black Mesa and in the Bradshaw, Santa Maria, and Juniper Mountains; ranging from 3.1 to 10.3 tritium units (mean =  $6.4 \pm 3.6$  TU;  $n = 11$ ). None of the samples appear to contain high levels of bomb-pulse tritium leftover from the 1950s and 1960s, suggesting that all of the water has been recharged since 1953. Samples from alluvial aquifers along major tributaries have less tritium activity and appear to be older relative to high-altitude springs. In Walnut Creek, a sample from a 150-ft well had a value of  $<0.7$  TU, and in Williamson Valley a 190-ft well and a spring sample had values of 1.3 and 3.8 TU, respectively. The age of the water in the Walnut Creek sample probably is pre-1953; whereas the two Williamson Valley sample values contain at least a fraction of water recharged since 1953.

Ground water from three wells in the northwestern Big Chino basin-fill aquifer (wells A, B, and C) had no detectable tritium, as did well H in the D-C zone of the carbonate aquifer north of Paulden. Two wells near Sullivan Lake (wells E and F) and one well near the confluence of Big Chino Wash with Williamson Valley (well D) had 1.2, 1.2, and 1.1 TU of

detectable tritium. Low levels of tritium suggest that direct recharge to the basin-fill aquifers is occurring along low-altitude ephemeral reaches. The largest tritium value of  $2.7 \pm 0.3$  TU measured for well L in the Little Chino basin-fill aquifer is from a 350-ft well in the Granite Creek flood plain. This sample also is heavily depleted in  $\delta^{18}\text{O}$  and  $\delta\text{D}$  (fig. E5), which is a further indication that high-altitude runoff has infiltrated beneath the ephemeral reach of Granite Creek.

Low levels of tritium detected in springs near the outlets of the basin-fill aquifers indicate recharge of intermittent storm runoff. Along the uppermost reach of the Verde River, tritium activities ranged from  $<0.5$  to 2.3 TU (Appendix B). At Paulden, north of Sullivan Lake and near the outlet for the Big Chino basin-fill aquifer, a sample from a basalt well B(17-02)02 CAC had a tritium activity of 0.8 TU, just above the reported detection level for that sample. This well is along the main flowpath between Paulden and upper Verde River springs, as indicated by water-level gradients presented by Wirt and DeWitt (Chapter D, this volume). Tritium values for seven different samples from upper Verde River springs collected during May–June 2000 ranged from  $<0.7$  to 1.1 TU. During the same time, five samples from Lower Granite Spring and Del Rio Springs had values ranging from 0.9 to 1.6 TU. Following extended drought conditions, two samples at Stillman Lake had  $<0.7$  TU in May and June of 2000. After a large regional storm in September 2001, Stillman Lake had a tritium activity of  $2.3 \pm 0.6$  TU on January 16, 2002. Similarly, Summer Spring in Sycamore Canyon at stream level had a low but detectable value of  $1.1 \pm 0.3$  TU. The large spring at Mormon Pocket had  $<0.6$  TU. This spring discharges above all but the highest floods in this reach.

In summary, water from high-altitude springs and major tributaries had the highest tritium activities and youngest apparent ages. None of the tritium values exceed 10 TU, a level that would indicate that some portion of precipitation was recharged during atmospheric nuclear testing of the 1950s and 1960s, or post fallout during the 1970s. Samples from wells greater in depth than 500 ft in northwestern Big Chino Valley and from the carbonate aquifer had no detectable tritium, indicating that ground water was recharged before 1953. The presence of low-level tritium in springs and wells near streams indicates that modern direct recharge is occurring along Williamson Valley Wash, southeastern Big Chino Wash, middle and lower Granite Creek, and in the areas near Sullivan and Stillman Lakes. Major springs near the outlets of Big and Little Chino Valleys tend to have tritium activities slightly above the analytical detection limit, which is consistent with low-altitude recharge occurring along low-gradient stream segments.

### Carbon-14 and Carbon-13

Carbon-14 was analyzed for samples from fourteen wells and low-altitude springs. Because high-altitude springs represent modern recharge, as indicated by elevated tritium activities, none of these samples were further analyzed for  $^{14}\text{C}$ .

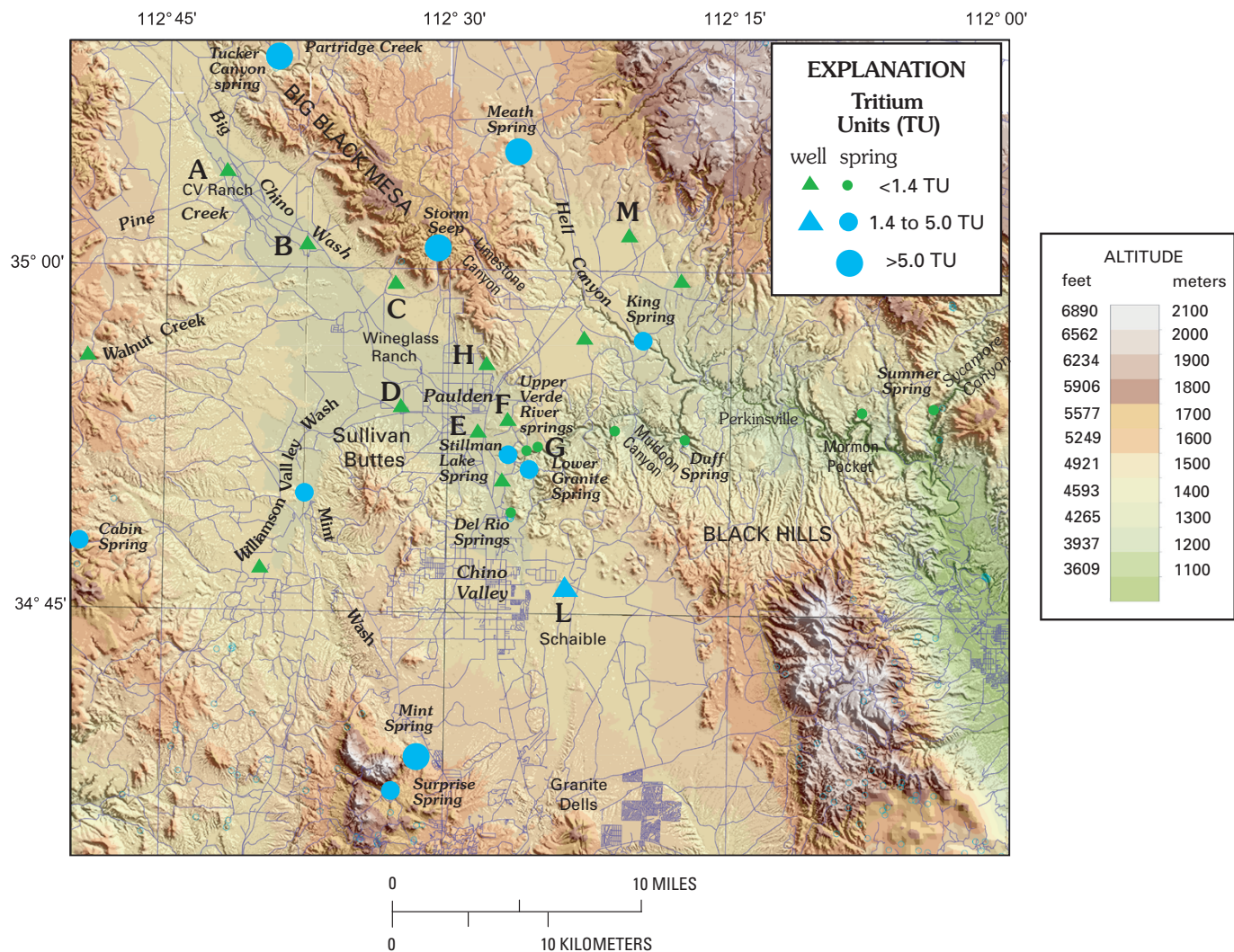


**Figure E7.** Map showing tritium activities measured in this study, upper Verde River headwaters region. Base is from 1:100,000 U.S. Geological Survey digital data. Circle is spring sample, triangle is well sample. Lettered location corresponds to samples plotted in graphs on figure E9. Data are reported in Appendix B.

The highest  $^{14}\text{C}$  activities > 65 percent modern carbona (pmc), indicative of younger ground water, are found along major tributaries adjacent to high-altitude recharge areas receiving the most precipitation (fig. E8). A sample from a 150-ft well in Walnut Creek contained  $81.1 \pm 0.6$  percent modern carbon (pmc) and a 190-ft well and spring in Williamson Valley Wash contained  $79.1 \pm 0.7$  and  $106.5 \pm 0.8$  pmc, respectively. The latter  $^{14}\text{C}$  value exceeding 100 pmc is similar to that measured for air in southern Arizona in 2002 (Eastoe and others, 2004).

Carbon-13 for the entire study area ranged from  $-1.9$  to  $-15.2\text{‰}$  (average =  $-8.6$ ;  $n = 45$ ). As mentioned in the methods section, the primary source of  $\delta^{13}\text{C}$  in ground water is  $\text{CO}_2$  in the soil gas of the recharge zone (Bullen and Kendall, 1998). The lowest  $\delta^{13}\text{C}$  values generally were measured from springs in riparian areas and from well samples having detectable tritium and also having among the highest  $^{14}\text{C}$  activity. All

three samples from Williamson Valley and Walnut Creek had > 75 pmc  $^{14}\text{C}$  and moderately depleted  $\delta^{13}\text{C}$  of  $-11.2$ ,  $-11.9$  and  $-12.2\text{‰}$ , respectively.

Other high  $^{14}\text{C}$  activities were measured for the 350-ft well in the Granite Creek flood plain in Little Chino Valley (73 pmc;  $\delta^{13}\text{C} = -7.9$ ) and a 250-ft well south of Sullivan Lake (87 pmc;  $\delta^{13}\text{C} = -11.7$ ). Ground water from the Little Chino basin-fill aquifer is progressively younger toward the Verde River, as evidenced by  $^{14}\text{C}$  activities of 66, 81, and 97 pmc for Del Rio Springs, Lower Granite Spring, and Stillman Lake, respectively. This increasing trend is evidence of direct recharge of runoff to ground water beneath low-gradient stream channels, consistent with the results for the tritium data.

The lowest  $^{14}\text{C}$  activities indicating the oldest water were measured from well samples having no detectable tritium and relatively enriched  $\delta^{13}\text{C}$ . Five samples from the

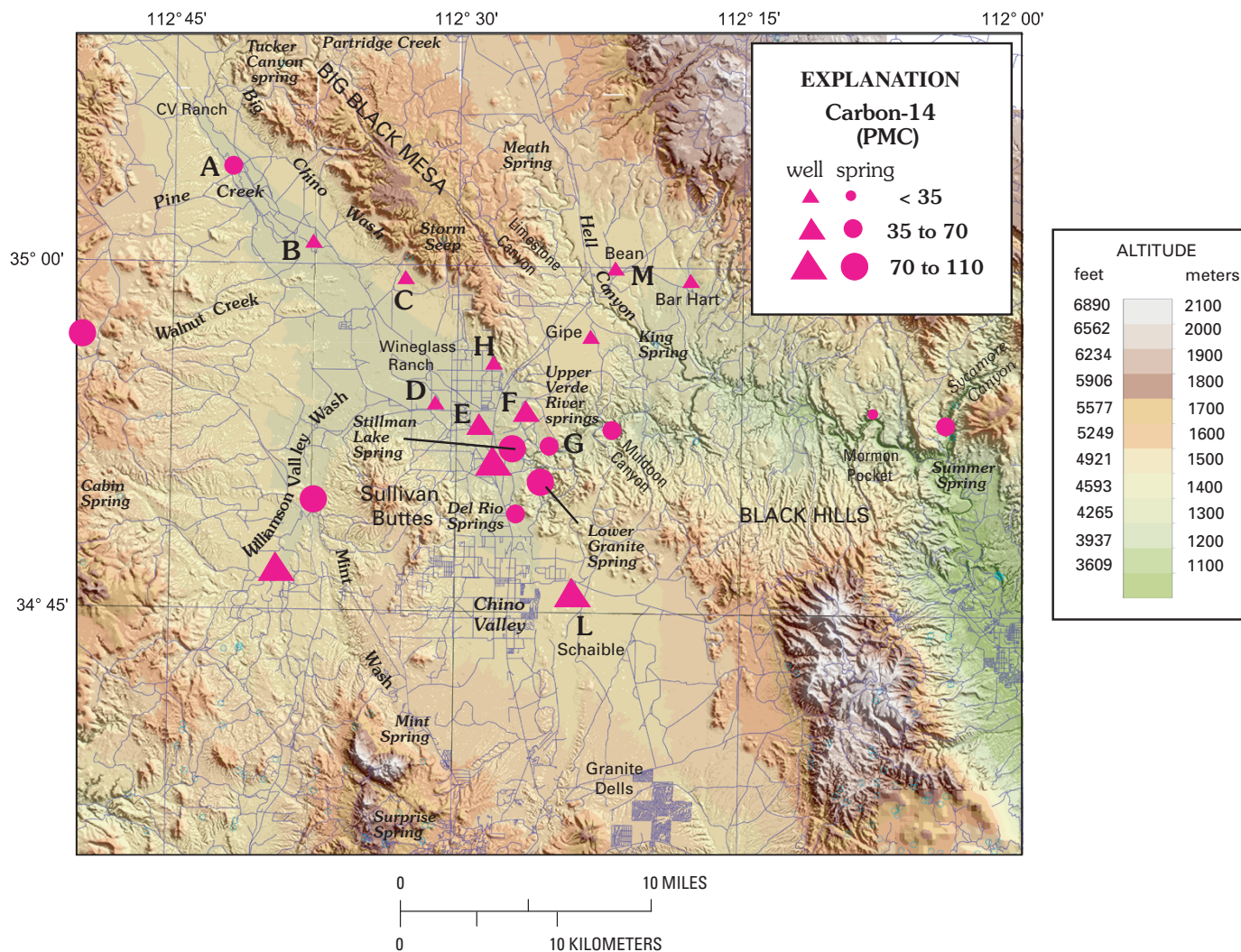
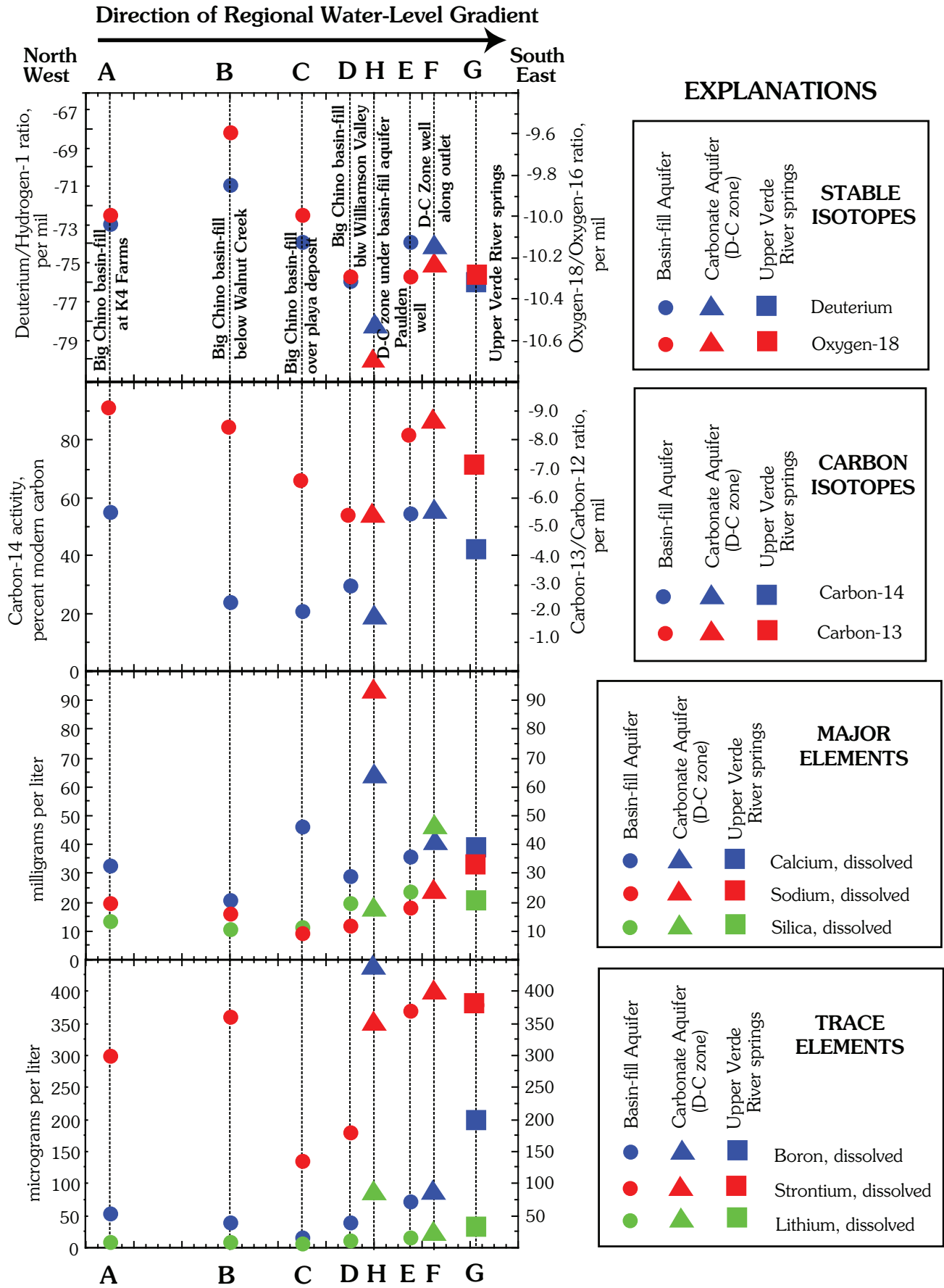


**Figure E8.** Map showing carbon-14 activities measured in this study, upper Verde River headwaters region. Base is from 1:100,000 U.S. Geological Survey digital data. PMC, percent modern carbon; circle is spring sample, triangle is well sample. Lettered location corresponds to samples plotted in graphs on figure E9. Data are reported in Appendix B.

carbonate aquifer north of the Verde River had values of 18.6 to 36.4 pmc and  $-7.7$  to  $-2.0$   $\delta^{13}\text{C}$  ( $\delta^{13}\text{C}$  average =  $-6.0 \pm 2.3$ ;  $n=5$ ). Ground water with a similar range of  $^{14}\text{C}$  activity was measured for two out of six wells sampled in Big Chino Valley. The lowest measured  $^{14}\text{C}$  activity of  $18.0 \pm 0.2$  pmc was measured for a sample from well H north of Paulden ( $\delta^{13}\text{C} = -5.6$ ; figs. E8 and E9), which was completed in the carbonate aquifer underlying the Big Chino basin-fill aquifer. The 346-ft well is near the terminus of the Big Chino Fault and was drilled through alluvial fan sediment into what is interpreted as the D-C zone of the carbonate aquifer. A second low value of  $21.0 \pm 0.2$  pmc and  $-6.7\%$   $\delta^{13}\text{C}$  was measured for a 190-ft well (site C) completed in alluvial fan sediment near the Big Chino Fault at the base of Big Black Mesa. One explanation for the two samples essentially having the same  $^{14}\text{C}$  activity is that they could be along a similar flowpath roughly

parallel to the Big Chino Fault. A second possible explanation is that, in both cases, the local ground water is in contact with carbonate rock or carbonate sediments and that the dissolution of carbonate minerals has contributed “dead” carbon to the ground water. Thus, it is unclear whether the ground water is really old or whether there has been an addition of dead carbon resulting in values that appear older. Geochemical modeling is needed to correct for the presence of dead carbon and to calculate numerical ages for the ground water samples.

If the Big Chino basin-fill aquifer were a closed aquifer system, one would expect ground water to appear progressively older along the valley axis from northwest to southeast. But because the aquifer is an open system, ground water changes in age in relation to depth and distance from recharge sources such as Big Chino Wash and



its major tributary streams. The apparent age of ground water in the basin-fill aquifer varies not only along the axis of the basin, but in relation to many factors such as the distance from recharge sources, rates of ground-water movement, changes in the lithology of water-bearing units, and the depth of the well screen. Sampling limitations make it impossible to determine a possible relation between water chemistry and depth. In addition, no wells were sampled across the wide confluence of Williamson Valley with Big Chino Valley.

In northwestern Big Chino Valley,  $^{14}\text{C}$  activity decreases along the axis of the upper basin from  $55.0 \pm 0.6$  to  $24.1 \pm 0.5$  pmc between Partridge Creek and Walnut Creek (between well A and well B shown on figs. E8 and E9). Near the center of the basin, one might predict that relatively younger water from Walnut Creek and Williamson Valley Wash would enter and mix with the Big Chino basin-fill aquifer and that the next sample along the axis of the basin should be younger. In fact, the value of  $29.8 \pm 0.6$  pmc for well D north of Sullivan Buttes in Quaternary and Tertiary alluvium is only slightly higher, or younger than the sample upgradient from Walnut Creek. That the value is not substantially higher (indicating apparently younger water) may be because the thickness of the aquifer decreases along its axis from at least 2,000 ft in the deepest part of the basin to several hundred ft or less in the southeastern part of the valley (Langenheim and others, Chapter C, this volume). Deeper circulating ground water may migrate upward along preferential flowpaths, particularly along fault-bounded margins on the north and south sides of the basin. This hypothesis would explain the relatively lower  $^{14}\text{C}$  activity for wells D and H and also might explain in part why many productive wells have been developed in lower Big Chino Valley near the distal end of the aquifer. East of Wineglass Ranch, yields exceeding 1,000 gallons per minute have been reported for wells completed in basin-fill alluvium, in basin-fill basalt, and in the carbonate aquifer underlying the basin-fill aquifer (Water Resources Associates, 1989; 1990; Chapter D, this volume). All of these aquifer units are thought to be hydraulically connected.

The hydrogeologic framework for southeastern Big Chino Valley is briefly summarized here from Chapter D (Wirt and DeWitt, this volume) for the area downgradient from Wineglass Ranch. Ground water from Williamson Valley merges with the Big Chino basin-fill aquifer near Wineglass Ranch. As ground water moves down the axis of Big Chino Valley toward the main ground-water outlet near Paulden, it encounters buried basalt flows within the alluvium. The buried

basalt is 500 ft in depth with a thickness of 90 ft in a borehole west of Wineglass Ranch (DeWitt and others, Chapter B, this volume). The basalt exposed at Sullivan Lake is about 350 ft thick. The water-level gradient of the Big Chino basin-fill aquifer near Paulden slopes gently east or southeast, toward upper Verde River springs, the main point of discharge for the Big Chino aquifer (Chapter D, this volume). The Big Chino basin-fill aquifer and the D-C zone are strongly interconnected in this part of the basin as shown by a dashed basin-fill aquifer boundary east of Paulden (fig. E1). This interpretation is supported by a gently-sloping water-level gradient that extends over a broad area from Paulden on the west, to upper Verde River springs and the Verde River on the south, to King Spring on the east, and at least 2.0 mi north of Drake (Chapter D, fig. D7). Ground water leaving Big Chino Valley near Paulden travels approximately 1.5 mi through the carbonate aquifer (which includes a basalt paleochannel) before reaching upper Verde River springs.

The main flowpath between Paulden and upper Verde River springs is indicated by the lack of change in  $^{14}\text{C}$  activity and  $\delta^{13}\text{C}$  ratio for wells E and F (fig. E8) that is consistent with the water-level gradient. Well E near Paulden (at B-17-02 04 DDC) is 200 ft in depth and produces from the basin-fill aquifer. Well F is 1.5 mi north of upper Verde River springs (site G), 480-ft deep, and produces from the carbonate aquifer just east of the Big Chino basin boundary. Both wells E and F penetrate the same correlated basalt units, are less than 1.5 mi apart, and have essentially the same  $^{14}\text{C}$  activity ( $54.7 \pm 0.8$  versus  $55.5 \pm 0.6$  pmc) and  $\delta^{13}\text{C}$  ratio ( $-8.2$  versus  $-8.8\%$ ). Continuing along the flowpath, ground water discharging to the main spring G in the upper Verde River springs network has a  $^{14}\text{C}$  activity of  $42 \pm 0.3$  pmc ( $-7.0\%$   $\delta^{13}\text{C}$ ). The slightly lower  $^{14}\text{C}$  value may be due in part from dissolution of dead carbon from carbonate rocks along the final leg of the flowpath. Alternately, mixing with a small amount of apparently older ground water such as that for well H in the D-C zone north of Paulden, with a  $^{14}\text{C}$  activity of  $18.0 \pm 0.3$  pmc and  $-5.6\%$   $\delta^{13}\text{C}$ , would also account for the slight decrease in  $^{14}\text{C}$  activity and  $\delta^{13}\text{C}$  content at upper Verde River springs. Mixing versus water-rock interaction processes are further addressed in the following section and in Chapter F (this volume).

## Multiple Lines of Geochemical Evidence along a Flowpath

Stable-isotopes alone do not always uniquely identify water sources. Where more than one interpretation is possible, knowledge of water-level gradients, geological factors, and other geochemical evidence can help to rule out unlikely scenarios. The most likely scenario can be identified when all chemical and isotopic data are considered in their geologic and hydrologic context. Water-chemistry and isotope data presented in this chapter have been used to characterize the basin-fill aquifers, stratigraphic units and geographical areas within

---

**Figure E9 (facing page).** Graphs showing changes in water chemistry along regional water-level gradient from upper to lower Big Chino Valley and from the Big Chino basin-fill aquifer near Paulden through the carbonate aquifer to upper Verde River springs. Letter on x-axis corresponds to sample location shown in figure E8. Horizontal spacing is proportional to map distance.

the carbonate aquifer, high-altitude recharge areas, and major springs discharging to the upper Verde River and its tributaries. Chemical and isotopic data provide integrated information for ground water discharging from the major aquifers. Different geochemical constituents help to constrain hypotheses regarding the nature of water-rock interactions and possible end-members involved in mixing processes.

To summarize the different lines of geochemical evidence presented thus far in this chapter, upper Verde River springs and Little Chino basin-fill aquifer are easily distinguished from each other on the basis of trace-element concentrations and stable-isotope ratios. Del Rio Springs and Lower Granite Spring are ~0.4‰ heavier in  $\delta^{18}\text{O}$ , and have strontium concentrations exceeding 450  $\mu\text{g/L}$  compared with moderate Sr (346 to 440  $\mu\text{g/L}$ ) for upper Verde River springs. Ground-water discharge from the Little Chino basin-fill aquifer has more contact with Sr-rich volcanic rocks and less exposure to sedimentary rocks in the D-C zone. In contrast, upper Verde River springs contain moderately high concentrations of 17–29  $\mu\text{g/L}$  As, 136–270  $\mu\text{g/L}$  B, and 28–49  $\mu\text{g/L}$  Li. This compares with 7–17  $\mu\text{g/L}$  As, 40–80  $\mu\text{g/L}$  B, and 7–17  $\mu\text{g/L}$  Li for samples from Del Rio Springs, lower Granite Creek, and Stillman Lake.

Ground water from upper Verde River springs and the M-D sequence also are easily distinguished from one another. The isotope composition of upper Verde River springs is enriched by about 1.3‰ and 7.9‰ in  $\delta^{18}\text{O}$  and  $\delta\text{D}$  relative to the M-D sequence north of the Verde River (fig. E6; table E2). The M-D sequence also has relatively low levels of trace-elements (101–120  $\mu\text{g/L}$  Sr, 2–10  $\mu\text{g/L}$  As, 12–71  $\mu\text{g/L}$  B, and 3–15  $\mu\text{g/L}$  Li; fig. E3); however, these elements could be acquired later through contact with the D-C zone. A substantial contribution from the M-D sequence of the carbonate aquifer would be expected to deplete the  $\delta^{18}\text{O}$  of upper Verde River springs, but this argument is not compelling given the degree of variation in the data. A small amount of mixing, within the margin of analytical uncertainty for the  $\delta^{18}\text{O}$ , cannot be ruled out with a simple mass-balance approach. The M-D sequence could provide up to about 15 percent of the total discharge to upper Verde River springs without changing the  $\delta^{18}\text{O}$  by more than 0.2‰. Recharge from Big Black Mesa has been estimated at about 5 percent of base flow at the Paulden gauge, based on its aerial extent and rate of precipitation (Ford, 2002; Chapter A, this volume; fig. A16). A mixing contribution on this scale could not be confirmed or rejected by the stable-isotope evidence alone and therefore this hypothesis will be further tested by inverse geochemical modeling at the end of the following chapter (Chapter F, this volume). Trends in major and trace-element concentrations presented here indicate that water-rock interaction, as opposed to mixing with the M-D sequence, is the major process occurring along the Big Chino outlet flowpath.

A conceptual summary of water chemistry along the main ground-water flowpath—down the axis of northwestern Big Chino Valley to southeastern Big Chino Valley, and from the Big Chino basin-fill aquifer through the carbonate aquifer

to upper Verde River springs—is presented on fig. E9 (sample locations shown on fig. E8). Samples A and B were collected from deep irrigation wells in the Big Chino basin-fill aquifer upgradient of Walnut Creek. Samples from wells C and D were collected near the northern and southern margins of the central basin, respectively. Preferential flow out of the basin-fill aquifer is thought to occur along a flowpath from wells E, to F, to G. The basin-fill aquifer at E predominantly consists of buried basalt layers at Paulden. Sample F also penetrates basalt within the carbonate aquifer east of Paulden. Sample G is the largest spring in the upper Verde River springs network. Sample H is from the area along the Big Chino Fault and represents water that has had extensive contact with the D-C zone.

In the uppermost graph,  $\delta^{18}\text{O}$  and  $\delta\text{D}$  ratios initially increase and then become more depleted with distance along the conceptual flowpath down the axis of Big Chino Valley. East of Wineglass Ranch, the  $\delta^{18}\text{O}$  and  $\delta\text{D}$  values for well samples D, E, and F are within analytical precision of upper Verde River springs (G), suggesting a major flowpath that approximately follows this route. The  $\delta^{18}\text{O}$  and  $\delta\text{D}$  at the outlet of the Big Chino aquifer (sample E on fig. E9) closely matches well F and upper Verde River springs (G). Samples F and H are within the D-C zone along the outlet flowpath but differ slightly to within 0.4‰  $\delta^{18}\text{O}$  and 4.0‰  $\delta\text{D}$  (2-sigma analytical uncertainty) of upper Verde River springs. The mean stable-isotope ratio for nine samples from upper Verde River springs, however, closely match that for five samples from the D-C zone within 0.1‰  $\delta^{18}\text{O}$ , which is within 1-sigma analytical uncertainty of 0.2‰ (table E2). Sample H is the most depleted in  $\delta^{18}\text{O}$  and  $\delta\text{D}$  of all the samples from the D-C zone (fig. E6). Consequently, a small amount of mixing of the D-C zone with the Big Chino basin-fill aquifer—even if one were to use the most depleted result—would not produce a significant shift in the stable isotope composition of upper Verde River springs.

In the second graph (fig. E9),  $^{14}\text{C}$  activities decrease along the valley axis from samples A to C, then increase from D to F. The increase in modern  $^{14}\text{C}$  toward the basin outlet corresponds with the increase in measurable tritium activity (fig. E7), indicating that direct recharge from infrequent runoff probably is occurring along Big Chino Wash, lower Williamson Valley Wash, and near Sullivan Lake. A slightly lower  $^{14}\text{C}$  activity at upper Verde River springs (G) might be caused by mixing with older deeper water near the outlet for the basin-fill aquifer, or by dissolution of carbonate rocks contributing ‘dead’ carbon, if this process were occurring. A proportionate decrease in  $\delta^{13}\text{C}$  from –8.8 to –7.0‰ from samples E and F to G corresponds with the lithology change along the flowpath from basalt to limestone and suggests that a small amount of mixing or dissolution of carbonate rocks is occurring.

The third graph (fig. E9) shows concentrations of dissolved calcium, sodium, and silica (as Si). Dissolution of calcite and dolomite in the carbonate aquifer would be expected to calcium concentrations from well E to spring G; yet the concentrations remain nearly constant along this flowpath. Using NETPATH (Plummer and others, 1994), saturation

indices for calcite of  $-0.78$  and  $-0.37$  were calculated for two samples from upper Verde River springs (spring G or SP1700). This indicates that the ground water is near saturation or slightly undersaturated with respect to calcite. Cation exchange with clay minerals, common in shale (Potter and others, 1980), also might account for the lack of change in Ca concentration, which is accompanied by an increase in Na concentration from well E to spring G. Mixing or contact in the D-C zone (represented by well H) results in a Ca concentration about one third higher and a Na concentration 6 times higher than the concentrations at upper Verde River springs (spring G). In addition, dissolved silica is slightly higher near Paulden than the rest of big Chino Valley, but is about twice as high at well F, which intercepts the basalt paleochannel. This is consistent with dissolution of silicate minerals in igneous rock. Disproportionate changes in major ion concentrations (or lack thereof) are more likely caused by water-rock interaction and are difficult to explain solely by mixing.

In contrast to Ca and Si, concentrations of Na, B, and Li increase from well D to spring G, also presumably the result of water-rock interactions. Between well E and spring G there are 189 and 188 percent increases in the concentrations of Na and Li, respectively (probably the result of a correlated dissolution processes). Boron increases from well D to spring G by 274 percent, likely caused by a different process or solid-phase distribution. Both B and Li sorb weakly and tend to remain in the dissolved state (Hem, 1985); hence these disproportionate changes in the concentrations of these constituents are best explained by water-rock interaction as opposed to mixing. This observation is reinforced by the lack of significant change in  $\delta^{18}\text{O}$  and  $\delta\text{D}$  values along the same flowpath (well D to spring G). Stable-isotope ratios of oxygen and hydrogen are the parameters most likely to behave conservatively (fig. E9) and these also support the interpretation that little mixing is occurring (within the analytical precision of the technique).

Lastly, elevated Sr concentrations are most strongly linked to volcanic rocks, although a playa source is possible for some wells in middle and lower Big Chino Valley. Strontium concentrations are moderately high in the northwest and southeast parts of the Big Chino basin-fill aquifer, where there is spatial proximity downgradient from buried basalt flows (wells A, B, and E). Strontium concentrations are lowest for wells C and D near the northern and southern basin margins where there is no contact with the playa deposit or buried basalt. Strontium concentrations are similar for the Big Chino basin-fill aquifer near its outlet (well E) and the D-C zone (F and H), suggesting that a playa or igneous source of Sr is upgradient from the D-C zone. Basalt-filled paleochannels may also provide an additional source of strontium to well F and spring G. Conversely, mixing of ground water from the low-Sr M-D sequence with ground water traveling through the D-C zone would be expected to produce a lower Sr concentration at spring G. This does not appear to be the case and there again is a lack of geochemical evidence to support mixing.

In conclusion, the results of the geochemistry investigation reinforce the hydrogeologic framework conceptual model that the Big Chino basin-fill aquifer and underlying carbonate aquifer are strongly interconnected along the basin outlet flowpath near Paulden and appear to function as a single source of ground water to upper Verde River springs. Overall, the results from this geochemical study indicate considerable vertical and horizontal heterogeneity of the Big Chino basin-fill aquifer and its underlying carbonate aquifer that need to be considered when establishing a regional ground-water model. Paleozoic rocks are presumed to underlie all or most of Big Chino Valley, although there are no ground-water samples from the lower carbonate aquifer except for those from the D-C zone north of Paulden along the trend of the Big Chino Fault. Overall similarities among the stable-isotope ratios measured for the Big Chino basin-fill aquifer and D-C zone near Paulden (fig. E6) indicates similar or overlapping recharge source areas and a common outlet flowpath. Along the outlet flowpath, the carbonate aquifer functions primarily as a conduit, as opposed to a new source of ground water. That Na, Li, and B increase disproportionately along the flowpath, while Ca,  $\delta^{18}\text{O}$ , and  $\delta\text{D}$  values vary relatively little, points to water-rock interaction with rocks chemically similar to the Bright Angel Shale or Chino Valley Formation as opposed to mixing—although a small amount of mixing with the M-D sequence on the order of about 15 percent or less cannot be ruled out. Variations in the concentrations of elements are attributed to differences in ground-water residence time, or to slight differences in the length or direction of the flowpath, or to variations in the mineralogy of individual rock units. Geochemical trends presented here indicate preferential flow from the Big Chino aquifer near Paulden through fractures in basalt and karst in the D-C zone of the carbonate aquifer, to upper Verde River springs. In the following chapter, these geochemical trends will be further evaluated to calculate the relative contributions from each major aquifer to base flow in the upper Verde River.

## References Cited

- Baedecker, P.A., Grossman, J.N., and Buttleman, K.P., 1998, National Geochemical Data Base; PLUTO Geochemical data base for the United States: U.S. Geological Survey Digital Data Series DDS-47, CD-ROM.
- Benson, Larry, and Peterman, Zell, 1995, Carbonate deposition, Pyramid Lake subbasin, Nevada: The use of  $^{87}\text{Sr}$  values in carbonate deposits (tufas) to determine the hydrologic state of paleolake systems: Elsevier Science, *Palaeogeography, Palaeoclimatology, Palaeoecology* 119, p. 201–213.
- Bierman, P.R., Albrecht, Achim, Bothner, M.H., Brown, E.T., Bullen, T.D., Gray, L.B., and Turpin, Laurent, 1998, Erosion, Weathering, and Sedimentation, *in* Kendall, Carol and McDonnell, J.J., eds., *Isotope Tracers in Catchment Hydrology*: Elsevier, New York, p. 647–678.

- Bowie, S. H. U., Dawson, J., Gallagher, M. J., Ostle, D., Lambert, R. St. J., and Lawson, R.I., 1966, Potassium-rich sediments in the Cambrian of northwest Scotland: Institution of Mining and Metallurgy, Transactions, Section B: Applied Earth Science, v. 75, p.125–145.
- Bowie, S. H. U., Dawson, J., Gallagher, M. J., and Ostle, D., 1967, Potassium-rich sediments in the Cambrian of northwest Scotland [discussion]: Institution of Mining and Metallurgy, Transactions, Section B: Applied Earth Science, v. 76, p.60–69.
- Briggs, P.H., and Fey, D.L., 1996, Twenty-four elements in natural and acid mine waters by inductively coupled plasma-atomic emission spectrometry, *in* Arbogast, B.F., ed., Analytical methods manual for the Mineral Resources Surveys Program: U.S. Geological Survey Open-File Report 96-525, p. 95–101.
- Bryson, J.R., Ekwurzel, Brenda, and Hoffmann, J.P., 2004, Determination of ground-water flowpaths using stable isotopes as geochemical tracers: Upper and Middle Verde River Watersheds, Arizona, USA: 2004 Annual Meeting, Geological Society of America Abstracts, v. 36, Paper No. 243-3.
- Bullen, T.D., and Kendall, Carol, 1998, Tracing of weathering reactions and water flowpaths: A multi-isotope approach, *in* Kendall, Carol and McDonnell, J.J., eds., Isotope Tracers in Catchment Hydrology: Elsevier, New York, p. 611–646.
- Coleman, M.L., Shepherd, T.J., Durham, J.J., Rouse, J.E., and Moore, G.R., 1982, Reduction of water with zinc for hydrogen isotope analysis: *Anal. Chem.* 54, p. 993–995.
- Craig, Harmon., 1957, Isotopic standards for carbon and oxygen and correction factors for mass spectrometric analysis of carbon dioxide: *Geochim. Cosmochim. Acta.* v. 12, p. 133–149.
- Craig, Harmon, 1961, Isotopic variations in meteoric waters: *Science*, v. 133, p. 1702–1703.
- Coplen, T.B., 1993, Uses of environmental isotopes, *in* Alley, W.M., Regional ground-water quality: New York, Van Nostrand Reinhold, 634 p.
- Coplen, T.B., 1994, Reporting of stable hydrogen, carbon, and oxygen isotopic abundances: *Pure and Applied Chemistry*, v. 66, no. 2. p. 273–276.
- Coplen, T.B., Herczeg, A.L., and Barnes, C.J., 2000, Isotope Engineering—using stable isotopes of the water molecule to solve practical problems, *in* Cook, P.G., Herczeg, A.L., eds., Environmental tracers in subsurface hydrology: Boston, Kluwer Academic Press, p. 70–110.
- Corkhill, E.F., and Mason, D.A., 1995, Hydrogeology and simulation of ground-water flow: Prescott Active Management Area, Yavapai County, Arizona: Arizona Department of Water Resources Modeling Report No. 9, 143 p.
- Dansgaard, W., 1964, Stable isotopes in precipitation: *Tellus*, v. 16, p. 436–468.
- d'Angelo, W.M., and Ficklin, W.H., 1996, Fluoride, chloride, nitrate, and sulfate in aqueous solution by chemically suppressed ion chromatography, *in* Arbogast, B.F., ed., Analytical methods manual for the Mineral Resources Surveys Program: U.S. Geological Survey Open-File Report 96-525, p. 149–153.
- Drever, J.I. 1988, *The geochemistry of natural waters*: Prentice Hall, Englewood, New Jersey, p. 367–381.
- Eastoe, C.J., Gu, Ailiang, and Long, Austin, 2004, The origins, ages, and flow paths of ground water in Tucson Basin: Results of a study of multiple isotope systems, *in* Hogan, J.F., Phillips, F.M., and Scanlon, B.R., eds., Ground-water Recharge in a Desert Environment: The Southwestern United States, American Geophysical Union, Washington, D.C., p. 217–234.
- Emsley, John, 1991, *The Elements*. Second Edition: Oxford University Press, New York, 251 p.
- Ewing, D.B., Osterberg, J.C., and Talbot, W.R., 1994, Big Chino ground-water study: Bureau of Reclamation Technical Report, 3 sections.
- Fritz, P., and Fontes, J.C., 1980, *Handbook of Environmental Isotope Geochemistry*: Elsevier Scientific Publishing Company, New York, v. 1, 545 p.
- Ford, J.R. 2002, Big Chino Valley ground water as the source of the Verde River: *in* Ground Water/Surface Water Interactions, July 1–3, 2002, American Water Resources Association summer specialty conference, 6 p.
- Gehre, M., Hoefling, R., Kowski, P. and Strauch, G., 1996, Sample preparation device for quantitative hydrogen isotope analysis using chromium metal: *Anal. Chem.* 68, p. 4414–4417.
- Hereford, Richard, 1975, Chino Valley Formation (Cambrian?) in northwestern Arizona: Geological Society of America Bulletin, v. 86, p. 677–682.
- Hem, J.D., 1985, Study and interpretation of the chemical characteristics of natural water: U.S. Geological Survey Water-Supply Paper 2254, 263 p.



- Hutcheon, Ian; Bloch, John; de Caritat, Patrice; Shevalier, Maurice; Abercrombie, Hugh; Longstaffe, Fred J.A.F., 1998, What is the cause of potassium enrichment in shales?, *in* Schieber, Juergen; Zimmerle, Winfried; Sethi, Parvinder, S., editors, *Shales and mudstones; II, Petrography, petrophysics, geochemistry, and economic geology*: E.
- Schweizerbart'sche Verlagsbuchhandlung Naegle u. Obermiller, Stuttgart, Federal Republic of Germany, 60 p.
- Ingraham, N.L., 1998, Isotopic variations in precipitation: *in* Kendall, Carol and McDonnell, J.J., ed., *Isotope tracers in catchment hydrology*: Elsevier, New York, Chap. 3, p. 87–118.
- International Atomic Energy Agency, 1994, Environmental isotope data No. 10, World survey of isotope concentration in precipitation (1988–1991): Technical Report Series No. 371, 214 p.
- International Atomic Energy Agency, 2001, Isotope Hydrology Information System. The ISOHIS Database: Vienna, Austria, International Atomic Energy Agency: accessed May 21, 2004 at URL: <http://ioshis.iaea.org>.
- Kalin, R.M., 1994, The hydrogeochemical evolution of the ground water of the Tucson Basin with application to 3-dimensional ground-water flow modeling: University of Arizona (Tucson), Ph.D. thesis, 510 p.
- Kendall, Carol, and Caldwell, E.A., 1998, Fundamentals of isotope geochemistry, *in* Kendall, Carol and McDonnell, J.J., ed., *Isotope tracers in catchment hydrology*: Elsevier, New York, Chap. 3, p. 51–86.
- Knauth, L.P., and Greenbie, Marnie, 1997, Stable isotope investigation of ground-water-surface-water interactions in the Verde River headwaters area: Arizona State University Department of Geology report in fulfillment of Arizona Water Protection Fund Grant #95-001, administered by Arizona Department of Water Resources, 28 p.
- Krieger, M.H., 1965, Geology of the Prescott and Paulden quadrangles, Arizona. U.S. Geological Survey Professional Paper 467, 127 p.
- Krieger, M.H., 1967, Reconnaissance geologic map of the Turkey Creek quadrangle, Yavapai and Coconino Counties, Arizona: U.S. Geological Survey Miscellaneous Geologic Investigations Map 1-501, scale 1:62,000.
- Lamothe, P.J., Meier, A.L., and Wilson, S.A., 1999, The determination of forty four elements in aqueous samples by Inductively Coupled Plasma—Mass Spectrometry: U.S. Geological Survey Open-File Report 99-151, 14 p.
- Lin, J.C., 1996, U-Th,  $^{14}\text{C}$  and Sr isotopic studies of Late Pleistocene hydrological events in Western Great Basin, Nevada and California: Columbia University (New York), 154 p.
- Lucas, L.L., and Unterweger, M.P., 2000, Comprehensive review and critical evaluation of the half-life of tritium: *Journal of Research of the National Institute of Standards and Technology*, v. 105, p. 541–549.
- Muller, A.B., and Mayo, A. L., 1986,  $^{13}\text{C}$  variation in limestone on an aquifer-wide scale and its effects on ground-water  $^{14}\text{C}$  dating models: *Radiocarbon*, v. 28, no. 3, p. 1041–1054.
- Parada, C.B., 1981, Isotopic composition of soil carbon dioxide in the Tucson basin: University of Arizona (Tucson), M.A. thesis, 85 p.
- Pearson, F.J.Jr., and Hanshaw, B.B., 1970, Sources of dissolved carbonate species in ground water and their effects on carbon-14 dating, *in* *Isotope Hydrology, 1970, Proceedings of the International Atomic Energy Association*, p. 271–286.
- Piper, A.M., 1944, A graphic procedure in the geochemical interpretation of water analyses: *American Geophysical Union Transactions*, v. 25, p. 914–923.
- Plummer, L.N., Prestemon, E.C., and Parkhurst, D.L., 1994, An interactive code (NETPATH) for modeling NET geochemical reactions along a flowpath, version 2.0: U.S. Geological Survey Water-Resource Investigations Report 94-4169, 130 p.
- Polach, H., Gower, J., and Fraser, I., 1973, Synthesis of high-purity benzene for radiocarbon dating, *in* Rafter, T.A. and Grant-Taylor, T., eds., *Proceedings of the 8th International  $^{14}\text{C}$  Conference*, v. 1. Wellington, Royal Society of New Zealand, p. B36–B49.
- Potter, P.E., Maynard, J.B., and Pryor, W.A., 1980, *Sedimentology of a Shale: Study guide and reference source*: Springer-Verlag, New York, 306 p.
- Remick, W.H., 1983, Maps showing ground-water conditions in the Prescott Active Management Area, Yavapai County, Arizona—1982. Arizona Department of Water Resources Hydrologic Map Series, Phoenix, Report Number 9.
- Robertson, F.K., 1991, Geochemistry of ground water in alluvial basins of Arizona and adjacent parts of Nevada, New Mexico, and California: U.S. Geological Survey Professional Paper 1406-C, 90 p.
- Schwab, K.J., 1995, Maps showing ground-water conditions in the Big Chino subvalley of the Verde River basin, Coconino and Yavapai Counties, Arizona—1992: Department of Water Resources, Hydrologic Map Series Report Number 28, Phoenix, Arizona, 1 sheet.
- Shaw, D.M., and Sturchio, N.C., 1991, Boron-lithium relationships in rhyolites and associated thermal waters of young silicic calderas, with comments on incompatible element

- behavior: *Geochimica et Cosmochimica Acta*: v. 56, p. 3723–3731.
- SAS Institute, 1998, StatView: Version 5.0.1, Cary, North Carolina.
- Theodórsson, P., 1996, Measurement of weak radioactivity: Singapore, World Scientific, 333 p.
- Tyner, G.N., 1984, Geology and petrogenesis of the Sullivan Buttes latite, Yavapai County, Arizona; field and geochemical evidence: Austin, University of Texas, Ph.D. dissertation, 286 p.
- Van Metre, P.C., Wirt, Laurie, Lopes, T.J., and Ferguson, S.A., 1997, Effects of uranium-mining releases on ground-water quality in the Puerco River Valley, Arizona and New Mexico: U.S. Geological Survey Water-Supply Paper 2476, 73 p.
- U.S. Geological Survey, 1999–2003, Annual Water Resources Data Reports: AZ-99-01, AZ-00-01, AZ-01-01, AZ-02-01, and AZ-03-01.
- Wallace, B. L., and Laney, R. L., 1976, Maps showing ground-water conditions in the lower Big Chino Valley and Williamson Valley areas, Yavapai and Coconino Counties, Arizona—1975–76: U.S. Geological Survey Water Resources Investigations 76-78 Open-File Report, 2 maps.
- Wallick, E.I., 1973, Isotopic and chemical considerations in radio-carbon dating of ground-water within the arid Tucson basin, Arizona: Ph.D. thesis, University of Arizona (Tucson), 184 p.
- Ward, S.A., 1993, Volcanic study of a portion of the Sullivan Buttes latite, Chino Valley, Arizona: Flagstaff, Northern Arizona University, M.S. Thesis, 60 p.
- Water Resources Associates, 1989, Hydrogeology investigation of Big Chino Valley, Yavapai County, Arizona: Phase I, Consultants reports for city of Prescott, City Attorney's Office, Prescott, Arizona, November 29, 1989, 2 volumes.
- Water Resources Associates, 1990, Hydrogeology investigation of Big Chino Valley, Yavapai County, Arizona: Phase II, Consultants reports for city of Prescott, City Attorney's Office, Prescott, Arizona, February 5, 1990, 3 volumes.
- Wilde, F.D., Radtke, D.B., Gibs, J., and Iwatsubo, R.T. (eds.), 1999, National field manual for the collection of water-quality data: Techniques of Water Resources Investigations TWI 09-A4, book 9, chap. A6, sections 6.0, 6.0.1, 6.0.2, 6.0.2.A, and 6.0.2B, 152 p.
- Wirt, Laurie, and Hjalmarsen, H.W., 2000, Sources of springs supplying base flow to the Verde River headwaters, Yavapai County, Arizona: U.S. Geological Survey Open-File Report 99-0378, 50 p.
- Wirt, Laurie, 1993, Isotopic content and water chemistry of ground water that supplies springs in the Verde headwaters, Yavapai, County, Arizona. Paper submitted at the Fifth Annual Symposium of the Arizona Hydrological Society, Sedona, Arizona, September 10-12, 1992.
- Wright, W.E., 2001,  $\delta D$  and  $\delta^{18}O$  in mixed conifer systems in the U.S. Southwest: the potential of  $\delta^{18}O$  in *Pinus ponderosa* tree rings as a natural environmental recorder: Unpublished Ph.D. Dissertation, University of Arizona (Tucson), 328 p.



# Sources of Base Flow in the Upper Verde River

By Laurie Wirt

Chapter F

## **Geologic Framework of Aquifer Units and Ground-Water Flowpaths, Verde River Headwaters, North-Central Arizona**

Edited by Laurie Wirt, Ed DeWitt, and V.E. Langenheim

Prepared in cooperation with the Arizona Water Protection Fund Commission

Open-File Report 2004–1411-F

**U.S. Department of the Interior**  
**U.S. Geological Survey**

**U.S. Department of the Interior**  
Gale A. Norton, Secretary

**U.S. Geological Survey**  
P. Patrick Leahy, Acting Director

U.S. Geological Survey, Reston, Virginia: 2005

For product and ordering information:  
World Wide Web: <http://www.usgs.gov/pubprod>  
Telephone: 1-888-ASK-USGS

For more information on the USGS--the Federal source for science about the Earth, its natural and living resources, natural hazards, and the environment:  
World Wide Web: <http://www.usgs.gov>  
Telephone: 1-888-ASK-USGS

Any use of trade, product, or firm names is for descriptive purposes only and does not imply endorsement by the U.S. Government.

Although this report is in the public domain, permission must be secured from the individual copyright owners to reproduce any copyrighted materials contained within this report.

***Suggested citation:***

Wirt, L., 2005, Sources of Base Flow in the Upper Verde River: *in* Wirt, Laurie, DeWitt, Ed, and Langenheim, V.E., eds., Geologic Framework of Aquifer Units and Ground-Water Flowpaths, Verde River Headwaters, North-Central Arizona: U.S. Geological Survey Open-File Report 2004-1411-F, 34 p.

# Contents

Abstract.....	1
Introduction.....	1
Purpose and Scope .....	4
Acknowledgments .....	5
Environmental Setting and Base-Flow Conditions .....	5
Methods and Approach.....	7
Discharge by Tracer-Dilution Method .....	7
Field Reconnaissance.....	8
Field Activities and Equipment .....	9
Gauge Readings and Current-Meter Measurements.....	9
Tracer-dilution Equipment .....	13
Automatic Samplers.....	13
Synoptic Sampling.....	15
Sample Processing, Analytical Methods, and Analytical Uncertainty.....	15
Results .....	15
Calculated Base Flow.....	15
Accuracy of Discharge Calculations.....	15
Changes in Water Chemistry with Distance Downstream.....	17
Field Parameters .....	17
Major Elements .....	20
Selected Trace Elements.....	23
Hydrogen and Oxygen Stable Isotopes.....	23
Inverse Geochemical Modeling to Determine Mixing Proportions at Upper Verde River Springs .....	26
Summary and Conclusions.....	31
References Cited.....	32

## Figures

<b>F1.</b> Map showing location of tracer-dilution sampling locations, upper Verde River, north-central Arizona.....	2
<b>F2.</b> Photographs showing sources of perennial flow in the upper Verde River at (A) Lower Granite spring, emerging through stream channel one mile upstream from mouth of Granite Creek, and (B) lower end of Stillman Lake showing cattail marsh and natural sediment levee.....	3
<b>F3.</b> Photographs of upper Verde River gaining reach (A) site of tracer injection (VR900) on June 15, 2000, and (B) beaver dam near inflow from large spring (SP1700) emerging in right foreground (north bank), taken in 2004 .....	6
<b>F4.</b> Graph showing diurnal variation in discharge at the USGS streamflow-gauging station near Paulden, Arizona, (09503700) near river mile 10 on June 14–20, 2000 (U.S. Geological Survey, 2000).....	7
<b>F5.</b> Schematic diagram showing mass-balance calculations in a gaining reach of stream with tributary and diffuse ground-water inflows .....	9

<b>F6.</b>	Graph showing relative chloride potential with distance along the tracer reach, which is inversely related to chloride concentration.....	13
<b>F7.</b>	Field notes and graph explaining variations in tracer concentrations versus time at each of three automatic samplers.....	14
<b>F8.</b>	Graph showing discharge calculated from tracer-dilution study versus distance downstream on June 18, 2000 .....	16
<b>F9.</b>	Graphs showing changes in (A) specific conductance, (B) water temperature, and (C) pH versus distance from Granite Creek/Verde River confluence.....	18
<b>F10.</b>	Graphs showing changes in (A) calcium, (B) magnesium, and (C) bicarbonate versus distance from Granite Creek/Verde River confluence.....	19
<b>F11.</b>	Graphs showing changes in saturation indices of (A) CO <sub>2</sub> gas, (B) calcite, and (C) dolomite versus distance from Granite Creek/Verde River confluence .....	21
<b>F12.</b>	Graphs showing changes in (A) chloride, (B) sodium, and (C) sulfate versus distance from Granite Creek/Verde River confluence.....	22
<b>F13.</b>	Graphs showing changes in (A) boron, (B) lithium, and (C) strontium versus distance from Granite Creek/Verde River confluence.....	24
<b>F14.</b>	Graphs showing changes in stable isotopes (left axis) of (A) oxygen, and (B) hydrogen, and base flow (right axis) versus distance from Granite Creek/Verde River confluence.....	25
<b>F15.</b>	Geology map showing the location of selected wells and springs used in inverse geochemical modeling of Big Chino basin outlet flowpath .....	28

## Tables

<b>F1.</b>	Field parameters and chemical analyses of water samples collected during synoptic sampling of the Verde River headwaters, June 17–19, 2000 .....	10
<b>F2.</b>	Chemical composition of selected ground waters from the Verde River headwaters representing the Big Chino basin-fill aquifer, the regional carbonate aquifer (D-C zone and M-D sequence) and upper Verde River springs .....	29
<b>F3.</b>	Saturation indices for mixing endpoints contributing to upper Verde River springs .....	29
<b>F4.</b>	Results of PHREEQC model simulations for mixing at upper Verde River springs.....	30

# Sources of Base Flow in the Upper Verde River

By Laurie Wirt

## Abstract

Base flow in the upper Verde River begins downgradient from Big and Little Chino valleys and the regional carbonate aquifer in three different locations—Stillman Lake, lower Granite Creek, and upper Verde River springs. The relative contribution of inflow from each of three aquifer sources is difficult to directly measure because most of the inflows occur diffusely through the streambed. A tracer-dilution study and synoptic water-chemistry sampling were conducted during low-flow conditions to identify locations of inflows and to determine the relative contribution from major aquifers. Discharge was determined using the analytical concentration of chloride tracer to calculate dilution. Ground-water inflows produced spatial trends in field parameters, major and trace elements, and stable isotopes of hydrogen and oxygen. Last, inverse modeling was used to constrain hypotheses regarding the nature of water-rock interactions and to determine the extent of mixing along the flowpath between the Big Chino aquifer near Paulden and upper Verde River springs.

Base flow at Stewart Ranch was  $19.5 \pm 1.0$  ft<sup>3</sup>/s, compared with  $21.2 \pm 1.0$  ft<sup>3</sup>/s downstream at the Paulden gauge during the same time interval. By subtraction, approximately 7 percent of base flow at the Paulden gauge was contributed downstream from the tracer reach, with some inflows observed in the vicinity of Muldoon Canyon. The Little Chino basin-fill aquifer contributed  $2.7 \pm 0.08$  ft<sup>3</sup>/s, or  $13.8 \pm 0.7$  percent, with upper Verde River springs contributing the remaining 86.2 percent of total base flow at Stewart Ranch. Most of the Little Chino inflow was derived from the Stillman Lake flowpath, as opposed to lower Granite Creek.

Inverse model simulations using the geochemical computer program PHREEQC indicate that discharge to upper Verde River springs upstream from Stewart Ranch is predominantly derived from a mixture of initial water types within lower Big Chino Valley. A small amount of mixing with the Mississippian-Devonian (M-D) sequence north of the Verde River is plausible, although none is required to account for the observed water chemistry. About 10 to 15 percent of discharge to upper Verde River springs is attributed to ground water from the Devonian-Cambrian (D-C) zone of the carbonate aquifer underlying and adjoining the Big Chino basin-fill aquifer near Paulden. Important reactions along the Big Chino basin outlet flowpath include the dissolution of silicate minerals

and degassing of carbon dioxide. Despite extensive contact with limestone, dissolution of carbonate minerals does not appear to be a dominant process along the outlet flowpath. Adjusted contributions from each aquifer source to base flow at the Paulden gauge are estimated as: (a) Little Chino basin-fill aquifer, 14 percent; (b) M-D sequence north of the Verde River, less than about 6 percent; and (c) the combined Big Chino basin-fill aquifer and underlying D-C zone of the carbonate aquifer, at least 80 to 85 percent.

## Introduction

Perennial base flow in the upper Verde River begins downgradient from three aquifers—the Big and Little Chino basin-fill aquifers and the carbonate aquifer north of the Verde River (Mississippian-Devonian, or M-D sequence). Base flow is defined as the sustained low-flow condition of a stream and is derived from ground-water inflow to the stream channel, in contrast to runoff from rainfall or snowmelt. Base flow emerges in three locations in the vicinity of the confluence of Granite Creek and the Verde River, including (a) Stillman Lake, (b) the cienaga in lower Granite Creek referred to in this report as “Lower Granite spring,” and (c) the gaining reach of the Verde River channel downstream from river mi 2.2, referred to here as “upper Verde River springs.” Because the inflows occur diffusely and the precise points of discharge are not always evident, the inflows are difficult to measure directly using a traditional current-meter approach. Consequently, the relative contribution and source(s) of the various inflows (particularly the M-D sequence of the carbonate aquifer) previously have not been well understood, allowing for conflicting interpretations.

Daily mean flow at the U.S. Geological Survey (USGS) streamflow gauging station near Paulden (09503700), which is referred to in this report as the “Paulden gauge” (fig. F1), is about 25 cubic ft per second (ft<sup>3</sup>/s) (1964 through 2003 water years, Fisk and others, 2004). Historically, perennial base flow in the upper Verde River was greater than it is now and began at Del Rio Springs (Wirt, Chapter A, this volume). At present, the first perennial segment of base flow in the Verde River is an impounded reach of river channel intercepting the water table, informally known as Stillman Lake (between river mi 1.0 and 2.0, fig. F1). The lake is dammed by a low levee of stream-deposited sediment upstream from

F2 Sources of Base Flow in the Upper Verde River

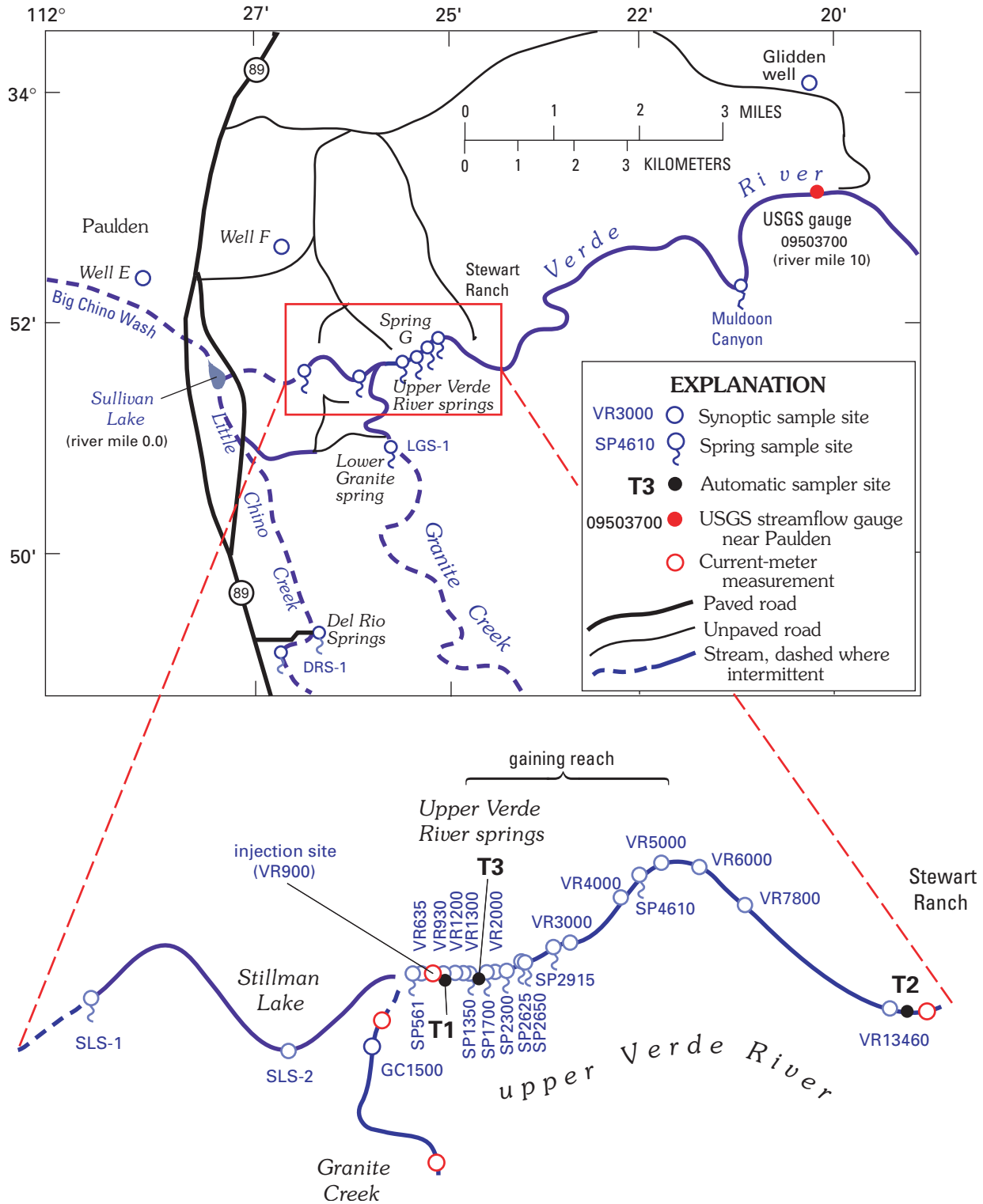


Figure F1. Map showing location of tracer-dilution sampling locations, upper Verde River, north-central Arizona.



the mouth of Granite Creek (fig. F2). A second point of perennial flow begins in lower Granite Creek. In June 2000, base flow in the lowermost mi of Granite Creek peaked at about 0.5 ft<sup>3</sup>/s before seeping into the stream alluvium near its confluence. As interpreted from stable-isotope data and strontium concentrations (Wirt and DeWitt, Chapter E, this volume) and water-level gradients (Wirt and others, Chapter D, this volume), the source of ground water discharging to Stillman Lake and lower Granite Creek is the Little Chino basin-fill aquifer. Below its confluence with Granite Creek, the Verde River was dry for more than more than 600 ft until flow reemerged as a cienaga (fig. F3A). Underflow from Stillman Lake and lower Granite Creek flowed beneath the ephemeral reach, discharging to the upper Verde River near site VR635 (fig. F1).

Downstream from site VR635, base flow in the upper Verde River was permanent and continuous, increasing to about 19 ft<sup>3</sup>/s within the next mi. Most of the gain came from a large, diffuse spring network discharging from the Martin Limestone near river mi 2.2, formerly referred to as “Big Chino Springs” (Wirt and Hjalmarson, 2000) and here as “upper Verde River springs.” Since 2000, beavers have intermittently dammed the Verde River near upper Verde River springs, creating a series of ponds and flooding the major spring outlet (fig. F3). Wirt and DeWitt (Chapter E, this volume) have shown that the water chemistry of upper Verde River springs is consistent with ground water from the Big Chino basin-fill aquifer that has been in contact with rocks in the Devonian Cambrian zone (D-C zone) of the carbonate aquifer. The D-C zone underlies lower Big Chino Valley and also lies between Big Chino Valley and upper Verde River springs. As demonstrated by water-level data (Wirt and others, Chapter D, this volume), the two aquifers are strongly interconnected at the ground-water outlet of the Big Chino basin-fill aquifer near Paulden. An unknown fraction of ground water from the M-D sequence of the carbonate aquifer north of the upper Verde River has been hypothesized to mix with Big Chino ground water before discharging to upper Verde River springs.

Estimates of the relative contribution from the Big Chino basin-fill aquifer to the upper Verde River have been an ongoing source of controversy (Hendrickson, 2000; Dodder, 2004). Wirt and Hjalmarson (2000) estimated that at least 80 percent of the base flow to the upper Verde River springs (formerly referred to as Big Chino Springs) was derived from the Big Chino basin-fill aquifer, with the remaining fraction largely attributed to the Little Chino basin-fill aquifer. Their estimate was based on two independent lines of evidence, namely (1) a mass-balance calculation using  $\delta^{18}\text{O}$  data from a 1991 seepage study (Ewing and others, 1994), and (2) a water-budget approach based on historical base-flow, precipitation, water-level, and water-use data. A separate contribution from the regional carbonate aquifer was not considered because the regional flow gradients were consistent with this interpretation. In addition, there was little water-chemistry information



**Figure F2.** Photographs showing sources of perennial flow in the upper Verde River at (A) Lower Granite spring, emerging through stream channel one mile upstream from mouth of Granite Creek, and (B) lower end of Stillman Lake showing cattail marsh and natural sediment levee. Photographs by Laurie Wirt and Charles Paradzick of the Arizona Game and Fish Department.

available north of the Verde River at the time of that study. In contrast, Knauth and Greenbie (1997) concluded that the major source of discharge to the upper Verde River was the carbonate aquifer north of the upper Verde River. Their interpretation was largely based on similarities between a few samples collected from the upper Verde River and the Glidden well (fig. F1) and the observation that most of the springs in the river canyon emerge from limestone. Subsequent sampling has shown that the stable-isotope results

from the regional carbonate aquifer north of the upper Verde River are more depleted and more variable than those for upper Verde River springs, which more closely resembles the chemistry of ground water at the Big Chino basin outlet near Paulden (Chapter E, this volume, fig. E5). The different conclusions reached by the two studies illustrates that although stable isotopes are useful natural tracers of water sources, a reliance on too few stable-isotope results in the absence of other supporting evidence sometimes will lead to an interpretation that is biased by the low number of samples, a limited distribution of samples, or one that does not fully reflect the full range of possible scenarios.

The goal of this chapter is to more precisely determine the contributions from each aquifer (as opposed to the contributions from a geographical area) to the upper Verde River. At the end of Chapter A in this report, an estimate of the relative contributions from each aquifer to base flow of the upper Verde River was compiled from the results of earlier studies (fig. A16, Chapter A, this volume). This simple water-budget approach suggests that the combined aquifers beneath Big Chino Valley and Big Black Mesa presently contribute about 92 percent of base flow at the Paulden gauge; Little Chino Valley contributes the remainder. Because the budget was compiled from several studies using various approaches, no precision or accuracy could be assigned to this working model. In addition, little information was available for the regional carbonate aquifer north of the upper Verde River between Big Black Mesa and Hell Canyon. This chapter will draw on the geologic and geophysical framework results (Chapters B and C, this volume), the hydrogeology (Chapter D, this volume), and geochemistry data for major aquifers and springs (Chapter E, this volume), to constrain flowpaths and quantify the contribution from specific aquifer units.

In this chapter, synoptic sampling and a tracer-dilution study provide more detailed spatial coverage than earlier studies by Knauth and Greenbie (1997) and Wirt and Hjalmarson (2000). Spatial trends in pH, specific conductance, temperature, major and trace elements, and stable isotopes are evaluated with distance along the gaining reach of the upper Verde River to identify trends (fig. F1). Next, inverse modeling using PHREEQC (Parkhurst and Appelo, 1999) is used to identify major geochemical processes occurring between the Big Chino basin-fill aquifer and the upper Verde River and to determine the degree of potential mixing with the regional carbonate aquifer. The geochemical modeling helps to integrate multiple lines of geochemical evidence and reduce the number of viable nonunique interpretations. Mass-balance estimates of mixing fractions identified by PHREEQC do not rely solely on stable-isotope data to the exclusion of other geochemical results, a problem with earlier interpretations. Moreover, the model results are interpreted in context with the geologic framework and geochemical processes that have been identified along the outlet flowpath.

## **Purpose and Scope**

The objectives of this study are to determine locations of ground-water inflows to the uppermost gaining reach of the Verde River and to quantify the relative contributions from each of the three major aquifers to base flow at Stewart Ranch. The tracer-dilution method (Kimball, 1997; Bencala and others, 1990; Broshears and others, 1993; Kimball and others, 1994) was used to locate and quantify inflows from springs discharging to the Verde River between the mouth of Granite Creek and Stewart Ranch (fig. F1). The study was conducted during low-flow conditions from June 15 to 19, 2000, which is now considered a period of extended drought (Betancourt, 2003). Field reconnaissance measurements of pH, specific conductance, and dissolved oxygen were used to select water-chemistry sampling sites. Multiple lines of geochemical evidence (field parameters, major and trace elements, and stable-isotopes of oxygen and hydrogen) are presented to characterize the inflows, identify their source(s), and indicate where mixing is occurring. Finally, inverse modeling of water-chemistry analyses along the major flowpath from Paulden to upper Verde River springs is used to determine major geochemical processes and the degree of mixing with the M-D sequence.

In this study, the rate of discharge (volume of fluid passing a point per unit of time) was determined using a dilution approach by continuously injecting a saturated sodium-chloride (NaCl) solution into the beginning of the reach until steady-state mixing had occurred throughout, followed by synoptic sampling. In a synoptic study, many discharge measurements are made within a short period, providing a “snapshot” in time. Once the tracer solution reached steady-state conditions, twelve flow-weighted streamflow synoptic samples were collected from a 2-mi reach of the upper Verde River within a 1-hour timeframe. In addition, twelve ground-water inflows were collected from discrete spring inflows along the upper Verde River, from the perennial reach of lower Granite Creek, and from different parts of Stillman Lake over a 3-day timeframe, for a total of 24 water-chemistry samples.

Characterization of the water chemistry of spring inflow data from the synoptic sampling presented in this chapter relies on the characterization of water chemistry of major aquifers, recharge areas, and springs presented earlier in Chapter E (this volume). Chapter E provides a detailed discussion of the water chemistry of the Big and Little Chino basin-fill aquifers as well as that of different areas within the carbonate aquifer. As in Chapter E, the regional carbonate aquifer within the Transition Zone geologic province is subdivided into the Mississippian-Devonian (M-D) sequence north of the upper Verde River and the Devonian-Cambrian (D-C) zone underlying the Big Chino basin-fill aquifer near Paulden. The four D-C zone samples, which are located along the fault-bounded margin of the Big Chino basin-fill aquifer (fig. E1, Chapter E, this volume), do not necessarily represent the water chemistry of the carbonate aquifer underlying the Big Chino basin-fill

aquifer in the middle of Big Chino Valley. The underlying carbonate aquifer is largely unsampled.

## Acknowledgments

This study was funded by the Arizona Water Protection Fund. Land access was granted by the Prescott National Forest and the Arizona Department of Game and Fish. The following local residents graciously granted permission for water-sampling activities: Billy Wells, Harley and Patty Shaw, and Ann Harrington. Field support was provided by David Christiana of the Arizona Department of Water Resources and by Tasha Lewis and Steve Acquafredda of the Department of Hydrology and Water Resources at the University of Arizona. USGS personnel who assisted the author in the field include Ken Leib, Jonathan Evans, Betsy Woodhouse, Owen Baynham, Bert Duet, and Ken Fossum. Most of all, the author is indebted to Pierre Glynn of the USGS for his help with PHREEQC and inverse modeling.

## Environmental Setting and Base-Flow Conditions

Base flow in the upper Verde River begins in three locations—at Stillman Lake, Lower Granite spring, and upper Verde River springs (figs. F1–A3). The geologic setting is a narrow canyon incised up to 250 ft in depth into Paleozoic sedimentary rocks and, in some places, Tertiary basalt. Most Paleozoic carbonate rocks and the Tertiary basalt have moderate to high permeability (Wirt and others, Chapter D, table D1). The Martin Limestone (Devonian) contains abundant northwest-striking high-angle joints near its base, which enhance its overall permeability. Locally, the Martin contains dissolution cavities and other small karst features. The bottom contact of the Martin Limestone is a stratigraphic nonconformity with the underlying Chino Valley Formation (where present) or Tapeats Sandstone. The Tapeats Sandstone (Cambrian) has low permeability, due to its strongly cemented nature. The Chino Valley Formation (Cambrian?), found above the Tapeats, has three units consisting of a lithic sandstone, a pebble conglomerate, and a red shaley dolomite. The Chino Valley is inferred to have low porosity owing to the high clay content of the shale (Chapter D, this volume), but its actual permeability is unknown.

Stillman Lake is an impounded section of channel between river mi 1.0 and 2.0 (fig. F1). The lake is less than 5 ft in depth. The downstream end of the lake terminates in a cattail marsh above the mouth of Granite Creek (fig. F2B and cover photograph). This mile-long curving channel receives occasional runoff whenever runoff overtops the dam at Sullivan Lake during large floods (Chapter A, this volume, fig. A13). The primary source of water in Stillman Lake, however, is ground water rather than surface water. The water level of Stillman Lake varies little between storm runoff events because it intersects the water table (Wirt and others, Chapter D, this volume, fig. D8). Stillman Lake is fed by ground water

from the Little Chino basin-fill aquifer. The lake water has undergone evaporation, based on the enrichment of the stable isotopes of oxygen and hydrogen (Wirt and DeWitt, Chapter E, this volume, fig. E4).

During this study, the upper Verde River was in the third year of a drought and little if any rainfall runoff had overtopped the dam at Sullivan Lake for more than a year (Tadayon and others, 2000 and 2001; MacCormack and others, 2002). The 2000 water year had an annual mean discharge of 22.5 ft<sup>3</sup>/s at the Paulden gauge (16,370 acre-ft/yr), which is the lowest annual discharge on record, as of this writing (MacCormack and others, 2002). This compares closely with the mean base flow of 16,000 acre-ft/yr calculated by Freethey and Anderson (1986) and 18,000 acre-ft/yr calculated by Wirt and Hjalmarson (2000). Both of these earlier studies estimated base flow using a hydrograph separation approach, but for differing time periods of record at the Paulden gauge. Because no runoff occurred in the 2000 water year, hydrograph separation is not required to estimate annual base flow.

A long, straight segment of the lake coincides with what Krieger (1965, pl. 2) mapped as a fault offsetting the Martin Limestone and Tapeats Sandstone or with what may instead be a unconformity between the Martin and Chino Valley Formation. Detailed field mapping is needed to determine the precise nature of this contact. Near the mouth of Granite Creek, the Chino Valley is a slope-forming unit that consists of thin alternating layers of sandstone, conglomerate, and a shaley dolomite (Hereford, 1975). Before being recognized as a separate unit, the Chino Valley was mapped as part of the Tapeats by Krieger (1965). The Chino Valley Formation, where present, lies between the Tapeats and the Martin.

Perennial flow in lower Granite Creek emerges from the stream channel about 1 mi upstream from the mouth near two small faults in the lower Paleozoic strata (Krieger, 1965, Plate 2). The spring is shown on U.S. Geological topography maps and is referred to informally in this report as “Lower Granite spring” or site LGS-1 (figs. F1–F2). Several large cottonwood trees grow west of the spring in a low-lying area between the two faults, indicating a high water table. Also, a large cottonwood tree grows east of the spring along the same trend, suggesting preferred availability of ground water along this orientation. Based on the geochemical evidence, the source of base flow in Granite Creek (as well as Stillman Lake) has been linked to the Little Chino basin-fill aquifer (Wirt and DeWitt, Chapter E, this volume). Parts of lower Granite Creek are a cienaga. Base flow in lower Granite Creek has been measured at 0.55 ft<sup>3</sup>/s in 1977 (Owen-Joyce and Bell, 1983), estimated at <0.5 ft<sup>3</sup>/s in 1991 (Boner and others, 1991, Ewing and others, 1994), and measured by Parshall flume at 0.13 ft<sup>3</sup>/s in 1996 (Knauth and Greenbie 1997). These data were collected by different parties at different times and locations. In this study, the flow in lower Granite Creek was measured twice at 0.5 ft<sup>3</sup>/s in two different locations. The quantity of underflow through alluvium flowing beneath lower Granite Creek is unknown, but probably is small because bedrock is shallow.

## F6 Sources of Base Flow in the Upper Verde River

Base flow in lower Granite Creek varies substantially in response to seasonal and temporal changes. In June 2000, diurnal changes in flow were relatively large owing to the small amount of stream discharge and large degree of evapotranspiration. In gaining and losing segments, much of the streamflow disappeared entirely during the heat of the day and reappeared at night and through the early morning. This especially was the case near its confluence with the Verde River canyon, which is a losing reach. Here, the precise point where streamflow disappeared into the loose, sandy gravel moved up and down the alluvial channel above the mouth of Granite Creek by more than 50 ft over the course of the day. During the cooler months, perennial flow in Granite Creek was considerably greater than in the summer and typically extended beyond the confluence to join perennial flow in the upper Verde River below Stillman Lake—presumably, in part, because riparian plants are less active during the winter, and less water is lost to evapotranspiration.

Downstream from the mouth of Granite Creek, the upper Verde River was dry throughout 1999–2001. In June 2000, the dry reach of the upper Verde River below the confluence extended 560 ft downstream from the natural sediment levee below Stillman Lake. From mi 2.1 onward, flow in the Verde River was permanent and continuous. Discharge increased to about 19 cubic ft per second ( $\text{ft}^3/\text{s}$ ) before reaching Stewart Ranch (Knauth and Greenbie, 1997; Wirt and Hjalmarson, 2000; and this study). Most of the gain occurred downstream from a large, unnamed spring (site SP1700; fig. F3B) that emerged on the north bank through Martin Limestone. Much of the inflow occurred diffusely through the streambed and could not be sampled directly.

Base flow in the upper Verde River, as in lower Granite Creek, is strongly influenced by evapotranspiration. During the tracer experiment, daily discharge at the USGS streamflow-gauging station near Paulden (station number 09503700; river mi 10) ranged from 19 to 21  $\text{ft}^3/\text{s}$  with a diurnal range of 2  $\text{ft}^3/\text{s}$ , or ten percent of the maximum daily flow occurring about every 12 hours (fig. F4). The daily peak at the Paulden gauge occurred each morning between 0400 and 1200 hours, based on pressure-transducer recordings at 15-minute intervals. The lowest discharge occurred between 1600 and 2400 hours in the evening. The timing of the peak and trough at the Paulden gauge lags a few hours behind what was observed 6 to 8 mi upstream in the study reach.

Near site VR635 at the beginning of the study reach (fig. F1), the highest observed flows occurred around daybreak (before 0700 AM) and the lowest flows were observed in the late afternoon following the hottest part of the day (after about 1700 PM until midnight). At daybreak, streamflow began more than 60 ft upstream from site VR635 near site VR561 and the discharge was visibly greater than that observed later in the day. Similarly, the flow in lower Granite Creek extended about 50 ft further downstream towards the confluence with the upper Verde River canyon in the morning than it did in the afternoon. These observations correspond with air temperature and photosynthesis activity of riparian



**Figure F3.** Photographs of upper Verde River gaining reach (A) site of tracer injection (VR900) on June 15, 2000, and (B) beaver dam near inflow from large spring (SP1700) emerging in right foreground (north bank), taken in 2004. Most ground-water inflows are diffuse and emerge through the streambed or are hidden by dense vegetation on either bank. Photographs by David Christiana and Charles Paradzick, respectively.

vegetation along the stream corridor. Based on these field observations, it was evident that synoptic samples needed to be collected as quickly as possible in order to minimize effects of diurnal changes in base flow.

The degree of evapotranspiration is related to the amount of upstream riparian vegetation at any given point along the stream. In general, the canyon and floodplain are narrow and the vegetation consisted of willow, cottonwood, mesquite, and mixed broadleaf plants (figs. F2 and F3). Using the integration method, Anderson (1976) calculated the annual consumptive

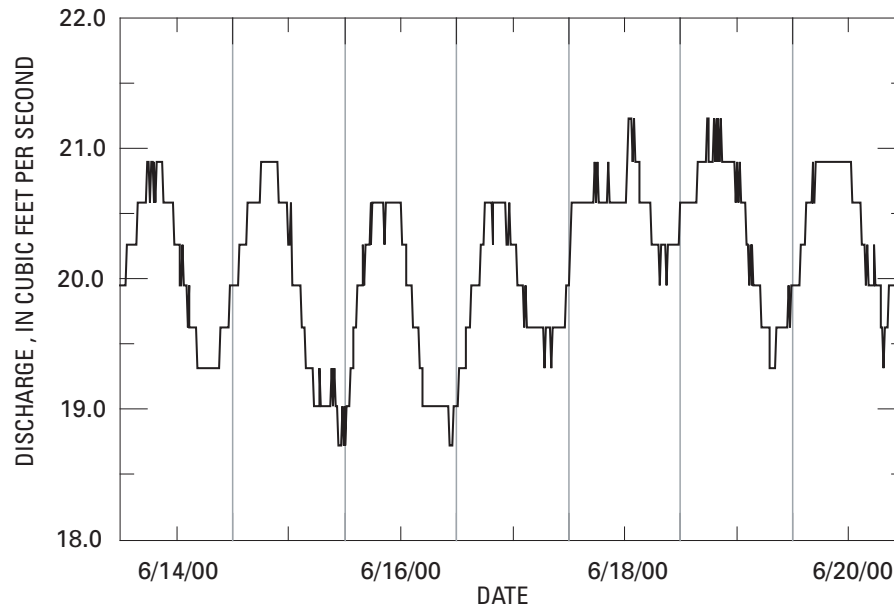


**Figure F4.** Graph showing diurnal variation in discharge at the USGS streamflow-gauging station near Paulden, Arizona, (09503700) near river mile 10 on June 14–20, 2000 (U.S. Geological Survey, 2000). Pressure-transducer data recorded every 15 minutes ( $\text{ft}^3/\text{s}$ ). Peak of diurnal flow occurred between 0400 and 1200 AM. Trough occurred between 1600 and 2400 PM.

use by riparian vegetation upstream from the Paulden gauge to be 600 acre-ft/yr over an area of 384 acres. This is equivalent to an average of 2.2 acre-ft per acre. Based on field observations, the occurrence of riparian vegetation and aquatic plants was denser in gaining reaches than in non-gaining reaches. For example, the presence of algal strands and nonnative water-cress growing on stream substrate was an excellent indicator of spring flow. Also, the wet part of the stream tended to be wider in marshy areas having seepage. From year to year, the density of trees and vegetation probably changes as a consequence of damage from large floods and beaver activity. Changes in vegetation could have a measurable effect on the amount of base flow lost to evapotranspiration.

## Methods and Approach

### Discharge by Tracer-Dilution Method

Dilution of a continuously injected chemical tracer provides a more accurate means to measure discharge than other methods in less-than-ideal stream cross sections. Current-meter measurements work well where the channel bottom and banks are smooth. They tend to be less accurate where the channel is irregular owing to large boulders or thick aquatic

vegetation, or where a large fraction of flow moves beneath the stream through what is known as the hyporheic zone (Ben-cala and others, 1990). Traditional measurements of discharge can thus miss a substantial percentage of the flow (Kimball, 1997; Kimball and others, 2000). In the upper Verde River, the marshy banks and vegetated stream bottom create wide, shallow cross sections with numerous obstructions, making it difficult to accurately measure flow using a current meter. Hyporheic flow probably is not an important issue within a gaining reach but could be important in other nongaining reaches further downstream. Another advantage of the tracer method is that synoptic samples can be collected much faster than it takes to complete the same number of current-meter measurements, allowing many discharge estimates to be made in a short timeframe over a long reach.

The choice of tracer generally is limited to anions (which tend to stay in solution) such as chloride, bromide, and sulfate, and to some organic dyes (Zellweger, 1996). Chloride was chosen for the tracer based on presynoptic data for the upper Verde River indicating that natural levels of chloride were low and varied little over the stream reach (Boner and others, 1991). Chloride is nontoxic and has little effect on the stream environment at low concentrations. Ninety-nine percent pure NaCl, obtained locally in a 50-lb sack as stock salt, was used to make the tracer solution because it was inexpensive and locally available.

## F8 Sources of Base Flow in the Upper Verde River

In the tracer-dilution approach, discharge is determined by adding a known quantity of salt tracer, such as NaCl, to a stream. Discharge is calculated by measuring the amount of dilution that occurs as the tracer moves downstream (Kimball, 1997). This technique is illustrated in figure F5 and described by the following mass-balance equation:

$$Q_s = \left( \frac{C_{INJ} Q_{INJ}}{C_B - C_A} \right) \quad (1)$$

where:

- $Q_s$  = stream discharge, in cubic ft per second;
- $C_{INJ}$  = tracer concentration in the injection solution, in mg/L;
- $Q_{INJ}$  = rate of tracer injection to the stream, in cubic ft per second;
- $C_B$  = tracer concentration downstream from injection point, in mg/L; and
- $C_A$  = tracer concentration upstream from injection point, in mg/L.

Streamflow discharge can be calculated at any site downstream from the injection site by using the instream tracer concentration and the concentration and injection rate of the tracer. Adjustment was made for the changes in chloride concentration from major sampled inflows as follows:

$$Q_F = Q_D \left( \frac{C_D - C_E}{C_F - C_E} \right) \quad (2)$$

where:

- $Q_F$  = stream discharge downstream from ground-water inflow, in cubic ft per second;
- $Q_D$  = stream discharge upstream from ground-water inflow, in cubic ft per second;
- $C_D$  = in-stream concentration of chloride upstream from ground-water inflow, in mg/L;
- $C_E$  = background concentration of chloride of ground-water inflow, in mg/L; and
- $C_F$  = in-stream concentration of chloride downstream from ground-water inflow, in mg/L.

Inflows include visible spring inflows that can be sampled directly and diffuse seeps in the form of ground-water discharge through the streambed that cannot be sampled directly. The magnitude of each inflow can be determined by the difference in streamflow between the mainstem sites immediately downstream and upstream from the inflow. Corrections were made for the background chloride in unsampled inflows by adjusting for sampled inflows upstream and downstream from diffuse inflows. The term “background” refers here to the amount of chloride that occurs naturally in local ground water (see fig. E3, Chapter E, this volume).

The dilution method assumes that mixing of the tracer is rapid and uniform, that the behavior of the tracer is

conservative, that no stream losses occur, and that background chloride concentrations from tributaries and inflows are less than the injected tracer concentrations. The term “conservative” is used to describe elements that are unlikely to undergo geochemical reactions or sorption. The method works best when conditions are constant or steady state; however, the method still can be applied when discharge is rising or falling—such as from diurnal changes in evapotranspiration, or runoff events from storms—if all tracer-dilution samples are obtained within a short timeframe by synoptic sampling. Synoptic samples are collected using flow-weighted sampling protocol (Shelton, 1994), to further ensure that tracer concentrations are representative of well-mixed conditions.

## Field Reconnaissance

In the 2 days preceding the synoptic sampling, detailed field reconnaissance was conducted in order to select the synoptic water-chemistry sample sites (fig. F1). The study benchmark was located at the natural sediment dam at the lower end of Stillman Lake. All taped distances were measured relative to this point. The study reach was measured and flagged by stretching a 200-ft tape measure along the thalweg or center of the stream. Latitude and longitude locations were determined by using a hand-held global positioning system (GPS); however, the steepness of the canyon walls limited the accuracy of those horizontal measurements to within 50 ft. Consequently, taped distances were deemed more accurate.

Field parameters were measured at 100–200 ft intervals in the first 2,200 ft below the benchmark and at 1,000–2,000 ft intervals thereafter (table F1). The greater frequency of measurements in the upper part of the tracer reach corresponds with the area having the greatest gain in discharge. Station numbers were assigned according to the taped distance downstream from the downstream end of Stillman Lake and the type of site. For example, site VR635 (which is the first point of seepage on the Verde River) is 635 ft downstream from the study benchmark at the center of the natural dam at Stillman Lake. Similarly, site SP1700 is a discrete spring outside the flowing river channel that is 1,700 ft downstream from the study benchmark.

Synoptic sample sites were chosen to bracket known springs in order to obtain discharge values above and below each inflow and to closely bracket unobserved inflows in the gaining reach. In reaches where no visible inflows were present, changes in pH, water temperature, specific conductance, and dissolved oxygen data were used as guides for selecting sample sites. These field reconnaissance measurements are presented in the “Results” section. Most discrete spring samples in the study reach were collected and processed immediately following the synoptic sampling. Samples from major springs and tributaries did not have to be collected at precisely the same time as the synoptic stream sampling because the water chemistry of these inflows was not potentially affected

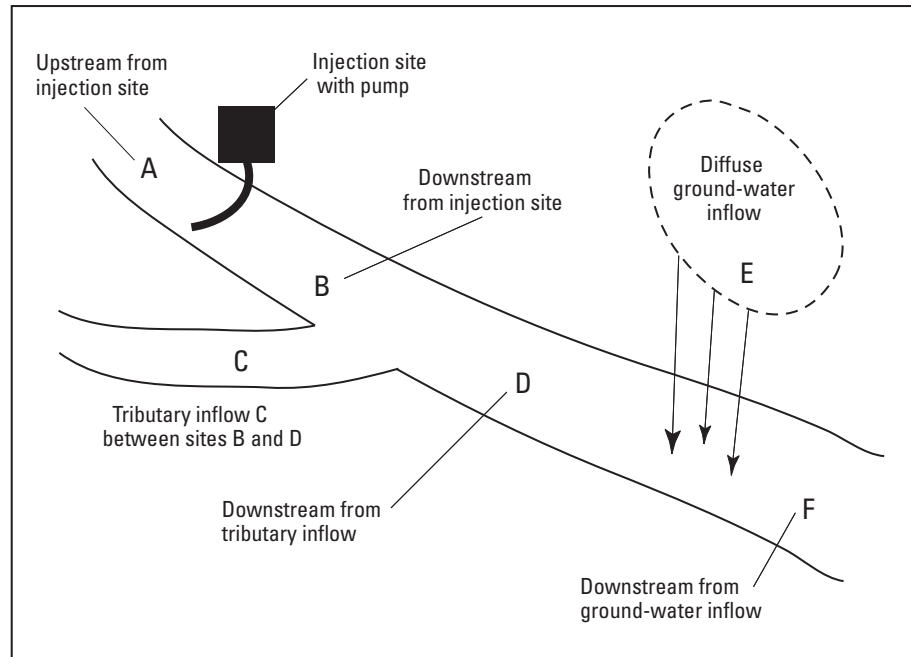


**Figure F5.** Schematic diagram showing mass-balance calculations in a gaining reach of stream with tributary and diffuse ground-water inflows. Diagram modified from Kimball and others (2000) to illustrate equations 1.0 and 2.0.

by diurnal variations in instream mixing. Samples from Del Rio Springs, Granite Creek, and Stillman Lake were collected from June 15–17, 2000.

After the injection of tracer solution had started, an ion-selective chloride probe was used to monitor relative changes in the tracer concentration with distance along the study reach (fig. F6). The relative potential is measured by the probe in millivolts and the value is inversely proportional to the amount of chloride present. Results from the selective-ion probe were used to determine the arrival time of the tracer at the end of the reach and to evaluate the degree of mixing of the tracer with distance through the reach. In addition, stream velocities were measured in the study reach by current meter. These values, ranging between 0.5 and 1.5 ft/s, also helped to predict arrival times of the tracer at the lower end of the reach.

The data from the selective ion probe were not used to calculate discharge because the analytical approach is more accurate for this purpose. The relative chloride potential measurements indicated rapid dilution of the chloride tracer between the injection point and site VR2000 before stabilizing within a narrow range (fig. F6). Because measurements were made at different times during the day, the variation in relative chloride potential values between sites VR6000 and VR13460 (fig. F1) is attributed largely to diurnal variations in flow. The reconnaissance measurements were collected by two teams over a 2-day period. Graphing these data in the field assisted in selection of synoptic sample sites.

## Field Activities and Equipment

Field activities and equipment described in this section include (a) continuous gauge readings and current-meter measurements, (b) the setup and operation of tracer injection equipment, (c) the setup and application of automatic samplers, and (d) synoptic sampling.

## Gauge Readings and Current-Meter Measurements

Stage readings at the Paulden gauge and manual current-meter measurements provided a means to estimate the concentration of tracer needed, as well as an independent cross check of discharge determined by tracer dilution. Although 6 mi downstream from Stewart Ranch, readings from the Paulden gauge helped to predict the timing and range of diurnal fluctuations. Discharge in the study reach was measured using an AA current meter as described by Rantz and others (1982a and 1982b). In order to improve the accuracy of the current-meter measurements, the cross-sectional shape of the channel was improved by removing aquatic vegetation and channeling the flow with a shovel. Equation 1 was used to estimate the concentration of injectate ( $C_1$ ) needed for the entire reach, based on the values for discharge ( $Q_s$ ) at the downstream end of the study reach (site

**Table F1.** Field parameters and chemical analyses of water samples collected during synoptic sampling of the Verde River headwaters, June 17-19, 2000. [ $\mu\text{S}/\text{cm}$ , microsiemens per centimeter; ND, not determined;  $\text{mg}/\text{L}$ , milligrams per liter;  $\mu\text{g}/\text{L}$ , micrograms per liter;  $\delta$ , del; \*, estimated]

Lab no.	Field ID	Site description and comments	Distance <sup>1</sup> (ft)	Date <sup>2</sup>	Time	Latitude (34°)	Longitude (112°)	GPS error (ft)
C-172501	FB-00	Field blank using deionized water from USGS laboratory		06/18/2000	0000	ND	ND	ND
C-172522	DRS-1	Del Rio Spring; collected upstream from southernmost culvert along main dirt road	ND	06/19/2000	1035	49.190	26.730	+18
C-172523	LGS-1	Lower Granite Creek Spring; north of large cottonwood grove; north bank near large fallen log	-5,000	06/17/2000	1115	51.020	25.449	+9.2
C-172524	SLS-1	Stillman Lake Spring; uppermost end of lake from small disconnected spring-fed pool	-4,000	05/07/2000	0930	51.530	26.267	+78
C-172525	SLS-2	Stillman Lake Spring; small pools were dry; sampled from uppermost end of lake; lots of algae	-4,000	06/17/2000	1400	51.530	26.267	+78
C-172502	SP561	Dry channel, ground-water sample from hand-dug pit in streambed	561	06/18/2000	0920	51.822	25.830	+410
C-172503	VR635	First standing water in Verde River channel amidst thick stand of aquatic and riparian plants	635	06/18/2000	0915	51.832	25.838	+29
C-172504	VR930	Verde River sample collected from well-defined channel with measurable current	920	06/18/2000	0910	51.877	25.793	+370
C-172505	VR1200	Verde River 1,200 ft downstream from confluence; gaining reach	1,200	06/18/2000	0900	51.914	25.750	+46
C-172506	VR1300	Verde River 1,300 ft downstream from confluence; gaining reach	1,300	06/18/2000	0917	51.914	25.728	+29
C-172507	SP1350	Spring-fed pool near south bank of Verde River; 3 X 6 X 2 ft in size; low dissolved oxygen	1,430	06/18/2000	0905	51.917	25.709	+44
C-172521	SP1700	Largest flowing spring emerging from Martin Limestone, north edge of canyon near overhead power line	1,700	06/17/2000	1610	51.550	25.800	+7.8
C-172508	VR2000	Verde River 2,000 ft downstream from confluence; below inflow from largest spring; gaining reach	2,000	06/18/2000	0905	51.913	25.623	+380
C-172509	SP2300	Large spring-fed pond on south edge of canyon at base of canyon wall; about 70 X 30 X 5 ft in size	2,300	06/17/2000	1535	51.915	25.589	+45
C-172510	SP2625	Flowing spring on north edge of stream channel, emerging from aquatic plants	2,625	06/18/2000	1050	51.925	25.528	+34
C-172511	SP2650	Flowing spring on south edge of stream channel	2,650	06/18/2000	1100	51.916	25.536	+56
C-172512	SP2915	Flowing spring on north edge of stream channel, emerging from aquatic plants	2,915	06/18/2000	1110	51.926	25.489	+55
C-172513	VR3000	Verde River 3,000 ft downstream from confluence	3,000	06/18/2000	0900	51.946	25.487	+29
C-172514	VR4000	Verde River, 4,000 ft downstream from confluence; near mouth of "Greenbie Gulch"	4,000	06/18/2000	1000	51.985	25.365	+27
C-172515	SP4610	South side of channel, small seep at upstream end of small shallow inlet; sampled with dipper	4,610	06/18/2000	1030	52.015	25.283	+33
C-172516	VR5000	Verde River 5,000 ft downstream from confluence	5,000	06/18/2000	0950	52.025	25.235	+31
C-172517	VR5000	Duplicate sample	5,000	06/18/2000	0950	52.025	25.235	+31
C-172518	VR6000	Verde River 6,000 ft downstream from confluence	6,000	06/18/2000	0940	52.033	25.097	+31
C-172519	VR7800	Verde River 7,000 ft downstream from confluence	8,000	06/18/2000	0930	52.091	24.875	+42
C-172520	VR13460	Verde River at Stewart Ranch 13,460 ft downstream from confluence, near gate in fence	13,660	06/18/2000	0900	52.080	24.019	+36
C-220225	MDN-1	Unnamed spring on north bank of Verde River near mouth of Muldoon Canyon, river mile 8	ND	05/16/2003	0200	86.710	35.450	+40



**Table F1.** Field parameters and chemical analyses of water samples collected during synoptic sampling of the Verde River headwaters, June 17-19, 2000. (Continued)[ $\mu\text{S/cm}$ , microsiemens per centimeter; ND, not determined; mg/L, milligrams per liter;  $\mu\text{g/L}$ , micrograms per liter;  $\delta$ , del; \*, estimated]

Lab no.	Field ID	Dissolved oxygen (mg/L)	pH	SC ( $\mu\text{S/cm}$ )	T	$\text{HCO}_3$ (mg/L)	Alkalinity (Lab)	Alkalinity (Field)	Dis-charge <sup>3</sup> (ft <sup>3</sup> /s)	Cl <sup>4</sup> (mg/L)	Ca (mg/L)	Mg (mg/L)	Na <sup>4</sup> (mg/L)	F (mg/L)	NO <sup>3</sup> (mg/L)
C-172501	FB-00	--	--	--	--	--	--	--		<1.2	<0.1	<0.1	<0.1	<0.08	<0.35
C-172522	DRS-1	5.55	7.55	345	18.5	151	123	124	ND	18.5	46	21	21	0.5	6.2
C-172523	LGS-1	2.48	7.30	458	18.9	226	253	185	ND	20.8	48	22	20	0.5	4.6
C-172524	SLS-1	0.83	6.84	546	15.2	293	245	240	ND	20.7	56	24	21	0.4	1.3
C-172525	SLS-2	5.87	8.13	454	28.0	251	157	206	ND	14.5	87	40	9.2	0.4	<0.35
C-172502	SP561	0.88	6.00	570	22.2	305	259	250	0.05*	<b>31.9</b>	64	25	<b>29</b>	0.4	0.6
C-172503	VR635	0.54	5.99	523	12.1	305	244	250	0.5*	20.4	52	22	21	0.4	<0.35
C-172504	VR930	4.50	6.90	451	17.0	238	197	190	1.0	<b>76.4</b>	46	20	<b>62</b>	0.4	2.9
C-172505	VR1200	3.06	7.17	439	19.5	229	190	187	2.3	<b>45.0</b>	40	18	<b>37</b>	0.4	4
C-172506	VR1300	10.13	7.48	439	19.7	244	193	200	2.7	<b>41.5</b>	40	18	<b>36</b>	0.4	4.1
C-172507	SP1350	0.97	7.40	598	20.4	354	284	290	ND	22.5	62	26	37	0.4	<0.35
C-172521	SP1700	6.87	7.41	552	19.8	285	--	234	0.5*	23.9	30	16	17	0.5	4.1
C-172508	VR2000	8.44	7.16	484	20.9	256	212	210	5.4	<b>29.7</b>	42	20	<b>37</b>	0.5	4.7
C-172509	SP2300	2.23	7.08	557	25.0	293	--	240	ND	20.0	43	23	46	0.5	1.3
C-172510	SP2625	5.72	7.06	579	21.1	305	240	250	ND	19.3	45	22	44	0.5	5.6
C-172511	SP2650	6.25	7.30	584	20.0	329	260	270	ND	19.4	42	21	44	0.5	5.9
C-172512	SP2915	0.57	6.88	663	24.7	354	293	290	ND	22.8	46	23	47	0.5	<0.35
C-172513	VR3000	5.39	7.00	553	21.1	281	198	230	13.8	<b>23.3</b>	43	21	<b>40</b>	0.5	5
C-172514	VR4000	7.83	7.06	596	21.7	334	260	270	13.7	<b>23.4</b>	44	22	<b>48</b>	0.5	5
C-172515	SP4610	1.16	7.33	642	21.4	354	303	290	ND	22.5	53	26	60	0.5	2.4
C-172516	VR5000	7.16	7.04	634	22.2	390	283	320	19.7	<b>23.9</b>	49	24	<b>57</b>	0.5	5
C-172517	VR5000	--	--	--	--	--	--	--	19.3	<b>24.0</b>	49	24	<b>58</b>	0.5	5
C-172518	VR6000	7.44	7.53	634	22.4	329	263	270	21.3	<b>23.7</b>	51	26	<b>61</b>	0.6	4.6
C-172519	VR7800	9.32	7.85	637	24.5	354	286	290	18.6	<b>24.1</b>	48	24	<b>57</b>	0.5	4.4
C-172520	VR13460	7.81	8.14	637	25.1	348	256	285	19.5	<b>23.8</b>	44	22	<b>59</b>	0.5	4.2
C-220225	MDN-1	4.40	6.80	704	18.2	330	--	270	<1*	<b>23.0</b>	0.5	25	<b>57</b>	0.5	<0.08

**Table F1.** Field parameters and chemical analyses of water samples collected during synoptic sampling of the Verde River headwaters, June 17-19, 2000. (Continued)

[µS/cm, microsiemens per centimeter; ND, not determined; mg/L, milligrams per liter; µg/L, micrograms per liter; δ, del; \*, estimated]

Lab no.	Field ID	SO <sub>4</sub> (mg/L)	Si (mg/L)	K (mg/L)	Al (µg/L)	As (µg/L)	B (µg/L)	Ba (µg/L)	Fe (µg/L)	Li (µg/L)	Mn (µg/L)	Sr (µg/L)	V (µg/L)	δ <sup>18</sup> O per mil	δD per mil
C-172501	FB-00	<1.6	<0.1	<0.1	<10	<100	14	<1	<50	<10	<10	<1	<10	--	--
C-172522	DRS-1	14	16	2.4	0.83	11	41	8.7	15	<10	14	500	15	-10.1	-72
C-172523	LGS-1	13	20	2.9	7.8	16	81	31	22	12	28	620	11	-9.7	-70
C-172524	SLS-1	15	18	3.8	8.2	12	80	170	61	17	260	540	<10	-8.7	-66
C-172525	SLS-2	13	16	2.5	3.6	6.7	70	92	44	15	1100	560	<10	-8.3	-65
C-172502	SP561	21	17	4.1	<10	<100	80	160	<50	17	780	650	17	-9.5	-69
C-172503	VR635	11	16	2.7	<10	<100	74	81	<50	<10	480	540	<10	--	--
C-172504	VR930	12	18	3	<10	<100	77	40	<50	15	12	480	12	-9.8	-71
C-172505	VR1200	12	18	2.8	<10	<100	82	32	<50	17	<10	410	12	-10.1	-72
C-172506	VR1300	12	19	2.8	<10	<100	85	32	<50	18	<10	410	12	-10.1	-72
C-172507	SP1350	5.8	30	5.3	1.6	13	150	95	82	27	320	560	<10	-9.2	-69
C-172521	SP1700	15	20	3	16	19	200	45	35	36	<10	390	13	-10.3	-75
C-172508	VR2000	13	20	2.9	<10	<100	120	38	<50	24	<10	410	13	-10.2	-73
C-172509	SP2300	14	13	4	4.8	17	200	49	30	39	18	380	<10	--	--
C-172510	SP2625	14	20	3	6.1	20	210	47	28	39	<10	380	13	-10.4	-75
C-172511	SP2650	14	19	2.8	7.4	21	200	45	28	37	<10	360	12	-10.4	-75
C-172512	SP2915	13	20	6.2	2.4	29	200	57	65	39	540	400	<10	-10.3	-74
C-172513	VR3000	13	20	2.9	<10	<100	170	41	<50	31	<10	400	13	-10.3	-74
C-172514	VR4000	14	19	3.1	<10	<100	210	47	<50	39	<10	380	12	-10.3	-74
C-172515	SP4610	16	21	3.3	8.6	29	270	60	34	49	11	440	13	-10.4	-75
C-172516	VR5000	15	20	3.2	<10	<100	250	52	<50	47	<10	390	12	-10.3	-75
C-172517	VR5000	15	20	3.3	<10	<100	240	53	<50	47	<10	410	13	--	--
C-172518	VR6000	15	21	3.4	<10	<100	260	55	<50	49	<10	430	13	-10.4	-75
C-172519	VR7800	15	19	3.2	<10	<100	240	52	<50	47	<10	390	12	-10.5	-74
C-172520	VR13460	15	20	3.2	<10	<100	250	55	<50	48	<10	420	12	-10.5	-75
C-220225	MDN-1	23	19	2.6	0.71	26	260	110	40	41	12	380	0.8	-10.0	-74.0

<sup>1</sup>Distance is the distance in feet downstream from the confluence with Granite Creek as defined by the center of the natural dam at Stillman Lake.

<sup>2</sup>Field parameters collected during field reconnaissance June 14-17, 2000.

<sup>3</sup>Calculated using chloride concentration, except where indicated by asterisks.

<sup>4</sup>Bold value indicates stream sample was downstream from the injection site (non-background).

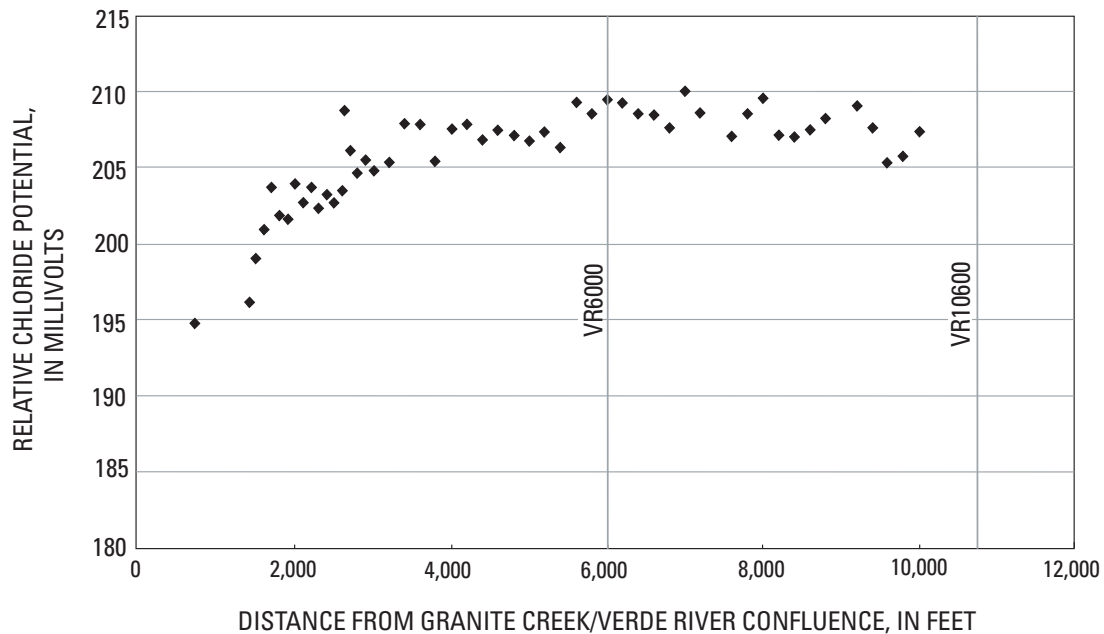


**Figure F6.** Graph showing relative chloride potential with distance along the tracer reach, which is inversely related to chloride concentration. In order to monitor the distribution of the chloride tracer, measurements of relative chloride potential were made using a selective-ion probe over a three-day timeframe. Variations in chloride distribution are related to the degree of mixing and to diurnal variations in discharge.

VR13640 at Stewart Ranch on June 13, 2000) and predetermined concentrations of chloride in the upper Verde River ( $C_A$  and  $C_B$ ) from an earlier seepage study (Boner and others, 1991). Current-meter measurements were made at the beginning and end of the study reach (sites VR930 and VR13460) and at two sites in lower Granite Creek with good channel control that were outside of the tracer reach. Discharge from Stillman Lake could not be determined using a current meter because the velocity of the lake current was too slow.

## Tracer-dilution Equipment

To prepare the tracer solution, granular NaCl was mixed with streamwater to saturation level several hours before the injection. A 500-gallon nalgene tank and thirty-five 50-lb bags of stock salt were shuttled to the injection site using an all-terrain vehicle. Small batches of injectate solution were premixed in a 55-gallon reservoir with a canoe paddle until the solution reached saturation and then transferred as needed to keep the larger reservoir tank filled. An excess of undissolved NaCl always was present in the bottom of the larger reservoir to maintain a state of saturation and the tank was periodically stirred. Injectate samples were collected throughout the tracer study to verify that the concentration of the solution remained fairly constant.

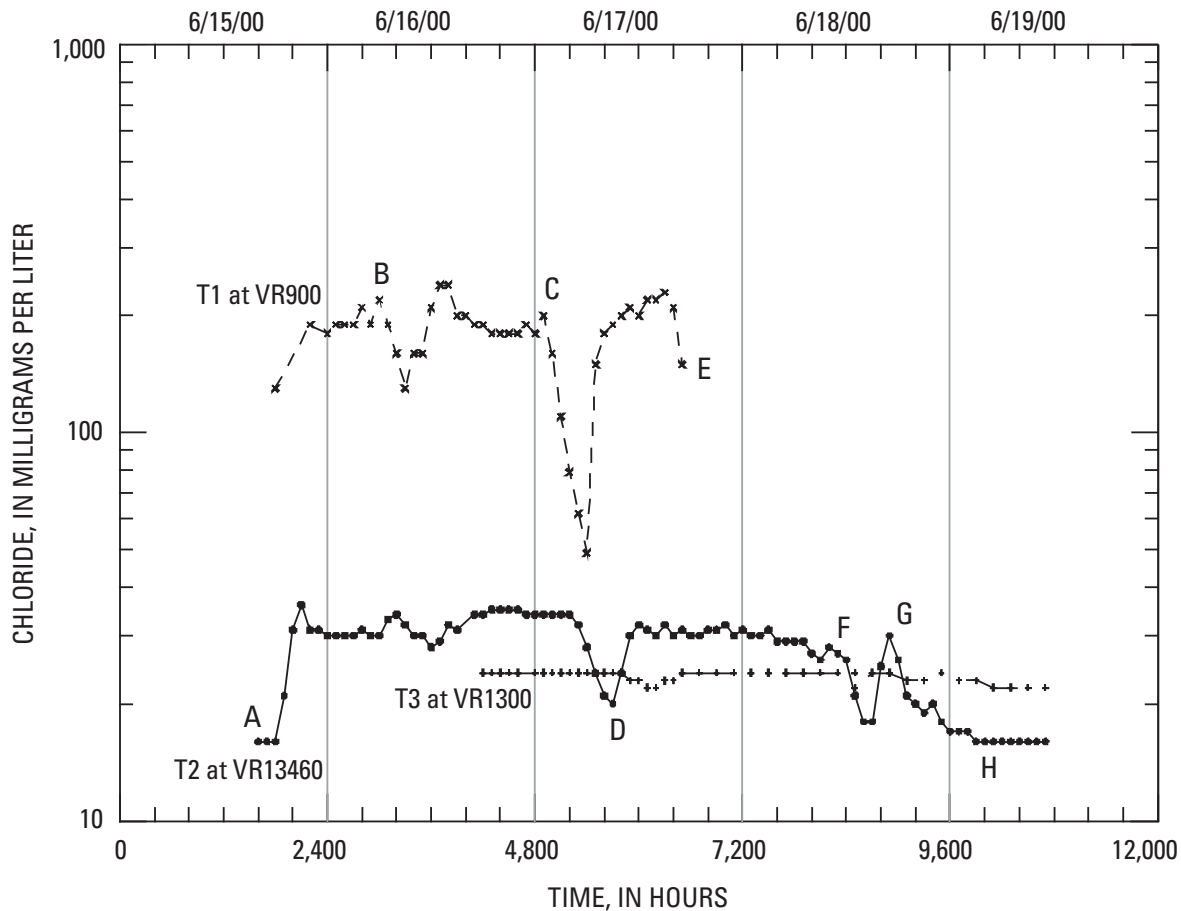
The injection apparatus consisted of a piston-core pump driven by an electric motor that was powered by a deep-cell

marine battery. Tracer solution (NaCl) was pumped from the large reservoir through plastic tubing to a prepump filter capsule and then through the pump to the stream. Injection of the tracer solution at site VR900 started at 1800 hours on June 15 and continued until 1200 on June 18. A bubble meter was used to monitor the rate of injection to ensure that the pump was working properly and that the flux of tracer was steady. In addition, the injection rate was measured periodically with a volumetric flask and stopwatch to make sure that it remained constant.

## Automatic Samplers

Hourly stream samples were collected by three ISCO®™ automatic samplers (sites T1, T2, and T3 in fig. F1) to monitor the concentration of the tracer solution in streamflow (fig. F7). The hourly samples were analyzed later for chloride concentrations at a USGS laboratory in Denver, Colorado (see discussion of analytical methods below) to determine tracer arrival and recovery times and to verify that the salt tracer was close to steady-state conditions during the synoptic sampling. Steady-state tracer conditions are required to accurately measure discharge.

Sampler T1 was deployed near the beginning of the reach below the injection point at site VR900 and T2 was deployed at the end of the study reach at Stewart Ranch (site VR13640). The intake for T3 at site VR1300 was inadvertently located at a



**EXPLANATION**

- A, Tracer injection begins at 1800 hours
- B, Pump battery dies before daybreak
- C, Pump battery disconnected by cow at about 1300 hours
- D, Lag time from VR900 to VR13460 about 2-3 hours (estimated)
- E, ISCO sampler at VR900 discontinued to conserve sample bottles
- F, Synoptic sampling from 0900 to 1000 hours on 6/18/2000.
- Tracer injection ends at 1000 hours
- G, Slug of remaining tracer solution from emptied tank
- H, Background conditions resumed

**Figure F7.** Field notes and graph explaining variations in tracer concentrations versus time at each of three automatic samplers. Samples were collected hourly. Locations of automatic samplers are shown on figure F1.

location where ground water was discharging to the bottom of the stream; consequently, the sampler collected unmixed inflow from upper Verde River springs instead of fully mixed stream-flow. This was not realized until much later when the analytical results became available. Apparently, the intake tubing rested on the streambed in a gaining area that displaced the tracer solution with no significant mixing. The T3 results were unintended but do show that concentrations of chloride in spring inflow did not vary substantially with time. The background concentration of chloride in ground water discharging near upper Verde River springs was  $23.5 \pm 0.7$  mg/L ( $n = 45$ ) and varied by 3 percent

between June 16 and 19, 2000, which is similar in magnitude to the reported analytical accuracy (discussed below).

An injection rate of 9.3 milliliters per second was maintained throughout the study, with the exception of two accidental power-supply interruptions (fig. F7). The first interruption occurred when the battery ran down on June 16 at 0400, shortly before dawn. A second interruption occurred on June 17 at about 0100, when a cow dislodged the wire cables between the pump and the battery. In each instance, the pump ceased for several hours, but the tracer resumed steady-state conditions quickly because of the rapid travel time through

the reach. Thus, neither interruption appears to have had a lingering effect on tracer concentrations during the synoptic sampling on the morning of June 18. At the time of the synoptic sampling, the injection of tracer had been continuous for more than 24 hours without interruptions. The rate of injection appears to have been declining gradually through the previous night, which is attributed to the pump batteries gradually losing their charge. Given the rapid travel time through the reach, however, the distribution of tracer appears to have been close to steady-state conditions and should have been well mixed in the slower moving parts of the channel.

As mentioned earlier, because chloride determinations by selective-ion probe are less accurate than by ion chromatography, the probe method was used primarily for reconnaissance to show the arrival of tracer and that the tracer solution was well mixed throughout the stream reach (fig. F6). Tracer concentrations at site VR13460 could only be verified much later when the analytical results for the T2 samples became available. Although initial velocity measurements indicated that the tracer solution could traverse the 2.5-mi reach in several hours, there was concern that the density of aquatic vegetation would prevent the tracer from evenly mixing through the water column. Most tracer-dilution studies have been conducted in high-gradient mountain streams (Zellweger, 1996; Kimball, 1997; Kimball and others, 1999; Walton-Day and others, 1999; Wirt and others, 2000; 2001) so the utility of the technique in a relatively low-gradient canyon setting having thick riparian vegetation was largely untested. How well the tracer would mix through the stream, given the dense aquatic vegetation at the upper end of the reach and the presence of a large-volume, slow-moving reach impounded by a beaver dam near site VR7800, was unknown. To compensate for these conditions, the injection of tracer was extended for 60 hours or as long as reasonably possible given staffing constraints. In hindsight (and without the power interruptions), 6 hours probably would have been adequate to reach and maintain steady-state conditions. The end result was that tracer conditions were fairly steady for 24 hours leading up to the synoptic study and are thought to have been well mixed at all sites (except possibly synoptic site VR7800, in deep, slow water behind a beaver dam).

## Synoptic Sampling

Synoptic samples were collected by three teams, between 0900 and 1000 hours on June 18, during what probably was close to the peak discharge of the diurnal cycle. The analytical results are reported in table F1. The injection pump was shut off as soon as the synoptic sampling was completed. Chloride concentrations at site VR13460 returned to background levels after approximately 2–3 hours (fig. F7).

Water-chemistry samples were collected at selected springs and all synoptic sites using standard USGS methods comparable to Wilde and others (1999). The width of the Verde River increased from about 3 to 20 ft over the reach. A representative sample was collected at each site by immersing

an open, hand-held 1- or 2-L plastic bottle in the centroid of flow or at multiple verticals as described by Shelton (1994).

## Sample Processing, Analytical Methods, and Analytical Uncertainty

Filtering and processing were done in the field, using standard USGS equipment and protocols (Horowitz and others, 1994). All samples were processed within a 12-hour period on the same day they were collected. Water samples were filtered using a 0.45- $\mu\text{m}$  syringe-mounted capsule filter. Sample splits for major-ion analysis were preserved by adding ultrapure nitric acid to a pH of  $< 2$ . Major elements were determined at a USGS laboratory in Denver, Colorado, by inductively coupled plasma-atomic emission spectrometry (ICP-AES; Briggs and Fey, 1996). Concentrations of the chloride, nitrate, fluoride, and sulfate were determined by ion chromatography from filtered, unacidified samples (d'Angelo and Ficklin, 1996). The quality of the laboratory analyses was assessed through analysis of laboratory blanks, sample duplicates, and USGS standard reference water samples (Long and Farrar, 1995). Field parameters and analytical data for dissolved cations and anions are listed in table F1. Stable isotope analyses were conducted by the Laboratory of Isotope Geochemistry at the University of Arizona in Tucson, Arizona.

The accuracy of chloride analyses in synoptic samples by ion chromatography was considered critical and was determined using USGS standard reference water samples (Long and Farrar, 1995). A low-range standard of 25.8 mg/L was run 4 times and had a standard deviation of  $\pm 1.4$  mg/L. A high-range standard of 65 mg/L was run twice with a standard deviation of  $\pm 2.1$  mg/L. Thus, the analytical uncertainty for the discharge measurements using the tracer-dilution technique is about  $\pm 5$  percent for low-range chloride concentrations and  $\pm 3$  percent for high-range chloride concentrations.

## Results

### Calculated Base Flow

A total base flow of  $19.5 \pm 1.0$  ft<sup>3</sup>/s was calculated for the end of the tracer reach at Stewart Ranch (during near-peak conditions), compared with a peak daily flow of  $21.2 \pm 1.0$  ft<sup>3</sup>/s at the Paulden gauge. By subtraction, approximately 7 percent of base flow at the Paulden gauge was contributed downstream from the tracer reach. Seepage has been observed on both banks of the Verde River downstream from the mouth of Muldoon Canyon (river mi 8), which is thought to account for most of the missing inflow. The Little Chino basin-fill aquifer delivered  $13.8 \pm 0.7$  percent of the total base flow ( $2.7 \pm 0.08$  ft<sup>3</sup>/s) upstream from site VR1200. This Little Chino fraction is substantially higher than the 8.4 percent contribution from the Little Chino basin-fill aquifer predicted

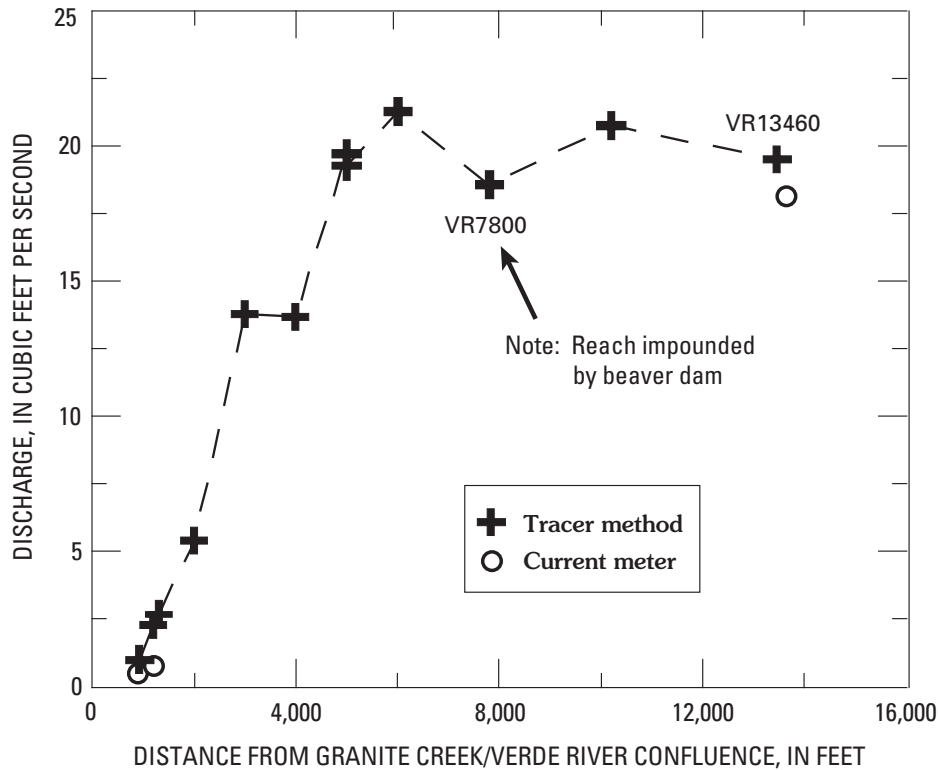


**Figure F8.** Graph showing discharge calculated from tracer-dilution study versus distance downstream on June 18, 2000. Synoptic sampling occurred between 0900 and 1000 hours. Current-meter measurement at VR13460 was made at 1343 hours and rated as good ( $\pm 5\%$ ).

by the conceptual 1990s water-budget model presented in the introductory chapter (Wirt, Chapter A, this volume, fig. A16 and table A4) and is thought to provide a more accurate baseline of current conditions.

### Accuracy of Discharge Calculations

Discharge was calculated from analytically determined concentrations of chloride at each synoptic stream site using equations 1.0 and 2.0 (figs. F5 and F8). Discharge values are most accurate in the first mile of the study reach where the tracer concentrations greatly exceed the natural chloride concentrations (fig. F8). In the beginning of the tracer reach, the contrast between tracer concentrations and background concentrations of chloride is large (table F1) and the method uncertainty approaches the uncertainty of the high-range analytical method for chloride, which was about 5 percent. Between sites VR3000 and VR13460, instream concentrations of chloride tracer approached the background concentrations of chloride measured from springs, although the low-range analytical uncertainty decreased to about 3 percent.

Tracer concentrations downstream from site VR3000 varied from 23.3 to 24.1 mg/L. In comparison, background chloride concentrations determined for upper Verde River

springs varied between 19.3 to 23.9 mg/L (table F1), with an average background value of 19.6 mg/L ( $n = 7$  springs). It was not possible to flowweight the background chloride levels from different spring inflows; however, the mean value was 15 percent less than the chloride range measured for the stream and is thought to accurately represent background conditions. Near site VR7800, slow-moving backwater behind a beaver dam may have caused incomplete mixing along the marshy edges of the wide, deep reach.

Potential tracer method uncertainty is the sum of (a) analytical uncertainty, (b) uncertainty of the range of variation in background chloride levels, (c) amount of change in stage attributed to diurnal changes, and (d) uncertainty of the degree of mixing of the tracer in the stream. The amount of analytical uncertainty is known, and an effort was made in the design of the study to minimize the effects of the other unknown factors by measuring background chloride in springs, by continuing the injection phase as long as feasible to establish steady-state conditions, and by restricting the synoptic sampling to 1 hour.

The analytically determined discharge is within 10 percent of that determined by current-meter measurements (fig. F8). By using the tracer-dilution method, the discharge calculated at the lower end of the tracer reach was  $19.5 \pm 1.0$  ft<sup>3</sup>/s at 0900 hours on June 18, 2000, at site VR13460. In comparison, a discharge of  $17.7 \pm 1.0$  ft<sup>3</sup>/s was measured using a current

meter at 1343 hours, almost 5 hours later on the same day. In addition,  $17.4 \pm 1.4$  ft<sup>3</sup>/s was measured using a current meter at 1110 hours on June 13, 2000. Given that the current-meter measurements were made 2 to 5 hours later on the falling limb of the diurnal cycle, the measurements are in reasonable agreement, although the tracer measurement is considered more representative of the peak daily discharge. An additional factor that may explain part of the disparity is that current-meter measurements tend to underestimate the amount of base flow by neglecting the fraction that occurs as hyporheic flow. Thus, the 2.1 ft<sup>3</sup>/s difference between the two methods is attributed to (1) falling stage resulting from diurnal variations, (2) a fraction of base flow occurring as hyporheic flow, (3) measurement uncertainties for both methods, or (4) a combination of these three factors.

## Changes in Water Chemistry with Distance Downstream

Spatial changes in stream chemistry result from a variety of simple processes. Physical changes in temperature, pH, and the concentration of dissolved gases occurred as ground water discharging to the stream equilibrated with the atmosphere. Water chemistry also changed in response to mixing between different sources of water and from geochemical processes such as leaching or dissolution of rock-forming minerals. This section presents downstream variation in field parameters and selected cations, anions, trace elements, and in the stable isotope composition of oxygen and hydrogen with distance along the study reach. Water-chemistry data are presented in figures F9–F14 and reported in table F1.

## Field Parameters

Specific conductance, water temperature, and pH were measured as part of the field reconnaissance of lower Granite Creek, Stillman Lake, and the upper Verde River. Reconnaissance field data were collected at many sites in addition to the synoptic sites (presented in table F1 and subsequent figures). Reconnaissance data in figure F9 were graphed in the field to select the synoptic sampling sites.

Specific conductance is the ability of a substance to conduct an electrical current, which in dilute solutions is directly related to the concentration of dissolved salts (Hem, 1992). Specific conductance increased along the length of lower Granite Creek from about 460 microSiemens per centimeter ( $\mu\text{S}/\text{cm}$ ) at Lower Granite Spring (site LGS-1) to about 550  $\mu\text{S}/\text{cm}$  near its mouth, as indicated by the dashed best-fit regression line (fig. F9A). The increase in dissolved salts is most likely caused by water-rock interaction but also could be caused by evaporation of surface water. The increasing trend extended beyond the mouth of Granite Creek toward two small seeps near the beginning of the first seepage in the upper Verde River channel (sites SP561 and SP1350, with 570 and 598  $\mu\text{S}/\text{cm}$ , respectively). Based on the field data, the

two seeps are interpreted to represent shallow ground water derived from the Granite Creek area, as indicated by their orange “X” symbols in figure F9.

A decreasing trend in conductance was observed over the length of Stillman Lake. Specific conductance ranged from about 550  $\mu\text{S}/\text{cm}$  at the upstream end of the lake to 360  $\mu\text{S}/\text{cm}$  at the downstream end. This is surprising in that evaporation or dissolution of rock-forming minerals would be expected to produce an increase rather than a decrease in specific conductance along the flow gradient. The simplest explanation for this occurrence is a high-conductance inflow discharging to the upstream end of the lake and a low-conductance inflow discharging to the downstream end of the lake.

Specific conductance of the initial flow in the upper Verde River at site VR635 (523  $\mu\text{S}/\text{cm}$ ) was more similar to that at the mouth of Granite Creek (550  $\mu\text{S}/\text{cm}$ ) than to that at the lower end of Stillman Lake (360  $\mu\text{S}/\text{cm}$ ). Conductance initially decreased between sites VR635 and VR900 from 523 to 410  $\mu\text{S}/\text{cm}$ . The decrease appears to be caused by mixing between ground-water inflows from Granite Creek and Stillman Lake. At site VR930, this trend was abruptly reversed, and specific conductance (and discharge) increased, owing to a third source of ground-water inflow from upper Verde River springs. Specific conductance for the upper Verde River springs network ranged between 550 and 642  $\mu\text{S}/\text{cm}$ . Downstream from site VR5000, specific conductance reached a plateau indicating no new inflows with distinct geochemical characteristics and what probably is the end of the gaining reach.

In ground-water studies, similar water temperatures can be an indication that ground waters have undergone a similar cooling regime, which provides one piece of evidence that the sources could be similar. Temperature is not a conclusive line of evidence because water temperatures can change in response to sunlight, air temperature, and other variables. Not surprisingly, the highest water temperatures were measured near the edges of Stillman Lake, where water was shallow, slow moving, and in direct sunlight (fig. F9B). The lowest temperatures of about 15 degrees Celsius ( $^{\circ}\text{C}$ ) were measured from the bottom of a small pool in lower Granite Creek (site GC1500) and a spring inflow at the upstream end of Stillman Lake (site SLS-1). The similarity of the water temperatures near two widely spaced inflows in Stillman Lake and lower Granite Creek (both having specific conductance of about 550  $\mu\text{S}/\text{cm}$ ) suggests a similar ground-water origin, although not at all conclusively. Similarities in the composition of hydrogen and oxygen stable isotopes and strontium concentrations presented in Chapter E (Wirt and DeWitt, this volume) and later in this chapter provide more compelling evidence that the common origin of ground-water discharge to lower Granite Creek and Stillman Lake is the Little Chino basin-fill aquifer. In general, the water temperature of Granite Creek increased with distance downstream from site GC1500 and also increased in a nonlinear fashion from the upstream to the downstream end of Stillman Lake.

Temperature variations suggest at least two ground-water inflows near the beginning of the upper Verde River.

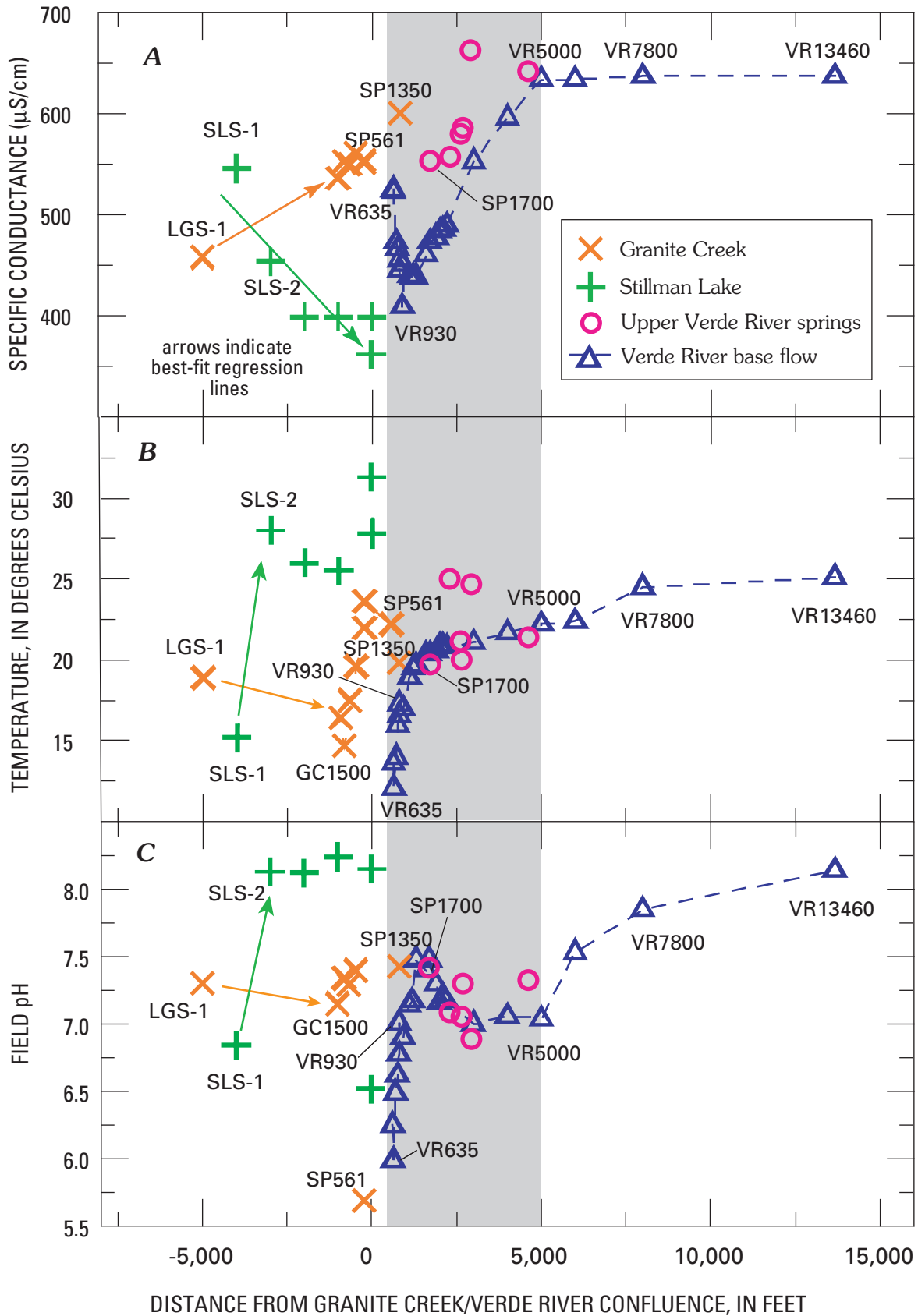


**Figure F9.** Graphs showing changes in (A) specific conductance, (B) water temperature, and (C) pH versus distance from Granite Creek/Verde River confluence. Shaded area indicates extent of gaining reach.



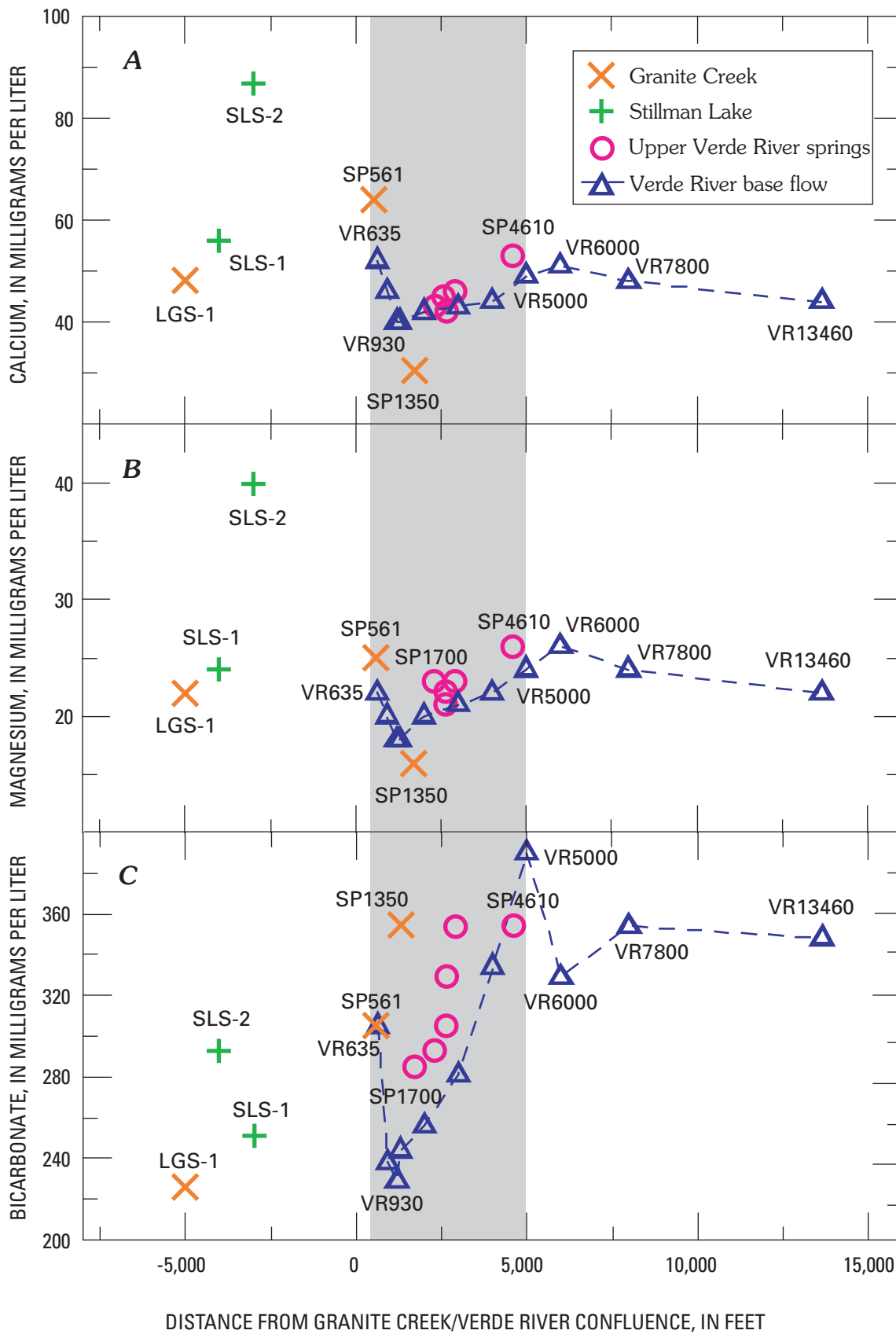


**Figure F10.** Graphs showing changes in (A) calcium, (B) magnesium, and (C) bicarbonate versus distance from Granite Creek/Verde River confluence. Shaded area indicates extent of gaining reach.

The lowest water temperature for the entire study of 12.1°C was at site VR635, in comparison to air temperatures measured in excess of 35°C during the day. The source of this colder inflow is attributed to a Little Chino source. In contrast, the minimum temperature measured for upper Verde River springs was 19.8 °C, with a mean water temperature of 21.7±2.2°C (n = 7) or nearly 10 degrees higher than at VR635. Downstream from the gaining reach, the streamflow temperature increased to 25.1°C at site VR13460, as base flow was warmed by air and sunlight.

Variations in pH in the Verde River correlated with the degree of contact that water has had with the atmosphere (fig. F9C). All pH values less than 7.0 were measured from sites where ground-water inflow was evident. Most of these sites were in the immediate vicinity of the confluence of Granite Creek and the Verde River. In Stillman Lake, the lowest pH value of 6.5 (site SLS-3 at the downstream end), which also had the lowest specific conductance within the study area (360 µS/cm), indicating unmixed inflow. In lower Granite Creek, a similar pH of 6.7 was measured near the mouth. The lowest pH of 6.0 for the entire study area was measured downstream at site VR635 in the Verde River, which also had the lowest measured temperature. All three sites had a Little Chino source and were in relatively close spatial proximity, although disconnected by a dry stream segment. In contrast, the highest pH measurements exceeded 8.0 along the edges of Stillman Lake and also at site VR13460. These were sites where no ground-water inflows were occurring and there was ample contact with the atmosphere allowing degassing of carbon dioxide.

Changes in pH (or hydrogen-ion activity) are related to temperature, alkalinity, and interrelated chemical reactions, particularly the degassing of CO<sub>2</sub> and the dissolution of calcite (Hem, 1992). The pH is a useful index of geochemical reactions in which the water participates. For example, dissolution of calcite (CaCO<sub>3</sub>) results in an increase in HCO<sub>3</sub><sup>-</sup> and a corresponding increase in pH. A decrease in dissolved CO<sub>2</sub>, which is produced from biological activity in the unsaturated zone, also will cause pH to increase. Because the concentration of CO<sub>2</sub> in the soil zone is often as high as 5 percent and the atmospheric concentration is about 0.03 percent, dissolved CO<sub>2</sub> is rapidly lost as shallow ground water seeps into a stream bed (Bullen and Kendall, 1998).

The pH increased from 6.0 to 8.1 in a non-linear pattern between sites VR635 and VR13460 (fig. F9C). An initial increase in pH from 6.0 to 7.5 between sites VR635 and VR1700 is attributed to rapid degassing of CO<sub>2</sub> from Granite Creek and Stillman Lake inflow. In the vicinity of upper Verde River springs, the stream pH decreased slightly to less than 7.2. Many of the spring inflows had dissolved oxygen values of less than about 5 mg/L (table F1), an indication that the ground water had not yet equilibrated with the atmosphere. The concentration of dissolved oxygen is a function of temperature and pressure and to a lesser degree, the concentration of other solutes (Hem, 1992). At 30°C, the saturation point of dissolved oxygen in fresh water is 7.54 mg/L (Hem, 1992).

Within 1.5 mi downstream from the gaining reach (site VR 13460), ground-water inflow had equilibrated with the atmosphere, as indicated by saturated conditions for dissolved oxygen (7.9 mg/L at site VR7800, table F1). The increase in the dissolved oxygen of the streamflow presumably was accompanied by degassing of CO<sub>2</sub>. Downstream from the gaining reach (sites VR5000 to VR13460), the pH of the streamflow further increased to 8.1, which also correlates with increasing water temperature and a lack of ground-water inflows. An additional possibility that will be tested by geochemical modeling later in this chapter, is that dissolution of carbonate minerals in the Martin Limestone could also contribute, in part, to the increase in pH through this reach.

## Major Elements

Ground waters in the upper Verde River headwaters area are predominantly calcium-bicarbonate waters with variable proportions of magnesium and sodium. Calcium (Ca<sup>+2</sup>) and bicarbonate (HCO<sub>3</sub><sup>-</sup>) typically are governed by the availability of carbonate minerals and by solution- and gas-phase equilibria involving carbon dioxide (Hem, 1992). Where dolomite is present, the behavior of dissolved magnesium (Mg<sup>+2</sup>) generally is related to carbonate reactions, although its behavior is more complicated than that of Ca<sup>+2</sup>.

In fig. F10, concentrations of Ca<sup>+2</sup>, Mg<sup>+2</sup>, and HCO<sub>3</sub><sup>-</sup> are plotted versus the distance above and below the Granite Creek/Verde River confluence. In the short reach between sites VR635 and VR930, Ca<sup>+2</sup> and Mg<sup>+2</sup> concentrations decreased, presumably as a result of mixing between Granite Creek and Stillman Lake inflows. Bicarbonate also decreased between sites VR635 to VR930, presumably from degassing of CO<sub>2</sub> and a corresponding increase in pH, as well as from mixing. In the middle segment between sites VR1300 and VR5000, Ca<sup>+2</sup>, Mg<sup>+2</sup>, and HCO<sub>3</sub><sup>-</sup> increased due to mixing with inflow from upper Verde River springs. Downstream from site VR6000, dissolved Ca<sup>+2</sup> and Mg<sup>+2</sup> concentrations decreased slightly, perhaps in response to a concurrent increase in pH (fig. F9). The increasing pH is largely attributed to degassing of CO<sub>2</sub> from emerging ground water. Bicarbonate sharply decreased from VR5000 to VR6000 in the absence of spring inflows, then stabilized between sites VR7800 and VR13460.

Concentrations of major cations generally are related to geochemical processes involving the distribution of minerals and the length of the ground-water flowpath. Mineral saturation indices (SI, where SI = log IAP/K; IAP is the ion activity product and K is the equilibrium constant) were calculated using the computer program NETPATH (Plummer and others, 1994). The plot of SI values for CO<sub>2</sub> gas, calcite, and dolomite along the tracer reach (fig. F11) shows that the partial pressure of CO<sub>2</sub> is decreasing downstream from gaining reaches. Near-surface degassing of CO<sub>2</sub> appears to be the most important factor controlling the distribution of carbonate species along the study reach.

Spatial variations in the concentrations of the major anions—chloride, sodium, and sulfate (Cl<sup>-</sup>, Na<sup>+</sup>, and SO<sub>4</sub><sup>-2</sup>)

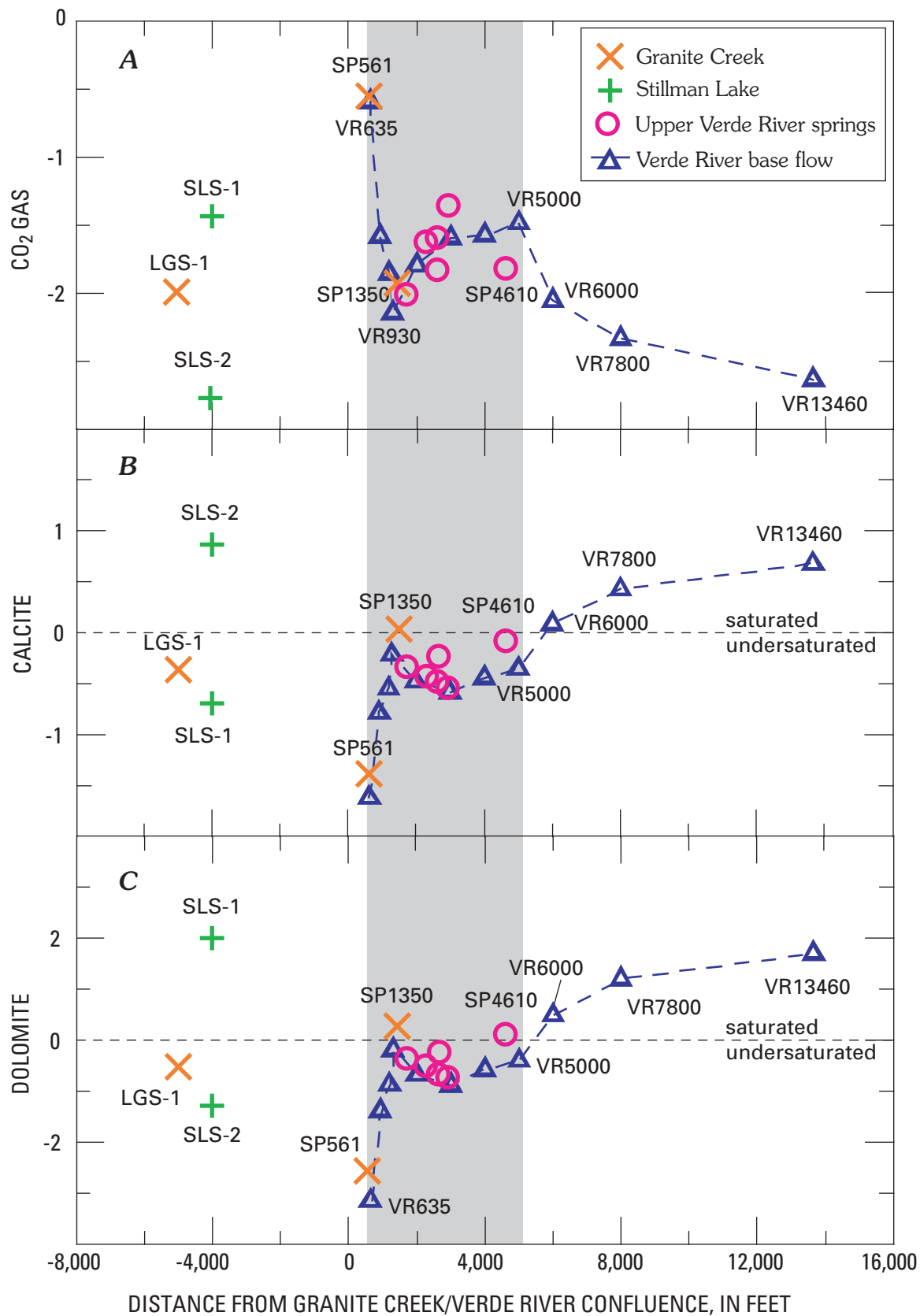


**Figure F11.** Graphs showing changes in saturation indices of (A) CO<sub>2</sub> gas, (B) calcite, and (C) dolomite versus distance from Granite Creek/Verde River confluence. Shaded area indicates extent of gaining reach.

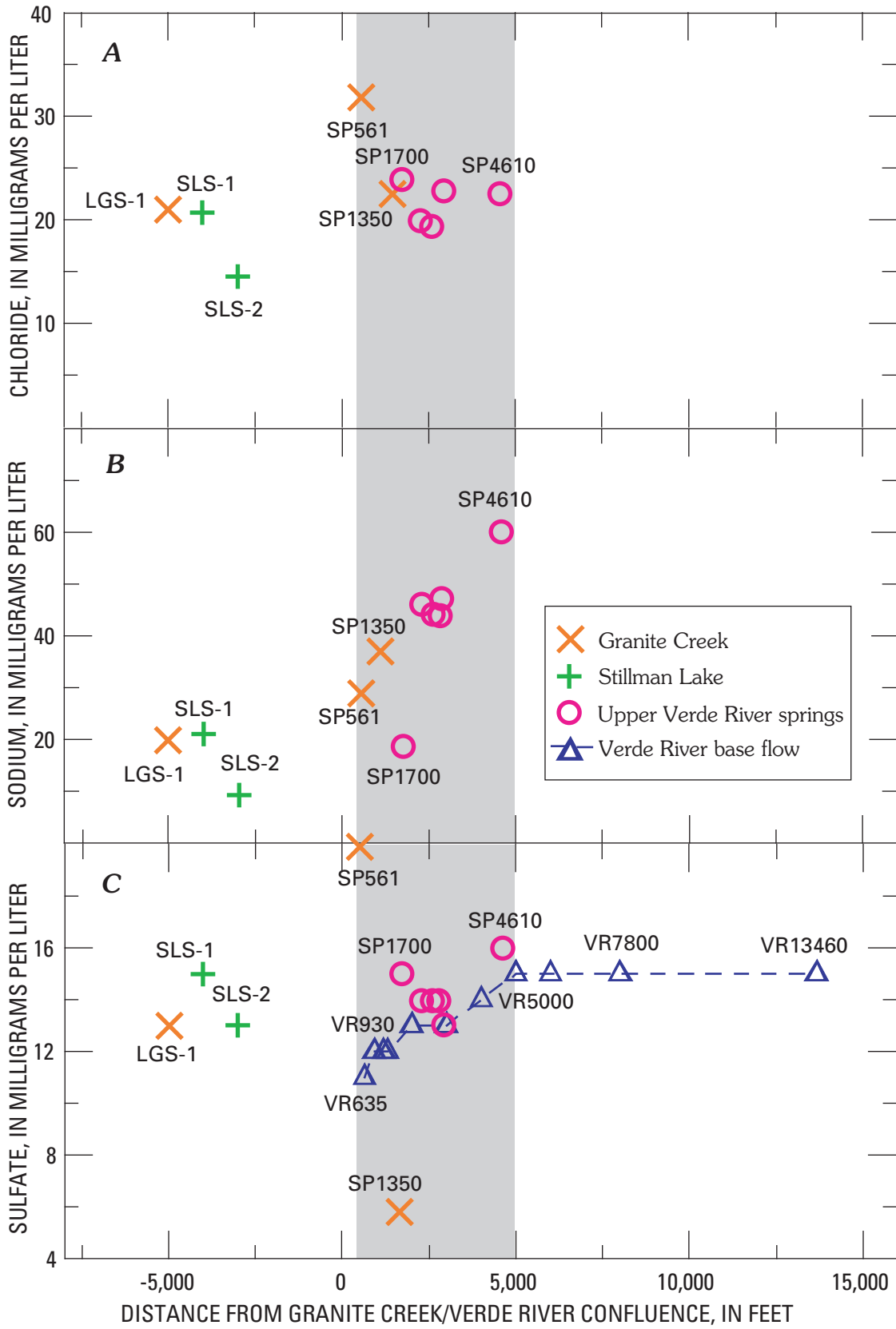


**Figure F12.** Graphs showing changes in (A) chloride, (B) sodium, and (C) sulfate versus distance from Granite Creek/Verde River confluence. Stream concentrations in the study reach are influenced by NaCl tracer and therefore instream values for Cl and Na are not shown. Shaded area indicates extent of gaining reach.

were plotted with distance along the tracer reach (fig. F12). Fortunately for the accuracy of the discharge calculations, background concentrations of chloride varied little, within a small range along the tracer reach, and the tracer reach values could be corrected for background contributions of chloride. The mean chloride concentrations for the upper Verde River springs network varied between 19.3 to 23.9 mg/L, with a mean concentration of 19.6 mg/L ( $n = 7$ ). Del Rio Springs, Stillman Lake, and Granite Creek had chloride concentrations between 14.5 and 20.8 mg/L. Instream  $\text{Cl}^-$  and  $\text{Na}^+$  concentrations in the Verde River were artificially influenced by the NaCl tracer and are not plotted in figure F13, although they are provided in table F1.

In contrast,  $\text{Na}^+$  concentrations in discharge from upper Verde River springs varied between 37 and 60 mg/L. Contact with shale of marine origin containing rhyolitic ash (such as the Chino Valley Formation or playa sediment) is the most likely source of elevated concentrations of  $\text{Na}^+$  (as well as As, B, Li, and K) in wells intercepting the D-C zone near the ground-water outlet of the Big Chino aquifer (Wirt and DeWitt, Chapter E, fig. E3, this volume). The Chino Valley Formation, where present, underlies the Martin Limestone and overlies the Tapeats Sandstone. The Chino Valley Formation is prominently exposed at the confluence of Stillman Lake and Granite Creek (southwest bank). It is thought to underlie the Martin Limestone beneath the north wall of the canyon and is the most likely source of dissolved  $\text{Na}^+$  in discharge to upper Verde River springs. Sulfate concentrations were relatively low (between 6 and 16 mg/L) but increased over the tracer reach as a consequence of mixing between Little Chino ground water and upper Verde River springs. Sulfate concentrations in discharge from upper Verde River springs varied little, between 13 and 16 mg/L.

## Selected Trace Elements

Elevated levels of boron (B) and lithium (Li) in upper Verde River springs are the highest in the headwaters region with the exception of the four Big Chino bedrock wells penetrating the D-C zone, described earlier in Chapter E. These bedrock wells have a distinct trace-element chemistry containing 330–460  $\mu\text{g/L}$  of B and 54–86  $\mu\text{g/L}$  of Li, respectively (Wirt and DeWitt, Chapter E, fig. E3; and Appendix A). The occurrence of these constituents is spatially associated with argillaceous rocks in the lower Paleozoic section. Strontium (Sr) is another trace element useful in indicating flowpath origin and is predominantly derived from the dissolution of feldspar minerals in igneous rocks (Wirt and DeWitt, Chapter E, fig. E3; and Appendix A). Some Sr also is present in carbonate rocks, but at relatively low levels in comparison to the Sr-rich volcanic rocks in the study area (Chapter E, this volume).

Concentrations of B and Li were lowest for Granite Creek and Stillman Lake samples but increased along the tracer reach more than threefold from 74 to 270  $\mu\text{g/L}$  and from 15 to 49  $\mu\text{g/L}$ , respectively (fig. F13). In contrast to Li and B, concentrations of Sr were highest in the Granite Creek and Stillman

Lake samples (540 to 620  $\mu\text{g/L}$ ;  $n = 3$ ). Strontium concentrations for upper Verde River springs samples were significantly lower, ranging between 360 and 440  $\mu\text{g/L}$  Sr. The higher Sr concentrations are attributed to Little Chino source water in contact with Tertiary latite-andesite, whereas the Sr content in upper Verde River springs probably is related to contact with the Tertiary 5-myra basalt unit. Basalt flows partly cover the Paleozoic rocks in the confluence area and extend beneath surficial alluvial deposits in lower Big Chino Valley (fig. B8, Chapter B, this volume). The buried playa deposit in the center of Big Chino Valley is also a possible source of dissolved strontium along this flowpath.

Trace-element concentrations provide evidence for water-rock interactions along ground-water flowpaths. Elevated levels of B and Li are interpreted as having water/rock contact within the lower Martin/Chino Valley/Tapeats interface. High concentrations of Sr in Stillman Lake samples are interpreted as evidence for contact with volcanic igneous rocks along the ground-water outlet of northern Little Chino Valley.

## Hydrogen and Oxygen Stable Isotopes

The composition of hydrogen and oxygen stable isotopes provides some of the most definitive geochemical evidence for identifying the source areas of springs and their aquifers. These isotopes are particularly useful in tracing ground-water flowpaths because they are part of the water molecule and can be assumed to behave conservatively once the water has reached the saturated zone and no longer has contact with the atmosphere. Evaporation and condensation of atmospheric precipitation and moisture in the unsaturated zone are the most significant physical processes that affect the proportions of these isotopes. The effects of evaporation were significant for most of the samples collected from Stillman Lake and, to a lesser degree, from lower Granite Creek. A discussion of the effects of evaporation has been presented in Chapter E (Wirt and DeWitt, this volume). In their figure E4, samples from Del Rio Springs, Granite Creek, and Stillman Lake plot along a dashed regression line with a slope of approximately 4, showing ground water similar to that discharging at Del Rio Springs (the major point of discharge for the Little Chino basin-fill aquifer) as the ground-water source for Stillman Lake and Granite Creek. This interpretation is corroborated by the slope of the water-level gradient from Del Rio Springs toward the confluence area (Wirt and others, Chapter D, this volume, fig. D7). Thus, it is evident that ground water discharging upgradient from the Granite/Verde confluence has been subjected to varying degrees of evaporation.

In figure F14, the stable-isotope samples plot into two main groups, with most of the samples from Stillman Lake and lower Granite Creek enriched by evaporation and comparatively heavier than samples from upper Verde River Springs. The “Little Chino” sample collected closest to the point where it emerged from the ground and least likely to have been affected by evaporation (with the exception of Del Rio Spring) was Lower Granite spring (site LGS-1;  $-9.7\text{‰}$   $\delta^{18}\text{O}$  and  $-7\text{‰}$

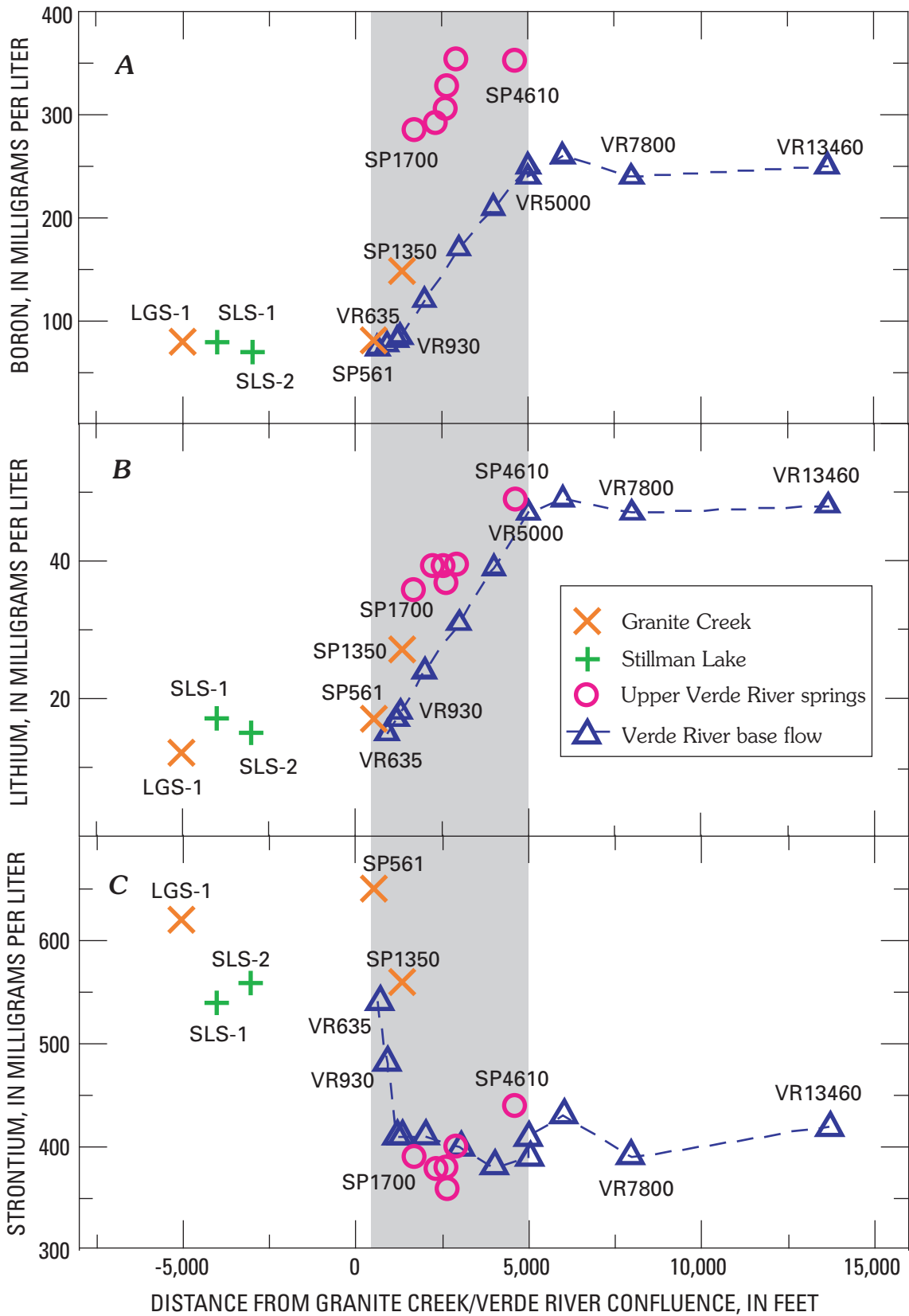


**Figure F13.** Graphs showing changes in (A) boron, (B) lithium, and (C) strontium versus distance from Granite Creek/Verde River confluence. Shaded area indicates extent of gaining reach.

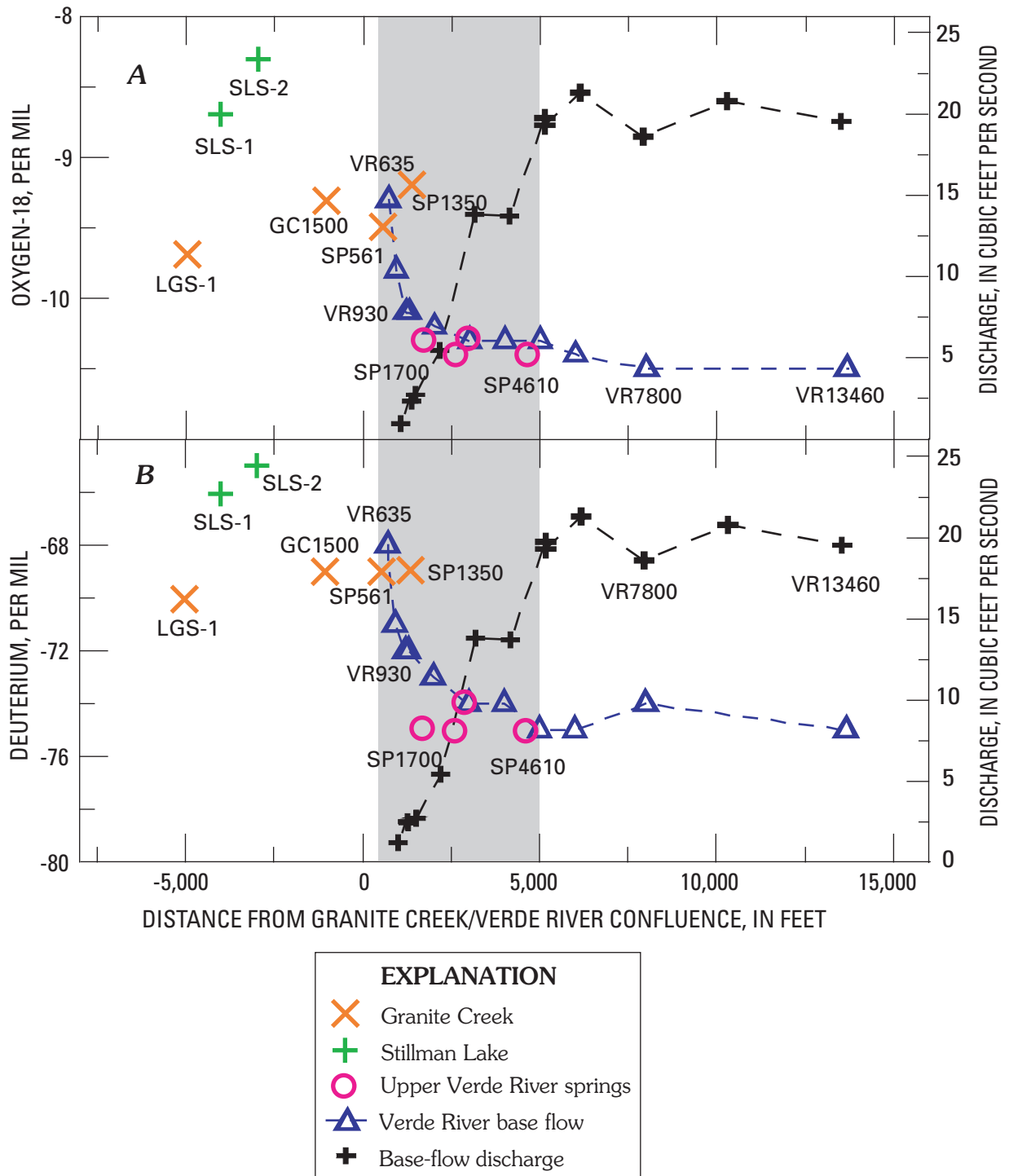


**Figure F14.** Graphs showing changes in stable isotopes (left axis) of (A) oxygen, and (B) hydrogen, and base flow (right axis) versus distance from Granite Creek/Verde River confluence. Shaded area indicates extent of gaining reach.

$\delta D$ ). In the uppermost reach of the Verde River, instream mixing of “Little Chino” sources of ground water with inflow from upper Verde River springs was the most important process downstream from site VR1200. The furthest point downstream from the confluence where Granite Creek inflow was identified was site SP1350, a small 3-ft radius pool that did not connect directly with the Verde River, at least on the ground surface. Based on supporting evidence from field-measured parameters (fig. F9) and the T3 automatic sampler (fig. F7), inflow from upper Verde River springs strongly emerges first in the vicinity of stream site VR1300. If one presumes that all inflow upgradient from site VR1200, with a discharge of  $2.7 \pm 0.08 \text{ ft}^3/\text{s}$ , originates as ground-water discharge from Granite Creek and Stillman Lake, then at least  $13.8 \pm 0.7$  percent of the total base flow of  $19.5 \pm 1.0 \text{ ft}^3/\text{s}$  at site VR13460 can be attributed to the Little Chino basin-fill aquifer.

Because the base flow of lower Granite Creek was about  $0.5 \text{ ft}^3/\text{s}$ , the remaining four-fifths of the  $2.7 \pm 0.08 \text{ ft}^3/\text{s}$  attributed the Little Chino aquifer is contributed along the Stillman Lake flowpath. This estimate is supported by the decrease in specific conductance between VR635 and VR1200, which shows mixing between the Stillman Lake and Granite Creek fractions (fig. F9 and table F1). The remaining 86.2 percent of total flow at Stewart Ranch is attributed to discharge from upper Verde River springs.

All lines of geochemical evidence show mixing between ground water from the Little Chino subbasin and upper Verde River springs immediately downstream from VR1200. At the lower end of the tracer reach, the  $\delta^{18}\text{O}$  of the final base-flow mixture ( $-10.5 \pm 0.2\text{‰}$  at site VR13460) should be intermediate to those for Lower Granite spring (site LGS-1,  $-9.7 \pm 0.2\text{‰}$ ) and upper Verde River springs (site SP4610,  $-10.4 \pm 0.2\text{‰}$ ). Instead, stream values for  $\delta^{18}\text{O}$  and  $\delta D$  between sites VR6000 and VR13460 cannot be distinguished from those reported for upper Verde River springs, as they are within analytical precision of one another. This is an indication that mixing may have occurred with unsampled inflow that is isotopically depleted with respect to the sampled inflows.

Perhaps, the most notable attribute of the upper Verde River springs sample group is the relative lack of analytical variation (table F1,  $n = 5$ ). Because some data from previous studies were analyzed by different laboratories, two standard-deviation analytical precisions of  $0.2\text{‰}$  for  $\delta^{18}\text{O}$  and  $2.0\text{‰}$  for  $\delta D$  have been used for all of the stable-isotope data in this study (Kendall and Caldwell, 1998; p. 75; Christopher J. Eastoe, oral commun., 2003)—yet the upper Verde River springs samples from the synoptic sampling varied by less than  $0.1\text{‰}$  for  $\delta^{18}\text{O}$  and  $1.0\text{‰}$  for  $\delta D$ . Differences between upper Verde River springs and the final base-flow mixture at Stewart Ranch (site VR-13460) differ within the margin of analytical uncertainty, which is about 15 percent. Mixing could be occurring at the scale of this uncertainty, but the amount cannot be determined with any confidence solely based on the stable-isotope results.

Wirt and DeWitt (Chapter E, this volume, table E2) show that the carbonate aquifer north of the Verde River (M-D

sequence) is substantially depleted (about  $1.3 \pm 0.2\text{‰}$ ) in  $\delta^{18}\text{O}$  relative to upper Verde River springs. Although none of the samples from upper Verde River springs were more depleted in  $\delta^{18}\text{O}$  and  $\delta D$  than samples of base flow at Stewart Ranch, some mixing of Big Chino ground water with isotopically depleted ground water as unsampled inflow appears likely. Inverse geochemical modeling is used next to evaluate the degree of mixing between the Big Chino basin-fill aquifer and the M-D sequence of the carbonate aquifer to produce the water chemistry observed at upper Verde River springs.

### Inverse Geochemical Modeling to Determine Mixing Proportions at Upper Verde River Springs

The hypothesis that upper Verde River springs is a mixture of ground water from the Big Chino basin-fill aquifer and the carbonate aquifer was tested by inverse geochemical modeling using the computer program PHREEQC (Parkhurst and Appelo, 1999). Inverse modeling uses existing geochemical analyses to account for chemical changes occurring as water evolves along a flowpath. Given two water analyses representing the starting and ending water composition along a flow path, inverse modeling will calculate the moles of minerals and gases that must enter or leave solution to account for differences in composition (Parkhurst and Appelo, 1999). If two or more initial waters mix and subsequently react, PHREEQC computes the mixing proportion and the net geochemical reactions to account for the observed composition of the final water. Every possible geochemical mass-balance reaction is examined between selected evolutionary waters for a set of chemical and isotopic constraints and a set of plausible phases in the system. This modeling approach has been described extensively by Parkhurst and Plummer (1993) and Appelo and Postma (1999).

An advantage of PHREEQC (Version 2; Parkhurst and Appelo, 1999) over earlier versions of PHREEQC and NET-PATH (Plummer and others, 1994) is the capability to consider uncertainties associated with individual element analyses (Glynn and Brown, 1996). The user is allowed to specify the analytical uncertainty range for each element or isotope entered in the model. In addition, PHREEQC will determine mass-transfer models that minimize the number of phases involved, referred to as “minimal models.” Unlike earlier mass-balance programs, PHREEQC includes a charge-balance constraint and water mass-balance constraint that allow additional adjustments to analytical element concentrations, alkalinity, and pH. These additional constraints are equivalent to including a mass balance on hydrogen or oxygen for changes that may result from water derived from mineral reactions, evaporation, or dilution.

In this study, PHREEQC was used (a) to calculate saturation indices and the distribution of aqueous species, (b) to identify net geochemical mass-balance reactions between initial and final waters along the outlet flowpath, and (c) to



calculate proportions of water types contributing to the final mixture. Extensive knowledge of the geologic framework and the geochemical system (detailed in Chapters D and E and the preceding part of this chapter) as well as an evaluation of cation-anion balances for individual wells was used to select representative initial and final waters for this modeling exercise. In brief, multiple flow lines within the lower Big Chino basin-fill aquifer converge toward Paulden (fig. F15; and fig. E9 of Chapter E, this volume) and the main flowpath continues through the D-C zone of the carbonate aquifer (well F) to upper Verde River springs (site G, fig. F15; sample SP1700, table F1). Well F is screened in a basalt-filled paleochannel north of the upper Verde River (Chapter B, fig. B8A; Chapter D, fig. D8) and occupies an intermediate location along the basin outlet flowpath (fig. F15).

In this exercise, mixing of four initial waters is allowed to occur between Paulden and upper Verde River springs (table F2, fig. F15). Initial waters include (a) well H representing the D-C zone of the regional carbonate aquifer underlying basin-fill alluvium near the outlet, (b) well E, representing basin alluvium and basalt facies of the Big Chino basin-fill aquifer near its outlet, (c) well F representing the carbonate aquifer between Big Chino Valley and upper Verde River springs, and (d) well M representing the M-D sequence of the carbonate aquifer north of the Verde River near Drake. The final endpoint is represented by ground water at spring G, which was the largest discrete spring in the upper Verde River springs network identified at the time of the synoptic sampling (site SP1700, table F1). All of the selected analyses have cation-anion balances lower than 5 percent.

The first step in inverse modeling was to examine trends in the water chemistry and thermodynamic state of the initial and final waters used in the model (tables F2 and F3). The most significant change between ground water near Paulden (well E) and upper Verde River springs (spring G) is a 91 percent increase in dissolved silica, as well as large increases in the concentrations of sodium (78 percent), boron (86 percent), and lithium (65 percent), as shown by the last column in table F2. In comparison, concentrations of calcium, magnesium, and sulfate increased slightly by 11 percent, 19 percent, and 21 percent, respectively. The only decreasing trend between well E and spring G was for strontium (−6.5 percent), which behaves independently of the other dissolved constituents discussed here.

Saturation indices (SIs) shown in table F3 indicate that calcite and dolomite are near or at saturation and that gypsum is undersaturated in all of the selected samples. Amorphous  $\text{SiO}_2$  (chalcedony) is near saturation or slightly undersaturated in the regional carbonate aquifer (wells H and M), but slightly oversaturated in the basin-fill aquifer and upper Verde River springs (well E and spring G). Trends for SIs of Mg-silicate minerals, such as talc and sepiolite, strongly correlate with those for chalcedony, consistent with one or more of a family of related secondary silicate minerals dissolving along the outlet flowpath.

Water chemistry for well F is quite different from that for well H, although both wells are considered part of the D-C zone. Ground water underlying the margin of the Big Chino basin-fill aquifer at well H is near saturation with respect to celestite, chalcedony, calcite, and dolomite (table F3). Well H also has the highest concentrations of  $\text{HCO}_3^-$ ,  $\text{Ca}^{+2}$ ,  $\text{Na}^+$ ,  $\text{SO}_4^{-2}$ ,  $\text{Cl}^-$ , Li, and B and is moderately depleted in  $\delta^{18}\text{O}$  and  $\delta\text{D}$  (table F2). In contrast, well F has dissolved-element concentrations far more similar to well E than well H, with the exception of silica. A trend of increasing silica from 22 to 44 mg/L from well E to well F is consistent with an abrupt change in rock type from basin-fill alluvium to fractured basalt. The silica concentration at well F is nearly the same as that at upper Verde River springs (spring G), indicating that a large fraction of the ground water discharging at upper Verde River springs evidently has been in contact with basalt, despite the observation of ground water emerging from limestone. The basalt paleochannel is interpreted as a preferential conduit for ground water movement in the local vicinity of well F.

In comparison to other samples along the ground-water outlet, the M-D sequence (represented by well M near Drake) had the lowest concentrations of Li and B and was the most depleted in  $\delta^{18}\text{O}$  and  $\delta\text{D}$ . Stable-isotope compositions of oxygen and hydrogen usually are one of the best geochemical constraints in mass-balance calculations, but their application may be limited by the range of spatial variation, seasonal variation, or analytical uncertainty, which may allow for multiple nonunique solutions. Because a multitude of mixing scenarios or flowpaths can produce the same observed water chemistry, uncertainty limits were placed on all constituents used in the model to better constrain the number of possible reactions and more accurately determine the fractions of mixing solutions.

A global uncertainty of  $\pm 5$  percent was assigned to all of the major and most of the trace-element analyses, consistent with cation-anion balances of less than  $\pm 5$  percent (table F2). A larger uncertainty of  $\pm 10$  percent was assigned to boron and lithium because they are known to behave nonconservatively in this system. Stable isotopes of oxygen, hydrogen, and carbon were assigned an uncertainty of 0.1‰  $\delta^{18}\text{O}$ , 1.0‰  $\delta\text{D}$ , and 2.0‰  $\delta^{13}\text{C}$ , respectively (consistent with their reported analytical uncertainty for these analyses in this study). Calcite and dolomite mineral phases were assigned a value of −2.0‰  $\delta^{13}\text{C}$ , based on a mean value of −1.85‰ ( $n = 36$ ) for analyses of nearly pure limestone samples from the Redwall Limestone in north central Arizona (Muller and Mayo, 1986). Carbon-dioxide gas was assigned a value of −18.0‰  $\delta^{13}\text{C}$ , based on the results of soil-gas samples collected from the Dripping Springs basin in central Arizona (Pierre Glynn, unpub. data, oral commun., 2005). The “minimal” option in PHREEQC was chosen to reduce the number of possible models and to provide only those models which are a best fit to the input data. In selecting this option, it is presumed that the simplest, least complicated models with the fewest phases are the most plausible models.

The model was required to evaluate mass transfers of the following 9 phases, which were chosen based on relative

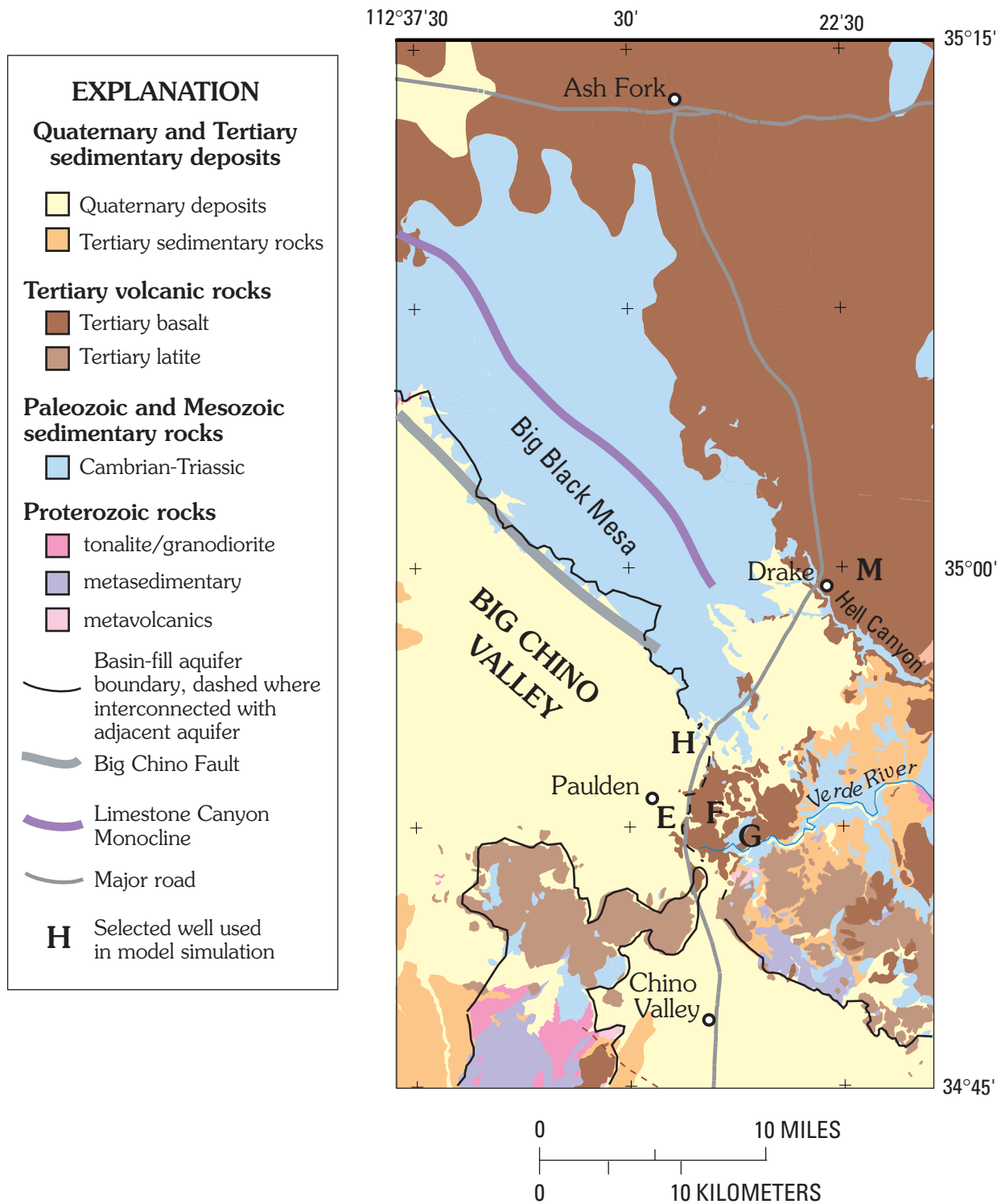


**Figure F15** Geology map showing the location of selected wells and springs used in inverse geochemical modeling of Big Chino basin outlet flowpath (geology simplified from DeWitt and others, in press). Base is from U.S. Geological Survey digital data 1:100,000.

**Table F2.** Chemical composition of selected ground waters from the Verde River headwaters representing the Big Chino basin-fill aquifer, the regional carbonate aquifer (D-C zone and M-D sequence) and upper Verde River springs. Sample locations shown on Figure F15.

[Concentrations in mg/L; isotopes expressed in per mil, and pH in pH units;  $\delta$ , delta;  $^{\circ}\text{C}$ , centigrade]

	Well E Big Chino basin-fill aquifer near outlet	Well H D-C zone beneath basin-fill aquifer	Well M M-D sequence near Drake	Well F D-C zone along main flowpath	Spring G Upper Verde River springs	Change between well E and spring G (%)
pH	7.8	7.0	7.7	7.7	7.8	
Dissolved oxygen	8.9	5.7	5.1	4.7	5.0	
Temperature ( $^{\circ}\text{C}$ )	18.7	25.9	23.6	18.2	19	
Alkalinity (as $\text{HCO}_3$ )	195	500	220	235	256	
Calcium	36	64	40	41	40	11
Magnesium	16	28	19	18	19	19
Sodium	18	93	6	21	32	78
Silica (as $\text{SiO}_2$ )	22	17	9	44	42	91
Strontium	0.370	0.350	0.101	0.408	0.346	-6.5
Sulfate	9.2	23	18	12	11.1	21
Chloride	13	27	7	15	17	31
Lithium	0.017	0.086	0.003	0.019	0.028	65
Boron	0.073	0.440	0.012	0.088	0.136	86
$^{18}\text{O}$	-10.3	-10.7	-10.9	-10.2	-10.3	
$^2\text{H}$	-73	-77	-80	-73	-75	
$^{13}\text{C}$	-8.2	-5.6	-2.0	-8.8	-7.0	
Cation/Anion balance percent error	1.68	0.38	-4.72	-1.00	0.43	

**Table F3.** Saturation indices for mixing endpoints contributing to upper Verde River springs. Positive numbers indicate saturation, negative numbers indicate undersaturation. Sample locations shown on Fig. F15.

[NC, not calculated]

Mineral phases	Chemical formula	Well E Big Chino basin-fill aquifer near outlet	Well H D-C zone beneath basin-fill aquifer	Well M M-D sequence near Drake	Well F D-C zone along main flowpath	Spring G Upper Verde River springs
Calcite	$\text{CaCO}_3$	0.12	0.00	0.18	0.14	0.27
Dolomite	$\text{CaMg}(\text{CO}_3)_2$	0.16	0.00	0.37	0.18	0.49
Strontianite	$\text{SrCO}_3$	-1.38	-1.82	-1.96	-1.37	-1.21
Gypsum	$\text{CaSO}_4 \cdot 2\text{H}_2\text{O}$	-2.83	-2.34	-2.52	-2.68	-2.74
Celestite	$\text{SrSO}_4$	-3.12	-0.01	-3.41	-2.98	-3.1
Chalcedony	$\text{SiO}_2$	0.19	-0.01	-0.26	0.5	0.46
$\text{SiO}_2$ (amorphous)	$\text{SiO}_2$	-0.67	-0.84	-1.10	-0.37	-0.4
Sepiolite	$\text{Mg}_2\text{Si}_3\text{O}_{7.50}\text{H} \cdot 3\text{H}_2\text{O}$	-1.7	-4.70	-3.01	-1.13	-0.74
Talc	$\text{Mg}_3\text{Si}_4\text{O}_{10}(\text{OH})_2$	0.93	-2.96	-0.46	1.6	2.26
Halite	$\text{NaCl}$	-8.18	-7.19	-8.94	-8.05	-7.82
Albite	$\text{NaAlSi}_3\text{O}_8$	NC	NC	NC	NC	NC
Anorthite	$\text{CaAl}_2\text{Si}_2\text{O}_8$	NC	NC	NC	NC	NC
Kaolinite	$\text{Al}_2\text{Si}_2\text{O}_5(\text{OH})_4$	NC	NC	NC	NC	NC
Carbon dioxide	$\text{CO}_2$ (gas)	-2.56	-1.32	-2.38	-2.38	-2.44

**Table F4.** Results of PHREEQC phase mole transfers and mixing model simulations for upper Verde River springs.

Model no.	Phase Mole Transfers*									No. of phases	Sum of residuals
	SiO <sub>2</sub> Chalcedony	CO <sub>2</sub> (gas)	NaCl Halite	CaMgCO <sub>3</sub> Dolomite	Mg <sub>3</sub> Si <sub>4</sub> O <sub>10</sub> (OH) <sub>2</sub> Talc	CaCO <sub>3</sub> Calcite	CaSO <sub>4</sub> Gypsum	CaF <sub>2</sub> Fluorite	SrSO <sub>4</sub> Celestite		
1		-2.31E-04					-2.94E-05	-2.89E-06		3	1.14E+01
2			8.42E-05		2.50E-05			-3.31E-06	-8.50E-07	4	1.78E+01
3	1.00E-04	-1.66E-04	8.42E-05					-3.31E-06	-8.50E-07	5	1.70E+01
4				6.03E-05			-2.94E-05	-3.09E-06	-5.78E-07	4	1.87E+01
5					2.49E-05		-2.17E-05	-3.53E-06		3	1.50E+01
6	1.00E-04		8.42E-05	5.69E-05				-3.31E-06	-8.50E-07	5	2.05E+01
7	1.27E-04			6.47E-05			-2.82E-05	-3.82E-06		4	1.97E+01
8			7.97E-05	5.41E-05			-3.50E-05	-1.93E-06		4	2.24E+01
9					2.25E-05		-2.31E-05	-2.65E-06	-6.25E-07	4	1.48E+01
10					2.04E-05	1.48E-05	-2.91E-05	-2.49E-06		4	1.71E+01
11			3.17E-05		2.16E-05		-2.67E-05	-2.27E-06		4	1.59E+01
12		-2.22E-04					-2.44E-05	-2.87E-06	-6.18E-07	4	7.88E+00
13			4.80E-05	5.17E-05			-2.58E-05	-2.02E-06	-6.44E-07	5	1.73E+01

\*Results in millimoles per kilogram of H<sub>2</sub>O. Positive numbers indicate moles entering solution, negative numbers indicate moles leaving solution owing to precipitation or degassing. Sample locations are shown on figure F15.

Model no.	Solution Fractions for Initial Waters													Final water
	Devonian-Cambrian Zone north of Paulden			Big Chino basin-fill aquifer at outlet near Paulden			Carbonate aquifer between Big Chino outlet and Verde River near Paulden			Sum of Big Chino initial waters	Carbonate aquifer north of upper Verde River (Mississippian-Devonian sequence)			
	Well H	Min	Max	Well E	Min	Max	Well F	Min	Max	H + E + F	Well M	Min	Max	
1	0.14	0.12	0.15	0.00	0.00	0.00	0.79	0.79	0.82	0.94	0.06	0.05	0.07	1.00
2	0.10	0.09	0.10	0.25	0.24	0.25	0.66	0.66	0.66	1.00	0.00	0.00	0.00	1.00
3	0.10	0.09	0.10	0.25	0.24	0.25	0.66	0.66	0.66	1.00	0.00	0.00	0.00	1.00
4	0.12	0.11	0.12	0.12	0.09	0.13	0.76	0.75	0.79	1.00	0.00	0.00	0.00	1.00
5	0.13	0.12	0.15	0.16	0.05	0.23	0.67	0.56	0.77	0.96	0.04	0.03	0.08	1.00
6	0.10	0.09	0.10	0.25	0.24	0.25	0.66	0.66	0.66	1.00	0.00	0.00	0.00	1.00
7	0.13	0.13	0.13	0.23	0.22	0.23	0.61	0.60	0.62	0.97	0.03	0.03	0.04	1.00
8	0.10	0.10	0.10	0.00	0.00	0.00	0.83	0.82	0.84	0.93	0.07	0.06	0.08	1.00
9	0.13	0.11	0.13	0.00	0.00	0.00	0.87	0.87	0.89	1.00	0.00	0.00	0.00	1.00
10	0.13	0.12	0.13	0.00	0.00	0.00	0.81	0.80	0.82	0.94	0.06	0.06	0.08	1.00
11	0.12	0.10	0.12	0.00	0.00	0.00	0.82	0.76	0.84	0.94	0.06	0.06	0.12	1.00
12	0.14	0.11	0.18	0.00	0.00	0.00	0.86	0.82	0.89	1.00	0.00	0.00	0.00	1.00
13	0.10	0.09	0.11	0.00	0.00	0.00	0.90	0.89	0.91	1.00	0.00	0.00	0.00	1.00

activities of major and trace dissolved species and on the calculated values of the SIs:

calcite (dissolution only)  
 dolomite (dissolution only)  
 chalcedony  
 CO<sub>2</sub> gas (exsolution only)  
 halite  
 talc  
 gypsum  
 fluorite  
 celestite

Calcite, dolomite, and quartz (chalcedony) are common rock-forming minerals in basin-fill alluvium, as well as in igneous and sedimentary rocks. As shown in fig. F11, CO<sub>2</sub> gas is an important phase for near-surface carbonate reactions. Gypsum and halite are common secondary minerals that were included to account for the presence of SO<sub>4</sub>, Na, and Cl, although other sources are possible. Similarly, fluorite is needed to provide a fluoride-bearing phase. Celestite was included to provide a strontium-bearing phase, and its presence is supported by SI data for well H (table F3). Saturation indices for common alumina-silicate minerals such as albite, anorthite and kaolinite were *not* calculated by the model because too little dissolved aluminum is present. Alternately, a nonaluminous mineral such as talc or sepiolite was selected to provide a Mg-silicate phase. Talc includes of a large family of minerals such as chlorite, mica, phyllite, or clays formed by alteration of igneous rocks. In addition, the model allows cation exchange to occur between Ca and Na.

Within the above constraints, thirteen plausible minimal models were identified by PHREEQC (table F4). It is noted that linear combinations of these models also represent possible models, and that by assigning larger uncertainties to the constraints, there could be a much greater number of nonunique models. The models shown here are the simplest models yielding the best fit for the given analytical data and the designated constraints.

All of the minimal models presented in table F4 require between three and five phase transfers. A few of the models call upon relatively large phase transfers of chalcedony or degassing of carbon-dioxide. Nearly half the models require phase transfers involving dissolution of halite, dolomite, or talc. All models include minor transfers of fluorite, and most of the models require minor transfers of gypsum and/or celestite. The fact that calcite is included in only one of the models is an important result indicating that other processes than carbonate dissolution are more likely to have an effect on concentrations of Ca<sup>+2</sup> and Mg<sup>+2</sup> along the outlet flowpath. This result is somewhat surprising, given the extensive exposure to limestone (and dolomite) along the outlet flowpath. For all of the models presented in table F4, the range of variability in the calculated uncertainty (sum of residuals) is within 3.5 percent. None of the models are favored over any of the other possible models; all are considered plausible.

Six out of thirteen minimal models support a small amount of mixing between Big Chino ground water and the M-D sequence of the carbonate aquifer. The sum of three initial waters from Big Chino Valley (wells H, E, and F) accounts for between 93 and 100 percent of total discharge at upper Verde River springs, with the M-D sequence outside of Big Chino Valley accounting for none to a maximum of 7 percent of total spring inflow. At the Big Chino outlet near Paulden (well H in table F4), the D-C zone of the underlying carbonate aquifer contributes on the order of 10 to 15 percent of the ground water discharging from Big Chino Valley.

In summary, all thirteen of the minimal inverse models are consistent with converging flow along the valley outlet near Paulden to produce the water chemistry at upper Verde River springs by means of one or more of the following processes: (a) near-surface degassing of carbon dioxide, (b) dissolution of silicate minerals, (c) precipitation of gypsum, or (d) dissolution of small amounts of relatively common minerals such as halite, dolomite, talc, or calcite. All of these possible model scenarios are accompanied by a minor phase transfer of fluorite and usually one of celestite. Despite contact with carbonate minerals, the models predict relatively little change in the saturation state of calcite and dolomite along the Big Chino basin outlet flowpath, contrary to what might be expected for evolution along a carbonate aquifer flowpath. Compositional variations in major dissolved species such as Ca<sup>+2</sup>, Mg<sup>+2</sup>, and HCO<sub>3</sub><sup>-</sup> can be entirely accounted for by simple mixing and water interaction with non-carbonate minerals. No mixing with the M-D sequence of the carbonate aquifer is necessary to account for the water chemistry at upper Verde River springs, although a small fraction (less than 7 percent) is plausible.

## Summary and Conclusions

Using the tracer-dilution method, base flow at Stewart Ranch during low-flow conditions of June 2000 was measured as 19.5±1.0 ft<sup>3</sup>/s. Most ground-water inflow to upper Verde River springs occurs within the first mile downstream from the mouth of Granite Creek. Base flow in the upper Verde River upstream from Stewart Ranch is predominantly derived from upper Verde River springs (86.2 percent) and, to a lesser extent, from the Little Chino basin-fill aquifer. The Little Chino basin-fill aquifer contributed 13.8±0.7 percent of the base flow (2.7±0.08 ft<sup>3</sup>/s) based on the trace-dilution approach. Approximately four-fifths of the Little Chino inflow appears to originate from beneath Stillman Lake, as opposed to from lower Granite Creek which had a base flow of about 0.5 ft<sup>3</sup>/s upstream from its mouth.

Inverse model simulations in PHREEQC indicate that discharge to upper Verde River springs upstream from Stewart Ranch is predominantly derived from mixing of initial water sources solely within Big Chino Valley. A small amount of mixing with the M-D sequence north of the Verde River is possible (less than about 7 percent), although none is required

by a majority of the model simulations. A potential contribution from the M-D sequence (if any) would be credited to the part of the carbonate aquifer north of the upper Verde River between Big Black Mesa and lower Hell Canyon. These model results are consistent with the Big Chino basin-fill aquifer and the D-C zone of the carbonate aquifer being strongly interconnected near the basin outlet and functioning together as a single source of ground water from beneath Big Chino Valley.

The contributions to the base flow at the Paulden gauge can be estimated by using a simplifying assumption. An additional 7 percent of Verde River base flow is contributed between Stewart Ranch and the Paulden gauge. The source of this inflow has not been determined, but a reasonable simplifying assumption is that the sources of inflow for the remaining 7 percent are in the same proportion as those at Stewart Ranch. This assumption is supported by relatively little variation in the stable-isotope composition of streamflow between Stewart Ranch and the Paulden gauge. The readjusted contributions from each aquifer source at the Paulden gauge are as follows: (a) Little Chino basin-fill aquifer, 14 percent; (b) M-D sequence north of the Verde River, less than 6 percent; and (c) the combined Big Chino basin-fill aquifer and D-C zone of the underlying carbonate aquifer, greater than 80 to as much as 86 percent.

The model estimates for the ground-water fraction from the M-D sequence north of the upper Verde River compares favorably with the estimate by Ford (2002), who determined recharge from the geographical area underlying Big Black Mesa at about 5 percent of the base flow at the Paulden gauge using nongeochemical methods. The M-D sequence is part of a 3-dimensional regional aquifer, whereas the Big Black Mesa defined by Ford (2002) is a geographical area. A contribution of about 5 percent from the M-D sequence seems entirely consistent with the conceptual geologic framework of the carbonate aquifer developed in the earlier chapters of this report.

In summary, the accuracy of the inverse model simulations depends on how well the selected initial waters and mineral phases reflect the mineralogy and water chemistry of the water-bearing units. A large number of nonunique models are possible, although only the best-fit "minimal" models for the data have been presented here. Important reactions identified by inverse modeling include the dissolution of silicates and degassing of carbon dioxide, processes supported by field and analytical data. The most likely cause of a two-fold increase in dissolved silica is water-rock interaction with the basalt-filled paleochannel east of Paulden. Variations in pH and bicarbonate along the tracer reach primarily are attributed to degassing of CO<sub>2</sub> where ground water is discharging to land surface. Calcite and dolomite minerals remain near or at saturation along the length of the basin outlet flowpath, indicating that the dissolution (or precipitation) of carbonate rocks is *not* a dominant process, despite extensive exposure to limestone and dolomite.

In conclusion, the water chemistry of upper Verde River springs is consistent with the evolution of ground water from the Big Chino basin-fill aquifer that has traveled a short distance through the carbonate aquifer to emerge in the upper Verde River canyon. Little or no mixing with ground water

from the M-D sequence of the carbonate aquifer north of the upper Verde River is required to create the water chemistry at upper Verde River springs. Inverse geochemical modeling constrains the potential contribution from the M-D sequence of the regional carbonate aquifer to less than about 6 percent of base flow at the Paulden gauge. Other lines of nongeochemical evidence indicate that a contribution on the order of about 5 percent is plausible, but uncertain. Adjusted contributions from each aquifer source to base flow at the Paulden gauge are estimated as: (a) Little Chino basin-fill aquifer, 14 percent; (b) M-D sequence north of the Verde River, less than about 6 percent; and (c) the combined Big Chino basin-fill aquifer and underlying D-C zone of the carbonate aquifer, at least 80 to 86 percent.

## References Cited

- Anderson, T.W., 1976, Evapotranspiration losses from floodplain areas in Central Arizona: U.S. Geological Survey Open-File Report 76-864, 91 p.
- Appelo, C.A.J., and Postma, D., 1999, Geochemistry, Groundwater, and Pollution: Balkema, Rotterdam, 536 p.
- Bencala, K.E., McKnight, D.M., and Zellweger, G.W., 1990, Characterization of transport in an acidic and metal-rich mountain stream based on a lithium tracer injection and simulations of transient storage: *Water Resources Research*, v. 26, no. 5., p. 989–1000.
- Betancourt, J.L., 2003, The current drought (1999–2003) in historical perspective: 2003 Southwest Drought Summit report, May 12–13, 2003, Northern Arizona University, Flagstaff, Arizona, <http://www.mpcer.nau.edu/>, accessed on May 19, 2004.
- Boner, F.C., Davis, R.G., and Duet, N.R., 1991, Water resources data, Arizona, water year 1991: U.S. Geological Survey Water-Data Report AZ-91-1.
- Briggs, P.H., and Fey, D.L., 1996, Twenty-four elements in natural and acid mine waters by inductively coupled plasma-atomic emission spectrometry, *in* Arbogast, B.F., ed., Analytical methods manual for the Mineral Resources Surveys Program: U.S. Geological Survey Open-File Report 96-525, p. 95–101.
- Broshears, R.E., Bencala, K.E., Kimball, B.A., and McKnight, D.M., 1993, Tracer-dilution experiments and solute-transport simulations for a mountain stream, Saint Kevin Gulch, Colorado: U.S. Geological Survey Water-Resources Investigations Report 92-4081, 18 p.
- Bullen, T.D., and Kendall, Carol, 1998, Tracing of weathering reactions and water flowpaths: A multi-isotope approach, *in* Kendall, Carol and McDonnell, J.J., eds., *Isotope Tracers in Catchment Hydrology*: Elsevier, New York, p. 611–646.

- d'Angelo, W.M., and Ficklin, W.H., 1996, Fluoride, chloride, nitrate, and sulfate in aqueous solution by chemically suppressed ion chromatography, *in* Arbogast, B.F., ed., Analytical methods manual for the Mineral Resources Surveys Program: U.S. Geological Survey Open-File Report 96-525, p. 149–153.
- DeWitt, Ed, Langenheim, V.E., Force, Eric, Vance, Kelley, and Lindberg, P.A., *with* a digital database by Doug Hirschberg, Guy Pinhassi, and Nancy Shock, *in press*, Geologic map of the Prescott National Forest and headwaters of the Verde River, Yavapai and Coconino Counties, Arizona, U.S. Geological Survey Miscellaneous Investigations Map, scale 1:100,000, two sheets.
- Dodder, Joanna, 2004, Study supports Big Chino contribution to river: The Daily Courier, April 22, 2004, Prescott, Arizona, p. 12A.
- Ewing, D.B., Osterberg, J.C., and Talbot, R.W., 1994, Ground-water Study of the Big Chino Valley—Hydrology and hydrogeology: Bureau of Reclamation Technical Report, Denver, Colorado, 14 p. plus 6 appendixes.
- Fisk, G.G., Duet, N.R., Evans, D.W., Angerth, C.E., Castillo, N.K., and Longworth, S.A., 2004, Arizona Water Resources Data—Water Year 2003: U.S. Geological Survey Water-Data Report AZ-03-1, 328 p.
- Ford, J.R., 2002, Big Chino Valley ground water as the source of the Verde River, *in* Ground Water/Surface Water Interactions, July 1–3, 2002: American Water Resources Association summer specialty conference, 6 p.
- Freethy, G.W., and Anderson, T.W., 1986, Predevelopment hydrologic conditions in the alluvial basins of Arizona and adjacent parts of California and New Mexico: U.S. Geological Survey Hydrologic Investigations Atlas HA-664.
- Glynn, Pierre, and Brown, James, 1996, Reactive transport modeling of acidic metal-contaminated ground water at a site with sparse spatial information, *in* Steefer, C.I., Lichtner, P., and Oelkers, E., eds., Reviews in Mineralogy: Mineralogical Society of America, Washington, D.C., v. 34, p. 377–438.
- Hem, J.D., 1992, Study and interpretation of the chemical characteristics of natural water: U.S. Geological Survey Water-Supply Paper 2254, 263 p.
- Hendrickson, Raquel, 2000, USGS report creates waves—Government agencies fence over Verde source: Verde Independent, Camp Verde, Arizona, (<http://www.verdevalleynews.com> on December 18, 2000).
- Hereford, Richard, 1975, Chino Valley Formation (Cambrian?) in northwestern Arizona: Geological Society of America Bulletin, v. 86, p. 677–682.
- Horowitz, A.J., Demas, C.R., and Fitzgerald, K.K., 1994, U.S. Geological Survey protocol for the collection and processing of surface-water samples for the subsequent determination of inorganic constituents in filtered water: U.S. Geological Survey Open-File report 94–539, 157 p.
- Kendall, Carol, and Caldwell, E.A., 1998, Fundamentals of isotope geochemistry, *in* Kendall, Carol and McDonnell, J.J., eds., Isotope tracers in catchment hydrology: Elsevier, New York, Chapter 3, p. 51–86.
- Kimball, B.A., 1997, Use of tracer injections and synoptic sampling to measure metal loading from acid mine drainage: U.S. Geological Survey Fact Sheet 245–96, 4 p.
- Kimball, B.A., Bencala, K.E., and Runkel, R.L., 2000, Quantifying effects of metal loading from mine discharge, *in* Fifth International Conference on Acid Rock Drainage, Denver, 2000, Proceedings: v. II, ICARD 2000, p. 1381–1390.
- Kimball, B.A., Broshears, R.E., Bencala, K.E., and McKnight, D.M., 1994, Coupling of hydrologic transport and chemical reactions in a stream affected by acid mine drainage: Environmental Science & Technology, v. 28, p. 2065–2073.
- Kimball, B.A., Runkel, R.L., Bencala, K.E., and Walton-Day, Katherine, 1999, Use of tracer-injection and synoptic-sampling studies to quantify effects of metal loading from mine drainage, *in* Morganwalp, D.W., and Buxton, H.T., eds., U.S. Geological Survey Toxic Substances Hydrology Program—Proceedings of the Technical Meeting, Charleston, South Carolina, March 8-12, 1999, Volume 1—Contamination from hardrock mining: U.S. Geological Survey Water-Resources Investigations Report 99–4018A.
- Knauth, L.P., and Greenbie, M., 1997, Stable isotope investigation of ground-water surface-water interactions in the Verde River headwaters area: Arizona State University Department of Geology report in fulfillment of Arizona Water Protection Fund Grant #95-001, administered by Arizona Department of Water Resources, 28 p.
- Krieger, M.H. 1965, Geology of the Prescott and Paulden quadrangles, Arizona: U.S. Geological Survey Professional Paper 467, 127 p.
- Long, H.K. and Farrar, J.W., 1995, Report on the U.S. Geological Survey's evaluation program for standard reference samples distributed in May 1995—T-135 (trace constituents), M-134 (major constituents), N-45 (nutrients), N-46 (nutrients), P-24 (low ionic strength), Hg-20 (mercury), and SED-5 (bed material): U.S. Geological Survey Open-File Report 95–395, 135 p.
- MacCormack, H.F., Fisk, G.G., Duet, N.R., Evans, D.W., and Castillo, N.K., 2002, Water Resources Data, Arizona, Water Year 2001: U.S. Geological Survey Water-Data Report AZ-01–1, p. 257.
- Muller, A.B., and Mayo, A.L., 1986,  $^{13}\text{C}$  variation in limestone on an aquifer-wide scale and its effects on groundwater  $^{14}\text{C}$  dating models: Radiocarbon, v. 28, no. 3., p. 1041–1054.

- Owen-Joyce, S.J., and Bell, C.K., 1983, Appraisal of water resources in the Upper Verde River area, Yavapai and Coconino Counties, Arizona: Arizona Department of Water Resources Bulletin 2, 219 p.
- Parkhurst, D.L., and Plummer, L.N., 1993, Geochemical models, *in* regional ground-water quality: Chapter 9 of Alley, W.M., ed., Van Nostrand Reinhold, New York, p. 199–225.
- Parkhurst, D.L., and Appelo, C.A.J., 1999, User's guide to PHREEQC (Version 2)—A computer program for speciation, batch-reaction, one-dimensional transport, and inverse geochemical calculations. U.S. Geological Survey Water-Resources Investigations Report 99–4259, 312 p.
- Plummer, L.N., Prestemon, E.C., and Parkhurst, D.L., 1994, An interactive code (NETPATH) for modeling NET geochemical reactions along a flowpath, version 2.0: U.S. Geological Survey Water-Resources Investigations Report 94–4169, 130 p.
- Rantz, S.E. (compiler), 1982, Measurement and Computation of Streamflow—v. 1, Measurement of stage; v. 2, Computation of discharge: U.S. Geological Survey Water-Supply Paper 2175, v. 1, 284 p.; v. 2, 346 p.
- Shelton, L.R., 1994, Field guide for collecting and processing of stream-water samples for the National Water-Quality Assessment Program: U.S. Geological Survey Open-File Report 94-455, 42 p.
- Tadayon, Saeid, Duet, N.R., Fisk, G.G., MacCormack, H. F., Partin, C.K., Pope, G.L., and Rigas, P.D., 2001, Water Resources Data, Arizona, Water Year 2000: U.S. Geological Survey Water-Data Report AZ-00–1, p. 250.
- Tadayon, Saeid, Duet, N.R., Fisk, G.G., MacCormack, H. F., Partin, C.K., Pope, G.L., and Rigas, P.D., 2000, Water Resources Data, Arizona, Water Year 1999: U.S. Geological Survey Water-Data Report AZ-99–1, p. 225.
- Walton-Day, Katherine, Runkel, R.L., Kimball, B.E., and Bencala, K.E., 1999, Application of the solute-transport models OTIS and OTEQ and implications for remediation in a watershed affected by acid mine drainage: Cement Creek, Animas River Basin, Colorado, *in* Morganwalp, D.W., and Buxton, H.T., eds., U.S. Geological Survey Toxic Substances Hydrology Program—Proceedings of the Technical Meeting, Charleston, South Carolina, March 8-12, 1999: Volume 1—Contamination from hardrock mining: U.S. Geological Survey Water-Resources Investigations Report 99-4018A.
- Wilde, F.D., Radtke, D.B., Gibb, Jacob, and Iwatsubo, R.T. (eds.), 1999, National field manual for the collection of water-quality data: Techniques of Water Resources Investigations TWI 09-A4, book 9, chap. A6, sections 6.0, 6.0.1, 6.0.2, 6.0.2.A, and 6.0.2B, 152 p.
- Wirt, Laurie, and Hjalmanson, H.W., 2000, Sources of springs supplying base flow to the Verde River headwaters, Yavapai County, Arizona: U.S. Geological Survey Open-file Report 99–0378, 50 p.
- Wirt, Laurie, Leib, Kenneth J., and Mast, M. Alisa, 2000, Chemical-constituent loads during thunderstorm runoff in a high-altitude alpine stream affected by acid drainage, *in* Fifth International Conference on Acid Rock Drainage, Denver, 2000, Proceedings: V. II, ICARD 2000, p. 1391–1401.
- Wirt, Laurie, Leib, Kenneth J., Bove, Dana, and Melick, Roger, 2001, Metal loading assessment of point and nonpoint sources in a small alpine subbasin characterized by acid drainage—Prospect Gulch, upper Animas River watershed, Colorado: U.S. Geological Survey Open-File Report 01–0258, 36 p.
- Zellweger, G.W., 1996, Tracer injections in small streams—why and how we do them, *in* Morganwalp, D.W., and Aronson, D.A., eds., U.S. Geological Survey Toxic Substances Hydrology Program—Proceedings of the Technical Meeting, Colorado Springs, Colo., September 20–24, 1993: U.S. Geological Survey Water-Resources Investigations Report 94–4015, v. 2, p. 765–768.





# **Synthesis of Geologic, Geophysical, Hydrological, and Geochemical Data**

By Laurie Wirt

Chapter G

## **Geologic Framework of Aquifer Units and Ground-Water Flowpaths, Verde River Headwaters, North-central Arizona**

Edited by Laurie Wirt, Ed DeWitt, and V.E. Langenheim

Prepared in cooperation with the Arizona Water Protection Fund Commission

Open-File Report 2004–1411-G

**U.S. Department of the Interior  
U.S. Geological Survey**

**U.S. Department of the Interior**  
Gale A. Norton, Secretary

**U.S. Geological Survey**  
P. Patrick Leahy, Acting Director

U.S. Geological Survey, Reston, Virginia: 2005

For product and ordering information:  
World Wide Web: <http://www.usgs.gov/pubprod>  
Telephone: 1-888-ASK-USGS

For more information on the USGS--the Federal source for science about the Earth, its natural and living resources, natural hazards, and the environment:  
World Wide Web: <http://www.usgs.gov>  
Telephone: 1-888-ASK-USGS

Any use of trade, product, or firm names is for descriptive purposes only and does not imply endorsement by the U.S. Government.

Although this report is in the public domain, permission must be secured from the individual copyright owners to reproduce any copyrighted materials contained within this report.

This report has not been reviewed for stratigraphic nomenclature.

***Suggested citation:***

Wirt, L., 2005, Synthesis of Geologic, Geophysical, Hydrological, and Geochemical Data: *in* Wirt, Laurie, DeWitt, Ed, and Langenheim, V.E., eds., Geologic Framework of Aquifer Units and Ground-Water Flowpaths, Verde River Headwaters, North-Central Arizona: U.S. Geological Survey Open-File Report 2004-1411-G, 17 p.

# Contents

Introduction.....	1
Acknowledgements.....	1
Hydrological Setting.....	1
Predevelopment Conditions.....	2
Water Use.....	2
Geologic Framework.....	2
Major Aquifers and Ground-Water Flowpaths.....	3
Regional Carbonate Aquifer.....	3
Little Chino Basin-Fill Aquifer.....	4
Big Chino Basin-Fill Aquifer.....	4
Water Chemistry.....	5
Tritium and Carbon-14.....	5
Trace Elements.....	5
Stable Isotopes of Hydrogen and Oxygen.....	6
Synoptic Sampling and Tracer-Dilution Studies.....	6
Inverse Modeling of Geochemical Data.....	6
Sources of Base Flow.....	7
Recommendations for Future Studies.....	9
Summary of Conclusions.....	10
References Cited.....	10

## Figures

<b>G1.</b> Pie charts showing sources of base flow to the upper Verde River, comparing water-budget estimates with those based on inverse modeling using geochemistry and tracer-study data.....	8
--	---

# Synthesis of Geologic, Geophysical, Hydrological, and Geochemical Data

By Laurie Wirt

## Introduction

The upper Verde River is a true desert river. Its surface flow begins—not high in the mountains—but instead from a network of diffuse springs at the bottom of a narrow bedrock canyon. In marked contrast to the headwaters of large rivers in more temperate climates where two or more mountain streams typically come together to form a river, base flow in the upper Verde River discharges from springs downgradient from large aquifers in Big and Little Chino Valleys. Near their topographic outlets, the Big and Little Chino basin-fill aquifers discharge to Paleozoic sedimentary rocks, which, in turn, are drained by an incised canyon. In addition, a carbonate aquifer underlies most of Big Chino Valley and the area north of the upper Verde River near Paulden.

Water resources of the Big and Little Chino basin-fill aquifers are under increasing pressure from population growth and residential development. The rural towns of Chino Valley and Paulden in Big Chino Valley are shifting from an economy of irrigated agriculture and ranching to one of suburban land use. In 2004, the city of Prescott purchased a ranch in upper Big Chino Valley with the intent to build a pipeline to import 8,717 acre-ft/yr of water into the Prescott Active Management Area, or PAMA (Southwest Ground-Water Consultants, 2004). The proposed water pipeline and accelerated rural development add to increasing concern about water-resource issues and the effects of pumping on base flow of the upper Verde River. Better understanding of relations between the three major aquifers and the river is needed to manage limited water resources. The stated goal of this report has been to describe the geologic framework of aquifer units and ground-water flowpaths in the Verde River headwaters region.

Together, the chapters in this report offer a synoptic summary, or snapshot in time, of the geologic, geophysical, and geochemical information presently available for the Verde River headwaters region. This framework of information is needed for future scientific investigations such as ground-water modeling, as well as for water-resource policy decisions. In this final chapter, the findings of six previous chapters are summarized and integrated according to the following topics: (a) hydrologic setting, (b) geologic framework, (c) major aquifers and ground-water flowpaths, and (d) water chemistry. Lastly, proportions of base flow from each of the three major source aquifers to the upper Verde River are reevaluated

based on a synthesis of new and preexisting data. Collectively, a synthesis of multidisciplinary evidence from varied and independent sources improves confidence in our knowledge of the hydrogeologic system and allows us to better define contributions from distinct source areas. This chapter serves as an executive summary of the findings in this report.

## Acknowledgments

Investigations in this report were coordinated with the Arizona Department of Water Resources, Arizona Water Protection Fund, Arizona Game and Fish Department, Prescott National Forest, Yavapai County Water Advisory Committee, U.S. Bureau of Land Management, and local land owners, all of whom are involved directly with or affected by water-resource planning activities within the watershed. Technical review for the Arizona Water Protection Fund was coordinated by John P. Hoffmann of the U.S. Geological Survey (USGS) and Frank Corkhill of the Arizona Department of Water Resources. Additional review by David Lindsey (USGS) helped to integrate the chapters and improve the readability of the overall manuscript. The authors especially would like to recognize all of those who have contributed to earlier studies in the Verde River watershed and, in turn, look forward to future studies that will build on the ideas presented here.

## Hydrological Setting

The Verde River is a major tributary of the Gila River watershed which is part of the Colorado River drainage. The Verde River headwaters region encompasses Big and Little Chino Valleys, which are part of the Transition Zone geologic province. The two valleys are bounded by the Bradshaw, Santa Maria, and Juniper Mountains to the south and west; and to the north by Big Black Mesa, which is the southernmost margin of the Colorado Plateau (figs. A1–A2, Chapter A, this volume; fig. D1, Chapter D, this volume). The 35-mi reach of the Verde River upstream from Verde Valley begins at the Sullivan Lake dam and ends at the mouth of Sycamore Creek. The reach referred to as the “upper Verde River” is considered here to be the uppermost 10-mi reach above the U.S. Geological Survey streamflow gauging station near Paulden (09503700), or “Paulden gauge.” The climate of the study area is arid to semiarid.

## Predevelopment Conditions

Present surface- and ground-water conditions no longer reflect predevelopment conditions in Big or Little Chino Valleys. Continuous perennial flow in the Verde River historically began at the confluence of Big Chino Wash and Williamson Valley Wash in Big Chino Valley and at Del Rio Springs in Little Chino Valley, but now begins 2–5 mi farther downstream. Ground-water pumping began in 1930 with the drilling of the first deep artesian well in Little Chino Valley. Predevelopment conditions are thought to have persisted in Little Chino Valley through 1937, when storage capacity in reservoirs increased, and pumping became more widespread (Schwalen, 1967). At present, year-round flow between Del Rio Springs and Sullivan Lake via Little Chino Creek has all but disappeared, and uppermost perennial flow now emerges downstream at three distinct spring networks within a 1-mi radius of the Granite Creek/Verde River confluence (fig. F1, Chapter F, this volume).

Little hydrologic information is available for Big Chino Valley before 1946, but segments of Big Chino Wash probably were intermittent or perennial before about 1950. Historical USGS topographic maps (1947) and aerial photographs indicate perennial segments (fig. A10A, Chapter A, this volume) and native fish were documented in upper Big Chino Wash in 1897 (Gilbert and Scofield, 1898) and again in 1950 (Winn and Miller, 1954). On the basis of these historical observations and modern water-level data, it is estimated that the water table in the vicinity of Sullivan Lake has declined by more than 80 ft since 1947 (fig. A10B, Chapter A, this volume). Streamflow records at the Paulden gauge began in 1963, long after diversions for irrigation and ground-water pumping had started, and thus true predevelopment base-flow conditions will never be accurately known.

## Water Use

Pre-existing water-use data for Big and Little Chino basins are confusing and sometimes inaccurate because of differences in the way the data are collected. Water-use data have been collected for different areas by different agencies using different approaches over different timeframes. In addition, estimates of agricultural water use vary widely depending on whether a consumptive use or water-duty reporting method is taken. Indirect measurements of consumptive use often have a large error component and are unreliable compared with direct approaches, such as gauging or metering (Chapter A, this volume).

In general, agricultural use is diminishing as residential use is expanding. In 1997, water use in Little Chino Valley was about one-half municipal (including residential, commercial, and industrial demand) and one-half agricultural (Arizona Department of Water Resources, 2000). Because most of the water used in the PAMA is either metered or gauged, estimates of water use in Little Chino Valley are fairly accurate. Since 1997, the PAMA overdraft in excess of recharge has been

reported variously between 6,610 and 9,830 acre-ft/year (Arizona Department of Water Resources, 1998, 1999a, 1999b, and 2000).

Water use in Big Chino Valley is more than 90 percent agricultural and has varied greatly since the 1950s. Irrigated agriculture probably peaked between 9,000 and 15,000 acre-ft/yr in the 1950s through the 1970s and steadily declined through the 1990s. Seventy percent of ground-water pumping prior to 1967 was in northern or “upper” Big Chino Valley (Bob Wallace, oral commun., 1989). Since about 1998 water use reportedly has increased (Arizona Department of Water Resources, 2000, p. 3–31), but current estimates of water use are largely based on indirect consumptive use estimates which are unreliable. Large discrepancies between various indirect estimates are attributed to differences in consumptive use factors, soil types, farming practices, delivery methods, and system efficiencies, as well as to differences in estimating the amount of land under cultivation (Chapter A, this volume). More accurate and direct methods such as metering are sorely needed.

## Geologic Framework

The basins beneath Big and Little Chino Valleys developed in late Tertiary time between 10 Ma to the present by crustal extension in central Arizona (Chapter B, this volume). They are the northernmost basins of the Transition Zone. Not as extensive or as deep as Basin-and-Range basins to the south and west, the Big and Little Chino basins are distinguished by fault-bounded margins, incorporation of volcanic material within the basin-fill deposits, and facies variations within the sediment fill.

Big Chino Valley, which is the larger of the two basins, is an elongate, northwest-trending, 45-km-long graben that is at least 700 m deep in the center and shallower around the northwestern, southeastern, and southwestern margins. Basalt flows entered the valley from the north, west, and southeast from 6.0 to 4.5 Ma. The basin contains Quaternary and late Tertiary sediment and is bordered by the Quaternary Big Chino Fault on the northeastern side of the valley. Fine-grained carbonate sediment indicates that the central part of the basin was a playa. Alluvial fans and major tributaries, predominantly Williamson Valley and Walnut Creek, contributed sediment to the margin of the playa from the south and west.

The basin underlying Little Chino Valley is smaller than the Big Chino basin and contains a thinner sequence of Quaternary and late Tertiary sediment. The deepest part of the basin trends northwest and is 18 km long. Maximum sediment thickness is about 200 m. Alluvial fans contributed sediment from the west, south, and southeast. The valley lacks proven playa deposits and young (4–6 Ma) basalt flows. Beneath the Quaternary and late Tertiary sediments are extensive basalt flows of the 10–15-Ma Hickey Formation, as well as the abundant flows, domes, and intrusive centers of 24-Ma latite-andesite (figs. B5 and B7, Chapter B, this volume). These volcanic rocks formed an irregular topographic surface on which the

Quaternary and late Tertiary sediment was deposited. Consequently, sediment thickness in Little Chino basin varies and mirrors the underlying relief of Tertiary volcanic rocks. Shallowly buried (<200–300 m) latite-andesite plugs in northern Little Chino Valley, detected as semicircular magnetic lows, probably act as barriers to ground-water flow. The complexity of volcanic facies beneath Little Chino Valley is the major cause of artesian conditions.

Gravity data indicate an asymmetric basin beneath Big Chino Valley at least 1–2 km deep and 3–4 km wide (fig. C13, Chapter C, this volume). The areal extent of the Big Chino gravity low coincides with a thick playa deposit that is corroborated by well data. The lack of a distinct gravity low in Little Chino Valley suggests that the sedimentary and volcanic fill is much thinner (< 1 km) than that of Big Chino Valley. As shown by gravity values in both basins, the basin-fill deposits thin and become narrower toward their topographical outlets in the direction of Sullivan Lake. The reduction of the basin-fill deposits toward their outlets coincides with the emergence of predevelopment discharge in lower Big Chino Wash and Little Chino Creek north of Del Rio Springs.

The Big Chino Fault is the largest structural feature in the study area, a northwest-trending fault with at least 1,100 m of displacement that forms the northern boundary of the basin graben. Where displacement is large, basin-fill deposits abut Proterozoic basement rocks beneath Big Black Mesa, which serve as a barrier to flow across the fault. The fault decreases in displacement to the southeast and dies in a series of horsetail splays north of Paulden, where there is connection between the basin-fill aquifer and the underlying and adjoining carbonate aquifer north of the upper Verde River (Chapter D, this volume).

Unlike Big Chino Valley, Little Chino Valley does not have large displacement faults. The pervasive magnetic grain within Little Chino Valley is northeast and northwest striking, but apparently none of the structures responsible for this grain have a large vertical offset like the Big Chino fault. Geophysical and borehole data suggest the presence of a northwest-striking, low-displacement fault in Little Chino Valley north of Del Rio Springs.

## Major Aquifers and Ground-Water Flowpaths

Three major aquifers in the headwaters study slope toward the upper Verde River. They are the Big and Little Chino basin-fill aquifers and the carbonate aquifer north of Big Black Mesa and the upper Verde River within the Transition Zone (fig. D2, Chapter D, this volume). Although smaller, the basin-fill aquifers have the large storage capacity of typical Basin-and-Range basin-fill aquifers and deliver steady, reliable discharge to perennial streams near their outlets. The part of the carbonate aquifer contributing to the Verde River headwaters is the eroded and exposed margin of an extensive regional aquifer that lies more than 3,000 ft beneath much of the southwestern Colorado Plateau (fig. D1, Chapter D, this volume).

Igneous and metamorphic Proterozoic basement rocks generally have very low permeability and define the bottom and edges of the basin-fill aquifers. Where basement rocks are absent or fractured, ground water can move into or out of the basins. The most permeable water-bearing units producing the largest well yields include medium- to coarse-grained Quaternary and Tertiary alluvium, some (but not all) Tertiary basalt flows, and Paleozoic carbonate rocks.

Recharge to the aquifers varies seasonally, temporally, and spatially throughout the headwaters area as a function of climate, stream gradient, and rock type. The greatest amounts of recharge generally are attributed to losing reaches of mountain-front areas having the most precipitation. Williamson Valley Wash, Walnut Creek, and Granite Creek are the largest tributaries draining mountain fronts to the south and west. Substantial amounts of recharge, however, also appear to occur along the valley floors. In lowland areas, direct recharge to the basin-fill aquifers along low-gradient stream reaches may be substantial, particularly near the basin outlets. The amount of recharge resulting from infrequent flooding of Williamson Valley Wash, lower Big Chino Wash, and Granite Creek may be underestimated, as indicated by decreasing apparent ground-water ages toward the valley outlets (figs. E7 and E8, Chapter E, this volume).

The degree of recharge also is influenced by the types of rocks exposed at the ground surface. Relatively impermeable igneous and metamorphic rocks in the Bradshaw and Santa Maria Mountains probably produce little high-altitude recharge, but supply the largest amounts of runoff to the basins where there is substantial low-gradient recharge beneath ephemeral streams overlying alluvium. In contrast, in high-altitude carbonate regions such as Big Black Mesa or the Juniper Mountains, the rate of infiltration is probably relatively higher owing to greater permeability of carbonate rocks and fractured basalts. The highest rates of infiltration are likely to occur where there is karst, and the water table is near land surface; for example, along Hell Canyon near King Spring.

In general, ground-water movement within the basin-fill aquifers is from the valley margins and tributaries toward the valley center and then down the longitudinal axis of the valley toward the basin outlet. Ground-water flowpaths within the basin-fill aquifers may deviate from surface-water drainage patterns (a) where confining conditions exist, (b) where fine-grained playa sediment or thick latite plugs create less-permeable obstructions to flow, and (c) near the outlets of the basins where ground water is transmitted through pre-Cenozoic rock units. Within the carbonate aquifer, preferential ground-water movement is caused by abrupt changes in the secondary porosity of the lithology caused by karst or extensive fracturing, which on a regional scale may be broadly associated with large structural features (such as faults or monoclines).

## Regional Carbonate Aquifer

The region north of the Big Chino Fault and the upper Verde River (in the Transition Zone and extending southward

from the Colorado Plateau) is a continuous expanse of Paleozoic sedimentary rocks that is partly overlain by Tertiary basalt flows. Eroded remnants of these same rocks also are exposed in the Juniper Mountains, Sullivan Buttes, and Black Hills. Paleozoic rocks also are concealed beneath Big Chino Valley and part of northern Little Chino Valley. Although largely disconnected from the carbonate aquifer beneath the Colorado Plateau, these remnants are considered part of the regional carbonate aquifer. Within the Transition Zone, the carbonate aquifer consists of many discrete zones which may be faulted or eroded and may or may not be interconnected. The carbonate aquifer typically discharges to lakes or springs at the bottom of incised canyons such as Stillman Lake, King Spring, and the springs in the Verde River/Granite Creek confluence area (fig. D8, Chapter D, this volume).

The crest of Big Black Mesa and the Mogollon Rim south of Bill Williams Mountain form a ground-water divide for the regional carbonate aquifer between the Colorado Plateau and the Transition Zone. North of Big Black Mesa, the Limestone Canyon Monocline, and the Mogollon Rim, Paleozoic rocks gently dip to the north or northeast (fig. D3, Chapter D, this volume). Although high-altitude surface-water runoff is produced on the Colorado Plateau overlying the carbonate aquifer, it typically reaches Big Chino Valley only a few times in any given decade. Consequently, little if any ground-water recharge to Big Chino Valley or the upper Verde River is contributed from the area north of Big Black Mesa and the Mogollon Rim (Chapter D, this volume).

In the study area, the primary water-bearing unit within the regional carbonate aquifer is the Martin Formation, followed to a lesser degree by the Redwall Limestone. The lower Martin contains abundant northwest-striking high-angle joints, dissolution cavities, and other small karst features that enhance its overall permeability. The underlying Tapeats Sandstone, due to its low overall porosity, forms a resistive layer to vertical ground-water movement from above. For this reason, springs such as those in the Verde River/Granite Creek confluence area preferentially emerge near the base of the Martin. The occurrence of elevated concentrations of lithium, boron, and arsenic are spatially associated with the presence of the Chino Valley Formation (Cambrian?) (Chapter E, this volume). This discontinuous sedimentary facies is found along the contact between the Martin and the Tapeats within the Devonian-Cambrian zone, or "D-C zone" in the Verde River/Granite Creek confluence area (Chapter E, this volume).

Basalt flows in the carbonate aquifer have high-overall permeability and provide important flowpaths, due in large part to extensive intersecting columnar joints or rubble zones. For example, a basalt-filled paleochannel in the Martin limestone (which intercepts the D-C zone) offers a preferential flowpath, as indicated by a two-fold increase in dissolved silica between the Big Chino basin-fill aquifer near Paulden and upper Verde River springs (table F2, Chapter E; this volume). The ground-water flow direction at Paulden is east or southeast, consistent with regional gradients and the Big

Chino aquifer as the major source of discharge to the Verde River (figs. D7–D8, Chapter D, this volume).

In the Paulden area, the carbonate aquifer acts as a conduit between Big Chino Valley and the Verde River, as indicated by water levels and water chemistry. The basin-fill aquifer and the D-C zone of the carbonate aquifer are strongly connected at the Big Chino outlet and function together as a single aquifer source (Chapter D, this volume). A small amount of mixing between the Big Chino aquifer units and the Mississippian-Devonian or M-D sequence of the carbonate aquifer may occur along this conduit (Chapter F, this volume). The M-D sequence contributes less than 6 percent of the base flow to the upper Verde River at the Paulden gauge, based on the results of the tracer study and inverse geochemical modeling.

### Little Chino Basin-Fill Aquifer

In Little Chino Valley, a complex sequence of alluvial and volcanic deposits forms a highly productive aquifer. The Little Chino basin-fill aquifer is connected on its southeastern boundary with the Agua Fria basin-fill aquifer and at its northern outlet near Stillman Lake and lower Granite Creek with the carbonate aquifer (fig D1, Chapter D, this volume). Artesian flow near the town of Chino Valley is attributed to multiple complex facies environments that include (a) trachyandesite overlying small pockets of irregularly distributed sediment, (b) volcanic-clastic sequences within the lati-andesite, (c) lati-andesite over sedimentary rock or alluvium, (d) permeable basalt beneath strongly cemented alluvium, and (e) unconsolidated alluvium beneath strongly cemented alluvium. The narrow basin outlet and low permeability of latite plugs restrict northern movement of ground water, which partly accounts for discharge at Del Rio Springs. From Del Rio Springs, northward flow is constricted by shallow basement south of Sullivan Lake. The most reasonable outlet flowpath is northeast through faulted Paleozoic rock and lati-andesite toward spring-fed Stillman Lake and Lower Granite Spring.

### Big Chino Basin-Fill Aquifer

The Big Chino basin contains (a) buried basalt flows in the northwest and southeast parts of the basin, (b) thick fine-grained playa deposits in the basin center, and (c) other basin-fill deposits. Ground-water flowpaths are locally influenced by the heterogeneous distribution of alluvial deposits (ranging from coarse-grained alluvial fans to the fine-grained playa sediment) and by the buried basalt flows. Williamson Valley is by far the largest source of tributary recharge, followed by Walnut Creek.

Much attention has been given to the role of the playa deposit as a potential obstruction to ground-water movement between the northern and southern ends of Big Chino Valley (Ewing and others, 1994; Ostenaar and others, 1993; Southwest Ground-water Consultants, 2004). Owing to a shortage of deep well logs, the full extent of the playa deposit cannot be mapped but can be approximately inferred by the inflection of

water-level contours around the center of the valley where the playa is known to be present (fig. D7, Chapter D, this volume). Preferred ground-water movement occurs down the axis of the valley along the western edge of the playa through coarser-grained sediment. Some ground water may flow beneath the playa through pre-Cenozoic rocks or above the playa deposit through alluvial fans that interfinger with and partly overlie the playa deposit along the Big Chino Fault. The full areal extent of the playa is poorly constrained, particularly where elongated along the Big Chino Fault, where it could extend as far northwest as Partridge Creek. Consequently, the productive part of the aquifer northwest of the playa could be substantially smaller than the area proposed in a recent ground-water model by Southwest Ground-water Consultants (2004). More work is needed to better define the vertical and lateral extent of the playa deposit in the center of Big Chino Valley.

The Big Chino basin-fill aquifer boundary is fairly impermeable where defined by contact with Proterozoic basement rocks (such as where the two are juxtaposed because of large vertical displacement along the Big Chino Fault) or with extensive occurrences of Sullivan Buttes latite-andesite. The mouth of Partridge Creek is such an area where substantial ground-water movement across the basin boundary is highly unlikely. On the other hand, the basin-fill aquifer is thought to be interconnected with carbonate units in several locations where basement rocks are absent. For example, the basin-fill aquifer abuts extensive erosional remnants of the carbonate aquifer along the base of the Juniper Mountains and in the graben block underlying the basin. The most obvious interconnected area is north of Paulden, where displacement along the Big Chino fault terminates. Here, the basin alluvium is shallowly underlain by the regional carbonate aquifer near its ground-water outlet. Buried basalt flows straddle both sides of the basin margin east of Paulden, creating another potential conduit between the two aquifers, and major joint sets in the Martin Formation parallel the trend of the Big Chino Fault. This combination of structures directs ground water out of the Big Chino basin-fill aquifer, through the D-C zone of the carbonate aquifer, and toward the incised canyon of the upper Verde River.

## Water Chemistry

Geochemical and isotopic methods were used to characterize the water chemistry of major aquifers and springs in the Verde River headwaters, to identify changes along the basin outlet flowpath in southeastern Big Chino Valley, and to determine sources of water contributing to the upper Verde River (Chapters E and F). Water-chemistry groups that were characterized include (a) high-altitude areas west and south of Big Chino Valley, (b) the carbonate aquifer north of Big Chino Valley and the upper Verde River (M-D sequence), (c) the Little Chino basin-fill aquifer, (d) the Big Chino basin-fill aquifer, (e) the carbonate aquifer underlying the Big Chino basin-fill aquifer (D-C zone), and (f) low-altitude springs discharging to the upper Verde River, including lower Granite

Creek, Stillman Lake, and upper Verde River springs (fig. E1, Chapter E, this volume). Characterization of water-chemistry groups helped to identify the sources of low-altitude springs and delineate major flowpaths near the basin outlets. This helped in selection of representative water compositions used in the inverse geochemical modeling, which is discussed in more detail at the end of this section.

## Tritium and Carbon-14

In general, water from high-altitude springs and major tributaries in the Verde River headwaters has the highest tritium activities and youngest apparent ages (fig. E7, Chapter E, this volume). None of the tritium values exceed 10 TU, a level that would have indicated that some portion of precipitation was recharged during atmospheric nuclear testing of the 1950s and 1960s or after radioactive fallout during the 1970s. Deep wells in northwestern Big Chino Valley and in the carbonate aquifer north of the Verde River have no detectable tritium, indicating that ground water in these areas was recharged before 1953. The presence of low-level tritium in springs and wells along low-altitude drainages indicates that modern recharge from storm runoff is occurring. Major springs near the outlets of Big and Little Chino Valleys often have tritium activities slightly above the analytical detection limit, which is interpreted as evidence for direct recharge along these low-gradient stream segments.

Likewise,  $^{14}\text{C}$  data also indicate that direct recharge to the basin-fill aquifers is occurring beneath major drainages. Some of the highest  $^{14}\text{C}$  activities occur along Walnut Creek and Williamson Valley Wash, which receive runoff from high-altitude areas having some of the highest rates of precipitation (fig. E8, Chapter E, this volume). Ground water in the northernmost part of the Little Chino basin-fill aquifer becomes progressively younger toward the Verde River. This trend indicates direct recharge from runoff along perennial tributaries and ephemeral stream channels near the valley outlets, consistent with the results from the tritium data.

## Trace Elements

Water/rock interaction with shales of marine or lacustrine origin or playa sediment is the most likely source for the unusual occurrence of elevated As, Li, and B in the Verde River/Granite Creek confluence area. Ground water sampled from the Martin/Chino Valley/Tapeats (D-C zone) of the carbonate aquifer beneath the basin-fill aquifer near Paulden has a distinctive water chemistry that is moderately mineralized, with the highest concentrations of As, Li, and B (fig. E3B, Chapter E, this volume). At upper Verde River springs, moderate concentrations of As, Li, and B are interpreted as evidence that water has had contact with Paleozoic rocks in the D-C zone. Disproportionate increases in B relative to Li along the Big Chino basin outlet from near Paulden to upper Verde River springs also suggests water-rock interaction as the predominant process, as opposed to mixing. In contrast, ground waters from the carbonate aquifer (M-D sequence) north



of the Verde River have low concentrations of these trace elements (fig. E2B, Chapter E, this volume).

Strontium concentrations are a useful indicator of Little Chino ground-water sources in the Verde River/Granite Creek confluence area. The amount of Sr represents the degree of contact ground water has had with Sr-rich igneous rocks, particularly latite-andesites. Water samples from Del Rio Springs, Lower Granite Springs and Stillman Lake are elevated substantially in strontium, owing to contact with Sr-rich latite-andesite in northern Little Chino Valley and the Sullivan Buttes. In central Big Chino Valley, the playa deposit (although largely unsampled) is thought to provide another potential source of elevated strontium concentrations. Water samples from upper Verde River springs contain moderate concentrations of Sr, between 350 to 420 micrograms per liter ( $\mu\text{g/L}$ ) Sr, compared with 460 to 620  $\mu\text{g/l}$  for the Little Chino basin-fill aquifer (fig. E3C, Appendix A). In contrast, water samples from the carbonate aquifer north of the Verde River (M-D sequence) are comparatively lacking in Sr (70 to 120  $\mu\text{g/L}$ ).

## Stable Isotopes of Hydrogen and Oxygen

Past stable-isotope interpretations have been a basis for conflicting conclusions about the source of upper Verde River springs. In Chapter E, stable isotopes of hydrogen and oxygen were used to show that many of the samples collected from spring-fed lakes (for example, Stillman Lake and King Spring) and some earlier well samples collected from stock tanks (for example, Hell well) had undergone substantial evaporation. Samples that had undergone evaporation could not be used to evaluate the degree of mixing with the carbonate aquifer.

Similarly, stable-isotope results for the basin-fill aquifers indicate considerable vertical and horizontal heterogeneity. Ground water from the basin-fill aquifers had a broad range of  $\delta^{18}\text{O}$  versus  $\delta\text{D}$  with substantial overlap between basins (figs. E5B and E6, Chapter E, this volume), as might be expected for samples collected on different dates, from different screened depths, and from different areas of the basins. Consequently, the mean stable-isotope values calculated for the basin-fill aquifers were not useful endpoints for mass-balance mixing calculations (fig. E6 and table E2, Chapter E, this volume). For this reason, samples collected near the outlets of the Big and Little Chino basin-fill aquifers were selected as volumetric composites of water leaving the aquifer. In Little Chino Valley, Del Rio Springs was used to represent the Little Chino basin-fill aquifer. In Big Chino Valley, a  $\delta^{18}\text{O}$  value of approximately  $-10.3\pm 0.2\text{‰}$  was used to trace the main flowpath backwards or upgradient from upper Verde River springs through the D-C zone of the carbonate aquifer to the outlet of the Big Chino basin-fill aquifer near Paulden (fig. E10, Chapter E, this volume). A well along the main basin outlet flowpath near Paulden was chosen to represent a volumetric composite of the Big Chino basin-fill aquifer.

No mixing of the Big Chino aquifer with another source is required to account for the stable-isotope composition at

upper Verde River springs, although a small amount of mixing within the range of analytical uncertainty for  $\delta^{18}\text{O}$  could not be rejected. Using a mass-balance approach, the maximum hypothetical contribution from the M-D sequence of the carbonate aquifer north of the Verde River that could occur without affecting the  $\delta^{18}\text{O}$  content of upper Verde River springs is about 15 percent. Consequently, mixing with the carbonate aquifer less than about 15 percent could not be determined with any confidence (Chapter E, this volume). Because of this large degree of uncertainty, the mixing hypothesis was tested further by inverse modeling (Chapter F, this volume), which relied on multiple lines of geochemical evidence rather than stable-isotope data alone.

## Synoptic Sampling and Tracer-Dilution Studies

Tracer-injection and water-chemistry synoptic studies were conducted during low-flow conditions to identify locations of diffuse springs and to quantify the relative contribution from each major aquifer source to base flow in the upper Verde River. Base flow begins downstream from Big and Little Chino Valleys in three different locations: Stillman Lake, lower Granite Creek, and 600 ft downstream from the Granite Creek/Verde River confluence. The relative contribution of flow from each source is difficult to measure directly because most of the inflows occur diffusely through the streambed.

By using the results of the tracer study and synoptic sampling, base flow was calculated at  $19.5\pm 1.0\text{ ft}^3/\text{s}$  at Stewart Ranch, compared with  $21.2\pm 1.0\text{ ft}^3/\text{s}$  measured at the Paulden gauge during the same time interval. By subtraction, approximately 7 percent of base flow at the Paulden gauge was contributed between Stewart Ranch and the Paulden gauge. Most of the undetected inflow presumably occurs in the vicinity of the Muldoon Canyon confluence where inflow has been observed from both banks. The Little Chino basin-fill aquifer contributed  $2.7\pm 0.08\text{ ft}^3/\text{s}$ , or  $13.8\pm 0.7$  percent, of total base flow at Stewart Ranch. Approximately four fifths of the Little Chino inflow was derived from the flowpath beneath Stillman Lake, as opposed to base flow from the Granite Creek area. By subtraction, discharge from upper Verde River springs contributed the remaining  $86.2\pm 0.7$  percent. Inverse modeling was used to determine the proportions of water types that contribute ground water to upper Verde River Springs.

## Inverse Modeling of Geochemical Data

Inverse modeling was used to constrain hypotheses regarding the nature of water-rock interactions and possible mixing along the flowpath between the Big Chino aquifer near Paulden and upper Verde River springs. The computer program PHREEQC (Version 2; Parkhurst and Appelo, 1999) was used (a) to calculate saturation indices and the distribution of aqueous species, (b) to identify net geochemical mass-balance reactions between initial and final waters along the outlet flowpath, and (c) to calculate proportions of water types contributing to the final mixture. PHREEQC allows the user

to specify the analytical uncertainty range for each element or isotope entered in the model. In addition, PHREEQC identified only the mass-transfer models that minimized the number of phases involved, referred to as “minimal models.”

Four initial water compositions were used in the model to represent (a) well H representing the D-C zone of the regional carbonate aquifer underlying basin-fill alluvium near the outlet, (b) well E, representing basin alluvium and basalt facies of the Big Chino basin-fill aquifer near its outlet, (c) well F representing the carbonate aquifer between Big Chino Valley and upper Verde River springs, and (d) well M representing the M-D sequence of the carbonate aquifer north of the Verde River near Drake. The final water composition was represented by the largest discrete spring contributing to upper Verde River springs. An uncertainty of  $\pm 5$  percent was assigned to concentrations of all the major and trace elements except boron and lithium because of their nonconservative behavior in this setting. Stable isotopes of oxygen, hydrogen, and carbon were assigned an uncertainty equal to the reported analytical precision. Although many plausible models were possible, the “minimal” option was used to identify only those models with the fewest phases that were a best fit for the input data.

Important reactions identified by the inverse modeling include the dissolution of silicate minerals and degassing of carbon dioxide, interpretations that are largely supported by field observations as well as analytical data. The most likely cause of a two-fold increase in dissolved silica is water-rock interaction with basalt along the outlet flowpath. Degassing of  $\text{CO}_2$  is inferred by variations in pH along gaining reaches of the Verde River and Granite Creek (fig. F11, Chapter F, this volume). Notably, calcite and dolomite minerals remain near or at saturation along the flow paths, indicating that dissolution of carbonate rocks is *not* a major process affecting concentrations of Ca, Mg, and  $\text{HCO}_3^-$ . Dissolution of silicate minerals and mixing of initial water types are the predominant processes affecting compositional variations in the major elements along the Big Chino basin outlet flowpath.

Six out of thirteen minimal models support a small amount of mixing between Big Chino ground water and the M-D sequence of the carbonate aquifer at upper Verde River springs. The sum of three initial waters from Big Chino Valley accounts for between 93 and 100 percent of total discharge at upper Verde River springs, with the M-D sequence outside of Big Chino Valley accounting for a maximum of 7 percent of total spring inflow (1,200 acre-ft/yr), if any. At the outlet of the Big Chino basin-fill aquifer near Paulden, the D-C zone of the underlying carbonate aquifer contributes on the order of 10 to 15 percent of the ground water discharging from Big Chino Valley.

Contributions from each aquifer source, readjusted for the Paulden gauge, are as follows: (a) the combined Big Chino basin-fill aquifer and D-C zone of the underlying carbonate aquifer, greater than 80 to 86 percent, (b) the D-C zone of the carbonate aquifer alone, 10 to 15 percent, (c) Little Chino basin-fill aquifer, 14 percent, (d) M-D sequence north of the

Verde River, less than 6 percent. Contributions of flow to the Verde River from each aquifer is presumed to vary seasonally and annually in response to climatic or anthropogenic variables, such as long-term drought or changes in the amount of pumping. The calculations presented here are based on synoptic measurements of June 2000, representing a snapshot in time during low-flow conditions.

## Sources of Base Flow

Previous estimates of the sources of base flow to the upper Verde River were reconciled with the hydrogeologic framework and geochemistry. Pie charts in fig. G1 compare the relative contributions to Verde River base flow based on previous studies using a water-budget approach (table A4 and fig. A16, Chapter A, this volume) with the results from the tracer study and inverse modeling (Chapter F, this volume). In accordance with the conceptual model developed in this study, the relative contributions are linked to three major aquifers (right pie chart) as opposed to less specific geographical areas for Big and Little Chino Valleys and Big Black Mesa (left and center pie charts). In addition, contributions from different parts of the regional carbonate aquifer are subdivided with respect to the D-C zone and M-D sequence.

Contemporary estimates presented in the 1990 and 2000 pie charts assume mean annual base flow at the Paulden gauge of 17,000 acre-ft/yr (Freethey and Anderson, 1986; Wirt and Hjalmarsen, 2000; Table A4, Chapter A, this volume), a level that is corroborated by mean annual flow during a drought year with no runoff of 16,370 acre-ft (MacCormack and others, 2002). Results of the tracer study (Chapter F, this volume) indicate that  $13.8 \pm 0.7$  percent of the base flow, or 2,350 acre-ft/year, was derived from the Little Chino basin-fill aquifer. Other recent studies (Arizona Department of Water Resources, 2000; Nelson, 2002) estimate that the amount of underflow from Little Chino Valley to the Verde River was about 2,100 acre-ft/yr during the mid-1990s. The tracer-study measurement is within 250 acre-ft/year of that by Nelson (2002), which is considered excellent agreement for independent results using different approaches. An important distinction in our conceptual understanding here is that not all outflow from the Little Chino basin-fill aquifer becomes inflow to the Big Chino basin-fill aquifer near Sullivan Lake.

Little Chino outflow travels north and east from Del Rio Springs and does not provide inflow to the Big Chino basin-fill aquifer. An indeterminate fraction of Little Chino outflow probably enters the Big Chino aquifer near Sullivan Lake. The proportion of Little Chino outflow discharging directly to Stillman Lake without first entering Big Chino Valley is still unknown, but appears to be substantial and probably represents the majority of contemporary outflow from the Little Chino basin-fill aquifer. Given that the Little Chino aquifer is out of safe yield (Arizona Department of Water Resources, 1998, 1999a, 1999b, and 2000) and in light of the historical loss of perennial base flow between Del

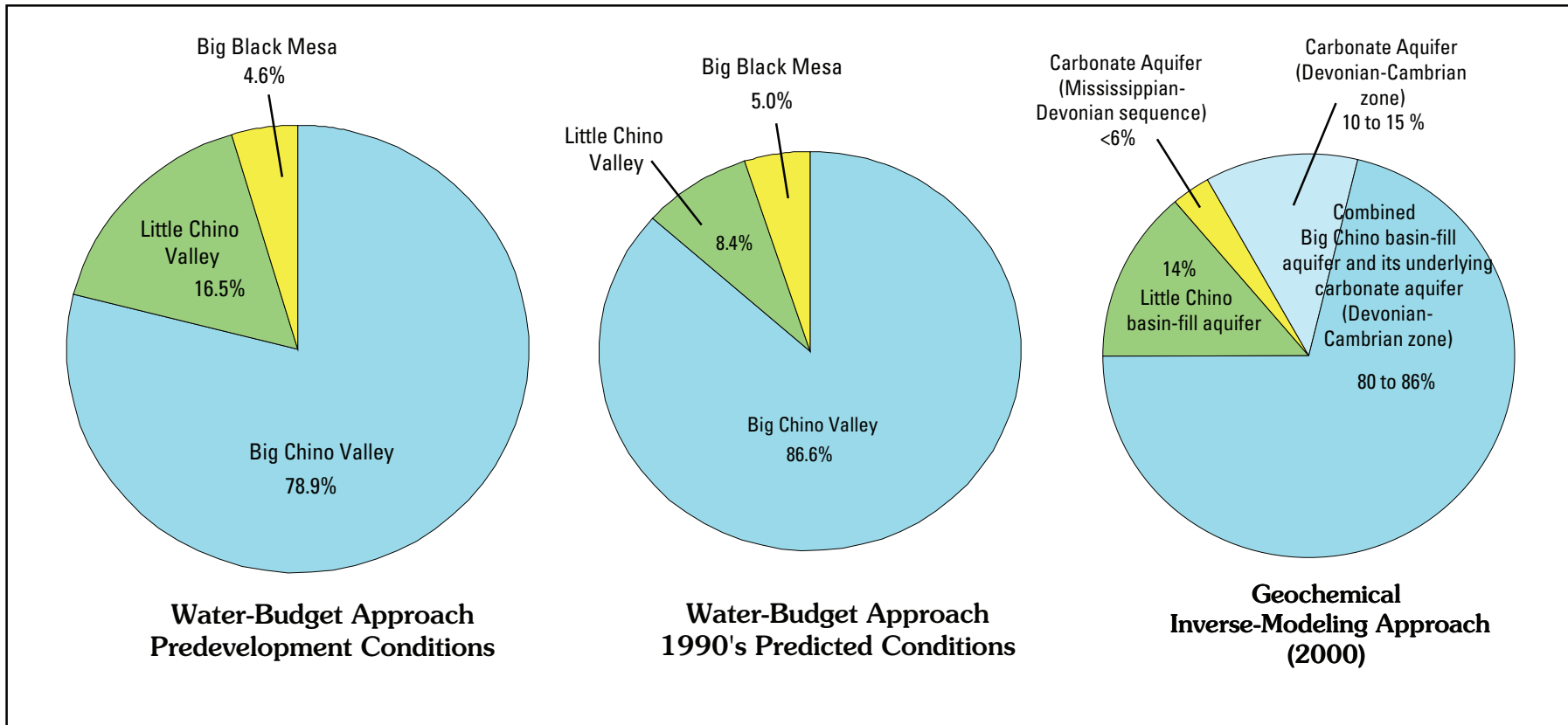


**Figure G1.** Pie charts showing sources of base flow to the upper Verde River, comparing water-budget estimates with those based on inverse modeling using geochemistry and tracer-study data. Data from previous studies is provided in table A4 and figure A16 (Chapter A, this volume). Note that the predevelopment pie diagram on the left is proportionately larger than those on the center and right.

Rio Springs and Sullivan Lake along the Little Chino Creek (Chapter A, this volume, fig. 10b), Little Chino outflow probably has declined more rapidly along the Sullivan Lake flowpath than along the Stillman Lake and lower Granite Creek flowpaths. This finding has significant implications for whether all of the Little Chino outflow ought to be counted as Big Chino inflow in a water-budget calculation, particularly if the budget is intended to represent modern conditions.

On the basis of the geologic framework and the tracer and inverse geochemical modeling results (Chapter F, this volume), the combined basin-fill aquifer and carbonate aquifer underlying Big Chino Valley are here estimated to contribute 80 to 86 percent, or between 13,600 and 14,650 acre-ft/yr of the mean base flow at the Paulden gauge. This compares favorably with data compiled from previous studies using a water-budget approach (Table A4, Chapter A, this volume), which were used to calculate that the Big Chino Valley area contributed about 78.9 percent of mean annual discharge at the Paulden gauge during predevelopment conditions and about 86.6 percent of mean annual discharge during 1990s conditions. Thus, estimates based on the tracer study and geochemical modeling approach independently corroborate the findings of earlier studies, although contributions from the Big and Little Chino basin-fill aquifers are presumed to be declining in response to increasing water usage. Unexpectedly, the tracer study directly measured a larger contribution from Little Chino Valley in 2000 (13.8 percent versus 8.4 percent) than that predicted with 1990s data using a water-budget approach. One possible explanation for this discrepancy is a delayed response to the effects of pumping, in which the predicted rate of decline in Little Chino base flow is lower than the observed rate. Whether discharge from the Big Chino aquifer has also decreased from predevelopment conditions cannot be quantified from the available data, though the results of the 2000 tracer study can be used to provide a baseline for making a point-in-time comparison in the future.

Based on the geochemical modeling, the geographical region south of the crest of Big Black Mesa and lower Hell Canyon near Drake is estimated to contribute less than 6 percent, or a maximum of about 1,200 acre-ft/year, of base flow to the Verde River—about the same as that estimated for Big Black Mesa by Ford (2002). Ford (2002) estimated Big Black Mesa recharge at 1,250 acre-ft/yr, by calculating the land area of the mesa exceeding 5,000 ft above sea level and applying a recharge rate based the rate of precipitation. Ford's (2002) estimate cannot be directly compared to the contribution from the regional carbonate aquifer north of the upper Verde River (M-D sequence) because the geographical extent of the two contributions is not the same. In addition, a substantial part of the recharge from the Big Black Mesa area probably enters the Big Chino basin-fill aquifer directly through alluvial fans along the Big Chino fault, or through the underlying carbonate aquifer near Paulden, and, thus, cannot be discriminated from the rest of the Big Chino basin-fill aquifer using a geochemical approach. Consequently, it is difficult to differentiate a Big

Black Mesa contribution as distinct from the Big Chino basin-fill aquifer and its underlying carbonate aquifer.

As a closing observation, previous studies of recharge (Ford, 2002; Ewing and others, 1994; Freethey and Anderson, 1986) have not rigorously addressed the issue that infiltration rates are spatially variable as a function of geology as well as of climate. Rates presumably are higher for Paleozoic carbonate rocks and Tertiary basalts in the Transition Zone region than for igneous and metamorphic rocks in the Bradshaw and Santa Maria Mountains, owing to their greater permeability and the short distance to water tables beneath deeply incised canyons such as Limestone Canyon and Hell Canyon (Chapter D, this volume). The amount of direct runoff infiltrating beneath low-gradient streams, during large but infrequent floods and seasonal runoff, is probably more substantial than thought earlier as indicated by elevated carbon-14 and tritium values along low-altitude stream segments near the basin outlets (figs. E7 and E8, Chapter E, this volume). Improved understanding and delineation of recharge areas could be used to protect important recharge areas or possibly to enhance recharge in certain areas. Additional stream monitoring and directed geologic studies of recharge are needed to address these and other data gaps listed below.

## Recommendations for Future Studies

1. Fill data gaps in streamflow records by maintaining the long-term gauging stations recently reestablished at Williamson Valley Wash, Walnut Creek, and Del Rio Springs. Add high-flow capability to gauging stations on Pine Creek, Partridge Creek, upper Big Chino Wash, and lower Granite Creek.
2. Provide more accurate water-use records in Big Chino Valley by direct measurements such as metering and gauging instead of indirect methods such as estimating consumptive use.
3. Improve definition of the vertical and lateral extent of the playa deposit and buried basalt flows in north central Big Chino Valley by using ground-based geophysical surveys and drilling of additional deep boreholes. Recommended geophysical approaches include audio-magneto telluric (AMT) and "mise-a-la-messe" direct-current (DC) methods that are able to identify water-bearing properties of geologic units and preferential flowpaths as a function of depth. The mise-a-la-messe approach has been used to determine discrete flowpaths through basalt rubble zones and karst.
4. Determine infiltration rates for selected geologic units and evaluate the effects of prominent structural features such as faults, monoclines, and prominent joint sets to improve estimates of recharge in different parts of the headwaters region.

5. Complete geochemical modeling to calculate ground-water ages of representative composite waters at the basin outlets, using the  $^{14}\text{C}$  activities measured in this study, to determine rates of ground-water movement.

## Summary of Conclusions

Multiple lines of evidence indicate that the major source of ground water to the upper Verde River is the Big Chino aquifer at its ground-water outlet near Paulden (80 to 86 percent) with the Little Chino aquifer providing about 14 percent of 17,000 acre-ft/yr. Flowpaths from the Big Chino basin-fill aquifer and its underlying carbonate aquifer converge north and east of Paulden. The Big Chino basin-fill aquifer and D-C zone of the carbonate aquifer are strongly connected between Paulden and upper Verde River springs. Here, the D-C zone of the carbonate aquifer acts as a conduit for outflow from Big Chino Valley and provides as much as 15 percent of ground water attributed to the Big Chino basin-fill aquifer. Distinctive water-chemistry changes along the Big Chino outlet flowpath are largely caused by dissolution of silicate minerals, leaching of trace elements, and mixing with ground water from the D-C zone of the carbonate aquifer. Inverse modeling constrains the potential contribution from the M-D sequence of the regional carbonate aquifer north of the upper Verde River to less than 6 percent of base flow at the Paulden gauge.

Numerous stratigraphic and structural features influence ground-water flowpaths and the location of springs supplying base flow to the upper Verde River. Prominent features that provide preferential flow in the regional carbonate aquifer include karst openings, faults and fractures (including the horsetail splays at the terminus of the Big Chino Fault), joint sets parallel to monoclines (such as the Limestone Canyon Monocline), and a basalt-fill paleochannel that straddles the basin-fill aquifer boundary near Paulden. Basalt flows have high-overall permeability and sometimes provide important flowpaths, owing to extensive columnar fractures and rubble zones. Igneous and metamorphic basement rocks usually have very low permeability and define the bottom and edges of the basin-fill aquifers.

Ground-water movement within the basin-fill aquifers is from the valley margins and tributaries toward the valley center and then down the longitudinal axis of the valley toward the basin outlet. Elongate basin-fill deposits tend to narrow and thin toward their topographic outlets, resulting in low-altitude springs that correspond spatially with the distal end of the aquifer. Major buried obstacles to ground-water movement include resistive latite-andesite plugs and shallow basement rocks in northern Little Chino Valley and a playa deposit in central Big Chino Valley. In lower Big Chino Valley, a basalt-filled paleochannel straddles the basin boundary between the basin-fill aquifer and the carbonate aquifer, offering an intermediate conduit between alluvium and carbonate aquifer units. Synthesis of independent data from a variety of geological, geophysical, hydrological, and geochemical sources provides a

more detailed conceptual understanding of the geologic framework, the aquifer units, and major ground-water flowpaths in the Verde River headwaters.

## References Cited

- Arizona Department of Water Resources, 1998, Preliminary report on the Safe-Yield Status of the Prescott Active Management Area: 44 p. plus appendixes.
- Arizona Department of Water Resources, 1999a, Report on the final decision and order that the Prescott Active Management area is no longer at safe-yield: January 12, 1999, 31 p.
- Arizona Department of Water Resources, 1999b, Third management plan for Prescott Active Management Area 2000–2010: [http://www.water.az.gov/adwr/Content/Publications/files/ThirdMgmtPlan/tmp\\_final/prescott/pre-toc.pdf](http://www.water.az.gov/adwr/Content/Publications/files/ThirdMgmtPlan/tmp_final/prescott/pre-toc.pdf)
- Arizona Department of Water Resources, 2000, Verde River Watershed Study: Arizona Department of Water Resources report, 208 p. plus appendixes.
- Ewing, D.B., Osterberg, J.C., Talbot, R.W., 1994, Groundwater Study of the Big Chino Valley—Hydrology and hydrogeology: Bureau of Reclamation Technical Report, Denver, Colorado, Sections I through III, including 6 appendixes.
- Ford, J.R. 2002, Big Chino Valley ground water as the source of the Verde River *in* Ground Water/Surface Water Interactions, July 1–3, 2002, American Water Resources Association summer specialty conference, 6 p.
- Freethy, G.W., and Anderson, T.W., 1986, Predevelopment hydrologic conditions in the alluvial basins of Arizona and adjacent parts of California and New Mexico: U.S. Geological Survey Hydrologic Investigations Atlas HA-664.
- Gilbert, C.H., and Scofield, N.B., 1898, Notes on a collection of fishes from the Colorado Basin in Arizona. Proceedings U.S. National Museum, v. 20, p. 287–499 (plates XXXVI–XXXIX).
- MacCormack, H.F., Fisk, G.G., Duet, N.R., Evans, D.W., and Castillo, N.K., 2002, Water Resources Data, Arizona, Water Year 2001: U.S. Geological Survey Water-Data Report AZ-01-1, p. 257.
- Nelson, Keith, 2002, Application of the Prescott Active Management Area—Ground-water flow model planning scenario 1999–2025: Arizona Department of Water Resources Modeling Report No. 12, 49 p.
- Ostenaar, D.A., Schimschal, U.S., King, C.E., Wright, J.W., Furgerson, R.B., Harrel, H.C., and Throner, R.H., 1993, Big Chino Valley Groundwater Study—Geologic Framework Investigations Seismotectonic Report 93–2, Bureau of Reclamation, Denver Office, 31 p.

- Parkhurst, D.L., and Appelo, C.A.J., 1999, User's guide to PHREEQC (Version 2)—A computer program for speciation, batch-reaction, one-dimensional transport, and inverse geochemical calculations. U.S. Geological Survey Water-Resources Investigations Report 99-4259, 312 p.
- Schwalen, H.C., 1967, Little Chino Valley artesian area and ground-water basin: Technical Bulletin 178, Agricultural Experiment Station, University of Arizona, Tucson, Arizona, 63 p.
- Southwest Ground-water Consultants, 2004, C.V./C.F. Ranch Acquisition hydrology report: prepared for the city of Prescott, June, 2004, 6 chapters plus Appendix.
- Twenter, F.R., and Metzger, D.G., 1963, Geology and ground water in Verde Valley—the Mogollon Rim region of Arizona: U.S. Geological Survey Bulletin 1177, 132 p.
- Winn, H.E., and Miller, R.R., 1954, Native post-larval fishes of the lower Colorado River Basin, with a key to their identification: California Fish and Game, v. 40, p. 273-285.
- Wirt, Laurie, and Hjalmarson, H.W., 2000, Sources of springs supplying base flow to the Verde River headwaters, Yavapai County, Arizona: U.S. Geological Survey Open-File Report 99-0378, 50 p.

# Glossary

This glossary is a compilation of geologic, geophysical, and hydrological terms used in this report which are found in the public domain. Geologic terms are from Bates and Jackson (1980). Geophysical terms also are from Bates and Jackson (1980) and from <http://www.geotech.org/survey/geotech/>. Hydrological terms are from previously published USGS reports and from Weight and Sonderegger (2001). The terms herein are not necessarily the only valid definitions for these terms.

**acre-foot (acre-ft, ac-ft).**—The volume of water required to cover 1 acre to a depth of 1 foot and is equal to 43,560 cubic feet or 325,851 gallons or 1,233.49 cubic meters.

**Active Management Area.**—A geographical area that has been designated by the Arizona state legislature as requiring active management of ground-water withdrawals from pumping.

**aeromagnetic.**—Relating to the study of the earth's magnetic fields, especially in relation to air surveys used to map local anomalies caused by variations in rock magnetization.

**alkali basalt.**—Critically silica-undersaturated basalt, containing normative nepheline, diopside, and olivine, with no normative hypersthene. Basalts with nepheline and/or acmite fall in this category.

**andesite.**—A dark-colored, fine-grained extrusive rock that, when porphyritic, contains phenocrysts composed primarily of zoned sodic plagioclase (esp. andesine) and one or more mafic minerals (e.g. biotite, hornblende, pyroxene), with a groundmass composed generally of the same minerals as the phenocrysts, although the plagioclase may be more sodic and quartz is generally present; the extrusive equivalent of *diorite*. Andesine grades into *latite* with increasing alkali feldspar and quartz.

**analcime.**—A mineral:  $\text{NaAlSi}_2\text{O}_6 \cdot \text{H}_2\text{O}$ . It is an isometric zeolite, commonly found in diabase and alkali-rich basalts.

**aquifer.**—A geologic formation, group of formations, or part of a formation that contain sufficient saturated permeable material to yield significant quantities to springs and wells.

**artesian.**—*See* confined aquifer.

**background concentration.**—A concentration of a substance in a particular environment that is indicative of minimal influence by human (anthropogenic) sources.

**basalt.**—A general term for dark-colored mafic igneous rocks, commonly extrusive but locally intrusive (e.g. dikes), composed chiefly of calcic plagioclase and clinopyroxene; the fine-grained equivalent of *gabbro*. Nepheline, olivine, and orthopyroxene, and quartz may be present, but not all simultaneously.

**bloedite.**—A white or colorless monoclinic mineral:  $\text{Na}_2\text{Mg}(\text{SO}_4)_2 \cdot 4\text{H}_2\text{O}$ .

**base flow.**—The sustained low flow of a stream, usually ground-water inflow to the stream channel.

**carbonate rocks.**—Rocks (such as limestone or dolostone) that are composed primarily of minerals (such as calcite and dolomite) containing the carbonate ion ( $\text{CO}_3^{2-}$ ).

**cienaga (cienega).**—A marshy area where the ground is wet due to the presence of seepage or springs.

**cgs.**—is the system of units based on measuring lengths in centimeters, mass in grams, and time in seconds. It is a *metric system*, although not the flavor of the metric system used most commonly. It was introduced by the British Association for the Advancement of Science in 1874, and was immediately adopted by many working scientists.

**clastic.**—Rock, such as sandstone, or sediment composed principally of broken fragments that are derived from preexisting rocks which have been transported from their place of origin.

**clinoptilolite.**—A zeolite mineral:  $(\text{Na}, \text{K}, \text{Ca})_{2-3}\text{Al}_3(\text{Al}, \text{Si})_2\text{Si}_{13}\text{O}_{36} \cdot 12\text{H}_2\text{O}$ . It is a potassium-rich variety of *heulandite*.

**columnar jointing.**—A phenomenon that occurs as lava contracts to form a solid. During the cooling process, polygonal prismatic shapes form to accommodate the escaping heat. The polygonal prismatic shapes extend down through the thickness of the lava flow to form columns.

**concentration.**—The ratio of the quantity of any substance present in a sample of a given volume or a given weight compared to the volume or weight of the sample.

**conductance.**—The product of conductivity and thickness. Indication of ease of current flow in a medium.

**conductivity.**—The ability of a material to conduct electrical current. In isotropic material, the reciprocal of resistivity. Units are in siemens per meter.

**conductivity, effective hydraulic.**—The rate of flow of water through a porous medium measured in gallons per day through a cross-section of one square foot under a unit hydraulic gradient.

**confined aquifer (artesian).**—An aquifer that is isolated by having confining layers to maintain the pressure in the system at a pressure greater than atmospheric pressure. This causes the water levels in cased wells to rise above the top of the aquifer. The pressure results from the weight of the water elevation near the recharge area to be propagated through the entire system.

**confining layers.**—Layers that have hydraulic conductivity two or three orders of magnitude less than a layer above or below.

**conglomerate.**—A coarse-grained sedimentary rock composed of fragments larger than 2 millimeters in diameter.

**contributing area.**—The area in a drainage basin that contributes water to streamflow or recharge to an aquifer.

**constituent.**—A chemical or biological substance in water, sediment, or biota that can be measured by an analytical method.

**consumptive use.**—The quantity of water that is not available for immediate reuse because it has been evaporated,

## 2 Geologic Framework of Aquifer Units, North-Central Arizona

transpired, or incorporated into products, plant tissue, or animal tissue. Also referred to as “water consumption”.

**core sample.**—A sample of rock, soil, or other material obtained by driving a hollow tube into the undisturbed medium and withdrawing it with its contained sample.

**crystalline rocks.**—Rocks (igneous or metamorphic) consisting wholly of crystals or fragments of crystals.

**cubic foot per second (ft<sup>3</sup>/s, or cfs).**—Rate of water discharge representing a volume of 1 cubic foot passing a given point during 1 second, equivalent to approximately 7.48 gallons per second or 448.8 gallons per minute or 0.02832 cubic meter per second. In a stream channel, a discharge of 1 cubic foot per second is equal to the discharge at a rectangular cross section, 1 foot wide and 1 foot deep, flowing at an average velocity of 1 foot per second.

**dacite.**—A fine-grained extrusive rock with the same general composition as *andesite* but having a less calcic plagioclase and more quartz; according to many, it is the extrusive equivalent of *granodiorite*.

**degree (° or deg).**—the standard unit of angle measure, equal to 1/360 circle, 60 minutes, 3600 seconds, or about 0.017 453 293 *radian*.

**density.**—The mass per unit volume of a substance, commonly expressed in grams/ cubic centimeter.

**detection limit.**—The concentration of a constituent or analyte below which a particular analytical method cannot determine, with a high degree of certainty, the concentration.

**direct runoff.**—The runoff entering stream channels promptly after rainfall or snowmelt.

**discharge.**—The volume of fluid passing a point per unit of time, commonly expressed in cubic feet per second, million gallons per day, gallons per minute, or seconds per minute per day. Ground-water outflow or streamflow, as in a stream, canal, or from a pumped well.

**dissolved constituent.**—Operationally defined as a constituent that passes through a 0.45-micrometer filter.

**dissolved oxygen.**—Oxygen dissolved in water; one of the most important indicators of the condition of a water body. Dissolved oxygen is necessary for the life of fish and most other aquatic organisms.

**diurnal.**—Having a daily cycle; showing periodic alteration of conditions with day and night.

**diversion.**—A turning aside or alteration of the natural course of a flow of water, normally considered physically to leave the natural channel. In some States, this can be a consumptive use direct from another stream, such as by livestock watering. In other States, a diversion must consist of such actions as taking water through a canal, pipe, or conduit.

**downgradient.**—The direction water flows by force of gravity.

**drainage area.**—The drainage area of a stream at a specified location is that area, measured in a horizontal plane, which is enclosed by a drainage divide.

**drainage basin.**—The land area drained by a river or stream.

**drought.**—A prolonged period of less-than-normal precipitation such that the lack of water causes a serious hydrologic imbalance.

**emu/cm<sup>3</sup> or emu/cc.**—a *CGS* unit of magnetization. In *SI* units, one emu/cm<sup>3</sup> can be interpreted either as 4pi/10 milliteslas (1.256 637 mT) as a unit of magnetic polarization or excess magnetic induction, or as 1000 *amperes* per meter as a unit of magnetic dipole moment per unit volume.

**endangered species.**—A species that is in imminent danger of becoming extinct.

**ephemeral stream.**—A stream or part of a stream that flows only in direct response to precipitation; it receives little or no water from springs, melting snow, or other sources; its channel is at all times above the water table.

**evapotranspiration.**—The process by which water is discharged to the atmosphere as a result of evaporation from the soil and surface-water bodies, and transpiration by plants.

**fanglomerate.**—A sedimentary rock consisting of slightly water-worn, heterogeneous fragments of all sizes, deposited in an alluvial fan and later cemented into a firm rock; it is characterized by persistence parallel to the depositional strike and by rapid thinning downdip.

**feldspar.**—A group of abundant rock-forming minerals of general formula: MAl(Al,Si)<sub>3</sub>O<sub>8</sub>, where M = K, Na, Ca, Ba, Rb, Sr, and Fe. Feldspars are the most widespread of any mineral group and constitute 60 percent of the Earth's crust; they occur as components of all kinds of rocks and as fissure minerals in clefts and druse minerals in cavities. Feldspars are usually white or nearly white and clear and translucent (they have no color of their own but are frequently colored by impurities), have a hardness of 6 on the Mohs scale, frequently display twinning, exhibit monoclinic or triclinic symmetry, and possess good cleavage in two directions. On decomposition, feldspars yield a large part of the clay of the soil and also the mineral kaolinite.

**flowpath (flow path).**—An underground route for ground-water movement, extending from a recharge (intake) zone to a discharge (output) zone such as a shallow stream.

**flow duration.**—Flow duration of daily mean discharge, expressed in percentage of time, are specified daily flow that were equaled or exceeded during the period of record.

**gaining stream.**—A stream or reach of stream that receives water from the inflow of ground water. Discharge occurs because the head in the ground-water system is higher than the stage elevation of the stream.

**gauging (gaging) station.**—A particular site on a stream, canal, lake, or reservoir where systematic observations of hydrologic data are obtained regularly by permanently installed equipment.

**geophysics.**—the study of the *earth* by quantitative *physical* methods, especially by *seismic reflection* and



*refraction, gravity, magnetic, electrical, electromagnetic, and radioactivity methods.*

**graben.**—An elongate, relatively depressed crustal unit or block that is bounded by faults on its long sides. It is a structural form that may or may not be geomorphologically expressed as a rift valley.

**gradient, hydraulic.**—The change of pressure per unit distance from one point to another in an aquifer. When an area is said to be “downgradient” it is at a lower level and water will flow in that direction.

**gravity anomaly.**—The value of gravity left after subtracting from a gravity measurement the reference value based on latitude, and possibly the free-air and Bouguer corrections.

**gravity survey.**—The measurement of gravity at regularly spaced grid points with repetitions to control instrument drift.

**gravitation.**— is the tendency of *masses* to move toward each other.

**ground water.**—In the broadest sense, all subsurface water; more commonly that part of the subsurface water in the saturated zone.

**ground-water flow system.**—The underground pathway by which ground water moves from areas of recharge to areas of discharge.

**headwater.**—The source and upper part of a stream, especially of a large stream or river, including the upper drainage basin.

**heterogeneous.** —See homogeneity.

**homogeneity.** —Relating to the physical properties of an aquifer from point A to point B, including packing, thickness, and cementation. Homogeneous units have similar properties from point A to point B and heterogeneous units differ in physical properties from point A to point B.

**hydraulic conductivity.**—The capacity of a rock to transmit water. It is expressed as the volume of water at the existing kinematic viscosity that will move in unit time under a unit hydraulic gradient through a unit area measured at right angles to the direction of flow.

**hydraulic gradient.**—The slope of the potentiometric surface. It is the rate of change of head per length of flow in a given direction.

**hydraulic head.**—The height of the free surface of a body of water above a given point beneath the surface.

**illite.**—A general name for a group of three-layer, mica-like clay minerals that are widely distributed in argillaceous sediments. They are intermediate in composition between *muscovite* and *montmorillonite*, and have the general formula  $(\text{H}_3, \text{O}, \text{K})_y(\text{Al}_4, \text{Fe}_4, \text{Mg}_4, \text{Mg}_6)(\text{Si}_{8-y}, \text{Al}_y)\text{O}_{20}(\text{OH})_4$ , with  $y$  less than 2 and frequently 1 to 1.5.

**impermeability.**—The condition of a rock, sediment, or soil that renders it incapable of transmitting fluids under pressure.

**infiltration.**—The process of precipitation water migrating into the soil horizon.

**intermittent or seasonal stream.**—A stream that flows only when it receives water from rainfall runoff or springs, or from some surface source such as melting snow.

**inverse modeling.**—The process of estimating model or desired parameters from measured data.

**ion.**—A positively or negatively charged atom or group of atoms.

**isopachs.**—A line drawn on a map through points of equal true thickness of a designated stratigraphic unit, or group of stratigraphic units.

**joints.**—Undisplaced fractures in rocks that have been subjected to tectonic forces.

**karst.**—A type of topography that results from dissolution and collapse of carbonate rocks such as limestone, dolomite, and gypsum, and that is characterized by closed depressions or sinkholes, caves, and underground drainage.

**latite.**—A porphyritic extrusive rock having phenocrysts of plagioclase and potassium feldspar (probably mostly sanidine) in nearly equal amounts, little or no quartz, and a finely crystalline to glassy groundmass, which may contain obscure potassium feldspar; the extrusive equivalent of *monzonite*. Latite grades into *trachyte* with an increase in the alkali feldspar content, and into *andesite* or *basalt*, depending on the presence of sodic or calcic plagioclase, as the alkali feldspar content decreases. It is usually considered synonymous with *trachyandesite* and *trachybasalt*, depending on the color.

**limestone.**—A sedimentary rock consisting chiefly of calcium carbonate, primarily in the form of the mineral calcite.

**losing stream.**—A stream or reach of a stream that contributes water to the zone of saturation.

**magnetic anomaly.**—The value of the local magnetic field remaining after the subtraction of the dipole portion of the Earth’s field.

**magnetic susceptibility.**—is the degree of *magnetization* of a material in response to a *magnetic field*.

**major ions.**—Constituents commonly present in water in concentrations exceeding 1.0 milligram per liter. Major cations are calcium, magnesium, sodium, and potassium; the major anions are sulfate, chloride, fluoride, nitrate, and those contributing to alkalinity (see alkaline), most generally assumed to be bicarbonate and carbonate.

**mean discharge (MEAN).**—As used by the U.S. Geological Survey, the arithmetic mean of individual daily mean discharges of a stream during a specific period, usually daily, monthly, or annually. The term “average” generally is reserved for average of record and “mean” is used for averages of shorter periods, namely, daily, monthly, or annual mean discharges.

**metapelitic.**—Derived by metamorphism of an argillaceous or a fine-grained aluminous sediment, such as consolidated volcanic ash consisting of clay-sized particles.

## 4 Geologic Framework of Aquifer Units, North-Central Arizona

**method detection limit.**—The minimum concentration of a substance that can be accurately identified and measured with current laboratory technologies.

**micrograms per liter ( $\mu\text{g/L}$ ).**—A unit expressing the concentration of constituents in solution as weight (micrograms) of solute per unit volume (liter) of water; equivalent to one part per billion in most streamwater and ground water. One thousand micrograms per liter equals one milligram per liter.

**milligal (mGal or mgal).**—a unit of acceleration used in geology to measure subtle changes in gravitational acceleration. One milligal equals 10 micrometers per second per second, or  $10^{-5}$  meters per second per second.

**micrograms per liter ( $\mu\text{g/L}$ ).**—A unit expressing the concentration of constituents in solution as weight (micrograms) of solute per unit volume (liter) of water; equivalent to one part per billion in most streamwater and ground water. One thousand micrograms per liter equals one milligram per liter.

**milligrams per liter (mg/L).**—A unit expressing the concentration of chemical constituents in solution as weight (milligrams) of solute per unit volume (liter) of water; equivalent to one part per million in most streamwater and ground water.

**minimum reporting level (MRL).**—The smallest measured concentration of a constituent that may be reliably reported using a given analytical method. In many cases, the MRL is used when documentation for the method detection limit is not available.

**montmorillonite.**—A group of expanding-lattice clay minerals of the general formula  $\text{R}_{0.33}\text{Al}_2\text{Si}_4\text{O}_{10}(\text{OH})_2 \cdot n\text{H}_2\text{O}$ , where R includes one or more of the cations  $\text{Na}^+$ ,  $\text{K}^+$ ,  $\text{Mg}^{+2}$ , and possibly others. The minerals are characterized by a three-layer crystal lattice, and by swelling when wetting (and shrinking on drying) due to the introduction of considerable interlayer water in the *c*-axis direction.

**mountain-front recharge.**—Natural recharge that occurs at the base of mountains and which then infiltrates into a permeable rock unit.

**muscovite.**—A mineral of the mica group:  $\text{KAl}_2(\text{AlSi}_3)\text{O}_{10}(\text{OH})_2$ . It is colorless to yellowish or pale brown, and is a common mineral in gneisses and schists, in most acid igneous rocks (such as granites and pegmatites), and in many sedimentary rocks (esp. sandstones).

**nanotesla (nT).**—a unit of magnetic field strength equal to  $10^{-9}$  tesla or  $10^{-5}$  gauss. The unit is used in geology to measure small changes in the Earth's magnetic field.

**ohm meter (ohm/m).**—a unit of resistivity, measuring the extent to which a substance offers resistance to passage of an electric current. The resistivity of a conductor in ohm meters is defined to be its resistance (in ohms) multiplied by its cross-sectional area (in square meters) divided by its length (in meters).

**overland flow.**—The flow of rainwater or snowmelt over the land surface toward stream channels.

**parts per billion (ppb).**—Unit of concentration equal to one billion units of water per unit of trace element or contaminant.

**parts per million (ppm).**—Unit of concentration equal to one milligram per kilogram or one milligram per liter.

**perched aquifer.**—An aquifer that occurs above the regional ground-water system with a vadose zone beneath it.

**perennial stream.**—One that flows continuously, year-round.

**permeability.**—The ability of a porous medium to transmit fluid under a given gradient.

**phreatophyte.**—A term that refers to plants that use ground water; often used as a synonym for “riparian plant.”

**picocurie (pCi).**—One trillionth ( $10^{-12}$ ) of the amount of radioactivity represented by a curie (Ci). A curie is the amount of radioactivity that yields  $3.7 \times 10^{10}$  radioactive disintegrations per second (dps). A picocurie yields 2.22 disintegrations per minute (dpm) or 0.037 dps.

**plagioclase.**—A group of triclinic feldspars of the general formula:  $(\text{Na}, \text{Ca})\text{Al}(\text{Si}, \text{Al})\text{Si}_2\text{O}_8$ . At high temperatures it forms a complete solid-solution series from albite,  $\text{Ab}(\text{NaAlSi}_3\text{O}_8)$ , to anorthite,  $\text{An}(\text{CaAl}_2\text{Si}_2\text{O}_8)$ . Plagioclase minerals are among the commonest rock-forming minerals, have characteristic twinning, and commonly display zoning.

**playa.**—A dry, flat area at the lowest part of an undrained desert basin in which water accumulates and is quickly evaporated; underlain by stratified clay, silt, or sand and commonly by soluble salts; term used in Southwestern United States.

**phenocrysts.**—Visible crystals in an igneous rock that are conspicuously larger than the surrounding matrix material.

**porosity.**—The volume of void space within earth materials. Primary porosity occurs with the formation of a rock mass. Secondary porosity represents void spaces that occur after the rock mass formed.

**potentiometric surface.**—A surface estimated by the level to which cased wells will rise. This surface represents total head, which includes elevation head and pressure head.

**precipitation.**—Any or all forms of water particles that fall from the atmosphere, such as rain, snow, hail, and sleet.

**recharge (ground water).**—The process involved in the absorption and addition of water to the zone of saturation; also, the amount of water added.

**recurrence interval.**—The average interval of time within which the magnitude of a given event, such as a storm or flood, will be equaled or exceeded once.

**resistivity.**—The property of a material that resists the flow of electrical current. Units are ohmmeters.

**return flow.**—That part of irrigation water that is not consumed by evapotranspiration and that returns to its source or another body of water.

**rhyolite.**—A group of extrusive igneous rocks, typically porphyritic and commonly exhibiting flow texture, with

phenocrysts of quartz and alkali feldspar in a glassy to cryptocrystalline groundmass; also, any rock in that group; the extrusive equivalent of *granite*. Rhyolite grades into *rhyodacite* with decreasing alkali feldspar content and into *trachyte* with a decrease in quartz.

**riparian.**—Pertaining to or situated on the bank of a natural body of flowing water.

**runoff.**—That part of precipitation or snowmelt that appears in streams or surface-water bodies.

**safe yield.**—A ground-water management goal which attempts to achieve and thereafter maintain a long-term balance between the annual amount of ground water withdrawn in an Active Management Area and the annual amount of natural and artificial recharge within a designated area.

**saturated zone (zone of saturation).**—A subsurface zone in which all the interstices or voids are filled with water under pressure greater than that of the atmosphere. See also *Water table*.

**shale.**—A fine-grained sedimentary rock formed by the consolidation of clay, silt, or mud.

**solution.**—Formed when a solid, gas, or another liquid in contact with a liquid becomes dispersed homogeneously throughout the liquid. The substance, called a solute, is said to dissolve. The liquid is called the solvent.

**sorption.**—General term for the interaction (binding or association) of a solute ion or molecule with a solid.

**sources.**—Contributions of water to a ground-water system, such as natural recharge from an aquifer unit or geographical area, precipitation, injection wells, or imported water.

**spring.**—A point where ground water intersects the land surface; a ground-water discharge point.

**standard deviation.**—Statistical measure of the dispersion or scatter of a series of values. It is the square root of the variance, which is calculated as the sum of the squares of the deviations from the arithmetic mean, divided by the number of values in the series minus 1.

**stream reach.**—A continuous part of a stream between two specified points.

**streamflow.**—The discharge of water in a natural channel.

**subbasin.**—An area which encloses a relatively hydrologically distinct body of ground water within a ground-water basin and which is described horizontally by surface description.

**surface runoff.**—Runoff that travels over the land surface to the nearest stream channel.

**surface water.**—An open body of water such as a pond, lake, river, or stream.

**synoptic survey.**—A detailed stream-gauging survey along a reach of stream, accounting for every gain or loss from diversion ditches or tributary inflows along a path. One can identify gaining or losing reaches if the values exceed the error limitations of the equipment. It is performed as a flux balance

approach to streamflow. Also, a short-term investigation of specific water-quality conditions during selected seasonal or hydrologic conditions, to provide improved spatial resolution for critical water-quality conditions.

**synoptic sites.**—Sites sampled during a short-term investigation of specific water-quality conditions during selected seasonal or hydrologic conditions, to provide improved spatial resolution for critical water-quality conditions.

**tholeiite.**—A silica-oversaturated (quartz-normative) basalt, characterized by the presence of low-calcium pyroxenes in addition to clinopyroxene and calcic plagioclase. Olivine may be present in the mode, but neither olivine nor nepheline appear in the norm.

**trace element.**—A chemical element that is present in minute quantities in a substance.

**tracer.**—A stable, easily detected substance or a radioisotope added to surface or ground water to follow the location of the substance in the environment to estimate hydraulic or hydrochemical properties.

**trachyte.**—A group of fine-grained, usually porphyritic, extrusive rocks having alkali feldspar and minor mafic minerals (biotite, hornblende, or pyroxene) as the main components, and possibly a small amount of sodic plagioclase; also, any member of that group; the extrusive equivalent of *syenite*.

**transmissivity.**—The rate at which water of the prevailing kinematic viscosity is transmitted through a unit width of an aquifer under a unit hydraulic gradient. It equals the hydraulic conductivity multiplied by the aquifer thickness.

**unconfined aquifer.**—An aquifer whose upper surface is a water table free to fluctuate under atmospheric pressure.

**unconsolidated deposit.**—Deposit of loosely bound sediment that typically fills topographically low areas.

**unsaturated zone.**—A subsurface zone above the water table in which the pore spaces may contain a combination of air and water.

**upgradient.**—Of or pertaining to the place(s) from which ground water originated or traveled through before reaching a given point in an aquifer.

**upland.**—A general term for nonwetland; elevated land above low areas along streams or between hills; any elevated region from which rivers gather drainage.

**water budget.**—An accounting of the inflow to, outflow from, and storage changes of water in a hydrologic unit.

**water demand.**—Water requirements for a particular purpose, such as irrigation, power, municipal supply, plant transpiration, or storage.

**water table.**—The top of the saturated zone of an unconfined aquifer where the pressure is at atmospheric pressure.

**watershed.**—The region or area drained by a river and its tributaries.

## **References**

Bates, R.L. and Jackson, J.A., (ed.), 1980, Glossary of Geology:  
American Geological Institute, Falls Church, Virginia, 749 p.

Weight, W.D., and Sonderegger, J.L., 2001, Manual of  
Applied Field Hydrogeology: McGraw-Hill, New York,  
New York, 608 p.

**Appendix A.** Water chemistry data for wells and springs (1981 to 2003), Verde River headwaters region, Arizona. Methods and laboratories described in Chapter E, this volume.

[E, estimated; nd, not determined; <, less than]

Local ID (Township, Range, Section)	STAID Station no.	Name(s) used in this report or other reports	Altitude of land surface (ft)	Depth of well (ft below land surface datum)	Altitude of water (ft)	Well log	Date (mm/dd/yyyy)	Sample start time	Dissolved oxygen, water, unfiltered (mg/L)
<b>High-Altitude Springs and Tributaries south and west of Big Chino Valley</b>									
B-13-03 14dcc	342934112322501	Aspen Creek spring	6,610				04/16/2001	1530	10.9
B-14-03 11cab	343614112324501	Surprise spring	5,750				06/21/2002	0945	
B-15-03 36baa		Mint Spring					05/11/2000	1400	8.0
B-16-04 15acd		LV-1 spring	4,620				05/28/2001	1100	3.5
B-15-04 03bcb		LV-2 well		190		X	05/28/2001		7.9
B-16-05 25cdd	344255112442001	Williamson Valley Wash HW-1	5,050				04/18/2001	1215	
B-16-05 06sbbc	344709112495501	Cabin Spring	5,570				04/18/2001	1430	nd
B-16-05 06sbbc	344709112495501	Cabin Spring	5,570				06/19/2002	1340	
B-18-06 09abb	345759112541601	Pine Spring	6,300				04/20/2001	1315	5.3
B-18-06 09abb	345759112541601	Pine Spring	6,300				06/19/2002	1305	4.8
B-18-06 20aac	345605112550901	Lee Spring	5,720				04/20/2001	1015	
B-18-06 20aac	345605112550901	Lee Spring	5,720				04/20/2001	1015	nd
B-18-06 24ddd	345525112503401	Walnut Creek well	5,150	150			06/13/1990	1145	4.7
B-18-06 24ddd	345525112503401	Walnut Creek well		150			04/19/2001	1430	3.4
<b>Low-Altitude Springs discharging to upper Verde River</b>									
B-17-02 26ccc	344914112264301	Del Rio Springs (C-3)	4,425				08/25/1991	1245	6.3
B-17-02 26ccc3	344911112264401	Del Rio Springs (C-3)	4,425				06/15/2000	1245	
B-17-02 26ccc3	344911112264401	Del Rio Springs (DRS-1)	4,425				06/19/2000	1035	5.6
B-17-02 26ccc3	344911112264401	Del Rio Springs (DRS-1)	4,425				04/17/2001	1800	5.5
B-17-02 26ccc3	344911112264401	Del Rio Springs (C-3)	4,425				12/19/2002	1330	
B-17-02 13ccb	345102112254101	Lower Granite Springs (LGS-1)	4,280				06/17/2000	1115	2.5
B-17-02 13ccb	345102112254101	Lower Granite Springs (LGS-1)	4,280				06/17/2000	1030	
B-17-02 13ccb	345102112254101	Lower Granite Springs (LGS-1)	4,280				05/30/2001	1900	3.8
B-17-02 13cbc	345103112254501	Stillman Lake (SLS-1)	4,285				12/19/2002	1130	
B-17-02 13cbc?	345103112254501?	Stillman Lake (SLS-1)	4,285				05/07/2000	0930	0.8
B-17-02 11cdd	345154112262701	Stillman Lake (SLS-2)	4,245				06/17/2000	1400	5.9
B-17-02 11cdd	345154112262701	Stillman Lake (SLS-2)	4,245				06/17/2000	1300	
B-17-02 12	SP1350	SP1350	4,240				06/17/2000	0905	
B-17-02 12ccb	345155112254801	Upper Verde River spring (BC-1)	4,240				06/15/2000	1350	
B-17-02 12ccb	345155112254801	Upper Verde River spring (SP1700) spring G	4,240				06/17/2000	1610	6.9
B-17-02 12ccb	345155112254801	Upper Verde River spring (BC-1)	4,240				04/20/2001	1600	6.9
B-17-02 12ccb	345155112254801	Upper Verde River spring (BC-1)	4,240				12/19/2002	1030	
B-17-02 12	SP2300	Upper Verde River spring (SP2300)					06/17/2000	1535	2.2
B-17-02 12	SP2625	Upper Verde River spring (SP2625)					06/18/2000	1050	5.7
B-17-02 12	SP2650	Upper Verde River spring (SP2650)					06/18/2000	1100	6.3
B-17-02 12	SP2915	Upper Verde River spring (SP2915)					06/18/2000	1110	0.6
B-17-02 12	SP4610	Upper Verde River spring (SP4610)					06/18/2000	1030	1.2
B-17-01 03cca	345243112212701	Unnamed spring near Muldoon Canyon					05/16/2003	0200	4.4

**Appendix A.** Water chemistry data for wells and springs (1981 to 2003), Verde River headwaters region, Arizona. Methods and laboratories described in Chapter E, this volume. (Continued)

pH, water, unfiltered (standard units)	Specific conductance, water, unfiltered ( $\mu\text{S}/\text{cm}$ @ 25°C)	Temperature, water (°C)	Bicarbonate, water, titration (mg/L)	Alkalinity, water, titration (mg/L as $\text{CaCO}_3$ )	Aluminum, water, filtered ( $\mu\text{g}/\text{L}$ )	Arsenic, water, filtered ( $\mu\text{g}/\text{L}$ )	Boron, water, filtered ( $\mu\text{g}/\text{L}$ )	Barium, water, filtered ( $\mu\text{g}/\text{L}$ )	Bromide, water, filtered (mg/L)	Calcium, water, filtered (mg/L)	Chloride, water, filtered (mg/L)	Fluoride, water, filtered (mg/L)
<b>High-Altitude Springs and Tributaries south and west of Big Chino Valley</b>												
6.1	136	8.5	67	55	<15		E11.38			15	3	
6.9	336	16.2	168	138	<15		23			36	8	
6.7	179	15.0	122	105	5.3	0.4	32	63		21	7	0.7
7.2	601	20.5	354	290			65	110		89	9	0.6
7.8	416	16.7	220	180	<0.01	<100	24	12		47	13	0.4
6.7	97	18.8	44	36	<15		33			10	3	
7.4	364	22.0	210	172			26			28	10	
6.8	358	22.5	206	169	<15		16			25	10	
7.2	959	8.0	639	524			32			72	11	
7.2	921	12.0	631	517	<15		33			76	11	
7.9	751	16.0	442	362	<15		39			71	24	
7.9	751	16.0	442	362			39			71	24	
7.6	580	16.5		297		2	30	36		68	12	0.9
7.0	589	16.6	357	294			24	32		71	10	1.2
<b>Low-Altitude Springs discharging to upper Verde River</b>												
8.3	330	20.0	136	111		17	40	10	0.14	30	19	0.3
7.6	376	19.8								29	22	0.3
7.6	345	18.5	151	124	0.83	11	41	8.7		46	21	0.5
7.7	367	18.6	155	127				8.7		25		
7.9	443	16.5		144	<15	11	40			36	25	
7.3	458	18.9	226	185	7.8	16	81	33		48	21	0.5
7.3	548	18.9								43	21	0.3
7.9	457	20.3	224	184								
8.0	474	16.1	246	292	<15	11	56			45	24	
6.8	546	15.2	293	240	3.6	7	80	170		56	16	0.4
8.1	454	28.0	251	206	8.2	12	70	92		87	14	0.4
8.1	454	28.0								43	16	0.3
7.4								86		51	23	0.4
7.2	654	20.5			1.6	13				44	20	0.4
7.4	552	19.8		285	16	19	200	45		30	24	0.5
7.3	549	19.5	329	270	16	19		49		39		
7.8	474	19.0	256	210	<15	19	136			40	17	
7.1	557	25.0	293		4.8	17	200	49		43	20	0.5
7.1	579	21.1	305	240	6.1	20	210	50		45	19	0.5
7.3	584	20.0	329	260	7.4	21	200	52		42	19	0.5
6.9	663	24.7	354	293	2.4	29	200	64		46	23	0.5
7.3	642	21.4	354	303	8.6	29	270	62		53	23	0.5
6.8	704	18.2	330	270	0.71	26	260	110		55	23	0.5

**Appendix A.** Water chemistry data for wells and springs (1981 to 2003), Verde River headwaters region, Arizona. Methods and laboratories described in Chapter E, this volume. (Continued)

Iron, water, filtered (µg/L)	Potassium, water, filtered (µg/L)	Lithium, water, filtered (µg/L)	Magnesium, water, filtered (mg/L)	Manganese, water, filtered (µg/L)	Sodium, water, filtered (µg/L)	Nitrate, water, filtered (mg/L as N)	Silica as Si, water, filtered (mg/L)	Silica as SiO <sub>2</sub> , water, filtered (mg/L)	Sulfate, water, filtered (mg/L)	Strontium, water, filtered (µg/L)	Uranium, water, filtered (µg/L)	Vanadium, water, filtered (µg/L)
<b>High-Altitude Springs and Tributaries south and west of Big Chino Valley</b>												
<10	0.5	<3.9	4	<3.2	5		17	28	2.8	123		<8
<10	0.6	19	11	14	16		31	50	13.6	192		<8
23	0.5	12	5	4	10	0.4	9	14	5.1	150	0.48	0.2
	1.7	7	19		18	2.4	14		11.0	440	3.17	10
<0.02	1.4	15	15	5	16	7.9	15		8.1	370	1.85	
<10	1.1	E2.37	3	6	3		23		3.3	69		<8
	1.4	25	18	172	21		43		2.8	191		<8
<10	0.9	28	18	3	22		35		4.7	147		<8
<10	0.4	E2.90	80	<3.2	8		11		17.7	96		<8
<10	0.7	E3.66	82	50	8		13		14.4	94		<8
<10	0.9	18	47	E2.46	20		28		20.2	150		E4.58
	0.9	18	47	3	20		28		20.2	150		4.6
4	0.9	23	28	<1	16		30		3.8	140		3
	1.0	18	29		17	3.6	15		4.7	140	3.81	10
<b>Low-Altitude Springs discharging to upper Verde River</b>												
4	2.6	10	15	<1	17			33	12.0	480		15
	2.5		16		17		33		14.4			
	2.4	10	21	14	21	6.2	16		14.0	500	1.81	15
15	1.9	7	12	13	13			24	9.3	460	1.44	12
<10	2.7	9	19	5	17		34		20.8	541		11.3
22	2.9	12	22	24	20	4.6	20	31	13.0	620	2.08	8.8
	2.9		21		21		43		14.7			
											2.51	
16	3.0	10	20	67	18		39		14.7	600		E5.87
61	3.8	17	24	220	21	1.3	18	28	15.0	540	0.63	2.5
44	2.5	15	40	900	9	0.4	16	26	13.0	560	1.83	0.6
	4.6		22		21		34		10.1			
82		21	20	260	28			46	4.0	490	0.45	0.6
	3.2		22		44		43		12.7			
	3.0	36	16	10	17	4.1	20		15.0	390		
35	2.5	32	17	0	34			34	9.7	380	3.34	11
<10	2.7	28	19	<2	32		42		11.1	346		11.8
30	4.0	39	23	16	46	1.3	13	21	14.0	380	2.69	7.4
28	3.0	39	22	4	44	5.6	20	35	14.0	380	3.08	10
28	2.8	37	21	0	44	5.9	19	35	14.0	360	2.91	11
65	6.2	39	23	520	47	0.4	20	37	13.0	400	2.91	1.5
34	3.3	49	26	11	60	2.4	21	36	16.0	440	2.91	10
40	2.6	41	25	12	57	<0.08		34	23.0	380	0.79	0.81

**Appendix A.** Water chemistry data for wells and springs (1981 to 2003), Verde River headwaters region, Arizona. Methods and laboratories described in Chapter E, this volume. (Continued)

Local ID (Township, Range, Section)	STAID Station no.	Name(s) used in this report or other reports	Altitude of land surface (ft)	Depth of well (ft below land surface datum)	Altitude of water (ft)	Well log	Date (mm/dd/yyyy)	Sample start time	Dissolved oxygen, water, unfiltered (mg/L)
<b>Low-Altitude Springs discharging to upper Verde River (continued)</b>									
A-17-01 07aaa UNSURV	345235112172501	Duff Spring	4,055				07/04/1991	1145	6.4
A-17-01 07aaa UNSURV	345235112172501	Duff Spring	4,055				06/13/2000	1200	
A-17-01 07aaa UNSURV	345235112172501	Duff Spring	4,055				12/18/2002	1640	
<b>Carbonate Aquifer north of upper Verde River (Mississippian-Devonian sequence)</b>									
B-19-02 19bdd	350107112305601	Storm Seep	5,580		5,400		05/07/2000	1700	
B-19-02 19bdd	350107112305601	Storm Seep	5,580				04/19/2001	1130	7.7
B-19-02 19bdd	350107112305601	Storm Seep	5,580				06/20/2002	1045	5.6
B-19-03 26adb	350022112324001	Pool Seep	5,380				04/19/2001	1345	6.1
B-20-02 35baa	350535112263601	Meath Spring	4,990		5,000		04/17/2001	1630	9.9
B-20-04 02cdb		Tucker Canyon Spring			4,830		05/11/2000	1030	2.6
B-18-01 06abb	345843112240201	Hell Well (BBM-04)		460			07/04/1987		
B-18-01 17aaa	345653112223701	Gipe well	4,643	620			08/18/1994	1230	
B-18-01 17aaa	345653112223701	Gipe well		620	4,220	X	05/31/2001	1300	9.2
B-19-01 16aca	350154112220001	Bean well, well M		720	4,240	X	05/26/2002	0940	5.1
A-19-01 33bbd	345905112174401	Bar Hart Ranch well	4,460	585			08/03/1994	1400	4.2
A-19-01 33bbd	345905112174401	Bar Hart Ranch well	4,460	585	3,926		05/24/2002	1830	7.8
A-18-01 18bbb	345644112193601	King Spring	4,200	Surface	4,200		05/05/2000	1630	3.4
A-17-01 02bba		Mormon Pocket spring	3,675	Surface	3,675		05/21/2002	0830	8.8
A-17-03 05caa		Summers Spring	3,640	Surface	3,640		05/20/2002	1500	7.1
<b>Little Chino Basin-fill Aquifer</b>									
B-15-02 23cbd	343938112263201	LC-10	5,071	578			05/06/1981	1530	
B-16-01 17ccb	344540112234301	Schaible well	4,764	305			05/07/1981	1000	
B-16-01 17ccb	344540112234301	Schaible well		305	nd		05/27/2001	1100	10.5
B-17-02 15acc		Arnold well		250	-4,260	X	04/17/2001	1430	6.4
B-17-02 15caa	345122112272601		4,390	170			05/07/2003	1100	5.6
B-17-02 15cad2	345115112273101		4,377	157			05/06/2003	1140	
<b>Big Chino Basin-fill Aquifer</b>									
B-17-02 04aaa	345342112281501	C-7	4,390	298			09/08/1991	1130	6.0
B-17-02 04aaa	345342112281501	C-7	4,390	298			03/05/2003	1140	4.8
B-17-02 04ddc		Smith/Texaco, well E	4,390	200	-4,260	X	06/01/2001	0900	8.9
B-17-02 09dba	345220112282501		4,380	190			03/04/2003	1130	6.1
B-17-02 09ddd2	345157112280701	C-2		130			09/08/1991	1330	6.8
B-17-02 10cac	345209112274001		4,393	310			03/07/2003	1220	4.1
B-17-02 S34bca4	345041112274501	C-1		57			09/08/1991	1245	6.8
B-17-02 S34bba	344822112274301	C-5		?			09/08/1991	0915	10.7



**Appendix A.** Water chemistry data for wells and springs (1981 to 2003), Verde River headwaters region, Arizona. Methods and laboratories described in Chapter E, this volume. (Continued)

pH, water, unfiltered (standard units)	Specific conductance, water, unfiltered ( $\mu\text{S}/\text{cm}$ @ 25°C)	Temperature, water (°C)	Bicarbonate, water, titration (mg/L)	Alkalinity, water, titration (mg/L as $\text{CaCO}_3$ )	Aluminum, water, filtered ( $\mu\text{g}/\text{L}$ )	Arsenic, water, filtered ( $\mu\text{g}/\text{L}$ )	Boron, water, filtered ( $\mu\text{g}/\text{L}$ )	Barium, water, filtered ( $\mu\text{g}/\text{L}$ )	Bromide, water, filtered (mg/L)	Calcium, water, filtered (mg/L)	Chloride, water, filtered (mg/L)	Fluoride, water, filtered (mg/L)
<b>Low-Altitude Springs discharging to upper Verde River (continued)</b>												
8.1	438	26.0	250	205				48	0.15	47	14	0.3
7.8	442	20.3								43	14	0.2
7.7	404	17.0	226	185	<15	41	68			42	14	
<b>Carbonate Aquifer north of upper Verde River (Mississippian-Devonian sequence)</b>												
8.3	471				6.4	1.2	33	38		64	4	0.1
7.8	511	10.5	325	267	<15		21			86	4	
7.6	386	13.0		169	<15		20			57	4	
8.1	655	12.0	333	271	<15		62			58	10	
9.2	159	20.6	71	53			19			20	3	
7.1	996	14.5	573	470	6.1	6	95	160		72	47	0.4
8.5	423			178			60			41	14	0.1
7.7	451	20.4	227	186			43	160		49	11	0.3
7.7	380	23.6	220	180	2.1	7.3	12	351		40	7	0.2
7.6	349	18.0		179		10	40	300	0.03	41	3	0.1
7.6	345	19.4	215	176	2.3	15	25	299		40	4	0.1
6.9	675	19.0	410	336	4.3	3	39	140		87	7	0.4
7.5	357	18.4	220	180	3.4	16	51	299		39	4	0.2
7.0	534	19.4	320	262	3.4	12	71	186		63	6	0.1
<b>Little Chino Basin-fill Aquifer</b>												
7.8	330						20			37	10	0.2
7.9	338			110		3	30			44	16	0.0
7.2	266	17.7	122	110			21	110		31	5	0.3
7.3	502	17.0	237	194			55	44		54	21	0.4
7.7	491	16.5	247	203	<15	11	52			55	23	
7.6	505	15.3	248	204	<15	11	61			55	25	
<b>Big Chino Basin-fill Aquifer</b>												
7.8	430	19.0	183	150		12	70	30	0.13	42	18	0.4
7.8	406	17.5	218	179	<15	13	73			41	14	
7.8	386	18.7	195	160			73	22		36	13	0.5
7.7	353	16.2	197	161	<15	14	75			36	12	
7.8	530	16.0	231	189		10	70	55	0.18	61	23	0.3
7.6	548	15.5	298	244	<15	5	79			58	23	
7.8	445	17.5	178	146		12	50	26	0.16	52	21	0.3
8.0	325	19.5	110	90		12	40	5	0.14	37	21	0.3

**Appendix A.** Water chemistry data for wells and springs (1981 to 2003), Verde River headwaters region, Arizona. Methods and laboratories described in Chapter E, this volume. (Continued)

Iron, water, filtered (µg/L)	Potassium, water, filtered (µg/L)	Lithium, water, filtered (µg/L)	Magnesium, water, filtered (mg/L)	Manganese, water, filtered (µg/L)	Sodium, water, filtered (µg/L)	Nitrate, water, filtered (mg/L as N)	Silica as Si, water, filtered (mg/L)	Silica as SiO <sub>2</sub> , water, filtered (mg/L)	Sulfate, water, filtered (mg/L)	Strontium, water, filtered (µg/L)	Uranium, water, filtered (µg/L)	Vanadium, water, filtered (µg/L)
<b>Low-Altitude Springs discharging to upper Verde River (continued)</b>												
	1.0		24		11		16		8.3	170		
	1.3		24		11		18		6.4			
<10	1.4	9	24	<2	11	3.4	19		5.8	162		8
<b>Carbonate Aquifer north of upper Verde River (Mississippian-Devonian sequence)</b>												
1600	0.5	10	16	9	3	7.9	5	9	23.0	82	0.52	1.8
<10	0.2	<3.9	16	36	3		9		22.2	74		<8
<10	0.5	<3.9	15	8	3		12		26.0	70		<8
<10	1.1	6	46	<3.2	10		12		51.1	86		E6.46
<10	3.8	<3.9	6	E1.80	3		17		3.2	130		9.2
<0.05	3.0	<10	88	130	34	0.4	17	25	27.0	360	1.50	1.9
10	1.3		21	1	11	1.2	16		7.5			
	1.1	12	19		10	7.9	7		6.9	110	0.82	
39	1.3	3	19	19	6	3.1	9	18	18.0	101	0.57	0.55
<3	1.4	6	16	<1	5		16		3.0	110		7
39	1.3	6	15	15	5	0.3	7	15	15.0	109	0.72	0.77
72	1.6	10	40	46	9	0.4	11	16	4.9	280	0.58	0.68
38	1.3	10	16	16	7	0.2	7	15	15.0	120	0.72	0.74
64	1.1	15	24	23	5	0.3	6	13	13.0	106	0.52	0.55
<b>Little Chino Basin-fill Aquifer</b>												
30	1.7		14	M	12		37		6.1			
20	1.1		9	M	10		22		14.0			
	1.2	7	9		9	26	10		8.2	340	0.91	
	3.1	13	20		20	7.5	18		16.0	560	4.11	14
<10	3.0	14	20	<2	19		39		17.2	583		14.7
<10	3.0	13	19	<2	22		39		18.7	555		18.5
<b>Big Chino Basin-fill Aquifer</b>												
4	3.1	20	18	<1	20			38	12.0	420		13
<10	3.1	18	18	<2	18		45		10.9	417		15.5
	3.0	17	16		18	5.4	22		9.2	370	2.56	16
<10	2.9	17	15	<2	17		48		7.7	366		17.7
5	3.2	15	21	<1	23			39	14.0	590		11
10	3.5	8	24	<2	24		33		21.0	430		9.1
3	2.6	14	16	<1	17			42	13.0	450		13
<3	1.6	9	9	<1	14			33	9.2	270		14

**Appendix A.** Water chemistry data for wells and springs (1981 to 2003), Verde River headwaters region, Arizona. Methods and laboratories described in Chapter E, this volume. (Continued)

Local ID (Township, Range, Section)	STAID Station no.	Name(s) used in this report or other reports	Altitude of land surface (ft)	Depth of well (ft below land surface datum)	Altitude of water (ft)	Well log	Date (mm/dd/yyyy)	Sample start time	Dissolved oxygen, water, unfiltered (mg/L)
<b>Big Chino Basin-fill Aquifer (continued)</b>									
B-18-02 31cdc		Prucha well, well D		300	~4,259	X	04/17/2001	1430	6.3
B-18-03 25cda	345442112315801	C-4		334			09/09/1991	0945	4.3
B-19-03 18ccc	350138112374101	C-9		200			09/09/1991	1030	6.4
B-19-03 28dac	350002112344201	T2 windmill, well C	4,639	190			06/13/1990	1100	4.2
B-19-03 28dac	350002112344201	T2 windmill, well C		190	4,467		05/24/2002	1600	nd
B-19-03 30bcb		T2, well B		750	4,470		05/30/2001	1600	6.6
B-19-04 04bdb		RWK, well A		569	4,520		05/30/2001	1100	6.8
B-19-04 04cac	350332112413701	C-8	4,547	500			08/26/1991	1230	5.8
B-19-04 04cac	350332112413701	C-8	4,547	500			06/08/1992	1230	6.3
B-19-04 04cac	350332112413701	C-8	4,547	500			05/24/1993	1200	9.1
B-19-04 04cac	350332112413701	C-8	4,547	500			07/14/1994	1130	4.6
B-19-04 04cac	350332112413701	C-8	4,547	500			06/20/1996	1100	5.4
B-19-04 04cac	350332112413701	C-8	4,547	500			06/12/1997	0915	5.6
B-19-04 04cac	350332112413701	C-8	4,547	500			06/22/1998	1345	5.4
B-19-04 04cac	350332112413701	C-8	4,547	500			05/30/2001	0930	5.3
B-21-02 14bcc	351207112283701	AF-06		1,700			08/26/1991	0930	nd
B-23-07 1ccc	352410112581001	BC-19	5,150	500			08/13/1986	0845	10.8
B-23-07 26dda	352045112583401	BC-10	5,207	474			06/11/1990	1400	4.8
<b>Carbonate Aquifer underlying Big Chino Basin-fill Aquifer (Devonian-Cambrian zone)</b>									
B-17-02 02cac	345302112264701	C-6/Wagner, well F	4,590	480			08/29/1991	0800	6.6
B-17-02 02cac	345302112264701	C-6/Wagner, well F	4,590	480			03/06/2003	1200	4.7
B-17-02 02cac	345302112264701	C-6/Wagner, well F	4,590	480	4,245	X	05/31/2001	1500	7.4
B-18-02 21acb		Reeves well, well H		346	~4,263	X	05/27/2001	1700	5.7
B-18-02 27cba	345459112275601	C-11		285			09/09/1991	0830	5.2
B-18-02 27cda	345440112274101	LS-12		3,010			08/29/1991	0930	6.3
B-18-02 28bab	345525112285201		4,490	335			05/08/2003	0955	4.8

**Appendix A.** Water chemistry data for wells and springs (1981 to 2003), Verde River headwaters region, Arizona. Methods and laboratories described in Chapter E, this volume. (Continued)

pH, water, unfiltered (standard units)	Specific conductance, water, unfiltered ( $\mu\text{S}/\text{cm}$ @ 25°C)	Temperature, water (°C)	Bicarbonate, water, titration (mg/L)	Alkalinity, water, titration (mg/L as $\text{CaCO}_3$ )	Aluminum, water, filtered ( $\mu\text{g}/\text{L}$ )	Arsenic, water, filtered ( $\mu\text{g}/\text{L}$ )	Boron, water, filtered ( $\mu\text{g}/\text{L}$ )	Barium, water, filtered ( $\mu\text{g}/\text{L}$ )	Bromide, water, filtered (mg/L)	Calcium, water, filtered (mg/L)	Chloride, water, filtered (mg/L)	Fluoride, water, filtered (mg/L)
<b>Big Chino Basin-fill Aquifer (continued)</b>												
7.6	548	15.5	298	244	<15	5	79			58	23	
7.8	445	17.5	178	146		12	50	26	0.16	52	21	0.3
8.0	325	19.5	110	90		12	40	5	0.14	37	21	0.3
7.8	277	18.5	110	90			41	22		29	8	0.5
8.0	430	19.0	165	135		nd	130	56	0.21	24	28	0.8
8.0	323	18.5	184	150		7	40	150	0.13	28	12	0.3
7.5	476	17.5		207		1	30	250		52	19	0.2
7.5	488		244	200	3.2	3	16	218		46	18	0.2
8.0	388	20.1	195	160			40	46		21	9	0.3
7.6	480	21.9	271	222			54	160		33	12	0.3
7.9	436	22.0	202	165		14	60	130	0.13	32	13	0.3
7.6	538	20.0	294	241			60			42	20	0.2
7.7	695	15.0		274			110			64	22	0.2
7.7	473	21.5		210			70			34	13	0.3
7.6	457	21.5		204			60			34	12	0.3
7.8	444	22.0		206			60			33	13	0.3
7.6	452	22.0		200			70			31	12	0.3
7.8	464	21.5		223			59			33	13	0.3
7.9	614	nd	nd	nd		nd	nd	43	0.20	54	30	0.3
7.4	387	20.0		174		3	60	94		39	10	0.2
7.7	432	19.0		220		2	40	350		46	16	0.2
<b>Carbonate Aquifer underlying Big Chino Basin-fill Aquifer (Devonian-Cambrian zone)</b>												
8.1	400	18.5	187	153		13	80	31	0.14	42	19	0.2
7.7	423	18.2	235	193	<15	14	88			41	15	
8.0	437	23.9	217	178			87	29		41	14	0.4
7.0	903	25.9	500	410			440	61	0.18	64	27	1.1
7.6	795	25.0	379	310		38	390	74	0.17	57	29	0.7
7.8	730	24.0	334	273		33	330	70		55	nd	0.8
7.3	699	23.5	411	337	<15	37	456			43	24	

**Appendix A.** Water chemistry data for wells and springs (1981 to 2003), Verde River headwaters region, Arizona. Methods and laboratories described in Chapter E, this volume. (Continued)

Iron, water, filtered (µg/L)	Potassium, water, filtered (µg/L)	Lithium, water, filtered (µg/L)	Magnesium, water, filtered (mg/L)	Manganese, water, filtered (µg/L)	Sodium, water, filtered (µg/L)	Nitrate, water, filtered (mg/L as N)	Silica as Si, water, filtered (mg/L)	Silica as SiO <sub>2</sub> , water, filtered (mg/L)	Sulfate, water, filtered (mg/L)	Strontium, water, filtered (µg/L)	Uranium, water, filtered (µg/L)	Vanadium, water, filtered (µg/L)
<b>Big Chino Basin-fill Aquifer (continued)</b>												
<3	1.4	12	10		12	18	20		7.3	180	1.02	10
<3	2.3	nd	22	<1	24			73	6.1	720		nd
<3	1.5	10	28	<1	13			22	7.1	230		15
24	1.1	12	26	<11	10		21		7.7	150		3
	1.2	7	24		9	15	10		10.0	135	1.46	
	2.2	8	26		16	10	10		5.4	360	0.74	22
	3.1	9	26		20	13	14		8.6	300	2.10	13
<3	2.5	12	26	<1	23			30	7.0	330		13
8	2.4		32	<1	21		27		16.0			
4	1.1		37	<1	35		30		35.0			
5	2.1		27	<1	24		31		9.9			
<3	2.5		27	<1	22		30		7.7			
<3	2.4		26	<1	20		30		7.0			
<10	2.5		27	4	22		29		7.2			
<2	2.3		26	<1	23		27		8.0			
nd	1.4	nd	19	nd	48			17	8.8	150		nd
12	2.9	11	21	6	7		17		5.0	190		8
<3	1.4	12	24	7	6		18		6.4	180		2
<b>Carbonate Aquifer underlying Big Chino Basin-fill Aquifer (Devonian-Cambrian zone)</b>												
7	2.9	21	18	<1	23			38	13.0	410		12
<10	3.0	19	18	<2	21		44		12.0	408		13.4
	3.0	19	18		23	6.7	20		11.0	400	2.69	12
	4.0	86	28		93	5.9	17		23.0	350	3.66	11
4	3.6	79	27	<1	84			40	16.0	390		10
9	3.3	66	26	1	77			34	30.0	380		11
E8.7	2.9	54	26	<2	71		34		16.4	419		17.9

**Appendix B.** Isotope data for wells and springs (1986 to 2003), Verde River headwaters, Arizona. Methods and laboratories described in Chapter E, this volume.

[E, estimated; nd, not determined; <, less than]

Local ID (Township, Range, Section)	STAID Station no.	Name(s) used in this report or other reports	Collecting agency	Date (mm/dd/yyyy)	Sample start time	Oxygen-18/ Oxygen-16 ratio, water, unfiltered (per mil)	Deuterium/ Protium ratio, water, unfiltered (per mil)	Carbon-13/ Carbon-12 ratio, water, unfiltered (per mil)	Carbon-14 activity, water, unfiltered (% modern carbon)	Carbon-14 2-sigma uncertainty, water, unfiltered (% modern carbon)	Tritium, water, unfiltered (picocuries/ L)	Tritium 2-sigma combined uncertainty (picocuries/ L)	Tritium, water, unfiltered (TU)	Tritium 2-sigma combined uncertainty (TU)
<b>High-Altitude Springs and Tributaries south and west of Big Chino Valley</b>														
B-13-03 14dcc	342934112322501	Aspen Creek spring	USGS	04/16/2001	1530	-11.1	-75.1							
B-14-03 11cab	343614112324501	Surprise spring	USGS	02/07/2002	1445	-11.1	-77.9			14.4	1.9	4.5	0.6	
B-14-03 11cab	343614112324501	Surprise spring	USGS	06/21/2002	0945	-11.1	-78.5							
B-15-03 36baa		Mint Spring	USGS	05/11/2000	1400	-7.1	-60	-8.2					9.9	0.5
B-15-04 03bcb		LV-2 well	USGS	05/28/2001		-10.6	-75.0	-11.9	79.1	0.7			1.3	0.3
B-16-04 14adb	344618112385901		USGS	01/17/2002	1230	-9.9	-72.4			1.0	1.0	0.3	0.3	
B-16-04 14dcd			ASU	12/1996		-10.6	-75.0							
B-16-04 15acd		LV-1 spring	USGS	05/28/2001	1100	-10.8	-77.0	-12.2	106.5	0.8			3.8	0.3
B-16-05 25cdd	344255112442001	Williamson Valley Wash HW-1	USGS	04/18/2001	1215	-10.0	-71.8							
B-16-05 06sbbc	344709112495501	Cabin Spring	USGS	04/18/2001	1430	-10.5	-74.7	-12.0					3.1	0.5
B-16-05 06sbbc	344709112495501	Cabin Spring	USGS	02/07/2002	1710	-11.2	-77.0			4.2	1.3	1.3	0.4	
B-16-05 06sbbc	344709112495501	Cabin Spring	USGS	06/19/2002	1340	-11.2	-78.6							
B-17-04 14cbd			ASU	05-12/		-10.8	-73.5							
B-17-04 36bcb			USGS	08/30/1987		-11.1	-77.0							
B-18-06 09abb	345759112541601	Pine Spring	USGS	04/20/2001	1315	-11.0	-78.5	-11.0					6.0	0.5
B-18-06 09abb	345759112541601	Pine Spring	USGS	06/19/2002	1305	-10.9	-80.2							
B-18-06 20aac	345605112550901	Lee Spring	USGS	04/20/2001	1015	-10.2	-74.3							
B-18-06 20aac	345605112550901	Lee Spring	USGS	04/20/2001	1015	-10.2	-74.3	-6.4					3.7	0.5
B-18-06 24ddd	345525112503401	Walnut Creek well	USGS	04/19/2001	1430	-10.7	-76.0	-11.2	81.1	0.6				
B-18-06 24ddd		Walnut Creek well	ASU	12/1996		-10.4	-73.0						0.7	0.6
<b>Low-Altitude Springs discharging to upper Verde River</b>														
B-17-02 26ccc	344914112264301	Del Rio Springs (C-3)	USGS	08/25/1991	1245	-9.9	-71.0	-11.5						
B-17-02 26ccc3	344911112264401	Del Rio Springs (C-3)	USGS	06/1993		-9.9	-72.0							
B-17-02 26ccc3	344911112264401	Del Rio Springs (DRS-1)	USGS	06/15/2000	1245	-10.0	-71.0							
B-17-02 26ccc3	344911112264401	Del Rio Springs (DRS-1)	USGS	06/19/2000	1035	-10.1	-72.0							
B-17-02 26ccc3	344911112264401	Del Rio Springs (C-3)	USGS	04/17/2001	1800	-10.0	-71.5	-10.7	66.4	1.0			1.0	0.4
B-17-02 26ccc3	344911112264401	Del Rio Springs (C-3)	USGS	12/19/2002	1330	-9.8	-70.0						1.0	0.4
B-17-02 13ccb	345102112254101	Lower Granite Spring (LGS-1)	USGS	06/17/2000	1115	-9.7	-70.0	-10.4						
B-17-02 13ccb	345102112254101	Lower Granite Spring (LGS-1)	USGS	06/17/2000	1030	-9.6	-69.2							
B-17-02 13ccb	345102112254101	Lower Granite Spring (LGS-1)	USGS	05/30/2001	1900	-9.7	-69.0	-11.3	81.5	0.4			1.8	0.9
B-17-02 13ccb	345102112254101	Lower Granite Spring (LGS-1)	USGS	12/19/2001	1200	-9.6	-70.3						1.3	1.0
B-17-02 13cbc	345103112254501	Stillman Lake	USGS	12/19/2002	1130	-9.4	-68.9							
B-17-02 10cdd		Stillman Lake (SLS-1)	USGS	05/07/2000	0930	-8.7	-66.0	-7.6					0.7	0.3
B-17-02 11cdd		Stillman Lake (SLS-2)	USGS	06/17/2000	1400	-8.3	-65.0	-5.6						
B-17-02 10cdd		Stillman Lake (SLS-1)	USGS	06/17/2000	1300	-7.9	-62.3			7.4	1.9	2.3	0.6	
B-17-02 13cbc	345103112254501	Stillman Lake	USGS	01/16/2002	1040	-8.5	-67.9							
B-17-02 12ccb	345155112254801	Upper Verde River spring (BC-1)	USGS	06/15/2000	1350	-10.1	-73.2							
B-17-02 12cca	345155112253601	Upper Verde River spring (BC-1)	USGS	01/16/2002	1500	-10.1	-73.8			1.6	0.7	0.5	0.2	
B-17-02 12cca	345155112253601	Upper Verde River spring (BC-1)	USGS	12/19/2002	1030	-9.9	-73.2							
B-17-02 12ccb	345155112254801	Upper Verde River spring G (SP1700)	USGS	06/17/2000	1610	-10.3	-75.0	-7.0					0.7	
B-17-02 12ccb	345155112254801	Upper Verde River spring (BC-1)	USGS	04/20/2001	1600	-10.3	-75.0	-3.6	42.1	0.3			0.7	0.9
B-17-02 12ccb	345155112254801	Upper Verde River spring (BC-1)	USGS	02/08/2002	1010	-10.1	-73.7			2.2	1.3	0.7	0.7	0.4
B-17-02 12ccb	345155112254801	Upper Verde River spring (SP2300)	USGS	12/19/2002	1030	-10.1	-73.8							
B-17-02 12ccb	34523311212701	Unnamed spring near Muldoon Canyon	USGS	05/16/2003	0200	-10.3	-75.0	-7.0	49.9	0.2				

**Appendix B.** Isotope data for wells and springs (1986 to 2003), Verde River headwaters, Arizona. Methods and laboratories described in Chapter E, this volume. (Continued)

Local ID (Township, Range, Section)	STAID Station no.	Name(s) used in this report or other reports	Collecting agency	Date (mm/dd/yyyy)	Sample start time	Oxygen-18/ Oxygen-16 ratio, water, unfiltered (per mil)	Deuterium/ Protium ratio, water, unfiltered (per mil)	Carbon-13/ Carbon-12 ratio, water, unfiltered (per mil)	Carbon-14 activity, water, unfiltered (% modern carbon)	Carbon-14 2-sigma uncertainty, water, unfiltered (% modern carbon)	Tritium, water, unfiltered (picocuries/ L)	Tritium 2-sigma combined uncertainty (picocuries/ L)	Tritium, water, unfiltered (TU)	Tritium 2-sigma combined uncertainty (TU)
<b>Low-Altitude Springs discharging to upper Verde River (continued)</b>														
B-17-02 12		SP2625	USGS	06/18/2000	1050	-10.4	-75.0						1.1	0.4
B-17-02 12		SP2650	USGS	06/18/2000	1100	-10.4	-75.0						0.8	0.4
B-17-02 12		SP2915	USGS	06/18/2000	1110	-10.3	-74.0						<0.4	
B-17-02 12		SP4610	USGS	06/18/2000	1030	-10.4	-75.0			0.3	0.6		0.1	0.2
B-17-01 03cca	345243112212701	Unnamed spring at Muldoon Canyon	USGS	05/16/2003		-10.0	-74.0	-7.0						
A-17-01 07aaa														
UNS	345235112172501	Duff Spring	USGS	07/04/1991	1145	-9.2	-67.0	-8.2						
A-17-01 07aaa														
UNS	345235112172501	Duff Spring	USGS	06/13/2000	1200	-9.2	-68.1							
A-17-01 07aaa														
UNS	345235112172501	Duff Spring	USGS	12/18/2002	1640	-9.3	-70.5							
<b>Carbonate Aquifer north of upper Verde River (Mississippian-Devonian sequence)</b>														
B-19-02 19bdd	350107112305601	Storm Seep	USGS	05/07/2000	1700	-11.6	-83.0	-6.0					5.2	0.4
B-19-02 19bdd	350107112305601	Storm Seep	USGS	04/19/2001	1130	-11.4	-81.0							
B-19-02 19bdd	350107112305601	Storm Seep	USGS	06/20/2002	1045	-10.8	-77.1							
B-19-03 26adb	350022112324001	Pool Seep	USGS	04/19/2001	1345	-11.0	-80.8						10.3	
B-20-02 35baa	350535112263601	Meath Spring	USGS	04/17/2001	1630	3.06	-16.5	-15.2					5.6	0.6
B-20-04 02cdb		Tucker Canyon Spring	USGS	05/11/2000	1030	-1.3	-40.0	-6.7						0.4
B-18-01 06abb	345843112240201	Hell well (BBM-04)	USGS	07/04/1987		-10.1	-73.5							
B-18-01 27aac		Glidden well (BBM-111)	ASU	09/1996		-10.5	-78.0							
B-18-01 27aac		Glidden well (BBM-111)	ASU	05/1996		-10.4	-70.0							0.3
B-18-01 17aaa	345653112223701	Gipe well	USGS	05/31/2001	1300	-11.2	-78.0	-7.7	34.2	0.6			0.5	
B-19-01 16aca	350154112220001	Bean well, well M	USGS	05/26/2002	0940	-10.9	-80.0	-2.0	18.6	0.2			0.6	0.6
A-19-01 33bbd	345905112174401	Bar Hart Ranch well	USGS	05/24/2002	1830	-12.0	-85.0	-6.2	24.9	0.2			0.5	0.4
A-18-01 18bbb	345644112193601	King Spring	USGS	05/05/2000	1630	-9.5	-73.0	-1.9					3.8	
		King Spring	USGS	06/15/2000	Surface	-8.8	-70.0							0.6
		King Spring	USGS	02/08/2002	Surface	-10.2	-76.3				7.4	1.9	2.3	0.6
A-17-01 02bba		Mormon Pocket spring	USGS	05/21/2002	0830	-12.0	-85.0	-7.0	25.6	0.2			0.6	0.3
A-17-03 05caa		Summers Spring	USGS	05/20/2002	1500	-12.0	-84.0	-7.1	36.4	0.3			1.1	
<b>Little Chino Basin-fill Aquifer</b>														
B-15-02 23cbd	343938112263201	LC-10	USGS	07/04/1987		-10.3	-73.0							
B-15-02 23cba			ASU	05-09/		-10.1	-68.0							
B-16-01 17ccb	344540112234301	Schaible well	USGS	05/27/2001	1100	-11.2	-78.0	-7.3	73.1	1.6			2.7	0.3
B-16-02 04cbb			ASU	12/1996		-10.0	-74.0							
B-16-02 14bcc			ASU	09/1996		-10.1	-73.0							
B-16-02 15ada			ASU	05-09/		-8.9	-66.5							
B-17-02 14ada			ASU	12/1996		-10.7	-70.0							
B-17-02 15acc		Arnold well	USGS	04/17/2001	1430	-9.8	-70.0	-11.7	87.2	0.9				
B-17-02 15caa	345122112272601		USGS	05/07/2003	1100	-9.7	-69.6						1.2	0.5

**Appendix B.** Isotope data for wells and springs (1986 to 2003), Verde River headwaters, Arizona. Methods and laboratories described in Chapter E, this volume. (Continued)

Local ID (Township, Range, Section)	STAID Station no.	Name(s) used in this report or other reports	Collecting agency	Date (mm/dd/yyyy)	Sample start time	Oxygen-18/ Oxygen-16 ratio, water, unfiltered (per mil)	Deuterium/ Protium ratio, water, unfiltered (per mil)	Carbon-13/ Carbon-12 ratio, water, unfiltered (per mil)	Carbon-14 activity, water, unfiltered (% modern carbon)	Carbon-14 2-sigma uncertainty, water, unfiltered (% modern carbon)	Tritium, water, unfiltered (picocuries/ L)	Tritium 2-sigma combined uncertainty (picocuries/ L)	Tritium, water, unfiltered (TU)	Tritium 2-sigma combined uncertainty (TU)
<b>Little Chino Basin-fill Aquifer (Continued)</b>														
B-17-02 15cad2	345115112273101		USGS	05/06/2003	1140	-9.6	-69.6							
B-17-02 15cdd			ASU	12/1996		-9.8	-72.0							
B-17-02 17aad			ASU	12/1996		-10.2	-72.0							
B-17-02 34aca			ASU	05-12/		-9.8	-67.5							
B-17-02 N34acc			USGS	07/04/1987		-10.2	-72.0							
B-17-02 35cda			ASU	12/1996		-9.4	-61.0							
<b>Big Chino Basin-fill Aquifer</b>														
B-17-02 S03cbb1			ASU	12/1996		-10.0	-69.0							
B-17-02 04aaa	345342112281501	C-7	USGS	09/08/1991	1130	-9.4	-71.5	-9.4						
B-17-02 04aaa		C-7	ASU	12/1996		-10.4	-69.0							
B-17-02 04aaa	345342112281501	C-7	USGS	03/05/2003	1140	-10.1	-72.0							
B-17-02 06aba			ASU	12/1996		-9.5	-65.0							
B-17-02 04ddc		Smith/Texaco, well E	USGS	06/01/2001	0900	-10.3	-73.0	-8.2	54.7	0.8		1.2	0.5	
B-17-02 09bbc			ASU	M-S-D-M		-10.1	-68.5							
B-17-02 09ccb			ASU	S-D-M		-9.6	-74.0							
B-17-02 09ccd			ASU	12/1996		-9.6	-71.0							
B-17-02 09dba	345220112282501		USGS	03/04/2003	1130	-10.1	-71.0							
B-17-02 09ddd2	345157112280701	C-2	USGS	09/08/1991	1330	-9.5	-69.5	-11.8						
B-17-02 10cac	345209112274001		USGS	03/07/2003	1220	-8.8	-66.3							
B-17-02 22bca4	345041112274501	C-1	USGS	09/08/1991	1245	-9.9	-71.0	-11.9						
B-17-02 N34acc	344846112271401		USGS	07/04/1987		-10.2	-72.0							
B-17-02 S34bba	344822112274301	C-5	USGS	09/08/1991	0915	-10.1	-71.5	-10.3						
B-18-02 31cdc		Prucha well, well D	USGS	04/17/2001	1430	-10.2	-75.0	-5.5	29.8	0.6		1.1	0.4	
B-18-02 27dda			ASU	05-09/1996		-10.2	-70.5							
B-18-03 26baa			ASU	05-09/		-10.3	-76.0							
B-18-03 03aaa			ASU	05/1996		-9.6	-65.0							
B-18-03 04ccc			ASU	05-09/		-10.1	-72.0							
B-18-03 25ada			ASU	05-09/		-10.5	-78.0							
B-18-03 25cda	345442112315801	C-4	USGS	09/09/1991	0945	-9.7	-72.0	-11.3						
B-19-03 18ccc	350138112374101	C-9	USGS	09/09/1991	1030	-10.0	-72.5	-8.0						
B-19-03 28dac	350002112344201	T2 windmill, well C	USGS	05/24/2002	1600	-9.7	-73.0	-6.7	21.0	0.2		0.5	0.6	
B-18-03 30bcb		T2, well B	USGS	05/30/2001	1600	-9.6	-70.0	-8.5	24.1	0.5		1.3	0.6	
B-19-04 04bdb		RWK, well A	USGS	05/30/2001	1100	-10.0	-72.0	-9.1	55.0	0.6		0.5	0.6	
B-19-04 04cac	350332112413701	C-8	USGS	08/26/1991	1230	nd	nd	-9.1						
B-19-04 09abd			ASU	09-03/		-9.4	-69.5							
B-19-04 15aac			ASU	05-09/		-10.1	-72.0							
B-20-04 32bba			ASU	05/1996		-9.8	-67.0							
B-21-02 14bcc	351207112283701	AF-06	USGS	08/31/1987		-10.1	-75.5							
B-21-02 14bcc	351207112283701		USGS	08/26/1991	0930	-10.1	-76.0	-7.1						
B-21-05 35aba			ASU	05/1996		-10.0	-71.0							
B-21-06 14ccd	351145112540001		USGS	07/06/1987		-9.9	-74.5							
B-22-07 25adb	351554112574001		USGS	07/04/1987		-10.4	-74.5							
B-23-07 1ccc	352410112581001	BC-19	USGS	07/05/1987		-9.6	-69.0							
B-23-07 26dda	352045112583401	BC-10	USGS	07/04/1987		-9.9	-72.5							



**Appendix B.** Isotope data for wells and springs (1986 to 2003), Verde River headwaters, Arizona. Methods and laboratories described in Chapter E, this volume. (Continued)

Local ID (Township, Range, Section)	STAID Station no.	Name(s) used in this report or other reports	Collecting agency	Date (mm/dd/yyyy)	Sample start time	Oxygen-18/ Oxygen-16 ratio, water, unfiltered (per mil)	Deuterium/ Protium ratio, water, unfiltered (per mil)	Carbon-13/ Carbon-12 ratio, water, unfiltered (per mil)	Carbon-14 activity, water, unfiltered (% modern carbon)	Carbon-14 2-sigma uncertainty, water, unfiltered (% modern carbon)	Tritium, water, unfiltered (picocuries/ L)	Tritium 2-sigma combined uncertainty (picocuries/ L)	Tritium, water, unfiltered (TU)	Tritium 2-sigma combined uncertainty (TU)
<b>Carbonate Aquifer underlying Big Chino Basin-fill Aquifer (Devonian-Cambrian zone)</b>														
B-18-02 21acb		Reeves well, well H	USGS	05/27/2001	1700	-10.7	-77.0	-5.6	18.0	0.3				
B-18-02 27cba	345459112275601	C-11	USGS	09/09/1991	0830	-10.3	-75.5	-6.6					0.9	0.3
B-18-02 27cda	345440112274101	LS-12	USGS	08/31/1987		-10.5	-74.0							
B-18-02 27cda	345440112274101	LS-12	USGS	08/29/1991	0930	-10.5	-76.0	-6.4						
B-18-02 28bab	345525112285201		USGS	05/08/2003	0955	-10.1	-74.0							
B-17-02 02cac	345302112264701	C-6/Wagner, well F	USGS	08/29/1991	0800	-10.0	-71.5	-9.6						
B-17-02 02cac	345302112264701	C-6/Wagner, well F	USGS	03/06/2003	1200	-9.9	-72.2							
B-17-02 02cac	345302112264701	C-6/Wagner, well F	USGS	05/31/2001	1500	-10.2	-73.0	-8.8	55.4	0.6			0.8	